

# ACTA PHYSICA

ACADEMIAE SCIENTIARUM  
HUNGARICAE

ADIUUVANTIBUS

Z. GYULAI, L. JÁNOSSY, I. KOVÁCS, K. NOVOBÁTZKY

REDIGIT

P. GOMBÁS

TOMUS IX



1959



# ACTA PHYSICA

## TOMUS IX

G. Schmidt: Electrical Discharges in High Vacuum. — Г. Шмит: Электрические разряды в высоком вакууме .....	1
I. Berkes: Effect of Magnetic Stray Field on the Location of Image in Nuclear Spectrometers. — И. Беркеш: Влияние рассеяния магнитного поля на изображение в ядерных спектрометрах .....	13
K. L. Nagy: Tomonaga's Intermediate Coupling Theory Using Configuration Space Methods. — К. Л. Надь: Метод средней связи Томонага, при использовании конфигурационно-пространственных методов .....	23
G. Domokos: Production of Heavy Unstable Particles in Extremely Energetic Nucleon-Nucleon Collisions. — Г. Домокош: Рождение тяжелых нестабильных частиц в соударениях нуклеонов большой энергии .....	49
L. Nagy: Shower Production at Small Thicknesses of Absorber — Л. Надь: Рождение ливней при малых толщинах Al, Fe, Cu, Pb.....	63
T. Tietz: Eine analytische Formel für die Theorie der Bildung der Elektronengruppen im periodischen System der Elemente. — Т. Титц: Аналитическое выражение для теории возникновения электронных групп в периодической системе элементов .....	73
R. Gáspár: Plane Wave Method with a Modified Potential Field — Р. Гашпар: Определение зонного энергетического спектра электронов в металлах.....	79
I. Dohán, T. Gémesy, T. Sándor und A. Somogyi: Bestimmung des Verhältnisses zwischen der Zahl der Photonen und der Zahl der Elektronen in den ausgedehnten Luftschauern der kosmischen Strahlung mittels einer Wilsonkammer. — И. Доган, Т. Гемеш, Т. Шандор и А. Шомоди: Определение отношения числа фотонов и электронов в широких атмосферных ливнях космического излучения камерой Вильсона .....	97
R. Gáspár und I. Tamásy-Lentei: The United Atom Model of the HF Molecule. — Р. Гашпар и И. Тамаш-Лентеи: Объединенная атомная модель молекул HF	105
K. Ladányi: Variational Method for the Solution of the Quantummechanical Many-Body Problem. — К. Ладани: Вариационный метод для решения проблем у многих тел в квантовой механике .....	115
I. Deézi: A Recent Rotational Analysis of the $\gamma$ Bands of the NO Molecule — Новый вращательный анализ $\gamma$ полос молекулы NO .....	125
I. Náray-Szabó: Zusammenhang zwischen der Struktur und den physikalischen Eigenschaften des Glases II. — И. Нарай-Сабо: Соотношение между структурой и физическими свойствами стекла II.....	151
T. Tietz: The Scattering of Electrons by Free Natural Atoms in the Thomas-Fermi Model. — Т. Титц: Рассеяние электронов свободными нейтральными атомами по моделями Томаса-Ферми .....	163
A. С. Давыдов и Г. Ф. Филиппов: Коллективные возбужденные состояния четно-четных атомных ядер. — A. S. Davydov and G. F. Filippov: Collective Excitations of the Even-Even Atomic Nuclei .....	169

(2) 775828  
6693  
3R

В. И. Гольданский: О $\gamma\gamma$ -реакциях с образованием основных состояний ядер. — V. I. Goldanskij: On ( $\gamma\gamma$ ) Reactions with Final Nuclei in the Ground State.....	177
Д. Ф. Курдгеладзе: Феноменологическое обобщение уравнения Томаса-Ферми- Дирака (ТФД) в случае теории металлов и его периодические решения. — D. F. Kurdgeladze: Phenomenological Generalization of the Thomas-Fermi-Dirac (TFD) Equation in Case of the Theory of Metals and its Periodic Solutions...	185
K. Sasvári: On the Crystal Structure of $AlCl_3$ — К. Шашвари: О кристаллической структуре $AlCl_3$ .....	195
P. Szépfalusy: On the Statistical Treatment of the Fermion Gas I. — П. Сепфалуши: О статистической трактовке фермион газа I. ....	203
Д. А. Петров: Некоторые вопросы, относящиеся к выращиванию монокристаллов полупроводников, их структуре и свойствам. — D. A. Petrov: Some Problems of Growth, Structure and Properties of Semiconductor Monocrystals .....	217
O. Stasiv: Die Lage der Absorptionsbanden von Störstellenelektronen in Ionengittern. — О. Стасив: Положение абсорбционных полос дефектных электронов в ионных решетках .....	229
E. Kapuy: Calculation of the Energy Expression in Case of a Wave Function Built up from two Electron Orbits .....	237
K. Novobátzky: E. L. Nikolai, Theoretische Mechanik Band I (Buchbesprechung)....	241
I. Fényes: Über das Verhältnis des wellenmechanischen Energieeigenwertproblems zur klassischen Mechanik. — И. Фенеш: О соотношении между квантовомеха- нической проблемой собственных значений энергии и классической меха- никой .....	245
G. Pócsik: $\hbar$ -Quantization of the Free Bilocal Bozon Field. — Г. Почик: $\hbar$ -квантов- ание свободного, билокального поля частиц Бозе .....	261
K. L. Nagy: Free Field Operators and the Yang-Feldman Formalism. — К. Л. Надь: Операторы свободного поля и формализм Янга-Фельдмана .....	269
F. Fáthy and F. Bukovszky: Elementary Method for the Calculation of the Lattice Energies of the NaCl Crystal II — Ф. Фати и Ф. Буковски: Элементарный метод вычисления энергии решетки кристалла NaCl II.....	275
P. Szabó: On the Calculation of Intensity Scattered by Fine-Crystalline Coals. — П. Сабо: О вычислении интенсивности, рассеянной мелкокристаллическими углями .....	285
А. Бекеши, Л. Пал и Л. Яноши: Методы определения флуктуации энергии и углового рассеяния быстрых ионизирующих частиц. — A. Békéssy, L. Jánossy and L. Pál: Methods of Determination of the Fluctuation of the Energy and the Distribution of Angles of Fast Ionizing Particles .....	297
E. Kapuy: Application of One-Center Wave Functions to Tetrahedral Symmetric Hydrid Molecules I. — Э. Капуй: Применение одноцентровой функции к молекулам гидридов с тетраэдрической симметрией I .....	317
P. Szépfalusy: On the Statistical Treatment of the Fermion Gas II — П. Сепфалуши: О статистической трактовке фермион-газа II, .....	335
O. Orient: Fatigue Effects on the Cathode of Self-Quenching GM Counters .....	343
G. Bozóki, E. Fenyves, T. Sándor and A. Somogyi: Further Investigation of Extensive Air Showers Containing Nuclear Active Particles .....	347
S. L. Malurkar: Further Studies of Cosmic Ray Bursts with Solar Activity. — Ш. Л. Малуркар: Дальнейшие исследования ливней космического излучения свя- занных с солнечной активностью .....	353
R. Gáspár, B. Koltay-Gyarmati and I. Tamássy-Lentei: Determination of Electrostatic Potentials by Series. — Р. Гашпар, Б. Колтай-Дьярматы и И. Тамаш- Лентеи: Определение электростатических потенциалов с помощью рядов	369



<i>F. Berencz</i> : Einige Zweizentrenintegrale zu Rechnungen auf Grund der Methode der korrelationsmässigen Molekülbahn. — <i>Ф. Беренц</i> : Некоторые биполярные интегралы для исчислений на основе метода коррелированных молекулярных орбит	381
<i>G. Marx</i> : The Fundamental Theorem of Continuous Transformations in the Quantum Theory. — <i>Г. Маркс</i> : О фундаментальной теореме непрерывных преобразований в квантовой теории	393
<i>I. Náray-Szabó</i> : Zusammenhang zwischen der Struktur und den physikalischen Eigenschaften des Glases III. Die Wärmeausdehnung des Glases. — <i>И. Нарай-Сабо</i> : Связь между структурой и физическими свойствами стекла. III. Термическое расширения стекла	403
<i>I. Kovács and O. Scari</i> : Intensity Formulae for ${}^2\Pi \leftrightarrow {}^2\Sigma$ Band. — <i>И. Ковач и О. Скари</i> : Формулы интенсивностей септетных полос	423
<i>E. Kapuy</i> : Application of One-Center Wave Functions to Tetrahedral Symmetric Hydrid Molecules II. Numerical Computations for Methane. — <i>Э. Капуй</i> : Применение одноцентральной волновой функции к молекулам гидридов с тетраэдрической симметрией. II. Нумерические вычисления для метана	445
<i>P. Gombás</i> : Statistische Behandlungsweise des $N_2$ -Moleküls. — <i>П. Гомбаш</i> : Статистическая трактовка молекулы $N_2$	461
<i>A. Mašín und V. Havel</i> : Über das Sichtbarmachen der Versetzungen an den Grenzen der Subkörner der Fe-Cr-Legierungen mittels Bombardierung durch Ionen.	471
<i>E. Kapuy</i> : Diamagnetic Susceptibility of Perturbed Systems	475



# ELECTRICAL DISCHARGES IN HIGH VACUUM\*

By

G. SCHMIDT\*\*

CENTRAL RESEARCH INSTITUTE OF PHYSICS, DEPARTMENT OF ATOMIC PHYSICS

(Received : IX. 20. 1955)\*\*\*

Measurements have been made to investigate the mechanism of the breakdown in high vacuum and of the discharge preceding the breakdown. The results of the measurements have been at variance with the theory of VAN DE GRAAFF and TRUMP as well as with that of CRANBERG and have clearly shown that the mechanism of a breakdown in high vacuum is identical with the events observed by BOYLE and al. at very low voltages. Thus it was found possible to form a uniform picture by which many already wellknown phenomena can be explained.

## 1. Introduction

When reducing the gas pressure in a discharge tube it is observed that at very low pressures, where the free path of the electrons is greater than the electrode distance, the character of the discharge changes fundamentally. This type of electric discharge is generally known as vacuum discharge. The character of the discharge is actually independent of the quality and pressure of the gas at an electrode distance of a few mm, resp. cm for pressures of less than  $10^{-4}$  mm Hg; dependence on these being observed only when surface qualities of the electrodes are effected. This gas discharge "without gas" makes it possible to examine the electrode events of a normal gas discharge on the one hand, and is of great practical importance when designing accelerating electrodes of electrostatic accelerators and when operating X-ray-blitz devices, on the other hand.

A vacuum discharge may occur at low voltage (a few kV) as well as at high voltage; the phenomena in the two groups being explained by different mechanisms. The problems in connection with discharges at high voltage are the most controversial and unclarified. The present paper contains a critical analysis of theories dealing with the latter effect. An attempt at interpretation of the phenomena leads to the conclusion that there is no essential difference between the breakdown at low or at high voltages.

## 2. The theory of the electron-ion exchange

The most natural explanation as to the mechanism of the phenomenon would be to attribute the vacuum breakdown to the cold emission electrons

\* Prepared for the press by L. Keszthelyi

\*\* Now at the Israel Institute of Technology, Haifa, Israel.

\*\*\* Revised version VII. 1. 1957

produced by the strong field occurring at the cathode. Measurements have been made by VAN DE GRAAFF and TRUMP concerning the breakdown occurring between a stainless steel ball and a plane electrode at voltages up to 700 kV [1]. They found that the field strength at the cathode producing a breakdown was more than 3 MV/cm at 0,1 mm distance of the electrodes, where as it was lower than 100 kV/cm at 70 mm distance. Thus it was assumed that the critical condition for breakdown depends not only on the field strength but also on the absolute value of the voltage. According to the assumption of these authors each electron emitted by the cathode produces a positive ion when impinging on the anode, these ions releasing in their from secondary electrons by their impact on the cathode. The critical state sets in when the number  $A$  of ions produced by one electron and the number  $B$  of electrons released by one ion fulfill the condition  $A \cdot B \geq 1$ . In such cases chain multiplication of the process initiates a breakdown.

VAN DE GRAAFF and his collaborators as well as other authors have made many measurements to determine  $A$  and  $B$  [1], [2], [3], [4] and [5]. The results of all these measurements contradict the above theory namely  $AB$  always proved to be much smaller than 1. All the same this theory has not yet been abandoned.

In order to check the correctness of the above assumption we have made measurements to determine the ratio of electrons and positive ions produced in a vacuum discharge. For this purpose we have perforated one of the two plane electrodes providing it with a grid; the particles passing through the grid were then captured by an insulated dial target (Fig. 1). Alternating

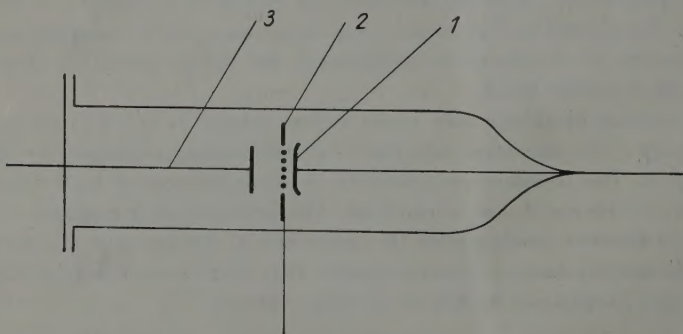
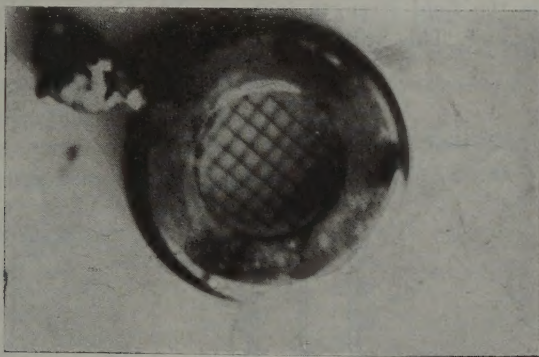


Fig. 1a. Apparatus for measuring electron/ion ratio. 1. High-voltage electrode, 2. Grounded grid electrode, 3. Target electrode

the polarity of the electrodes alternately positive ions and electrons were captured by the target. The distance between the electrodes was about 1 mm, the voltage 20—30 kV. In order to prevent a breakdown from destroying the



electrodes, we inserted a protective resistance of  $100\text{ M}\Omega$  in the circuit. The voltage was adjusted to obtain equal current at both polarities (e. g.  $100\text{ }\mu\text{A}$ ). As a result of the measurement the proportion of negative to positive particles was found to be  $1000:1$ .<sup>1</sup>



1b. Photograph of the grid electrode

The result of this measurement is in accordance with the published measurements of the coefficients  $A$  and  $B$  [1], [2] and [3] and disagrees with the theory of exchange. Theoretically, the low values ( $10^{-4}$ — $10^{-3}$ ) of the coefficient  $A$  are quite acceptable too since it is difficult to explain an energy transfer by an electron impinging on a metal ion about  $10^5$  times its mass which would force the ion to depart from the metal.

### 3. The clump theory

Cranberg's theory gives an entirely different explanation of the phenomenon of vacuum breakdown. According to his assumption owing to the strong field at the electrode surface macroscopic pieces are torn from the electrodes and these colliding with the other electrode produce there a high local rise in temperature. This would explain the critical condition of the breakdown being dependent both on the voltage and the field strength. To prove his statement CRANBERG has shown that the measurements of [1] and also other measurements can be interpreted by this theory. His assumption seems to be supported by measurements, where a material migration has been found before [7] and during [8] the breakdown.

<sup>1</sup> In the meantime a paper was published by BOURNE [9]. He measured the electron-ion ratio in a different way and obtained in respect of steel electrodes results in agreement with the above.

The main difficulty of this theory lies in the fact that very small electrostatic forces are at play, hardly capable of overcoming the cohesion forces of the material. For instance in measurement [1] a breakdown occurs at 100 kV/cm with a corresponding power density  $F = \frac{1}{2}\epsilon_0 E^2 = 4,4 \text{ g/cm}^2$ , but even supposing that at some part protruding due to the surface unevenness of the electrode the field strength increases 100 times we do not get more than  $F = 44 \text{ kg/cm}^2$ . This value is very small compared with the strength

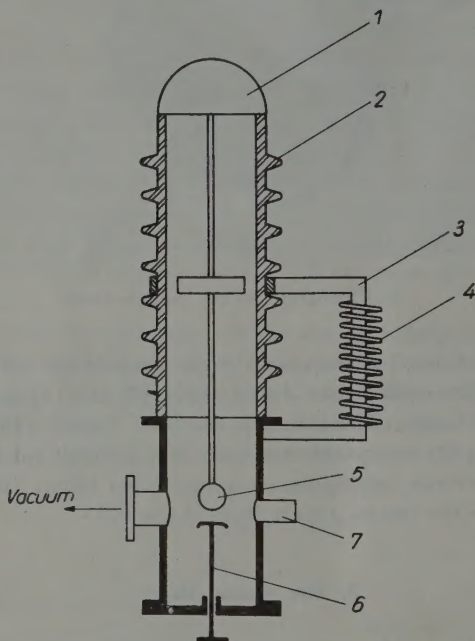


Fig. 2. 1. High-voltage terminal, 2. Porcellan insulator, 3. Iron yoke, 4. Magnetic coil, 5. High-voltage electrode, 6. Adjustable grounded electrode, 7. Vacuummeter

limit of the electrode materials ( $\sim 1000 \text{ kg/cm}^2$ ). Since, however, the theory gives a satisfactory explanation for the results reported in [1] we considered it worth while to carry out a control experiment.

The principle of measurement is the following. Using steel electrodes a magnetic field from a coil parallel to the electric field causes an effect opposite to the latter. The magnetic field makes the iron pieces stick to the electrode. If Cranberg's assumption is correct, breakdown must not occur, when applying an adequate magnetic field; or at least it should occur only at higher voltages. We calculated both the forces acting on a ball placed in an electric and a magne-

tic field, respectively and in respect of the latter verified our results experimentally. The magnetic field applied was about 350 Gauss, which compensates a tearing force produced by an electric field of about  $10^5$  V/cm. There was, however, no difference in the results from the measurements effected with and without magnetic field, nor in the currents preceding the breakdown or in the values of the breakdown voltage. The electrodes were similar to those used by VAN DE GRAAFF and TRUMP with the difference that the non-magnetizable stainless-steel electrodes had to be exchanged for normal steel electrodes. The measuring arrangement is shown in Fig. 2.

With the same arrangement we made the following measurement: the dark discharge prior to the breakdown is followed by an X-ray radiation.

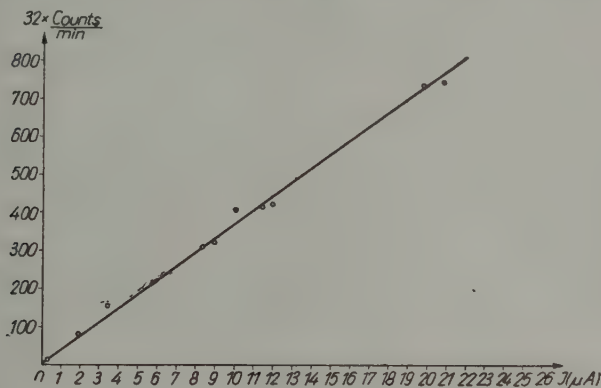


Fig. 3. Counts versus current curve

For a fixed voltage the flow of current varies with the electrode distance. The potential being constant the efficiency of producing bremsstrahlung, the geometry, etc have no effect, thus when measuring with a G. M.-counter the intensity of the X-ray radiation will be proportional to the number of electrons involved in the discharge. Results of such measurements are shown in Fig. 3. It can be seen, that the number of electrons is proportional to the current. These measurements while rendering the clump theory improbable at the same time also support our result, according to which the electrons are present in the discharge in an overwhelming majority as compared to the positive ions. According to some authors [10] the negative ions also play an important part in the discharge. This assumption too is contradicted by our measurements. Namely, it is hardly acceptable that the probability of electron emission and clump-tearing and ion emission, respectively should all depend in the same manner on the electric field (causing the change of the current).

All our measurement prove, in accordance with our assumption, that only the electrons play an important part in the phase of the discharge prior to the breakdown.

#### 4. Investigation of the pre-breakdown

Experience gained in investigations concerning the breakdown of accelerating electrodes in static accelerators shows that the breakdown is mostly preceded by the deterioration of the vacuum. This suggests that the pre-breakdown discharge involves to a high degree the release of gases and vapours and that the effective breakdown takes place in this gaseous space. Thus the breakdown can be divided into two independent sections.

1. Pre-breakdown discharge which consists in the release of the electrons from the cathode.

2. The pre-breakdown discharge releases vapour and gas from one (or both) of the electrodes, the pressure between the electrodes increases and thus the actual breakdown becomes a common gas discharge.

In order to study the mechanism of the pre-breakdown discharge we first examined whether the critical field strength decreases when greatly increasing the electrode distance. Critical field means here the gradient at the cathode at which a given current flows. The measurement was made with the equipment shown in Fig. 2 with electrodes similar to those in the above experiment. In the course of several measurements it has been proved that reproducible results could only be obtained at low intensities when the measurement was of short duration. Typical curves are shown in Fig. 4. It can be seen that the field intensity required to produce a given current shows first a tendency to decrease and later becomes nearly constant. This is in complete agreement with the work of BOYLE, KISLIUK and GERMER [11] whose paper has been published while our measurements were going on and who made similar measurements in connection with the problem of electric contacts at much lower voltages ( $< 2000$  V). As is also indicated by these authors such a small value and decrease of the field strength does not contradict the assumption that the current is of cold-emission origin. Owing to the unevenness of the cathode surface the maximum field strength produced at the emitting peaks is  $\beta$ -times the macroscopic cathode gradient  $E$ ,  $\beta$  increasing first rapid then more slowly with growing electrode distance.

To prove, however, directly that the pre-breakdown discharge has in fact the character of a cold emission, we have to show that the relation between the field strength and current intensity follows the Fowler-Nordheim law. For this purpose we plotted the current-voltage function at a given electrode distance, taking care that the recording of each point should take a short time



only as otherwise the results could not have been reproduced. In case of cold emission the curves  $\ln I - f(1/E)$  have to be almost linear [12], [13], [14] and [15] (Fig. 5). As we may notice this condition is fulfilled, the difference being that in case of high current intensities the curves deviate downwards from the linear. We shall return to the cause of this later on. Quite similar curves have been obtained by BOYLE and al. [11] at otherwise absolutely

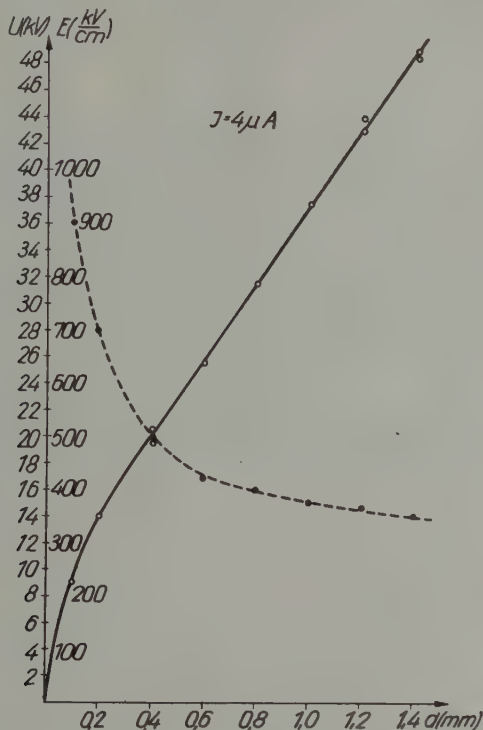


Fig. 4. Voltage (—) and cathode gradient (---) at constant current as a function of electrode separation

different conditions. The curves can be evaluated as usual. Assuming for work function  $V_a = 4 \text{ eV}$ , at  $d = 0.1 \text{ mm}$  we obtain  $\beta = 60$  and at  $d = 1.0 \text{ mm}$ .  $\beta = 190$  from the slopes of the straight lines. These values of  $\beta$  are too great in comparison with those obtained by SCHOTTKY who estimates them to be of the order of 10 [16]. His calculations however, are very rough and we have to take into consideration that among the million or so micropeaks that having the highest  $\beta$  will emit; certainly statistically even very pointed peaks must occur. There might also be places where  $V_a$  is considerably smaller than  $4 \text{ eV}$

due to the impurities. The values reported here, however, are within reasonable limits.

On the basis of the curves we have an other further possibility for checking the estimate for the  $\beta$ -s. The ratio of the  $\beta$ -s belonging to two different curves can also be obtained by plotting the ratio of the  $E$ -s corresponding to the points of the curves at  $I = \text{const.}$  (Here it was assumed that the area of emitting surfaces was identical for both curves.) This control also fully supported our statements.

From the intersection points of the straight lines with the  $1/E$  axis we

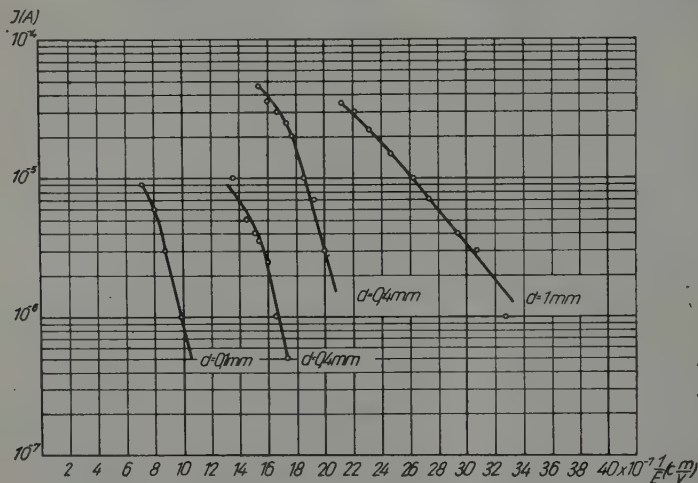


Fig. 5,  $\ln I$  versus  $1/E$  curves with different electrode separation as parameter

may draw conclusions as to the area of the emitting surface. The order of magnitude of the surfaces thus calculated is  $\sim 10^{-12} \text{ cm}^2$ . This result indicates that the emission takes place from very pointed peaks and thus the big values for  $\beta$  are justified.

The systematic deviation of the curves from the straight line is easy to explain on the basis of the above results.  $10^{-5} \text{ A}$  means a current density of  $10^7 \text{ A/cm}^2$  on a surface of  $10^{-12} \text{ cm}^2$ , where the emission is already limited by the space charge. This has already been observed on single well-defined peaks [14], [15].

Using the above results many phenomena which have up to now remained unexplained may now be accounted for. It is obvious for instance why in order to obtain reproducible results it is necessary to restrict oneself to small currents and short times of observation. As a matter of fact high current density is sufficient to melt the micropeak in consequence of which its surface

and form change. The emission in this case may be transferred to another peak, or it may continue on the same peak, but with a different value of  $\beta$ . The result of a measurement of longer duration (about half a minute per point)

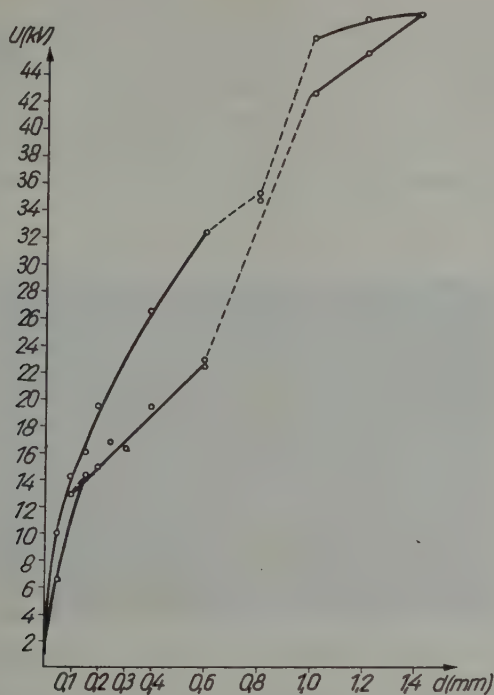


Fig. 6. Voltage versus electrode separation at constant current, obtained by prolonged measuring of every point. The arrows show the order of obtaining the individual points. The solid lines belong probably to different emitting peaks

is plotted in Fig. 6 which shows how the characteristic of the emission changes. The peaks flatten in general after the melting, the same current requires a higher voltage, the cathode "gets better". This is one physical reason for the long-used conditioning of electrodes of accelerating tubes.

## 5. The mechanism of the breakdown

On the basis of the mechanism of the pre-breakdown described above the process of the breakdown can be outlined as follows. The electrons produced by a small emitting peak hit the anode causing there a great local rise in temperature. Calculating for instance with a current of  $100 \mu A$  and a

voltage of 100 kV one obtains an output of 10 W which affects a very small area of the anode surface. This is quite sufficient to produce local outbreaks of gases and vapours. In the gaseous space thus produced the electrons are ionizing and the produced positive ions on the one hand increase the field intensity at the cathode by forming a space charge [11] while on the other hand they increase the electronic flux by inducing secondary electrons. The process multiplies automatically and soon generates so much gas that a regular gas discharge occurs. Thus we have a picture as to how the material of the anode migrates to the cathode and this explains why a smaller cathode gradient is needed to initiate a breakdown at higher voltage. In such cases small emission currents produce greater output on the anode, thus a release of gas starts al-

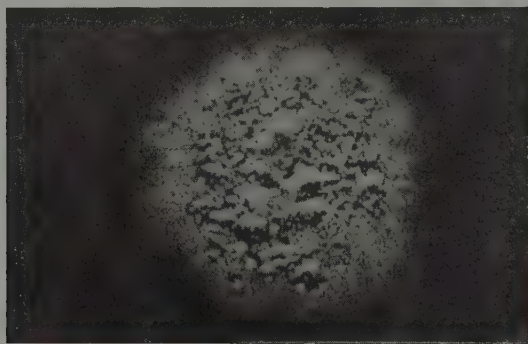


Fig. 7. Surface of an electrode after several vacuum breakdowns

ready at lower fields. Fig. 7 shows highgrade melting and destruction of the electrodes after a few breakdowns the electrodes originally showing a finely polished electrode surface.

It is interesting, however, that VAN DE GRAAFF and TRUMP have reported breakdown at very high voltages even at a very small cathode gradient. But a thorough examination of their curves shows that they did not plot the field strength occurring at the cathode but the mean field produced by the relation  $U/d$ . In case of a sphere and a plane electrode the maximum field strength on the surface of the sphere is higher at great distances than the one plotted. The corrected curve together with the original one is shown in Fig. 8. It is of interest to notice that the curves show an ascending tendency for greater distances. This can have several causes. First more gas is needed at a greater electrode distance, on the other hand the conditons of gas conductance, its pumping off by the pump are much better. Another cause may be higher scattering of the electrons emerging from the cathode at a greater electrode distance, thus impinging on a larger anode surface. For heating a larger anode



surface, however, a higher output is needed i.e. at greater electrode distances it is important to impart higher energy to the electrons. Evaluation of this problem requires further work.

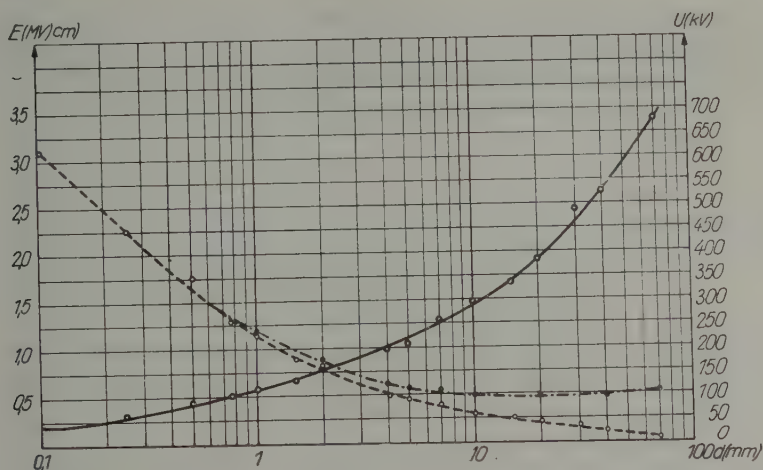


Fig. 8. The plot of TRUMP-VAN DE GRAAFF and the corrected critical cathode field strength curve. (—) voltage, (---) field strength, (-.-.-) corrected field strength

I wish to express my thanks to Prof. K. SIMONYI for his kind assistance and support, to Mr. L. Pócs who participated in some of the measuring work, to Mr. A. Rósa, laboratory assistant, for his kind help in building the apparatus and helping with the measurements and to the mechanical workshop of the Department for Atomic Physics for their careful work in executing the necessary equipment.

#### REFERENCES

1. J. G. TRUMP and R. J. VAN DE GRAAFF, *J. of Appl. Phys.*, **18**, 327, 1947.
2. J. G. TRUMP and R. J. VAN DE GRAAFF, *Phys. Rev.*, **75**, 44, 1949.
3. B. AARSET, R. W. CLOUD and J. G. TRUMP, *J. of Appl. Phys.*, **25**, 1364, 1954.
4. I. FILOSOFO and A. ROSTAGNI, *Phys. Rev.*, **75**, 1269, 1949.
5. R. J. VAN DE GRAAFF and J. G. TRUMP, *J. of Appl. Phys.*, **23**, 264, 1952.
6. L. CRANBERG, *J. of Appl. Phys.*, **23**, 518, 1952.
7. L. HEARD and H. LAUER, *Univ. Calif. Rad. Lab. Rep. N. O. UCRL-1622*, 1952.
8. H. W. ANDERSON, *El. Engng.*, **54**, 1315, 1935.
9. H. C. BOURNE, *J. of Appl. Phys.*, **26**, 625, 1955.
10. J. L. MC KIBBEN and K. BOYER, *Phys. Rev.*, **82**, 315, 1951.
11. W. S. BOYLE, P. KISLIUK and L. H. GERMER, *J. of Appl. Phys.*, **26**, 720, 1955.
12. R. H. FOWLER and L. W. NORDHEIM, *Proc. Roy. Soc. A.*, **119**, 173, 1928.
13. R. H. HAEFER, *Z. Phys.*, **116**, 604, 1940.
14. W. P. DYKE and J. K. TROLEN, *Phys. Rev.*, **89**, 799, 1953.
15. W. P. DYKE, J. K. TROLEN, E. G. MRATIN and J. P. BARBOUR, *Phys. Rev.*, **91**, 1043, 1953.
16. W. SCHOTTKY, *Z. Phys.*, **14**, 80, 1923.

## ЭЛЕКТРИЧЕСКИЕ РАЗРЯДЫ В ВЫСОКОМ ВАКУУМЕ

Г. ШМИТ

## Резюме

Производились измерения для исследования электрических разрядов в высоком вакууме. Результаты измерения противоречат теории Ван дэ Графа, Трумпа и Кранберга, и явно показывают, что механизм разряжения в высоком вакууме идентичен с явлениями, обнаруженными Бойлом и др. при малом напряжении. Это позволило развить единую теорию, которая может объяснить и другие, хорошо известные явления.

# EFFECT OF MAGNETIC STRAY FIELD ON THE LOCATION OF IMAGE IN NUCLEAR SPECTROMETERS

By

I. BERKES

DEPARTMENT FOR ATOMIC PHYSICS OF THE CENTRAL RESEARCH INSTITUTE FOR PHYSICS,  
HUNGARIAN ACADEMY OF SCIENCES, BUDAPEST

(Presented by L. Jánossy. — Received: V. 6. 1957)

In case of sectorial magnetic fields the location of image shifts from its geometrically calculated position on account of a fringing field. We have calculated the lateral displacement. This has been compensated for in actual measurements by altering the field intensity. The calculated alteration of field intensity has been checked experimentally.

Most mass spectrographs deflect the ion beam by means of a homogeneous sectorial magnetic field; some beta-spectrographs are built with a field arrangement, where both the source and the detector are outside the deflecting system. In the latter case the particle beam enters the homogeneous field by passing through a stray field, and similarly it travels again through a fringing field when leaving to reach the detector. The effect of the stray field is taken into account by a virtual increase  $d$  of the dimension of the magnet (Fig. 1). In the increased part of the sector one calculates with the total field intensity  $B_0$ , the rest being taken as 0. This pole increment  $d$  which is proportional to the gap separation  $k$  is determined in a way to leave the total angle of deflection unchanged, while the position of image relative to the object alters. Calculations as to the stray field correction for various locations of image have been made by COGGESHALL [1] and BAINBRIDGE [2], [3]. Other stray field corrections have been calculated by PLOCH and WALCHER [4]; they have shown at the same time the part played by stray fields in the aberration of the location of image. With a given arrangement the actual location of image with its defining slit can be made to coincide by moving the magnet in the direction marked in Fig. 1.

All methods, of course, postulate knowledge of the fringing field distribution  $h(\xi) = \frac{B}{B_0}$ . (For meaning of  $\xi$  see Fig. 3.) This can be determined either by actual measurements, or by some theoretical assumption of its course. COGGESHALL, for instance, determined it for poles of infinite dimensions without shielding by using the Schwartz-Cristoffel transformation. However, if shielding is applied  $h(\xi)$  has to be measured in any case.

It was shown by HERZOG [5] that the effect of the substituted virtual field will never be equivalent to that of the actual one. This is to say that by

choosing the substituted field to give a deflection angle corresponding to the geometrical angle (deflection of the idealized path), the object, resp. its image will not be located on the ideal path but will be shifted outwards. This has to be corrected by a corresponding adjustment of the geometry.

In most of the simple arrangements, however, the object and the location of image are fixed, and the image can be brought into the position determined by the image slit by increasing the magnetic field intensity. For this case, however,  $(B_0 \cdot r_0) \neq (B_0) \cdot (r_0)$ , where  $(B_0 \cdot r_0)$  is the particle momentum (ion, beta-particle, etc.),  $r_0$  the deflection radius determined by the geometrical dimensions and  $B_0$  the field intensity required for deflection;  $(B_0) \cdot (r_0)$  means the product of the values  $B_0$  and  $r_0$ , measured independently, while  $(B_0 r_0)$  is measured directly, for instance by means of beta-rays.

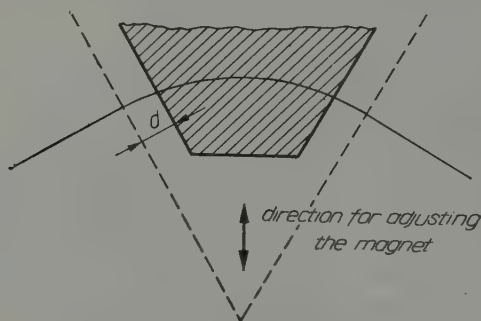


Fig. 1. Adjusting of magnet

The present paper deals with the quantitative determination of the deviation of  $(B_0 r_0)$  from  $(B_0) \cdot (r_0)$ . For simplicity's sake we shall restrict our considerations to the entry and exit of the ideal path normal to the virtual pole boundary, and we shall consider the beam travelling in the plane of symmetry only. In order to have a general case, we shall not assume a substituting field as determined by HERZOG's method, thus any exit angle of the actual beam is allowed. We do not stipulate anything as to the relation between the path lengths travelled in a homogeneous and a fringing field. As the virtual pole boundary may be chosen arbitrarily, the region lying between the straight lines drawn from the center of deflection to be normal on the ideal path (the enclosing angle being then the angle of deflection) will be taken for the virtual pole boundary.

Like BAINBRIDGE [3] we shall start by determining the location of image. The location of image shifts from its virtual position both in lateral and longitudinal direction. As for the longitudinal displacement we assume



that for the location of the image, as first approximation, the laws for location without fringing field hold.

According to HERZOG [6] for  $\varepsilon_1 = 0$

$$l_2 = r_0 \frac{r_0 \tan(\Omega - \varepsilon'') + l_1}{l_1 \tan(\Omega - \varepsilon'') - r_0 - [\tan(\Omega - \varepsilon'') r_0 + l_1] \tan \varepsilon''} \quad (1)$$

$\Omega$  being the geometrical deflection angle,  $l_1$  and  $l_2$  the distance of object resp. image from pole boundary (see. Fig. 3) and  $\varepsilon''$  the exit angle of the homo-

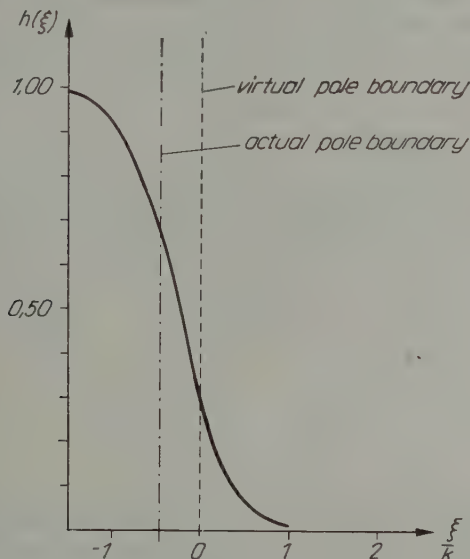


Fig. 2. Field intensity plot

geneous field. In the above equation the exit angle  $\varepsilon_i$  of the actual path, measured at the location of image, has to be substituted for  $\varepsilon''$ .  $\varepsilon_i$  can be obtained from equation (14).

Now let us consider the lateral displacement. By determining  $h(\xi)$  along the trajectory we obtain the curve shown in Fig. 2. The boundary of the field which inside the required accuracy of measurements and calculations is to be considered as homogeneous, may be chosen arbitrarily. In any case it is useful to regard the field as a stray field up to the values of  $h(\xi) \approx 0.98-0.99$ . Thus the particle travels in a fringing field from the point of the object to point 2 (cf. Fig. 3) and from point 3 to the point of location of image, whereas it travels in a homogeneous field in the section from point 2 to point 3.

The differential equation for the trajectory is

$$\frac{1}{r} = \frac{\eta''}{(1 + \eta'^2)^{3/2}} \sim \frac{\eta''}{1 + \frac{3}{2}\eta'^2}, \quad (2)$$

where  $r$  is the radius of deflection and  $\eta$  the lateral displacement of the beam (cf. Fig. 3). As

$$r_0 = \frac{mv}{eB_0}$$

(in MKS-units system), where  $mv$  is the momentum of the deflected particle,  $e$  the particle charge and  $B_0$  the field intensity measured in the homogeneous field:

$$r(\xi) = \frac{r_0}{h(\xi)}. \quad (3)$$

Knowing  $h(\xi)$  this differential equation can be solved by numerical calculation for the given initial conditions. Starting from the point of the object and from the point of the image, respectively,  $\eta'^2 \ll 1$  on a long section, hence

$$\frac{h(\xi)}{r_0} = \eta''$$

and thus

$$\eta(\xi) = \frac{1}{r_0} \int_0^\xi \int_0^\xi h(\xi) d\xi^2. \quad (4)$$

As will be seen from the following, the deviation is the difference between large values; it is therefore, better to calculate with the exact differential equation for  $\eta' > 0,1$ .

Let be  $\Delta_1, \Delta_2, \Delta_3, \Delta_i$  the deviations of the real path from the virtual one and  $\varepsilon_1, \varepsilon_2, \varepsilon_3, \varepsilon_i$  (Fig. 3) the deviations of the deflection angles. In Fig. 3 the continuous line represents the ideal and the dotted line the actual trajectory. The deflection angle in a homogeneous field measured on the virtual path is

$$\Phi = \Omega - 2\varphi,$$

where  $\varphi$  is the deflection of the virtual path in the stray field. By taking the fringing field effect as equal on both sides, an equal distance of object and image from the pole boundary is assumed, or if this is not the case, object and image may be assumed to be at distances from the sectorial field large enough to give  $h(\xi) < 0,01$  and thus there is no appreciable difference in the values of  $\eta_1$  and  $\eta_2$  as calculated from equation (4).

Between object and location of image an infinite number of trajectories are possible depending on the exit angle and the applied field intensity. We have to select one of them. This can be done by means of a defining slit which determines at the same time the angle of aperture. In the following the defining slit will be located at the beginning of the curvature of the virtual trajectory (point 1). Then  $\Delta_1 = 0$ .

$\Delta_1$  can be expressed in the following way :

$$\Delta_1 = -\frac{1}{r_0} \int_0^{\xi} \int_0^{\xi} h(\xi) d\xi^2 + \varepsilon_0 l_1, \quad (5)$$

where  $\varepsilon_0$  is the angle enclosed at the point of the object by the actual and the

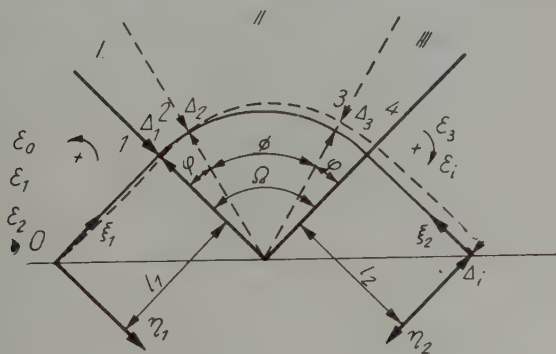


Fig. 3. Ideal and virtual paths

virtual paths. By numerical integration we obtain a value which is negligible as compared with the width of the defining slit. Consequently our above supposition means that we consider the trajectory for which  $\varepsilon_0 \sim 0$ . From this follows further (see Fig. 4)

$$\varepsilon_2 = \varphi - \arctan \eta_1(2), \quad (6)$$

$$\Delta_2 = \frac{r_0(1 - \cos \varphi) - \eta_1(2)}{\cos \varphi}. \quad (7)$$

In the sector 2-3 even the real path is circular. In Fig. 4 we have taken the origin of the coordinate system to be in the center of the virtual trajectory. The center of the real circular path is  $O_1$ ; by neglecting the second and higher order terms of  $\varepsilon_2$ ,  $\left(\frac{\Delta_2}{r_0}\right)^2$ ,  $\frac{\varepsilon_2 \Delta_2}{r_0}$  etc., the equation for the circular path becomes (cf. Fig. 4)

$$x^2 + y^2 - \varepsilon_2 2 r_0 x - \Delta_2 2 y = r_0^2. \quad (8)$$

By introducing  $m = \tan \left( \frac{\pi}{2} - \Phi \right)$  at point 3, the equation becomes

$$x^3 (1 + m^2) - 2x(r_0 \varepsilon_2 + m \cdot l_2) - r^3 = 0.$$

For the deviation at point 3 from the virtual trajectory, by neglecting again the second order terms, we obtain

$$l_3 = \frac{r_0 \varepsilon_2 + m \cdot l_2}{\sqrt{1 + m^2}}. \quad (9)$$

In order to determine  $\varepsilon_2$  we derive equation (8) :

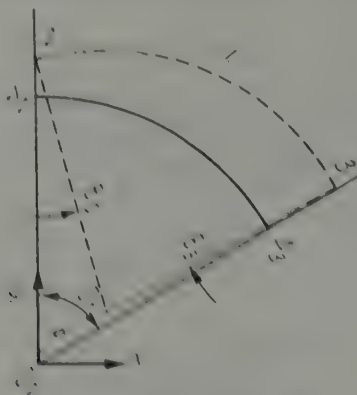


Fig. 4. Sector II from Fig. 3

$$y^2 = - \frac{x - r_0 \varepsilon_2}{y - l_2}.$$

If we want to calculate more accurately than with  $1\%$  accuracy the relative values of the second order terms have to be less than  $1\%$  when expanding the series, therefore the condition

$$\frac{l_2}{y} = \frac{l_2}{r_0 \cos \varphi} < 0,1 \quad (10)$$

has to be satisfied. Then

$$y^2 = - \frac{r}{y} - \frac{r \cdot l_2}{y^2} - \frac{r_0 \varepsilon_2}{y}. \quad (11)$$

It is evident that

6\*

$$y' = \tan [\pi - (\Phi - \varepsilon_3)] = -\tan (\Phi + \varepsilon_3),$$

$$-\frac{x}{y} = -\tan \Phi. \quad (12)$$

From (11) and (12) we obtain using the relations between circular functions and by further approximations

$$\varepsilon_3 = \sin \Phi \frac{A_2}{r_0} - \cos \Phi \varepsilon_2. \quad (13)$$

As indicated before, going from the location of image towards point 3 we have to carry out the same integration as going from the location of object to point 2. Denoting the angle of any given deflection measured from the image by  $\psi$ , the deflection angle of the location of image is represented by  $-\varepsilon_i$ , which is at the same time the angle formed by the actual and virtual trajectories at the location of image.

$$\psi = -\varepsilon_i + \arctan \eta'_2(\xi_2) \quad (14)$$

and hence

$$\psi_i = \varphi + \varepsilon_3 + \arctan \eta'_2(3) \quad (15)$$

and by (14) and (15)

$$\psi = \varphi - \varepsilon_3 - \arctan \eta'_2(3) + \arctan \eta'_2(\xi_2). \quad (16)$$

For

$$\eta'_2(3) = \eta'_1(2) \quad \text{and} \quad \eta' \tan (\varepsilon_2 - \varepsilon_3) \ll 1$$

this becomes

$$\int_i^3 \tan \psi d\xi = (\varepsilon_2 - \varepsilon_3)(l_2 + r_0 \sin \varphi) + \eta_2(3)$$

and thus

$$A_i = \int_i^{(3)} \tan \psi d\xi + A_3 \cos \varphi - r_0(1 - \cos \varphi). \quad (17)$$

The image of the object thus does not coincide with the location of image on the virtual trajectory and for a  $A_i$  of positive sign it falls farther away from the center of curvature.

By altering the magnetic field intensity from  $B_0$  to  $B'_0$ , the image shifts in a certain measure in the direction normal to the path. Introducing

$$\frac{B_0 - B'_0}{B_0} = \delta$$



and hence

$$r'_0 = (1 + \delta) r_0$$

the lateral displacement will be for an ideal sectorial field

$$\Delta \xi = r_0 \delta (1 - \cos \Omega) + l_g \frac{\delta}{1 + \delta} \sin \Omega. \quad (18)$$

In order to bring the image located with deviation  $l_i$  from the ideal position into the image slit that determines the location of image, the intensity of the magnetic field has to be increased in such a measure that  $l_i = \Delta \xi$ . From this  $\delta$ , and eventually  $B'_0$  may be determined.

The accuracy of the calculated increase in field intensity is limited by field intensity measurements, exactitude of calculations and approximations the latter may be taken in general to be 0,5–1%.

At the Department for Atomic Physics of the Central Research Institute of Physics we have built a magnetic deflector of  $90^\circ$  [7] for energy measurements of electrons accelerated by our free-air type Van de Graaff accelerator of 1 MeV. The magnetic field was measured by means of a ballistic galvanometer and the deflector calibrated by the K-line of Cs<sup>137</sup>. With the value of 3381 Gcm known from the literature we should have obtained  $B_0 = 375,5 \pm 15$  Gs for a deflection radius of 9 cm (the half-width of the K-line on account of the resolving power being about  $0,3\%$ ), the result of the direct measurement, however, has been  $B'_0 = 400,0 \pm 3,0$  Gs. (The measuring coil coupled to the ballistic galvanometer had been calibrated by magnetic nuclear resonance.) By means of the above calculations this difference may be explained as follows. In designing the deflector the effect of the stray field was taken into account by a virtual increase of the poledimensions of 0,7 k. In order however to eliminate the effect of the surrounding iron components and of other disturbing fields, the electrons travel in a shielding iron tube outside the pole pieces of the magnet. Although the magnet was moved toward the center of deflection during calibration, the above mentioned stray field effect could only partly be corrected. Using equ. (18) we find for  $\delta$  the value,

$$\delta = 7,6 \pm 0,5 \%$$

which is in agreement with the measured  $6,5 \pm 1\%$  inside the limits of measurements accuracy.

Finally we have to note that the measured deviations from the virtual trajectories are rather appreciable on the exit side of the deflector e.g.  $l_g = 4,55$  mm,  $l_i = 11,3$  mm. If in order to obtain better resolving power and determination of trajectories, slits are introduced here too, the increase in the field intensity results in bringing the actual path nearer the virtual one, however the intensity of the beam might then decrease.

The conditions under which the equation  $(B_0 r_0) = (B_0) \cdot (r_0)$  is satisfied give at the same time a criteriom for the best adjustment of the magnet.

I am indebted to Professor K. SIMONYI for helpful discussions.

#### REFERENCES

1. N. D. COCKESNALL, J. Appl. Phys., **18**, 855, 1947.
2. E. SEGRIÉ, Exp. Nucl. Phys., Wiley, 1953, p. 586.
3. K. T. BAINBRIDGE, Phys. Rev., **75**, 216, 1949.
4. W. PLOCH and W. WALCHER, ZS. f. Phys., **127**, 274, 1950.
5. K. HENZOG, Zs. f. Naturf., **10a**, 887, 1955.
6. K. HENZOG, ZS. f. Phys., **89**, 447, 1934.
7. I. BEKKER, KFKI Közl., **4**, 125, 1955.

#### ВЛИЯНИЕ РАССЕЯНИЯ МАГНИТНОГО ПОЛЯ НА ИЗОБРАЖЕНИЕ В ЯДЕРНЫХ СПЕКТРОМЕТРАХ

И. ПЕРКЕН

#### Резюме

В случае секторных магнитных полей вследствие влияния рассеянного магнитного поля положение изображения отличается от рассчитанного из геометрических соображений. В статье вычислен этот боковой сдвиг. В измерениях указанный сдвиг компенсирован изменением напряженности поля. Необходимое изменение напряженности поля было проверено экспериментально.



# TOMONAGA'S INTERMEDIATE COUPLING THEORY USING CONFIGURATION SPACE METHODS

By

K. L. NAGY

INSTITUTE FOR THEORETICAL PHYSICS OF THE ROLAND EÖTVÖS UNIVERSITY, BUDAPEST

(Presented by K. F. Novobátzky — Received : V. 24. 1957)

With the intermediate coupling theory — using the configuration space methods of the quantum theory of fields — we determine the state vector characterizing the real nucleon. We carry out our calculations for the case of interaction of the nucleon field described by the Dirac equation and the scalar, resp. pseudoscalar meson field. Pair creation is completely disregarded. Remaining within the frameworks of the configuration space method the recoil of the nucleon is considered. With the aid of the state vector we also calculate the mean value of some characteristic physical quantities. The use of the configuration space method — particularly in connection with the computation of local physical quantities — makes possible to form a very clear picture about the real nucleon.

## Introduction

For the quantum theoretical treatment of the interacting fields the covariant perturbation method proved to be very successful in quantum electrodynamics but it cannot be applied in case of strongly coupled fields. The results calculated with its aid do not agree with the experimental results owing to the bad convergence. Recently it has been becoming more and more obvious, that the renormalization method which can be unambiguously formulated with the aid of the  $S$ -matrix is not satisfactory, as after the renormalization physically inadmissible results occur. It is for this reason, that consideration of methods, other than the theory of the  $S$ -matrix, is of considerable importance.

In the following Tomonaga's intermediate coupling theory [1]—[21] is dealt with in the case of a nucleon field, described by the Dirac equation, being in interaction with the scalar resp. symmetrical pseudoscalar meson field. The state vectors characterizing the real nucleons are determined in an adequate approximation. Our calculations are based on configuration space methods, and throughout the interaction picture is made use of.

The four-momentum of interacting fields is

$$P_{\mu}[\sigma] = P_{\mu}^0 - \frac{1}{c} \int_{\sigma} H(x) d\sigma_{\mu}(x), \quad (1)$$

where  $P_{\mu}^0$  is the sum of the four-momenta of the individual interacting fields

and thus the operator of the infinitesimal displacement for the interaction picture operators.

According to (1) the energy-momentum eigenvalue equation is

$$P_\mu |\sigma\rangle = \Pi_\mu |\sigma\rangle, \quad (2)$$

where in case of a neutral scalar coupling

$$H(x) = g : \bar{\psi}(x) \psi(x) \Phi(x) :. \quad (3)$$

In case of the symmetric pseudoscalar field pseudoscalar coupling according to the DYSON-FOLDY theorem [22], [23]

$$H(x) = \frac{ig}{2\kappa} : \left( \bar{\psi} \gamma_\mu \gamma_5 \sqrt{2} \tau_- \psi \partial_\mu \Phi + \bar{\psi} \gamma_\mu \gamma_5 \sqrt{2} \tau_+ \psi \partial_\mu \Phi^* + \bar{\psi} \gamma_\mu \gamma_5 \tau_3 \psi \partial_\mu \Phi_3 \right) : + \\ + \lambda \frac{g^2}{2Mc^2} : \bar{\psi} \psi (2\Phi \Phi^* + \Phi_3^2) :, \quad (4)$$

where  $\delta$ -like interaction terms were neglected,  $\lambda$  serves for the pair suppression suggested by BRÜCKNER and others [24], [25], according to BRÜCKNER its most probable value is 0.2. Here  $:$  denotes, as is usual, a normal product. It is known that the pseudoscalar coupling is preferred as against pseudovector coupling owing to its renormalizability. Recently the possibility of the renormalization of pseudovector coupling was also suggested [26], [27]. Thus the substitution  $\lambda = 0$  is justified too.

The state vector of the field according to the configuration space method [28], [29] applied here (detailed literature in the latter) in case of a nucleon and neutral scalar meson field is

$$|\sigma\rangle = \sum_{n, n', m} (i)^{n+n'} \left( \frac{i}{\hbar c} \right)^m \int \dots \int_{\sigma} |x^1, \dots, x^n; x'^1, \dots, x'^{n'}; y^1, \dots, y^m\rangle \\ \prod \gamma_{vi}^{(i)} d\sigma_{vi}(x^i) \prod \gamma_{uj}^{(j)} d\sigma_{uj}(x'^j) \prod^m d_{ek}(y^k) d\sigma_{ek}(y^k) \\ \langle x^1, \dots, x^n; x'^1, \dots, x'^{n'}; y^1, \dots, y^m | \sigma \rangle, \quad (5)$$

in case of a nucleon and symmetrical pseudoscalar meson field

$$|\sigma\rangle = \sum_{n, n', \dots, m^+, m^-, m^3} (i)^{n+n'} \left( \frac{i}{\hbar c} \right)^{m^+ + m^- + m^3} \int \dots \int_{\sigma} |x^1, \dots, x^n; x'^1, \dots, x'^{n'}; \\ \xi^1, \dots, \xi^{m^+}; \eta^1, \dots, \eta^{m^-}; \zeta^1, \dots, \zeta^{m^3}\rangle \\ \prod^n \gamma_{vi}^{(i)} d\sigma_{vi} \prod^{n'} \gamma_{uj}^{(j)} d\sigma_{uj} \prod^{m^+} d_{ei} d\sigma_{ei} \prod^{m^-} d_{ek} d\sigma_{ek} \prod^{m^3} d_{ee} d\sigma_{ee} \\ \langle x^1, \dots, x^n; x'^1, \dots, x'^{n'}; \xi^1, \dots, \xi^{m^+}; \eta^1, \dots, \eta^{m^-}; \zeta^1, \dots, \zeta^{m^3} | \sigma \rangle. \quad (6)$$



Here

$$d_v = \left( \frac{\overleftarrow{\partial}}{\partial x_v} - \frac{\overrightarrow{\partial}}{\partial x_v} \right).$$

The state vectors and through them the amplitudes are defined by

$$\begin{aligned} |x^1, \dots, x^n; x'^1, \dots, x'^{n'}; y^1, \dots, y^m\rangle &= (n! n'! m!)^{-\frac{1}{2}} \bar{\psi}^{(+)}(x^1) \dots \bar{\psi}^{(+)}(x^n), \\ &\bar{\psi}'^{(+)}(x'^1) \dots \bar{\psi}'^{(+)}(x'^{n'}) \Phi^{(-)}(y^1) \dots \Phi^{(-)}(y^m) |0\rangle. \end{aligned} \quad (7)$$

resp.

$$\begin{aligned} |x^1, \dots, x^n; x'^1 \dots x'^{n'}; \xi^1, \dots, \xi^{m+}; \eta^1, \dots, \eta^{m-}; \zeta^1, \dots, \zeta^{m^1}\rangle &= \\ &= (n! n'! m^+! m^3!)^{-\frac{1}{2}} \bar{\psi}^{(+)}(x^1), \dots, \bar{\psi}'^{(+)}(x'^1) \dots \Phi^{(+)*}(\xi^1) \dots \\ &\dots \Phi^{(-)}(\eta^1) \dots \Phi_3^{(-)}(\zeta^m) |0\rangle. \end{aligned}$$

resp.

$$\psi^{(+)}(x) |0\rangle = \psi'^{(+)}(x) |0\rangle = \Phi^{(+)}(x) |0\rangle = 0, \quad \langle 0 | 0 \rangle = 1 \quad (8)$$

where  $|0\rangle$  is the vacuum state:

$$\psi^{(+)}(x) |0\rangle = \psi'^{(+)}(x) |0\rangle = \Phi_3^{(+)}(x) |0\rangle = \Phi^{(-)*}(x) |0\rangle = 0, \quad \langle 0 | 0 \rangle = 1.$$

Solving the eigenvalue equation (2) just means the determination of all the amplitudes  $\langle x^1, \dots | \sigma \rangle$  occurring in (5) resp. (6). In the following we shall determine these amplitudes in a suitable approximation. With the help of these amplitudes we may — since they have a direct probability meaning in the coordinate space and at the same time determine also the number of mesons — form a clear picture about a real nucleon. Our picture can be completed by determining the mean value of some physical quantities characterizing the system. From this point of view the local quantities are of particular interest. Thus in the environment of the real nucleon, the mean values of the meson potential, the electric charge density, as well as the energy density will be determined.

### The intermediate coupling theory

The intermediate coupling theory is the variational method in the quantum theory of fields. According to this instead of the exact solution of the eigenvalue equation (2) only the mean value of  $-ic \langle \sigma | P_4[\sigma] | \sigma \rangle$  is minimized, satisfying the condition  $\langle \sigma | \sigma \rangle = 1$ , with the help of suitable trial functions. In this paper pair creation is disregarded throughout; thus in (5) resp. (6) — and everywhere, where this may occur in the course of

the calculations zero is written for all amplitudes  $x^1, \dots; x'^1, \dots | \sigma \rangle$  containing at least one antinucleon.

In the following we examine such states in which a specified number of real nucleons (say  $A$ ) is contained. Then owing to the neglect of pair creation in the state vectors only such amplitudes can occur which characterize (apart from possible mesons) exactly  $A$  bare nucleons. We carry out our calculations first for the case the nucleon and the scalar field.

### 1. The nucleon and the neutral scalar meson field

Our aim is now to determine the state vector describing  $A$  real nucleons and to calculate for this state the values of some characteristic physical quantities. Neglecting pair creation, from (1), (3) and (5) using the formulae (7), (11) as well as the properties of the functions  $S$  and  $T$  occurring in the commutation relations we obtain:

$$\begin{aligned}
 a | P_n | a | | a &= \sum_n i^A \left( \frac{i}{\hbar c} \right)^n \int_0^\infty \dots \int_0^\infty \langle \sigma | x^1, \dots, x^A; y^1, \dots, y^n \\
 &\quad \prod_{i=1}^A \gamma_{\nu i} d\sigma_{\nu i}(x^i) \prod_{j=1}^n d_{\mu j} d\sigma_{\mu j}(y^j) \cdot \\
 &\quad \cdot \frac{\hbar}{i} \left\{ \sum_{i=1}^A \frac{\Theta}{\Theta x_{\mu i}^1} + \sum_{j=1}^n \frac{\Theta}{\Theta y_{\mu j}^1} \right\} \langle x^1, \dots, x^A; y^1, \dots, y^n | \sigma \rangle = - \\
 &= \frac{4(i)^{A+1}}{c} \sum_n (n+1)^{1/2} \int_0^\infty d\bar{\sigma}_\mu(v) \left( \frac{i}{\hbar c} \right)^n \int_0^\infty \dots \int_0^\infty \langle \sigma | x, x^2, \dots, x^A; y^1, \dots, y^n \rangle \cdot \\
 &\quad \prod_{i=1}^A \gamma_{\nu i}^{(1)} d\sigma_{\nu i}(v^i) \prod_{j=1}^n d_{\mu j} d\sigma_{\mu j}(y^j) = x, x^2, \dots, x^A; x, y^1, \dots, y^n | \sigma \rangle = - \\
 &= \frac{4(i)^{A+1}}{c} \sum_n n^{1/2} \int_0^\infty d\bar{\sigma}_\mu(v) \left( \frac{i}{\hbar c} \right)^{n-1} \int_0^\infty \dots \int_0^\infty \langle \sigma | x, x^2, \dots, x^A; x, y^2, \dots, y^n \rangle \cdot \\
 &\quad \prod_{i=1}^A \gamma_{\nu i}^{(1)} d\sigma_{\nu i}(v^i) \prod_{j=1}^n d_{\mu j} d\sigma_{\mu j}(y^j) = x, x^2, \dots, x^A; y^2, \dots, y^n | \sigma \rangle. \quad (9)
 \end{aligned}$$

Similarly

$$\begin{aligned}
 a | M | a &= \sum_n n (i)^A \int_0^\infty \dots \int_0^\infty \left( \frac{i}{\hbar c} \right)^n \int_0^\infty \dots \int_0^\infty \langle \sigma | x^1, \dots, x^A; y^1, \dots, y^n \rangle \cdot \\
 &\quad \prod_{i=1}^A \gamma_{\nu i}^{(1)} d\sigma_{\nu i}(v^i) \prod_{j=1}^n d_{\mu j} d\sigma_{\mu j}(y^j) = x^1, \dots, x^A; y^1, \dots, y^n | \sigma \rangle. \quad (10)
 \end{aligned}$$

where  $M = \frac{i}{\hbar c} \int d^3x d_\nu \Phi^{(1)} d_\nu \Phi^{(1)}$  is the operator of the meson number. Similarly

$$\begin{aligned}
\langle \sigma | \Phi(x) | \sigma \rangle &= \sum_n (i)^A \int_{\sigma} \dots \int_{\sigma} \left( \frac{i}{\hbar c} \right)^n \int_{\sigma} \dots \int_{\sigma} (n+1)^{1/2} \cdot \sigma(x^1, \dots, x^A; x, y^1, \dots, y^n) \\
&\cdot \prod \gamma_{vi}^{(i)} d\sigma_{vi}(x^i) \prod_{j=2}^n d\mu_j d\sigma_{\mu_j}(y^j) \cdot x^1, \dots, x^A; y^1, \dots, y^n \cdot \sigma \dots \\
&+ \sum_n (i)^A \int_{\sigma} \dots \int_{\sigma} \left( \frac{i}{\hbar c} \right)^{n-1} \int_{\sigma} \dots \int_{\sigma} n^{1/2} \cdot \sigma(x^1, \dots, x^A; y^2, \dots, y^n) \\
&\prod \gamma_{vi}^{(i)} d\sigma_{vi}(x^i) \prod_{j=2}^n d\mu_j d\sigma_{\mu_j}(y^j) \cdot x^1, \dots, x^A; x, y^2, \dots, y^n \cdot \sigma \dots \quad (11)
\end{aligned}$$

The normalization condition is now

$$\begin{aligned}
\langle \sigma | \sigma \rangle &= 1 = \sum_n (i)^A \int_{\sigma} \dots \int_{\sigma} \left( \frac{i}{\hbar c} \right)^n \int_{\sigma} \dots \int_{\sigma} \cdot \sigma(x^1, \dots, x^A; y^1, \dots, y^n) \cdot \\
&\prod \gamma_{vi}^{(i)} d\sigma_{vi}(x^i) \prod_{j=2}^n d\mu_j d\sigma_{\mu_j}(y^j) \cdot x^1, \dots, x^A; y^1, \dots, y^n \cdot \sigma \dots \quad (12)
\end{aligned}$$

In the above expression  $\sigma$  is not affected by the differentiation. Later when going over to the plane  $\sigma \rightarrow t = \text{const.}$ , the substitutions

$$\begin{aligned}
d_4 &\rightarrow 2(-\Delta + \mu^2)^{1/2} \\
-i\hbar\partial_4 &\rightarrow i\hbar\gamma_4\gamma_t\partial_t + i\hbar\gamma_4 \times \\
-i\hbar\partial_4 &\rightarrow i\hbar(-\Delta + \mu^2)^{1/2} \quad (13)
\end{aligned}$$

may therefore be introduced to advantage. According to (7) and (8), because  $\psi$  and  $\Phi$  are operators in the interaction picture, these are permissible.

#### a) The intermediate coupling theory without considering the nucleon recoil

Disregarding the pair creation our equations are yet exact. In the following a single real nucleon is investigated and we assume

$$\langle x; y^1, \dots, y^n | \sigma \rangle = C_n(\sigma) \varphi(x) \prod f(y^i). \quad (14)$$

The functions  $\varphi$  and  $f$  may also depend on  $\sigma$ , which can be chosen arbitrarily, however, we do not especially denote this dependence. Substituting (14) into (9) we obtain

$$\begin{aligned}
\langle \sigma | P_{\mu}[\sigma] | \sigma \rangle &= \sum_n C_n^*[\sigma] C_n[\sigma] \{p_{\mu} + n k_{\mu}\} + \\
&+ \sum_n (n+1)^{1/2} C_n^*[\sigma] C_{n+1}[\sigma] a_n + \\
&+ \sum_n n^{1/2} C_n^*[\sigma] C_{n-1}[\sigma] \beta_n, \quad (15)
\end{aligned}$$

where

$$\begin{aligned} p_\mu &= i \int_{\sigma} \bar{\varphi} \gamma_\nu (-i \hbar) \partial_\mu \varphi d\sigma_\nu, & i \int_{\sigma} \bar{\varphi} \gamma_\nu \varphi d\sigma_\nu &= 1 \\ k_\mu &= \frac{i}{\hbar c} \int_{\sigma} f^* d_\nu (-i \hbar) \partial_\mu f d_\nu, & \frac{i}{\hbar c} \int_{\sigma} f^* d_\nu f d\sigma_\nu &= 1 \\ a_\mu &= -\frac{g}{c} \int_{\sigma} d\sigma_\mu \bar{\varphi} \varphi f, & \beta_\mu &= -\frac{g}{c} \int_{\sigma} d\sigma_\mu \bar{\varphi} \varphi f^*. \end{aligned} \quad (16)$$

The normalization condition  $\langle \sigma | \sigma \rangle = 1$  is fulfilled if

$$\sum C_n^* C_n = 1. \quad (17)$$

We now go over to the plane  $t = \text{const.}$  and change denotation, so that  $x, y \dots$  etc. are now the vectors of the threedimensional space;  $dx = dx_1 dx_2 dx_3$ . Besides, the mean values of operators at an arbitrarily chosen time will be denoted instead of by  $\langle t | \Omega | t \rangle$  frequently by  $\langle \Omega \rangle$ . Neither will the dependence on time following from the transition  $\sigma \rightarrow t$  in (14) be denoted.

Taking into account the condition (17) and varying  $-ic \langle P_4 \rangle$  with respect to  $C_n$  we obtain

$$C_n \{E + n\varepsilon - W\} + C_{n+1} (n+1)^{1/2} \alpha + C_{n-1} n^{1/2} \alpha^* = 0, \quad (18)$$

where

$$\begin{aligned} E &= \frac{c}{i} p_4 = \int \bar{\varphi} (\hbar c \gamma_i \partial_i + M c^2) \varphi dx, \\ \varepsilon &= \frac{c}{i} k_4 = 2 \int f^* (-A + \mu^2) f dy, \\ a &= \frac{c}{i} a_4 = g \int \bar{\varphi} \varphi f dx. \end{aligned} \quad (19)$$

Transforming equation (18) according to the method of GLAUBER and LUTINGER [3] to the problem of the harmonical oscillator, it can be easily solved. The solution is

$$W^{(\nu)} = E + \nu \varepsilon - \frac{\alpha \alpha^*}{\varepsilon}, \quad (20)$$

$$C_n^{(\nu)} = e^{-\frac{\alpha \alpha^*}{2\varepsilon^2}} \sum_{l=0}^{\nu} \frac{(\nu!)^{1/2} (n!)^{1/2} (-1)^{n-\nu+l}}{l! (\nu-l)! (n-\nu+l)!} \left( \frac{\alpha^*}{\varepsilon} \right)^{n-\nu+l}. \quad (21)$$

With the aid of the solution thus obtained the mean value of the meson number operator (10) can be calculated in the  $\nu$ -th state. From (14), (16) and (21) we obtain



$$\langle M \rangle^{(v)} = \frac{\alpha \alpha^*}{\epsilon^2} + v. \quad (22)$$

Now we determine the meson amplitude in the ground state ( $v = 0$ ). For this we vary  $W^{(0)}$  with respect to  $f$ . The condition (16) need not be taken into consideration when varying, because  $f$  is determined by (20) except for an indefinite constant. Varying (20) we obtain

$$\bar{\varphi} \varphi - \frac{\int \bar{\varphi} \varphi f^* dx}{\int f^* (-\Delta + \mu^2) f dx} (-\Delta + \mu^2) f = 0, \quad (23)$$

the solution of which is

$$f(x) = a (-\Delta + \mu^2)^{-1} \bar{\varphi}(x) \varphi(x). \quad (24)$$

From here we can already calculate the mean value of the meson potential in the ground state. Substituting into (11) and (16) the quantities determined above, we finally obtain

$$\langle \Phi(x) \rangle = -g (-\Delta + \mu^2)^{-1} \bar{\varphi}(x) \varphi(x) \quad (25)$$

as expected. Using (24) the mean value of the meson number operator in the ground state according to (22) is

$$\langle M \rangle = \frac{g^2}{2 \hbar c} \int \bar{\varphi} \varphi (-\Delta + \mu^2)^{-\frac{n}{2}} \bar{\varphi} \varphi dx. \quad (26)$$

The energy of the fields from (20) and (24) is thus

$$W^{(0)} = E - \frac{g^2}{2} \int \bar{\varphi} \varphi (-\Delta + \mu^2)^{-1} \bar{\varphi} \varphi dx. \quad (27)$$

Finally minimizing this with respect to  $\varphi$  and taking into account the normalization condition (16) referring to  $\varphi$  we obtain that the energy of the fields is minimal, assuming

$$(\hbar c \gamma_4 \gamma_i \partial_i + \gamma_4 M c^2 - g^2 \gamma_4 (-\Delta + \mu^2)^{-1} \bar{\varphi} \varphi) \varphi = \lambda \varphi. \quad (28)$$

According to (7) here and further on for similar equations only solutions giving positive frequency are to be taken into consideration.

As regards the interpretation of the above formulae the following idea is due to G. HEBER [12], [13], [20], [21]. It seems to be clear at once from (27) — at least qualitatively — that for some suitable  $g$ ,  $W$  has a minimum in case of a concentrated  $\varphi$  packet. This has of course to be determined from (28). Thus the following idea may be formed about the real nucleon: each real nucleon consists of a core concentrated into a

small volume which is swarmed around by mesons. When the nucleons are treated in other calculations as plane waves, then these plane waves have nothing to do with the present  $\varphi$  — this is always concentrated into a small volume — but it describes simply the centre of mass of the  $\varphi$  packet.

The working out of the qualitative picture requires naturally detailed calculations. The result of such calculations does not seem very convincing. Ensurance of the nucleon concentration requires an unusually high value of  $g$  and on the other hand as was shown later by HEBER the recoil of the nucleon also counteracts concentration (see further below).

The other more common possibility is the renormalization. Indeed, the interaction Hamiltonian [3] completed by the term  $-\delta M c^2 \bar{\psi} \psi$  can be easily checked to give back formulae (24)–(26) unchanged, expression (27), however, is modified

$$W^{(0')} = E - \frac{g^2}{2} \int \bar{\varphi} \varphi (-\Delta + \mu^2)^{-1} \bar{\varphi} \varphi dx - \delta M c^2 \int \varphi \varphi dx, \quad (27')$$

where now in  $E$  the experimentally observed mass occurs. Assuming

$$\delta M = -\frac{g^2}{2c^2} \int \bar{\varphi} \varphi (-\Delta + \mu^2)^{-1} \bar{\varphi} \varphi dx / \int \bar{\varphi} \varphi dx \quad (29)$$

the energy of the fields is just  $E$ , which has a minimum if  $\varphi$  satisfies the energy eigenvalue equation

$$(\hbar c \gamma_4 \gamma_i \partial_i + \gamma_4 M c^2) \varphi = \lambda \varphi \quad (28')$$

containing now already the real mass.

The mass correction  $\delta M$ , however, depends strongly on the form of the bare nucleon, showing that our solution is not exact, the trial function (14) is too simple. Nevertheless accepting the normalization as an approximation, according to the foregoing we may form the following picture about the real nucleon in a coordinate system moving with the nucleon. According to (20) and (27) the total energy of the field is  $M c^2$ , where  $M$  is the real mass of the nucleon. According to (26) if the state function  $\varphi$  of the bare nucleon is normalized to the volume  $V$  the mean value of the meson number is  $g^2/2\hbar c \mu^3 V$ . (25) gives the mean value of the meson potential as  $-g/\mu^2 V$ . The mean value of the energy of the mesons surrounding the bare nucleon is from (16), (19) and (24)  $m c^2$ , their momenta are zero. From (15) follows that the mean value of the momentum of the field is also zero and from (29) that the mass correction is  $\delta M = -g^2/2c^2 V \mu^2$ .

\* \* \*

Our method may be applied without encountering difficulties to the case of many nucleons as well. For the amplitudes, similarly to (14) we now assume:

$$\langle x^1, \dots x^A; y^1, \dots y^n | t \rangle = C_n \varphi(x^1, \dots x^A) \prod^n f(y^i). \quad (30)$$

Owing to (7)  $\varphi$  must be antisymmetric. Repeating our calculations with the trial function (30) instead of (24) we obtain

$$f(x) = a(-\Delta + \mu^2)^{-1} A \bar{\varphi}(x) \varphi(x),$$

$$\bar{\varphi}(x) \varphi(x) = \int \dots \int \bar{\varphi}(x, x^2, \dots x^A) \gamma_4^{(2)} dx^2 \dots \gamma_4^{(A)} dx^A \varphi(x, x^2, \dots x^A) \quad (31)$$

from which the mean value of the meson number operator becomes

$$\langle M \rangle = \frac{g^2 A^2}{2 \hbar c} \int \bar{\varphi} \varphi (-\Delta + \mu^2)^{-\frac{3}{2}} \bar{\varphi} \varphi dx \quad (32)$$

and the mean value of the energy of the field

$$W^{(0)} = A E - \frac{g^2 A^2}{2} \int \bar{\varphi} \varphi (-\Delta + \mu^2)^{-1} \bar{\varphi} \varphi dx. \quad (33)$$

For atomic nuclei in zeroth approximation  $\varphi \varphi = 1/V = 3/4r_0^3 \pi A$ . In this case  $W^0$  is indeed proportional to  $A$  and the average meson number (32) becomes.

$$\langle M \rangle = \frac{g^2}{2 \hbar c} \frac{A^2}{V \mu^3} \approx \frac{g^2}{4 \pi \hbar c} A \quad \text{if} \quad \mu = \mu_\pi.$$

#### b) The intermediate coupling theory considering the nucleon recoil

Now the recoil of the nuclon will be considered. This may be done remaining within the framework of the method, by the modification of the trial function (14). Considering the recoil be now

$$\langle x; y^1, \dots y^n | t \rangle = C_n \varphi(x) \prod^n f(y^i - x). \quad (34)$$

Taking into account the normalization conditions

$$\sum C_n^* C_n = 1, \quad \int \bar{\varphi} \gamma_4 \varphi dx = 1, \quad \frac{2}{\hbar c} \int f^* (-\Delta + \mu^2)^{\frac{1}{2}} f dx = 1 \quad (35)$$

[compare equ. (16)] and calculating the mean value of the momentum of the fields from (9) we obtain

$$\langle P_i \rangle = \int \bar{\varphi} \gamma_4 (-i \hbar) \partial_i \varphi dx. \quad (36)$$

i.e. while according to (15) the total momentum of the field depends also on the momenta of the mesons, here the mean value of the total momentum of the field is determined only by the bare nucleon. Hence we may say that when a meson is emitted the momentum of the bare nucleon decreases to just the necessary extent (see Appendix).

Let us calculate the mean value of the energy. Using (9), (34) and (35) we obtain

$${}^c_i \langle P_4 \rangle = \sum_n C_n^* C_n (E + n(\varepsilon - \beta)) + \sum_n C_n^* C_{n+1} (n+1)^{1/2} a + \sum_n C_n^* C_{n-1} n^{1/2} a^*, \quad (37)$$

where [compare (19)]

$$\begin{aligned} E &= \int \bar{\varphi} (\hbar c \gamma_i \partial_i + M c^2) \varphi dx, \\ \varepsilon &= 2 \int f^* (-\Delta + \mu^2) f dx, \\ \alpha &= g f(0) \int \bar{\varphi} \varphi dx, \\ \beta &= \hbar c \int \bar{\varphi}(x) \gamma_j \varphi(x) dx \int f^*(y) \partial_j f(y) dy = -i \hbar \int f^* \nabla f dy. \end{aligned} \quad (38)$$

Repeating the calculations carried out in the first part we obtain successively

$$W^{(v)} = E + v(\varepsilon - \beta) - \frac{\alpha a^*}{\varepsilon - \beta}, \quad (39)$$

$$C_n^{(v)} = e^{-\frac{\alpha a^*}{2(\varepsilon - \beta)^2}} \sum_{l=0}^v \frac{(\nu!)^{1/2} (n!)^{1/2} (-1)^{n-\nu+l}}{l! (\nu-l)! (n-\nu+l)!} \left( \frac{\alpha^*}{\varepsilon - \beta} \right)^{n-\nu+l}, \quad (40)$$

$$\langle M \rangle^{(v)} = \frac{\alpha a^*}{(\varepsilon - \beta)^2} + v. \quad (41)$$

Varying (39) with respect to  $f$  we obtain in the ground state

$$f(x) = a \left( -\Delta + \mu^2 + \frac{i \hbar}{2} i \cdot \nabla \right)^{-1} \delta(x). \quad (42)$$

In the following only nucleons at rest will be dealt with ( $i = 0$ ). From (39) and (42) the total energy of the field is obtained as

$$W^{(0)} = E - \frac{g^2}{2} \left( \int \bar{\varphi} \varphi dx \right)^2 \int \delta(x) (-\Delta + \mu^2)^{-1} \delta(x) dx. \quad (43)$$

Completing the interaction Hamiltonian (3) for the sake of mass renormalization the second term of (43) can again be made to vanish if



$$\delta M = -\frac{g^2}{2c^2} \int \bar{\varphi} \varphi d\mathbf{x} \int \delta(\mathbf{x}) (-\Delta + \mu^2)^{-1} \delta(\mathbf{x}) d\mathbf{x}. \quad (44)$$

Because  $\delta M$  is yet weakly depending on the form of the bare nucleon, the solution is exact only for particles of infinite masses, in other cases it is an approximation.

The mean value of the meson potential from (11) and (42) is thus

$$\langle \Phi(\mathbf{x}) \rangle = -g \int \bar{\varphi} \varphi d\mathbf{x} (-\Delta + \mu^2)^{-1} \bar{\varphi}(\mathbf{x}) \gamma_4 \varphi(\mathbf{x}) \quad (45)$$

and the mean value of the meson number

$$\langle M \rangle = \frac{g^2}{2\hbar c} \left( \int \bar{\varphi} \varphi d\mathbf{x} \right)^2 \int \delta(\mathbf{x}) (-\Delta + \mu^2)^{-\frac{3}{2}} \delta(\mathbf{x}) d\mathbf{x}. \quad (46)$$

Summarizing the results: after renormalization in case of a real nucleon in a coordinate system moving with the nucleon the total energy of the field is  $Mc^2$  and its momentum zero. The mean value of the meson potential is  $-g/\mu^2 V$  and that of the meson number infinite.

For the determination of the meson-mode belonging to the  $\nu$ -th excited state of the nucleon we obtain from (39) ( $i = 0$ ):

$$f(\mathbf{x}) = \left[ \left( \frac{2\varepsilon\nu}{\alpha g} + \frac{2\alpha^*}{\varepsilon g} \right) (-\Delta + \mu^2) + \frac{2\lambda\varepsilon}{\hbar c \alpha g} (-\Delta + \mu^2)^{\frac{1}{2}} \right]^{-1} \delta(\mathbf{x}),$$

where  $\lambda$  is the Lagrange factor belonging to the normalization condition referring to  $f$ . In case of strong coupling the present  $f$  agrees with (42), namely then only the second term of the bracket remains ( $\alpha \sim g$ ).

Let us finally examine the energy distribution in the environment of a real nucleon in the ground state. Let us thus determine the mean value of the energy density:

$$\varrho = : \frac{1}{2} [\nabla \Phi \nabla \Phi - \partial_4 \Phi \partial_4 \Phi + \mu^2 \Phi^2] + \hbar c \bar{\psi} (\gamma_i \partial_i + \kappa) \psi + g \bar{\psi} \psi \Phi - \\ - \delta M c^2 \bar{\psi} \psi :$$

Similarly to the preceding methods we obtain with the aid of the state vector determined before

$$\langle \varrho \rangle = \frac{g^2}{2} \left( \int \bar{\varphi} \varphi d\mathbf{x} \right)^2 \int \bar{\varphi}(\mathbf{x}^1) \gamma_4 \varphi(\mathbf{x}^1) \left\{ \nabla (-\Delta + \mu^2)^{-1} \delta(\mathbf{x} - \mathbf{x}^1) \nabla (-\Delta + \mu^2)^{-1} \delta(\mathbf{x} - \mathbf{x}^1) + \mu^2 (-\Delta + \mu^2)^{-1} \delta(\mathbf{x} - \mathbf{x}^1) (-\Delta + \mu^2)^{-1} \delta(\mathbf{x} - \mathbf{x}^1) \right\} d\mathbf{x}^1 + \\ + \hbar c \bar{\varphi}(\mathbf{x}) (\gamma_i \partial_i + \kappa) \varphi(\mathbf{x}) - \frac{g^2}{2} \int \bar{\varphi} \varphi d\mathbf{x} \cdot \bar{\varphi}(\mathbf{x}) \varphi(\mathbf{x}) (-\Delta' + \mu^2)^{-1} \delta(\mathbf{x}') \Big|_{\mathbf{x}'=0} - \\ - \frac{g^2}{2} \int \bar{\varphi} \varphi d\mathbf{x} \bar{\varphi}(\mathbf{x}) \varphi(\mathbf{x}) (-\Delta' + \mu^2)^{-1} \delta(\mathbf{x}') \Big|_{\mathbf{x}'=0} - \delta M c^2 \bar{\varphi}(\mathbf{x}) \varphi(\mathbf{x}). \quad (47)$$

According to (44) the last two terms just cancel each other. It can be similarly seen, that forming  $\int \varrho dx$ , the first and third terms also become zero. Compensation of these terms, however, does not take place locally, thus finally

$$\begin{aligned} \langle \varrho(x) \rangle = & \hbar c \bar{\varphi}(x) (\gamma_i \partial_i + \kappa) \varphi(x) + \frac{g^2}{2} \int \bar{\varphi} \varphi dx \left\{ \int \bar{\varphi} \varphi dx \int \bar{\varphi}(x^1) \gamma_4 \varphi(x^1) \right. \\ & \left[ \left( \mu + \frac{1}{|x - x^1|} \right)^2 + \mu^2 \right] \cdot (-\Delta + \mu^2)^{-1} \delta(x - x^1) (-\Delta + \mu^2)^{-1} \delta(x - x^1) dx^1 - \\ & \left. - \bar{\varphi}(x) \varphi(x) (-\Delta' + \mu^2)^{-1} \delta(x') \right|_{x'=0} \}. \end{aligned}$$

Hence the energy density depends — with the exception of  $g$  — only on the form of the bare nucleon. If this is prescribed, then from the above equation the energy density can be determined.

Earlier ВНАВНА [30] carried out calculations concerning the theory of cosmic showers assuming, that the energy of the nucleon is concentrated into two regions, in an internal region of the order of a nucleon Compton wave length and an external meson region of the order of a meson Compton wave length in the proportion of  $(1-\varepsilon)Mc^2$  resp.  $\varepsilon Mc^2$ . Let us examine now how much energy falls — according to our calculations — in the case of our present model into the individual regions. Let us suppose as an approximation that the bare nucleon is pointlike:  $\bar{\varphi}(x)\gamma_4\varphi(x)=\delta(x)$  and  $\int \varphi\varphi dx=1$ . We then obtain a lower limit for the energy falling into the external region. Thus ( $m$  is the  $\pi$  meson mass,  $g=5e$ ,  $M=6,8 m$ ):

$$\begin{aligned} \int_{x^2 \geq \left(\frac{\hbar}{Mc}\right)^2} \langle \varrho(x) \rangle dx = & \frac{g^2}{4\pi\hbar c} \frac{e^{-\frac{2m}{M}}}{2} (m+M) c^2 \approx \frac{g^2}{4\pi\hbar c} 0,43 M c^2 = \\ & = 0,08 M c^2. \end{aligned}$$

\* \* \*

Let us deal now with the many-nucleon problem. As a generalization of (34) let us take the trial function in the following form:

$$\langle x^1, \dots, x^A; y^1, \dots, y^n | t \rangle = C_n \varphi(x^1, \dots, x^A) \prod \left\{ \sum_{j=1}^A f(y^i - x^j) \right\}. \quad (48)$$

Here according to (7)  $\varphi$  is antisymmetric. The normalization condition (12) is now

$$\begin{aligned} \sum C_n^* C_n l(n) &= 1, \\ l(n) &= \int \dots \int B(x^1, \dots, x^A)^n \bar{\varphi}(x^1, \dots, x^A) \prod^A \gamma_4^{(i)} dx^{(i)} \varphi(x^1, \dots, x^A), \\ l(0) &= 1, \end{aligned} \quad (49)$$

where

$$B(x^1, \dots, x^A) = \frac{2}{\hbar c} \left[ A \int f^*(y) (-\Delta + \mu^2)^{1/2} f(y) dy + \sum_{\substack{i,j \\ i \neq j}} \int f^*(y - x^i) (-\Delta + \mu)^{1/2} f(y - x^j) dy \right] = D + b(x^1, \dots, x^A). \quad (50)$$

According to (9) the mean value of the total momentum of the field is

$$\langle P_i \rangle = \sum_n C_n^* C_n \int \dots \int B(x^1, \dots, x^A)^n \bar{\varphi}(x^1, \dots, x^A) \prod_A \gamma_4^{(i)} dx^{(i)} \frac{\hbar}{i} \sum_i \frac{\partial}{\partial x_i} \varphi(x^1, \dots, x^A). \quad (51)$$

Let us determine the mean value of the energy. From (10) we obtain

$$\frac{c}{i} \langle P_4 \rangle = \sum_n C_n^* C_n (AE(n) + n \varepsilon(n)) + \sum_n C_n^* C_{n+1} (n+1)^{1/2} \alpha(n) + \sum_n C_n^* C_{n-1} n^{1/2} \alpha^*(n-1)$$

$$\begin{aligned} E(n) &= \int \dots \int B(x^1, \dots, x^A)^n \varphi(x^1, \dots, x^A) \prod_A \gamma_4^{(i)} dx^{(i)} \\ &\quad (\hbar c \gamma_4^{(1)} \gamma_4^{(1)} \partial_i + \gamma_4^{(1)} M c^2) \varphi(x^1, \dots, x^A) \\ \varepsilon(n) &= 2 \int \dots \int B(x^1, \dots, x^A)^{n-1} \bar{\varphi}(x^1, \dots, x^A) \prod_A \gamma_4^{(i)} dx^{(i)} \varphi(x^1, \dots, x^A) \\ &\quad \sum_{i,j} \int f^*(y - x^i) (-\Delta + \mu^2) f(y - x^j) dy \\ \alpha(n) &= A g \int \dots \int dx B(x, x^2, \dots, x^A)^n \bar{\varphi}(x, x^2, \dots, x^A) \prod_{i=2}^A \gamma_4^{(i)} dx^{(i)} \varphi(x, x^2, \dots, x^A) \\ &\quad \cdot \left( \sum_{j=2}^A f(x - x^j) + f(0) \right), \end{aligned} \quad (52)$$

where the terms corresponding to  $\beta$  of the expression (37) were omitted. Considering the normalization condition (49) and varying we obtain

$$C_n \left( A \frac{E(n)}{l(n)} + n \frac{\varepsilon(n)}{l(n)} - W \right) + C_{n+1} (n+1)^{1/2} \frac{\alpha(n)}{l(n)} + C_{n-1} n^{1/2} \frac{\alpha^*(n-1)}{l(n)} = 0. \quad (53)$$

Now the coefficients of the  $C_n$ -s depend yet on  $n$ . The coefficients will all be independent of  $n$ , if it is assumed that when substituting (50) into any integral of (52)  $b$  may be neglected against  $D$ . Further be  $f$  normalized:  $D=1$ . Thus

$$\begin{aligned}
\frac{E(n)}{l(n)} &\rightarrow E = \int \dots \int \bar{\varphi}(x^1, \dots, x^A) \prod_{i=2}^A \gamma_4^{(i)} d x^{(i)} (\hbar c \gamma_4^{(1)} \gamma_l^{(1)} \partial_i + \gamma_4^{(1)} M c^2) \varphi(x^1, \dots, x^A), \\
\frac{\varepsilon(n)}{l(n)} &\rightarrow \varepsilon = 2 \int \dots \int \bar{\varphi}(x^1, \dots, x^A) \prod_{i=2}^A \gamma_4^{(i)} d x^{(i)} \varphi(x^1, \dots, x^A) \\
&\quad \sum_{i,j} f^*(y - x^i) (-\Delta + \mu^2) f(y - x^j) d y, \\
\frac{\alpha(n)}{l(n)} &\rightarrow \alpha = A g \int \dots \int d x^1 \bar{\varphi}(x^1, \dots, x^A) \prod_{i=2}^A \gamma_4^{(i)} d x^{(i)} \varphi(x^1, \dots, x^A) \\
&\quad \left( \sum_{j=2}^A f(x^1 - x^j) + f(0) \right), \quad \frac{\alpha^*(n-1)}{l(n)} \rightarrow \alpha^*. \quad (54)
\end{aligned}$$

Using these expressions the solution of equation (53) is as before

$$\begin{aligned}
W^{(\nu)} &= A E - \frac{\alpha \alpha^*}{\varepsilon} + \nu \varepsilon, \\
C_n^{(\nu)} &= e^{-\frac{\alpha \alpha^*}{2 \varepsilon^2}} \sum_{l=0}^{\nu} \frac{(\nu!)^{\frac{1}{2}} (n!)^{\frac{1}{2}} (-1)^{n-\nu+l}}{l! (\nu-l)! (n-\nu+l)!} \left( \frac{\alpha^*}{\varepsilon} \right)^{n-\nu+l}. \quad (55)
\end{aligned}$$

$f$  can be again determined by the variation of  $W$ . Thus the solution is for the ground state

$$f(x) = \alpha (-\Delta + \mu^2)^{-1} \delta(x),$$

if only  $\bar{\varphi} \gamma_4 \approx \bar{\varphi}$

Using this the total energy of the field becomes

$$\begin{aligned}
W^{(0)} &= A E - \frac{g^2}{2} A \int \dots \int d x \bar{\varphi}(x, x^2, \dots, x^A) \prod_{i=2}^A \gamma_4^{(i)} d x^{(i)} \varphi(x, x^2, \dots, x^A) \\
&\quad \sum_{j=2}^A (-\Delta + \mu^2)^{-1} \delta(x - x^j), \quad (56)
\end{aligned}$$

here the self-energies were left out. Finally varying  $W^{(0)}$  with respect to  $\varphi$  we obtain, that the total energy of the field is minimal, if

$$\begin{aligned}
\sum_j \left[ \hbar c \gamma_4^{(j)} \gamma_l^{(j)} \partial_l^{(j)} + \gamma_4^{(j)} \left( M c^2 - \frac{g^2}{2} (-\Delta^{(j)} + \mu^2)^{-1} \sum_{\substack{i,j \\ i \neq j}} \delta(x^j - x^i) \right) \right] \varphi(x^1, \dots, x^A) = \\
= \lambda \varphi(x^1, \dots, x^A), \quad (57)
\end{aligned}$$

where  $\lambda$  is the Lagrangian factor belonging to the normalization condition (49) [ $l(0) = 1$ ]. In the equation resulting from iterating (57) as it has been shown by G. MARX and G. SZAMOSI [32], [33] relativistical repulsive and many-body forces occur which might result the saturation.

The mean value of the meson number from (11), (48), (49) and (55) is

$$\langle M \rangle = \frac{\alpha^* \alpha}{\varepsilon^2} = \frac{g^2 A}{2 \hbar c} \int \delta(y) (-A + \mu^2)^{-1/2} \delta(y) dy \simeq A \langle M \rangle_{\text{one nucleon}},$$

hence our approximation used in this part means essentially the omission of the mesons giving rise to the interaction between the individual nucleons, against those belonging to the self-fields of the nucleons.

According to the foregoing the divergent self-energies can be approximately eliminated by mass renormalization, other quantities, however, remain divergent. For the elimination of these the usual method is the cutting-off method. This can be explained according to the considerations of part a) by attributing to the bare nucleon a finite extension. As against this from the calculations performed taking into consideration the recoil, it is evident that if the cut-off is to be justified, (3) cannot be of general validity.

Thus we obtain from (46) for a nucleon at rest if the cutting-off is carried out at a value  $\delta\mu = \kappa \approx 6,8 \mu$  with  $g = 5e$

$$\langle M \rangle = 0,09.$$

## 2. The nucleon and the symmetrical pseudoscalar meson field

In our calculations here we consider only the recoil of the nucleon, simplest calculations not taking into account the recoil can be carried out similarly. Let us first of all consider the mean value of  $\langle \sigma | P_\mu [\sigma] | \sigma \rangle$ .

We obtain from (1), (4) and (6) similarly to (9)

$$\begin{aligned} \langle \sigma | P_\mu [\sigma] | \sigma \rangle &= i \int_{\sigma} \sum \left( \frac{i}{\hbar c} \right)^{n^+ + n^- + n^3} \dots \int \langle \sigma | \bar{x}; \xi^1 \dots \xi^{n^+}; \eta^1, \dots \eta^{n^-}; \xi^1, \dots \xi^{n^3} \rangle \\ &\quad \cdot \prod d_{v_i} d\sigma_{v_i}(\xi^i) \prod d_{v_i} d\sigma_{v_i}(\eta^i) \prod d_{v_k} d\sigma_{v_k}(\xi^k) \gamma_v d\sigma_v(x) \cdot \\ &\quad \frac{\hbar}{i} \left\{ \frac{\partial}{\partial x_\mu} + \sum \frac{\partial}{\partial \xi_\mu^i} + \sum \frac{\partial}{\partial \eta_\mu^j} + \sum \frac{\partial}{\partial \xi_\mu^k} \right\} \langle x; \xi^1, \dots \xi^{n^+}; \eta^1, \dots \eta^{n^-}; \xi^1, \dots \xi^{n^3} | \sigma \rangle - \\ &\quad - \frac{ig}{2\kappa c} \int_{\sigma} d\sigma_\mu(x) \sum \left( \frac{i}{\hbar c} \right)^{n^+ + n^- + n^3} \dots \int \langle \sigma | x; \xi^1, \dots \xi^{n^+}; \eta^1, \dots \eta^{n^-}; \xi^1, \dots \xi^{n^3} \rangle \\ &\quad \prod d_{v_i} d\sigma_{v_i}(\xi^i) \prod d_{v_j} d\sigma_{v_j}(\eta^j) \prod d_{v_k} d\sigma_{v_k}(\xi^k) \gamma_e \gamma_5 \frac{\partial^{(1)}}{\partial x_0} \left\{ \sqrt{2} \tau_- (n^+ - 1)^{1/2} \cdot \right. \end{aligned}$$



$$\begin{aligned}
& \cdot \langle x; x, \xi^1, \dots, \xi^{n^+}; \eta^1, \dots, \eta^{n^-}; \zeta^1, \dots, \zeta^{n^3} | \sigma \rangle + \sqrt{2} \tau_+ (n^- - 1)^{1/2} \cdot \\
& \cdot \langle x; \xi^1, \dots, \xi^{n^+}; x, \eta^1, \dots, \eta^{n^-}; \zeta^1, \dots, \zeta^{n^3} | \sigma \rangle + \tau_3 (n^3 - 1)^{1/2} \cdot \\
& \cdot \langle x; \xi^1, \dots, \xi^{n^+}; \eta^1, \dots, \eta^{n^-}; x, \zeta^1, \dots, \zeta^{n^3} | \sigma \rangle \} + c. c. - \\
& - \lambda \frac{\xi^2}{2 M c^2} 2 \int_{\sigma} d \sigma_{\mu}(x) \sum \left( \frac{i}{\hbar c} \right)^{n^+ + n^- + n^3 - 1} \int_{\sigma} \dots \int_{\sigma} \{ n^+ \\
& \langle \sigma | x; x, \xi^2, \dots, \xi^{n^+}; \eta^1, \dots, \eta^{n^-}; \zeta^1, \dots, \zeta^{n^3} \rangle \\
& \quad \prod_{i=2}^{n^+} d v_{vi} d \sigma_{vi}(\xi^i) \prod_{j=1}^{n^-} d v_j d \sigma_{vj}(\eta^j) \prod_{k=1}^{n^3} d v_{vk} d \sigma_{vk}(\zeta^k) \cdot \\
& \cdot \langle x; x, \xi^2, \dots, \xi^{n^+}; \eta^1, \dots, \eta^{n^-}; \zeta^1, \dots, \zeta^{n^3} | \sigma \rangle + \quad (58)
\end{aligned}$$

+ analogous terms for  $n^-$  and  $n^3 + 2$  mesons more + 2 mesons less. Here the exclamation mark over  $\frac{\partial}{\partial x_Q}$  indicates, that the succeeding amplitude should be differentiated with respect of the meson coordinate only. Further on the last two terms of (58) which are there not given explicitly are everywhere omitted, because they contribute nothing to the approximation to be dealt with below. In (58)  $x, \xi, \eta, \zeta$  etc. are again four-dimensional vectors.

Before making an assumption concerning the trial functions, it is worth while to consider the following. A bare nucleon can be characterized by its parity, isotope spin and spin and these values remain the same for the real nucleon.

Earlier for a scalar field these requirements were fulfilled automatically, here in the choice of the trial function special attention has to be paid to these considerations. The only possibility to avoid the difficulties encountered in the calculation owing to this fact is not to allow around the real nucleon an arbitrary number of mesons.

Calculations were also carried out by taking into account several mesons [17]. To illustrate the configurational method we go only as far as the one-meson states, however, the recoil as well as the term of the form  $\bar{\psi}\psi\Phi^2$  of the interaction energy are taken into account. Accordingly, only the following amplitudes can be chosen as differing from zero (again in the case of a  $t = \text{const}$  plane and by changing notation) :

$$\begin{aligned}
\langle x | t \rangle &= C_0 \varphi_{\frac{1}{2}, \frac{1}{2}}(x, 1/2, 1/2) \\
\langle x; \xi | t \rangle &= C_1 \left[ \sqrt{\frac{2}{3}} \left\{ \sqrt{\frac{1}{3}} f_{1,1}(\xi - x, 1, 0) \varphi_{\frac{1}{2}, -\frac{1}{2}}(x, 1/2, 1/2) + \right. \right. \\
& \quad \left. \left. + \sqrt{\frac{2}{3}} f_{1,1}(\xi - x, 1, 1) \varphi_{\frac{1}{2}, -\frac{1}{2}}(x, 1/2, -1/2) \right\} \right]
\end{aligned}$$

$$\begin{aligned} \langle x; \zeta, t \rangle = C_1 \left\{ \sqrt{\frac{1}{3}} \left\{ \sqrt{\frac{1}{3}} f_{1,0}(\zeta - x, 1, 0) \varphi_{\frac{1}{2}, \frac{1}{2}}(x, \frac{1}{2}, \frac{1}{2}) + \right. \right. \\ \left. \left. + \sqrt{\frac{2}{3}} f_{1,0}(\zeta - x, 1, 1) \varphi_{\frac{1}{2}, \frac{1}{2}}(x, \frac{1}{2}, -\frac{1}{2}) \right\} \right\} \quad (59) \end{aligned}$$

for a proton and

$$\begin{aligned} \langle x | t \rangle &= C_0 \varphi_{\frac{1}{2}, -\frac{1}{2}}(x, \frac{1}{2}, \frac{1}{2}) \\ \langle x; \eta | t \rangle &= C_1 \left\{ \sqrt{\frac{2}{3}} \left\{ \sqrt{\frac{1}{3}} f_{1,-1}(\eta - x, 1, 0) \varphi_{\frac{1}{2}, \frac{1}{2}}(x, \frac{1}{2}, \frac{1}{2}) + \right. \right. \\ &\quad \left. \left. + \sqrt{\frac{2}{3}} f_{1,-1}(\eta - x, 1, 1) \varphi_{\frac{1}{2}, \frac{1}{2}}(x, \frac{1}{2}, -\frac{1}{2}) \right\} \right\} \\ \langle x; \zeta | t \rangle &= C_1 \left\{ \sqrt{\frac{1}{3}} \left\{ \sqrt{\frac{1}{3}} f_{1,0}(\zeta - x, 1, 0) \varphi_{\frac{1}{2}, -\frac{1}{2}}(x, \frac{1}{2}, \frac{1}{2}) + \right. \right. \\ &\quad \left. \left. + \sqrt{\frac{2}{3}} f_{1,0}(\zeta - x, 1, 1) \varphi_{\frac{1}{2}, -\frac{1}{2}}(x, \frac{1}{2}, -\frac{1}{2}) \right\} \right\} \quad (60) \end{aligned}$$

for a neutron. Here the outer indices of  $\varphi$  and  $f$  mean the isotope spin and its third component for the nucleon resp. the meson. By our choice the problems related to the isotope spin have been solved. The inner indices of  $\varphi$  refer to the angular momentum and its projection, and have in the usual representation of the  $\gamma$ -s the following form

$$\varphi_{\frac{1}{2}, \frac{1}{2}}(x, \frac{1}{2}, \frac{1}{2}) = \begin{pmatrix} \varphi_1 \\ 0 \\ \varphi_2 \\ 0 \\ 0 \\ 0 \\ 0 \\ 0 \end{pmatrix}, \quad \varphi_{\frac{1}{2}, \frac{1}{2}}(x, \frac{1}{2}, -\frac{1}{2}) = \begin{pmatrix} 0 \\ -\varphi_1 \\ 0 \\ -\varphi_2 \\ 0 \\ 0 \\ 0 \\ 0 \end{pmatrix}$$

$\varphi_{\frac{1}{2}, -\frac{1}{2}}(\frac{1}{2}, \frac{1}{2})$  and  $\varphi_{\frac{1}{2}, -\frac{1}{2}}(\frac{1}{2}, -\frac{1}{2})$  are the same, but their elements differ from zero at the lower 4 places.  $\varphi_1$  and  $\varphi_2$  are arbitrary spherical symmetric functions. Each  $\varphi$  is normalized to 1, and they are orthogonal to each other. For given  $\varphi_i$ , the values  $\bar{\varphi}\varphi$ ,  $\bar{\varphi}\gamma_4\varphi$  and  $\int \bar{\varphi}(\hbar c\gamma_i\partial_i + Mc^2)\varphi dx$  are independent of the indices of the  $\varphi$ -s. This will be made use of later on. It is to be expected that the inner indices of the functions  $f$  will refer also to the angular momentum and its projection. For the moment let us consider them simply as distinguishing indices. Be the  $f$ -s normalized and the functions with different inner indices orthogonal to each other:

$$\frac{2}{\hbar c} \int f^* (-\Delta + \mu^2)^{\frac{1}{2}} f dx = 1,$$

$$\int f_{1,0}^* (x, 1, 0) (-\Delta + \mu^2)^{1/2} f_{1,0} (x, 1, 1) dx = 0 \quad \text{etc.} \quad (61)$$

In this case the normalization condition  $\langle t | t \rangle = 1$  is the following :

$$C_0^* C_0 + C_1^* C_1 = 1. \quad (62)$$

Substituting (59) into (58) and making use of what has been said about the  $\varphi$ -s and  $f$ -s we obtain

$$\frac{c}{i} \langle P_4 \rangle = C_0^* C_0 E + C_1^* C_1 (E + \varepsilon) + C_0^* C_1 \alpha + C_1^* C_0 \alpha^* + C_1^* C_1 \gamma, \quad (63)$$

where

$$E = \int \bar{\varphi} (\hbar c \gamma_i \partial_i + M c^2) \varphi dx.$$

$$\begin{aligned} \varepsilon = 2 \int \left\{ \frac{1}{3} \frac{1}{3} f_{1,0}^* (1, 0) (-\Delta + \mu^2) f_{1,0} (1, 0) + \frac{1}{3} \frac{2}{3} f_{1,0}^* (1, 1) (-\Delta + \mu^2) f_{1,0} (1, 1) + \right. \\ \left. + \frac{2}{3} \frac{1}{3} f_{1,1}^* (-\Delta + \mu^2) f_{1,1} (1, 0) + \frac{2}{3} \frac{2}{3} f_{1,1}^* (1, 1) (-\Delta + \mu^2) f_{1,1} (1, 1) \right\} dx, \end{aligned}$$

$$\begin{aligned} \alpha = \frac{g}{2\kappa} \left\{ \left| \sqrt{\frac{2}{3}} \right| \sqrt{\frac{1}{3}} a_{1,1} (1, 0)_i \int f_{1,1} (x, 1, 0) \partial_i \delta (x) dx + \right. \\ \left. + \left| \sqrt{\frac{2}{3}} \right| \sqrt{\frac{2}{3}} a_{1,1} (1, 1)_i \int f_{1,1} (x, 1, 1) \partial_i \delta (x) dx + \right. \\ \left. + \left| \sqrt{\frac{1}{3}} \right| \sqrt{\frac{1}{3}} a_{1,0} (1, 0)_i \int f_{1,0} (x, 1, 0) \partial_i \delta (x) dx + \right. \\ \left. + \left| \sqrt{\frac{1}{3}} \right| \sqrt{\frac{2}{3}} a_{1,0} (1, 1)_i \int f_{1,0} (x, 1, 1) \partial_i \delta (x) dx \right\}, \end{aligned}$$

$$a_{1,1} (1, 0)_i = \{0, 0, \sqrt{2}\},$$

$$a_{1,1} (1, 1)_i = \{\sqrt{2}, -i\sqrt{2}, 0\},$$

$$a_{1,0} (1, 0)_i = \{0, 0, 1\},$$

$$a_{1,0} (1, 1)_i = \{1, -i, 0\},$$

$$\begin{aligned} \gamma = \lambda \frac{g^2}{2M c^2} 2b \left[ \frac{2}{3} \frac{2}{3} \int f_{1,1}^* (x, 1, 1) f_{1,1} (x, 1, 1) \delta (x) dx + \right. \\ \left. + \frac{2}{3} \frac{1}{3} \int f_{1,1}^* (x, 1, 0) f_{1,1} (x, 1, 0) \delta (x) dx + \right. \end{aligned}$$

$$\begin{aligned}
& + \frac{1}{3} \frac{1}{3} \int f_{1,0}^* (x, 1, 0) f_{1,0} (x, 1, 0) \delta (x) dx + \\
& + \frac{1}{3} \frac{2}{3} \int f_{1,0}^* (x, 1, 1) f_{1,0} (x, 1, 1) \delta (x) dx \Big], \\
& b = \int \bar{\varphi} \varphi dx.
\end{aligned} \tag{64}$$

Here it has been used that  $\int \bar{\varphi} \gamma_4 \gamma_5 \varphi dx \approx 0$ , and also the term corresponding to the  $\beta$  of equation (37) has been omitted.

Varying (63) with respect to  $C^*$ , and considering (62) we obtain

$$\begin{aligned}
C_0 (E - W) + C_1 \alpha &= 0, \\
C_0 \alpha^* + C_1 (E + \varepsilon + \gamma - W) &= 0.
\end{aligned} \tag{65}$$

This system of equations has a nontrivial solution if  $\text{Det} \neq 0$ . From this the lower energy value is

$$W = E + \frac{\varepsilon + \gamma - (\varepsilon + \gamma) \sqrt{1 + \frac{4 \alpha \alpha^*}{(\varepsilon + \gamma)^2}}}{2} \approx E - \frac{\alpha \alpha^*}{\varepsilon + \gamma} \tag{66}$$

and the amplitudes belonging to this state

$$C_0 = \frac{1}{\sqrt{1 + \frac{\alpha \alpha^*}{(\gamma + \varepsilon)^2}}}, \quad C_1 = -\frac{\alpha^*}{\varepsilon + \gamma} C_0. \tag{67}$$

From here it may be seen, that the approximation used in (66) for the extraction of the root does not make use of the small value of  $g$ , but of the fact, that the probability of single-meson states is small, compared with the bare-nucleon state. On the basis of the conclusions to be drawn from the preceding paragraph we may, however, hope that by permitting arbitrarily many mesons we would obtain essentially the same energy.

The determination of the  $f$ -s remains to be carried out. We determine the  $f$ -s also here from (66) by variation. The auxiliary conditions (61) should also be taken into account for the variation. However in our present approximation they are disregarded, although the  $f$ -s obtained as solution are to satisfy the conditions.

The solution of the set of equations obtained by variation is

$$f_{1,1} (x, 1, 0) = \frac{a}{\sqrt{2}} \left( -\Delta + \mu^2 + \lambda \frac{g^2}{2 M c^2} b \delta (x) \right)^{-1} a_{1,1}^* (1, 0)_i \partial_i \delta (x),$$

$$\begin{aligned}
 f_{1,1}(x, 1, 1) &= \frac{a}{2} \left( -\Delta + \mu^2 + \lambda \frac{g^2}{2Mc^2} b \delta(x) \right)^{-1} a_{1,1}^* (1, 1)_i \partial_i \delta(x), \\
 f_{1,0}(x, 1, 0) &= a \left( -\Delta + \mu^2 + \lambda \frac{g^2}{2Mc^2} b \delta(x) \right)^{-1} a_{1,0}^* (1, 0)_i \partial_i \delta(x), \\
 f_{1,0}(x, 1, 1) &= \frac{a}{\sqrt{2}} \left( -\Delta + \mu^2 + \lambda \frac{g^2}{2Mc^2} b \delta(x) \right)^{-1} a_{1,0}^* (1, 1)_i \partial_i \delta(x).
 \end{aligned} \tag{68}$$

The normalization factor  $a$  can be determined from any  $f$  and we obtain always the same value. Similarly we may satisfy ourselves about the fact that the  $f$ -s of different inner indices are orthogonal.

Using (68) finally the energy of the field is in case of one proton

$$W = E - \left( \frac{g}{2\kappa} \right)^2 \frac{3}{2} \int \partial_i \delta(x) \left( -\Delta + \mu^2 + \lambda \frac{g^2}{2Mc^2} b \delta(x) \right)^{-1} \partial_i \delta(x) dx. \tag{69}$$

For a neutron the calculations can be carried out in the same way. Finally we receive back the functions (68) ( $f_{1,1} \rightarrow f_{1,-1}$ ) and the energy (69).

Formulating the state vector of the total system from (6), (59), (60) and (68) it may be seen, that the determined state is the eigenstate of the total angular momentum and its projection, further on because the mesons are created in the  $p$  state also of the parity with correct eigenvalues.

In the present approximation the state vector characterizing the real nucleon has already been determined, so that now the value of an arbitrary operator characterizing the field can be determined. Below the magnetic momentum of the nucleon is calculated. The operator of the magnetic momentum is

$$\mathfrak{M} = : \frac{e\hbar}{2Mc} \int \bar{\psi} \gamma_4 \frac{1 + \tau_3}{2} \sigma \psi dx + \frac{ie}{2\hbar c} \int (\Phi[x, \nabla] \Phi^* - \Phi^*[x, \nabla] \Phi) dx : \tag{70}$$

From the obtained state functions we obtain the relation found by SACHS [45]

$$\langle \mathfrak{M} \rangle_P + \langle \mathfrak{M} \rangle_N = \frac{e\hbar}{2Mc} \left( 1 - \frac{4}{3} C_1^* C_1 \right). \tag{71}$$

The numerical values of the magnetic momentum with a cutting off at  $\delta\mu$  become in case of  $\frac{g^2}{4\pi\hbar c} = 15$ :



$$\begin{array}{llll}
\langle \mathfrak{M} \rangle_P = 0,98 & \langle \mathfrak{M} \rangle_N = -0,40 & C_1^* C_1 = 0,32 & \text{if } \delta = 4 \\
= 1,04 & = -0,29 & = 0,19 & = 3 \\
= 1,04 & = -0,14 & = 0,08 & = 2
\end{array}$$

In case of  $\lambda = 0,2$  :

$$\langle \mathfrak{M} \rangle_P = 1,02 \quad \langle \mathfrak{M} \rangle_N = -0,20 \quad C_1^* C_1 = 0,14, \quad \delta = 3.$$

These are in accordance with the earlier statements of SACHS: permitting only single meson states we obtain for the anomalous magnetic momentum of the nucleon wrong results. Taking into account the term of the interaction energy proportional to  $\lambda$  does not alter this fact either.

Let us determine now the electron charge distribution of the nucleon. Let us form with the determined state vector the mean value of the charge density-operator

$$\varrho(x) = : e \bar{\psi} \gamma_4 \frac{1 + \tau_3}{2} \psi + \frac{e}{\hbar c} \Phi^* d_4 \Phi :$$

Similarly to our other methods we obtain by considering what has been said about  $\varphi$

$$\begin{aligned}
\langle \varrho(x) \rangle_P &= C_0^* C_0 e \bar{\varphi}(x) \gamma_4 \varphi(x) + \frac{1}{3} C_1^* C_1 \bar{\varphi}(x) \gamma_4 \varphi(x) + \frac{2}{3} C_1^* C_1 \frac{e}{\hbar c} \int \left\{ \right. \\
&\quad \frac{1}{3} f_{1,1}^*(x - x^1, 1, 0) 2(-\Delta + \mu^2)^{1/2} f_{1,1}(x - x^1, 1, 0) + \frac{2}{3} f_{1,1}^*(x - x^1, 1, 1) \cdot \\
&\quad \cdot 2(-\Delta + \mu^2)^{1/2} f_{1,1}(x - x^1, 1, 1) \left. \right\} \varphi(x^1) \gamma_4 \varphi(x^1) dx^1, \\
\langle \varrho(x) \rangle_N &= \frac{2}{3} C_1^* C_1 e \bar{\varphi}(x) \gamma_4 \varphi(x) - \frac{2}{3} C_1^* C_1 \frac{e}{\hbar c} \int \left\{ \frac{1}{3} f_{1,-1}^*(x - x^1, 1, 0) \cdot \right. \\
&\quad \cdot 2(-\Delta + \mu^2)^{1/2} f_{1,-1}(x - x^1, 1, 0) + \frac{2}{3} f_{1,-1}^*(x - x^1, 1, 1) \cdot 2(-\Delta + \mu^2)^{1/2} \cdot \\
&\quad \cdot f_{1,-1}(x - x^1, 1, 1) \left. \right\} \bar{\varphi}(x^1) \gamma_4 \varphi(x^1) dx^1. \tag{72}
\end{aligned}$$

From here making use of the fact that the  $\varphi$ -s with the same inner indices are identical functions, it can be read that the mesonic charge cloud of the real proton and neutron, — disregarding the sign — are the same.

$$\langle \varrho(x) \rangle_P + \langle \varrho(x) \rangle_N = e \bar{\varphi}(x) \gamma_4 \varphi(x).$$

Finally from (72) in case of  $\lambda = 0$  with the determined quantities the mesonic charge cloud becomes

$$e C_0^* C_0 \frac{g^2}{4 \pi \hbar c} - \frac{\mu}{8 \pi^2 \kappa^2} \int \left\{ \frac{\partial}{\partial x_i} \frac{e^{-\mu|x-x^1|}}{|x-x^1|} \frac{\partial}{\partial x_i} \frac{K_1(\mu|x-x^1|)}{|x-x^3|} \right\} \bar{\varphi}(x^1) \gamma_4 \varphi(x^1) dx^1.$$

Let us finally calculate the mean value of the energy density of the field. With the aid of the determined state vector and in the approximation used in equation (66) we obtain that the energy density of the meson field is in the environment of the real nucleon

$$\begin{aligned} \langle \varrho^M(x) \rangle = & \left( \frac{g}{2\kappa} \right)^2 \frac{3}{2} \frac{1}{2} \int \bar{\varphi}(x^1) \gamma_4 \varphi(x^1) \left\{ \partial_i \partial_j (-\Delta + \mu^2)^{-1} \delta(x-x^1) \right. \\ & \partial_i \partial_j (-\Delta + \mu^2)^{-1} \delta(x-x^1) + \sqrt{-\Delta + \mu^2} \partial_j (-\Delta + \mu^2)^{-1} \\ & \delta(x-x^1) \sqrt{-\Delta + \mu^2} \partial_j (-\Delta + \mu^2)^{-1} \delta(x-x^1) + \\ & \left. + \mu^2 \partial_j (-\Delta + \mu^2)^{-1} \delta(x-x^1) \partial_j (-\Delta + \mu^2)^{-1} \delta(x-x^1) \right\} dx^1. \end{aligned} \quad (73)$$

Indeed its integral over the whole volume agrees apart from the sign to the self-energy term of expression (69). In analogy with (47) it may however be assumed that taking into account the many-meson states the energy density of the field can be better approximated by the expression

$$\begin{aligned} \langle \varrho^M(x) \rangle = & \left( \frac{g}{2\kappa} \right)^2 \frac{3}{2} \int \bar{\varphi}(x^1) \gamma_4 \varphi(x^1) \left\{ \partial_i \partial_j (-\Delta + \mu^2)^{-1} \delta(x-x^1) \partial_i \partial_j \cdot \right. \\ & \cdot (-\Delta + \mu^2)^{-1} \delta(x-x^1) + \mu^2 \partial_j (-\Delta + \mu^2)^{-1} \delta(x-x^1) \partial_j (-\Delta + \mu^2)^{-1} \delta(x-x^1) \left. \right\} dx^1, \end{aligned} \quad (74)$$

the integral of which taken over the total volume agrees also with the second term of (69). From (74) in case of a point-like nucleon with  $g^2/4 \pi \hbar c = 15$  we obtain

$$\int_{x^1 \geq \left( \frac{\hbar}{Mc} \right)^2} \langle \varrho(x) \rangle dx = \frac{g^2}{4 \pi \hbar c} 0,99 M c^2 = 14,8 M c^2,$$

namely only the energy of the meson field extends to the considered part of the space. Since the total energy of the field is (neglecting the kinetic energy of the Dirac field)  $M c^2$ , thus in such cases the energy present in the internal region is  $-13,8 M c^2$ . It might be of interest to repeat the calculations of ВНАВНА by considering our present results.

My thanks are due to Dr. G. MARX for his advices given during the preparation of this work and for his continuous interest. Similarly I am indebted to Prof. Dr. G. HEBER (Jena) for his valuable remarks.

## Appendix

Earlier the recoil of the nucleon was taken into consideration. Here the calculations taking into account the recoil are carried out in the momentum space. The present discussion shows clearly why the choice of trial function (34) means just the consideration of the recoil of the nucleon. Let us write (34) in the following form

$$\langle x^1; y^1, \dots, y^n | \rangle = \\ = C_n \frac{1}{(2\pi\hbar)^{3/2}} \frac{1}{(2\pi\hbar)^{3n/2}} \int \varphi_n(p) e^{\frac{i}{\hbar} p x} d p \prod_{i=1}^n \sqrt{\frac{\hbar^2 c^2}{2\omega_i}} f(k^i) e^{\frac{i}{\hbar} k^i x} d k^i, \quad (1)$$

where the recoil has to be taken into consideration by

$$\varphi_n(p) = \sum_s a_s \left( p + \sum_{i=1}^n k^i \right) u_s(p). \quad (2)$$

$u_s(p)$  is owing to (7) an unit spinor characterizing a nucleon with momentum  $p$ , polarisation  $s$  (spin, isotope spin) and positive frequency, its explicit form is in the usual representation of the  $\gamma$ -s

$$\left( 1 + \frac{c^2 p^2}{(E + M c^2)^2} \right)^{-1/2} \begin{pmatrix} \delta_{1s} \\ \delta_{1s} \\ \frac{c(\sigma p)_{1s}}{E + M c^2} \\ \frac{c(\sigma p)_{2s}}{E + M c^2} \\ 0 \\ 0 \\ 0 \\ 0 \end{pmatrix} \quad \begin{array}{l} s = 1, 2 \\ \text{in case of } s = 3, 4, \text{ elements } \neq 0 \text{ are} \\ \text{at the lower 4 places.} \end{array} \quad (3)$$

$$\sum_s \int a_s^*(p) a_s(p) d p = 1,$$

$$\omega = \sqrt{c^2 k^2 + m^2 c^4}$$

$$\int f^*(k) f(k) d k = 1. \quad (4)$$

From (2) and (3) it can be seen, that neglecting the small components of the  $u$ -s (1) just agrees with (34). From the normalization condition  $\langle t | t \rangle = 1$  it again follows that

$$\sum C_n^* C_n = 1. \quad (5)$$

Let us first calculate the mean value of the momentum of the field. From (10) on the basis of the above we obtain

$$\langle P_i \rangle = \sum_s \int p_i a_s^*(p) a_s(p) dp. \quad (6)$$

Similarly the mean value of the energy of the field is

$$\begin{aligned} \frac{c}{i} \langle P_4 \rangle = & \sum_n C_n^* C_n \sum_s \int \dots \int a_s^*(p) \prod^n f^*(k^j) \sqrt{c^2(p - \sum k^j)^2 + M^2 c^4} + \\ & + \sum^n \sqrt{c^2 k^{j2} + m^2 c^4} \cdot a_s(p) \prod^n f(k^j) dp \prod^n dk^j + \\ & + g \sum_n (n+1)^{1/2} C_n^* C_{n+1} \sum_{s,s'} \int \dots \int a_s^*(p) \prod^n f^*(k^j) f(k^j) dk^j \cdot \\ & \cdot \bar{u}_s(p - \sum^n k^j) u_{s'}(p - q - \sum^n k^j) a_{s'}(p) \frac{1}{(2\pi\hbar)^{3/2}} \sqrt{\frac{\hbar^2 c^2}{2\omega_q}} f(q) dq dp + C \cdot C. \end{aligned} \quad (7)$$

Here the terms under the integral are still depending on  $n$ , thus GLAUBER and LUTTINGER's method cannot be applied to the solution of the equation obtained after the variation, therefore further approximations are used. By expansion we obtain

$$\sqrt{c^2(p - \sum k^j)^2 + M^2 c^4} \approx \sqrt{c^2 p^2 + M^2 c^4} + \frac{1}{2M} (\sum k^j)^2 - \frac{1}{M} p \sum k^j.$$

Assuming further that  $a(p)$  and  $f$  are spherical symmetric, then the first term is

$$\sum_n C_n^* C_n \left[ E + n \left( \varepsilon + \frac{\bar{k}^2}{2M} \right) \right],$$

of course here

$$E = \sum_s \int a_s^*(p) \sqrt{c^2 p^2 + M^2 c^4} a_s(p) dp,$$

$$\varepsilon = \int f^*(k) \sqrt{c^2 k^2 + m^2 c^4} f(k) dk,$$

$$\bar{k}^2 = \int f^*(k) k^2 f(k) dk.$$

In the second term using the approximation (compare [5])

$$\begin{aligned} \bar{u}_s(p - \sum k^j) u_{s'}(p - q - \sum k^j) &\rightarrow \bar{u}_s(p) u_{s'}(p) = \\ &= \frac{1 - \frac{c^2 p^2}{(E + M c^2)^2}}{1 + \frac{c^2 p^2}{(E + M c^2)^2}} \delta_{s,s'} = g(p) \delta_{s,s'} \end{aligned}$$

we obtain from (7) in such an approximation

$$\begin{aligned} \frac{c}{i} \langle P_4 \rangle = \sum C_n^* C_n \left[ E + n \left( \varepsilon + \frac{\hbar^2}{2M} \right) \right] + \sum_n (n+1)^{\frac{1}{2}} C_n^* C_{n+1} a + \\ + \sum_n n^{\frac{1}{2}} C_n^* C_{n-1} a^* \\ a = g \frac{1}{(2\pi\hbar)^{3/2}} \overline{g(p)} \int \sqrt{\frac{\hbar^2 c^2}{2\omega_q}} f(q) dq, \end{aligned} \quad (8)$$

Our method is from here already the usual one, thus in the ground state we obtain

$$W^{(0)} = E - \frac{a a^*}{\varepsilon + \frac{k^2}{2M}}. \quad (9)$$

This also minimizing with respect to  $f$  we obtain the solution for  $f$

$$f(k) = a \frac{1}{\sqrt{\omega_k}} \cdot \frac{1}{\omega_k + \frac{k^2}{2M}}. \quad (10)$$

From here the energy of the field is

$$W^{(0)} = E - \frac{g^2}{2} \overline{g(p)}^2 \frac{\hbar^2 c^2}{(2\pi\hbar)^3} \int \frac{1}{\omega_k \left( \omega_k + \frac{k^2}{2M} \right)} dk. \quad (11)$$

## REFERENCES

1. S. TOMONAGA, Progr. Theor. Phys., **2**, 6, 63, 1947.
2. K. WATSON and F. HART, Phys. Rev., **79**, 918, 1950.
3. P. T. MATTHEWS and A. SALAM, Phys. Rev., **86**, 715, 1952.
4. T. D. LEE and D. PINES, Phys. Rev., **92**, 883, 1953.
5. Z. MAKI, M. SATO and S. TOMONAGA, Progr. Theor. Phys., **9**, 607, 1953.
6. F. H. HARLOW and B. A. JACOBSON, Phys. Rev., **93**, 333, 1954.
7. R. J. RIDELL and B. D. FRIED, Phys. Rev., **94**, 1736, 1954.
8. T. D. LEE and R. CHRISTIAN, Phys. Rev., **94**, 1760, 1954.
9. G. TAKEDA, Phys. Rev., **95**, 1078, 1954.
10. G. HEBER, Ann. d. Phys., (6), **15**, 157, 1955.
11. G. HEBER, Ann. d. Phys., (6), **15**, 174, 1955.
12. G. HEBER, Ann. d. Phys., (6), **16**, 43, 1955.
13. G. HEBER, ZS. f. Naturforsch., **10a**, 103, 1955.
14. M. H. FRIEDMANN and R. CHRISTIAN, Phys. Rev., **100**, 1494, 1955.
15. K. HALLER and M. H. FRIEDMANN, Phys. Rev., **100**, 1501, 1955.
16. H. HASEGAWA, Progr. Theor. Phys., **13**, 47, 1955.
17. D. ITO, Y. MIYAMOTO and Y. WATANABE, Progr. Theor. Phys., **13**, 594, 1955.
18. Y. WATANABE, Progr. Theor. Phys., **13**, 603, 1955.
19. Y. NOGAMI and H. HASEGAWA, Progr. Theor. Phys., **15**, 137, 1956.
20. G. HEBER, Ann. d. Phys., (6), **17**, 102, 1956.



21. G. HEBER, *ZS. f. Phys.*, **144**, 39, 1956.
22. F. J. DYSON, *Phys. Rev.*, **73**, 929, 1948.
23. L. L. FOLDY, *Phys. Rev.*, **84**, 168, 1951.
24. K. A. BRUECKNER and K. M. WATSON, *Phys. Rev.*, **92**, 1023, 1953.
25. A. BETHE, F. DE HOFFMANN and S. S. SCHWEBER, *Mesons and Fields I—II*. Row Peterson and Co., New-York, 1955.
26. R. ARNOWITZ and S. DESER, *Phys. Rev.*, **100**, 349, 1955.
27. H. S. GREEN, *Nuclear Physics*, **1**, 360, 1956.
28. M. JEAN, *Ann. Phys.*, **8**, 338, 1953.
29. A. S. WIGHTMANN and S. S. SCHWEBER, *Phys. Rev.*, **98**, 812, 1955.
30. H. J. ВНАВНА, *Proc. Roy. Soc. A.*, **219**, 293, 1953.
31. G. SZAMOSI and G. MARX, *Acta Phys. Hung.*, **4**, 219, 1954.
32. M. A. ZIEGLER and G. SZAMOSI, *Acta Phys. Hung.*, **6**, 67, 1956.
33. R. G. SACHS, *Phys. Rev.*, **87**, 1100, 1952.

## МЕТОД СРЕДНЕЙ СВЯЗИ ТОМОНАГА, ПРИ ИСПОЛЬЗОВАНИИ КОНФИГУРАЦИОННО-ПРОСТРАНСТВЕННЫХ МЕТОДОВ

К. Л. НАДЬ

### Резюме

Определяются векторы состояния, характеризующие реальные нуклоны, методом средней связи, используя методы конфигурационного пространства в квантовой теории полей. Рассматривается взаимодействие между нуклонным полем, описываемым уравнением Дирака, и скалярным или псевдоскалярным мезонным полем. Образование пар пренебрегается. В рамках конфигурационного метода учитывается и отдача нуклонов. С помощью вектора состояния определяются средние значения некоторых физических величин в состоянии реального нуклона. Из-за конфигурационного метода, — особенно при расчете локальных физических величин — получается очень наглядная картина реального нуклона.

# PRODUCTION OF HEAVY UNSTABLE PARTICLES IN EXTREMELY ENERGETIC NUCLEON-NUCLEON COLLISIONS

By

G. DOMOKOS

CENTRAL RESEARCH INSTITUTE FOR PHYSICS, DEPARTMENT OF COSMIC RAYS, BUDAPEST

(Presented by L. Jánossy. — Received: V. 24. 1957)

The problem of multiple production of heavy unstable particles is analyzed. Possible reaction schemes are established on the basis of Gell-Mann's theory. In order to apply the Fermi-Landau thermodynamical model to the production of heavy unstable particles, their interaction with pions is investigated. Some characteristic quantities of the two-proton system are calculated by making use of the aforesaid model. The results seem not to contradict experimental results.

## 1. Introduction

In recent years several publications have been appearing on the production of heavy unstable particles in extremely energetic nuclear collisions. Although the statistics of experimental data is rather poor, and there are already some theoretical papers on the subject<sup>1</sup> we hope it may not be superfluous to carry out some investigations concerning the production mechanism of these particles.

Choosing a simple model, we shall deal with central, totally inelastic collisions of two nucleons at very high energies. (For the justification of this model, see the work of FEINBERG and CHERNAVSKI [1]). We assume further, that the nucleon has a pionic proper field, the linear dimensions of which are  $\sim 1/\mu$  ( $\mu$  stands for the mass of pions; in the course of the present paper we put  $\hbar = c = 1$ ) and similarly a K-mesonic proper field with linear dimensions  $\sim 1/m$  ( $m$  = mass of K-mesons). During a collision the two nucleons are assumed to form an intermediate state with highly excited proper fields. The latter ones give up their energy by emission of several quanta of the pionic, nucleonic and K-mesonic fields respectively. If the lifetime of the "intermediate state" is sufficiently long, we are allowed to assume that in the proper fields a statistical equilibrium exists and we may try to calculate the number of different particles produced by methods of statistical physics. This idea of FERMI [2]<sup>2</sup> was modified by LANDAU [3], [4], who states that during the first

<sup>1</sup> We mention only the early work of HABER-SCHAIM, YEIVIN and YEKUTIELI, Phys. Rev., **94**, 184 (1954) applying Fermi's theory and BELENKI's papers, quoted in ref [4].

<sup>2</sup> In FERMI's and LANDAU's papers only the pionic proper field of the nucleon is dealt with. The above-mentioned model seems to be a natural extension of the former. We do not introduce, however, hyperonic proper fields; we shall regard for sake of simplicity hyperons as "composite particles" — e. g. according to the model of GYÖRGYI [5]. This assumption does not affect seriously our later considerations.

stage of its decay, the intermediate state consists of a continuously varying-number of particles, since, because of strong interactions the number of particles is not a "good quantum number". Only at a later stage, when the particles have got out of the influence of each other, may we speak of a fixed number of particles and apply formulae of statistical mechanics. LANDAU defines a "critical temperature" of the system at which we can consider the particles as free.

According to LANDAU's calculations, the latter temperature for pions and nucleons is given by

$$T_c^{(\pi)} = a \cdot \mu$$

in energy-units, where  $a$  is a numerical factor near to unity.

Now the following problems arise :

a) Do multiple processes play a role in the production of  $K$ -mesons and hyperons, and if so, which are the reaction equations.

b) If we want to describe the production of the heavy unstable particles by means of the Fermi-Landau model, what is the critical temperature for the latter.

In connection with a) we remark, that if multiple production of heavy unstable particles takes place at all, then conservation laws allow the following reactions :

$$N + N \rightarrow \left\{ \begin{array}{l} N + N \\ \Lambda + N + K \\ \Sigma + N + K \\ \Xi + N + 2K \\ \Xi + \Lambda + 3K \\ \Lambda + \Sigma + 2K \\ \Xi + \Sigma + 3K \\ 2\Lambda + 2K \\ 2\Sigma + 2K \\ 2\Xi + 4K \end{array} \right. + \left\{ \begin{array}{l} \dots K + \bar{K} \\ \dots N + \bar{N} \\ \dots \Lambda + \bar{\Lambda} \\ \dots \end{array} \right. + \left\{ \begin{array}{l} \dots \Xi + \bar{N} + 2K \\ \dots \Xi + \bar{\Lambda} + K \\ \dots \Xi + \bar{Z} + K + \dots \pi \\ (+ \text{ch. conj.}) \end{array} \right.$$

Concerning problem b) we expect that either the interaction of  $\kappa$ -mesons and hyperons with pions and nucleons is weak in relation to that of pions and nucleons or it is nearly of the same strength. In the first case the critical temperature would be  $T_c^{(K)} \sim m$ , while in the second one we expect that

$$T_c^{(K)} \sim T_c^{(\pi)}$$

In sections 2 and 3 in order to answer problem b) we deal with the  $\pi, \pi$ ) and  $(\kappa, \pi)$  interaction ; while in the fourth and fifth sections we calculate

different observable quantities on the basis of the Fermi-Landau-model and try to compare them with experimental results.

## 2. The $(\pi, \pi)$ interaction

The  $(\pi, \pi)$  interaction seems to be an experimentally observable fact. Although we have no direct experiment yet, the analysis of the reactions [6]

$$\pi + N \rightarrow \pi + \pi + N \quad (2,1)$$

carried out by ITO and MINAMI [7] gives indirect evidence for the existence of such an interaction.

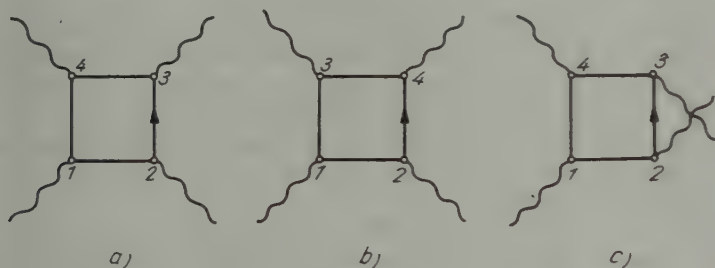


Fig. 1

From a theoretical point of view, this interaction is similar to the photon-photon scattering, *scil.*, it also is a vacuum effect and is described by the same types of Feynman-diagrams. Photon-photon scattering has been investigated theoretically in detail by KARPLUS and NEUMANN [8], [9]. We want to give here a rough estimation of the  $(\pi, \pi)$ -cross section for high energies, using  $ps(ps)$  meson theory and lowest order perturbation approximation. We neglect isobaric variables, and consider a neutral pion field only. In such a rough calculation this simplification seems to be justified. The basic interaction diagrams, describing the process are given in Fig. 1.

To each of these diagrams corresponds another, equivalent one, with the nucleon loop in the opposite direction.

In order to estimate the behavior of the cross section, we shall calculate the S-matrix element corresponding to diagram a) only, since interference terms will not affect seriously the order of magnitude.

In the center-of-mass system and momentum representation we obtain apart from numerical factors

$$S^{(4)} = G^4 \frac{\delta \left( \sum_{i=1}^4 k_i \right)}{\omega^2} \int d^4 p \, Sp \left\{ \gamma_5 \frac{i \gamma p - M}{p^2 + M^2} \gamma_5 \frac{i \gamma (p - k) - M}{(p - k)^2 + M^2} \cdot \right. \\ \left. \cdot \gamma_5 \frac{i \gamma (p - k_2 - k_3) - M}{(p - k_2 - k_3)^2 + M^2} \cdot \gamma_5 \frac{i \gamma (p + k_1) - M}{(p + k_1)^2 + M^2} \right\},$$

where  $M$  stands for the nucleon mass,  $k_i$  is the momentum four-vector of the  $i$ -th pion (choosing the signs in such a way as if all the pions were outgoing ones)  $G$  is the dimensionless coupling constant between the pion and nucleon field;  $\gamma p \equiv p_\mu \gamma^\mu$  and  $\omega^2 = k^2 + \mu^2$ . We perform the integration in (2, 1) using FEYNMAN's method [10]. Having carried through the transformations, quoted above, we find, that there is occurring a logarithmically divergent integral, namely

$$\int \frac{(p^2)^2 d^4 p}{(p^2 + a^2)^4}. \quad (2,2)$$

(After having taken the trace, we can neglect odd powers of  $p$  since they give zero in a symmetrical integration over the angles in the  $p$ -space; cf. FEYNMAN, *loc. cit.* or JAUCH's and ROHRICH's Quantum Electrodynamics [11].) We separate now the physically meaningless divergence in a well-known manner.

Using the identity

$$\frac{1}{a^n} - \frac{1}{\beta^n} = - \int_0^1 \frac{n(a - \beta) dz}{[(a - \beta)z + \beta]^{n+1}} \quad (2,3)$$

we find

$$\int \frac{(p^2)^2 d^4 p}{(p^2 + a^2)^4} = \int \frac{(p^2)^2 d^4 p}{(p^2 + M^2)^4} - 4 \int_0^1 du \int d^4 p \frac{(a^2 - M^2)(p^2)^2}{[p^2 + M^2 \cdot u + a^2(1 - u)]^5} \quad (2,4)$$

The second integral on the right side is already convergent. The first one is divergent, but can be removed *e. g.* by the formalistic regularization method of PAULI and VILLARS [12]. We have chosen the latter method for sake of simplicity; we do not attribute to it any physical interpretation, but regard it as an invariant cut-off procedure only.

Calculation from here on runs along the same lines as the one by KARPLUS and NEUMANN, *loc. cit.* We calculate the asymptotic expression for high energies of the forward-scattering amplitude. The total cross section is then obtained making use of the well known "optical theorem":

$$\sigma(\omega) = \frac{4\pi}{\omega} \operatorname{Im}(a(\omega)), \quad (2,5)$$

where  $a(\omega)$  is the forward-scattering amplitude.



The calculation yields, apart from some numerical factors

$$\sigma_{\pi\pi}(\omega) \sim \frac{G^4}{M^2} \frac{M^2}{\omega^2} \left( \ln \frac{\omega}{M} \right)^2 \quad (2,6)$$

The form of this expression agrees with that of the cross section for high-energy light quanta, and was obtained first by ACHESER (see KARPLUS, NEUMANN, *loc. cit.*)

### 3. The $(K, \pi)$ interaction

We turn now to the investigation of the interaction between  $K$ -mesons and pions, assuming an "elementary" interaction between  $(K, N)$  and  $(\pi, N)$  fields only.

We neglect again isobaric variables, and treat a scalar  $K$ -meson field with scalar coupling. The interaction-operator between the  $K$ -meson and nucleon field then will be of the form

$$W = g/m (\bar{\psi} \psi) (\bar{x} x), \quad (3,1)$$

where  $\psi$  is the field operator of the nucleon and  $x$  that of the  $K$ -meson field,  $g$  is the dimensionless interaction constant. Both  $\psi$  and  $x$  are isospinors of the first kind.<sup>1</sup>

The basic graph in lowest, non-vanishing order for an interaction is shown in Fig. 2. The corresponding  $S$  matrix element, — again apart from numerical factors — reads :

$$s \sim \frac{\delta(\Sigma p_i) G_g^2}{\sqrt{\omega_1 \omega_2 \omega_3 \omega_4}} \cdot \frac{1}{4m} \int Sp \gamma_5 \frac{i\gamma(k+p_4) - M}{(k+p_4)^2 + M^2} \gamma_5 \frac{i\gamma(k+p_4-p_1) - M}{(k+p_4-p_1)^2 + M^2} \cdot \frac{i\gamma k - M}{k^2 + M^2} d^4 k \quad (3,2)$$

Taking the trace under the integral, one can transform the denominator according to the standard method, indicated in the preceding section, and separate a logarithmically divergent term

$$\int \frac{k^2 d^4 k}{(k^2 + M^2)^3}$$

which can be removed by the Pauli-VILLARS regularization procedure.

All further calculations are carried out in the same manner, as has been shown in the preceding section. They give for the high-energy limit of the  $(K \pi)$  cross section :

<sup>1</sup>. An interaction Lagrangian of this form has been proposed by GYÖRGYI, *loc. cit.*

$$\sigma_{K\pi} \sim G^2 g \frac{M}{m} \frac{1}{\omega^2}. \quad (3,3)$$

Compared with the  $(\pi\pi)$  cross section, and taking some reasonable value for the coupling constants [17], we see, that  $\sigma_{K\pi}$  is comparable with  $\sigma_{\pi\pi}$  within a factor of the order of unity. (In this comparison we have taken into account some numerical factors, not written down explicitly in (2, 6) and (3, 31).

The consequence of this for the following thermodynamical calculation is, that the critical temperature for  $K$ -mesons will be nearly the same as for pions. Since the critical temperature varies rather slowly with the cross section [4], we shall choose both temperatures for sake of simplicity, exactly equal.



Fig. 2

We want to call attention once again to the very rough character of our calculations: we have used the high-energy limit of the cross sections, calculated by perturbation theory in the case of moderate energies and rather strongly coupled fields. Indeed, there are some indications [13], that  $(\pi\pi)$  cross section may have a different energy dependence than obtained by us. We hope, however, that the *ratio* of these cross sections is of the correct order of magnitude, and the qualitative conclusions drawn from the calculation are not false.

#### 4. Thermodynamical model of particle production

According to the programme outlined in sec. 1 we are going to calculate some observable quantities of the two-nucleon system, on the basis of the Fermi-Landau-model. We shall follow — as far as possible — the notations of [4].

From secs. 2 and 3 we conclude that at high energies — where thermodynamical approximation has any meaning at all —  $K$ -mesons and — possibly — hyperons interact strongly with pion and nucleon fields. Therefore, we choose in the Fermi-Landau-model

$$T_c^{(\pi)} = T_c^{(K)} = \mu. \quad (4,1)$$

(The value of the constant factor before  $\mu$  is obtained by means of a graphical estimation, based on the results of [4]).

The density of particles of type  $i$  is given by

$$n_i = w_i \int_0^{\infty} \frac{4\pi p^2 dp / (2\pi)^3}{\exp(\sqrt{p^2 + m_i^2}/T_c) \mp 1}, \quad (4,2)$$

where  $w_i$  is a weight factor arising from summations over spin, isobaric spin etc.  $m_i$  is the mass of the particle; the sign in the denominator depends on the statistics followed by the particle.

The latter formula can be written in the more convenient form

$$n_i = w_i / 2\pi^2 T_c^3 F^{\mp}(\xi_i),$$

$$\xi_i = m_i/T_c; \quad F^{\mp}(z) = z^3 \int_0^{\infty} \frac{x^2 dx}{\exp(z\sqrt{1+x^2}) \mp 1}. \quad (4,3)$$

( $F^{\mp}(z)$  and similar functions are tabulated in reference [4].) Conservation laws can be taken into account by means of the multiplier method. If there is one integral of motion, then  $F^{\mp}(z)$  should be replaced by

$$F^{\mp}(z, y) = z^3 \int_0^{\infty} \frac{x^2 dx}{\exp(z\sqrt{1+x^2-y}) \mp 1}, \quad (4,4)$$

where  $y$  is the corresponding multiplier. (5, 4) can be generalized for the case of several integrals of motion in a straightforward manner. For small values of  $y$

$$F^{\mp}(\xi, y) \approx e^y F^{\mp}(\xi). \quad (4,4a)$$

The multipliers can be determined from the equations expressing the conservation of the quantity in question. These can be written in the following form. If  $i, j$  are two kinds of particles, and the numbers of particles are denoted by capital letters, so, if  $T_c^{(i)} = T_c^{(j)}$ , then  $N_i/N_j = n_i/n_j$ .

Further, if the conserved quantity is  $\omega$ , its value for particle  $i$  is  $\omega_i$ , then the conservation equation reads

$$\omega_{N_1} + \omega_{N_2}/N_i = \sum_k n_k \omega_k / n_i. \quad (4,5)$$

( $N_1, N_2$  stands for the two colliding nucleons.)

We consider as an example the collision of two protons. Denote by  $y, z, u$  the multipliers, corresponding to  $N, T_3, U$  respectively. (It can be shown, that the neglect of the conservation of  $T$  introduces a very small error.)

Regarding the  $N$ ,  $T_3$ ,  $U$ -values of the different particles and (4, 4a), the conservation-equations are found to be,

$$(N) : n_{\pi_0}/N_{\pi_0} = n_N^0 \operatorname{sh}(y+z+u) + n_N^0 \operatorname{sh}(y-z+u) + n_A^0 \operatorname{sh} y + \\ + n_{\Sigma}^0 \operatorname{sh}(y+z-u) + n_{\Sigma}^0 \operatorname{sh}(y-z-u) + n_{\Sigma}^0 \operatorname{sh}(y+2z) + \\ + n_{\Sigma}^0 \operatorname{sh} y + n_{\Sigma}^0 \operatorname{sh}(y-2z);$$

$$(2T_3) : n_{\pi_0}/N_{\pi_0} = n_N^0 \operatorname{sh}(y+z+u) - n_N^0 \operatorname{sh}(y-z+u) + n_K^0 \operatorname{sh}(z-u) + \\ + n_K^0 \operatorname{sh}(z+u) + n_{\Sigma}^0 \operatorname{sh}(y+z-u) - n_{\Sigma}^0 \operatorname{sh}(y-z-u) + \\ + 2n_{\pi}^0 \operatorname{sh} 2z + 2n_{\Sigma}^0 \operatorname{sh}(y+2z) - 2n_{\Sigma}^0 \operatorname{sh}(y-2z);$$

$$(u) : n_{\pi_0}/N_{\pi_0} = n_N^0 \operatorname{sh}(y+z+u) + n_N^0 \operatorname{sh}(y-z+u) + \\ + n_K^0 \operatorname{sh}(z+u) - n_K^0 \operatorname{sh}(z-u) - n_{\Sigma}^0 \operatorname{sh}(y+z-u) - \\ - n_{\Sigma}^0 \operatorname{sh}(y-z-u).$$

Here we have chosen neutral pions as "reference-particles" and  $n_i^0 = w_i/2\pi^2 \cdot T^3 F^\mp(\xi_i)$ .

The approximate roots of the system (4, 6) are :<sup>1</sup>

$$y = 7,667/N_{\pi_0}, \quad z = 0,2131/N_{\pi_0}, \quad u = 0,8407/N_{\pi_0}.$$

We see, that for very high energies, as a rough estimation, we may put :

$$n_i \approx n_i^0. \quad (4,7)$$

As another important quantity, the average energy which is carried away by a definite kind of particles is calculated. The energy-density is given by

$$\varepsilon_i = T^4 w_i/2\pi^2 \Phi^\mp(\xi_i),$$

$$\Phi^\mp(\xi_i) = \xi_i^3 \int_0^\infty \frac{x^2 \sqrt{1+x^2} dx}{\exp(\xi_i \sqrt{1+x^2}) \mp 1} \quad (4,8)$$

and a corresponding function, if some conservation laws are taken into account. Similarly, as in (4, 4a) and (4, 7), we may put

$$\Phi^\mp(z, y) \approx e^y \Phi^\mp(z). \quad (4,9)$$

The result of the calculation, outlined here, without making use of the approximations (4, 7), (4, 9), is plotted in Table I. Columns 2—3 give the density, resp.

<sup>1</sup> The relative error of the approximation decreases with energy as  $(N_{\pi_0})^2$ . Since the most important role is played by the conservation of  $N$ , our further considerations apply — at least qualitatively — to  $(N, P)$  and  $(P, P)$  collisions as well.

energy density of the particle, indicated in column 1, divided by a common factor. Column 4 gives the average energy of one particle in the c. m. system, according to the approximate expression  $\langle E \text{ c. m.} \rangle \approx \varepsilon/n$ . Column 5 gives the fraction of the total available energy, carried away by the particles in question; while the last column gives the relative number of emitted particles. In columns 5 and 6 the approximation (4, 7) and the similarity  $\varepsilon_i \sim \varepsilon_i^0$  is used.

Table I

1	2	3	4	5	6
Particle	$n (T^{3/2} \pi^2)^{-1}$	$\varepsilon (T^{3/2} \pi^2)^{-1} *$	$\langle E \text{ c. m.} \rangle$ [Be V]	$\varepsilon/\sum_j \varepsilon_j **$	$n/\sum_j n_j$
$\pi^0$ $\pi^+$ $\pi^-$	$\left. \begin{array}{l} 1 \\ \exp (0,462/N_{\pi^0}) \\ \exp (-0,462/N_{\pi^0}) \end{array} \right\} \cdot 1,78$	$\left. \begin{array}{l} \\ \\ \end{array} \right\} \cdot 5,90$	1,12	0,23	0,19
$K^0$ $\bar{K}^0$ $\bar{K}^+$ $K^-$	$\left. \begin{array}{l} \exp (0,628/N_{\pi^0}) \\ \exp (-0,628/N_{\pi^0}) \\ \exp (1,054/N_{\pi^0}) \\ \exp (-1,054/N_{\pi^0}) \end{array} \right\} \cdot 0,478$	$\left. \begin{array}{l} \\ \\ \\ \end{array} \right\} \cdot 2,39$	1,71	0,062	0,078
$N^0$ $\bar{N}^0$ $P^+$ $\bar{P}^-$	$\left. \begin{array}{l} \exp (8,29/N_{\pi^0}) \\ \exp (-8,29/N_{\pi^0}) \\ \exp (8,72/N_{\pi^0}) \\ \exp (-8,72/N_{\pi^0}) \end{array} \right\} \cdot 0,0714$	$\left. \begin{array}{l} \\ \\ \\ \end{array} \right\} \cdot 0,606$	2,88	0,009	0,020
$\Lambda^0$ $\bar{\Lambda}^0$	$\left. \begin{array}{l} \exp (7,67/N_{\pi^0}) \\ \exp (-7,67/N_{\pi^0}) \end{array} \right\} \cdot 0,023$	$\left. \begin{array}{l} \\ \end{array} \right\} \cdot 0,23$	3,34	0,003	0,074
$\Sigma^+$ $\Sigma^0$ $\Sigma^-$ $\bar{\Sigma}^+$ $\bar{\Sigma}^0$ $\bar{\Sigma}^-$	$\left. \begin{array}{l} \exp (8,09/N_{\pi^0}) \\ \exp (7,67/N_{\pi^0}) \\ \exp (7,24/N_{\pi^0}) \\ \exp (-7,24/N_{\pi^0}) \\ \exp (-7,67/N_{\pi^0}) \\ \exp (-8,09/N_{\pi^0}) \end{array} \right\} \cdot 0,015$	$\left. \begin{array}{l} \\ \\ \\ \\ \\ \end{array} \right\} \cdot 0,15$	3,40	0,002	0,0048
$\Xi^0$ $\Xi^0$ $\Xi^-$ $\Xi^+$	$\left. \begin{array}{l} \exp (7,04/N_{\pi^0}) \\ \exp (-7,04/N_{\pi^0}) \\ \exp (6,61/N_{\pi^0}) \\ \exp (-6,61/N_{\pi^0}) \end{array} \right\} \cdot 0,007$	$\left. \begin{array}{l} \\ \\ \\ \end{array} \right\} \cdot 0,076$	3,69	0,0009	0,0024

\* The figures of column 3 have to be multiplied by the same exponential factor as the corresponding figures in column 2.

\*\* Columns 5 and 6 are calculated in the high-energy limit:  $N_{\pi^0} \sim \infty$

The number of a definite kind of particles is obtained by multiplying its density with the interaction volume.

The latter is expressed by  $N_i / \sum_j n_j$ , where  $N_i$  is the total number of emitted particles. Thermodynamical calculations show (cf. [2] [4]), that,  $N_i$  is proportional to the fourth root of the primary energy in the  $L$ -system :

$$N_i \approx 2 (E_p/M)^{1/4}.$$

So the average number of particle  $i$  becomes

$$N_i \approx 2n_i / \sum_j n_j (E_p/M)^{1/4} \quad (4,10)$$

and in particular

$$N_{\pi^0} \approx 0,38 (E_p/M)^{1/4}. \quad (4,11)$$

Consider an example. Let be,  $E_p = 10^5$  BeV, then our calculations give the results  $N_i \approx 35$ ; we quote the average numbers of some "interesting" particles :

$$N_{K^0} = 2,3; \quad N_{\bar{K}}^0 = 1,9; \quad N_{K^+} = 2,4; \quad N_{\bar{K}^-} = 1,7; \quad N_{\Lambda^0} = 0,31; \\ N_{\Sigma^+} \approx N_{\Sigma^0} \approx N_{\Sigma^-} \approx 0,2; \quad N_{\Xi^0} \approx N_{\Xi^-} \approx 0,07.$$

(The latter figure indicates, that the correction to the counted number of neutral pions due to the  $\gamma$ -decay of  $\Xi^0$ -cf. BRISBOUT et al.'s work, quoted later — is very small.) One observes further that the number nucleon-antinucleon pairs is rather *small*.

Similarly, the number of antihyperons is considerably smaller than that of their charge-conjugate pairs.

The fraction of energy, carried away by heavy particles (heavy mesons, nucleons, hyperons) is about 50%.

## 5. Comparison with experimental results

Now we try to compare our results with the experiments; we do not intend to give a full account of experiments and discuss the experimental procedure, but we aim rather at obtaining some information about the power and limitations of our model.

A measurable quantity is the ratio of neutral pions to charged shower particles.

Measurements have been carried out by several authors (of [14]—[19]). Some of their results are summarized in Table II.

We see that the  $R$ -values agree within the — rather large — statistical errors, and further that  $R$  is approximately constant in a large range of pri-



Table II

Ratio  $R$  of neutral pions to charged shower particles in jets

Author	$R = N_{\pi^0}/N_{\pm}$
Daniel et al. [14] .....	0,33 $\pm$ 0,07
Mulvey [15] .....	0,25 $\pm$ 0,1
Naugle et al. [16] .....	0,44 $\pm$ 0,14
Kaplon et al. [17] .....	0,46 $\pm$ 0,09
Lal et al. [18] .....	0,40 $\pm$ 0,08
Brisbout et al. [19] .....	0,383 $\pm$ 0,044
Weighted average .....	0,375 $\pm$ 0,029

mary energy ( $50 \leq E_p \leq 3000$  BeV/nucleon). The possible variation of  $R$  is obscured by statistical uncertainties.

From  $R$  we obtain the ratio of the non-pionic charged shower particles to charged pions, if we assume that  $N_{\pi^0}/N_{\pi^{\pm}} = 0,5$ , which is a very good approximation.

The above-mentioned ratio from the weighted average of Table II is

$$\bar{f} = \left( \frac{N_s - N_{\pi^{\pm}}}{N_{\pi^{\pm}}} \right) = 0,33 \pm 0,10.$$

Our calculated result is (summing over charged particles, which are not pions)

$$f_{th} = 0,33.^1$$

Concerning the ratio of charged to neutral heavy unstable particles, we quote the works of LEIGHTON and TRILLING [20] and of GIACCONI et al. [21], who have carried out measurements with cloud chamber and *lead* absorber. According to their measurements this ratio is approximately

$$\frac{N_u^+}{N_u^0} = 0,21 \pm 0,03,$$

while Table I yields

$$\frac{N_u^+}{N_u^0} = 0,9$$

in significant contradiction with the experimental result. We mention, however, that the quoted measurements were carried out with Pb target nuclei, so, the possibility of explaining the discrepancy between theory and experiment by secondary effects, does not seem excluded.

<sup>1</sup> Our model predicts a variation for  $f$  of about 10% in the energy-range  $50 \text{ BeV} < E_p < \infty$ ; this — if it really exists — is completely obscured by uncertainties of present experiments.

## 9. Discussion and conclusion

We want to stress once again the main assumptions, made in this paper :

a) To consider collisions to be central collisions only.  
 b) To regard interaction between heavy unstable particles and pions resp. nucleons as strong.

c) To consider it possible to apply thermodynamic calculations. We believe, that the validity of hypothesis a) is rather doubtful, but as long as a correct field theory is not constructed, we cannot consider non-central collisions.

Hypothesis c) is partly dependent on b) ; we do not want to discuss its validity in detail, but refer the reader to the works of FERMI and the LANDAU-school, already-quoted.

Looking at Table I and (4, 10), one observes, that the multiplicity of heavy unstable particles is not too high ; therefore, the application of thermodynamics may be a very rough approximation.

Bearing the aforesaid comments in mind, it might appear strange, that this model could give an — at least qualitative — agreement with experiment.

We believe this in great part to be due to the uncertainties of the experiments. We only mention here, that even the estimation of the *primary energy* of a jet from the angular distribution is a procedure of rather doubtful accuracy. Further, we do not have sufficient information as to the mass spectrum of shower particles. The above-mentioned experiments give only a ratio of non-pions to pions or similar "composite" ratios.

We try to point out some features of our model, which it will perhaps be possible to test experimentally.

a) The variation of the ratio of the numbers of different particles with primary energy might be investigated. In our model this depends apart from the exponential factor arising from conservation equations — on the variation of interaction cross sections in the "cloud" around the nucleon. (Variation of  $T_c$ ).

b) The fraction of energy, carried away by heavy particles, decreases — although rather slowly — with primary energy. Its variation becomes faster at primary energies of the order of ten or hundred BeV. In this region, however, our model breaks down, and we cannot make quantitative predictions. (In the region of only a few BeV-s, one can easily understand the increase of the big fraction of energy, carried away by nucleons : there the *elastic* part of the cross section becomes large, and the energy is carried away by the *original* nucleons.)

Concerning the problems mentioned in the introduction, we cannot assert definitely, that *multiple* production of heavy unstable particles really does take place, but this uncertainty might be due to the fact, that at energies

available at present, their multiplicity is rather low; so, we might expect, that extension of experiments to the region of still higher energies, will yield a definite answer.

A simple model, assuming excited self-fields around the colliding nucleons is not in qualitative contradiction with present experimental data.<sup>1</sup>

We hope to have the opportunity of returning to some of the problems concerning this subject.

The author has the pleasure to express his thanks to Prof. L. JÁNOSSY, for his valuable critical remarks, to Dr. E. FENYVES, for several interesting discussions on the subject, and to Miss M. GOMBOSI, for having performed numerical computations.

## REFERENCES

1. E. L. FEINBERG and D. S. CHERNAVSKIJ, Доклады А. Н., **91**, 511, 1953.
2. E. FERMI, Prog. Theor. Phys., **5**, 570, 1950.
3. L. D. LANDAU, Изв., А. Н. **17**, 51, 1953.
4. S. Z. BELENKIJ and L. D. LANDAU, У. Ф. Н. **56**, 309, 1955. (the same paper in English: Nuvo Cim. Suppl., **3**, 15, 1956)
5. G. GYÖRCSY, ЖЭТФ, **28**, 152, 1957.
6. L. M. EISBERG, W. B. FOWLER, R. M. LEA, W. D. SHEPHARD, R. P. SHUTT, A. M. THORNDIKE and W. L. WHITTEMORE, Phys. Rev., **97**, 797, 1955.
7. D. ITO and S. MINAMI, Prog. Theor. Phys., **14**, 482, 1955.
8. R. KARPLUS and M. NEUMANN, Phys. Rev., **80**, 380, 1950.
9. R. KARPLUS and M. NEUMANN, Phys. Rev., **83**, 776, 1951.
10. R. P. FEYNMAN, Phys. Rev., **76**, 769, 1949.
11. J. M. JAUCH and F. ROHRICH, The Theory of Photons and Electrons, Addison—Wesley, Cambridge, 1955.
12. W. PAULI and F. VILLARS, Rev. Mod. Phys., **21**, 434, 1949.
13. Z. KOBA, Prog. Theor. Phys., **15**, 461, 1956.
14. R. R. DANIEL, J. H. DAVIES, J. H. MULVEY and D. H. PERKINS Phil. Mag., **43**, 753, 1952.
15. J. H. MULVEY, Proc. Roy. Soc., **221**, 367, 1954.
16. J. E. NAUGLE and P. S. FREIER, Phys. Rev., **92**, 1086, 1953.
17. M. F. KAPLON and D. M. RITSON, Phys. Rev., **88**, 386, 1952.  
M. F. KAPLON, W. D. WALKER and M. KOSHIBA, Phys. Rev., **93**, 1424, 1954.
18. D. LAL, YASH PAL and RAMA, Nuovo Cim. Suppl., **12**, 347, 1954.
19. F. A. BRISBOUT, C. DAHANAYAKE, A. ENGLER, Y. FUJIMOTO and D. H. PERKINS, Phil. Mag., **1**, 605, 1956.
20. LEIGHTON and TRILLING, Proc. 6<sup>th</sup> Rochester Conf. Interscience, New York, 1956.
21. R. GIACCONI, A. LOVATI, A. MURA and C. SUCCI, Nuovo Cim., **4**, 827, 1956.

<sup>1</sup> After this work had been finished, the author got acquainted with a paper, reporting of the multiple emission of heavy unstable particles, from stars in photographic emulsion. (TSAI-CHÜ, MORAND, Phys. Rev., **104**, 1943, 1956). The reported event is not a jet. The authors assume a reaction

$$N + N \rightarrow \Sigma^+ + \Sigma^- + K^- + 3\theta^0 + \pi^+$$

or

$$\pi^- + N \rightarrow \Sigma^+ + \bar{\Sigma}^- + K^- + \theta^0 + N$$

leading to the emission of heavy unstable particles. A further question remains, however namely, whether the quoted events may not be explained by two separate reactions, each of them being a "simple" associated production.

Recently, DEBENEDETTI et al (Nuovo Cim., **4**, 1142, 1956) reported the value of  $R$  (see p. 27) to be  $0.426 \pm 0.06$ , measured on a single event. The author is indebted to Dr. TSAI-CHÜ for information about their event and the Turin-group for having sent him a reprint.

## РОЖДЕНИЕ ТЯЖЕЛЫХ НЕСТАБИЛЬНЫХ ЧАСТИЦ В СОУДАРЕНИЯХ НУКЛЕОНОВ БОЛЬШОЙ ЭНЕРГИИ

Г. ДОМОКОШ

## Резюме

Рассматривается проблема множественного рождения тяжелых нестабильных частиц. Устанавливаются возможные схемы реакций на основе теории Гелл—Манн. Исследуется взаимодействие тяжелых нестабильных частиц с  $\pi$ -мезонами, на основании которого образование тяжелых нестабильных частиц рассматривается применением термодинамической модели Ферми—Ландау. С помощью этой модели вычисляются некоторые характеристические величины системы, состоящей из двух протонов. Результаты повидимому не противоречат данным опытов.

# SHOWER PRODUCTION AT SMALL THICKNESSES OF ABSORBER

By

L. NAGY

CENTRAL RESEARCH INSTITUTE FOR PHYSICS, DEPARTMENT OF COSMIC RAYS, BUDAPEST

(Presented by L. Jánossy. — Received : VI. 20. 1957)

We have investigated the shape of the first part of the Rossi curve in the case of Al, Fe, Cu and Pb absorbers separating showers generated by mesons, electrons and photons

## Introduction

It has been established experimentally by several authors [1—3], that the production cross section of showers, generated by the soft component of the cosmic radiation, is proportional to the second power of the atomic number of the material in which the shower is produced. HU CHIEN SHAN [2] expressed the thickness of an absorber in terms of  $nZ^2$ , where  $n$  means the number of atoms per  $\text{cm}^2$  and  $Z$  is the atomic number of the absorber. He found that the numbers of showers observed with different absorbers, lie in nearly a straight line, when plotted as a function of  $nZ^2$ .

According to the calculations of ARLEY [4], and the experimental investigations of TRUMPY [5] concerning the photon component, however, the Rossi curves for different materials do not coincide but separate at already very small thicknesses.

In ARLEY's opinion, the curves obtained by HU with different materials, may have coincided, because HU did not investigate showers produced by the soft component only, as in his experiment showers were generated by the meson component as well, and this may have made separation of the curves indistinct.

JÁNOSSY [6] has explained the contradiction by the fact, that the calculations of ARLEY and the experiments of TRUMPY relate to *small* showers, while showers, observed with the usual GM-counter arrangement contain many particles.

The above-mentioned contradiction led us to investigate anew the problem sketched above employing an apparatus which was used already in earlier investigations concerning the Rossi curve.

### Experimental arrangement

The geometry used in our first series of measurement is similar to that of HU, i.e. five GM-counters were placed under an absorber in the vertices of a pentagon, the area of the absorber being  $42 \times 120 \text{ cm}^2$ . At least three ionizing particles were necessary in order to make all the five counters to respond. Such showers were registered by a five-fold coincidence arrangement.

The arrangement used in the second series of measurement was — apart from minor modifications — identical with that described in detail in an earlier paper [7], so that we may confine ourselves here to a short description.

The arrangement of absorbers and GM-counters is to be seen in Fig. 1. The simultaneous response of the five counters *B* indicated that in the absorber  $S_1$  above them, a shower had been produced, such that at least one ionizing particle passed through every counter *B*. Coincidences ( $B_1 B_2 B_3 B_4 B_5$ ) were registered by a fivefold coincidence arrangement. Counters *A* placed on the two sides of  $S_1$  and connected in parallel with each other were connected in anticoincidence with the fivefold coincidence arrangement.

Thus the anticoincidence arrangement registered those fivefold coincidences, which were not accompanied by a response of counters *A*, i. e. when no ionizing particles arrived simultaneously with the shower-producing particle, which could have made respond counters *A*. By this arrangement dense air showers could be eliminated [7].

### Results

As absorber  $S_1$ , in both series of experiments, were used aluminium, iron, copper and lead.

The results obtained in the first series of experiments are plotted in Fig. 2. Ordinate values are the numbers of fivefold coincidences per hour, the abscissa gives the thickness of the absorber. The number of fivefold coincidences includes the showers produced by both the soft and hard components. Our result, as can be seen from the Figure, is identical with that of HU: the points obtained at small thicknesses of absorber lie on the same straight line. Further on the curves separate: they lie the higher, the greater the atomic number of the absorber.

The results of the second series of experiments are summarized in the following table.

The significance of the letters at the heads of the columns of the Table is as follows:

$K'$  = fivefold coincidences ( $B_1 B_2 B_3 B_4 B_5$ ), i. e. the sum of the number of showers per hour, produced by the soft and hard component. Here the



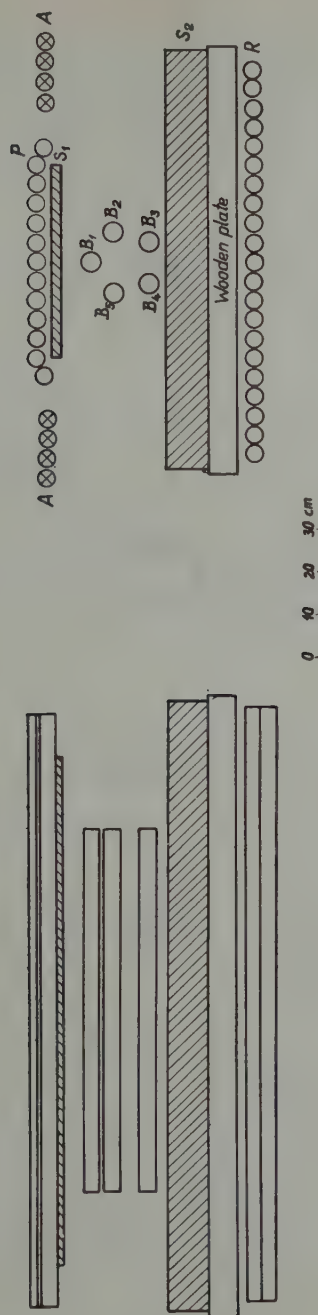


Fig. 1. Geometry of the experimental arrangement in the second series of measurements. In the first series the apparatus consisted of absorber  $S_1$  and counts  $B$  only

same events have been registered, as in the first series, the only difference being, that here the counters  $P$  were placed above the absorber.

$K$  = anticoincidence ( $B_1 B_2 B_3 B_4 B_5 - A$ ), i. e. the number of showers registered without simultaneous response of counters  $A$ .

$I$  = twofold coincidences ( $KP$ ), i. e. the number of showers per hour, produced by ionizing particles.

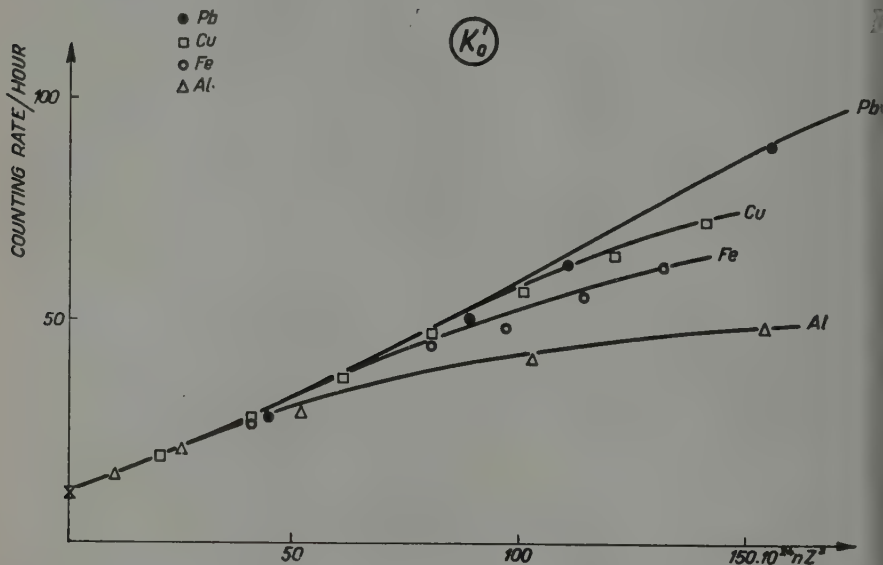


Fig. 2. Curves obtained in the first series of measurement: showers initiated by the soft and hard component.  $Z$  is the atomic number of the absorber,  $n$  the number of atoms per  $\text{cm}^2$

$M$  = twofold coincidences ( $KR$ ), i. e. the number of showers per hour, generated by mesons.

$E$  = difference between  $I$  and  $M$ , i. e. the number of showers per hour, generated by electrons.

$F$  = difference between events  $K$  and  $I$ , i. e. the number of showers per hour, generated by photons.

The numbers of the various events listed in the Table are plotted in Figures 3—8 as function of the absorber thickness in  $nZ^2$ .

One can see from the Figures, that the points, obtained for different absorbers, fall on the same straight line, when the thickness of absorber is small, while the curves separate for greater thicknesses of absorber — except curves  $M$  and  $F$  — and lie the higher, the greater the atomic number of the absorber.

Table I

Ab- sorber	cm	$nZ^2/10^{24}$	Time of measurement (hours)	K'	K	I	M	E	F
Without absorber			109	$19,3 \pm 0,4$	$8,6 \pm 0,3$	$8,4 \pm 0,3$	$1,6 \pm 0,1$	$6,8 \pm 0,2$	$0,2 \pm 0,04$
Al	1,0	10,3	91	$22,5 \pm 0,5$	$11,1 \pm 0,3$	$10,5 \pm 0,3$	$2,0 \pm 0,1$	$8,5 \pm 0,3$	$0,6 \pm 0,1$
	2,5	25,7	90	$25,8 \pm 0,5$	$13,8 \pm 0,4$	$12,9 \pm 0,4$	$2,6 \pm 0,2$	$10,3 \pm 0,3$	$0,9 \pm 0,1$
	5,0	51,3	93	$34,3 \pm 0,6$	$20,0 \pm 0,5$	$17,7 \pm 0,4$	$4,2 \pm 0,2$	$13,4 \pm 0,4$	$2,3 \pm 0,2$
	7,5	77,0	139	$40,7 \pm 0,5$	$25,1 \pm 0,4$	$21,4 \pm 0,4$	$5,4 \pm 0,2$	$16,1 \pm 0,3$	$3,7 \pm 0,2$
	10,0	102,7	90	$43,9 \pm 0,7$	$27,4 \pm 0,6$	$22,5 \pm 0,5$	$5,6 \pm 0,2$	$16,9 \pm 0,4$	$5,0 \pm 0,2$
Fe	0,3	17,2	92	$23,5 \pm 0,5$	$12,0 \pm 0,4$	$11,1 \pm 0,3$	$1,9 \pm 0,1$	$9,2 \pm 0,3$	$0,9 \pm 0,1$
	0,7	40,1	107	$33,7 \pm 0,6$	$18,7 \pm 0,4$	$17,0 \pm 0,4$	$3,3 \pm 0,2$	$13,7 \pm 0,4$	$1,7 \pm 0,1$
	1,0	57,3	107	$39,9 \pm 0,6$	$23,9 \pm 0,5$	$21,5 \pm 0,4$	$3,9 \pm 0,2$	$17,6 \pm 0,4$	$2,4 \pm 0,2$
	1,4	80,2	139	$50,6 \pm 0,6$	$31,2 \pm 0,5$	$28,0 \pm 0,4$	$5,3 \pm 0,2$	$22,7 \pm 0,4$	$3,3 \pm 0,2$
	1,7	97,4	93	$56,9 \pm 0,8$	$36,6 \pm 0,6$	$31,5 \pm 0,6$	$6,2 \pm 0,3$	$25,2 \pm 0,5$	$5,1 \pm 0,2$
	2,0	114,6	155	$62,1 \pm 0,6$	$40,8 \pm 0,5$	$35,0 \pm 0,5$	$6,7 \pm 0,2$	$28,3 \pm 0,4$	$5,8 \pm 0,2$
	2,3	131,8	103	$68,3 \pm 0,8$	$46,1 \pm 0,7$	$38,8 \pm 0,6$	$8,3 \pm 0,3$	$30,5 \pm 0,5$	$7,3 \pm 0,3$
Cu	0,3	20,2	158	$26,4 \pm 0,4$	$13,5 \pm 0,3$	$12,6 \pm 0,3$	$2,3 \pm 0,1$	$10,3 \pm 0,3$	$0,9 \pm 0,1$
	0,6	40,3	111	$36,0 \pm 0,6$	$20,0 \pm 0,4$	$18,3 \pm 0,4$	$3,5 \pm 0,2$	$14,8 \pm 0,4$	$1,8 \pm 0,1$
	0,9	60,5	93	$42,8 \pm 0,7$	$25,8 \pm 0,5$	$22,8 \pm 0,5$	$4,0 \pm 0,2$	$18,8 \pm 0,4$	$3,0 \pm 0,2$
	1,2	80,6	88	$52,8 \pm 0,8$	$34,1 \pm 0,6$	$29,9 \pm 0,6$	$5,5 \pm 0,3$	$24,4 \pm 0,5$	$4,2 \pm 0,2$
	1,5	100,8	87	$59,5 \pm 0,8$	$39,7 \pm 0,7$	$34,8 \pm 0,6$	$6,4 \pm 0,3$	$28,4 \pm 0,6$	$4,9 \pm 0,2$
Pb	1,8	120,9	110	$68,8 \pm 0,8$	$46,5 \pm 0,7$	$39,6 \pm 0,6$	$8,2 \pm 0,3$	$31,4 \pm 0,5$	$6,9 \pm 0,3$
	2,1	141,1	138	$75,7 \pm 0,7$	$52,3 \pm 0,6$	$44,0 \pm 0,6$	$8,8 \pm 0,3$	$35,2 \pm 0,5$	$8,4 \pm 0,2$
	0,1	22,2	109	$29,1 \pm 0,5$	$15,6 \pm 0,4$	$14,5 \pm 0,4$	$2,6 \pm 0,2$	$11,9 \pm 0,3$	$1,2 \pm 0,1$
	0,2	44,3	86	$37,0 \pm 0,7$	$21,8 \pm 0,5$	$20,0 \pm 0,5$	$3,3 \pm 0,2$	$16,7 \pm 0,4$	$1,8 \pm 0,1$
	0,3	66,5	189	$53,4 \pm 0,5$	$33,2 \pm 0,4$	$29,9 \pm 0,4$	$5,0 \pm 0,2$	$24,9 \pm 0,4$	$3,3 \pm 0,1$
	0,4	88,7	132	$60,2 \pm 0,7$	$38,5 \pm 0,5$	$34,3 \pm 0,5$	$5,6 \pm 0,2$	$28,8 \pm 0,5$	$4,2 \pm 0,2$
	0,5	110,8	80	$76,0 \pm 1,0$	$52,6 \pm 0,8$	$45,5 \pm 0,8$	$7,7 \pm 0,3$	$37,8 \pm 0,7$	$7,1 \pm 0,3$
	0,7	155,2	61	$99,7 \pm 1,3$	$68,1 \pm 1,1$	$58,3 \pm 1,0$	$9,4 \pm 0,4$	$48,9 \pm 0,9$	$9,8 \pm 0,4$

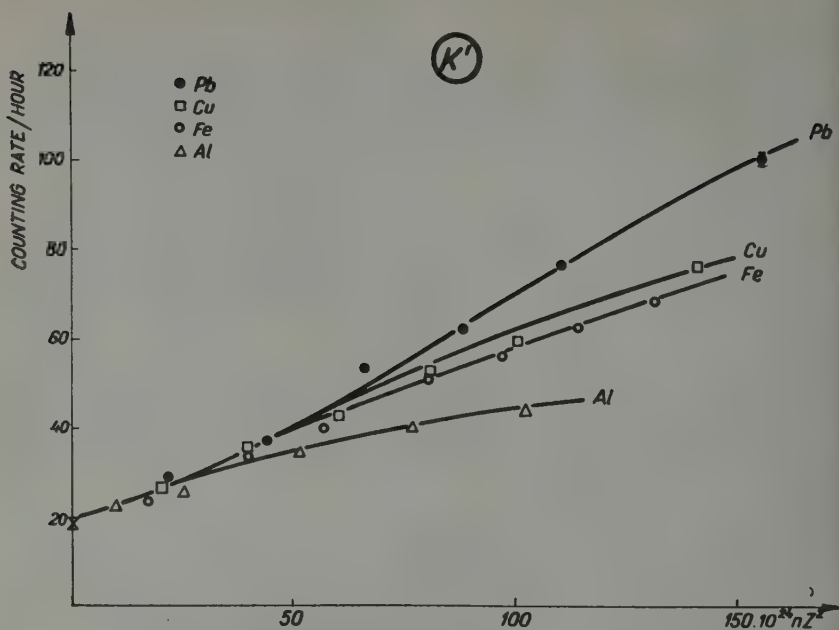


Fig. 3. The number of showers, generated by the soft and hard component obtained in the second series of measurement

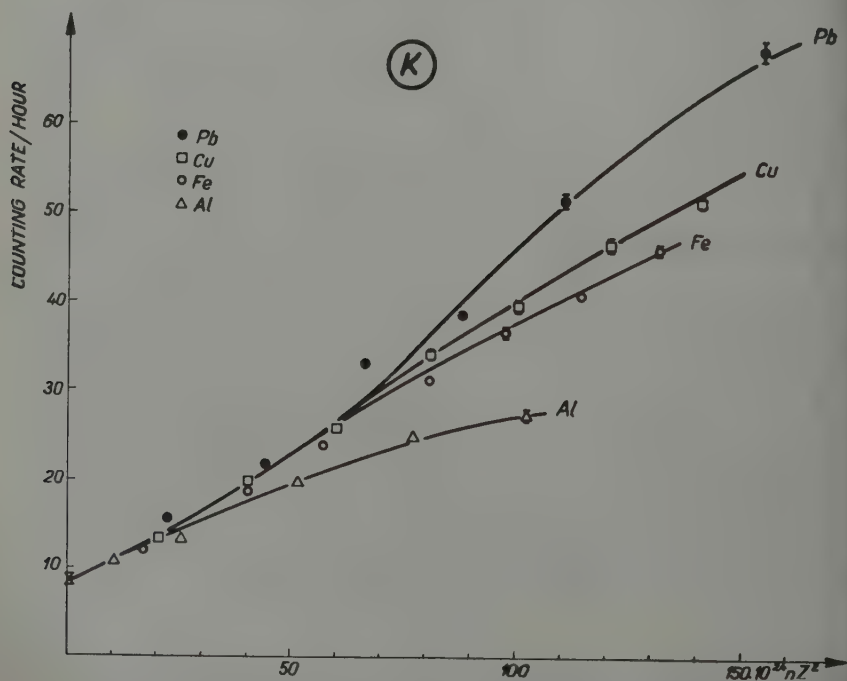


Fig. 4. Number of showers, generated by soft or hard primary. The primary falling onto the absorber is not connected with a dense air shower

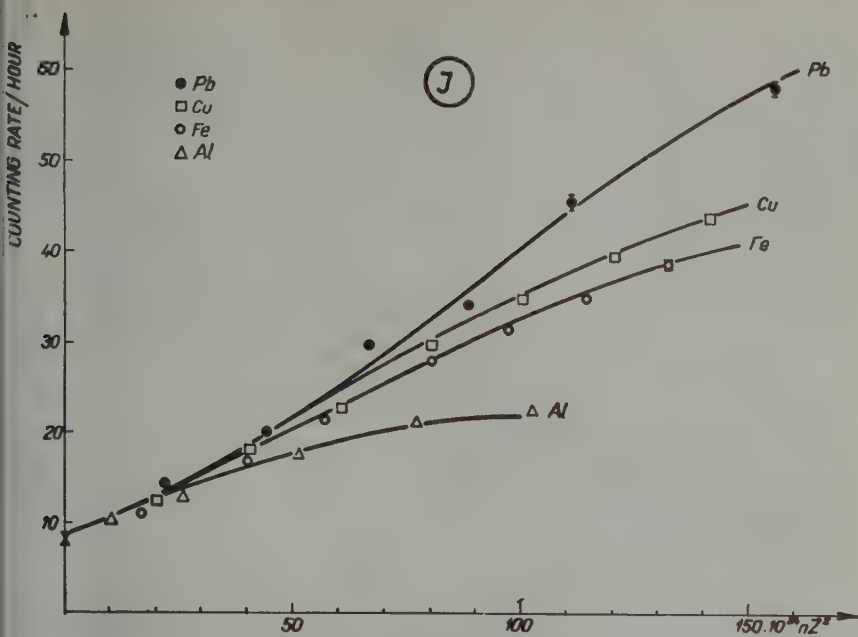


Fig. 5. Number of showers generated by ionizing particles

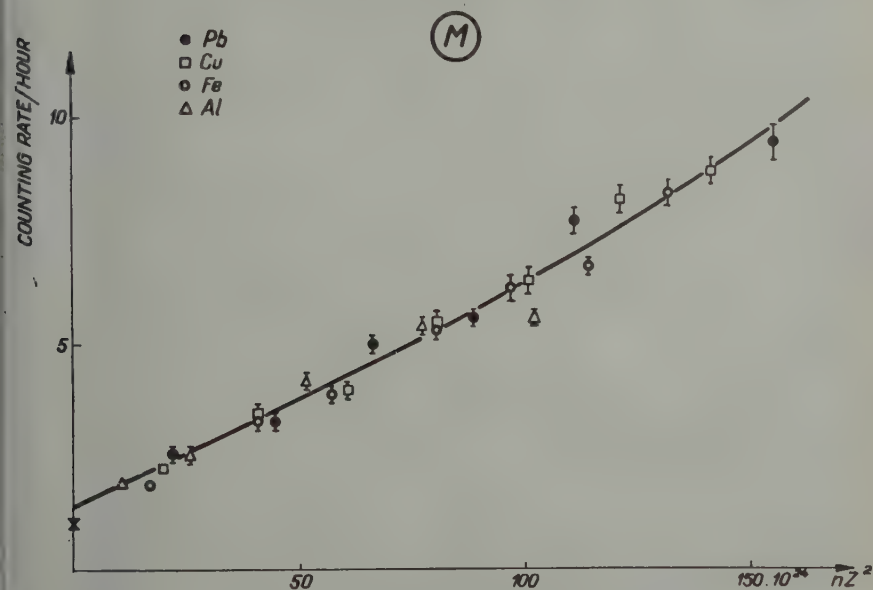


Fig. 6. Number of showers generated by mesons

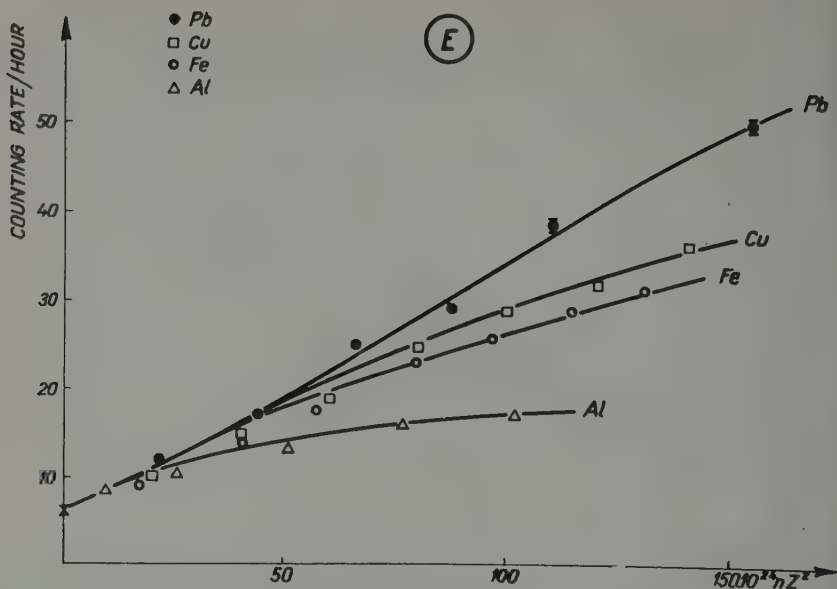


Fig. 7. Number of showers generated by electrons

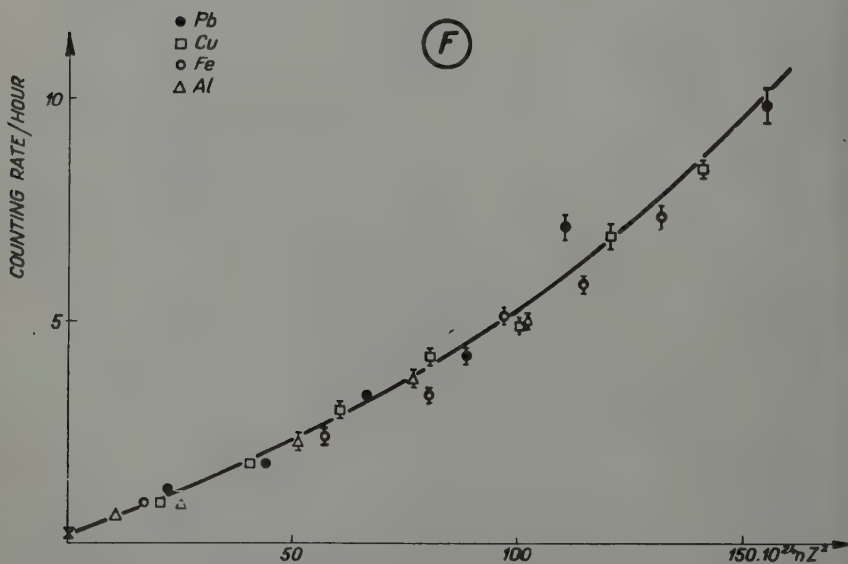


Fig. 8. Number of showers generated by photons



This result renders it probable, that ARLEY's calculations are valid at most for small showers.

We note in particular that the counting rates of showers initiated by mesons lie for the various absorbers on one curve (Fig. 6). The definite proportionality to  $Z^2$  is demonstrated in this case by Fig. 9, where absorber thicknesses are plotted in  $nZ^{3/2}$  units, instead of  $nZ^2$ ; the curves separate already at small thicknesses, and the separation is significant.

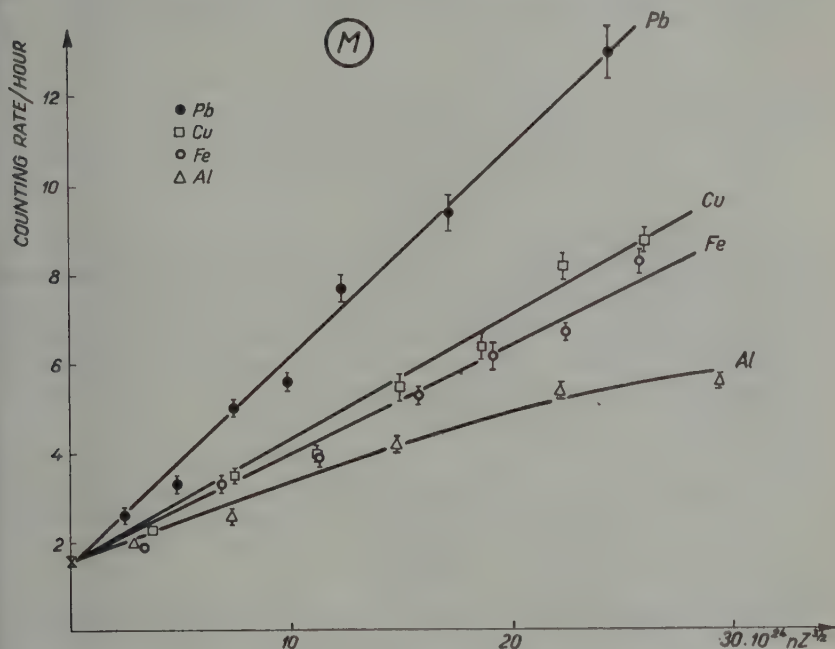


Fig. 9. Number of showers generated by mesons. The thickness of the absorber is expressed as a function of  $nZ^{3/2}$

### Control of the apparatus

In the second series of measurements a great number of GM counters and electron tubes were used and thus continuous control of the apparatus was of particular importance.

Two of the checking methods may be briefly described.

Into the electronic units of counters  $P$  and  $R$  were fed the signals of two counters  $B$  (e. g.  $B_1$  and  $B_2$ ) instead of their own pulses. If, at the same

time the voltage of counters  $A$  is under operating voltage then all the output stages ought to count the same rates in this case namely, together with every coincidence pulse ( $B_1 B_2 B_3 B_4 B_5$ ), the twofold mixers belonging to counters  $P$  and  $R$  receive a pulse from counters  $B_1$  and  $B_2$  resp. and because of the non-operation of counters  $A$ , as well from the anticoincidence arrangement, which is connected to the coincidence arrangement.

As a further check instead of counters  $A$  one of the counters  $B$  was connected as well with the anticoincidence stage. In this case the latter and consequently the twofold mixers belonging to counters  $P$  and  $R$  must not count.

The author is greatly indebted to Prof. L. JÁNOSSY for his valuable advice.

#### REFERENCES

1. J. E. MORGAN and W. M. NIELSEN, *Phys. Rev.*, **50**, 882, 1936; W. M. NIELSEN and J. E. MORGAN, *Phys. Rev.*, **52**, 568, 1937.
2. HU CHIEN SHAN, *Proc. Roy. Soc., A* **158**, 581, 1937; HU CHIEN SHAN, B. B. KISILBASCH and D. KETILADGE, *Proc. Roy. Soc., A* **161**, 195, 1937.
3. J. CLAY and H. K. J. JONKER, *Physica*, **7**, 921, 1940.
4. N. ARLEY, *Proc. Roy. Soc., A* **168**, 519, 1938; N. ARLEY and B. ERIKSEN, *D. Kgl. Danske Vidensk. Selskab, Mat.-fys. Medd.*, **17**, 11, 1940.
5. B. TRUMPY, *D. Kgl. Danske Vidensk. Selskab, Mat.-fys. Medd.*, **20**, 6, 1943.
6. L. JÁNOSSY, *Cosmic Rays*, Oxford, 1952, p. 265.
7. L. JÁNOSSY and L. NAGY, *Acta Phys. Hung.*, **6**, 467, 1956.

#### РОЖДЕНИЕ ЛИВНЕЙ ПРИ МАЛЫХ ТОЛЩИНАХ Al, Fe, Cu, Pb

Л. НАДЬ

#### Резюме

Исследован ход первой части кривой Росси при разных поглотителях. Выделены ливни, вызваны мезонами, электронами и фотонами.

# EINE ANALYTISCHE FORMEL FÜR DIE THEORIE DER BILDUNG DER ELEKTRONENGRUPPEN IM PERIODISCHEN SYSTEM DER ELEMENTE

Von

T. TIETZ

INSTITUT FÜR THEORETISCHE PHYSIK DER UNIVERSITÄT LÖDZ, POLEN

(Vorgelegt von P. Gombás. — Eingegangen: 4. IX. 1957)

In dieser Arbeit geben wir eine analytische Formel für die untere Grenze der  $Z$ -Werte, bei der  $s$ -,  $p$ -,  $d$ -,  $f$ -Elektronen erstmalig in Erscheinung treten. Unsere analytische Formel bestimmt gut die Ordnungszahlen, bei welchen mit dem Einbau der  $s$ -,  $p$ -,  $d$ -,  $f$ -Elektronengruppen begonnen wird.

Wie bekannt, werden die  $K$ -,  $L$ -,  $M$ -,  $N$ -, ... Schalen mit den Hauptquantenzahlen  $n = 1, 2, 3, 4, 5, \dots$  nicht durchweg sukzessiv mit Elektronen besetzt, sondern das neu hinzukommende Elektron bevorzugt an einigen Stellen einen  $s$ - oder  $p$ -Quantenzustand mit höherer Hauptquantenzahl, obwohl in den Schalen mit tieferen Hauptquantenzahlen noch freie  $d$ - oder  $f$ -Quantenzustände vorhanden sind. Diese Unregelmässigkeiten im Atombau des periodischen Systems der Elemente finden sich z. B. bei der  $M$ -Schale (der Einbau der  $p$ -Elektronen der  $M$ -Schale beginnt nicht bei Kalium,  $Z = 19$ , sondern erst bei Scandium,  $Z = 21$ ) und bei der  $N$ -Schale (die Besetzung der  $N$ -Schale mit  $f$ -Elektronen beginnt statt bei Indium,  $Z = 49$ , erst bei Cerium,  $Z = 58$ ).

Diese Unregelmässigkeiten im periodischen System hat zuerst Fermi [1] auf Grund des statistischen Atommodells sehr befriedigend erklärt. Fermi leitete eine Formel für die Gesamtzahl  $N_K$  der Elektronen eines Atoms mit der Ordnungszahl  $Z$  für die Quantenzustände  $s$ -,  $p$ -,  $d$ -,  $f$  ab. Die Fermische Formel für  $N_K$  ist

$$N_K = 2 \left( \frac{6Z}{\pi^2} \right)^{1/3} k \Phi(\alpha), \quad \alpha = \left( \frac{4}{3\pi Z} \right)^{2/3} K^2. \quad (1)$$

In dieser Formel ist  $K$  die azimutale Quantenzahl, welche für die  $s$ -,  $p$ -,  $d$ -,  $f$ -Quantenzustände nur die diskreten Werte  $\frac{1}{2}, \frac{3}{2}, \frac{5}{2}, \frac{7}{2}$  annehmen kann.

Die von Fermi eingeführte Funktion  $\Phi(\alpha)$  welche in der Formel für  $N_K$  vorkommt, hat folgende Form:

$$\Phi(\alpha) = \int_0^1 [1 - \psi(x) - \alpha]^{1/2} \frac{dx}{x} \quad \text{mit} \quad \alpha = \left( \frac{4}{3\pi Z} \right)^{2/3} K^2. \quad (2)$$

Das Integral in (2) ist über alle positiven  $x$ -Werte zu erstrecken, für die der Ausdruck unter der Wurzel positiv ist. In der letzten Formel ist  $\varphi(x)$  die Thomas-Fermi-Funktion des neutralen Atoms. Zum Vergleich mit der Erfahrung hat FERMI die Funktion  $\Phi(\alpha)$  tabelliert und weiter die Gesamtzahl der Elektronen mit der azimutalen Quantenzahl  $K$  als Funktion von  $Z$  graphisch dargestellt. Um eine analytische Formel für die  $N_K$  zu erhalten, ersetzen wir in der Formel (2) die Thomas Fermi-Funktion  $\varphi(x)$  durch unsere Approximation [2],

$$\varphi(x) = \frac{1}{(1+ax)^2} \quad \text{mit } a = \left(\frac{\pi}{8}\right)^{2/3}. \quad (3)$$

Mit diesem einfachen Ausdruck kann man das Integral  $\Phi(\alpha)$  exakt lösen. In unserem Falle hat die Funktion  $\Phi(\alpha)$  folgende Form

$$\Phi(\alpha) = \int_{x_1}^{x_2} \frac{[-\alpha a^2 x^2 + (1-2a)x - \alpha]^{1/2}}{x(1+ax)} dx \quad (4)$$

mit

$$x_1 = \frac{1-2a\alpha - \sqrt{1-4a\alpha}}{2a^2 a}, \quad (4)$$

$$x_2 = \frac{1-2a\alpha + \sqrt{1-4a\alpha}}{2a^2 a}.$$

Für  $\alpha \geq \frac{1}{4a}$  verschwindet die Funktion  $\Phi(\alpha)$ , weil in diesem Falle der Ausdruck unter der Wurzel im Integrand von (4) negativ ist. Für den Fall  $\alpha = 0$  ist in (4)  $x_1 = 0$  und  $x_2 = \infty$  zu setzen. Eine ziemlich lange aber leichte Rechnung zeigt, dass für  $1-4a\alpha < 0$

$$\begin{aligned} \Phi(\alpha) = & \left| -\frac{1}{\sqrt{a}} \arcsin \frac{-2\alpha + (1-2a)x}{x\sqrt{1-4a\alpha}} + \right. \\ & + \frac{1}{\sqrt{a}} \arcsin \frac{(1-2a\alpha) - 2a^2 \sigma x}{\sqrt{1-4a\alpha}} + \\ & \left. + \frac{1}{\sqrt{a}} \arcsin \frac{ax-1}{(1+ax)\sqrt{1-4a\alpha}} \right|_{x_1}^{x_2}. \end{aligned} \quad (6)$$

Setzt man weiter in der letzten Formel für  $x_1$  und  $x_2$  ihre Werte gemäss Formel (5) ein, so bekommt man für die Funktion  $\Phi(\alpha)$  folgenden Ausdruck :

$$\Phi(\alpha) = -2\pi\alpha^{1/2} + \frac{\pi}{\sqrt{a}}, \quad \text{für } 0 \leq \alpha < \frac{1}{4a}, \quad (7)$$

$$\Phi\left(\alpha \geq \frac{1}{4a}\right) \equiv 0.$$

Zuerst vergleichen wir unsere Werte für die Funktion  $\Phi(\nu)$  mit den numerischen Werten von Fermi. Den Vergleich zeigt Tab. I. Aus der Tabelle

**Tabelle I**  
Die Funktion  $\Phi(\alpha)$

$\alpha$	0,0	0,1	0,2	0,3	0,4	0,49
$\Phi(\alpha)$ nach FERMI	3,2	2,2	1,48	0,88	0,36	0,00
$\Phi(\alpha)$ gemäss Formel (7)	4,3	2,3	1,48	0,85	0,32	0,00

ist ersichtlich, dass nur für  $\alpha = 0$  ein grösserer Unterschied zwischen unseren und den Fermischen Werten besteht. Der Unterschied rührt daher, dass

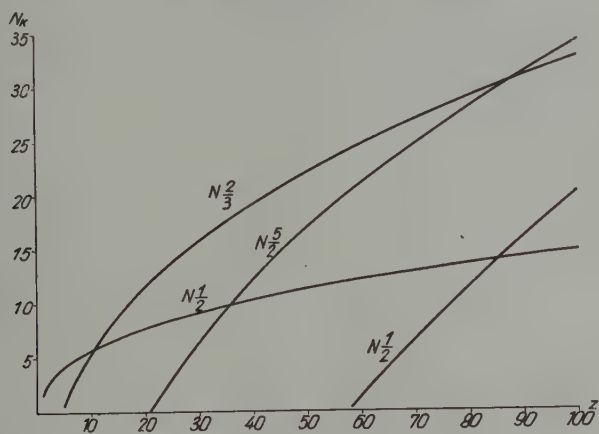


Abb. I

unsere Approximation (3) der Thomas Fermi-Funktion nicht das richtige Verhalten im Unendlichen zeigt. Zum Vergleich mit der Erfahrung stellen wir  $N_K$  als Funktion von  $Z$  graphisch dar. Wir bringen unsere Resultate in Abb. 1. In dieser Abbildung ist  $N_K$  als Funktion von  $Z$  für die  $s$ -,  $p$ -,  $d$ - und  $f$ -Elektronen, also für  $K = \frac{1}{2}, \frac{3}{2}, \frac{5}{2}, \frac{7}{2}$  dargestellt. Die Funktion  $N_K$  hat in unserem Falle folgende einfache Form :

$$N_K = 4(6Z)^{1/3} K \left[ 1 - \left( \frac{4}{3Z} \right)^{1/3} K \right]. \quad (8)$$

Die Abb. 1 zeigt, dass der Verlauf unserer Kurven sehr befriedigend ist. Unsere Kurven geben einen sehr guten Mittelwert der mehrfach gebrochenen Linien,

die sich erfahrungsgemäss aus den Stonerschen Tabellen ergeben. Unsere Kurven zeigen weiter praktisch denselben Verlauf wie die von Fermi gezeichneten Kurven.

Bei Anwendung der statistischen Theorie zur Berechnung der verschiedenen Eigenschaften der Atome hat man sich ständig vor Augen zu halten, dass die statistische Theorie ihrem Charakter gemäss den von Element zu Element stark schwankenden Atomgrössen nicht folgen kann, sondern über diese hinwegmittelt. Das ist der Grund, warum in unserem Falle die Formel (8) feinere Einzelheiten in der Bildung der Elektronengruppen nicht wiedergeben kann. In Tabelle II haben wir einige Werte für unsere  $N_K$  als Funktion von  $Z$  angegeben.

Tabelle II

Die Gesamtzahl der Elektronen  $N_K$  mit der azimutalen Quantenzahl  $K$  als Funktion der Ordnungszahl  $Z$

$Z$	$N_{1/2}$	$N_{3/2}$	$N_{5/2}$	$N_{7/2}$	$N_{9/2}$
3	3,2	0	0	0	0
4	3,8	0	0	0	0
5	4,2	0,7	0	0	0
6	4,8	1,8	0	0	0
16	7,2	9,5	0	0	0
20	8,0	11,6	0	0	0
21	8,0	12,1	0,1	0	0
22	8,2	12,6	0,91	0	0
24	8,5	13,5	2,4	0	0
30	9,3	15,9	6,5	0	0
40	10,4	19,3	12,1	0	0
50	11,4	22,2	16,9	0	0
55	11,8	23,5	19,1	0	0
58	12,1	24,2	20,3	0,5	0
59	12,1	24,4	20,7	1,0	0
65	12,6	25,9	23,0	4,3	0
70	13,0	26,9	24,9	6,8	0
80	13,7	29,0	28,3	11,6	0
90	14,3	30,9	31,4	16,0	0
100	14,9	32,6	34,3	20,0	0
103	15,0	33,1	35,2	21,3	0

Weiter geben wir in Tabelle III die untere Grenze der  $Z$ -Werte, bei der  $s$ -,  $p$ -,  $d$ - und  $f$ -Elektronen erstmalig in Erscheinung treten. Diese Zahlen sind diejenigen  $Z$ -Werte der Abb. 1 und Tab. I, für welche die  $N_K$  der Wert 1 annimmt.



men. Tabelle III bestätigt sehr gut den empirischen Befund für die untere Grenze der  $Z$ -Werte, bei der die  $s$ -,  $p$ -,  $d$ - und  $f$ -Elektronen erstmalig in Erscheinung treten.

Für die  $d$ - und  $f$ -Elektronen ergibt sich allerdings eine geringe Abweichung von der Erfahrung, da, wie die Erfahrung zeigt, die  $d$ -Elektronen schon bei Scandium ( $Z = 21$ ) und die  $f$ -Elektronen bei Cerium ( $Z = 58$ ) beginnen.

Unsere Formel (8) gibt hier etwas grössere Werte, es ist aber zu beachten, dass unsere theoretischen Werte,  $Z = 22$  und  $Z = 59$  den empirischen Werten,  $Z = 21$  und  $Z = 58$  bedeutend näher liegen als  $Z = 19$  und  $Z = 47$ , wo man bei einem vollständig regelmässigen Aufbau das erstmalige Auftreten der  $p$ - und  $f$ -Elektronen erwarten sollte.

Tabelle III

Die untere Grenze der  $Z$ -Werte, bei der  $s$ -,  $p$ -,  $d$ -, und  $f$ -Elektronen erstmalig in Erscheinung treten

	Die untere Grenze der $Z$ -Werte für			
	$s$ -Elektronen	$p$ -Elektronen	$d$ -Elektronen	$f$ -Elektronen
Erfahrung.....	1	5	21	58
nach FERMI.....	1	5	21	55
nach Gleichung(8) .....	1	5	22	59

Herrn Prof. F. J. WIŚNIEWSKI danke ich für sein Interesse an dieser Arbeit.

# LITERATUR

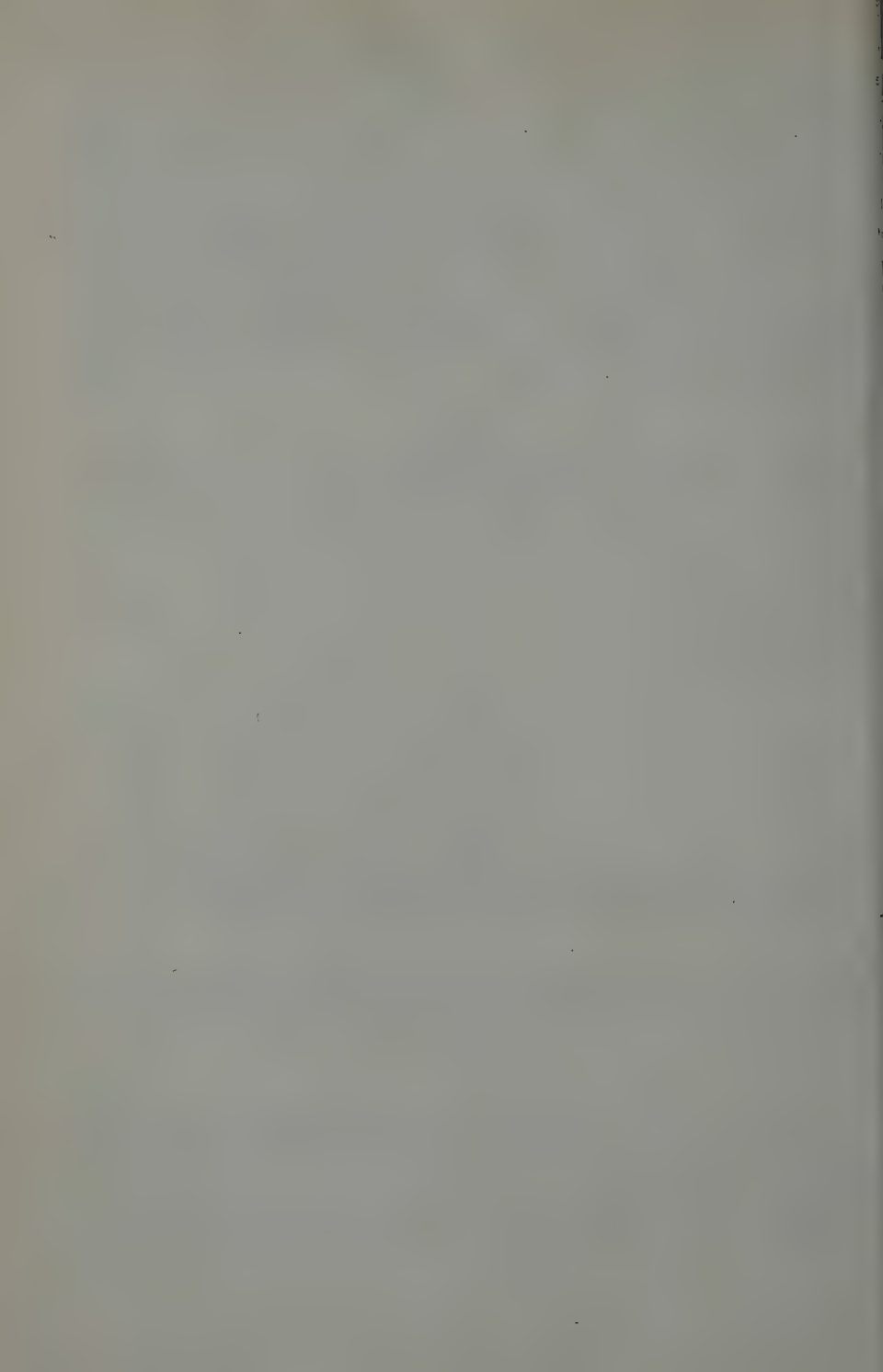
1. E. FERMI, ZS. f. Phys., **48**, 73, 1928; Nature, London, **121**, 502, 1928; Rend. Acc. Lincei [6], **7**, 342, 1928; für weitere Einzelheiten vgl. P. GOMBÁS, Die statistische Theorie des Atoms und ihre Anwendungen, Springer Verlag Wien, 1949.
2. T. TIETZ, Ann. d. Phys., **15**, 186, 1955.

## АНАЛИТИЧЕСКОЕ ВЫРАЖЕНИЕ ДЛЯ ТЕОРИИ ВОЗНИКНОВЕНИЯ ЭЛЕКТРОННЫХ ГРУПП В ПЕРИОДИЧЕСКОЙ СИСТЕМЕ ЭЛЕМЕНТОВ

Т. ТИТЦ

### Резюме

В этой работе даются аналитические выражения для таких минимальных значений  $Z$ , при которых первый раз встречаются  $s$ ,  $p$ ,  $d$ ,  $f$ -электроны. Указанное аналитическое выражение хорошо определяет те атомные номера, у которых начинают заполняться  $s$ ,  $p$ ,  $d$ ,  $f$  группы электронов.



# PLANE WAVE METHOD WITH A MODIFIED POTENTIAL FIELD

By

R. GÁSPÁR

INSTITUTE FOR THEORETICAL PHYSICS, KOSSUTH LAJOS UNIVERSITY, DEBRECEN, AND RESEARCH GROUP  
FOR THEORETICAL PHYSICS OF THE HUNGARIAN ACADEMY OF SCIENCES, BUDAPEST

(Presented by P. Gombás. — Received : IX. 7. 1957)

A new method is developed for the determination of the energy band spectrum of metal electrons. An essential advantage of the method is that it applies plane waves. This is made possible by the introduction of a "repulsive" potential, which takes care of the high kinetic energy of the eigenfunction oscillating in the neighbourhood of the nuclei. Thus the valence electrons can be treated as if they filled the Brillouin zones gradually from the lowest Brillouin zone. This also means that in this model the eigenfunctions of the metal electrons can be well approximated by the linear combination of a few plane waves. The number of the rows and columns of the secular equations arising at the degenerate points in the neighbourhood of the boundaries of the Brillouin zones is low. The problems associated with the repulsive potential in the matrix components of the secular equation are investigated in detail. It is shown that these matrix components are such that they do not alter the qualitative structure of the secular equation. The value of the matrix components of the Hamiltonian varies in the Brillouin zone from place to place. This fact considerably increases the numerical work as compared to the older free-electron model. As compared to the newer methods, however, this disadvantage, is not peculiar to the method presented here as they, although for other reasons, also involve tedious numerical work.

## Introduction

In the electronic theory of solids the quantitative determination of the energy spectrum presents a very important problem, a satisfactory solution of which has up to now been obtained only for a few metals. The method of WIGNER and SEITZ [1] is simple and yields good results for the lower edge of the energy band of metal electrons. However, the generalization of this method given by SLATER [2] can be applied to alkali metals only, because, as was shown by SHOCKLEY [3], the method involves an error, which makes the qualitative results doubtful already for the upper edge of the highest filled band. Although the recent extension of the method by LACE and BETHE [4] increased the accuracy it also involved a considerable increase in work. Another method by SLATER [5] is easier to apply to higher energies, but it is very tiresome. The method described in the present paper is a generalization of GOMBÁS's [6] method and is based partly on the statistical theory. Thus it can be well used, particularly for the treatment of heavier metals and can be regarded as a natural supplement to HERRING's method [7] which is mainly applicable to lighter metals. The chief advantage of the method to be described is that it proceeds on a mathematically well prepared way and is thus easy to apply.

## 1. Electronic structure of solids and the valence electrons

If we want to draw a comparison between the electrons of free atoms and those of solids (excluding solids, which contain transition elements) we have to classify them into two main groups, namely 1. the core electrons, which form a noble gas like  $(ns)^2 (np)^6$  or a  $(nd)^{10}$  shell and exhibit to good approximation, an identical distribution in the free atom and in the solid. 2. the valence electrons, the possible energy values of which in the stationary states of the free atom show the characteristic distribution of a discrete spectrum. In the solids the energy of the same electrons have a band spectrum. A further essential difference between the two groups is that whereas in solids for the core electrons the grouping according to the orbital quantum number can be regarded as a good approximation just as for the core electrons in the free atom, no definite orbital quantum number can be assigned in solids (in good approximation) to the valence electrons apart from some exceptional cases. The physical reason for this is the following. In solids it is a common property of the electrons that in principle none of them belongs to a definite atom, they wander from atom to atom. The essential difference between the core electrons bound in the inner shell and the valence electrons is that the density maximum of the former is in the neighbourhood of the nucleus and thus the probability for these electrons to approach a "foreign" atom is small. For the valence electrons the outer density maximum is in the region midway between the atoms and thus they cannot be localized around an atom not even for a short period. One of the consequences of the properties mentioned here is that the electrons in the inner shell's keep the quantum numbers assigned to them in the atom in the solid too and these play an essential role in the description of their eigenfunctions, while for valence electrons these quantum numbers may have but symbolic significance if any. The classification of the core electrons according to the orbital quantum number plays an important role in the statistical theory of metallic bond and thus it is absolutely necessary to investigate how the theoretical determination of the energy band spectrum of valence electrons can be carried out with regard to this fact.

In most solids, owing to the high constancy of the potential field, the eigenfunctions of valence electrons can be described by few plane waves in the  $7/8$  th of the elementary cell. In the  $1/8$  th of the cell around the nucleus the eigenfunctions of valence electrons have nodal surfaces and oscillate intensely, which is due to their orthogonality to the eigenfunctions of the electrons of the ionic core. This intense oscillation increases the kinetic energy and thus the total energy (the sum of the kinetic and potential energies) is comparatively great ensuring that the valence electrons remain in the very high-lying valence band. Thus it can be seen that the region around the ionic core, which is at equilibrium nuclear distance about  $1/8$  th of the elementary cell is very signi-

ficant. If the energetical conditions of the valence electrons of solids are to be treated the above mentioned increase of the kinetic energy must be taken into account. Here we restrict ourselves to the cases where the initial eigenfunctions are plane waves. This condition ensures namely that the eigenfunction with any arbitrary wave number vector can be set up readily and besides in  $7/8$  th of the elementary cell already the zeroth approximation yields excellent values. In this connection we may refer to two methods, that of orthogonalized plane waves developed by HERRING and the one to be developed here, which is not orthogonalized, i. e. it works with simple plane waves, but investigates the motion of electrons in a modified potential field. As in the construction of the modified potential field the classification of electrons according to their orbital quantum numbers plays an important role, we shall investigate the behaviour of an electron represented by a plane wave from the point of view of classification according to the orbital quantum number.

Be the eigenfunction of the electronic state in a space of volume  $\Omega$

$$\psi_{\mathbf{f}} = \frac{1}{\Omega^{1/2}} e^{i(\mathbf{f} \cdot \mathbf{r})} \quad (1)$$

with the wave number vector  $\mathbf{f}$ , and the kinetic energy of this electron

$$E = \frac{1}{2} |\mathbf{f}|^2, \quad (2)$$

where  $\mathbf{r}$  is the radius vector. There exists a close relation between the plane wave (1) and the spherical harmonics occurring in the classification of electrons in the centrally symmetrical potential field of the free atom. The plane wave can thus be expanded in a series

$$\psi_{\mathbf{f}} = \frac{e^{i(\mathbf{f} \cdot \mathbf{r}_n)}}{\Omega^{1/2}} \sum_{l=0}^{\infty} (2l+1) i^l j_l(kr) P_l(\cos \vartheta) \quad (3)$$

[8];  $r = |\mathbf{r} - \mathbf{r}_n|$ ,  $\vartheta$  and  $\varphi$  are polar coordinates around the  $n$ -th nucleus as centre and have an axis parallel to the direction of  $\mathbf{f}$ .  $k = |\mathbf{f}|$ ,  $\mathbf{r}_n$  is the radius vector drawn to the  $n$ -th nucleus,  $P_l(x)$  is a Legendre polynomial and

$$j_l(x) = \left( \frac{\pi}{2x} \right)^{1/2} J_{l+\frac{1}{2}}(x); \quad (4)$$

$J_{l+\frac{1}{2}}(x)$  is a Bessel polynomial. From (3) we obtain after multiplication by the conjugate complex and averaging over all possible values of the  $\vartheta$

and  $\varphi$  the weight of the electrons of orbital quantum number  $l$  at a distance  $r$  from the nucleus

$$a_l = \frac{4\pi}{\Omega} (2l+1) j_l^2(kr). \quad (5)$$

Or, by introducing the normalized probability  $a'_l$  corresponding to the assumption  $\sum_l a'_l = 1$  we obtain

$$a'_l = (2l+1) j_l^2(kr). \quad (5')$$

Fig. 1 shows the probabilities  $a'_l$  plotted as functions of  $kr$ . It is clear that a

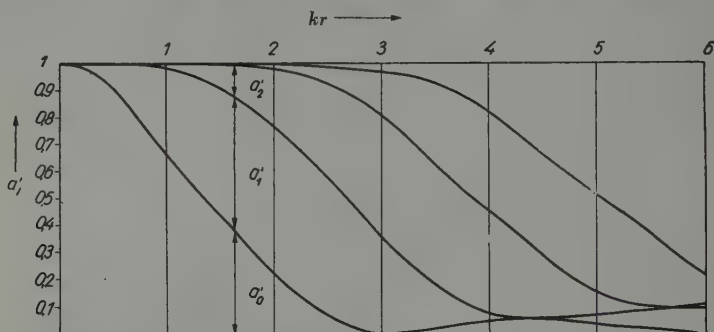


Fig. 1. The quantities  $a'_l$  occurring in the expansion of the plane wave in terms of spherical harmonics. The quantities in the figure are given in atomic units

small values of  $kr$  the  $s$  states prevail, whereas at places near the edge of the elementary cell, especially at higher values of the wave number vector, the states of higher orbital quantum numbers predominate.

## 2. General characteristics of the matrix elements of operators in the valence electron states in solids

The most important problem of the electronic theory of solids is the determination of the energy spectrum. With the aid of the latter the other data can be obtained by direct methods. To determine the energy spectrum the average values and matrix elements, respectively, of the operators must be evaluated. We now want to discuss the problems associated with these.

The situation is the simplest in the cases where the operator to be averaged over is spherically symmetrical around each of the nuclei, i. e. it depends on  $r$  only (the potential energies are mostly of this kind, e. g. the Coulomb interaction with the nucleus, the average field of the other electrons etc.). In such



a case averaging over the angles can be carried out immediately and the matrix elements can be obtained by a single integration over  $r$  [9].

A more difficult case is where the operator also depends on the angles and contains just the differential operators with respect to these angles. An operator of such a type is e. g. that of the kinetic energy and that of the square of the total angular momentum. Consider a prototype of such operators in detail. Be our operator, which we denote for brevity by  $\kappa$ , defined by the equation

$$\kappa = \begin{cases} M^2, & \text{if } r \leq R, \\ 0, & \text{if } r > R, \end{cases} \quad (6)$$

where

$$M^2 = \hbar^2 \left[ \frac{1}{\sin \vartheta} \frac{\partial}{\partial \vartheta} \left( \sin \vartheta \frac{\partial}{\partial \vartheta} \right) + \frac{1}{\sin^2 \vartheta} \frac{\partial^2}{\partial \varphi^2} \right]$$

is the operator of the square of the total angular momentum. Thus the operator essentially is one of the square of the total angular momentum within a sphere of radius  $R$ , whereas outside this sphere it is the operator of the multiplication by the constant 0. Let us form the average value of the operator  $\kappa$  over a sphere of radius  $r_0$  ( $R < r_0$ ). [In the theory of solids this sphere is as a rule the so-called elementary sphere (see later)]. With (6) and (3) we obtain

$$\bar{\kappa} = \sum_l A_l \hbar^2 l(l+1), \quad (7)$$

where

$$A_l = \frac{3\pi}{4} \frac{2l+1}{kr_0} \left( \frac{R}{r_0} \right)^2 \left\{ J_{l+\frac{1}{2}}^2(kR) - J_{l-\frac{1}{2}}(kR) J_{l+\frac{3}{2}}(kR) \right\}. \quad (8)$$

In the detailed examination of the weight factors  $A_l$  we take into account the dependence of the wave number factor on  $r_0$ . As the wave number vectors are defined in the reciprocal lattice, we may write

$$k = \frac{b}{r_0}, \quad (9)$$

where  $b$  under the normal conditions is a number of the order of 1. With the aid of (9) (8) may be written in the form

$$A_l = \frac{3\pi}{4} \frac{2l+1}{b} \left( \frac{R}{r_0} \right)^2 \left\{ J_{l+\frac{1}{2}}^2 \left( b \frac{R}{r_0} \right) - J_{l-\frac{1}{2}} \left( b \frac{R}{r_0} \right) J_{l+\frac{3}{2}} \left( b \frac{R}{r_0} \right) \right\}. \quad (10)$$

It is obvious that (10) can be regarded as a function of the quantities  $b \frac{R}{r_0} = y$  and  $b$ , where  $b$  solely depends on the type of lattice and the place

occupied by the valence electrons in the band but does not depend on the lattice constant. The dependence of  $A_l$  on the lattice constant as well as on the radius  $R$  in the definition of the operator  $\kappa$  is involved in  $y$ . In Fig. 2 the so-called normalized  $A'_l$ -s are exhibited in accordance with the representation of Fig. 1. The normalization was carried out in such a way that

$$\sum_l A'_l(y) = 1.$$

Thus we only want to know how the ratios of the  $s, p, d, f, g, \dots$ -states vary,

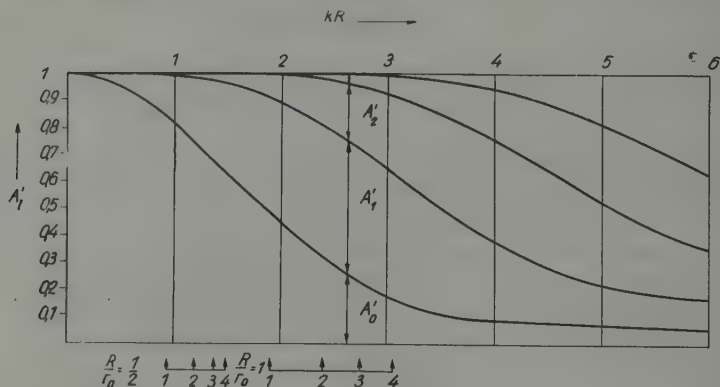


Fig. 2. The auxiliary quantities  $A'_l$  necessary for the determination of the matrix element for the operator  $\kappa$ . The quantities in the figure are given in atomic units

for the time being the variation of the absolute value of the weight factors not investigated. Accordingly

$$A'_l = \frac{3\pi}{4} \frac{2l+1}{y} \left\{ J_{l+\frac{1}{2}}^2(y) - J_{l-\frac{1}{2}}(y) J_{l+\frac{3}{2}}(y) \right\}, \quad (11)$$

which is already a function of  $y$  only.

Under the Figure there are several scales with arrows showing the places corresponding to various values of  $b$  at various values of  $R/r_0$ . The arrows marked 1, 2, 3 etc. indicate the radii of the Fermi sphere at 1, 2, 3 etc. electrons per atom. It is clear that at lower values of  $R/r_0$  the weight of the states of lower orbital quantum numbers (mainly that of the  $s$ -state) are great. This is very important from the point of view of the repulsive potentials because (see later) these take values different from zero only within the ionic core, which is a region of small radius near the nucleus.  $R$ , which can be defined in connection with the repulsive potentials, is smaller than  $r_0/2$ , which

makes it plausible that the weight of these states greatly increases. This was confirmed in the case of the Al metal [10] that carrying out the calculation associated with the metallic bond, even with the aid of an  $s$  type repulsive potential, results not very different from the experimental data were obtained.

### 3. The free electron method and the difficulties involved

In principle the theory of the electronic structure of solids [11] can be developed simplest by building up the total eigenfunctions of metal electrons of plane waves of the form

$$\psi = e^{i(\mathbf{k}\mathbf{r})}, \quad (12)$$

where  $\mathbf{k}$  is the wave number vector of a free electron. In the periodic potential field

$$V = \sum_{h_1, h_2, h_3}^{+\infty} V_h e^{2\pi i(\mathbf{h}, \mathbf{r})} \quad (13)$$

the eigenfunction of an electron can be written in the form

$$\psi = \sum_{h_1, h_2, h_3}^{+\infty} a_h e^{i[(\mathbf{k} + 2\pi\mathbf{h}), \mathbf{r})} \quad (14)$$

In (13) and (14)

$$\mathbf{h} = h_1 \mathbf{b}_1 + h_2 \mathbf{b}_2 + h_3 \mathbf{b}_3 \quad (15)$$

is the lattice vector of the reciprocal lattice and  $\mathbf{b}_1, \mathbf{b}_2, \mathbf{b}_3$  are the basic vectors determining the axes of this lattice. The eigenfunction  $\psi$  satisfies the Schrödinger equation

$$\Delta\psi + \frac{2m}{\hbar^2} (E - V) \psi = 0, \quad (16)$$

if the  $a_h$ -coefficients satisfy the homogeneous linear equations

$$\left[ E - V_{000} - \frac{\hbar^2}{2m} |\mathbf{k} + 2\pi\mathbf{h}|^2 \right] a_h - \sum_{\mathbf{h}'} a_{\mathbf{h}-\mathbf{h}'} V_{\mathbf{h}'} = 0. \quad (17)$$

(17) has a solution only if the determinant which can be formed from the coefficients vanishes. The determinantal equation thus provides a defining equation for  $E$  which so far is unknown: the solution of this equation thus immediately gives the energy of the electron belonging to the wave number vector  $\mathbf{k}$ . Inserting the value of  $E$  into (17) and solving this equation for the  $a_h$  coefficients we obtain the unknown coefficients of the eigenfunction. In

the course of the actual determination of the energy eigenvalue we cannot of course take all Fourier coefficients  $V_g$  into account but have to select those the order of magnitude of which is relevant for the secular equation. According to (17) those Fourier coefficients for which the condition

$$E_{2\pi g} - E_0 \gg |V_g| \quad (18)$$

is fulfilled can be neglected. In (18)

$$E_{2\pi g} = \frac{\hbar^2}{2m} |2\pi g|^2 + V_{000}. \quad (19)$$

For metals occurring in nature  $E_{2\pi g} - E_0 \sim 20\text{eV}$ , when for  $g$  its smallest possible value is taken into account. If the potential is the potential of the ionic core and that of the valence electrons without any repulsive potential then there are many Fourier coefficients  $V_g$  the order of magnitude of which agrees with that of  $E_{2\pi g} - E_0$  and thus the free electron method in this form is not suitable for the determination of either the energy or the eigenfunction.

Let us consider the real reason for the inapplicability of the method in some more detail. Retaining in the system of equations (17) but a few coefficients, (the largest of them), the smallest root of the secular equation gives a rough approximate value for the energy of the valence electrons. Taking more and more coefficients into account the lowest root of the secular equation does not approximate the energy of a valence electron but that of a core electron of smaller energy, while the energy of valence electrons is approximated by a larger root of the secular equation. Thus the above formulation of the problem is too general, demanding, that the method yield the energy and eigenfunctions of the core electrons too. This is, however, not necessary at all, since we already know these to an accuracy satisfactory for our purpose. The excessive generality of the method becomes still more obvious if the situation is examined from the standpoint of eigenfunctions. The assumption of the eigenfunction in the form (14) is based on the assumption that the approximate eigenfunction can be well approximated at least partly by plane waves. This is the case for electrons in the valence band and in the conduction bands. For the core electrons, however, the case is essentially different. The eigenfunction of the core electron keeps its atomic character and is no plane wave, it is exponential far from the nucleus and oscillates inside near him. To approximate such an eigenfunction by plane waves is of course very difficult and most of the difficulties associated with the method treated above are due to this fact. The solution is obvious: the method has to be modified so as to be applicable to valence electrons and conduction electrons only, which are interesting for us in any case.

Let us now proceed to investigate the eigenfunctions of valence and conduction electrons in some more detail. As has been mentioned above the eigenfunction of these electrons can be well approximated by a plane wave in the greater part (about 85%) of the elementary cell, as there the potential is constant. Significant deviation from the plane wave eigenfunction can only be experienced in the immediate neighbourhood of the nucleus where the eigenfunction begins to oscillate just like the atomic eigenfunctions. What is the immediate reason for this? In this region the potential changes very rapidly and near the nucleus tends to infinity as  $Ze/r$ . Owing to the smallness of the average value taken over this region the potential energy of the electron is very small (its absolute value is very large). The valence electron is in a state of higher energy; this is made possible by the average value of the operator of the kinetic energy taken in the inner region for the oscillating part of the eigenfunction. The situation can be described in this way if the energy relations are considered only in a formal manner.

It is due to the Pauli principle that the electrons in the atom occupy states of higher and higher energies. It has to be considered in detail how the difficulties associated with the eigenfunction can be overcome, if the kinetic energy increase due to the Pauli principle is taken explicitly into account.

#### 4. Reduction of the problem to the treatment of valence and conduction electrons

As has been shown above the most obvious solution of the problems would be to eliminate the core electrons from our treatment and to simplify our method to such an extent that it becomes suitable but for the treatment of valence and conduction electrons only. As the eigenfunctions of the core electrons are practically the same for the free atom and the solid, these could, if necessary, be used for the above simplification.

For this simplification several methods present themselves. Among these we mention those which aim at the correction of the plane wave. HERRING orthogonalized the plane waves to the eigenfunctions of the core electrons and achieved thus the appropriate behaviour of the eigenfunctions in the neighbourhood of the nucleus; further the orthogonality secures the necessary smallness of the matrix components of the potential energy. The second possible method was suggested by SLATER [13]. The essence of the method is to retain the plane wave far from the ionic core and to replace it inside a sphere of radius  $R$  around the nucleus by the linear combination of core electron solutions having the energy of the plane wave. Whereas HERRING's method has already been tried out in the theoretical treatment of several metal and semiconductor SLATER's method has not been applied yet.



Both these methods require an essential modification of the plane wave eigenfunction in order that the matrix components satisfy relation (18). This results in the loss of the most desirable property of the older methods, their comparatively simple structure and easiness to handle. We shall attempt to modify the free electron method in such a manner which makes possible to start from the plane wave eigenfunctions of the free electrons when treating the valence and conduction electrons.

The solution of the problem is made possible by the fact that for the valence and conduction electrons a modified potential field can be given

$$V' = V + \Phi, \quad (20)$$

which possesses several important properties.

1. The operator  $\Phi$  in (20) is such that if the density and the wave function of the core electrons of the free atom are given, the operator can immediately be determined with their aid.

2. The average value of the potential field taken over not too small regions does not, in the regions near the nucleus, significantly decrease below the average value over the regions far from the nucleus. In this connection we may refer to our investigations into the binding and electronic structure of the K metal [9].

3. Consequently, the eigenfunctions of the valence and conduction electrons can be well approximated by plane waves all over the sphere (including the  $1/8$  th part of the volume around the nucleus).

## 5. Introduction of the repulsive potential and the total potential

For the calculation of atomic term values and for the treatment of monovalent metals a certain form of the repulsive potential has been used for a long time, the kinetic energy increase due to the Pauli principle having been taken into account in the form of a potential energy [6]. The potential of this energy is

$$\Phi_l = -\gamma_0 (\varrho^{2/3} - \varrho_l^{2/3}) \quad (21)$$

In (21)  $\varrho$  is the total electron density of the ionic core and  $\varrho_l$  the density of the electrons which occupy states of energy lower than that of the lowest possible energy of the electron to be treated,  $l$  is the orbital quantum number of this electron and  $\gamma_0 = \frac{1}{2} (3\pi^2)^{2/3} e a_0$  is a constant. As has been shown by some recent investigations [14] the modified potential field obtained with the aid of (21) yields good approximation only if the outermost closed shell of



the ionic core is an  $(ns)^2 (np)^6$ , a so-called noble gas like shell. According to GOMBÁS the repulsive potential

$$\Phi_l' = - \frac{\pi^2 e a_0}{8 (2l+1)^2} D_l^2 - \frac{1}{4} \frac{e a_0}{r^2} \quad (22)$$

is correct not only for noble gas like ionic cores, but it is correct for other ones, e. g. for a closed  $(nd)^{10}$  core. In (22)  $D_l$  is the radial density of the electrons with the orbital quantum number  $l$  of the ion and  $e$  is the charge of the proton.  $a_0$  is the first Bohr hydrogen radius.

The above repulsive potentials (21) and (22) were introduced with the aid of statistical methods. Several authors have dealt with their wave-mechanical foundations [15].

To a good approximation the atomic electrons move in a central symmetrical potential field and as a result the states of these electrons can be characterized by the magnitude of the total angular momentum and one of its components, i. e. by the orbital and magnetic quantum numbers. Accordingly the repulsive potentials vary with these quantum numbers of the electrons. In solids the central field remains for the electrons of the ionic cores a good approximation i. e. it remains practically the same as in the free atom and thus the form of the repulsive potentials remains as given by the expressions (21) and (22). However, we want to characterize the metal electrons by plane waves and for these the momentum and not the angular momentum is well defined. It is thus necessary to replace the repulsive potential by an operator which can be applied to an arbitrary eigenfunction and leads in the special case of atoms to the former well proved form. Be the operator  $\Phi$  diagonal in the system of spherical harmonics and its eigenvalues the repulsive potentials (21) and (22) respectively, i. e.

$$\Phi Y_l^m = \Phi_l(r) Y_l^m, \quad (23)$$

where  $Y_l^m$  is the spherical harmonic with indices  $l$  and  $m$ . It is certain that operator  $\Phi$  is hermitic as its eigenvalues are real. Assuming that it is linear too, it can be written in the form

$$\Phi(r, \vartheta, \varphi) = \frac{1}{c_l^2} \Phi_l(r) M^2, \quad (24)$$

where  $M^2$  is the operator of the square of the total angular momentum and  $c_l^2 = \hbar^2 l(l+1)$  is its eigenvalue. Thus in the case of atoms operator  $\Phi$  leads to the same repulsive potentials as the selection according to orbital quantum numbers. For a valence electron, as will be shown later, it can be well applied

too. The author has already used the operator  $\Phi$  for investigations on the binding of the Al metal [10] and the results obtained were in good agreement with experiment.

To set up the total potential is a very delicate task, as the first term of expression (20) is composed of several parts

$$V = V_c^{\text{ion}} + V_{\text{ex}}^{\text{ion}} + V_{\text{kor}}^{\text{ion}} + V_c^{\text{electron}} + V_{\text{ex}}^{\text{electron}} + V_{\text{k.r.}}^{\text{electron}} \quad (25)$$

The first three terms of (25) are the Coulomb, the exchange and correlation potentials due to the ion with closed shell. The second three terms denote the corresponding terms due to the valence electrons except the one in question. Here we do not deal with the individual terms in detail, but will refer to them in connection with their practical application further below. In any case it is evident that the modified potential which is the sum of (25) and (24) is a very intricate function consisting of many terms and thus we will describe a simpler semi-empirical method by which it is easier to determine the potential of the ionic core.

For the treatment of alkali metals HELLMANN [16] succeeded in applying a semi-empirical method which essentially consists of the following: The part due to the ions of the periodic potential can also be determined by using the term values of the atom or ion (ionic core and one electron). Hellmann's method will be generalized for the determination of the resultant of the ionic potentials.

In the investigation of the structure of solids ions of its atoms with closed electron shells play a great role. Supplementing each shell with one valence electron it forms an atom or ion the term values of which are known from the study of arc and spark spectra. Knowing the term values we can always construct a potential function with the aid of which, in the case of an adequate form of the eigenfunction we can reproduce the term values. In practice, however, the method set up in this way is too general, because the few term values do not uniquely determine the potential function owing to the great variety of possible forms of the eigenfunction. Taking however, the experience gained from the calculations of atomic and ionic eigenfunctions into account, in the region far from the nucleus the form of the eigenfunction can qualitatively be well given as an exponentially decreasing function, provided however, that the eigenfunctions of the electrons of the ionic core are known. Then the requirement that the eigenfunction of the valence electron should be orthogonal to those of the same orbital quantum number of the ionic core, determines the form of the eigenfunction comparatively well. Naturally, the eigenfunctions of the electrons of the ionic core are generally not available. Then we may proceed in such a manner that we neglect the internal oscillation of the eigenfunction of the valence electron and take the kinetic energy thus neglected in

the form of a potential energy into account. From all this follows that the potential set up in this way for states of various orbital quantum numbers will differ from state to state. Again be  $r$  the distance from the nucleus and  $ze$  the charge of the ion, then the simplest form of the potential is

$$V_l = \frac{ze}{r} - A_l r^{n_l} e^{-a_l r} \quad (n_l \geq -1). \quad (26)$$

The first term of (26) represents the Coulomb-like potential outside the ionic core, and the second term, the deviation from the former inside the ionic core, the non-Coulomb-like part.  $A_l$  and  $a_l$  are constants the values of which must be determined with the aid of the experimental atomic terms of the orbital quantum number  $l$ .  $n_l$  is an integer, which will be determined in advance in concrete cases on the basis of trivial considerations. The second term in (26) actually involves all the non-Coulomb-like electrostatic terms as well as the repulsive potentials taking account of the missing kinetic energy. Writing (24) in the form

$$V_l = V_{\text{coulomb}} + \omega_l. \quad (27)$$

the formalism of the theory set up on the basis of the former repulsive potentials can be applied with the difference that the role of the  $\Phi_l$ -s in it is formally played by the  $\omega_l$ -s. Of course, we want to emphasize that the  $\Phi_l$ -s and the  $\omega_l$ -s differ greatly from each other. The  $\Phi_l$ -s occur but in the operator representing the repulsive potential while the  $\omega_l$ -s include the non-Coulomb-like interaction with the ionic core, the exchange interaction with the core electrons, the correlation interaction due to the electrostatic forces and still other possible interactions which would otherwise be very difficult to take into account.

## 6. The matrix elements of the Hamiltonian

The one-electron Hamiltonian occurring in the determination of the energy of the electrons is now

$$H = -\frac{\hbar^2}{2m} \Delta - Ve - \Phi_e \quad (28)$$

and its matrix element which can be most generally defined is

$$\begin{aligned} H_{\mathfrak{h}\mathfrak{h}'}^{\mathfrak{t}} &= \frac{1}{\Omega} \int e^{-i[(\mathfrak{l}+2\pi\mathfrak{h})r]} H e^{i[(\mathfrak{l}+2\pi\mathfrak{h}')r]} d\tau \\ &= \Delta_{\mathfrak{h}\mathfrak{h}'}^{\mathfrak{t}} - e V_{\mathfrak{h}\mathfrak{h}'} - e \Phi_{\mathfrak{h}\mathfrak{h}'}^{\mathfrak{t}}, \end{aligned} \quad (29)$$

where the integration is to be carried out over the total volume  $\Omega$ . In the following we assume that  $\Omega$  is a so-called basic region of the solid i. e.  $\Omega$  represents the period of the wave function occurring in the averaging and the possible values of  $\mathfrak{k}$  form a quasi-continuous discrete set. Taking this into account the matrix element of the operator of the kinetic energy is

$$\Delta_{\mathfrak{h}\mathfrak{h}'} = \frac{\hbar^2}{2m} |\mathfrak{k} + 2\pi\mathfrak{h}|^2 \delta_{\mathfrak{h}\mathfrak{h}'}, \quad (30)$$

where  $\delta_{\mathfrak{h}\mathfrak{h}'}$  is the Weierstrass symbol. The matrix element of the electrostatic type potentials can be very easily determined

$$V_{\mathfrak{h}\mathfrak{h}'} = \frac{1}{\Omega} \int V e^{2\pi i [(\mathfrak{h}' - \mathfrak{h}) \cdot \mathbf{r}]} d\mathbf{r} = V_{\mathfrak{g}}, \quad (31)$$

as  $\mathfrak{h}' - \mathfrak{h} = \mathfrak{g}$  is a lattice vector of the reciprocal lattice and thus (31) is a coefficient of the Fourier expansion of the potential  $V$ . (31) is in general independent of  $\mathfrak{k}$  and thus it need be determined only once, regardless of the value of  $\mathfrak{k}$ .

The matrix element of the operator of the repulsive potential is

$$\Phi_{\mathfrak{h}\mathfrak{h}'}^{\mathfrak{k}} = \frac{1}{\Omega} \int e^{-i [(\mathfrak{k} + 2\pi\mathfrak{h}) \cdot \mathbf{r}]} \Phi e^{i [(\mathfrak{k} + 2\pi\mathfrak{h}') \cdot \mathbf{r}]} d\mathbf{r}. \quad (32)$$

Taking (23) and (24) into account and using relations

$$\frac{2n+1}{2} P_n(\cos \omega) = \sum_{m=-n}^{+n} \bar{P}_n^m(\cos \vartheta) \bar{P}_n^m(\cos \vartheta_0) e^{im(\varphi - \varphi_0)} \quad (33)$$

and

$$\bar{P}_n^m = \sqrt{\frac{2n+1}{2} \frac{(n-m)!}{(n+m)!}} P_n^m(x) \quad (34)$$

and by integrating over the angles we obtain

$$\Phi_{\mathfrak{h}\mathfrak{h}'}^{\mathfrak{k}} = \frac{4\pi}{\Omega} \sum_{l=0}^{\infty} (2l+1) P_l(\cos \omega) \int_0^{r_0} \Phi_l(r) j_l(kr) j_l(k'r) r^2 dr \quad (35)$$

In (35)  $k = |\mathfrak{k} + 2\pi\mathfrak{h}|$ ,  $k' = |\mathfrak{k} + 2\pi\mathfrak{h}'|$  and  $\omega$  is the angle formed by the vectors  $\mathfrak{k} + 2\pi\mathfrak{h}$  and  $\mathfrak{k} + 2\pi\mathfrak{h}'$ . For sake of clearness the quantities in integral (32) are shown in Fig. 3.





With regard to (36) it is evident that the integrals in (35) are the same for all the  $\Phi_{\mathfrak{h}\mathfrak{h}'}^{\mathfrak{k}}$  matrix elements in the secular equation. Thus the  $\Phi_{\mathfrak{h}\mathfrak{h}'}^{\mathfrak{k}}$  matrix elements differ from each other only owing to the different values of  $\omega$ . The value of  $\omega$ , however, as is shown in Fig. 3, depends on the  $g$  only as the sides of the angles are, owing to (37) all equal and the third side of the triangle is  $2\pi g$ . Thus we have proved that  $\Phi_{\mathfrak{h}\mathfrak{h}'}^{\mathfrak{k}}$ , owing to (36) and (37) as well as to the relation  $(k + 2\pi \mathfrak{h}') - (\mathfrak{k} + 2\pi \mathfrak{h}) = 2\pi (\mathfrak{h}' - \mathfrak{h}) = 2\pi g$ , does not change the structure of the secular equation although it is a function of the three quantities indicated by the indices.

### Discussion

In the preceding sections it was shown how to determine the eigenfunctions and energy eigenvalues of the valence and conduction electrons by our method. Of course, the practical applicability of the method depends on whether the simplification introduced decreases the number of rows and columns of the secular equations by a sufficient order of magnitude.

In this respect valence electrons can be classified into two groups: *a*) Valence electrons for which the overlap of atomic eigenfunctions on neighbouring atoms is great, such as the *s* and *p* electrons of the outermost shell. The eigenfunction of these can be well approximated in the whole elementary cell by a plane wave, if the end point of the wave number vector is not in the neighbourhood of any of the boundary surfaces of the Brillouin zone. However, even in the latter case the linear combination of a few plane waves will yield a satisfactory result, as even in the most intricate case, when the planes bounding the zone cut each other, there are at most four Brillouin zones and not many more reciprocal lattice vectors determining the former. *b*) As belonging to the second group we may classify the *d* and *f* electrons of transition metals. In our approximation these can of course also be described by an eigenfunction which is free of internal nodal surfaces and here our method also provides for a significant simplification. In the case of these electrons a greater difficulty lies in that the eigenfunctions of *d* and *f* electrons keep their atomic character and form, rather than do those of the other electrons. This is due to the fact that the spatial dimensions of the *d* and *f* atomic eigenfunctions are smaller than that of the outermost *s* and *p* electrons. The difficulty here lies in the fact that for the description of these states such a linear combination of plane waves must be selected, which is similar to the eigenfunctions of the atomic *d* electrons in the greater part of the elementary cell (particularly in most part of the neighbourhood of the nuclei). To this end, of course, several plane waves must be superimposed. Further investigations would be necessary to decide whether the difficulties encountered here are significant.



## LITERATURE

1. E. WIGNER and F. SEITZ, *Phys. Rev.*, **43**, 804, 1933.  
For the more recent literature cf. e. g. F. SEITZ: *The Modern Theory of Solids*, McGraw-Hill Book Company, London, 1940.
2. J. C. SLATER, *Phys. Rev.*, **45**, 794, 1934.
3. W. SHOCKLEY, *Phys. Rev.*, **52**, 866, 1937.
4. F. G. VON DER LAGE and H. A. BETHE, *Phys. Rev.*, **71**, 612, 1947.
5. J. C. SLATER, *Phys. Rev.*, **51**, 846, 1937.
6. See e. g. P. GOMBÁS, *Statistische Theorie des Atoms und ihre Anwendungen*, Wien, Springer, 1949, p. 299, where the older literature can be found.
7. C. C. HERRING, *Phys. Rev.*, **57**, 1169, 1940.
8. See e. g. N. F. MOTT and I. N. SNEDDON, *Wave Mechanics and Its Applications*, Oxford Clarendon Press, 1948, p. 235.
9. See e. g. R. GÁSPÁR, *Acta Debreceniensis*, **2**, 151, 1955.
10. R. GÁSPÁR, *Acta Phys. Hung.*, **2**, 31, 1952.
11. See e. g. GEIGER—SCHEELS, *Handbuch der Physik*, XXIV/2, 2. Aufl., Springer, Berlin, 1933, p. 370.
12. For the definition of the reciprocal lattice see e. g. l. c. [11] and other books on the theory of solids, e. g. l. c. [1].
13. J. C. SLATER, *Phys. Rev.*, **92**, 603, 1953.
14. P. GOMBÁS, *Acta Phys. Hung.*, **1**, 285, 1952.
15. S. FLÜGGE, *Encyclopaedia of Physics*, XXXVI, Springer Verlag, Berlin, 1956. p. 109.  
P. GOMBÁS's article on "Statistische Behandlung des Atoms".
16. H. HELLMANN, *Acta Physicochimica URSS*, **1**, 913, 1935.

## ОПРЕДЕЛЕНИЕ ЗОННОГО ЭНЕРГЕТИЧЕСКОГО СПЕКТРА ЭЛЕКТРОНОВ В МЕТАЛЛАХ

Р. ГАШПАР

### Резюме

В работе выработан новый метод для определения зонного спектра электронов в металлах. Существенное преимущество метода, что он пользуется чистыми плоскими волнами. Это достигается тем, что в случае плоских волн вводится дополнительный потенциал для возмещения большой кинетической энергии собственных функций, осциллирующих в близости атомных ядер. Таким образом электроны проводимости можно трактовать так, как будто бы они заполняли зоны Бриллюэна постепенно, начиная от низшей. Это значит, что собственные функции металлических электронов хорошо аппроксимируются комбинацией нескольких плоских волн. Степень секулярных уравнений на вырожденных местах вблизи границы зон Бриллюэна является низкой. Детально исследованы в работе проблемы секулярного уравнения в связи с дополнительным потенциалом. Показано, что матричные элементы дополнительного потенциала таковы, что они не изменяют качественную структуру секулярного уравнения. Значение матричных элементов гамильтониана меняется в зоне Бриллюэна с места на место. Этот факт значительно увеличивает объем исчислительной работы по отношению к старшей модели со свободными электронами. По отношению к более новым методам, это не является недостатком, так как — хотя по этой причине — там встречается подобное же положение.



# BESTIMMUNG DES VERHÄLTNISSSES ZWISCHEN DER ZAHL DER PHOTONEN UND DER ZAHL DER ELEKTRONEN IN DEN AUSGEDEHNTEN LUFTSCHAUERN DER KOSMISCHEN STRAHLUNG MITTELS EINER WILSONKAMMER

Von

I. DOHÁN,\* T. GÉMESY, T. SÁNDOR und A. SOMOGYI

ZENTRALFORSCHUNGSINSTITUT FÜR PHYSIK DER UNGARISCHEN AKADEMIE DER WISSENSCHAFTEN  
BUDAPEST, ABTEILUNG FÜR KOSMISCHE STRAHLEN

(Vorgelegt von L. Jánossy. — Eingegangen : 14. X. 1957)

In eine Wilsonkammer, deren effektiver Querschnitt  $300 \text{ cm}^2$  war, wurden 7 Bleiplatten von insgesamt 33 mm Dicke gelegt. Die Kammer wurde von einer Apparatur für ausgedehnte Luftschauer gesteuert, und die Zahl der primären Elektronen und primären Elektronenpaare gezählt. Nach Anbringung einer Korrektur für die Anzahl der durchdringenden Photonen wurde das Verhältnis der Zahl der Photonen zu der Zahl der Elektronen in den ausgedehnten Luftschauern zu  $1,16 \pm 0,04$  erhalten.

## I

Eine grosse Zahl von Forschern beschäftigte sich bereits mit der Bestimmung des Verhältnisses der Zahl der Photonen zu der Zahl der Elektronen in den ausgedehnten Luftschauern [1]—[7], jedoch kann die Frage noch nicht als endgültig gelöst angesehen werden. Die bisherigen Messungen nämlich, die ausschliesslich mit Zählrohren durchgeführt wurden, ergaben für dieses Verhältnis einen meist wesentlich kleineren Wert als 1, obwohl man auf Grund der Theorie einen 1 nahestehenden Wert erwarten sollte.

Unsere neuerdings mit der Zählrohrmethode durchgeführten Messungen [6] weisen auf eine prinzipielle Schwierigkeit dieser Methode hin, die kaum zu überwinden ist. In dem folgenden Abschnitt geben wir eine kurze Beschreibung dieser Schwierigkeit.

## II

Die Bestimmung des Verhältnisses der Anzahl von Photonen zur Anzahl der Elektronen in ausgedehnten Luftschauern (im folgenden: der Quotient  $p/e$ ) mit Hilfe von Zählrohren beruht, wie bekannt, auf der Messung des sogenannten Übergangsfaktors, mit welchem Namen wir die Grösse

$$R(\theta) = p(\theta) + a q(\theta) \quad (1)$$

bezeichnen.  $p(\theta)$  bedeutet hier die Wahrscheinlichkeit dafür, dass ein Elektron entweder selbst eine Bleischicht der Dicke  $\theta$  durchdringt oder in dieser Schicht

\* Äusserer Mitarbeiter.

wenigstens ein solches ionisierendes Sekundärteilchen erzeugt, das die Schicht durchdringen kann.  $q(\theta)$  bedeutet die Wahrscheinlichkeit, mit welcher ein Photon in der Bleischicht  $\theta$  wenigstens ein solches ionisierendes Sekundärteilchen erzeugt, das die Bleischicht zu durchdringen vermag, und endlich  $\alpha$  bedeutet den Quotienten  $p/e$ . Die Werte von  $p(\theta)$  und  $q(\theta)$  sind auf Grund der Berechnungen von ARLEY [8] als bekannt vorausgesetzt. Es sei hier bemerkt, dass ARLEY diese Berechnungen nicht für das Energiespektrum der Elektronen und Photonen der ausgedehnten Luftschauer, sondern für das Energiespektrum der Elektronen- und Photonenkomponenten der totalen kosmischen Strahlung durchgeführt hat.

Der Wert von  $R(\theta)$  kann experimentell ermittelt werden und mittels  $R(\theta)$ ,  $p(\theta)$  und  $q(\theta)$  kann  $\alpha$  aus (1) bestimmt werden. Antikoinzidenzmessungsgestatten auch die experimentelle Bestimmung von  $\alpha q(\theta)$ . Die Berechnung des  $\alpha$  Wertes aus  $\alpha q(\theta)$  geschieht prinzipiell ebenso wie aus  $R(\theta)$ .

Die Messung von  $R(\theta)$  kann folgendermassen durchgeführt werden: Man misst die Anzahl der ausgedehnten Luftschauer pro Stunde mit einer bestimmten Apparatur ohne Absorber [ $C(0)$ ], und dann diese Anzahl mit derselben Apparatur, jedoch unter einer Bleischicht der Dicke  $\theta$ . [ $C(\theta)$ ]. Wie bekannt ist dann

$$C(\theta)/C(0) = R(\theta)^\gamma,$$

wo  $\gamma$  den Exponenten des Dichtespektrums der ausgedehnten Luftschauer bedeutet.

Unsere Messungen ergaben, dass der Quotient  $C(\theta)/C(0)$  von der Grösse der Oberfläche der Beobachtungszählrohre abhängt. Ein ähnliches Resultat, obzwar weniger ausgeprägt, erhielten bereits andere Verfasser [1], [2]. Ein solcher Effekt kann möglicherweise durch die Geometrie der Anordnung hervorgerufen werden, z. B. Streuung und Multiplikation der Schauerteilchen im Blei. Der Effekt kann aber auch eine Folge der Struktur der ausgedehnten Luftschauer sein, d. h. es ist möglich, dass der Übergangsfaktor der Luftschauer verschiedener durchschnittlicher Dichte tatsächlich verschieden ist. Unsere Kontrollmessungen und die ausführliche Analyse, durchgeführt von einem der Verfasser [7], ergaben, dass der Effekt in erster Linie mit der Struktur der ausgedehnten Luftschauer verknüpft ist. Dies bedeutet aber, dass die Berechnungen von ARLEY für die Ermittlung von  $p(\theta)$  und  $q(\theta)$  nicht benützt werden können; und weiter dass der Quotient  $p/e$  wohl kaum aus dem Übergangsfaktor bestimmt werden kann.

### III

Diese Bedenken führten uns dazu, den Quotienten  $p/e$  mit der Wilsonkammer zu bestimmen. Die Wilsonkammermethode erübrigt theoretische Berechnungen: der Quotient  $p/e$  kann durch einfache Abzählung der Elek-

tronenspuren und der von Photonen stammenden Elektronenpaare leicht ermittelt werden. Ausser der Bestimmung des Quotienten  $p/e$  ist die Wilsonkammer prinzipiell auch zur direkten Messung des Übergangsfaktors geeignet und bietet so eine Möglichkeit zur Prüfung der mit Zählrohren erhaltenen Resultate, also zur Entscheidung dessen, ob der Übergangsfaktor tatsächlich von der Schauerstruktur abhängig ist. Andererseits treten bei der Wilsonkammermethode gewisse Schwierigkeiten auf: Wegen der endlichen Ausdehnung der Kammer und der Wirkung der die Kammer umhüllenden Materie müssen gewisse nicht leicht abschätzbare Korrekturen gemacht werden.

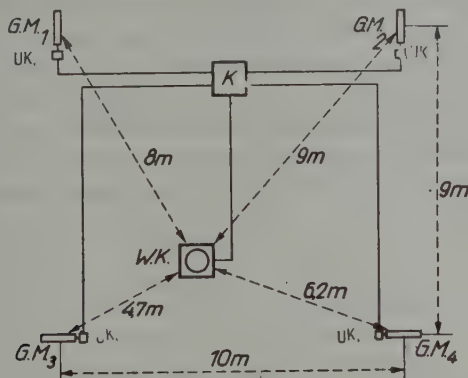


Abb. 1. Anordnung der Wilsonkammer und der GM-Rohre

GM — G.M. Zählrohre  
 UK — Umformungskreis  
 K — Koinzidenzgerät  
 WK — Wilsonkammer

Wir haben nun mit der Wilsonkammer zunächst den Quotienten  $p/e$  bestimmt. Wir setzten in unsere Zylinderförmige Wilsonkammer von  $300 \text{ cm}^2$  Oberfläche 3 Stück 3 mm dicke und 4 Stück 6 mm dicke Bleiplatten untereinander ein. Die Glaswand der Kammer hatte eine Dicke von  $0,8 \text{ g/cm}^2$ , und die Dicke des Deckels des temperierten Holzkastens, der die Kammer enthielt, betrug ungefähr  $1 \text{ g/cm}^2$ , während der Deckel der Holzkiste, in welcher sich der ganze Apparat befand, ungefähr eine Dicke von  $8 \text{ g/cm}^2$  hatte. Die Materiemenge über dem wirksamen Volumen der Kammer betrug somit etwa  $10 \text{ g/cm}^2$ . Die Messungen erfolgten in 410 m Meereshöhe. Eine ausführliche Beschreibung der Konstruktion und der technischen Angaben der Wilsonkammer ist in den Arbeiten [9] zu finden.

Die Kammer wurde von einem Viererkoinzidenzsignal gesteuert, welches von den vier Zählrohren von je  $320 \text{ cm}^2$  Oberfläche einer Messanordnung für ausgedehnte Luftschauer kam. Die Zählrohre befanden sich in den Ecken eines Quadrats von 10 m Seitenlänge (siehe Abb. 1).

Die Messungen wurden im Herbst 1956 begonnen und mit einer Unterbrechung von etwa 3 Monaten bis April 1957 fortgesetzt. Im Laufe dieser Zeit machten wir während 970 Stunden insgesamt 2350 Aufnahmen. Wir haben jene Aufnahmen die nur ein Primärteilchen aufwiesen, ausser acht gelassen, denn abgesehen von den von der Radioaktivität der Umgebung stammenden Spuren, die leicht erkennbar sind, besteht noch immer eine ungefähr 10%-ige Wahrscheinlichkeit dafür, dass auf einer Aufnahme ein »fremdes« Teilchen aus der kosmischen Strahlung vorkommt, d. h. ein solches, das mit dem ausgedehnten Luftschauer, der die Kammer steuert, nichts zu tun hat. Auch jene Aufnahmen wurden nicht ausgewertet, die mehr als 7 Primärelektronen zeigten. Auf solchen Aufnahmen kann nämlich die Zahl der Primärphotonen nicht bestimmt werden, da man nicht eindeutig feststellen kann, ob ein Elektronenpaar aus einem Primärphoton oder aber aus einem durch die Elektronen erzeugten Sekundärphoton entstanden ist.

Die Zahl der mit diesen Beschränkungen ausgewerteten Aufnahmen betrug 948. Tabelle I enthält die Gruppierung dieser Aufnahmen nach der

Tabelle I

$\begin{array}{c} e \\ \backslash \\ P \end{array}$	0	1	2	3	4	4—7
0			80	19	3	0
1		222	82	27	7	0
2	127	105	44	33	16	1
3	31	40	26	21	9	2
4	9	6	8	8	12	4
4—7	0	0	1	1	1	3

Anzahl der auf denselben sichtbaren Primärelektronen und Photonen. Von den weggelassenen Aufnahmen waren 1016 solche, auf denen gar kein Luftschauerteilchen zu beobachten war, 332 wiesen nur ein Primärteilchen auf und 54 konnten wegen der grossen Zahl der Primärteilchenspuren nicht ausgewertet werden.

Infolge der erwähnten Bedingungen zeigten die ausgewerteten Aufnahmen ausgedehnten Luftschauer, deren durchschnittliche Dichte zwischen 30 Elektronen/m<sup>2</sup> und 200 Elektronen/m<sup>2</sup> lag. Auf den Aufnahmen wurden insgesamt 1635 primäre Elektron-Positron Paare und 1458 primäre Elektronenspuren gezählt. Der Wert des Quotienten  $p/e$  ergibt sich daher ohne jedwede Korrektur zu  $1,12 \pm 0,04$ .



## IV

Der auf diese Weise ermittelte Zahlenwert bedarf jedoch aus mehreren Gründen einer Korrektur.

a) Die wichtigste Korrektur ist darauf zurückzuführen, dass in den Bleiplatten der Kammer nicht alle Primärphotonen Elektronenpaare erzeugen. Die in der Kammer angebrachten 3 Stück 3 mm dicken und 4 Stück 6 mm dicken Platten entsprechen ungefähr 5,75 Kaskadeneinheiten (siehe die in [10] mitgeteilten Daten). Die Wahrscheinlichkeit dafür, dass ein Photon, das eine Energie über 1 MeV besitzt, im Blei der besagten Dicke weder durch einen Compton-effekt noch durch Paarbildung ein Elektron erzeugt, schwankt je nach der Energie zwischen 28% und 1,1%. Der zuerst erwähnte Wert bezieht sich auf Photonen von 2,6 MeV, der zweiterwähnte auf Photonen von einer Energie über  $10^3$  MeV. Wenn man annimmt, dass die durchschnittliche Energie der Photonen der auf die Luft bezogenen kritischen Energie, d. h. 84 MeV [10], gleich ist, so erhält man für die Wahrscheinlichkeit des spurlosen Durchdringens von über 5,75 Kaskadeneinheiten 3,4%.

Die durchschnittliche Reichweite der Photonen im Blei ist teils wegen der Form der Kammer, teils zufolge dessen, dass Schauer auch aus seitlichen Richtungen eintreffen, prinzipiell nicht gleich den vorher erwähnten 33 mm. Annähernde Berechnungen ergeben aber, dass die Grösse der Reichweite dennoch in der Nähe von 33 mm liegt, und zwar wahrscheinlich weil das Anwachsen der Reichweite in den einzelnen Platten — was die Folge der schrägen Einfälle ist — grösstenteils durch die Abnahme der Reichweite jener aus Seitenrichtungen einfallenden Photonen, die nicht jede einzelne Platte durchlaufen, kompensiert wird.

b) Auch der etwaige Effekt der über der Kammer angebrachten Materie muss in Betracht gezogen werden. Dieser Effekt kann zweierlei sein. Reine Absorption (ohne Aussendung eines Sekundärteilchens) oder Umwandlung von Elektronen in Photonen und vice versa.

Die reine Absorption hat zur Folge, dass der von uns ermittelte Quotient  $p/e$  nur die Anzahl jener Photonen und Elektronen darstellt, die eine Materiemenge von mehr als  $10 \text{ g/cm}^2$  zu durchdringen vermögen; dies bedeutet, dass der ganz niedrigen Energien entsprechende Spektralbereich durch die über der Kammer befindliche Materie absorbiert wird.

Die gegenseitige Umwandlung von Elektronen und Photonen hat auf den Quotienten  $p/e$  keinen bedeutenden Einfluss, da der in Rede stehende Absorber von  $10 \text{ g/cm}^2$  zum grössten Teil aus Holz d. h. aus leichten Elementen besteht, also insgesamt höchstens  $1/3$  Kaskadeneinheit darstellt. Es sei noch bemerkt, dass der grösste Teil ( $8 \text{ g/cm}^2$ ) des Absorbers ziemlich hoch (2,5 m) über der Kammer liegt und dass deshalb auch der Einfluss des Dichteeffektes vernachlässigt werden kann.

## V

Aus unseren Messungen und mit der im Kapitel IV/a erwähnten Korrektur ergibt sich das Verhältnis zwischen der Anzahl von Photonen und Elektronen der Reichweite über  $10 \text{ g/cm}^2$  in ausgedehnten Luftschauern, deren mittlere Dichte zwischen  $30 \text{ Elektronen/m}^2$  und  $200 \text{ Elektronen/m}^2$  liegt zu

$$\alpha = 1,16 \pm 0,04,$$

wenn bei der Abschätzung der Anzahl der unbeobachtet gebliebenen Photonen als durchschnittliche Photonenenergie  $84 \text{ MeV}$  angenommen wird. Der angegebene Fehler ist der statistische. Berücksichtigt man die für Photonen über  $10^3 \text{ MeV}$  Energie gültige Korrektur, so erhält man  $p/e = 1,13 \pm 0,04$ . Berücksichtigung der Korrektur, die sich auf die Photonen grössten Durchdringungsvermögens (von der Energie um  $2,6 \text{ MeV}$ ) bezieht, ergibt  $p/e = 1,43 \pm 0,04$ . Der genaue Korrektionswert könnte nur errechnet werden, wenn das Energiespektrum der Photonen bekannt wäre. Die Wilsonkammer ist im Prinzip zur Bestimmung dieses Spektrums geeignet und wir haben die Absicht, unsere Untersuchungen in dieser Richtung zu erweitern.

Es sind uns keine früheren mit Wilsonkammern durchgeführte Messungen von  $p/e$  in ausgedehnten Luftschauern bekannt und wir können daher zum Vergleich nur die Messresultate der mit Zählrohren durchgeführten Messungen angeben (Tabelle II).

Tabelle II

Verfasser	Oberfläche der Beobachtungszählrohre	Gemessene $p/e$ Werte
BASSI, BIANCHI,	$400 \text{ cm}^2$	$\sim 0,3$
MANDUCHI [1]	$1200 \text{ cm}^2$	$\sim 0,12$
MILONE [2]	$600 \text{ cm}^2$	$0,75 \pm 0,15$
	$1800 \text{ cm}^2$	$0,75 \pm 0,20$
MASSALSKI [4]	$3000 \text{ cm}^2$	$\sim 1$

Das Messresultat der Wilsonkammermethode zeigt eine erhebliche Divergenz gegenüber dem der Zählrohrmessungen. Es ist beachtenswert, dass das Ergebnis der Wilsonkammermessungen mit der Kaskadentheorie, nach welcher der Wert des Quotienten  $p/e$  nahe 1 liegt, gut übereinstimmt. Die Abweichung zwischen den Resultaten der beiden Methoden ist wahrscheinlich der bei den Zählrohren verwendeten Messmethode zuzuschreiben; die im

Kapitel II beschriebene Mangelhaftigkeit dieser Methode mag wohl der Grund der grossen Abweichung sein.

Die Verfasser sind Herrn Professor L. JÁNOSSY für seine wertvollen Hinweise zu Dank verpflichtet.

#### LITERATUR

1. P. BASSI, A. M. BIANCHI und T. MANDUCHI, *Nuovo Cimento*, **8**, 735, 1951; **9**, 358, 1952.
2. C. MILONE, *Nuovo Cimento*, **9**, 549, 1952; **11**, 241, 1954 und *Phys. Rev.*, **87**, 680, 1952.
3. D. D. MILLAR, *Nuovo Cimento*, **8**, 279, 1951.
4. J. M. MASSALSKI, *Bull. Ac. Pol. Sci.*, **2**, 335, 1954.
5. BRUIN, Thesis, Amsterdam, 1952.
6. L. JÁNOSSY, T. SÁNDOR und A. SOMOGYI, *Acta Phys. Hung.*, **6**, 455, 1957.
7. A. SOMOGYI, *Acta Phys. Hung.*, **7**, 189, 1957.
8. N. ARLEY, *On the Theory of Stochastic Processes*, Wiley, New York, 1948, p. 165.
9. K. KÁNTOR, *Mitteilungen des Zentralforschungsinstitutes für Physik, Budapest*, **2**, 155, 1954; und K. KÁNTOR—K. ZSDÁNSZKY, *Magyar Fizikai Folyóirat*, im Druck.
10. B. ROSSI, *High-Energy Particles* (Prentice Hall, New York, 1952); p. 295.

#### ОПРЕДЕЛЕНИЕ ОТНОШЕНИЯ ЧИСЛА ФОТОНОВ И ЭЛЕКТРОНОВ В ШИРОКИХ АТМОСФЕРНЫХ ЛИВНЯХ КОСМИЧЕСКОГО ИЗЛУЧЕНИЯ КАМЕРОЙ ВИЛЬСОНА

И. ДОГАН, Т. ГЕМЕШИ, Т. ШАНДОР и А. ШОМОДИ

#### Резюме

В камере Вильсона, с эффективной поверхностью 300 см<sup>2</sup>, было помещено 7 пластин свинца с общей толщиной 33 мм. Камера управлялась аппаратурой для широких атмосферных ливней, затем производился счет первичных электронов и электронно-позитронных пар, принимая во внимание поправку из-за проникающих фотонов, полученное отношение числа фотонов к электронам в широких атмосферных ливнях составляет  $1,16 \pm 0,04$ .



# THE UNITED ATOM MODEL OF THE $HF$ MOLECULE

By

R. GÁSPÁR and I. TAMÁSSY-LENTEI

INSTITUTE OF THEORETICAL PHYSICS OF THE KOSSUTH LAJOS UNIVERSITY OF SCIENCES, DEBRECEN

(Presented by P. Gombás. — Received : XI. 3. 1957)

The united atom, which was used by the spectroscopists at the estimation of molecular-term values for more than two decades, is a suitable model in quantum chemistry too. The main features of the model are as follows : 1. Generally the nuclei are not moved adiabatically in one point, as they do in the united atom of spectroscopists, but hold their original equilibrium position or make little deviations from it. 2. The molecular eigenfunction is built up of one center one electron eigenfunctions according to the SLATER method. Excepting the geometrical configuration of the nuclei there is not any empirical or semiempirical parameter in this model. The calculations are extended to the treatment of the molecule  $HF$ . The theoretical values of the total energy, the dissociation energy and the equilibrium nuclear separation are in good agreement with the experimental ones.

## Introduction

It is relatively not very difficult to calculate the energy at atoms of small atomic number by the aid of quantummechanical methods — at least — if the precision required is not too great. The problem is, however, far more complicated regarding molecules, since the orbitals of the electrons in the molecules extend to more atoms, which with the methods hitherto used results in the eigenfunctions having more centers. Thus more-center integrals occur in the calculation of the energy, and the evaluation of these are generally very cumbersome. In investigations concerning molecules, beside the natural demand of obtaining as precise values as possible, another not less important requirement is that the time necessary for the accomplishment of the calculations should not be too long. Therefore in the following such approximations will be used when calculating the eigenfunctions of the molecules, that the numerical work will be essentially no greater than in the case of atoms.

For this purpose the united atom treatment for example seems to be very suitable, which has been adapted recently by MATSEN [1] for the determination of the excited states of the  $H_2^+$  molecule-ion. Further investigations [2] showed, that considering more configurations, the energy of the ground state of both the  $H_2^+$  molecule-ion and the  $H_2$  molecule can be determined well, though neither of these molecules can be taken in "good approximation" to be atomlike. Considering, that in the course of this treatment the molecule is always taken for a system having one center, i. e. for an "atom", good

results by this approximation can be expected chiefly for such molecules, where one of the centers is of far more importance than the others, i. e. where the molecule is more atom-like. Diatomic molecules of such kind are the halogen-hydride molecules, where the perturbing effect of the proton results in distortions in the spherically symmetrical, atom-like charge distribution of the negatively charged halogen ion. The calculations were carried out for the HF molecule.

### The method

The energy of the molecule will be calculated by the aid of the variational method. As is well known,

$$E = \frac{\int \Psi^* H \Psi dv}{\int \Psi^* \Psi dv},$$

where  $H$  is the Hamiltonian operator of the HF molecule and  $\Psi$  denotes its eigenfunction. The HF molecule has ten electrons. The Hamiltonian operator is thus

$$H = \sum_i H_i + \sum_{i > k} \frac{1}{r_{ik}} + \frac{Z}{R}, \quad (i, k = 1, 2, \dots, 10)$$

where  $H_i$  is the Hamiltonian operator of the  $i$ -th electron, disregarding the interaction between the electrons, that is

$$H_i = -\frac{1}{2} \Delta_i - \frac{Z}{r_i} - \frac{1}{r_{Hi}}$$

and

$$\Delta_i \equiv \frac{\partial^2}{\partial x_i^2} + \frac{\partial^2}{\partial y_i^2} + \frac{\partial^2}{\partial z_i^2}.$$

$R$  is the distance between the F and H nuclei;  $r_i$  is the distance of the  $i$ -th electron from the nucleus of the F-atom,  $r_{Hi}$  the distance of the  $i$ -th electron from the H nucleus,  $r_{ik}$  the distance between the  $i$ -th and  $k$ -th electron, and  $Z = 9$  is the charge on the nucleus of the F-atom. Throughout these calculations atomic units will be used; thus the electric charge will be expressed in  $e$ , the distance in  $a_0$  and the energy in  $e^2/a_0$  units, where  $e$  is the charge of the proton and  $a_0$  the radius of the first Bohr orbit in the hydrogen atom; these may all be found e. g. on page 10 of l. c. [3].

The trial eigenfunction of the HF molecule is built up of such one-electron eigenfunctions, that the distance  $r$ , occurring in their radial parts, is measured from the nucleus of the F-atom. The trial eigenfunction of the system is con-



structed of these and of the spin functions  $\alpha$  and  $\beta$  according to the well-known procedure of SLATER [4], and it is a determinant with ten rows and columns being antisymmetrical against the exchange of the electrons. This has the results, that in this theory the exchange interaction is considered.

The orthonormalized one-electron eigenfunctions were as follows :

$$\begin{aligned}\psi_{1s} &= R_{10}(r) Y_{00}(\vartheta, \varphi) = 2 a^{3/2} e^{-ar} \frac{1}{\sqrt{4\pi}}, \\ \psi_{2s} &= R_{20}(r) Y_{00}(\vartheta, \varphi) = \left( \frac{12 b^5}{a^2 - ab + b^2} \right)^{1/2} \left[ 1 - \frac{1}{3}(a+b)r \right] \frac{1}{\sqrt{4\pi}}, \\ \psi_{2px} &= R_{21}(r) \frac{Y_{11}(\vartheta, \varphi) + Y_{1,-1}(\vartheta, \varphi)}{\sqrt{2}} = \left( \frac{c^5}{24} \right)^{1/2} r e^{-\frac{cr}{2}} \sqrt{\frac{3}{4\pi}} \sin \vartheta \cos \varphi, \\ \psi_{2py} &= R_{21}(r) \frac{Y_{11}(\vartheta, \varphi) - Y_{1,-1}(\vartheta, \varphi)}{i \sqrt{2}} = \left( \frac{c^5}{24} \right)^{1/2} r e^{-\frac{cr}{2}} \sqrt{\frac{3}{4\pi}} \sin \vartheta \sin \varphi, \\ \psi_{2pz} &= R_{21}(r) Y_{10}(\vartheta, \varphi) = \left( \frac{d^5}{24} \right)^{1/2} r e^{-\frac{dr}{2}} \sqrt{\frac{3}{4\pi}} \cos \vartheta.\end{aligned}$$

Here  $a$ ,  $b$ ,  $c$  and  $d$  are the variational parameters, which have been determined so as to satisfy the requirement to reduce the total energy to a minimum. Considering that the  $z$ -axis was taken as the axis of the molecule, the electron distribution in the ground state may be assumed to be symmetrical around the  $z$ -axis and consequently the parameters of the functions  $\psi_{2px}$  and  $\psi_{2py}$  may be chosen to be equal.

Calculating the energy, which is the mean value of the operator  $H$ , we have the following types of integrals :

$$\left. \begin{aligned}I_j &= \int \psi_j^*(i) \left( -\frac{1}{2} \Delta_i - \frac{Z}{r_i} \right) \psi_j(i) d v_i, \\ C_{jl} &= \int \psi_j^*(i) \psi_l^*(k) \frac{1}{r_{ik}} \psi_j(i) \psi_l(k) d v_i d v_k, \\ A_{jl} &= \int \psi_j^*(i) \psi_l^*(k) \frac{1}{r_{ik}} \psi_l(i) \psi_j(k) d v_i d v_k, \\ L_j &= \int \psi_j^*(i) \frac{1}{r_{Hi}} \psi_j(i) d v_i.\end{aligned} \right\} \quad (*)$$

Here  $I$  denotes the term due to the kinetic energy of the electron and its Coulomb interaction energy with the nucleus of the F-atom;  $C$  is the Coulomb

interaction energy of the electrons,  $A$  the exchange energy and  $L$  a term resulting from the Coulomb attraction of the electron and the H nucleus. Three of the integrals  $I$ ,  $C$  and  $A$  are usual types occurring also in atomic problems. Only  $L$  is a two-center integral. A detailed expression for the energy will be given in the Appendix.

### Results

As a result of the variation the following values were obtained for the energy of the HF molecule in the ground state :

$$E_{HF} = -99,016$$

for the following values of the variational parameters :

$$a = 8,7; \quad b = 3,1; \quad c = 4,9; \quad d = 4,4.$$

The distance  $R$  between the nuclei naturally has been also taken for a variational parameter. (Thus there have been five parameters including  $R$ .) The value obtained for  $R$  is :

$$R = 1,57.$$

The experimental values of the energy and of the equilibrium nuclear separation are [5]:  $E = -100,489$ ,  $R = 1,73$ . The agreement with the experimental data can be considered as good.

A further aim of the calculations was to determine the dissociation energy of the HF molecule. The halogen hydrides in general dissociate into atoms and so does the HF too. This implies, that it would be necessary to calculate the energy of the F atom to the same approximation as was done for the HF molecule so as to obtain the dissociation energy. Instead of this it was simpler, however, to calculate the dissociation energy by the aid of a Born cycle from the energy of the  $F^-$  and  $H^+$  ions, taking into account the electron affinity of the F atom and the ionization energy of the H atom; since the  $F^-$  ion is a system having ten electrons just as the HF molecule, the neglects due to the approximations in both processes are similar.

Having obtained the analytical formulas for the energy of the HF molecule, the energy of the  $F^-$  ion can be easily obtained also with the variational method. The Hamiltonian of the  $F^-$  ion differs from that of the molecule only in so far as the energy term due to the Coulomb interaction between the electrons and the H nucleus, i. e.  $1/r_{Hi}$ , and the Coulomb interaction energy term of the nuclei, i. e.  $Z/R$ , do not occur in it. Then we have

$$H = \sum_i \left( -\frac{1}{2} \Delta_i - \frac{Z}{r_i} \right) + \sum_{i>k} \frac{1}{r_{ik}} \quad (i, k = 1, 2, \dots, 10)$$

The approximate eigenfunction of the  $F^-$ -ion has evidently to be constructed of the same one-electron eigenfunctions as were used in the treatment of the molecule. However, the electron configuration of the  $F^-$ -ion is like that of a rare gas, i. e.  $(1s)^2(2s)^2(2p)^6$ , and thus the charge density is spherically symmetrical. Consequently not only the variational parameters of the functions  $\psi_{2px}$  and  $\psi_{2py}$  agree, but that of  $\psi_{2pz}$  is also the same ( $c = d$ ) and there will be only three variational parameters. When taking the mean value of the Hamilton operator, integrals of the same type occur as before, except for the  $L$ . The detailed energy expression is also to be found in the Appendix.

As the result of the variational procedure the best parameter values obtained were

$$a = 8,7, \quad b = 3,1, \quad c = d = 4,6$$

and the energy

$$E_{F^-} = -98,468.$$

The electron affinity of the  $F^-$ -ion was determined experimentally [6] to be  $0,15_0$  and consequently the dissociation energy of the HF molecule i. e. the energy, which is necessary for the dissociation of the HF molecule into an F and an H atom is easily obtained with the aid of the Born cycle as

$$D = 0,19_8.$$

The experimental value of the dissociation energy is  $D = 0,23_5$  [5] and thus the deviation from it is approximately 15 per cent.

### Discussion

Calculations have been made by several authors to obtain certain data of the HF molecule. CH. R. MUELLER [7] used semilocalized orbitals and his result for the binding energy is better ( $0,1648$ ), than those obtained by the valence-bond or the molecular-orbital method. Zs. NÁRAY [8] has determined the energy of dissociation into the  $F^-$  and  $H^+$  ions and the equilibrium nuclear separation of the molecule by the aid of a special wave-mechanical perturbation theory with an error of not more than 10–11 per cents. Calculations of similar character have been carried out also by INGA FISCHER-HJALMARS [9] concerning the dipolmoment of the HF molecule.

When the eigenfunction of the HF molecule is selected as in atomic problems with central symmetry, the calculated energy and dissociation energy of the molecule show good agreement with the experimental data. The results are comparable with those obtained by the methods with many center molecular orbitals. The eigenfunction constructed of one-electron eigenfunctions having one center of reference only gives a good approximation when calculating the energy. It is to be noted, however, that comparing for example the radial charge density of the electrons of the  $F^-$  ion with that of the HF molecule, no essential difference is obtained. The charge density of the molecule is almost spherically symmetrical. The charge density of the  $F^-$  ion is naturally obtained by the method presented here — as

it is in reality — as spherical symmetrical. The charge density of the HF molecule, however, is deformed by the presence of the proton. The united atom model in its present form, however, cannot take this effect sufficiently into account, and in this model the charge density of the electrons merely extends in the direction of the  $z$ -axis and slightly contracts perpendicular to it. The charge density of the molecule is also symmetrical with respect to the nucleus of the  $F^-$  ion and the model cannot give the great electron density near to the proton in the molecule. This short-coming plays evidently an essential role in the discrepancy between the calculated energy of the molecule and its experimental value. It follows further that the calculated value of the equilibrium nuclear separation must be less than the experimental one, is a natural consequence of the united atom model. From this it may be already suspected, that such constants of the molecule, for which the charge density of the electron itself is essential, will be obtained less precisely. So e. g. nearly the double of the experimental value is obtained for the dipolmoment of the HF molecule.

The method can be improved when the one-electron eigenfunctions  $\psi_{1s}$ ,  $\psi_{2s}$  and  $\psi_{2p}$  or at least those, which are important from the point of view of the molecule formation, are constructed by the superposition of two or more functions. In the model of the molecule presented here it seemed suitable for example to use the linear combination  $\psi_{2pz} + c \psi_{3dz}$  instead of  $\psi_{2pz}$ . In this way, namely, not only one spherical harmonic occurs in the one-electron eigenfunctions, and this can favorably influence the distribution of the charge density near the proton. Naturally the symmetry characteristics of the molecule have to be taken into consideration in the selection of the new eigenfunction. As our calculations have shown the results really improved, consequently, such eigenfunctions are more suitable for the description of the properties of the molecule. The calculations have naturally been considerably more complicated, since the introduction of a new term in the one-electron eigenfunction implies the introduction of two more variational parameters, which considerably increased the numerical work.

## Appendix

In the energy expression of the HF molecule, integrals of the type  $I_j$ ,  $C_{jl}$ ,  $A_{jl}$  and  $L_j$  occur in the equation (\*). Evaluating the integrals  $C_{jl}$  and  $A_{jl}$ ,  $1/r_{ik}$  has been as usually expanded into a series in terms of the Legendre polynomials in the following manner

$$\frac{1}{r_{ik}} = \sum_{h=0}^{\infty} \sum_{m=-h}^h \frac{(h-|m|)!}{(h+|m|)!} \frac{r_{<}^h}{r_{>^{h+1}}} P_h^{(m)}(\cos \vartheta_i) P_h^{(m)}(\cos \vartheta_k) e^{im(\varphi_i - \varphi_k)}.$$

The integral  $C_{jl}$  by this expansion becomes

$$C_{jl} = \sum_{h=0}^{\infty} a^h(l, m_l; l', m_{l'}) F^h(n, l; n', l'),$$

where

$$F^h(n, l; n', l') = \int_0^{\infty} \int_0^{\infty} R_{nl}^2(r_i) R_{n'l'}^2(r_k) \frac{r_{<}^h}{r^{h+1}} r_i^2 r_k^2 dr_i dr_k$$

and

$$a^h(l, m_l; l', m_{l'}) = \frac{(2l+1)(l-|m_l|)!}{2(l+|m_l|)!} \cdot \frac{(2l'+1)(l'-|m_{l'}|)!}{2(l'+|m_{l'}|)!} \times$$

$$\times \int_0^{\pi} \{P_l^{m_l}(\cos \vartheta_i)\}^2 P_h(\cos \vartheta_i) \sin \vartheta_i d\vartheta_i \int_0^{\pi} \{P_{l'}^{m_{l'}}(\cos \vartheta_k)\}^2 P_h(\cos \vartheta_k) \sin \vartheta_k d\vartheta_k.$$

Entirely in the same way is obtained

$$A_{jl} = \sum_{h=0}^{\infty} b^h(l, m_l; l', m_{l'}) G^h(n, l; n', l'),$$

where

$$G^h(n, l; n', l') = \int_0^{\infty} \int_0^{\infty} R_{nl}(r_i) R_{n'l'}(r_i) R_{nl}(r_k) R_{n'l'}(r_k) \frac{r_{<}^h}{r^{h+1}} r_i^2 r_k^2 dr_i dr_k$$

and

$$b^h(l, m_l; l', m_{l'}) = \frac{(h-|m_l-m_{l'}|)!(2l+1)(l-|m_l|)!(2l'+1)(l'-|m_{l'}|)!}{4(h+|m_l-m_{l'}|)!(l+|m_l|)!(l'+|m_{l'}|)!} \times$$

$$\times \int_0^{\pi} P_l^{m_l}(\cos \vartheta) P_{l'}^{m_{l'}}(\cos \vartheta) P_h^{|m_l-m_{l'}|}(\cos \vartheta) \sin \vartheta d\vartheta^2.$$

The value of the coefficients  $a$  and  $b$  is to be found for example in the quoted work of SLATER [4].

Among the integrals only the  $L$ -integrals do not occur in atomic problems, but only in the case of molecules. The evaluation of such integrals of the two-center type does not present any serious difficulty (see for example GOMBÁS [3]). Where it was necessary, the expansion of  $1/r_{Hi}$  into a series mentioned above, was here also adapted. Otherwise the  $L$ -integrals can be easily evaluated in many cases by the introduction of elliptical coordinates.

Keeping in mind the above statements the following expressions were finally obtained for the energy of the HF molecule:

$$E = 2(I_{1s} + I_{2s} + I_{2px} + I_{2py} + I_{2pz}) +$$

$$+ F^0(1s; 1s) + 4F^0(1s; 2s) + 4F^0(1s; 2p_x) + 4F^0(1s; 2p_y) + 4F^0(1s; 2p_z) +$$

$$+ F^0(2s; 2s) + 4F^0(2s; 2p_x) + 4F^0(2s; 2p_y) + 4F^0(2s; 2p_z) +$$

$$\begin{aligned}
& + F^0(2p_x; 2p_x) + \frac{1}{25} F^2(2p_x; 2p_x) + 4 F^0(2p_x; 2p_y) + \frac{4}{25} F^2(2p_x; 2p_y) + \\
& + F^0(2p_y; 2p_y) + \frac{1}{25} F^2(2p_y; 2p_y) + 4 F^0(2p_x; 2p_z) - \frac{8}{25} F^2(2p_x; 2p_z) + \\
& + 4 F^0(2p_y; 2p_z) - \frac{8}{25} F^2(2p_y; 2p_z) + F^0(2p_z; 2p_z) + \frac{4}{25} F^2(2p_z; 2p_z) + \\
& - 2 \left( G^0(1s; 2s) + \frac{1}{3} G^1(1s; 2p_x) + \frac{1}{3} G^1(1s; 2p_y) + \frac{1}{3} G^1(1s; 2p_z) + \right. \\
& + \frac{1}{3} G^1(2s; 2p_x) + \frac{1}{3} G^1(2s; 2p_y) + \frac{1}{3} G^1(2s; 2p_z) + \frac{6}{25} G^2(2p_x; 2p_y) + \\
& + \frac{3}{25} G^2(2p_x; 2p_z) + \left. \frac{3}{25} G^2(2p_y; 2p_z) \right) \\
& - 2(L_{1s} + L_{2s} + L_{2px} + L_{2py} + L_{2pz}) + Z/R.
\end{aligned}$$

From symmetry considerations follows that the corresponding terms containing the functions  $\psi_{2px}$  and  $\psi_{2py}$  are here identical.

The evaluation of the energy of the  $F^-$  ion can be accomplished in the same way as that one of the HF molecule, since both systems have ten electrons. The explicit form of the energy will also be the same, only the terms containing  $L$  and  $Z/R$  will not occur. Because of the spherical symmetry of the ion naturally not only the terms containing  $\psi_{2px}$  and  $\psi_{2py}$  agree, but also those containing  $\psi_{2pz}$  are the same.

## REFERENCES

1. F. A. MATSEN, J. Chem. Phys., **21**, 928, 1953.
2. R. GÁSPÁR, Acta Phys. Hung., **7**, 151, 1957. — Acta Phys. Hung., **7**, 447, 1958.
3. P. GOMBÁS, Theorie und Lösungsmethoden des Mehrteilchenproblems der Wellenmechanik, Birkhäuser, Basel, 1950.
4. J. C. SLATER, Phys. Rev., **34**, 1233, 1929.
5. G. HERZBERG, Molecular Spectra and Molecular Structure. I. Spectra of Diatomic Molecules, D. Van Nostrand Company, Inc., New York, 1953.
6. LANDOLT-BÖRNSTEIN, Zahlenwerte und Funktionen, Bd. **1**, Teil I, Springer, Berlin, 1950.
7. CH. R. MUELLER, J. Chem. Phys., **19**, 1498, 1951.
8. ZS. NÁRAY, Magyar Fizikai Folyóirat, **1**, 85, 1953.
9. INGA FISCHER-HJALMARS, Arkiv för Fysik, **7**, 165, 1953.



## ОБЪЕДИНЕННАЯ АТОМНАЯ МОДЕЛЬ МОЛЕКУЛЫ HF

Р. ГАШПАР и И. ТАМАШИ-ЛЕНТЕИ

## Резюме

Объединенный атом, хорошо использованный спектроскопами для оценки положений молекулярных уровней, является и подходящей моделью для трактовки некоторых молекул. Существенные черты метода следующие: 1. Атомные ядра молекулы — в отличие от модели, использованной спектроскопами — сохраняют свои геометрические конфигурации и в процессе вариации они только мало смещаются с этого положения. 2. Собственная функция молекулы построена из одноцентровых — одноэлектронных собственных функций по методу Слетера. В методе эмпирическими или полуэмпирическими параметрами — кроме принятого геометрического расположения ядер — не пользуется. Вычисления произведены для молекулы HF. В этом случае полная энергия, энергия диссоциации и равновесное расстояние ядер хорошо согласуется с опытом.



# VARIATIONAL METHOD FOR THE SOLUTION OF THE QANTUMMECHANICAL MANY-BODY PROBLEM

By

K. LADÁNYI

RESEARCH GROUP FOR THEORETICAL PHYSICS OF THE HUNGARIAN ACADEMY OF SCIENCES, BUDAPEST

(Presented by P. Gombás. — Received XI. 4. 1957)

This paper gives a generalization of the variational method proposed by MACKE in the case of an outer potential of spherical symmetry. For a great number of particles and slowly changing potential this process becomes essentially the generalization of the statistical method based on grouping of the particles according to their azimuthal quantum number, however, it is well adaptable also for a few particles without any great difficulty. So as to lessen numerical difficulties three approximations will be given. Calculations made for the Ar atom disregarding the exchange effect, the calculated energy agrees with the semi-empirical value of SLATER within 5%.

## Introduction

As is well known the treatment of the wave-mechanical many-body problem is very complicated, so even the realization of the Hartree-Fock approximation needs a great deal of numerical calculations. Therefore it seems very useful to develop methods processes simpler than that of Hartree-Fock. For that purpose it is obvious to introduce approximations which enable the decreasing of the number of the various three-dimensional functions occurring in the density matrix or energy expression. Such approximation methods are essentially the Thomas-Fermi statistics and its generalizations too, where only one three-dimensional function in the energy expression is to submit to the variation [1—2]. However, the Thomas-Fermi method as well as its generalization introduced by WEIZSÄCKER gives slightly incorrect values for the energy in the case of atoms. GOMBÁS has shown, that the Thomas-Fermi method can be further developed in the framework of the statistical theory so as to give results which agree very well with the experimental data [3]. Many papers have recently been dealing with the wave mechanical foundation and developing of the theory [4, 5, 6]. In the present paper the foundation and generalization of the Thomas-Fermi method introduced by MACKE is essential [7]. On the base of the Ritz-method MACKE approximates the one-particle eigenfunctions with such variational assumptions, which give automatically the ortogonality relations. The closer investigation of the method in the case of reletively few particles is of great interest. The calculations for the one-dimensional case have been given by

MARCH, who has adapted the method for the harmonic linear oscillator. MARCH has mentioned calculations to be in preparation applying the method to the three-dimensional case too [8]. The present paper shows the possibility of generalization of this method for the treatment of problems of spherical symmetry.

### The foundation of the method

In the following a system of  $N$  particles will be discussed and its eigenfunctions will be approximated by the aid of a determinant. Since according to our assumptions the outer potential should have spherical symmetry, the one-particle eigenfunctions are to be taken in the form

$$\psi_i(q) = \frac{1}{2} R_{n_i l_i}(r) Y_{l_i m_i}(\vartheta, \varphi) \eta_i(\sigma), \quad (1)$$

where  $R_{n_i l_i}(r)$  is the radial eigenfunction,  $Y_{l_i m_i}(\vartheta, \varphi)$  the surface spherical harmonics, while  $\eta_i(\sigma)$  is the spinfunction in the  $i$ -th state. Taking  $N_{l_i}$  for the number of the occupied states belonging to the azimuthal quantum number  $l_i$  the following variational assumptions are introduced for the approximate determination of the radial eigenfunctions as well as of the energy:

$$R_{n_i l_i} = \frac{1}{\sqrt{N_{l_i}}} u_{l_i}(r) \varphi_{n_i}[y_{l_i}(r)], \quad (2)$$

where

$$\int u_{l_i}^2 dr = N_{l_i}, \quad (3)$$

$$\frac{dy_{l_i}}{dr} = \frac{1}{N_{l_i}} u_{l_i}^2, \quad (4)$$

and

$$y_{l_i}(0) = 0 \quad (5)$$

$$n_i = 0, 1, 2, \dots, \quad (6)$$

the functions  $\varphi_n$  form a real orthogonal system in the interval  $0 \leq y \leq 1$ .

$$\int_0^1 \varphi_{n_i}(y) \varphi_{n_j}(y) dy = \delta_{n_i n_j}. \quad (7)$$

By the aid of the expression (7) it is easy to show the fulfillment of the following orthogonality relations

$$\int R_{n_i l_i} R_{n_j l_j} dr = \delta_{n_i n_j}.$$

Then the radial density of the system averaged over the angular coordinates becomes

$$D = 4 \pi r^2 \rho = \sum_i u_i^2 s_i, \quad (8)$$

where  $\rho$  is the density averaged over the angular coordinates, further

$$s_i = \frac{1}{N_i} \sum_l^{(i)} |\varphi_{n_l}|^2.$$

In the above expression as well as in the following  $\sum^{(i)}$  means summation over the states with the azimuthal quantum number  $l_i$ .

Investigating the ground state of the system in the  $i$ -th one-particle state the quantum numbers  $n_i, l_i$  and the amplitudes  $u_{l_i}(r)$  are to be determined so, that fulfilling the orthogonality relations

$$\int \psi_i^*(q) \psi_j(q) d\tau = \delta_{ij}, \quad (9)$$

the energy should be minimum. It is evident, that the orthogonality relations (9) are realized in the case of arbitrary normalized functions  $u_{l_i}$  with proper values of  $n_i$  and  $l_i$  because of the orthogonality of the surface spherical harmonics.

It is to be noted, that for the above problem another method was proposed by MACKE which was based on the system of the eigenfunctions of a three-dimensional potential sphere [7]. However, the method presented here as well as its approximations to be discussed in the following seem to be easier to carry through.

With the above variational assumptions regarding the eigenfunctions the following terms give the kinetic energy  $E_K$  of the system

$$E_K = E_W + E_R + E_r + E_\varphi, \quad (10)$$

where  $E_W$  is the inhomogeneity correction,  $E_R$  is the analogous term to the radial part of the Fermi-energy,  $E_r$  is a correction of the radial kinetic energy and  $E_\varphi$  gives the azimuthal kinetic energy. The different energy terms can be brought into the following forms

$$E_W = \frac{\hbar^2}{2m} \sum_i \int \left| \frac{du}{dr} \right|^2 s_i dr \quad (11)$$

$$E_R = \frac{\hbar^2}{2m} \sum_i \int u_i^2 \frac{1}{N_i} \sum_l^{(i)} \left| \frac{d\varphi_{n_l}}{dr} \right|^2 dr, \quad (12)$$

$$E_i = \frac{1}{2} \frac{\hbar^2}{2m} \sum_l \int \frac{d u_l^2}{d r} \frac{d s_l}{d r} d r, \quad (13)$$

$$E_\varphi = \frac{\hbar^2}{2m} \sum_l \int \frac{l(l+1)}{r^2} u_l^2 s_l d r. \quad (14)$$

Proper choice of the functions  $\varphi_{n_i}(y_{l_i})$  is essential. In the present paper the following system of orthogonal functions will be used :

$$\begin{aligned} \varphi_{n_i}[y_{l_i}(r)] &= 1, & \text{when } n_i = 0, \\ \varphi_{n_i}[y_{l_i}(r)] &= \sqrt{2} \cos[\pi n_i y_{l_i}(r)], & \text{when } n_i \neq 0. \end{aligned} \quad (15)$$

With the above choice of the system of  $\varphi_n$  satisfactory analytic approximation of the functions  $u_l$  causes no serious difficulty neither in the vicinity of the nucleus nor for great values of  $r$ .

It has to be emphasized, that in the approximation discussed the  $R_{n_{i l_i}}$  functions cannot be regarded as the approximation of the radial one-particle eigenfunctions of Hartree  $R_{n_i+1, l_i}^{(H)}$ . Nevertheless the determinant constructed of the functions  $\psi_i(q)$  given by relation (1) is the approximation of the wave function of the whole system. Finally it is to be noted, that taking a sufficient number of particles, all the functions  $R_{n_i l_i}^{(H)}$  can be approximated by a suitable linear combination of the functions  $R_{n_i l_i}$

$$R_{n_i+1, l}^{(H)} \simeq \sum_j {}^{(l)} C_{n_i l, n_j l} R_{n_j l}.$$

Now the evaluation of the energy term based on the variation assumption (15) can be carried out. Taking into consideration the relation (4)

$$E_R = \sum_l \int \kappa_l(r) u_l^6 d r,$$

where

$$\kappa_l(r) = \frac{\hbar^2}{2m} \frac{\pi^2}{N_l^3} \sum_i {}^{(l)} n_i^2 2 \sin^2[\pi n_i y_l(r)];$$

further

$$E_r = - \frac{\hbar^2}{2m} \sum_l \frac{\pi}{N_l^2} \int u_l^2 \frac{d u_l^2}{d r} \sum_i {}^{(l)} n_i \sin[2\pi n_i y_l(r)] d r.$$

In the case of a great number of particles and slowly changing outer potential the following approximations can be introduced (statistical approximation)



$$\begin{aligned}
 s_l &\cong 1, \\
 E_R &\cong \sum_l \kappa_l \int u_l^6 d\mathbf{r}, \\
 \kappa_l &= \frac{\hbar^2}{2m} \frac{\pi^2}{N_l^3} \sum_i^{(l)} n_i^2.
 \end{aligned} \tag{16}$$

Finally

$$E_r \cong 0.$$

The above statistical approximation is essentially identical with HELLMANN's generalization of the statistical model based on grouping of the particles according to their azimuthal quantum number [1, 2, 9, 10, 11]. The only difference apart from the introduction of the inhomogeneity correction is in the constant value of  $\kappa_l$ . It is to be noted, that the well-known divergences of HELLMANN's generalization naturally do not appear because of the Weizsäcker term.

Since the energy expression (11) as well as the evaluation of the proper statistical approximation is generally complicated, three more approximations are introduced. In the first, apart from the use of the statistical approximation, the following relations are to be fulfilled

$$\frac{u_0^2}{N^0} = \frac{u_1^2}{N_1} = \dots = \frac{u_{l_\mu}}{N_{l_\mu}} = \frac{u^2}{N} \tag{17}$$

for all the orbital quantum numbers  $l$ . As can be easily seen the terms of the kinetic energy are as follows :

$$\begin{aligned}
 E_w^{(1)} &= \frac{\hbar^2}{2m} \int \left| \frac{d u}{d \mathbf{r}} \right|^2 d\mathbf{r}, \\
 E_R^{(1)} &= \kappa \int u^6 d\mathbf{r}, \\
 \kappa &= \frac{\hbar^2}{2m} \frac{\pi^2}{N^3} \sum_l n_l^2, \\
 E_\varphi^{(1)} &= \mu \int \frac{u^2}{r^2} d\mathbf{r}, \\
 \mu &= \frac{\hbar^2}{2m} \frac{1}{N} \sum_l l_i(l_i + 1).
 \end{aligned}$$

The above first approximation is applied to atoms, for that purpose as a rough estimation, the following variational assumption is introduced :

$$u^2 = 4\pi A r^2 e^{-2\lambda r}, \tag{18}$$

where  $A$  is the normalizing constant and  $\lambda$  the variational parameter. In the Table I there are given the energies of the Ar, Kr and X atoms based on the first approximation and the Thomas-Fermi-Weizsäcker theory, further the semi-empirical energy values of SLATER. The Thomas-Fermi-Weizsäcker approximation was also determined on the basis of the variational assumption (18).

Table I  
Energies of some rare-gas atoms in  $e^2/a_0$  units

	First assumption	TFW approximation	Semi-empirical
Ar	— 283,5	— 291,4	— 525,36
Kr	—1263,3	—1547,9	—2703,6
X	—3192,0	—4087,0	—7079,4

The chief reasons for the extraordinary great discrepancies in the first approximation apart from the inadequacy of the assumption (18) are the following: *a*) the approximation (16) is not applicable because of the small number of particles and of the very great strength field near the nucleus. *b*) The shape of the curve of eigenfunctions belonging to azimuthal quantum numbers  $l \neq 0$  is not appropriate in the vicinity of the nucleus because of equation (17).

To obtain the proper shape in the vicinity of the nucleus of the eigenfunctions, in a second approximation — retaining at the same time the statistical approximation — the amplitudes giving the states  $l = 0$  and  $l \neq 0$  are varied separately.

More precisely: only the fulfillment of condition

$$\frac{u_1^2}{N_1} = \frac{u_2}{N_2} = \dots = \frac{u_{l,\mu}^2}{N_{l,\mu}} = \frac{u_\lambda^2}{N_\lambda} \quad (19)$$

is required.  $N_\lambda$  is the number of occupied states belonging to the azimuthal quantum number  $l \neq 0$ .

At last as a third approximation the energy is determined directly on the basis of the relations (10) and (15), taking always into consideration the assumption (19) (without the introduction of the statistical approximation).

The second and the third approximation is sketched here for the Ar atom, introducing the following variational assumptions

$$u_0^2 = 4\pi (A'_1 r^{2n_1} e^{-2\lambda_1 r} + A'_2 r^{2n_2} e^{-2\lambda_2 r} + A'_3 r^{2n_3} e^{-2\lambda_3 r}), \quad (20)$$

$$u_1^2 = 4\pi (A''_2 r^{2n_2} e^{-2\lambda_2 r} + A''_3 r^{2n_3} e^{-2\lambda_3 r}). \quad (21)$$

The variation of the energy term can be accomplished with the use of the following subsidiary assumptions

$$\int u_0^2 dr = N_0,$$

$$\int u_1^2 dr = N_1.$$

For the purpose of simplifying the calculations the following values are introduced (in atomic units):

$$\begin{aligned} n_1 &= 1, & n_2 &= 2, & n_3 &= 3; \\ \lambda_1 &= 17,69, & \lambda_2 &= 6,55, & \lambda_3 &= 2,25; \\ A'_2 &= c A''_2, & A'_3 &= c A''_3. \end{aligned}$$

As will be seen later a good energy value can be obtained with the third approximation by choosing the variational parameters as follows:

$$\begin{aligned} A'_1 &= 2114,6, & A'_2 &= 2451,1, & A'_3 &= 11,91, \\ A''_2 &= 6127,8, & A''_3 &= 29,776. \end{aligned}$$

Determination of the second approximation of the energy can be carried out, with the exception of  $E_w^{(2)}$ , in an analytical way. The accomplishment of the calculations does not present any serious difficulty, although it is cumbersome to some degree, when calculating the electrostatical interaction energy  $E_i^{(2)}$ . The energy term  $E_c^{(2)}$  can be brought into the following form:

$$E_e^{(2)} = 8\pi^2 e^2 \sum_{i=1}^3 \sum_{j=1}^3 a_{ij} \left\{ \frac{(2n_i)!(2n_j-1)!}{(2\lambda_j)^{2n_i+1}(2\lambda_j)^{2n_j}} - \frac{(2n_i)!(2n_{j-1})}{(2\lambda_i)^{2n_i+1}(2\lambda_i+2\lambda_j)^{2n_j}} - \right.$$

$$\left. - \sum_{v=1}^{2n_i-1} \frac{(2n_i-1)!(2n_i+2n_j-v-1)!}{(2n_i-v)!(2\lambda_i)^{v+1}(2\lambda_i+2\lambda_j)^{2n_i+2n_j-v}} \right\},$$

where

$$a_{11} = \left(1 - \frac{1}{N_0}\right) A_1'^2,$$

$$a_{12} = a_{21} = \left(1 - \frac{1}{N_0}\right) A_1' A_2' + A_1' A_2'',$$

$$a_{13} = a_{31} = \left(1 - \frac{1}{N_0}\right) A_1' A_3' + A_1' A_3'',$$

$$a_{22} = \left(1 - \frac{1}{N_0}\right) A_2'^2 + A_2' A_3'' + \left(1 - \frac{1}{N_\lambda}\right) A_2''^2,$$

$$a_{23} = a_{32} = \left(1 - \frac{1}{N_0}\right) A_2' A_3' + A_2' A_3'' + A_2'' A_3' + \left(1 - \frac{1}{N_\lambda}\right) A_2'' A_3'',$$

$$a_{33} = \left(1 - \frac{1}{N_0}\right) A_3'^2 + 2 A_3' A_3'' + \left(1 - \frac{1}{N_\lambda}\right) A_3''^2.$$

The third approximation of the energy term was obtained numerically. Based on the mean value theorem of the integral calculus the calculations are easily to be carried out for intervals of suddenly varying integrand too (for example in the vicinity of the nucleus). It is astonishing, that in the field of the nucleus the second and third approximation of the potential energy  $E_p$  differ considerably. The results are given in the Table II, while the densities  $D(r)$ , furthermore the Hartree's distribution are plotted in Figure 1.

**Table II**  
The energy members of the Ar atom and its energy in  $e^2/a_0$  units

	$E_W$	$E_R$	$E_r$	$E$	$E_p$	$E_s$	$E$
Second approximation	240,8	38,1	0	73,4	— 913,7	184,8	—376,6
Third approximation	327,2	33,4	4,25	97,2	—1149,7	184,0	—503,6
Semi-empirical							—525,36

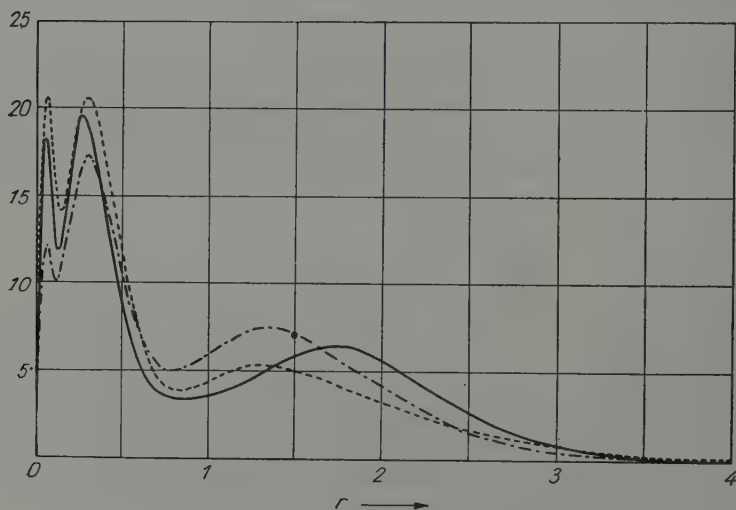


*Fig. 1.* Radial electron density of the Ar atom

— · — · — calculated on the basis of the second approximation  
 — calculated on the basis of the third approximation  
 ..... radial electron density of HARTREE

# Discussion

There has been given a variational method, which can be used relatively easily for the approximate determination of the ground state of a particle system placed in a central symmetrical outer potential field. The method can be generalized without any difficulty also for excited stationary states. The calculations have been carried out for the Ar atom in three approximations, only the third approximation giving a satisfactory result. Therefore the approximation (16) as well as the assumed proportionality of amplitudes  $u_0$  and  $u_1$  does not seem reasonable. The third approximation of the radial density ( $D$ ) has been determined on the basis of the variational assumptions (20) and (21). The result is satisfactory, though it is not impossible, that the agreement of the exact solution of the third approximation with the Hartree's distribution would be somewhat worse. Naturally, the agreement of the energy values can definitely only improve, though it is not too probable, that the energy values given in the Table II will vary considerably. The oscillations of the functions  $u_1^2$  may be caused by the analytical structure of the variational assumption, it being very probable, that the correct solution has only one maximum and the exact density  $u^2 = u_0^2 + u_1^2$  two maxima. In the third approximation the density  $D$  shows naturally the same maxima as the Hartree's distribution. At last it is to be noted, that the correction  $E_k$  can become considerably bigger (not necessarily positive) in the course of the variation than the values given in Table II. In another article we hope to introduce a further simplification of the above variational procedure.

I am very indebted to Professor Dr. P. GOMBÁS for his interest and discussions on this paper. Thanks are due to Mrs. J. JEANPLONG, Miss O. KUNVÁRY and Miss E. MÁCORY for the accomplishment of the numerical calculations.

# REFERENCES

1. P. GOMBÁS, Die statistische Theorie des Atoms und ihre Anwendungen, Springer, Wien, 1949.
2. P. GOMBÁS, Statistische Behandlung des Atoms, Handbuch der Physik, Springer, Berlin, Göttingen, Heidelberg, XXXVI, 1956.
3. P. GOMBÁS, Acta Phys. Hung., **3**, 105, 1953; Acta Phys. Hung., **3**, 127, 1953.
4. T. S. PLASKETT, Proc. Phys. Soc., A, **66**, 178, 1953.
5. W. J. SWIATECKI, Proc. Phys. Soc., A, **68**, 285, 1955.
6. N. H. MARCH and F. S. PLASKETT, Proc. Roy. Soc., A, **235**, 419, 1956.
7. W. MACKE, Phys. Rev., **100**, 992, 1955; Ann. d. Phys., **17**, 1, 1955.
8. N. H. MARCH, Proc. Phys. Soc., A, **70**, 169, 1957.
9. H. HELLMANN, Acta Physicochim. U. R. S. S., **4**, 225, 1936.
10. I. FÉNYES, Csillagászati Lapok (Budapest), **7**, 57, 1944; Múzeumi Füzetek (Kolozsvár), **3**, 3, 1945; **3**, 25 1945; Z. Physik, **125**, 336, 1948.
11. P. GOMBÁS, Acta Phys. Hung., **1**, 295, 1952.

ВАРИАЦИОННЫЙ МЕТОД ДЛЯ РЕШЕНИЯ ПРОБЛЕМ У МНОГИХ ТЕЛ  
В КВАНТОВОЙ МЕХАНИКЕ

К. ЛАДАНИ

## Резюме

Дается обобщение вариационного метода, разработанного Макке, на случай сферически симметричного внешнего потенциала. В случае большого числа частиц и медленно изменяющегося потенциала, метод переходит в обобщенную статистическую модель, в которой частицы группированы по орбитальным квантовым числам, настоящий метод без больших затруднений применим и в случае малого числа частиц. Для уменьшения нумерических трудностей даются три приближения. Вычисления сделаны в случае атома аргона, без учета обмена; вычисленная энергия совпадает с семиэмпирическим значением по Слетеру в пределах 5%.



# A RECENT ROTATIONAL ANALYSIS OF THE $\gamma$ BANDS OF THE NO MOLECULE

INCLUDING THE UNPUBLISHED DATA OF R. SCHMID<sup>†</sup> and L. GERŐ<sup>†</sup>

By

IRÉN DEÉZSI <sup>†</sup>

HUNGARIAN ACADEMY OF SCIENCES, CENTRAL RESEARCH INSTITUTE FOR PHYSICS, DEPARTMENT FOR SPECTROSCOPY, BUDAPEST

(Presented by L. Jánossy. — Received: XI. 14. 1957)

The present paper contains the rotational analysis of 16 bands of the  $\gamma$  band-system of the NO molecule. The constants in the electronic state  $A^2\Sigma^+$  of the molecule, obtained from the analysis extended to relatively high rotational quantum numbers, are the following:  $B_e = 1,9977 \text{ cm}^{-1}$ ,  $a_e = 0,0198 \text{ cm}^{-1}$ ,  $D_e = -6,2 \cdot 10^{-6} \text{ cm}^{-1}$ ,  $\beta_e = 0,3 \cdot 10^{-6} \text{ cm}^{-1}$ ,  $r_e = 1,063 \cdot 10^{-8} \text{ cm}$ ,  $I_e = 14,0076 \cdot 10^{-40} \text{ gcm}^2$ . The constants obtained for the ground state  $X^2\Pi$  are in agreement with the data of R. H. GILLETTE and H. EYSTER [1], within the margin of error. The dissociation energy is 6,603 eV, on the basis of the rotational analysis, as seen later. This value is somewhat higher (i. e. 6,50 eV) than that mentioned recently in a paper by G. HERZBERG, A. LAGERQVIST and E. MIESCHER [2]. From this the present writer was led to the conclusion that the predissociation on the upper electronic state of the  $\beta$  bands does not occur above the level  $v' = 6$ , as was suggested by several authors but there should exist in emission even the level  $v' = 7$ .

## § 1. Historical outline

In 1943, R. SCHMID and L. GERŐ, those two prominent pioneers of the Hungarian spectroscopical research work, set as their aim the intensive study of the ultraviolet and visible bands of the NO molecule, which can be photographed in air. Up to 1943 the rotational analysis of the bands involved had been carried out only with the prism spectrograph. The results issuing from photographs taken with prisms, however, were not found adequate to solve a number of unsettled questions concerning the NO molecule. The photographs of 1943 were taken with a 6,5 m grating spectrograph. After the sudden death of R. SCHMID in 1943, L. GERŐ published two short informative papers [3], [4] on the photographing of the bands of the NO molecule. Apart from the description of the experimental arrangement, these papers deal mainly with the scientific conclusions drawn from the analysis of the bands developed to high rotational quantum numbers. These conclusions concern the energy states of the NO molecule. Since in 1943 the vibrational levels of the upper electronic states of the  $\beta$  bands had been known only up to  $v' = 4$ , GERŐ's conclusions in relation to the dissociation energy of the NO molecule call for modification. Since then it has become well known that the  $v' = 5$  and  $v' = 6$  levels of the  $B^2\Pi$  state can also be excited in emission [5], [6], [7], [8].

In addition to the  $\gamma$  bands, some  $\varepsilon$  and  $\beta$  bands appeared as well on the plates of SCHMID and GERŐ, the rotational analysis of which is included

in the dissertation of C. F. SZILY [9] and C. BALLENEGGER [10]. The paper mentioned informs us of the photographing of  $\gamma$  bands and of the execution of the rotational analysis, but the publication of the analysis could, not be carried out. L. Gerő disappeared in 1945 and the paper he was preparing is likely to have been destroyed owing to the devastations of the war. However, on the basis of a manuscript which has been discovered J. VALATIN published [11] the rotational analysis of three  $\gamma$  bands, their predissociations found on the spectrum and suggestions, now to be modified — as I have mentioned before — concerning the dissociation energy of NO.

Since 1943, quite naturally, a considerable number of papers have been published on the bands of the NO molecule and the rotational analysis of a good many bands have been carried out by the Japanese researcher OGAWA [7]. No such paper has been published, however, which would have contained as many  $\gamma$  bands with as high rotational quantum numbers as the analysis of SCHMID and GERŐ. The re-discovery of these invaluable records could have been of high importance with regard to the exact calculation of rotational constants and the study of predissociation phenomena.

## § 2. Analysis

From the photographs and manuscripts found among the ruins it was possible to make up a collection of data, the partial rotational analysis of 18 bands, and spectrograms made in all spectrum ranges with the exception of the Schumann-range.

The present paper includes the rotational analysis of 16  $\gamma$  bands, with the omission of the data [11] already published. These bands are as follows :

(0,0) (0,1) (0,2) (0,3) (0,4) (0,5)  
 (1,1) (1,3) (1,4) (1,5) (1,6)  
 (2,2) (2,3) (2,7)  
 (3,4) (3,5)

First of all it was ascertained in the following way how the manuscripts and spectrograms found corresponded to each other one of my co-workers re-measured the lines of the (0,2) band and detected the branches ; then the results obtained in this way were compared with the data found. The agreement was excellent. After this I prepared the so-called Loomis and Wood diagram [12] for all bands. By means of this I succeeded, on the one hand, in checking the correctness of the analysis already done and, on the other hand, I was able to extend a good many branches towards higher quantum numbers. The first part of the (0,5) band was not to be found in the collection of data.

The gap has been filled by supplementary measurement and the analysis extended towards the band-head as well. The  ${}^0P_{12}$  branch had to be supplied in its entirety. Further branches missing were the  ${}^0P_{12}$  and  ${}^5R_{21}$  in the (1,5) band, the  ${}^5R_{21}$  in the (2,7) band and the  $P_1$  and  $R_2$  in the (3,4) band, all are now being fully supplied. In the following Tables the data of SCHMID and GERÖ are given in Roman type and those calculated recently by the present author in italics. The correctness of the supplements have been checked by enlarged copies made from the plates, apart from the comparison of combination differences.

Through the analysis completed in this way, I have calculated the rotational constants. The constants relating to the ground state  $X^2\Pi$  correspond to the data of GILLETTE and EYSTER [1] within a permissible margin of error. The following constants have been obtained for the electronic state  $A^2\Sigma^+$ :

$$\begin{aligned} B'_e &= 1,9977 \text{ cm}^{-1} \\ \alpha'_e &= 0,0198 \text{ cm}^{-1} \\ D'_e &= -6,2 \cdot 10^{-6} \text{ cm}^{-1} \\ \beta'_e &= 0,3 \cdot 10^{-8} \text{ cm}^{-1} \\ r'_e &= 1,0630 \cdot 10^{-8} \text{ cm} \\ I'_e &= 14,0076 \cdot 10^{-40} \text{ g cm}^2. \end{aligned}$$

### § 3. Dissociation Energy

According to the dissertations mentioned [9], [10], in previous reports [3], [4] and VALATIN's publication [11] the dissociation energy of the NO molecule had been determined by SCHMID and GERÖ as 4,29 eV. This was based on the fact that the  $\beta$  bands cease to exist above  $v' = 4$  owing to predissociation. SCHMID and GERÖ observed predissociation on the  $\gamma$  bands at the energy value  $53750 \text{ cm}^{-1}$ . The difference between the two predissociation limits corresponded to the energy difference between the atomic term combinations  $N(^4S) + O(^1D)$  and  $N(^2D) + O(^3P)$ . The coordination of the above atomic term combinations and predissociations seemed to be obvious. Thus the atomic term combination  $N(^4S) + O(^3P)$  lying lower by  $15868 \text{ cm}^{-1}$  than the atomic term combination  $N(^4S) + O(^1D)$ , has been placed to an energy level corresponding to 4,28 eV. The so-called accidental predissociation phenomena [4], [10], [11], [13], [14], allegedly arising in the rotational structure of the  $\gamma$  bands, were also interpreted as predissociation of the  $\beta$  bands occurring above  $v' = 4$ .

In the meantime, however, photographs were taken [5], [6], [7], [8] of such  $\beta$  bands whose upper vibrational levels are  $v' = 5$  and  $v' = 6$ . Even through a careful study of the spectrum, I could not find a satisfactory confirmation of the existence of the phenomena explained by accidental predissociation.

On the basis of the breaking-off of the vibrational terms of the  $\beta$  bands at  $v' = 6$  as well as by taking account of the dissociation energy of the  $N_2$  molecule, M. BROOK and J. KAPLAN [6] have fixed the limit of predissociation at 6,48 eV. This value was accepted by several authors. The predissociation was ascribed to the interaction of the repulsive term  $^2\Sigma^+$  arising from the atomic term combination  $N(^4S) + O(^3P)$  placed on that energy level.

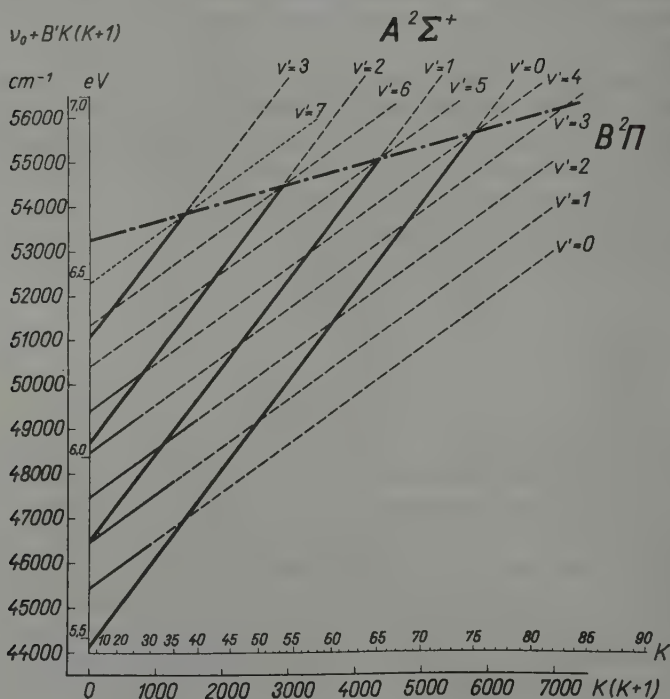


Fig. 1. Rotational term series of the electronic states  $A^2\Sigma^+$  and  $B^2\Pi$  of the NO molecule

Fig. 1. shows the term series of  $\gamma$  and  $\beta$  bands plotted against  $K(K + 1)$  drawn in a continuous line, to the quantum number I could reach in the course of the analysis. The breaking-off of the rotational terms in the  $\gamma$  bands indicates quite clearly the limiting curve of dissociation. As is seen, the limiting curve intersects the energy axis at 53 266  $\text{cm}^{-1}$  which corresponds to 6,603 eV. This value may deviate — according to my calculations — from the dissociation energy of NO by no more than 0,04 eV ( $\sim 300 \text{ cm}^{-1}$ ), inasmuch as the above energy value belonging to the above point of intersection is the lower limit for the dissociation limit [15]. As is seen from the Figure, apart

From this value of dissociation there may exist in emission the vibrational level  $v' = 7$  of the  $\beta$  bands.

Fig. 2. shows the position of the vibrational levels in the excited electronic states of the NO molecule with the atomic term combination coordinated to the predissociation limit.

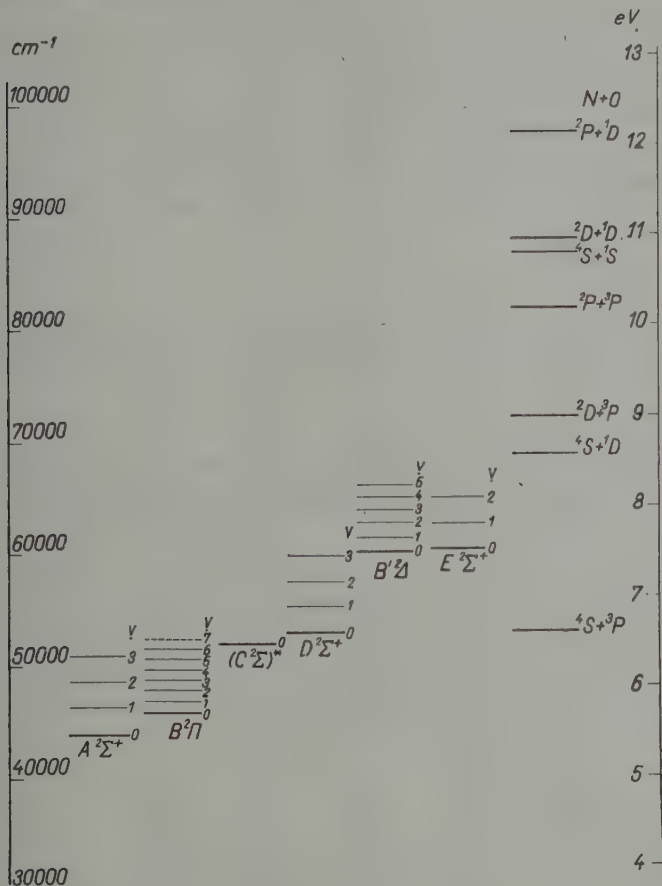


Fig. 2. The excited energy levels of the NO molecule

I feel deeply obliged to pay the tribute of respect to my beloved masters, R. SCHMID and L. GERŐ.

I should like to express my thanks to EDIT KOCZKÁS and L. CSÁSZÁR for their help and assistance in the tiresome work of calculation.

\* According to the paper [2] of G. HERZBERG, A. LAGERQVIST and E. MIESCHER the C state is not  $^2\Sigma$  but  $^2\Pi$ .

## REFERENCES

1. R. H. GILLETTE and H. EYSTER, *Phys. Rev.*, **56**, 1113, 1938.
2. G. HERZBERG, A. LAGERQVIST and E. MIESCHER, *Can. J. Phys.*, **34**, 622, 1956.
3. R. F. SCHMID and L. GERŐ, *Csillagászati Lapok*, **6**, 3, 1944.
4. R. F. SCHMID and L. GERŐ, *Mat. és Term. Tud. Ért.*, **62**, 408, 1943.
5. A. G. GAYDON, *Proc. Phys. Soc.*, **56**, 160, 1944.
6. M. BROOK and J. KAPLAN, *Phys. Rev.*, **96**, 1540, 1954.
7. M. OGAWA, *Science of Light*, **3**, 90, 1955.
8. I. DEÉZSI and T. MÁTRAI, *Acta Phys. Hung.*, **7**, 111, 1957.
9. K. F. SZILY, *Dissertation*, Budapest, 1943.
10. K. BALLENEGGER, *Dissertation*, Budapest, 1944.
11. L. GERŐ and R. SCHMID, *Proc. Phys. Soc.*, **60**, 533, 1948.
12. F. W. LOOMIS and R. W. WOOD, *Phys. Rev.*, **32**, 223, 1928.
13. I. KOVÁCS and A. BUDÓ, *J. Chem. Phys.*, **15**, 166, 1947.
14. I. DEÉZSI, *Magyar Fizikai Folyóirat*, **4**, 489, 1956.
15. G. HERZBERG, *Molecular Spectra and Molecular Structure*, I, 432, 1950.

НОВЫЙ ВРАЩАТЕЛЬНЫЙ АНАЛИЗ  $\gamma$  — ПОЛОС NO МОЛЕКУЛЫ

И. ДЕЖИ

## Резюме

Настоящая работа содержит вращательный анализ 16 полос  $\gamma$  системы NO молекулы. Постоянные  $A^2\Sigma'$  в электронном состоянии молекулы получены из анализа, расширенного на высокие вращательные квантовые числа, следующие:

$$B_e = 1,9977 \text{ cm}^{-1} \quad a_e = 0,0198 \text{ cm}^{-1} \quad D_e = -6,2 \cdot 10^{-6} \text{ cm}^{-1}, \\ \beta_e = 0,3 \cdot 10^{-6} \text{ cm}^{-1} \quad r_e = 1,063 \cdot 10^{-8} \text{ cm} \quad I_e = 14,0076 \cdot 10^{-40} \text{ g. cm}^2.$$

Постоянные получены для основного состояния  $X^2\Pi$  совпадают с данными Р. Г. Жилета и Г. Эйстера [1] в пределах ошибок. Энергия диссоциации, как показывается в дальнейшем, на основе вращательного анализа, составляет 6,603 eV. Это значение выше, чем данное недавно в работе Г. Герцберга, А. Лагерквиста и Е. Мицера [2] (т. е. 6,50 eV). Автор делает из этого вывод, что преддиссоциации на высших электронных состояниях  $\beta$  полос не происходит выше уровня  $v' = 6$ , как это было предсказано некоторыми авторами, а в эмиссии должен существовать  $v' = 7$ .



Table 1

(0,0)  $\gamma$ -band of NO

J	$^{\circ}P_{12}$	$P_2$	$Q_2$	$R_2$	$P_1$	$Q_1$	$R_1$	$^{\circ}R_{21}$
$\frac{1}{2}$	—	—	—	—	—	44 199,21	44 203,49	
	44 074,26	44 078,59	44 086,15	—	44 194,29	197,98	206,03	
	069,60	077,95	089,56	44 105,72	189,80	197,98	209,69	
	065,40	077,58	093,39	113,52	186,07	197,98	213,81	
	061,77	077,95	097,68	121,52	183,02	199,21	218,55	
$5\frac{1}{2}$	058,80	078,59	102,72	130,42	180,58	200,13	223,95	44 252,05
	056,49	080,32	108,17	140,13	178,53	202,36	230,23	261,79
	054,22	082,33	114,15	149,83	177,28	204,96	236,86	272,49
	052,78	084,83	120,71	160,46	176,85	208,38	244,30	283,28
	052,03	087,98	127,68	171,19	176,85	212,25	252,05	295,79
$10\frac{1}{2}$	052,03	091,56	135,31	183,02	177,28	217,00	260,93	308,22
	052,03	095,70	143,44	194,93	178,53	222,24	269,92	321,38
	052,78	100,45	152,17	207,81	180,58	228,00	279,65	335,22
	054,22	105,72	161,32	220,78	183,02	234,47	290,12	349,51
	056,16	111,50	171,19	234,47	186,07	241,68	301,17	365,00
$15\frac{1}{2}$	058,33	117,84	181,38	249,10	189,80	249,10	312,82	380,21
	061,30	124,74	192,18	264,24	194,29	257,54	325,12	396,60
	064,66	132,16	203,49	278,96	199,21	266,44	337,97	413,05
	068,69	140,13	215,46	294,38	204,96	275,98	351,46	430,56
$20\frac{1}{2}$	073,21	148,68	228,00	311,13	211,21	286,10	365,55	448,65
	078,59	157,73	241,13	328,22	217,73	296,87	380,21	467,16
	084,33	167,31	254,52	345,86	225,26	308,22	395,56	486,41
	090,28	177,28	268,65	363,61	233,24	320,28	411,51	506,13
	097,18	188,16	283,28	382,31	241,68	332,92	428,01	526,75
$25\frac{1}{2}$	104,59	199,21	298,56	401,45	251,31	345,86	445,05	547,80
	112,34	211,21	314,35	421,02	260,93	359,81	462,71	569,86
	120,71	223,95	330,62	441,26	271,53	374,12	481,26	591,53
	129,98	236,86	347,45	462,07	282,69	389,23	500,09	614,41
	140,13	250,17	365,00	483,40	294,38	404,77	519,47	637,85
$30\frac{1}{2}$	149,83	264,24	382,93	505,24	306,57	421,02	539,74	661,86
	160,46	278,96	401,45	527,76	319,69	437,77	560,38	686,59
	—	294,38	420,73	550,89	332,92	455,09	581,73	711,69
	184,08	309,89	440,23	574,03	347,45	473,15	603,58	737,46
	195,91	326,20	460,45	598,17	361,81	491,75	626,16	763,28
$35\frac{1}{2}$	—	343,01	481,26	622,97	377,09	510,92	649,12	789,81
	—	360,38	502,61	648,22	393,03	530,67	672,76	818,26
	—	378,49	524,55	673,94	409,50	550,89	697,12	846,11
	—	397,04	546,76	700,02	426,61	571,93	722,14	874,81
$40\frac{1}{2}$	—	416,27	569,86	727,04	444,40	593,46	747,37	904,54
	—	435,89	593,46	754,43	462,71	615,72	773,43	934,51
	—	456,12	617,56	782,57	481,26	638,53	799,89	964,99
	—	477,03	642,54	810,99	500,84	661,86	827,22	996,37
	—	498,37	667,87	839,97	520,84	685,82	855,00	—
	—	520,50	693,29	869,57	541,60	710,27	883,35	45 059,71
$45\frac{1}{2}$	—	543,03	719,64	900,10	562,99	735,22	912,31	—
	—	566,32	746,77	930,87	584,77	761,12	941,90	125,88
	—	589,82	774,11	962,16	607,18	787,26	971,96	160,13
	—	614,41	802,52	994,16	630,24	814,21	—	194,26
	—	638,53	830,88	45 026,71	653,90	841,72	45 033,87	229,55
	—	664,30	860,07	059,71	677,93	869,57	—	—
$50\frac{1}{2}$	—	690,17	890,06	093,30	702,38	898,31	—	—
	—	717,29	920,26	127,00	728,06	927,62	—	—
	—	744,53	951,42	—	754,43	957,38	—	—
	—	772,40	983,25	—	780,99	—	—	—
	—	—	45 015,54	—	808,20	—	—	—

(9,0)  $\gamma$ -band of NO

J	$^{\circ}P_{12}$	$P_2$	$Q_2$	$R_2$	$P_1$	$Q_1$	$R^s$	$^sR_{21}$
$55\frac{1}{2}$					835,71 864,16 893,03 922,68 952,81 983,25			
$60\frac{1}{2}$								

Table 2

(0,1)  $\gamma$ -band of NO

J	$^{\circ}P_{12}$	$P_2$	$Q_2$	$R_2$	$P_1$	$Q_1$	$R_1$	$^sR_{21}$
$\frac{1}{2}$	—	—	—	—	—	42322,42	42 326,69	—
	42 198,07	42 201,96	42 209,97	42 221,85	42 317,74	321,29	329,67	—
	193,43	201,44	213,36	229,25	313,64	321,29	333,11	—
	189,58	201,44	217,40	237,15	309,74	321,29	337,63	—
	186,32	201,96	221,85	245,88	306,85	322,42	342,46	—
$5\frac{1}{2}$	783,56	203,08	227,12	254,66	304,63	324,34	348,02	—
	181,19	204,79	232,80	264,50	302,88	326,69	354,37	42 386,21
	179,45	207,18	239,11	274,71	301,81	329,67	361,20	397,08
	178,31	209,97	245,88	285,49	301,81	333,11	368,91	408,32
	177,74	213,36	253,36	296,89	301,81	337,63	377,11	420,83
$10\frac{1}{2}$	177,74	217,40	261,38	308,95	302,88	342,46	386,21	433,52
	178,31	221,85	269,69	321,29	304,63	348,02	395,46	447,35
	179,45	227,12	278,73	334,51	306,85	354,37	405,78	461,47
	181,19	232,80	288,51	348,02	309,74	361,20	416,51	476,32
	183,56	239,11	298,89	362,19	313,64	368,91	428,48	491,86
$15\frac{1}{2}$	186,32	245,88	309,74	377,11	317,74	377,11	440,56	507,54
	189,82	253,36	321,29	392,35	322,42	386,21	453,45	524,65
	194,14	261,38	333,11	408,32	328,27	395,46	467,26	542,56
	198,84	270,10	345,56	424,88	334,51	405,78	481,12	—
	204,22	279,39	358,74	441,98	341,29	416,51	495,92	—
$20\frac{1}{2}$	209,97	289,25	372,46	459,54	348,63	427,90	511,32	598,15
	216,50	299,62	386,74	477,99	357,13	440,07	527,36	618,40
	223,45	310,60	401,79	496,77	365,89	452,76	544,19	638,99
	231,14	322,42	417,19	516,27	375,14	466,10	561,41	660,43
	239,11	334,51	433,52	536,28	385,38	480,25	579,42	682,28
$25\frac{1}{2}$	248,23	347,19	450,07	556,81	396,00	494,86	598,15	704,83
	257,63	360,49	467,26	577,95	407,56	510,20	617,45	727,90
	267,54	374,47	485,32	599,93	419,76	526,29	637,30	751,73
		389,03	503,73	622,34	432,29	542,56	657,88	776,31
		404,13	522,80	645,25	445,57	560,04	679,00	801,20
$30\frac{1}{2}$		419,76	542,56	668,85	459,54	577,95	700,82	827,08
		436,11	562,76	692,98	474,06	596,48	723,26	853,04
		452,76	583,52	717,71	489,33	615,57	746,21	880,09
		470,54	604,92	743,03	505,28	635,41	769,81	907,20
		488,77	627,03	769,12	521,80	655,55	794,07	—
$35\frac{1}{2}$		507,54	649,65	795,33	538,94	676,85	819,16	964,54
		527,36	672,92	822,46	556,81	698,67	844,58	994,03
		546,69	696,70	850,07	575,07	721,07	870,70	43 023,93
		567,27	721,07	878,31	594,19	743,70	897,55	054,52
		588,34	746,21	907,20	613,80	767,27	924,94	085,90
$40\frac{1}{2}$		610,06	771,86	936,67	634,21	791,38	952,84	117,88
		632,50	797,92	966,67	655,55	816,23	981,48	150,28

(0,1)  $\gamma$ -band of NO

J	$^0P_{12}$	$P_1$	$Q_2$	$R_2$	$P_1$	$Q_1$	$R_1$	$^sR_{21}$
$45\frac{1}{2}$		655,55	824,72	997,21	676,85	841,55	43 010,83	183,39
		679,00	852,03	43028,43	698,67	867,61	040,48	216,68
		703,19	880,09	060,40	722,06	894,32	071,07	
		727,90	908,67	092,58	745,22	921,63	102,19	
		753,28	937,88	125,46	769,12	949,51	133,87	
		779,35	967,61	158,96	749,07	977,07	166,11	
		805,82	997,99	193,00	819,16	43 007,07	199,14	
$50\frac{1}{2}$		832,99	43 028,78	227,85	845,27	036,84	232,84	
		860,92	060,40	263,56	871,88	067,17	266,84	
		889,14	092,58	299,42	999,10	098,17	301,80	
		918,12	125,46	335,79	926,90	129,84	337,00	
		947,73	158,96	373,64	955,31	161,96	373,64	
		977,97	193,00	411,16	984,33	194,92	410,23	
		43 008,66	227,85	449,57	43 014,01	228,27	447,72	
$60\frac{1}{2}$		040,48	262,68	488,62	044,37	262,68	485,23	
		072,20	298,49	528,13	075,32	297,30	523,70	
		104,84	334,86	568,23	106,80	332,49	562,91	
		138,08	372,57	608,94	138,96	369,12	602,43	
		171,82	410,23	650,29	171,82	405,61	642,84	
		206,29	448,57	692,25	205,32	442,71	683,86	
		241,61	487,01	734,44	239,43	480,37	725,03	
$65\frac{1}{2}$		277,16	526,52	777,87	274,03	518,79	767,35	
		313,10	566,45	821,70	309,34	557,79	810,08	
		351,20	607,05	865,91	345,15	597,35		
		388,49	648,25	910,73		637,28		
		426,56	690,67	956,06		678,57		
		465,23	732,58	44002,59		720,07		
		504,87	775,74	049,19		762,12		
$70\frac{1}{2}$		544,61	819,28			805,03		
		585,27	863,47			848,02		
		626,52	908,38			891,97		
		668,15	954,07			936,61		
		710,78	44 000,03			981,60		
		753,56	046,82			44 027,60		
		797,18						

Table 3

(0,2)  $\gamma$ -band of NO

J	$^0P_{12}$	$P_1$	$Q_2$	$R_2$	$P_1$	$Q_1$	$R_1$	$^sR_{21}$
$\frac{1}{2}$	—	—	—	—	—	—	—	—
$5\frac{1}{2}$	40 349,30	40 353,57	40 361,24	40 373,73	—	—	40 481,18	—
	344,83	353,11	364,78	381,56	40 464,55	—	485,15	—
	341,07	353,11	369,05	388,87	461,18	40 473,30	489,13	—
	337,62	353,57	373,73	397,65	458,36	474,38	494,40	—
	335,20	355,02	379,03	406,56	456,40	476,17	500,22	40 528,25
	333,24	356,83	384,80	516,81	454,92	478,95	506,90	538,62
	331,80	359,53	391,51	427,44	454,35	482,13	514,01	549,71
$10\frac{1}{2}$	330,91	362,74	398,59	438,32	454,35	486,00	521,97	561,39
	330,91	366,52	406,46	450,16	454,92	490,59	530,53	572,95
	330,91	370,96	414,76	462,53	456,40	495,90	540,04	587,06
	331,80	376,08	423,75	475,49	458,36	501,94	549,71	601,09
	333,72	381,56	433,33	489,13	461,18	508,70	560,55	616,07
	336,05	387,90	443,56	503,26	464,55	516,12	571,83	631,37
	338,88	394,62	454,35	517,90	468,71	524,19	584,03	647,39
$15\frac{1}{2}$	342,50	402,17	465,79	533,50	473,30	533,05	596,59	664,09

(0,2)  $\gamma$ -band of NO

J	$^oP_{11}$	$P_2$	$Q_3$	$R_2$	$P_1$	$Q_1$	$R_1$	$^sR_{21}$
20 $\frac{1}{2}$	346,52	410,25	477,87	549,51	478,95	542,43	610,16	681,23
	351,24	418,94	490,59	565,96	485,15	552,52	624,39	699,51
	356,83	428,31	503,72	583,24	492,02	563,23	638,87	718,28
	362,74	438,32	517,90	601,09	499,79	574,82	654,52	737,59
	369,05	448,75	532,37	619,47	507,92	587,06	671,12	757,72
	376,65	459,98	547,46	638,87	516,77	599,93	687,44	778,37
	384,80	471,71	563,23	658,24	526,46	613,48	704,98	799,94
25 $\frac{1}{2}$	392,96	484,20	579,52	678,55	536,76	627,79	723,10	821,96
	402,17	497,38	596,59	699,51	547,46	642,73	741,92	844,74
	411,85	511,03	613,95	720,93	559,35	658,24	761,49	868,23
	422,15	525,39	632,49	743,24	571,83	674,45	781,71	892,60
	433,33	540,04	651,24	765,93	584,66	691,48	802,62	917,79
	444,77	555,81	671,12	789,42	598,34	709,06	824,11	942,75
	457,17	571,83	690,98	813,34	612,80	727,30	846,24	968,54
30 $\frac{1}{2}$	470,17	589,01	711,63	838,03	627,79	746,31	869,10	995,47
	484,20	606,37	733,06	863,32	643,35	765,93	892,60	41022,71
	498,06	624,39	755,08	889,40	659,93	786,17	916,87	050,70
	512,79	642,73	777,77	915,71	676,86	807,13	941,56	079,53
	528,25	662,59	800,90	942,75	694,71	828,71	967,17	109,10
	544,41	682,64	824,79	970,63	713,02	850,98	993,30	139,21
	561,39	703,18	849,34	998,78	732,21	873,99	41020,10	169,98
40 $\frac{1}{2}$	578,71	724,55	874,58	41028,09	751,87	897,54	047,71	200,85
	596,59	746,31	900,35	057,66	772,23	921,86	075,76	232,87
	—	769,11	926,83	088,03	793,36	946,64	104,52	265,55
	634,69	792,23	953,89	118,74	815,09	972,40	133,95	298,95
	654,52	816,03	981,44	150,44	837,63	998,78	164,32	333,15
	675,52	840,55	41009,99	182,56	860,60	41025,62	195,00	367,53
	696,75	865,66	038,83	215,45	884,23	052,97	226,10	402,75
45 $\frac{1}{2}$	—	891,47	068,69	248,71	908,55	081,36	258,22	439,03
	—	917,79	098,68	282,83	933,50	110,20	291,03	475,15
	—	944,73	129,58	317,49	959,40	139,84	324,49	512,64
	—	972,40	161,15	352,76	985,84	169,98	358,31	550,57
	41000,90	193,23	388,92	41012,98	200,85	393,08	393,08	588,76
	—	029,83	226,10	425,22	040,48	232,41	428,33	627,98
	—	059,48	259,45	462,38	069,03	264,47	464,36	667,65
50 $\frac{1}{2}$	—	089,81	293,48	500,40	098,13	297,33	501,02	708,69
	—	120,67	328,20	538,45	127,66	330,78	538,45	749,02
	—	152,17	363,47	577,79	157,98	364,92	576,15	—
	—	184,53	399,61	617,86	189,00	399,61	614,69	—
	—	217,02	436,26	657,95	220,54	435,20	653,97	—
	—	250,61	473,55	699,04	252,98	471,22	693,79	—
	—	284,79	511,14	740,53	286,13	508,09	734,34	—
60 $\frac{1}{2}$	—	319,59	549,78	782,91	319,59	545,46	775,39	—
	—	354,85	588,76	825,60	353,82	583,39	817,29	—
	—	390,82	628,62	869,17	388,92	622,17	859,56	—
	—	427,73	669,06	913,17	424,57	661,51	902,77	—
	—	464,95	710,16	958,09	460,82	701,48	946,32	—
	—	502,95	751,83	42003,29	497,72	742,27	990,82	—
	—	541,71	794,27	049,73	535,36	783,54	42035,77	—
65 $\frac{1}{2}$	—	580,94	837,28	096,12	573,24	825,60	081,49	—
	—	620,91	880,82	143,55	612,51	868,01	127,78	—
	—	661,51	925,15	191,16	652,03	—	—	—
	—	702,71	970,12	240,25	692,26	—	—	—
	—	744,69	42015,61	289,25	733,38	—	—	—
	—	787,84	061,67	—	774,92	—	—	—
	—	831,50	108,61	—	817,29	—	—	—
70 $\frac{1}{2}$	—	876,08	156,10	—	—	—	—	—
	—	921,27	—	—	—	—	—	—
	—	967,20	—	—	—	—	—	—

Table 4

(0,3)  $\gamma$ -band of NO

J	$^{\circ}P_{12}$	$P_2$	$Q_2$	$R_2$	$P_1$	$Q_1$	$R_1$	$^{\circ}R_{21}$
$1\frac{1}{2}$	—	—	—	—	—	38 654,14	38 658,59	38 666,46
	38 530,52	38 535,23	38 542,54	38 554,21	38649,54	653,62	661,99	673,62
	526,20	534,35	545,97	562,21	645,59	653,62	665,57	681,31
	522,45	534,35	550,36	570,17	642,23	654,14	670,06	689,87
	519,43	535,23	555,20	579,16	639,23	655,48	675,39	699,20
$5\frac{1}{2}$	516,90	536,86	560,76	589,16	637,53	657,47	681,31	709,18
	515,20	539,05	566,74	598,59	636,21	660,30	688,05	719,71
	514,36	541,87	573,65	609,47	636,21	663,87	695,85	731,12
	513,68	545,35	581,08	620,78	636,21	667,97	703,86	743,71
	513,68	549,41	589,16	632,85	637,53	672,95	712,71	756,20
$10\frac{1}{2}$	514,36	554,21	597,89	645,59	639,23	678,63	722,32	770,38
	515,95	559,59	607,27	658,59	641,30	684,98	732,70	784,25
	517,96	565,69	617,30	672,95	644,62	692,21	743,71	799,24
	520,66	572,32	628,06	687,13	648,46	699,92	755,67	814,98
	524,06	579,69	639,23	702,80	653,17	708,51	768,17	831,42
$15\frac{1}{2}$	528,18	587,73	651,25	719,02	658,59	717,83	781,38	848,45
	532,90	596,39	663,87	735,11	664,48	727,70	795,37	866,60
	538,29	605,69	677,12	752,38	671,30	738,73	810,09	885,24
	544,28	615,63	691,06	770,38	678,63	749,99	825,56	904,73
	550,97	626,30	705,60	788,48	687,13	762,13	841,49	924,83
$20\frac{1}{2}$	558,40	637,53	720,88	807,99	695,85	775,01	858,58	945,61
	566,74	649,54	736,70	827,78	705,60	788,48	876,08	967,09
	574,96	661,99	753,33	848,33	716,06	802,89	894,41	989,24
	584,29	675,39	770,38	869,49	727,09	817,91	913,55	39 012,17
	594,33	689,33	788,48	891,28	738,73	833,65	933,02	035,75
$25\frac{1}{2}$	604,97	703,86	806,80	913,55	751,57	850,26	953,45	060,06
	616,17	719,02	826,00	936,76	764,64	867,45	974,51	084,84
	628,06	735,11	845,83	960,59	778,61	885,24	996,30	110,70
	—	751,57	866,60	985,15	793,26	903,85	39 018,75	137,14
	654,14	768,85	887,66	39 009,99	808,47	923,12	041,94	164,41
$30\frac{1}{2}$	667,97	786,73	909,52	035,75	824,61	943,12	065,87	191,93
	682,96	805,30	931,96	062,13	841,49	963,81	090,51	220,29
	698,34	824,61	955,18	089,18	859,05	085,15	115,84	249,75
	714,30	844,57	978,87	116,99	877,31	39 007,31	141,73	279,69
	731,12	865,14	39 003,39	145,24	896,21	030,22	168,43	310,16
$35\frac{1}{2}$	748,37	886,51	028,44	174,23	915,83	053,62	195,80	341,35
	766,46	908,35	054,24	203,83	936,19	077,77	223,89	373,31
	785,18	931,02	080,87	234,36	957,19	102,77	252,60	405,96
	804,41	954,29	108,13	265,34	978,87	128,27	282,15	439,48
	824,61	978,33	135,97	296,86	39001,30	154,53	312,14	473,30
$40\frac{1}{2}$	845,83	39 003,01	164,41	329,11	024,43	181,50	343,21	507,79
	868,45	028,44	193,51	362,24	048,25	209,14	374,97	543,40
	—	054,24	223,29	396,03	072,87	237,61	407,01	579,55
	—	080,87	253,88	430,24	098,05	266,59	439,48	616,45
	—	108,13	285,03	465,37	123,91	296,47	473,30	653,72
$45\frac{1}{2}$	—	135,97	316,92	500,92	150,58	326,91	507,79	692,15
	—	164,89	349,39	537,13	177,83	358,18	542,64	730,62
	—	194,09	382,59	574,14	205,71	389,99	578,59	770,23
	—	223,89	416,53	611,96	234,36	422,44	614,76	810,34
	—	255,11	450,92	650,29	264,11	455,53	651,73	—
$50\frac{1}{2}$	—	286,22	486,04	689,30	294,13	489,49	689,33	—
	—	318,68	522,07	728,98	324,79	524,31	727,88	—
	—	351,21	558,75	769,28	356,12	559,58	767,05	—
	—	384,64	595,71	810,34	388,67	595,71	806,83	—
	—	418,78	633,79	851,81	421,66	632,27	847,12	—



(0,3)  $\gamma$ -band of NO

J	$^0P_{12}$	$P_2$	$Q_2$	$R_2$	$P_1$	$Q_1$	$R_1$	$^5R_{21}$
$55\frac{1}{2}$		453,52	672,42	894,20	455,53	669,69	888,44	
		488,94	711,69	937,36	489,49	707,74	930,09	
		525,05	751,60	980,88	524,31	746,53	972,74	
		562,06	792,12	40 025,26	560,14	785,76	40 016,20	
		599,52	833,26	070,36	596,59	826,04	059,96	
$60\frac{1}{2}$		638,00	875,36	116,04	633,79	866,92	104,52	
		676,56	918,07	162,38	671,55	908,42	149,82	
		715,91	961,46		710,00	950,76		
		776,56	40 005,31		749,14	993,56		
		797,60	050,14		789,27	40 037,16		
$65\frac{1}{2}$		838,98	095,56		829,55	081,51		
		881,60	141,57		870,83	126,50		
		924,34	188,10		912,58	172,08		
		968,19	235,25		955,63	218,12		
		40 012,59	283,09		998,91	264,93		
$70\frac{1}{2}$		057,63	331,80		—	312,47		
		103,49	381,56		40088,00	360,48		
		149,82	431,30		133,20			
		197,10	482,13		179,04			
					225,94			
					273,16			

Table 5

(0,4)  $\gamma$ -band of NO

J	$^0P_{12}$	$P_2$	$Q_2$	$R_2$	$P_1$	$Q_1$	$R_1$	$^5R_{21}$
$\frac{1}{2}$	—	—	—	—	—	36 862,74	36 866,76	—
	36 739,17	36743,06	36 751,11	36 763,04	36 858,13	862,02	869,89	—
	737,92	742,89	754,86	770,68	854,06	862,02	873,91	—
	731,29	743,06	759,24	778,97	850,79	862,74	878,66	—
	728,44	744,37	764,09	788,11	848,28	864,34	884,12	—
$5\frac{1}{2}$	726,20	746,10	769,76	797,60	846,62	866,48	890,14	—
	724,46	748,46	776,20	808,10	845,85	869,37	897,16	—
	723,72	751,45	783,40	819,00	845,47	873,02	904,89	—
	723,72	755,23	791,07	830,68	845,85	877,59	913,40	—
	724,11	759,69	799,48	843,15	847,24	882,80	922,60	—
$10\frac{1}{2}$	725,15	764,93	808,57	856,12	849,31	888,84	932,70	36 980,18
	727,03	770,68	818,37	869,89	851,92	895,66	943,40	994,89
	729,60	777,25	828,76	884,12	855,78	903,24	954,92	37 010,28
	732,81	784,48	839,96	899,34	860,10	911,64	967,16	026,56
	736,67	792,29	851,92	915,33	865,13	920,61	880,18	043,54
$15\frac{1}{2}$	741,40	800,90	864,34	931,72	871,06	930,37	993,96	061,33
	746,45	810,17	877,59	948,77	877,59	940,85	37 008,51	079,79
	752,54	820,04	891,40	966,67	885,11	952,29	023,92	099,07
	759,24	830,68	905,97	985,36	893,26	964,40	039,91	119,18
	766,74	841,93	921,22	37 004,46	902,15	977,26	056,63	139,75
$20\frac{1}{2}$	774,75	854,06	937,26	024,26	911,64	990,81	074,22	161,22
	783,40	866,76	953,92	044,92	922,24	37 005,10	092,53	183,11
	793,12	880,12	971,26	066,18	933,32	020,23	111,70	206,51
	803,19	894,26	989,33	088,11	945,21	036,08	131,31	230,37
	814,10	909,05	37 008,03	110,77	957,72	052,64	151,80	254,80



(0,4)  $\gamma$ -band of NO

J	$P_2$	$P_1$	$Q_2$	$R_1$	$P_1$	$Q_1$	$R_1$	$\delta R_1$
$25\frac{1}{2}$	825.59	924.53	027.52	134.14	971.26	069.99	173.12	280.02
	837.96	940.85	047.59	158.26	985.36	088.11	195.30	305.85
	850.79	957.72	068.41	183.04	37 000.36	106.90	218.02	332.79
	864.34	975.17	089.96	208.52	015.97	126.47	241.54	360.01
	878.66	993.53	112.08	234.68	032.30	146.69	265.79	388.41
$30\frac{1}{2}$	894.26	37012.51	135.02	261.62	049.49	167.84	290.82	416.97
	909.81	032.30	158.61	289.05	067.39	189.79	316.54	446.58
	926.32	052.64	183.04	317.36	086.04	212.26	343.12	476.83
	943.40	073.81	208.30	345.97	105.40	235.58	370.10	508.37
	961.38	095.59	233.95	375.75	125.46	259.58	397.96	
$35\frac{1}{2}$	980.18	118.06	260.41	406.26	146.15	284.42	426.55	
	999.61	141.37	287.45	437.12	167.84	309.84	456.17	
	37 019.50	165.25	315.44	469.01	190.28	336.09	486.05	
	039.91	189.79	343.90	501.20	113.42	362.83	516.91	
	061.87	215.53	373.14	534.34	237.35	390.69	548.63	
$40\frac{1}{2}$	084.06	241.54	403.11	568.64	261.62	419.00	580.81	
	106.90	268.31	433.85	602.67	287.45	448.20	613.73	
		295.94	465.16	638.01	313.32	478.13	647.57	
		324.27	497.31	673.63	340.07	508.81	681.83	
		353.11	530.15	710.22	367.44	540.06	716.88	
$45\frac{1}{2}$		382.69	563.80	747.38	395.84	572.08	752.81	
		413.06	597.90	785.53	424.65	604.83	789.25	
		444.40	632.66	824.08	454.44	638.45	826.76	
		476.05	668.22	863.65	484.94	672.78	864.64	
		508.81	704.52	903.64	516.03	707.70	903.64	
$50\frac{1}{2}$		541.78	741.31	944.14	547.97	743.09	943.18	
		575.74	779.22	986.09	580.81	779.66	983.46	
		610.39	817.53	38 028.54	613.78	816.93	38 024.27	
		645.67	856.78	071.42	—	854.79	066.07	
		681.83	896.07	114.98	683.03	893.14	108.67	
$55\frac{1}{2}$		718.31	937.17	159.08	718.31	932.69	151.59	
		755.85	—	204.03	754.52	973.15	195.55	
		794.16	38 020.55	249.80	791.45	38 013.68	239.91	
		833.10	063.37	296.32	829.42	055.19	285.13	
		873.08	106.71	—	867.86	097.27	331.08	
$60\frac{1}{2}$		913.64	150.90	—	907.15	140.34	377.75	
			195.55	—	947.10	184.02	425.13	
			241.20	—	987.85	228.35	473.29	
			287.42	—	38 029.41	273.54	—	
			334.46	—	071.42	319.29	—	
$65\frac{1}{2}$			381.96	—	—	365.69	—	
						412.90		

Table 6

(0,5)  $\gamma$ -band of NO

J	$P_2$	$P_1$	$Q_2$	$R_1$	P	$Q_1$	R	$\delta R_1$
$1\frac{1}{2}$	—	—	—	—	—	—	35 103.40	—
	34 974.69	—	34 986.77	—	—	—	106.40	—
	071.80	—	991.50	—	35 090.23	—	110.55	—
	068.64	34 979.62	—	—	087.04	35 099.16	110.33	—
	065.37	081.24	35 001.14	35 025.78	085.23	100.97	121.12	—
$5\frac{1}{2}$	063.57	063.14	006.94	034.98	083.55	103.40	127.23	—
	061.00	085.81	013.56	044.97	082.89	106.40	134.48	—

(0,5)  $\gamma$ -band of NO

J	$^0P_{12}$	$P_2$	$Q_2$	$R_2$	$P_1$	$Q_1$	$R_1$	$^sR_{21}$
$10\frac{1}{2}$	961,33	989,05	021,03	056,42	082,89	110,55	142,49	—
	961,99	993,32	028,96	068,53	083,55	115,33	151,22	—
		998,11	037,85	081,52	085,23	121,12	160,70	—
	963,57	35003,51	047,31	095,06	087,64	127,23	171,20	—
	966,21	009,74	957,51	109,16	090,94	134,48	182,29	—
	969,22	016,79	068,53	124,25	095,06	142,49	194,44	—
	972,89	024,55	080,22	139,75	099,70	151,22	207,13	—
	977,18	032,83	092,51	155,87	105,38	160,70	220,83	—
$15\frac{1}{2}$	982,36	042,10	105,38	—	112,13	171,20	234,97	—
	988,36	051,82	119,43	190,63	119,43	182,29	250,20	—
		062,46	133,86	209,46	127,23	194,44	266,06	—
	35 002,23	073,69	149,18	228,62	135,98	207,13	282,71	—
$20\frac{1}{2}$	010,64	080,02	165,14	248,54	145,47	220,83	300,10	—
	019,34	098,64	—	269,10	155,87	234,97	318,26	—
	028,96	112,13	199,28	290,41	167,07	250,21	337,31	—
	039,19	126,35	217,71	312,49	178,90	266,06	357,20	35 452,98
$25\frac{1}{2}$	050,20	141,22	236,55	335,47	191,61	282,71	377,90	577,64
	061,90	157,05	256,10	358,92	204,49	300,10	398,98	502,47
	074,64	173,44	276,62	383,13	218,86	318,26	420,82	—
	087,64	190,63	297,77	408,21	233,87	337,32	444,08	555,49
$30\frac{1}{2}$	101,81	208,33	319,20	433,77	250,21	357,20	467,89	583,27
	116,33	227,23	341,78	460,27	266,82	377,90	492,14	611,51
	131,82	246,96	365,04	487,22	284,68	398,98	517,39	640,31
	148,06	266,82	389,12	515,13	302,71	420,82	543,64	670,51
$35\frac{1}{2}$	165,14	287,56	413,81	543,64	321,46	444,08	570,25	700,95
	182,29	309,03	439,25	573,14	340,80	467,27	597,80	732,27
		331,40	465,29	603,24	361,92	491,71	626,12	764,04
		354,39	492,14	634,24	383,13	516,90	655,34	—
$40\frac{1}{2}$		377,90	520,08	665,69	405,45	542,90	685,24	830,84
		402,93	548,45	697,93	428,18	569,67	715,95	865,29
		428,18	577,71	731,12	451,62	597,27	747,23	900,73
		453,81	607,68	764,94	476,04	625,60	779,30	936,95
$45\frac{1}{2}$		480,54	638,24	799,39	501,08	654,58	812,07	973,39
		508,31	669,68	834,69	527,25	684,39	846,01	36 011,15
		536,44	701,91	870,73	554,01	715,05	880,58	049,43
		565,53	734,77	907,43	581,47	746,40	915,75	088,42
$50\frac{1}{2}$		595,25	768,39	945,00	609,72	778,52	951,76	128,18
		625,60	802,77	983,18	638,89	811,37	988,57	168,42
		657,17	837,95	36 022,02	668,56	845,11	36 025,62	209,97
		689,32	873,77	061,70	699,30	879,48	063,88	251,79
$55\frac{1}{2}$		721,96	910,43	102,18	730,75	914,70	103,27	295,18
		755,42	947,85	143,01	762,86	950,72	143,01	333,88
		789,78	985,89	185,20	795,54	987,44	183,53	382,37
		824,87	36 024,89	227,66	829,33	36 024,89	224,59	—
$60\frac{1}{2}$		860,86	064,27	270,98	863,83	063,13	266,65	—
		897,22	104,74	315,09	899,14	102,18	309,76	—
		934,50	145,77	360,18	935,14	142,00	353,09	—
		972,52	187,43	405,70	971,93	182,49	397,56	—
$65\frac{1}{2}$		36011,15	229,72	452,01	36009,36	223,45	442,59	—
		050,85	273,56	499,01	047,71	265,80	488,25	—
		090,99	317,62	546,77	086,63	308,55	534,96	—
		132,29	362,43	595,50	126,70	352,29	582,78	—
$70\frac{1}{2}$		174,18	407,95	644,69	167,22	396,61	630,42	—
		217,10	454,30	694,89	208,48	441,69	679,26	—
		260,59	501,28	—	250,48	487,41	—	—
		304,76	549,24	—	293,13	534,25	—	—
$75\frac{1}{2}$			597,82	—		581,80	—	—
			647,19	—		629,83	—	—

(0,5)  $\gamma$ -band of NO

J	$^0P_{13}$	$P_2$	$Q_2$	$R_2$	$P_1$	$Q_1$	$R_1$	$^5R_{21}$
$65\frac{1}{2}$			697,55 648,46			678,68 728,44 778,97		
$70\frac{1}{2}$						882,08 934,63 987,96 37 042,23 096,98		

Table 7

(1,1)  $\gamma$ -band of NO

J	$^0P_{13}$	$P_2$	$Q_2$	$R_2$	$P_1$	$Q_1$	$R_1$	$^5R_{21}$
$\frac{1}{2}$	—	—	—	—	—	44 664,30	44 668,68	—
	44 539,74	44 543,47	44 552,08	—	44 660,17	663,58	671,40	—
	535,51	543,03	555,34	—	655,80	663,58	675,19	
	531,41	543,03	559,11	—	652,03	663,58	679,37	
	527,76	543,47	563,60	—	649,12	664,30	683,88	
$5\frac{1}{2}$	522,64	546,47	574,03	—	646,52	665,79	689,49	
	524,78	544,84	568,33	—	644,51	667,87	695,62	
	518,52	548,29	579,72	—	643,22	670,70	702,38	
	519,47	550,89	586,22	—	642,54	673,94	709,57	
	518,52	553,99	593,46	44 636,42	642,54	677,93	717,29	
$10\frac{1}{2}$	518,52	557,51	600,70	648,22	643,22	682,52	725,90	
	518,52	561,70	608,85	660,17	644,51	687,75	735,22	
	519,47	566,32	617,56	672,76	646,52	693,29	744,53	
	520,84	571,33	626,56	685,82	649,12	700,02	755,05	
	522,64	577,41	636,42	699,34	652,03	706,98	766,05	44 828,61
$15\frac{1}{2}$	524,78	583,75	646,52	713,31	655,80	714,67	777,66	843,63
	527,76	590,63	657,39	728,06	660,17	722,90	789,81	860,07
	531,41	598,17	668,68	743,47	665,27	731,74	802,52	876,87
	535,51	605,95	680,70	759,23	670,70	741,29	816,01	894,40
	539,74	614,41	693,29	775,19	677,05	751,24	829,94	912,31
$20\frac{1}{2}$	544,84	623,55	706,00	792,22	683,88	762,02	844,62	930,87
	550,89	633,15	719,64	809,71	691,19	773,43	860,07	949,98
	—	643,22	733,54	827,22	699,34	785,34	875,64	969,49
	563,60	653,90	748,13	846,11	707,73	797,88	892,10	989,85
	571,33	665,27	763,28	865,12	717,29	810,99	909,32	45 010,92
$25\frac{1}{2}$	579,00	677,05	779,02	884,84	727,04	824,55	926,98	
	587,57	689,49	795,29	904,54	737,46	838,97	945,10	
	596,64	702,38	812,06	925,36	748,13	853,95	963,81	
		715,73	829,35	946,69	760,32	869,57	983,25	
		729,80	847,27	968,58	772,40	885,47	45 003,04	
$30\frac{1}{2}$		744,53	865,61	990,82	785,34	902,26	023,48	
		759,23	884,84	45 013,84	798,62	919,79	045,41	
		775,19	904,54	037,34	812,66	937,66	067,46	
		791,42	924,52	061,43	827,22	956,19	089,56	
		808,20	945,10	085,88	842,61	975,26	112,46	
$35\frac{1}{2}$		825,68	966,34	110,84	858,38	994,95	135,50	
		843,63	988,13	136,31	874,81	45 015,54	160,13	

(1.)  $\gamma$ -band of NO

J	$^0P$	$P_2$	$Q_2$	$R_2$	$P_1$	$Q_1$	$R_1$	$^2R_{21}$
$40\frac{1}{2}$		862,14	45 010,92		892,10	036,44	184,84	
		881,30	033,87			057,84	210,06	
		900,85	057,31			079,92	236,28	
		921,05	081,18			102,62	263,13	
		941,90	106,12			125,88	289,84	
$45\frac{1}{2}$			131,30			—		
			156,84			173,98		
			183,39			199,12		
			210,66			224,74		
			237,61			250,57		
$50\frac{1}{2}$			265,52			277,62		
			293,99			304,97		
			323,17			332,87		
			353,24			361,50		
						390,21		
						420,12		
						450,48		
						481,39		

Table 8

(1,3)  $\gamma$ -band of NO

J	$^0P_{13}$	$P_2$	$Q_2$	$R_2$	$P_1$	$Q_1$	$R_1$	$^2R_{21}$
$\frac{1}{2}$	—	—	—	—	—	—	41 000,21	—
$5\frac{1}{2}$	40 872,42	40 876,60	40 884,23	40 896,57	40 991,66	40 995,47	003,59	—
	868,23	876,03	887,70	903,59	987,98	995,47	007,14	—
	864,37	876,03	891,47	911,65	984,25	—	011,74	—
	860,60	876,60	896,57	920,34	981,44	997,05	016,78	—
	858,29	878,14	901,54	929,06	979,34	998,78	022,71	—
$10\frac{1}{2}$	856,61	880,19	907,63	939,22	977,81	41 001,84	029,19	41 060,23
	855,47	882,69	914,24	949,66	976,85	004,70	036,28	071,66
	854,45	885,90	921,86	961,02	976,85	008,40	044,06	083,34
	854,45	889,40	929,06	972,40	977,81	012,98	052,97	095,84
	854,45	893,96	937,31	984,25	979,34	018,42	061,91	109,10
$15\frac{1}{2}$	855,47	998,96	946,64	997,05	981,44	024,64	071,66	122,71
	857,19	904,58	955,81	41 010,84	984,25	031,02	082,24	137,42
	859,93	910,91	965,87	024,64	987,98	038,83	093,78	152,17
	863,32	917,79	976,85	039,63	991,66	046,38	105,60	168,52
		925,09	987,98	055,12	997,05	055,12	118,27	184,53
$20\frac{1}{2}$		933,50	41 000,21	070,63	41 001,84	064,71	131,72	201,87
		941,56	012,98	087,36	008,40	074,77	145,75	219,91
		951,19	025,62	104,52	015,10	085,45	160,64	238,74
		961,02	039,63	122,02	022,71	097,14	175,70	258,22
		972,40	054,07	140,50	031,02	109,10	191,87	277,90
$25\frac{1}{2}$		982,68	069,03	159,49	039,63	122,02	208,48	298,42
		994,65	084,94	179,01	049,21	135,46	226,10	319,59
		41 007,14	101,21	199,22	059,48	149,75	243,94	341,73
		020,10	118,27	219,91	070,63	164,32	262,74	
		033,83	135,46	241,32	082,24	179,96	282,28	
		047,71	153,81	263,33	094,42	196,10	302,14	
		062,69	172,57	286,13	107,39	212,79	322,78	

(1,3)  $\gamma$ -band of NO

J	$^oP_{1,2}$	$P_2$	$Q_2$	$R_2$	$P_1$	$Q_1$	$R_1$	$^oR_{2,1}$
$30^{1/2}$		078.34	191.87	309.36	120.67	230.37	344.33	
		094.42	211.88	333.15	135.46	248.71	366.33	
		111.27	232.87	357.02	150.44	267.52	388.92	
		128.67	254.09	382.87	166.05	286.93	412.54	
		146.73	275.94	408.62	182.56	307.23	436.26	
$35^{1/2}$		165.56	298.42	435.20	199.22	328.20	461.09	
		184.53	321.57	462.38	217.02	349.62	486.61	
		204.64	345.43	489.67	235.20	371.78	512.64	
		225.17	369.88	518.10	254.09	394.78	539.20	
		246.44	394.78	546.86	273.91	418.15	566.71	
$40^{1/2}$		268.17	420.56	576.15	294.30	442.34	594.69	
		291.03	446.91	606.37	315.25	467.06	623.21	
		313.89	473.55	637.30	336.98	492.60	652.51	
		337.63	501.02	669.06	359.20	518.69	682.66	
		362.04	529.64	700.87	382.41	545.46	713.29	
$45^{1/2}$		387.07	558.48	733.38	405.74	573.24	744.69	
		412.54	588.13	766.65	430.22	601.13	776.80	
		439.03	617.86	800.51	455.13	629.94	809.05	
		465.82	648.70	834.95	480.84	659.40	842.11	
		493.53	680.23	870.36	507.18	689.46	876.08	
$50^{1/2}$		521.78	712.47	906.00	533.88	720.13	910.92	
		550.57	745.27	942.02	561.65	751.83	943.75	
		580.24	778.34	979.41	589.85	783.54		
		610.20	812.13	42 017.30	619.02	816.38		
		641.19	846.70	056.17	648.70	849.83		
$55^{1/2}$		672.59	881.79		678.84	883.81		
		704.76	917.95		709.53	918.44		
		737.62	953.99			953.99		
		770.74	991.29			989.72		
		805.23	42 029.21			42026.56		
$60^{1/2}$		839.66	067.67			063.67		
			106.55			101.34		
			146.09			139.95		
			186.32					
			227.12					

Table 9

(1,4)  $\gamma$ -band of NO

J	$^oP_{1,2}$	$P_1$	$Q_1$	$R_1$	$P_2$	$Q_2$	$R_2$	$^oR_{2,1}$
$1^{1/2}$	—	—	—	—	—	—	—	—
$5^{1/2}$	39 076.50	39 085.58	39 093.92	39 105.30	—	—	39 211.80	—
	072.87	084.84	096.29	112.09	—	—	215.00	39 231.20
	069.91	085.58	105.30	120.05	39 191.93	39 203.88	219.66	239.46
	067.37	087.24	110.70	128.27	189.91	205.71	225.51	248.74
	065.87	089.18	116.99	138.17	187.82	207.54	231.20	258.36
	—	092.25	123.91	147.96	186.49	210.29	237.61	269.28
	064.44	095.71	131.15	159.12	—	113.60	245.26	280.65
	099.91	139.18	182.42	170.41	186.49	218.00	253.88	292.75
				182.42	187.82	223.29	262.26	305.44



(1,4)  $\gamma$ -band of NO

F	$^0P_{12}$	$P_2$	$Q_2$	$R_2$	$P_2$	$Q_1$	$R_1$	$^0R_{21}$
$10\frac{1}{2}$	065,87	104,69	147,96	194,95	189,16	228,62	271,90	318,93
	066,96	110,07	157,28	208,32	191,11	234,77	282,15	333,15
	068,88	115,84	167,19	221,81	194,95	242,06	293,14	348,19
	071,72	122,74	177,83	236,81	198,89	249,75	305,08	363,76
	075,16	130,06	189,16	252,04	203,83	258,36	317,48	380,16
$15\frac{1}{2}$	079,19	138,17	200,99	267,70	209,14	267,70	330,66	397,11
	083,93	146,78	213,60	184,42	215,00	277,56	344,54	415,02
	089,18	156,05	226,75	301,59	221,81	288,29	359,05	433,65
	095,71	166,01	240,60	318,93	229,22	299,67	374,57	452,90
	102,02	176,61	255,11	337,64	237,61	311,94	390,47	472,01
$20\frac{1}{2}$	109,28	187,82	270,37	356,59	246,43	324,79	407,01	493,32
	117,52	199,75	286,22	376,21	256,02	338,15	424,71	514,86
	126,06	212,31	302,55	396,66	266,59	352,53	442,86	537,13
	135,97	225,51	319,74	417,69	277,56	367,42	461,65	559,58
	145,24	239,19	337,64	439,48	289,31	383,08	481,30	583,19
$25\frac{1}{2}$	156,05	253,88	356,12	461,65	301,59	399,47	501,47	607,18
	167,19	269,28	374,97	484,56	314,99	416,53	522,52	632,27
	179,41	285,03	394,77	508,24	329,11	434,41	544,28	657,40
	191,93	301,59	415,02	532,53	343,21	452,90	566,69	683,82
	205,71	318,93	436,23	557,28	359,05	472,01	589,74	710,85
$30\frac{1}{2}$	219,66	336,78	457,97	583,19	374,97	491,94	613,60	738,54
	234,36	355,35	480,52	609,48	391,65	512,60	638,00	767,05
	249,75	374,57	503,53	636,37	409,13	533,90	663,26	796,00
		394,40	527,39	663,82	427,27	555,92	689,33	826,04
		415,02	551,85	695,15	445,99	578,59	715,91	856,24
$35\frac{1}{2}$		436,23	576,90	721,14	465,37	602,28	743,07	887,14
		457,97	602,28	750,76	486,04	626,27	771,02	919,50
		480,52	628,92	780,94	507,01	651,10	799,66	951,32
		503,53	656,00	811,91	528,53	675,56	828,96	984,62
		527,39	683,82	843,26	551,15	702,78	859,01	
$40\frac{1}{2}$		551,85	712,16	875,36	574,14	729,68	889,68	
		577,45	741,30	908,42	597,81	757,20	921,16	
		603,38	771,02	941,95	622,31	785,76	953,25	
		629,96	801,44	976,12	647,61	814,48	986,11	
		657,40	832,42	40 011,10	673,36	844,18	40 019,62	
$45\frac{1}{2}$		685,24	864,16	046,72	699,94	874,46	053,63	
		713,83	896,72	082,94	727,04	905,54	088,58	
		743,07	929,77	119,79	755,19	937,36	124,26	
		773,14	963,51	157,09	783,81	969,96	160,38	
		803,67	997,98	195,21	812,93	40 003,07	197,10	
$50\frac{1}{2}$		834,83	40 032,99	234,07	843,26	037,16		
		866,92	068,88	273,16	873,96	071,37		
		900,03	105,35		905,54	106,67		
		933,04	142,61		937,36	142,61		
		967,22	180,30		970,30	179,04		
$55\frac{1}{2}$		40 001,98			40 003,80	215,87		
		037,16			038,35			
		073,33			073,33			
		110,26			108,72			
		147,72			145,10			
$60\frac{1}{2}$		185,63						
		224,14						



Table 10

(1,5)  $\gamma$ -band of NO

J	$^{\circ}\text{P}_{12}$	$\text{P}_2$	$\text{Q}_2$	$\text{R}_2$	$\text{P}_1$	$\text{Q}_1$	$\text{R}_1$	$^{\text{S}}\text{R}_{21}$
$\frac{1}{2}$	—	—	—	—	—	37440,74	37444,40	—
	—	37321,39	37329,32	37340,74	—	440,08	448,20	—
	37313,32	321,39	332,79	347,91	—	440,08	451,84	—
	309,84	321,39	337,25	356,28	—	440,74	456,17	—
	306,79	322,57	342,31	365,96	—	442,12	461,89	—
$\frac{5}{2}$	304,72	324,27	347,91	375,75	—	444,40	468,08	—
	303,08	326,75	354,28	385,81	—	447,36	475,05	37506,98
	302,27	329,89	361,33	396,72	—	451,07	482,66	518,00
	302,27	333,68	368,99	408,36	37423,81	455,48	491,10	530,15
	303,08	338,20	377,37	420,36	425,53	460,91	500,44	543,58
$10\frac{1}{2}$	304,04	343,12	386,45	433,85	427,64	466,92	510,33	557,57
	305,85	349,04	396,26	447,36	430,52	473,65	520,98	572,08
	308,37	355,61	406,67	461,89	433,85	481,19	532,48	587,43
	311,71	362,83	417,83	476,83	438,60	489,52	544,66	603,47
	315,44	370,56	429,61	492,50	443,79	498,73	557,57	620,32
$15\frac{1}{2}$	320,22	379,19	442,12	508,81	449,56	508,37	571,55	638,01
	325,64	388,41	455,48	526,01	456,17	518,90	585,86	656,39
	331,73	398,34	469,01	543,58	463,61	530,15	601,12	675,57
	338,20	408,98	483,65	562,19	471,79	542,26	617,08	695,52
$20\frac{1}{2}$	345,97	420,36	498,73	581,26	480,81	555,08	633,78	715,81
	354,28	432,30	514,83	601,12	490,35	568,64	651,27	737,21
	362,83	444,97	531,42	621,57	500,44	582,95	669,45	759,62
	372,10	458,44	548,63	642,85	511,90	597,90	688,55	782,34
	382,26	472,54	566,75	664,57	523,74	613,73	708,01	805,79
	393,25	487,32	585,50	687,22	536,31	630,42	728,33	830,05
$25\frac{1}{2}$	404,96	502,76	604,83	710,47	549,77	647,57	749,53	855,02
	416,97	518,90	624,90	734,23	563,80	665,58	771,48	880,88
	429,61	535,89	645,67	758,97	578,86	684,38	794,16	907,15
	443,79	553,40	667,07	784,23	594,49	703,80	817,53	934,53
	458,44	571,55	689,24	810,25	610,78	723,98	841,66	962,75
$30\frac{1}{2}$	473,65	590,79	712,09	836,82	627,94	744,89	866,53	991,33
	489,52	610,39	735,45	863,65	645,67	766,67	892,15	38020,57
	505,61	630,94	759,67	892,15	664,57	789,25	918,46	051,13
	522,84	651,78	784,56	921,25	683,72	812,29	945,42	081,90
	540,69	673,63	810,25	950,67	703,80	836,33	973,15	113,59
$35\frac{1}{2}$	559,38	696,06	836,82	980,98	724,28	860,87	38001,87	146,11
	578,86	719,08	863,65	38011,90	745,94	886,26	031,06	178,74
	598,78	743,09	891,53	043,43	768,24	912,45	060,95	212,82
	619,64	767,70	919,94	075,87	791,45	939,34	091,79	
	640,19	792,98	949,18	108,67	815,07	966,92	123,16	
$40\frac{1}{2}$	663,31	818,97	978,97	142,33	839,63	995,20	155,41	
		845,67	38009,51	176,83	864,64	38024,27	188,13	
		873,08	040,84	211,72	890,83	054,10	221,86	
		901,48	072,87	247,52	917,48	084,64	256,08	
		930,26	105,46	284,01	944,87	115,83	291,06	
$45\frac{1}{2}$		959,67	138,91	321,17	973,15	147,89	326,77	
		990,19	172,97	358,95	38001,87	180,38	363,29	
		38021,00	207,70	397,50	031,65	213,98	400,51	
		052,81	243,31	436,90	062,29	247,98	438,42	
		085,25	279,52	476,94	093,03	282,89	476,94	
$50\frac{1}{2}$		118,45	316,28	517,96	234,90	318,54		
		152,21	353,97	559,59	157,75	354,93		
		186,78	392,29		190,75	391,90		
		221,86	431,29		224,69	429,62		
		258,28	471,14		259,68	468,17		
$55\frac{1}{2}$		294,83	511,46		294,83	507,28		

(1,5)  $\gamma$ -band of NO.

J	$^0P_{11}$	$P_2$	$Q_2$	$R_2$	$P_1$	$Q_1$	$R_1$	$^5R_{21}$
$60\frac{1}{2}$		332,41	552,70		331,34	547,27		
		370,33	594,33		368,12	587,73		
		409,33			405,73	629,21		
		448,92			444,26	671,30		
		499,05			483,46	714,30		
		530,52			523,51	757,85		
		572,32			563,87	802,22		
						847,21		
						892,97		
						939,42		

Table 11

(1,6)  $\gamma$ -band of NO

J	$^0P_{12}$	$P_2$	$Q_2$	$R_2$	$P_1$	$Q_1$	$R_1$	$^5R_{21}$
$1\frac{1}{2}$	—	—	—	—	—	35704,69	35708,44	35715,95
$5\frac{1}{2}$	35582,39	35585,93	35593,98	35605,38	35700,22	704,17	711,60	723,22
	577,71	585,57	597,27	612,77	696,34	704,17	715,95	731,12
	574,30	585,93	601,61	621,38	693,28	704,69	720,87	740,05
	571,38	587,19	606,93	630,49	690,70	706,62	726,39	749,84
	569,67	589,17	612,77	640,31	689,32	708,86	732,91	760,18
$10\frac{1}{2}$	568,09	591,82	619,46	650,87	688,68	712,06	740,05	771,20
	567,72	595,25	626,70	662,06	688,68	715,95	747,93	783,09
	567,72	599,29	634,63	673,96	689,32	720,87	756,64	795,54
	568,54	604,14	643,42	686,73	690,70	726,39	766,00	808,96
	570,25	609,72	652,84	700,22	693,63	732,91	776,38	823,31
$15\frac{1}{2}$	572,59	615,89	663,09	714,19	696,94	740,05	787,06	838,53
	575,72	622,85	673,96	728,98	700,95	747,93	799,39	854,28
	579,38	630,49	685,60	744,47	705,90	756,64	812,07	871,08
	584,00	638,89	697,93	760,73	711,60	766,35	825,56	888,37
	589,17	648,04	710,95	777,71	718,00	776,70	839,76	906,47
$20\frac{1}{2}$	595,25	657,88	724,73	795,54	724,73	787,70	854,88	925,49
	601,61	668,56	739,23	813,79	732,91	799,78	870,73	945,00
	609,16	679,80	754,40	832,87	741,92	812,38	887,38	965,63
	617,28	691,77	770,33	852,76	751,47	825,92	904,80	987,04
	626,12	704,69	787,06	873,24	761,88	840,24	922,86	36009,06
$25\frac{1}{2}$	635,66	718,00	804,36	894,61	773,03	855,27	941,88	031,84
	645,76	732,27	822,53	916,67	784,97	871,08	961,73	055,40
	656,47	747,23	841,33	939,36	797,72	887,73	982,14	079,96
	668,56	762,86	860,86	962,70	811,37	905,06	36003,41	104,74
	681,17	779,30	881,22	987,04	825,56	923,29	025,62	130,85
$30\frac{1}{2}$	694,51	796,39	902,29	36011,82	840,24	942,21	048,35	157,68
	708,44	814,18	924,04	037,46	856,40	961,96	072,07	185,20
	723,22	832,87	946,49	063,88	873,24	982,51	096,31	213,33
	738,42	852,19	969,75	090,99	890,41	36003,74	121,51	242,24
	754,40	872,25	993,66	118,70	908,62	025,85	147,34	
$35\frac{1}{2}$	771,67	893,10	36018,38	147,34	927,56	048,66	174,18	
	789,78	914,70	043,76	176,56	947,39	072,07	201,42	
	807,90	936,95	069,94	206,31	967,80	096,31	229,72	
	827,29	959,99	096,65	237,09	989,05	121,51	258,72	
	847,06	983,78	124,44	268,64	36011,15	147,34	288,46	
$35\frac{1}{2}$	867,65	36008,26	152,79	300,80	034,01	174,18	318,96	
	889,25	033,53	181,75	333,79	057,65	201,42	350,34	

(1,6)  $\gamma$ -band of NO,

J	$^0P_{12}$	$P_2$	$Q_2$	$R_2$	$P_1$	$Q_1$	$R_1$	$^5R_{21}$
$40\frac{1}{2}$	911,38	059,55	211,55	367,44	081,98	229,72	382,37	
	934,50	086,31	242,24	401,91	107,03	258,72	415,21	
	957,92	113,73	273,56	437,07	133,01	288,46	448,76	
	982,51	142,00	305,73	473,06	159,66	318,96	483,14	
	36007,51	171,08	338,48	509,63	187,05	350,34	518,21	
$45\frac{1}{2}$		200,57	372,07	546,77	215,19	382,37	554,13	
		231,07	406,32	584,79	244,30	415,21	590,55	
		262,31	441,05	623,78	273,97	448,76	627,95	
		294,30	477,16	663,34	304,76	483,14	666,29	
		327,10	513,75	703,53	336,04	518,21	705,22	
$50\frac{1}{2}$		360,77	550,95	744,75	367,98	554,13	744,75	
		394,71	589,07	786,58	400,94	590,79	785,39	
		429,71	627,95		434,53	628,26	826,43	
		465,43	667,34		469,15	666,29	868,33	
		502,15	707,66		504,19	705,22		
$55\frac{1}{2}$		538,98	748,46		540,09	744,75		
		576,93	790,25		576,93	785,39		
		615,96	832,62		614,31	826,43		
		655,39	875,78		652,54	868,33		
		695,57	919,76		691,45			
$60\frac{1}{2}$		736,67	964,40		731,29			
		778,34			771,60			
		820,85			812,94			
		864,34			854,99			

Table 12

(2,2)  $\gamma$ -band of NO

J	$^0P_{12}$	$Q_3$	$Q_2$	$R_2$	$P_1$	$Q_1$	$R_1$	$^5R_{21}$
$\frac{1}{2}$	—	—	—	—	—	—	—	—
$5\frac{1}{2}$	45002,15	45006,48	45013,84	—	—	45124,98	45132,97	—
	44997,55	005,41	016,82	—	—	124,98	136,31	—
	993,60	005,41	020,67	—	—	124,98	140,57	—
	990,03	005,41	024,99	—	—	125,88	145,55	—
	986,73	006,48	029,91	45057,31	45107,84	127,00	150,81	—
$10\frac{1}{2}$	984,35	007,84	035,19	066,04	106,12	129,58	156,84	—
	982,65	009,94	041,15	076,10	104,75	132,18	163,51	—
	981,31	012,58	047,56	086,38	104,75	135,50	170,55	—
	980,56	015,54	054,57	097,49	104,75	139,27	178,49	—
	980,56	019,23	062,00	108,48	104,75	143,94	186,91	—
$15\frac{1}{2}$	980,56	023,48	070,20	120,79	106,12	149,15	195,95	—
	981,31	028,11	078,78	132,97	108,48	154,74	205,70	—
	982,65	033,42	087,81	146,26	110,84	161,19	215,98	—
	984,35	039,14	097,49	160,13	113,89	168,29	226,91	—
	986,73	045,41	107,84	173,98	117,65	175,82	238,30	—
$20\frac{1}{2}$	990,03	052,25	118,41	188,60	123,09	184,21	250,57	—
	993,60	059,71	129,58	203,54	127,00	193,03	263,13	—
	997,55	067,46	141,51	219,32	132,18	202,43	276,49	—
	45002,15	076,10	153,99	235,62	138,68	212,53	290,44	—
		085,19	166,84	252,49	145,55	223,29	304,97	45390,21
		094,74	180,33	269,54	153,05	234,33	320,10	409,23

(2,2)  $\gamma$ -band of NO

J	$^0P_{12}$	$P_2$	$Q_2$	$R_2$	$P_1$	$Q_1$	$R_1$	$^S R_{21}$
$25\frac{1}{2}$		104,75	194,26	287,42	161,19	246,49	335,97	428,90
		115,37	208,79	305,87	169,72	258,78	352,28	448,95
		125,88	223,94	324,56	178,49	271,96	369,32	470,03
		138,68	239,57	344,22	188,60	285,54	386,66	491,11
		150,81	255,69	364,38	199,12	299,86	404,90	—
		163,51	272,49	384,74	210,06	314,68	423,63	535,68
		177,19	289,84	405,79	221,63	330,09	442,75	559,00
$30\frac{1}{2}$		191,13	307,58	427,37	233,76	345,98	462,84	582,62
		205,70	325,96	449,78	246,49	362,96	483,19	606,49
		221,02	344,85	472,49	260,16	380,13	504,26	—
		236,28	364,38	495,79	274,46	397,89	525,93	—
		252,49	384,74	519,76	289,02	416,22	548,17	—
$35\frac{1}{2}$		269,54	404,90	543,85	304,15	435,38	570,82	—
		286,64	426,19	568,97	320,10	455,04	594,34	—
		304,97	447,89	594,34	335,97	475,22	618,37	—
		323,17	470,03	620,41	353,24	495,79	642,85	—
		342,10	493,33	646,97	370,92	517,29	668,30	—
$40\frac{1}{2}$		361,50	516,38	674,52	389,01	538,81	693,95	—
		382,02	540,18	701,97	407,38	561,78	720,20	—
		402,65	564,71	730,40	427,37	585,03	747,23	—
		423,63	589,60	759,06	447,11	608,38	774,79	—
		445,42	615,44	788,33	467,51	632,85	802,85	—
$45\frac{1}{2}$		467,51	645,97	818,28	488,72	657,77	831,17	—
		490,12	668,30	—	510,52	683,28	860,69	—
		513,89	695,71	—	532,96	709,24	890,30	—
		—	723,58	—	555,52	735,88	920,52	—
		—	751,96	—	579,02	—	—	—
$50\frac{1}{2}$		—	781,02	—	—	—	—	—
		—	810,84	—	—	—	—	—
		—	840,82	—	—	—	—	—
		—	871,56	—	—	—	—	—
		—	—	—	—	—	—	—

Table 13

(2,3)  $\gamma$ -band of NO

J	$^0P_{12}$	$P_2$	$Q_2$	$R_2$	$P_1$	$Q_1$	$R_1$	$^S R_{21}$
$\frac{1}{2}$		—	—	—	—	43306,25	43310,04	—
		—	—	—	—	305,15	313,30	—
		—	—	—	—	305,15	316,61	—
		—	—	—	—	305,15	320,98	—
		—	—	—	—	306,25	325,88	—
$5\frac{1}{2}$		—	—	—	—	307,94	331,44	—
		—	—	—	—	310,04	337,71	—
		—	—	—	—	313,30	344,29	—
		—	—	—	—	316,61	352,14	—
		—	—	—	—	320,98	360,17	—
$10\frac{1}{2}$		—	—	—	—	325,88	369,12	—
		—	—	—	—	331,44	378,48	—
		—	—	—	—	337,71	388,49	—
		—	—	—	—	344,29	399,30	—
		—	—	—	—	352,14	410,23	—
$15\frac{1}{2}$		—	—	—	—	360,17	422,58	—

(2,3)  $\gamma$ -band of NO

J	$^0P_{12}$	$P_2$	$Q_2$	$R_2$	$P_1$	$Q_1$	$R_1$	$^8R_{21}$
$20\frac{1}{2}$	—	—	43303,78	—	—	369,12	435,35	—
	—	—	315,91	—	—	378,48	448,57	—
	—	—	328,32	—	—	388,49	462,51	—
	—	—	341,28	—	—	399,30	477,04	—
	—	—	354,95	43440,49	43332,98	410,23	492,29	—
	—	—	369,12	458,26	341,28	422,58	508,11	—
$25\frac{1}{2}$	—	—	383,86	477,04	350,23	435,35	524,45	—
	—	43306,25	399,30	495,84	360,17	448,57	541,65	—
	—	318,37	415,13	516,06	369,12	462,51	559,31	—
	—	331,44	431,69	536,40	380,17	477,04	577,51	—
	—	344,29	448,57	557,79	391,62	492,29	596,61	—
	—	358,20	466,61	578,84	403,28	508,11	616,26	—
$30\frac{1}{2}$	—	—	372,57	485,23	601,16	524,45	637,28	—
	—	—	387,55	503,71	623,80	541,65	658,16	—
	—	—	403,28	523,70	647,37	559,31	679,43	—
	—	—	419,38	543,20	671,57	577,51	701,48	—
	—	—	435,96	563,80	695,63	596,61	—	—
	—	—	453,63	585,27	—	616,26	—	—
$35\frac{1}{2}$	—	—	471,48	607,05	746,09	636,06	—	—
	—	—	490,03	629,39	772,10	657,07	—	—
	—	—	509,19	652,31	799,41	678,57	—	—
	—	—	529,04	676,11	827,11	700,77	—	—
	—	—	549,61	700,77	—	723,38	—	—
	—	—	570,87	725,01	—	—	—	—
$40\frac{1}{2}$	—	—	592,11	750,61	—	770,70	—	—
	—	—	614,41	776,35	—	795,28	—	—
	—	—	637,28	802,98	—	820,54	—	—
	—	—	660,43	830,24	—	846,41	—	—
	—	—	683,86	857,82	—	872,54	—	—
	—	—	707,67	886,48	—	899,85	—	—
$45\frac{1}{2}$	—	—	732,58	915,24	—	927,76	—	—
	—	—	657,69	945,06	—	956,06	—	—
	—	—	—	975,66	—	984,83	—	—
	—	—	44006,30	—	—	44014,34	—	—
	—	—	037,43	—	—	—	—	—
	—	—	069,60	—	—	—	—	—
$50\frac{1}{2}$	—	—	102,72	—	—	—	—	—

Table 14

(2,7)  $\gamma$ -band of NO

J	$^0P_{12}$	$P_2$	$Q_2$	$R_2$	$P_1$	$Q_1$	$R_1$	$^8R_{21}$
$\frac{1}{2}$	—	—	—	—	—	36305,73	36309,76	—
	—	—	36187,26	36194,77	36300,80	304,76	313,02	—
	—	—	186,85	198,29	213,79	304,76	317,04	—
	—	—	187,26	202,71	222,23	305,73	321,53	—
	—	—	188,45	207,99	231,07	307,45	327,10	—
	—	—	190,42	213,79	241,32	309,76	333,51	—
$5\frac{1}{2}$	—	—	193,04	220,44	251,79	313,02	340,58	—
	—	—	196,52	227,66	262,73	317,04	348,44	—
	—	—	200,57	235,66	274,73	321,92	357,11	—
	—	—	205,41	244,30	287,30	327,49	366,62	—
	—	—	—	—	292,73	—	—	—
	—	—	—	—	—	—	—	—

(2,7)  $\gamma$ -band of NO

J	$oP_{12}$	$P_2$	$Q_2$	$R_2$	$P_1$	$Q_1$	$R_1$	$sR_{21}$
$10\frac{1}{2}$	36172,23	211,01	253,71	300,80	295,18	333,79	376,92	—
	174,18	217,10	263,88	314,52	298,64	341,02	387,71	—
	—	224,16	274,73	329,29	302,34	348,96	399,83	—
	181,14	231,86	286,41	344,87	307,45	357,68	412,57	—
$15\frac{1}{2}$	185,58	240,19	298,64	361,04	313,02	367,44	425,85	—
	190,94	249,28	311,66	377,66	319,36	377,66	440,12	—
	196,82	259,17	325,47	395,40	326,77	388,67	455,06	36524,94
	203,63	269,73	339,93	413,74	334,53	400,58	470,83	544,51
$20\frac{1}{2}$	211,01	281,00	355,04	432,78	343,33	413,30	487,41	565,08
	219,14	293,13	370,95	452,62	353,09	426,83	504,69	586,22
	227,66	305,73	387,71	473,06	363,38	441,05	522,83	608,15
	237,60	319,36	404,88	494,17	374,45	455,95	541,64	630,81
$25\frac{1}{2}$	248,02	333,51	423,00	516,07	386,46	471,80	561,12	654,30
	259,17	348,44	441,69	538,98	399,17	488,25	581,80	678,68
	270,98	364,05	461,27	562,34	412,57	505,67	602,99	703,53
	283,35	380,58	481,49	586,22	426,83	524,00	624,98	729,60
$30\frac{1}{2}$	296,66	397,56	502,39	611,10	441,69	542,69	647,69	756,21
	310,35	415,21	524,00	636,63	457,82	562,34	671,26	783,40
	325,47	434,12	546,77	662,97	474,43	582,78	695,57	811,47
	340,58	453,34	569,82	689,81	491,74	604,04	720,64	840,56
$35\frac{1}{2}$	357,11	473,37	593,79	717,55	509,96	626,00	746,45	869,89
	374,45	494,17	618,25	746,10	528,87	648,76	773,03	900,66
	391,64	515,72	643,64	774,75	548,56	672,27	800,54	931,72
	410,22	537,98	669,73	804,97	569,12	696,56	828,76	—
$40\frac{1}{2}$	—	561,12	696,56	835,70	590,55	721,63	857,33	996,60
	—	584,79	724,11	866,76	612,36	747,38	887,06	37029,91
	—	609,17	752,54	898,41	634,97	774,10	917,44	064,01
	—	634,40	781,46	931,72	658,76	801,46	948,77	099,07
$45\frac{1}{2}$	—	660,44	811,47	965,38	683,02	829,63	—	135,02
	—	—	841,93	999,61	708,21	—	37013,13	171,26
	—	714,21	873,02	37034,73	—	888,12	046,67	208,52
	—	742,89	904,89	071,01	760,76	918,56	080,79	—
$50\frac{1}{2}$	—	771,60	937,26	108,06	788,11	949,77	115,80	—
	—	801,46	971,26	145,11	816,19	981,63	151,80	—
	—	831,96	37006,12	183,04	845,47	37014,42	188,19	—
	—	—	—	—	874,95	047,59	226,02	—
$55\frac{1}{2}$	—	—	—	—	905,97	082,06	263,77	—
	—	—	—	—	937,26	116,95	303,08	—
	—	—	—	—	969,69	152,86	343,12	—
	—	—	—	—	37002,69	188,84	383,45	—
—	—	—	—	—	—	226,02	—	—

Table 15

(3,4)  $\gamma$ -band of NO.

J	$oP_{12}$	$P_1$	$Q_2$	$R_2$	$P_1$	$Q_1$	$R_1$	$sR_{21}$
$\frac{1}{2}$	—	—	—	—	—	43790,45	43794,46	—
	—	43671,57	43679,43	—	—	789,30	797,18	—
	—	670,77	682,10	—	—	789,30	800,90	—
	—	670,77	686,24	—	—	789,30	805,03	—
$5\frac{1}{2}$	—	670,77	690,27	—	—	790,45	810,08	—
	—	671,57	694,87	—	—	791,91	815,53	—
	—	673,51	700,77	—	—	794,46	821,70	—
	—	676,11	706,71	—	—	797,18	828,44	—



(3,4)  $\gamma$ -band of NO.

J	$^0P_{12}$	$P_2$	$Q_2$	$R_2$	$P_1$	$Q_1$	$R_1$	$^8R_{21}$
$10\frac{1}{2}$		678,57	713,11	—	—	800,90	835,99	
		682,10	720,07	—	—	805,03	844,08	
		686,24	728,62	—	—	810,08	852,87	
		690,27	737,11	—	—	815,53	862,30	
		695,63	746,09	—	—	821,70	872,54	
		701,48	755,59	—	—	828,44	883,09	
$15\frac{1}{2}$		707,67	765,80	43827,11	—	835,99	894,48	
		714,64	776,35	842,03	—	844,08	906,31	
		722,12	787,49	856,70	—	852,87	919,00	
		730,55	799,41	872,54	—	862,30	932,22	
		738,95	812,02	888,48	—	872,54	946,09	
		747,85	825,19	905,10	—	883,09	960,60	
$20\frac{1}{2}$		757,69	838,59	023,11	—	894,48	975,66	
		768,02	852,87	—	—	906,31	991,55	
		778,75	867,46	—	—	919,00	44007,99	
		790,45	883,09	978,87	43844,08	932,22	024,91	
		802,98	998,60	998,61	854,55	946,09	042,57	
		815,53	915,24	44018,97	864,66	960,60	061,30	
$25\frac{1}{2}$		828,44	932,22	039,86	876,49	975,66	080,32	
		842,03	949,93	061,30	888,48	991,55	100,45	
		856,70	968,08	082,33	901,45	44007,99	120,71	
		871,48	986,67	—	915,24	024,91		
		886,48	44006,30	—	929,31	042,57		
			026,28	—	944,08			
$30\frac{1}{2}$			046,82	—	959,19			

Table 16

(3,5)  $\gamma$ -band of NO.

J	$^0P_{12}$	$P_2$	$Q_2$	$R_2$	$P_1$	$Q_1$	$R_1$	$^8R_{21}$
$\frac{1}{2}$		—	—	—	—	—	42031,17	
		41907,38	41914,24	—	—	—	034,39	
		906,63	917,95	—	—	—	037,11	
		906,63	921,87	—	—	—	041,76	
		907,38	926,97	—	—	—	046,28	
		908,78	932,19	—	—	42029,21	052,14	
$5\frac{1}{2}$		910,92	937,59	—	—	031,17	058,38	
		913,17	944,10	41978,51	42007,61	034,39	065,21	
		916,43	951,08	989,72	007,61	038,79	073,27	
		920,18	958,57	42000,68	008,37	042,78	081,49	
		925,15	967,20	013,05	009,52	048,23	090,75	
		929,50	975,89	026,56	011,76	053,20	100,64	
$10\frac{1}{2}$		935,40	985,23	039,35	014,78	060,83	111,34	
		941,51	995,34	053,20	017,91	068,12	121,89	
		948,18	42005,86	067,67	022,41	076,03	133,94	
		955,42	017,30	082,69	026,56	084,71	147,27	
		963,89	029,21	098,41	032,66	094,12	159,94	
		973,01	041,76	114,85	038,79	104,10	173,68	
$15\frac{1}{2}$		981,84	055,09	132,39	046,28	114,85	187,83	
		992,18	068,12	149,31	053,20	126,21	203,09	

(3,5)  $\gamma$ -band of NO

$J$	$^2P_{1,2}$	$P_2$	$Q_2$	$R_2$	$P_1$	$Q_1$	$R_1$	$^2R_{1,2}$
$20\frac{1}{2}$		42002,24	082,69	167,60	061,67	138,15	219,08	
		013,05	097,84	186,32	069,94	150,94	235,74	
		024,67	113,18	204,79	079,74	163,62	—	
		037,11	129,54	224,82	090,01		270,10	
		049,73	146,09	245,88	100,64		288,51	
$25\frac{1}{2}$		063,67	163,62	267,54	112,03			
		077,80		289,25	124,06			
		092,88		311,53				
		108,61		334,51				
		124,06		358,74				
$30\frac{1}{2}$		140,71		383,06				
		158,21						
		175,98						
		194,14						
$35\frac{1}{2}$		213,36						

# ZUSAMMENHANG ZWISCHEN DER STRUKTUR UND DEN PHYSIKALISCHEN EIGENSCHAFTEN DES GLASES

## II. MITTEILUNG

Von

I. NÁRAY-SZABÓ

CHEMISCHES ZENTRALFORSCHUNGSINSTITUT DER UNGARISCHEN AKADEMIE DER WISSENSCHAFTEN,  
BUDAPEST

(Vorgelegt von P. Gombás. — Eingegangen: 15. XI. 1957)

In Verfolgung der in der I. Mitteilung erkannten Gesetzmässigkeiten wurden Gleichungen für das Sauerstoffionenvolumen in Gläsern mit vier und mehr Komponenten angegeben, die endlich zu 4 Gleichungen zusammengezogen werden können. Diese gelten 1. für Gläser auf Natronsilikatgrundlage, 2. für Gläser auf Kalisilikatgrundlage, 3. für Gläser auf Natronborosilikatgrundlage und 4. für Gläser auf Kaliborosilikatgrundlage. Mit diesen Gleichungen kann man das Sauerstoffionenvolumen und damit die Dichte von Gläsern, deren Zusammensetzung zwischen gewissen Grenzen bleibt, mit befriedigender Genauigkeit berechnen.

### Das Sauerstoffionenvolumen in Silikatgläsern mit vier oder mehr Komponenten

Wie in der ersten Mitteilung dieser Reihe [1] gezeigt wurde, kann man für das Volumen  $v$ , welches im Glas von einem  $O^{2-}$ -Ion in Anspruch genommen wird, einfache lineare Gleichungen angeben, die aus der Zusammensetzung die Berechnung dieses Volumens mit ziemlicher Genauigkeit gestatten. Für Gläser mit zwei oder drei Komponenten konnte hierfür ein Beweis erbracht werden. Bei der Fortsetzung dieser Arbeit habe ich gefunden, dass solche Gleichungen auch für Gläser mit mehr als drei Komponenten aufgestellt werden können.

Die Grundgleichungen bleiben diejenigen der I. Mitteilung u. zw. für Natronsilikatgläser

$$v = 3,8 R + 14,9$$

und für Kalisilikatgläser

$$v = 12 R - 1,2.$$

( $R$  ist  $O/Si+B+Al+\dots$ )

Bei der Einführung von weiteren Komponenten in das Glas werden diese Grundgleichungen in derselben Weise modifiziert wie bei den Gläsern mit drei Komponenten, d. h. proportional den eingeführten Grammionen. Die Proportionalitätsfaktoren sind für jedes Ion charakteristisch, sie bleiben in Gläsern auf Natronsilikatgrundlage konstant und unabhängig von der Gegenwart anderer Komponenten. Für Kalisilikatgläser gelten wieder andere, von einander unabhängige, konstante Faktoren. Die Prüfung dieser Zusammenhänge an dem vorhandenen experimentellen Material hat erwiesen, dass sie

zwischen gewissen Grenzen gültig sind. Bei Natronborosilikatgläsern muss auch der Natriumgehalt in Betracht gezogen werden, und die additive Konstante wird durch die Anwesenheit gewisser Ionen etwas modifiziert.

Betrachten wir zunächst die Natronsilikatgläser, die zwei Alkaliionen und ein Erdalkaliumion enthalten. Tabelle 1 zeigt Natrium—Lithium—Calciumsilikatgläser. Die mit einem Stern versehenen chemischen Symbole bedeuten jeweils die Zahl der Grammionen des betreffenden Elements in 100 g Glas.

Tabelle 1

Na<sub>2</sub>O—Li<sub>2</sub>O—CaO—SiO<sub>2</sub>—Gläser (2)

SiO <sub>2</sub> %	Na <sub>2</sub> O%	Li <sub>2</sub> O%	Li <sub>2</sub> O Mole	CaO%	CaO Mole	Dichte g/cm <sup>3</sup>	Volum von 100 g Glas cm <sup>3</sup>	O <sup>2-</sup> -Grammionen pro 100 g	R	Volumen pro O <sup>2-</sup> -Ion Å <sup>3</sup>		Diff.
										gem.	ber.	
74,89	0	15	0,500	10,02	0,179	2,454	40,75	3,169	2,542	21,32	21,26	—0,06
74,94	2	13	0,433	9,94	0,178	2,456	40,72	3,137	2,513	21,57	21,48	—0,09
74,96	4	11	0,367	10,08	0,180	2,463	40,60	3,106	2,491	21,70	21,70	± 0
75,02	6	9	0,300	10,00	0,179	2,466	40,55	3,072	2,462	21,91	21,92	+0,01
75,14	9	6	0,200	9,93	0,177	2,475	40,40	3,022	2,418	22,19	22,25	+0,06
74,96	11	4	0,133	10,02	0,179	2,484	40,26	2,983	2,392	22,40	22,43	+0,03
75,10	13	2	0,067	9,91	0,177	2,484	40,26	2,954	2,363	22,62	22,68	+0,06
75,00	14	1	0,033	10,25	0,183	2,482	40,29	2,938	2,354	22,76	22,77	+0,01
75,08	14,75	0	0	10,22	0,183	2,482	40,29	2,919	2,337	22,91	22,86	—0,05

Die mit der Gleichung

$$v = 3,8 R - 2,4 \text{ Li}^* - 5 \text{ Ca}^* + 14,9 \quad (1)$$

berechneten Werte zeigen eine maximale Abweichung von 0,42% gegenüber den gemessenen im Bereich von  $R = 2,337 - 2,542$ .

Natrium—Kalium—Calciumsilikatgläser enthält die Tabelle 2.

Tabelle 2

Na<sub>2</sub>O—K<sub>2</sub>O—CaO—SiO<sub>2</sub>—Gläser (3)

SiO <sub>2</sub> %	Na <sub>2</sub> O%	K <sub>2</sub> O%	K <sub>2</sub> O Mole	CaO%	CaO Mole	Dichte g/cm <sup>3</sup>	Volum von 100 g Glas cm <sup>3</sup>	O <sup>2-</sup> -Grammionen pro 100 g	R	Volumen pro O <sup>2-</sup> -Ion Å <sup>3</sup>		Diff.
										gem.	ber.	
75,07	12,94	1,94	0,020	9,98	0,178	2,477	40,37	2,906	2,327	23,06	23,03	+0,03
75,02	11,06	4,12	0,044	9,87	0,176	2,473	40,44	2,894	2,319	23,19	23,19	± 0
75,04	8,97	6,11	0,065	10,03	0,179	2,467	40,54	2,885	2,312	23,31	23,32	+0,01
74,97	5,98	9,00	0,096	10,00	0,179	2,460	40,65	2,867	2,298	23,52	23,51	—0,01
74,86	4,13	11,17	0,119	10,07	0,180	2,454	40,75	2,858	2,293	23,66	23,67	—0,01
75,15	1,85	13,04	0,138	10,13	0,181	2,442	40,95	2,850	2,280	23,84	23,78	—0,06

Kalium übt auf Natronsilikatglas eine ausdehnende Wirkung aus, entsprechend der Gleichung

$$v = 3,8 R + 4 K^* - 5 Ca^* + 14,9 \quad (2)$$

mit einem maximalen Fehler von 0,25% im Bereich von  $R = 2,280 - 2,327$ . Einfache Natron-Kalisilikatgläser wurden noch nicht untersucht, doch ist der Faktor, welcher aus obstehenden Gläsern abgeleitet wurde, auch für andere Gläser mit Natronsilikatunterlage gültig.

Bariumhaltige Natron-Kalisilikatgläser sind in Tabelle 3 angeführt.

Tabelle 3

$Na_2O-K_2O-BaO-SiO_2$ -Gläser (4)

$SiO_2\%$	$Na_2O\%$	$K_2O\%$	$K_2O$ Mole	$BaO\%$	$BaO$ Mole	Dichte g/cm <sup>3</sup>	Volum von 100 g Glas cm <sup>3</sup>	$O^{2-}$ - Gramm- ionen pro 100 g	$R$	Volumen pro $O^{2-}$ -Ion Å <sup>3</sup>		Diff.
										gem.	ber.	
70	12,5	12,5	0,133	5	0,033	2,528	39,56	2,698	2,316	24,33	24,49	+0,15
70	10	10	0,106	10	0,065	2,545	39,29	2,662	2,285	24,50	24,16	-0,34
70	7,5	7,5	0,080	15	0,098	2,634	37,97	2,629	2,257	23,96	23,82	+0,14
65	12,5	12,5	0,133	10	0,065	2,652	37,71	2,564	2,370	24,40	24,70	+0,30
65	10	10	0,106	15	0,098	2,705	36,97	2,529	2,337	24,26	24,34	+0,08
65	7,5	7,5	0,080	20	0,130	2,752	36,34	2,495	2,306	24,17	23,99	-0,18
60	10	10	0,106	20	0,130	2,834	35,29	2,393	2,398	24,47	24,55	+0,08
60	7,5	7,5	0,080	25	0,163	2,881	34,71	2,360	2,365	24,13	24,20	+0,07
60	5	5	0,053	30	0,196	2,949	33,91	2,336	2,341	24,09	23,87	+0,22
50	10	10	0,106	30	0,196	3,038	32,92	2,127	2,556	25,69	25,11	-0,58
50	7,5	7,5	0,080	35	0,228	3,227	30,99	2,093	2,516	24,58	24,74	+0,16

Die Gleichung

$$v = 3,8 R + 4 K^* - 0,5 Ba^* + 14,65 \quad (3)$$

ergibt einen maximalen Fehler von 1,39% für  $R = 2,257 - 2,516$ . Über  $R = 2,516$  nehmen die Abweichungen von Gl. (3) zu und bei einem BaO-Gehalt von über 40% ist die Gleichung nicht mehr brauchbar.

Magnesium- und calciumhaltige Natrongläser finden wir in Tabelle 4.

Für diese Gläser gilt die Gleichung

$$v = 3,8 R - 5 Mg^* - 5 Ca^* + 14,9 \quad (4)$$

mit einem maximalen Fehler von 0,52% im Bereich von  $R = 2,307 - 2,325$ .

Es wurden auch strontium- und aluminiumhaltige Natrongläser dargestellt, die in Tabelle 5 ersichtlich sind.

Tabelle 4

Na<sub>2</sub>O—MgO—CaO—SiO<sub>2</sub>—Gläser (5)

SiO <sub>2</sub> %	Al <sub>2</sub> O <sub>3</sub> %	Na <sub>2</sub> O %	MgO %	MgO Mole	CaO %	CaO Mole	O <sup>2-</sup> - Gramm- ionen pro 100 g Glas	Dichte g/cm <sup>3</sup>	Volum von 100 g Glas	R	Volumen pro O <sup>2-</sup> -Ion Å <sup>3</sup>		Diff.
											gem.	ber.	
74,76	1,01	14,84	1,64	0,041	7,52	0,134	2,932	2,467	40,58	2,320	22,97	22,85	-0,12
74,74	1,08	14,98	2,58	0,064	6,43	0,115	2,942	2,454	40,70	2,323	22,96	22,84	-0,12
75,58	0,94	14,48	3,66	0,091	5,48	0,098	2,966	2,450	40,82	2,325	22,84	22,80	-0,04
76,32	0,94	14,58	4,10	0,102	3,82	0,068	2,972	2,436	41,05	2,307	22,92	22,82	-0,10
76,00	0,98	14,98	4,85	0,120	3,14	0,056	2,977	2,426	41,22	2,317	22,91	22,83	-0,08

Tabelle 5

Na<sub>2</sub>O—SrO—Al<sub>2</sub>O<sub>3</sub>—SiO<sub>2</sub>—Gläser (6)

SiO <sub>2</sub> %	Al <sub>2</sub> O <sub>3</sub> %	Na <sub>2</sub> O%	SrO%	SrO Mole	Dichte g/cm <sup>3</sup>	Volumen von 100 g Glas cm <sup>3</sup>	O <sup>2-</sup> - Gramm- ionen pro 100 g	R	Volumen pro O <sup>2-</sup> -Ion, Å <sup>3</sup>		Diff.
									gem.	ber.	
74,7	2,0	17,1	6,0	0,058	2,480	40,32	2,880	2,245	23,24	23,26	+0,02
70,5	2,0	17,3	10,1	0,097	2,557	39,11	2,782	2,293	23,34	23,33	-0,01
66,6	2,1	17,3	13,6	0,131	2,636	37,94	2,689	2,338	23,42	23,40	-0,02
74,8	4,0	17,2	4,0	0,039	2,452	40,78	2,923	2,209	23,16	23,17	+0,01
70,6	4,0	17,2	8,0	0,077	2,536	39,43	2,821	2,251	23,19	23,22	+0,03
66,8	4,0	17,2	11,7	0,113	2,606	38,37	2,731	2,295	23,33	23,29	-0,04
76,1	2,0	15,8	6,1	0,059	2,467	40,54	2,906	2,225	23,15	23,18	+0,03
72,2	2,1	15,5	10,1	0,097	2,546	39,28	2,812	2,262	23,19	23,21	+0,02
68,0	2,0	15,7	14,0	0,135	2,625	38,10	2,712	2,314	23,32	23,30	-0,02
74,3	4,1	15,5	6,1	0,059	2,478	40,36	2,901	2,204	23,09	23,10	+0,01
70,1	4,1	15,5	10,1	0,097	2,554	39,15	2,799	2,246	23,22	23,15	+0,07
66,1	4,1	15,5	14,0	0,135	2,633	37,98	2,705	2,292	23,32	23,21	-0,11
77,7	2,1	13,9	6,1	0,059	2,449	40,98	2,942	2,204	23,11	23,10	-0,01
73,5	2,0	14,1	10,0	0,097	2,526	39,59	2,830	2,241	23,22	23,15	-0,07
69,6	2,0	14,1	13,9	0,134	2,609	38,33	2,737	2,285	23,24	23,19	-0,05
75,4	4,0	14,2	6,1	0,059	2,464	40,58	2,915	2,187	23,11	23,04	-0,07
71,5	4,1	14,2	10,0	0,097	2,538	39,40	2,826	2,225	23,14	23,07	-0,07
67,9	4,1	14,2	13,9	0,134	2,616	38,23	2,743	2,267	23,13	23,12	-0,01

Hier ist die Gleichung

$$v = 3,8 R - 3 \text{ Sr}^* + 14,9 \quad (5)$$



gültig, wo Aluminium natürlich zu den gerüstbildenden Ionen zu rechnen ist. Der maximale Fehler beträgt 0,47% im Bereich von  $R = 2,187 - 2,338$ .

Eisenhaltige Gläser enthalten immer Ferro- und Ferriion nebeneinander; solche Gläser sind in Tabelle 6 ersichtlich.

Tabelle 6  
 $\text{Na}_2\text{O} - \text{FeO} - \text{Fe}_2\text{O}_3 - \text{SiO}_2$ -Gläser (7)

$\text{SiO}_2$ %	$\text{Al}_2\text{O}_3$ %	$\text{Na}_2\text{O}$ %	$\text{FeO}$ %	$\text{FeO}$ Mole	$\text{Fe}_2\text{O}_3$ %	$\text{Fe}_2\text{O}_3$ Mole	Dichte g/cm <sup>3</sup>	Volumen von 100 g Glas cm <sup>3</sup>	$\text{O}^{2-}$ - Gramm- ionen pro 100 g	$R$	Volumen pro $\text{O}^{2-}$ -Ion, Å.		Diff.
											gem.	ber.	
72,18	0,41	24,00	0,63	0,009	2,21	0,014	2,481	40,31	2,852	2,375	23,46	23,56	+0,10
71,33	0,58	21,42	0,84	0,012	4,84	0,030	2,515	39,76	2,839	2,391	23,25	23,38	+0,13
69,02	0,70	22,42	1,05	0,015	6,52	0,041	2,540	39,37	2,827	2,463	23,12	23,24	+0,12
70,00	0,80	17,48	1,05	0,015	9,95	0,062	2,546	39,28	2,836	2,434	22,99	22,89	-0,10
69,25	1,01	17,25	1,89	0,026	10,16	0,064	2,565	38,99	2,830	2,456	22,86	23,08	+0,22
66,63	0,66	15,40	1,78	0,025	15,42	0,096	2,580	38,76	2,798	2,524	22,99	23,01	+0,02
65,64	0,42	14,46	4,20	0,058	15,03	0,094	2,599	38,48	2,768	2,535	23,07	22,96	-0,11
63,72	0,97	13,72	3,88	0,054	17,19	0,108	2,620	38,17	2,747	2,592	23,06	22,94	-0,12
63,69	0,86	11,57	3,36	0,047	20,50	0,128	2,633	37,98	2,763	2,607	22,81	22,80	-0,01
62,97	0,52	10,67	3,99	0,056	21,90	0,134	2,644	37,82	2,741	2,617	22,90	22,82	-0,08

### Die Gleichung

$$v = 3,8 R - 4 \text{ Fe}^{\text{II}*} - 6,5 \text{ Fe}^{\text{III}*} + 14,8 \quad (6)$$

ergibt bei diesen Gläsern  $v$  mit einem maximalen Fehler von 0,96% im Bereich von  $R = 2,363 - 2,625$ . Man sieht, dass Ferrieisen eine stärkere zusammenziehende Wirkung besitzt als Ferroeisen.

Natrongläser, die auch Kalium und Blei enthalten, finden sich in Tabelle 7.

### Die Gleichung

$$v = 3,8 R + 4 \text{ K}^* + 0,5 \text{ Pb}^* + 14,9 \quad (7)$$

gibt eine maximale Abweichung gegen die gemessenen Werte von 0,64% im Bereich von  $R = 2,268 - 2,400$ ; darüber hinaus werden die Abweichungen höher.

Kaligläser mit zwei anderen Kationen wurden ebenfalls berechnet. Tabelle 8 enthält solche mit Lithium- und Calciumgehalt.

Tabelle 7

Na<sub>2</sub>O—K<sub>2</sub>O—PbO—SiO<sub>2</sub>—Gläser (8, 9)

SiO <sub>2</sub> %	Na <sub>2</sub> O%	K <sub>2</sub> O%	K <sub>2</sub> O Mole	PbO%	PbO Mole	Dichte g/cm <sup>3</sup>	Volumen von 100 g Glas cm <sup>3</sup>	O <sup>2-</sup> -Grammionen pro 100 g	R	Volumen pro O <sup>2-</sup> -Ion, Å <sup>3</sup>		Diff.
										gem.	ber.	
70	10	10	0,106	10	0,045	2,570	38,92	2,648	2,268	24,45	24,49	+0,04
65	10	10	0,106	15	0,067	2,714	36,85	2,498	2,309	24,48	24,56	+0,08
60	10	10	0,106	20	0,090	2,845	35,15	2,353	2,358	24,78	24,77	—0,01
50	10	10	0,106	30	0,134	3,123*	32,02	2,065	2,482	25,73	25,26	—0,47
40	10	10	0,106	40	0,179	3,427	29,18	1,777	2,668	27,25	25,98	—1,27
30	10	10	0,106	50	0,224	3,742	26,74	1,489	2,979	29,79	27,19	—2,80
69,2	7,14	10,82	0,116	12,86	0,058	2,623	38,13	2,603	2,251	24,30	24,42	+0,12
61,3	6,33	9,61	0,102	22,77	0,102	2,884	34,64	2,350	2,300	24,48	24,51	+0,03
55,0	5,77	8,62	0,092	30,65	0,137	3,126	32,00	2,150	2,350	24,66	24,65	—0,01
49,9	5,15	7,84	0,083	37,10	0,166	3,339	29,95	1,994	2,400	24,92	24,76	—0,16
42,1	4,35	6,61	0,070	46,9	0,210	3,676	27,20	1,750	2,500	25,80	25,07	—0,73
36,4	3,76	5,71	0,060	53,1	0,242	3,952	25,30	1,572	2,598	26,70	25,38	—1,32

\* Diese Dichte ist offenbar zu klein (vgl. das folgende Glas mit 55,0% SiO<sub>2</sub> etc, welches bei bedeutend weniger Alkaligehalt und fast gleichem PbO-Gehalt eine etwas höhere Dichte hat).

Tabelle 8

K<sub>2</sub>O—Li<sub>2</sub>O—CaO—SiO<sub>2</sub>—Gläser (10)

SiO <sub>2</sub> %	K <sub>2</sub> O%	Li <sub>2</sub> O%	Li <sub>2</sub> O Mole	CaO %	CaO Mole	Dichte g/cm <sup>3</sup>	Volumen von 100 g Glas cm <sup>3</sup>	O <sup>2-</sup> -Grammionen pro 100 g	R	Volumen pro O <sup>2-</sup> -Ion, Å <sup>3</sup>		Diff.
										gem.	ber.	
75,04	3	12	0,401	10,02	0,179	2,449	40,83	3,110	2,490	21,79	21,81	+0,02
75,09	6	9	0,301	9,95	0,177	2,444	40,93	3,040	2,434	22,34	22,38	+0,04
75,18	9	6	0,201	9,90	0,177	2,442	40,95	2,976	2,379	22,84	22,92	+0,08
75,06	11	4	0,134	9,91	0,177	2,441	40,97	2,926	2,343	23,24	23,29	+0,05
75,02	13,5	1,5	0,050	9,99	0,178	2,438	41,02	2,868	2,298	23,74	23,74	±0
75,04	14	1	0,033	9,93	0,177	2,437	41,03	2,857	2,287	23,84	23,82	—0,02
75,04	14,5	0,5	0,017	10,07	0,180	2,436	41,05	2,849	2,281	23,91	23,91	±0
74,92	14,95	0	0	10,04	0,179	2,436	41,05	2,832	2,272	24,06	24,01	—0,05

Aus der Grundgleichung (4) der I. Mitteilung erhalten wir unter Berücksichtigung der zusammenziehenden Wirkung des Li und Ca die Gleichung

$$v = 12 R - 12 \text{ Li}^* - 12 \text{ Ca}^* - 1,1 \quad (8)$$

und diese gibt eine maximale Abweichung von 0,42% zwischen den berechneten und gefundenen  $v$ -Werten im Bereich von  $R = 2,272 - 2,490$ .

Durch die Einführung von Rubidium werden die Kaligläser ausgedehnt. da das Rubidiumion grösser als das Kaliumion ist. Wir ersehen dies aus der Tabelle 9.

Tabelle 9  
 $K_2O-Rb_2O-CaO-SiO_2$ -Gläser (11)

SiO <sub>2</sub> %	K <sub>2</sub> O%	Rb <sub>2</sub> O%	Rb <sub>2</sub> O Mole	CaO%	CaO Mole	Dichte g cm <sup>3</sup>	Volumen von 100 g Glas cm <sup>3</sup>	O <sup>2-</sup> -Grammionen pro 100 g Glas	— R	Volumen pro O <sup>2-</sup> -Ion Å <sup>3</sup>		Diff.
										gem.	ber.	
74,78	13	2	0,011	10,09	0,180	2,448	40,85	2,817	2,264	24,03	24,05	+0,02
74,87	10	5	0,027	10,14	0,181	2,470	40,49	2,806	2,252	23,96	23,96	± 0
75,09	7	8	0,043	10,00	1,178	2,490	40,16	2,793	2,236	23,90	23,86	—0,04
75,13	4	11	0,059	10,08	0,180	2,508	39,87	2,781	2,225	23,73	23,78	—0,05
74,89	0	15	0,080	10,01	0,178	2,539	39,39	2,750	2,207	23,73	23,66	—0,07

Die Gleichung

$$v = 12 R + 4 Rb^* - 12 Ca^* - 1,2 \tag{9}$$

stimmt sehr gut für die gemessenen Volumina; der maximale Fehler beträgt 0,29% im Bereich von  $R = 2,207 - 2,264$ .

Wie wir aus diesen Gleichungen sehen, bleiben die Faktoren der gerüstmodifizierenden Kationen bei vierkomponentigen Gläsern dieselben, wie die in der I. Mitteilung bereits gefundenen. In der folgenden Tabelle 10 sind fünfkomponentige Borosilikatgläser angeführt, die nebeneinander Natrium und Kalium enthalten. Dieser Fall ist etwas komplizierter ; doch konnten auch hier Gleichungen aufgestellt werden, die  $v$  mit befriedigender Genauigkeit ergeben.

Alle Gläser der Tabelle 10 enthalten Natrium und Kalium nebeneinander. Obzwar die Molenzahl des Natriums in fast allen Fällen grösser als die des Kaliums ist, muss man das Volumen  $v$  dieser Gläser auf Grundlage der Kaliumsilikatgläser berechnen. Bei  $R > 2,00$  gilt die Gleichung

$$v = 12 R - 3 Na^* - 12 Ca^* - 1,2 \tag{10a}$$

und zwischen  $R = 1,887 - 2,00$

$$v = 12,35 R - 2,5 Na^* - 12 Ca^* - 1,2. \tag{10b}$$

Diese Gleichungen ergeben einen maximalen Fehler von 1,28% bei (10a)

**Tabelle 10**  
 $\text{Na}_2\text{O}-\text{K}_2\text{O}-\text{CaO}-\text{SiO}_2-\text{B}_2\text{O}_3$ -Gläser (12)

SiO <sub>2</sub> %	Al <sub>2</sub> O <sub>3</sub> %	B <sub>2</sub> O <sub>3</sub> %	Na <sub>2</sub> O%	K <sub>2</sub> O%	K <sub>2</sub> O Mole	CaO%	CaO Mole	Dichte g/cm <sup>3</sup>	Volumen von 100 g Glas, cm <sup>3</sup>	O <sup>2-</sup> - Gramm- ionen pro 100 g	R	Volumen pro O <sup>2-</sup> -Ion Å <sup>3</sup>		Diff.
												gem.	ber.	
75,38	0,52	0,66	6,84	0,110	8,02	0,085	8,52	2,465	40,57	2,890	2,251	23,30	23,33	+0,03
73,38	0,72	2,05	6,14	0,099	9,38	0,100	8,40	2,484	40,26	2,905	2,240	23,01	23,29	+0,28
69,06	0,99	5,44	7,54	0,122	8,22	0,087	8,64	2,517	39,73	2,943	2,201	22,45	22,63	+0,18
68,20	0,74	7,90	7,00	0,113	7,56	0,080	8,70	2,519	39,70	3,002	2,158	21,97	22,16	+0,19
66,50	0,74	9,58	7,04	0,114	7,40	0,079	8,72	2,526	39,59	3,014	2,130	21,80	21,82	+0,02
64,58	1,00	10,78	7,50	0,121	7,42	0,079	8,60	2,525	39,60	3,031	2,124	21,69	21,70	+0,01
64,42	0,70	13,65	6,26	0,101	8,06	0,086	8,90	2,529	39,54	3,075	2,088	21,34	21,35	+0,01
56,76	1,00	19,43	7,38	0,119	7,14	0,076	8,54	2,523	39,64	3,159	2,025	20,83	20,56	-0,27
53,26	1,28	22,54	6,74	0,109	6,98	0,074	9,10	2,522	39,65	3,194	1,991	20,61	20,90	+0,29
49,50	0,88	25,70	7,00	0,113	7,50	0,080	9,08	2,513	39,79	3,215	1,970	20,54	20,63	+0,09
45,66	1,74	29,57	6,36	0,103	8,06	0,086	8,62	2,487	40,21	3,308	1,925	20,18	20,21	+0,03
41,98	1,80	33,79	6,52	0,105	7,38	0,078	8,56	2,472	40,45	3,345	1,887	20,07	19,76	-0,31

Industrielle und experimentelle Gläser (14)  
(Zusammensetzung in Gewichtsprozenten)

No.	SiO <sub>2</sub>	B <sub>2</sub> O <sub>3</sub>	Al <sub>2</sub> O <sub>3</sub>	Na <sub>2</sub> O	K <sub>2</sub> O	MgO	CaO	BaO	ZnO	PbO	Andere Oxyde	Dichte g/cm <sup>3</sup>	R	Volumen pro O <sup>+</sup> - Ion, Å <sup>3</sup>		Diff.
														gem.	ber.	
1.	96,3	2,9	0,4	—	—	—	—	—	—	—	—	2,18	1,973	22,76	22,75	-0,01
2.	80,5	12,9	2,2	3,8	0,4	—	—	—	—	—	—	2,23	1,920	21,52	21,74	+0,22
3.	71,0	14,0	5,0	10,0	—	—	—	—	—	—	—	2,370	1,974	21,33	21,51	+0,18
4.	72,86	10,43	6,24	10,17	0,10	—	—	—	—	—	—	2,370	1,972	21,72	21,95	+0,23
5.	68,2	10,0	—	10,0	9,5	—	—	—	2,5	—	—	2,47	2,100	22,49	22,59	+0,10
6.	70,6	—	—	17,0	—	—	—	—	12,0	—	—	2,572	2,358	23,28	23,18	-0,10
7.	69,0	2,5	—	4,0	16,0	—	8,0	—	—	—	—	2,49	2,280	23,97	24,06	-0,09
8.	64,6	2,7	—	5,0	15,0	—	—	10,2	2,0	—	—	2,580	2,254	24,75	24,55	-0,20
9.	47,73	3,90	0,65	1,14	7,16	—	0,15	29,88	8,61	—	—	3,21	2,369	23,79	23,86	+0,07
10.	73,8	—	3,5	10,5	—	—	7,0	—	5,0	—	—	2,479	2,247	22,96	22,88	-0,08
11.	70,2	12,0	4,5	10,3	—	3,0	—	—	—	—	—	2,378	2,017	21,62	21,74	+0,12
12.	67,9	—	1,0	16,8	—	—	—	—	5,8	8,1	—	2,629	2,320	23,66	23,60	-0,06
13.	66,58	0,91	3,84	14,8	—	—	7,18	—	6,24	—	—	2,585	2,324	22,83	22,54	-0,29
14.	64,4	12,0	4,5	8,0	—	11,0	—	—	—	—	—	2,424	2,125	21,42	21,28	-0,14
15.	58,7	—	—	—	33,0	—	8,0	—	—	—	—	2,518	2,506	27,26	27,15	+0,11
16.	55,0	—	17,0	14,0	14,0	—	—	—	—	—	—	2,480	2,184	24,73	24,59	-0,14
17.	54,8	—	—	—	28,0	—	—	—	17,0	—	—	2,668	2,555	26,69	26,74	+0,05
18.	73,0	14,0	1,7	4,4	—	—	—	—	—	5,7	—	2,35	1,926	22,25	22,15	-0,10
19.	74,6	18,0	1,0	4,2	1,7	—	0,3	—	—	—	—	2,27	1,898	21,67	21,72	+0,05
20.	77,3	12,8	1,7	1,4	6,6	—	—	—	—	—	As <sub>2</sub> O <sub>3</sub> 0,2	2,28	1,935	22,28	22,47	+0,19
21.	58,5	3,0	22,5	—	0,8	8,9	6,3	—	—	—	P <sub>2</sub> O <sub>5</sub> 4,6	2,50	2,051	21,56	21,31	-0,25
22.	51,3	1,0	25,3	—	—	4,2	8,3	5,3	—	—	—	2,62	2,049	21,43	21,55	+0,12
23.	67,5	22,0	2,0	6,5	2,0	—	—	—	—	—	—	2,25	1,884	21,84	21,99	+0,15
24.	65,1	1,8	5,1	12,0	3,3	—	7,8	4,9	—	—	—	2,57	2,264	23,17	23,27	+0,10
25.	70,5	—	1,0	16,0	1,0	3,9	5,4	2,0	—	—	Sb <sub>2</sub> O <sub>3</sub> 0,7	2,52	2,380	23,06	23,05	-0,01
26.	55,6	—	—	4,0	8,0	—	—	—	—	32,4	—	3,06	2,318	25,27	25,08	-0,19
27.	62,69	—	0,60	6,7	8,26	—	—	—	—	21,75	—	2,84	2,283	24,36	24,51	+0,15
28.	57,4	—	1,3	3,9	7,6	—	—	—	—	29,3	—	3,06	2,267	24,38	24,57	+0,19
29.	53,9	—	1,2	5,3	7,5	—	—	3,6	—	28,5	—	3,10	2,330	24,93	25,03 <sup>1</sup>	+0,10
30.	70,7	—	1,9	15,7	—	3,9	7,6	—	—	—	—	2,491	2,385	23,05	22,99	-0,06
31.	73,0	14,0	2,3	7,5	—	—	3,0	—	—	—	—	2,29	1,970	22,19	21,85	-0,34
32.	65,1	16,3	2,4	4,9	2,3	—	—	—	4,6	—	Sb <sub>2</sub> O <sub>3</sub> 3,8 As <sub>2</sub> O <sub>3</sub> 0,7	2,40	1,930	21,98	22,19	+0,21
33.	67,9	18,9	2,4	6,8	4,0	—	—	—	—	—	—	2,24	1,918	22,48	22,27	-0,19
34.	68,3	—	3,7	10,0	7,9	—	6,6	3,5	—	—	—	2,520	2,288	23,79	23,86	+0,07
35.	70,3	—	—	16,9	1,2	3,6	5,2	2,0	—	—	—	2,52	2,410	23,38	23,24	-0,14
36.	73,6	—	—	17,2	—	3,7	5,4	—	—	—	—	2,47	2,381	23,07	23,00	-0,07
37.	69,9	—	2,9	16,1	0,4	2,9	7,7	—	—	—	—	2,502	2,364	23,00	23,05	+0,05
38.	81,1	12,2	2,0	4,4	—	—	—	—	—	0,3	—	2,24	1,929	22,08	22,15	+0,07
39.	70,0	—	2,0	16,2	0,8	3,5	5,5	2,0	—	—	—	2,51	2,372	23,15	23,24	+0,09
40.	68,8	1,7	3,5	9,5	7,2	0,2	3,2	4,1	—	—	Sb <sub>2</sub> O <sub>3</sub> 1,1	2,57	2,209	23,15	23,15	± 0
41.	55,6	—	1,1	5,2	8,3	—	—	—	—	28,9	—	3,04	2,307	25,00	24,98	-0,02
42.	70,2	—	3,3	12,1	8,1	—	6,3	—	—	—	—	2,47	2,292	23,78	23,94	+0,16
43.	65,2	—	2,5	6,2	14,7	—	6,5	5,0	—	—	—	2,54	2,336	24,67	24,74	+0,07
44.	56,2	—	1,7	4,1	7,9	—	0,2	—	—	29,7	—	3,052	2,278	24,63	24,63	± 0
45.	63,1	—	0,3	7,6	5,6	—	1,0	—	—	20,2	Mn <sub>2</sub> O <sub>3</sub> 1,0	2,85	2,294	24,04	23,98 <sup>2</sup>	-0,06
46.	55,6	—	—	4,1	8,0	—	—	—	—	32,4	—	3,06	2,320	25,27	25,08	-0,19

<sup>1</sup> Als Kaliglas berechnet.  
<sup>2</sup> Faktor für Mn\* : 6.





und 1,55% bei (10b). Bei Borosilikatgläsern übt übrigens die Wärmebehandlung einen viel grösseren Einfluss auf die Dichte aus, als bei einfachen Silikatgläsern.

### Industrielle und experimentelle Gläser

Auf Grund der bisher entwickelten Gleichungen kann man nun die Dichten der in der Praxis vorkommenden Gläser berechnen. Hier genügt auch die Kenntnis des Volumens  $v$  des betreffenden Glases, da aus diesem und aus der Zusammensetzung des Glases die Dichte in einfacher Weise folgt.

Ich habe die Dichte einer Anzahl von solchen Gläsern unter Beibehaltung der schon bestimmten Faktoren berechnet. Man kann so zu Gleichungen kommen, die einen breiten Gültigkeitsbereich haben:

1. Für einfache Silikatgläser (wo bis 6%  $B_2O_3$ ,  $Al_2O_3$ ,  $P_2O_5$  oder kleinere Mengen  $As_2O_3$  bzw.  $Sb_2O_3$  zugegen sein können), wenn Na-Ionen vorherrschen, also in höchster Grammionenzahl vorhanden sind

$$v = 3,8R - 2,4Li^* + 4K^* - 5Mg^* - 5Ca^* - 3Sr^* - 0,5Ba^* - 2Zn^* + 0,5Pb^* - 4Fe^{II*} - 6,5Fe^{III*} - 9Bi^* - 11Ti^* - 10Zr^* + 14,9. \quad (11)$$

2. Für einfache Silikatgläser, wenn K-Ionen vorherrschen

$$v = 12R - 12Li^* - 2Na^* + 4Rb^* - 13Mg^* - 12Ca^* - 9Ba^* - 9Pb^* - 1,2. \quad (12)$$

3. Für Borosilikatgläser auf Na-Grundlage, wenn Na *stark* vorherrscht, also wenigstens zweimal so viele Na-Ionen als K-Ionen vorhanden sind

$$v = 3,8R - 2Na^* + 4K^* - 5Mg^* - 5Ca^* - 0,5Ba^* - 2Zn^* + 14,65. \quad (13)$$

4. Für Borosilikatgläser, wo die Zahl der K-Ionen mehr als die Hälfte der Zahl der Na-Ionen ausmacht, gelten die Gleichungen (10a) und (10b).

5. Für die additive Konstante bei Natronsilikatgläsern gelten folgende Regeln:

Ist mehr als 6,0% ZnO zugegen, so wird die additive Konstante 14,5 (statt 14,9). Wenn weniger ZnO vorhanden ist, dagegen 2,0% oder mehr  $Al_2O_3$ , so wird die additive Konstante 15,1.

In allen Gleichungen werden B, Al, P, As und Sb zu den gerüstbildenden Ionen gerechnet.

Alkalifreie Gläser sowie Bleiborosilikatgläser und silikatfreie Gläser werden in einer folgenden Mitteilung behandelt.

Die Tabelle 11 enthält eine Anzahl von Gläsern, die die hier behandelten Bedingungen erfüllen. Es gibt noch gewisse Grenzen für Schwermetalloxyde,

so kann  $v$  von Gläsern mit mehr als 40% PbO oder BaO oder B<sub>2</sub>O<sub>3</sub> mit der angegebenen Gleichungen nicht erfasst werden.

Es ist gelungen, das Sauerstoffionenvolumen von Gläsern mit bis zu 9 Komponenten mit befriedigender Genauigkeit, d. h. mit einem Fehler von unter 1,5% zu berechnen. Natürlich sind die Analysen und Dichtebestimmungen oft nicht sehr genau, somit kann man bessere Übereinstimmung nur dann erwarten, wenn Analyse und Dichtebestimmung exakt sind. Die Differenz zwischen gemessenen und berechneten  $v$ -Werten gestaltet sich folgendermassen:

Zahl der Gläser	Differenz
14	0 — 0,3 %
11	0,31 — 0,50 %
16	0,51 — 1,0 %
5	1,01 — 1,53 %

Ausser den hier angeführten Gläsern wurde noch eine Anzahl weiterer berechnet und ergab ebenfalls befriedigende Ergebnisse.

Somit ist die Möglichkeit der Vorausberechnung der Dichte von Gläsern aus der Zusammensetzung auf weiten Gebieten u. zw. bei der grossen Mehrheit der praktisch gebrauchten Gläser gesichert.

Die theoretische Deutung der entwickelten Gleichungen erfolgt in einer weiteren Mitteilung.

*Nachtrag bei der Korrektur.* Eine neue Arbeit von DIETZEL u. SHEYBANY (Verres et réfract. 2, 63, 1948) gibt die Dichten von Li<sub>2</sub>O—SiO<sub>2</sub>-Gläsern; sie können durch die Gleichung  $v = 26,1 - 1,95R$  wiedergegeben werden, wobei die maximale Differenz 0,7% beträgt (7 Gläser). — Die Dichten von 78 verschiedenen Na<sub>2</sub>O—K<sub>2</sub>O—SiO<sub>2</sub>-Gläsern nach YOUNG, GLAZE, FAICK und FINN (J. Res. Nat. Bureau of Standards 22, 453, 1939) wurden nach der Gleichung  $v = 3,8R + 4K^* + 14,9$  berechnet, wobei die maximale Abweichung 1,5% betrug.

#### LITERATUR

1. I. NÁRAY-SZABÓ, Acta Phys., **8**, 37, 1957.
2. S. C. WATERTON and W. E. S. TURNER, J. Soc. Glass Tech., **18**, 268, 1934.
3. S. C. WATERTON and W. E. S. TURNER, J. Soc. Glass Tech., **18**, 268, 1934.
4. C. J. PEDDLE, J. Soc. Glass Tech., **5**, 228, 1921.
5. S. ENGLISH and W. E. S. TURNER, J. Soc. Glass Tech., **6**, 228, 1922.
6. Owens-Illinois Glass Company, J. Am. Ceram. Soc., **31**, 1, 1948.
7. S. ENGLISH, H. W. HOWES, W. E. S. TURNER and F. WINKS, J. Soc. Glass Tech., **12**, 31, 1928.
8. C. J. PEDDLE, J. Soc. Glass Tech., **4**, 320, 1920.
9. C. J. PEDDLE, J. Soc. Glass Tech., **4**, 330, 1920.
10. S. C. WATERTON and W. E. S. TURNER, J. Soc. Glass Tech., **18**, 268, 1934.
11. S. C. WATERTON and W. E. S. TURNER, J. Soc. Glass Tech., **18**, 268, 1934.
12. W. E. S. TURNER and F. WINKS, J. Soc. Glass Tech., **9**, 389, 1925.
13. Die Daten der Gläser No. 1—17. sind in G. W. MOREY, Properties of Glass, II<sup>nd</sup> Ed., New York, 1954., S. 16—17. u. 80—84. zu finden. Die Gläser No. 18—46 stammen aus der Industrie.

СООТНОШЕНИЕ МЕЖДУ СТРУКТУРОЙ И ФИЗИЧЕСКИМИ СВОЙСТВАМИ  
СТЕКЛА

II сообщение

И. НАРАИ-САБО

## Резюме

На основе закономерностей выясненных в первом сообщении, выводятся линейные уравнения для объема иона  $O^-$  — в четыре — и более компонентных силикатных стеклах. Эти уравнения в конечном счете могут быть сведены на четыре общие уравнения для стекол со следующими основами: 1) кремнистый натрий, 2) кремнистый калий, 3) борокремнистый натрий, 4) борокремнистый калий. С помощью этих уравнений объем иона  $O^-$  в стеклах и таким образом их плотность может быть определена с достаточной точностью на основании состава.



# THE SCATTERING OF ELECTRONS BY FREE NEUTRAL ATOMS IN THE THOMAS-FERMI MODEL

By

T. TIETZ

DEPARTMENT OF THEORETICAL PHYSICS UNIVERSITY ŁÓDŹ, POLAND

(Presented by P. Gombás. — Received: XII. 6. 1957)

In this paper using the approximate solution of the Thomas-Fermi equation for free neutral atom given by BUCHDAHL we derive an analytical formula for the scattered intensity by a group of free atoms. The scattered intensity concerns the elastic and inelastic scattering for singly scattered electrons by free atoms in the Thomas-Fermi model. A comparison with the numerical results shows that our formula for the scattered intensity is very accurate.

## I. Introduction

When a beam of electrons strikes a free atom, the intensity of scattered electrons varies with the scattering angle in a way dependent upon the nuclear charge and electronic structure of the atom, and the energy of the incident electrons. In this paper we obtain an analytical formula for the scattered intensity  $I(s)$  by a group of free atoms. BORN<sup>1</sup> and MOTT<sup>2</sup>, as known, were the first, who obtained the scattered intensity  $I(s)$  for elastic scattering, MORSE<sup>3</sup> extended the Born approximation to include inelastic scattering, obtaining the expression for singly scattered electrons

$$I(s) = \frac{I_0 N}{R^2} \left( \frac{8\pi^2 m e^2}{h^2} \right)^2 \frac{1}{s^4} \{ [Z - F(s)]^2 + Z S(s) \}, \quad (1)$$

where  $I_0$  is the intensity of the incident electron beam,  $N$  the number of independently scattering atoms intercepted by the beam,  $R$  the distance between the point of observation of the scattered electrons,  $s$  the variable  $\left( 4\pi \sin \frac{1}{2} \Theta \right) / \lambda$ ,  $\lambda$  is the de Broglie wavelength of the incident beam,  $\Theta$  the scattering angle,  $Z$  the atomic number of the atoms,  $F(s)$  the  $x$ -ray atomic scattering factor of the atoms, and  $S(s)$  the  $x$ -ray incoherent scattering function of the atoms. The term  $[Z - F(s)]^2$  represents the elastic scattering and the term  $S(s)$  represents the inelastic scattering.

<sup>1</sup> M. BORN, Z. Phys., **38**, 803, 1926.

<sup>2</sup> N. P. MOTT, Proc. Roy. Soc. (London) (A), **124**, 425, 1928 ; **127**, 658, 1930.

<sup>3</sup> P. M. MORSE, Z. Phys., **33**, 443, 1932.

## II. Theory

Since the exact values of the Thomas-Fermi function  $\varphi_0(x)$  are given only for the discrete values of the argument  $x$ , the evaluation of the atom form factor  $F(s)$  of the Thomas-Fermi atom<sup>4</sup> of the atomic number  $Z$

$$F(s) = \int_0^{\infty} \frac{\sin sr}{sr} \varrho 4\pi r^2 dr \quad (2)$$

$$= Z \left[ 1 - s\mu \int_0^{\infty} \sin s\mu x \cdot \varphi_0(x) dx \right], \quad (3)$$

where  $\mu$  is the Thomas-Fermi unit, was carried out by BRAGG and WEST<sup>5</sup> in such a way that exact values were taken for  $\varphi_0$  and the integral was approximated by a sum. The results can be given naturally only in tabular form, so that the dependence on  $Z$  as well as on  $s$  is at first sight not clear except the similarity rule that the  $F$ -curves for an atom  $Z_0$  is transformed so as to be suitable for any other atom  $Z$  by multiplying  $F$  and  $s$  by  $Z/Z_0$  and  $(Z/Z_0)^{1/3}$ , respectively. Moreover, owing to the oscillating nature of sine, it is necessary to take the summation in as small steps as possible. The term  $S(s)$  responsible for the inelastic scattering, as known<sup>6</sup>, is given by

$$S(s) = 1 - \int_0^{x_0} \left\{ \left[ \frac{\varphi_0(x)}{x} \right]^{1/2} - w \right\}^2 \left\{ \left[ \frac{\varphi_0(x)}{x} \right]^{1/2} + \frac{1}{2} w \right\} x^2 dx, \quad (4)$$

where  $w$  is defined by

$$w = \frac{0,176 \cdot 10^{-8} \text{ cm}}{Z^{2/3}} s, \quad (5)$$

and  $x_0$  is the root of the following equation

$$\left[ \frac{\varphi_0(x)}{x} \right]^{1/2} = w. \quad (6)$$

<sup>4</sup> P. GOMBÁŠ, Die statistische Theorie des Atoms und ihre Anwendungen, Vienna 1949; p. 245.

<sup>5</sup> W. L. BRAGG and J. WEST, Z. Krist. u. Mineral., **69**, 118, 1929.

<sup>6</sup> W. HEISENBERG, Phys. Z., **51**, 213, 1932.



### III. Procedure and result

Since the exact solution of the Thomas-Fermi equation

$$\varphi_0''(x) = \varphi_0^{3/2}(x)/x^{1/2} \quad (7)$$

is available only numerically, its approximate expression in a closed analytical form is desirable for practical purposes. Hitherto<sup>7</sup> several different forms have been given. A detailed consideration of the author has shown that the best approximate solutions of the Thomas-Fermi equation (7) for free neutral atoms which fulfil the boundary conditions

$$\varphi_0(0) = 1, \quad \varphi_0(\infty) = 0, \quad \varphi_0'(0) = \text{const.} \quad (8)$$

are the Tietz<sup>8</sup> approximate solution

$$\varphi_{Ti}(x) = (1 + ax + bx^2)^{-3/2}$$

with

$$a = 0.7105, \quad b = 0.03919. \quad (9)$$

and the Buchdahl<sup>9</sup> approximate solution

$$\varphi_{Bn}(x) = \frac{1}{(1 + Ax)(1 + Bx)(1 + Cx)} \quad (10)$$

where  $A$ ,  $B$  and  $C$  are constants namely  $A = 0.9288$ ,  $B = 0.1596$  and  $C = 0.05727$ . The Tietz approximation has the same degree of accuracy as the Buchdahl approximation. The Buchdahl approximation is more convenient in practical calculations of the atom form factor. At first we re-write the Buchdahl approximate solution of the Thomas-Fermi equation in the following form

$$\varphi_{Bn}(x) = \frac{\alpha}{1 + Ax} + \frac{\beta}{1 + Bx} + \frac{\gamma}{1 + Cx}, \quad (11)$$

where the constants  $\alpha$ ,  $\beta$ ,  $\gamma$  are given by

$$\alpha = \frac{A^2}{(A - B)(A - C)}, \quad \beta = \frac{B^2}{(A - B)(C - B)}, \quad \gamma = \frac{C^2}{(A - C)(B - C)}. \quad (12)$$

A simple calculation shows that the constants  $\alpha$ ,  $\beta$ ,  $\gamma$  fulfil the following relations

<sup>7</sup> K. UMEDA, J. Phys. Soc., Japan, **10**, 750, 1955.

<sup>8</sup> T. TIETZ, Il Nuovo Cimento, **4**, 1192, 1956.

<sup>9</sup> H. A. BUCHDAHL, Ann. d. Phys., **17**, 238, 1956.

$$a + \beta + \gamma = 1, \quad \frac{a}{A} + \frac{\beta}{B} + \frac{\gamma}{C} = 0, \quad \frac{a}{A^2} + \frac{\beta}{B^2} + \frac{\gamma}{C^2} = 0. \quad (13)$$

Using eq. (3) and eq. (11) we obtain for the atom form factor  $F(s)$  the following expression

$$\begin{aligned} F(s) = Z \left[ 1 - s\mu \left\{ \frac{a}{A} \left( \cos \frac{s\mu}{A} \left( \frac{\pi}{2} - \text{Si} \frac{s\mu}{A} \right) + \sin \frac{s\mu}{A} \text{Ci} \frac{s\mu}{A} \right) + \right. \right. \\ \left. \left. + \frac{\beta}{B} \left( \cos \frac{s\mu}{B} \left( \frac{\pi}{2} - \text{Si} \frac{s\mu}{B} \right) + \sin \frac{s\mu}{B} \text{Ci} \frac{s\mu}{B} \right) + \right. \right. \\ \left. \left. + \frac{\gamma}{C} \left( \cos \frac{s\mu}{C} \left( \frac{\pi}{2} - \text{Si} \frac{s\mu}{C} \right) + \sin \frac{s\mu}{C} \text{Ci} \frac{s\mu}{C} \right) \right\} \right], \end{aligned} \quad (14)$$

where the symbol  $\text{Si}(x)$  and  $\text{Ci}(x)$  have the following meaning

$$\text{Si}(x) = \int_0^x \frac{\sin t}{t} dt; \quad \text{Ci}(x) = - \int_x^\infty \frac{\cos t}{t} dt. \quad (15)$$

In Table I we give a comparison of our results for  $f_0(s)$  with the numerical results. The symbol  $f_0(s)$  is given by  $F(s) = Zf_0(s)$ .

Table I

A comparison of our results for  $f_0(s)$  with the numerical results of  $f_0(s)$  (see reference<sup>4</sup>)

$s\mu$	0	0,15	0,31	0,46	0,62	0,77	0,93	1,08	1,24	1,39
Numerical $f_0$	1,000	0,922	0,796	0,684	0,589	0,522	0,469	0,422	0,378	0,342
Equation (14) $f_0$	1,000	0,942	0,793	0,693	0,609	0,538	0,469	0,420	0,389	0,348
$s\mu$	1,55	1,70	0,201	2,32	2,63	2,94				
Numerical $f_0$	0,309	0,284	0,240	0,205	0,175	0,156				
Equation (14) $f_0$	0,305	0,278	0,234	0,198	0,169	0,149				

Table I shows that our results for  $f_0(s)$  are in good agreement with the numerical  $f_0(s)$  data. In order to calculate the term  $S(s)$  which is responsible for the inelastic scattering we re-write eq. (4) as follows

$$S(s) = 1 - \int_0^{x_0} \left[ x^{1/2} \varphi_0^{3/2}(x) - \frac{3}{2} w x \cdot \varphi_0(x) + \frac{1}{2} w^3 x^2 \right] dx. \quad (16)$$

Taking into consideration the Thomas-Fermi equation (7), the boundary conditions for  $\varphi_0(x)$  given by eq. (8) and the relation (6), we see that the integration by parts gives us for  $S(s)$  the following formula.

$$S(s) = \varphi_0(x) - x_0 \varphi'_0(x) - \frac{1}{6} (w x_0)^3 + \frac{3}{2} w \int_0^{x_0} x \varphi_0(x) dx. \quad (17)$$

Substituting for  $\varphi_0(x)$  the Buchdahl approximation given by eq. (11) we obtain for  $S(s)$  the following expression

$$S(s) = \frac{\alpha(1 + 2Ax_0)}{(1 + Ax_0)^2} + \frac{\beta(1 + 2Bx_0)}{(1 + Bx_0)^2} + \frac{\gamma(1 + 2Cx_0)}{(1 + Cx_0)^2} - \frac{3}{2} w \left[ \frac{a}{A^2} \ln(1 + Ax_0) + \frac{\beta}{B^2} \ln(1 + Bx_0) + \frac{\gamma}{C^2} \ln(1 + Cx_0) \right] - \frac{1}{6} (w x_0)^3. \quad (18)$$

In Table II we give a comparison of our results for  $S(s)$  with the numerical results for  $S(s)$  of BEVILOGUA<sup>10</sup> for several  $w$ .

Table II

A comparison of our results\* for  $S(\omega)$  given by eq. (18) with the numerical results of  $S(\omega)$  given by BEVILOGUA

	$\omega$	0	0,001	0,003583	0,025	0,05	0,1	0,2	0,3	0,4	0,6	0,8	$\infty$
Equation (18)	$x_0$	$\infty$	99,149	49,716	15,751	9,907	5,923	3,352	2,306	1,725	1,103	0,7762	0,000
	$S(\omega)$	0	0,0123	0,0412	0,198	0,321	0,486	0,667	0,783	0,840	0,915	0,964	1
Numerical data	$S(\omega)$	0	—	—	0,199	0,319	0,486	0,674	0,776	0,839	0,909	0,944	1

\*  $S(\omega)$  has the same meaning as  $S(s)$ .

Table II shows that our data for  $S(s)$  are in good agreement with the numerical data for  $S(s)$  of BEVILOGUA.

For small values of  $s$  the atom form factor  $F(s)$  as given by eq. (14) is quadratic in  $s$ , namely

$$F(s \ll 1) = [1 - \text{const } s^2 Z^{-2/3}] \quad (19)$$

and for large values of  $s$  the atom form factor  $F(s)$  vanishes inversely quadratically in  $s$ , namely

<sup>10</sup> L. BEVILOGUA, Phys. Z., **32**, 740, 1931.

$$F(s \gg 1) = \text{Const} \frac{Z^{5/3}}{s^2}. \quad (20)$$

Relations (13) and (6) show that the term  $S(s)$  which is given in our case by eq. (18) has the correct behaviour for  $w \rightarrow 0$  and  $w \rightarrow \infty$  as is shown by Table II. The author's point of view is that the approximate analytical formulas, eq. (14) and eq. (18), are the best approximate analytical expressions known hitherto for the atom form factor and the x-ray incoherent scattering function  $S(s)$ .

Formula (14) for the atom form factor  $F(s)$  has a number<sup>11</sup> of less accurate corresponding formulas. Formulae for  $S(s)$  given by eq. (18) has been unknown in the physical literature. It is necessary to stress that using the approximate solution for the Thomas-Fermi function (9) proposed by the author one can obtain, using eq. (17), an analytical expression for  $S(s)$ . The results which will be obtained for  $S(s)$  are the same as those given by formula (18).

Formulas (14) and (18) allow the calculation of the scattering intensity when inserted in eq. (1).

The author is indebted to Prof. F. J. WISNIEWSKI for his interest in this note.

## РАССЕЯНИЕ ЭЛЕКТРОНОВ СВОБОДНЫМИ НЕЙТРАЛЬНЫМИ АТОМАМИ ПО МОДЕЛЯМ ТОМАС—ФЕРМИ

Т. ТИТЦ

### Резюме

В работе выведена аналитическая формула для определения рассеянной группой свободных атомов интенсивности, используя приблизительное решение Бухдала для уравнения Томаса—Ферми. Рассеянная интенсивность содержит упругое и неупругое рассеяние электронов, рассеянных один раз свободными атомами модели Томаса—Ферми. Сравнение с численными результатами показывает, что полученная формула рассеянной интенсивности является очень точной.

<sup>11</sup> K. UMEDA, J. Faculty of Science Hokkaido University, VI., 57, 1951; T. TIETZ, J. Chem. Phys., 23, 1965, 1955.

# КОЛЛЕКТИВНЫЕ ВОЗБУЖДЕННЫЕ СОСТОЯНИЯ ЧЕТНО-ЧЕТНЫХ АТОМНЫХ ЯДЕР

А. С. ДАВЫДОВ и Г. Ф. ФИЛИППОВ

МОСКОВСКИЙ ГОСУДАРСТВЕННЫЙ УНИВЕРСИТЕТ МОСКВА, СССР

(Поступило 13 декабря 1957. г.)

Рассматривается проблема коллективных возбуждений четно-четных ядер аксиальной. В расчетах не предполагается, что ротационная энергия много раз меньше чем вибрационная. Исчислены отношения энергий возбужденных коллективных состояний и последовательность спинов. Показано, что энергия двух параметров:  $\alpha_0 = \sqrt{\frac{C}{B}}$  и  $\delta = \beta_0 (Be/\hbar^2)^{1/4}$ . В области  $\delta \wedge 2,5$  спектр может быть представлен как система ротационно-вибрационных полос. В области  $\delta < 2,5$  энергия возбуждения не может быть разделена на вибрационные и ротационные части. В области  $\delta < 0,4$  возможны некоторые специальные возбуждения, соответствующие отрицательным квадрупольным моментам возбужденных состояний.

Результаты сравнены с данными экспериментов.

Атомное ядро представляет собой систему сильно взаимодействующих нуклонов. Для описания некоторых свойств стационарных состояний такой системы используются те или иные модельные представления. В последнее время при описании малых возбужденных состояний четно-четных ядер наибольшего успеха добилась так называемая обобщенная модель ядра, предложенная *Огге Бором* и *Моттelsonом*. В обобщенной модели предполагается, что нуклоны, находящиеся вне заполненных оболочек, можно описать используя одночастичное приближение, а нуклоны, входящие в состав полностью заполненных оболочек (остов ядра) проявляют себя только через свои коллективные свойства.

У четно-четных ядер частоты, соответствующие одно-частичным возбуждениям, превышают частоты коллективных движений. Поэтому можно произвести усреднение полного гамильтониана ядра по состояниям движения внешних нуклонов при фиксированных значениях координат, характеризующих коллективные степени свободы ядра. Таким образом удастся получить оператор энергии ядра, выраженный через коллективные координаты  $\beta$  и  $\gamma$ , введенные *О. Бором* для описания коллективных движений нуклонов

$$H = \frac{B}{2} (\dot{\beta}^2 + \beta^2 \dot{\gamma}^2) + \frac{C}{2} \beta^2 + \frac{\hbar^2}{4} \left( \frac{1}{I_1} + \frac{1}{I_2} \right) [J(J+1) + D] + A \beta \cos \gamma, \quad (1)$$

где

$$I_{1,2} = 4 B \beta^2 \sin^2 \left( \gamma \pm \frac{2\pi}{3} \right).$$

В (1) величина  $B$  и  $C$  являются параметрами, характеризующими коллективные движения,  $A$  и  $D$  — величины, зависящие от состояния движения внешних нуклонов.

Гамильтониан (1) был получен в работе Форда [1] при предположении, что ядро имеет аксиальную симметрию и проекции угловых моментов внешних нуклонов на ось симметрии ядра являются хорошими квантовыми числами

$$(J_3 = \sum_i j_{i3} = 0).$$

В нашей работе проведено исследование энергетических уровней системы, описываемой гамильтонианом (1) при предположении, что аксиальная симметрия ядра не нарушается. Потенциальная энергия в гамильтониане (1) имеет минимум при значениях  $\gamma = 0, \pi$  и

$$\beta = \beta_0 = -\frac{A}{C} + \frac{\hbar^2 D}{3 C B \beta_0^3} \quad (\text{при } J = 0) \quad (2)$$

Существенно, что потенциальная энергия имеет полюс в точке  $\beta = 0$ . Наличие этого полюса соответствует тому, что момент инерции ядра стремится к нулю при  $\beta \rightarrow 0$ .

Если в ядре имеются нуклоны вне заполненных оболочек, то даже при равном нулю полном угловом моменте момент количества движения остова и суммарный момент внешних нуклонов не являются интегралами движения и не равны нулю в отдельности.

Разлагая потенциальную энергию, входящую в (1), в ряд относительно отклонений от положения равновесия (при  $\gamma = 0$ ) получим уравнение Шредингера, определяющее энергию ( $\epsilon$ ) системы.

$$\left[ \hat{T} + \frac{C}{2} (\beta - \beta_0)^2 - \epsilon \right] \psi(\beta \theta \Phi) = 0, \quad (3)$$

где  $\theta, \Phi$  — углы, определяющие ориентацию оси симметрии ядра в пространстве;  $\hat{T}$  — оператор кинетической энергии:

$$\hat{T} = -\frac{\hbar^2}{2 B \beta^2} \left\{ \frac{\partial}{\partial \beta} \left( \beta^2 \frac{\partial}{\partial \beta} \right) + \frac{1}{\sin \theta} \frac{\partial}{\partial \theta} \left( \sin \theta \frac{\partial}{\partial \theta} \right) + \frac{1}{\sin^2 \theta} \frac{\partial^2}{\partial \Phi^2} \right\}. \quad (4)$$



Представляя решение (3) в виде

$$\psi(\beta, \theta, \Phi) = \sum_J \frac{U_J(\beta)}{\beta} Y_{JM}(\theta, \Phi), \quad J = 0, 2, \dots \quad (5)$$

$$U_J(0) = 0,$$

получаем уравнение для функции  $U_J(\beta)$

$$-\frac{\hbar^2}{2B} \frac{d^2 U_J}{d\beta^2} + \frac{C_J}{2} (\beta - \beta_J)^2 U_J - [\varepsilon - V_J(\beta_J)] U_J = 0, \quad (6)$$

где  $\beta_J = \xi \beta_0$  — новое положение равновесия, определяемое из условия

$$\xi^3 (\xi - 1) = \frac{J(J+1)}{3\delta^4}; \quad (7)$$

$\delta$  — безразмерный параметр теории, определяемый соотношением

$$\delta = \beta_0 \left( \frac{BC}{\hbar^2} \right)^{1/4} = \beta_0 \sqrt{\frac{B\omega_0}{\hbar}}, \quad (8)$$

$$\omega_0 = \sqrt{\frac{C}{B}}; \quad C_J = C_0 \left( 1 + \frac{J(J+1)}{\delta^4 \xi^4} \right).$$

$$V_J(\beta_J) = \hbar \omega_0 \left[ \delta^2 (\xi - 1)^2 + \frac{J(J+1)}{6\delta^2 \xi^2} \right].$$

Для решения уравнения (6) удобно ввести новую переменную

$$\zeta = \xi \delta \frac{\beta - \beta_J}{\beta_J},$$

изменяющуюся в пределах

$$-\xi \delta \leq \zeta < \infty \quad (9)$$

и новую функцию  $V(\zeta)$ , определяемую соотношением

$$U(\beta) = V(\zeta) \exp(-\zeta^2/2). \quad (10)$$

Тогда функция  $V(\zeta)$  будет удовлетворять уравнению

$$\frac{d^2 V}{d\zeta^2} - 2\zeta \frac{dV}{d\zeta} + 2\nu V(\zeta) = 0 \quad (11)$$

и граничным условиям

$$V(-\delta \xi) = 0 \text{ и } e^{-\xi^2/2} V(\xi) \rightarrow 0, \text{ если } \xi \rightarrow \infty. \quad (12)$$

Решения уравнения (11) с граничными условиями (12) выражаются через функции Эрмита

$$V_\nu(\xi) = \frac{\text{const}}{2 \Gamma(-\nu)} \sum_{k=0}^{\infty} \frac{(-1)^k \Gamma\left(\frac{k-\nu}{2}\right)}{k!} (2\xi)^k. \quad (13)$$

Число  $\nu$  вычисляется из трансцендентного уравнения

$$V(-\delta \xi) = 0. \quad (14)$$

При этом энергия системы определяется равенством

$$\frac{\varepsilon}{\hbar \omega_0} = (\nu + 1/2) \left[ 1 + \frac{J(J+1)}{\delta^4 \xi^4} \right]^{1/2} + \left[ \frac{1}{2} \delta^2 (\xi - 1)^2 + \frac{J(J+1)}{6 \delta^2 \xi^2} \right]. \quad (15)$$

Таким образом при заданном  $J$  энергия зависит только от двух параметров:  $\omega_0$  и  $\delta$ . Напомним, что согласно (8) безразмерный параметр  $\delta = \beta_0 \sqrt{\frac{B \omega_0}{\hbar}}$  где  $\beta_0$  — характеризует отклонение ядра от сферической формы;  $\omega_0$  — частота поверхностных колебаний;  $B$  — массовый коэффициент, который в случае гидродинамической модели выражается через массовое число ( $A$ ), массу нуклона ( $M$ ) и радиус ядра ( $R$ ) формулой

$$B = \frac{3}{8\pi} A M R_0^2, \text{ или } B = \frac{15}{16\pi} I_0,$$

где  $I_0$  — момент инерции твердого тела массы  $MA$  и радиуса  $R_0$ .

График зависимости  $\frac{\varepsilon}{\hbar \omega_0}$  для значений параметра  $\delta \geq 1$  приведен на рис. 1. Из этого рисунка видно, что при  $\delta > 2,5$  энергетический спектр коллективных возбуждений четно-четных ядер разбивается на систему вращательно-колебательных полос. В таблице 1 приведено сравнение полученных теоретических значений энергии возбуждения первой и второй вращательных полос возбужденных состояний некоторых ядер с экспериментальными

данными. Там же приведены значения параметров  $\hbar \omega_0$  и  $\delta$ , которые использовались при вычислении теоретических значений энергии возбуждения.

В таблице II приведены отношения  $\frac{\varepsilon_{2I}}{\varepsilon_{1I}}$ ,  $\frac{\varepsilon_{2II}}{\varepsilon_{1II}}$ ,  $\frac{\varepsilon_{1II}}{\varepsilon_{1I}}$  в зависимости от значения  $\delta$ , где  $\varepsilon_{1I}$ ,  $\varepsilon_{2I}$ ,  $\varepsilon_{1II}$ ,  $\varepsilon_{2II}$  соответственно энергии первого и второго (1,2) вращательных подуровней в первой и второй (I, II) полосах вращательных состояний ядра.

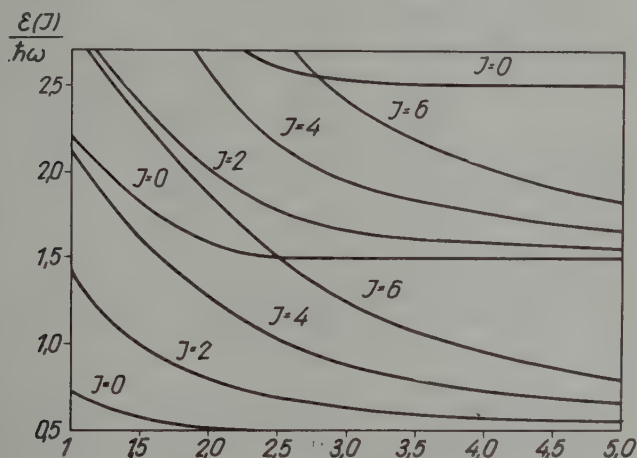


Рис. 1

При достаточно больших  $\delta$  энергия коллективных возбуждений (15) может быть представлена в виде

$$E_{nJ} = n \hbar \omega_0 + A J(J+1) - g J^2(J+1)^2, \quad (16)$$

где 
$$A = \frac{\hbar^2}{2I}, \quad g = \frac{a}{(\hbar \omega_0)^2} \left( \frac{\hbar}{I} \right)^3.$$

Эта формула уже предлагалась в работах *О. Бора* и *Моттельсона*. Она дает хорошее согласие с экспериментом, если  $A$  и  $g$  рассматривать как параметры в каждой полосе возбужденных состояний ядра. Таким образом при описании коллективных возбуждений ядер, указанных в таблице I, требовалось бы 5 параметров, а не 2, как это следует из формулы (15).

При  $\delta < 2,5$  разделение коллективных возбуждений на вращательные и колебательные невозможно. На рис. 2. приведена схема уровней для значения  $\delta < 1$ . В этом случае наряду с решениями, соответствующими  $\gamma = 0$

Таблица I

Ядро	J	Энергетический уровень		$\hbar\omega_0$	$\delta$
		Теория	Экспер.		
$W^{182}$	2	100,09	100,09	1101	3,48
	4	320,3	329,36		
	6	641,6	677,06		
	0	1101	—		
	2	1222	1222		
	4	1481	1488,6		
$Th^{232}$	2	50	50	710	3,98
	4	163	165		
	6	332	—		
	0	710	—		
	2	770	770		
	4	901	—		
$U^{234}$	2	43	43	803	4,48
	4	141	142		
	6	290	295		
	0	803	803		
	2	855	—		
	4	966	—		
$Pu^{238}$	2	44,2	44,2	935	4,74
	4	147,7	146		
	6	304,8	303		
	0	935	935		
	2	986	986		
	4	1100	1073		

Таблица II

$\delta$	1	2	3	4	5
$\frac{\varepsilon_{2I}}{\varepsilon_{1I}}$	2,17	2,70	3,02	3,27	3,33
$\frac{\varepsilon_{2II}}{\varepsilon_{1II}}$	1,76	2,43	2,94	3,25	3,31
$\frac{\varepsilon_{1II}}{\varepsilon_{1I}}$	1,48	1,36	1,26	1,16	1,11

возникают возбужденные состояния с  $\gamma = \pi$ , изображенные на рис. 2 пунктирными линиями. Эти возбужденные состояния соответствуют отрицательному знаку квадрупольного момента ядра, находящегося в возбужденном состоянии. В связи с тем, что предположения, положенные в основу теории

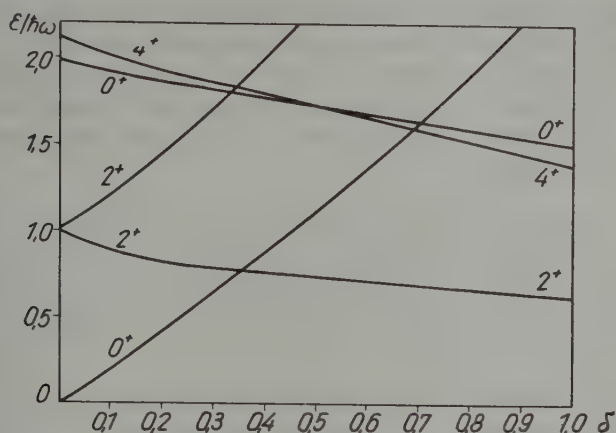


Рис. 2

нарушаются при малых значениях  $\delta$ , не вполне ясно, могут ли в действительности реализовываться такие возбужденные состояния.

Если допустить, что выводы теории можно применять до значений  $\delta \geq 0,2$ , то для некоторых ядер (см. табл. III) можно получить при соответ-

Таблица III

Ядро	Относительная энергия уровня		Спин уровня		
	Экспер.	Теория.	Экспер.	Теория	
$\text{Pt}^{192}$	—	0,65	—	[0]	0,25
	1,00	1,00	2	2	
	1,93	1,93	2	[2]	
	2,48	2,32	4	4,0	
$\text{Ge}^{72}$	0,82	0,82	0	[0]	0,29
	1,00	1,00	2	2	
	1,74	2,15	2	[2]	
$\text{Cd}^{114}$	—	0,86	—	[0]	0,3
	1,00	1,00	2	2	
	2,17	2,18	2	[2]	
	2,30	2,30	4	0	
	2,34	2,34	0	4	

ствующем выборе  $\delta$  удовлетворительное согласие с наблюдаемым экспериментально отношением энергии первых возбужденных уровней к энергии первого уровня, имеющего спин 2. При этом теория дает и правильную последовательность значений спинов уровней. Спины уровней энергии, соответствующие отрицательным значениям квадрупольных моментов заключены в квадратные скобки. Если эта интерпретация правильна, то следует ожидать, что вероятность переходов между состояниями, соответствующими разному знаку квадрупольного момента должны быть меньше, чем вероятности переходов между состояниями, соответствующими одному знаку квадрупольного момента ядра.

## ЛИТЕРАТУРА

1. K. Ford, Phys. Rev., **90**, 29, 1953.

## COLLECTIVE EXCITATIONS OF THE EVEN-EVEN ATOMIC NUCLEI

By

A. S. DAVYDOV and G. F. FILIPPOV

## Summary

The problem of collective excitations in an even-even nucleus possessing axial symmetry is considered. During the calculation it has not been assumed that a rotational energy is much smaller than a vibrational energy.

For different deformation parameters the energy ratios of the collective excitations and the succession of spins have been computed. It is shown that the energy of the collective

excitations can be represented as the function only of two parameters:  $a_0 = \sqrt{\frac{c}{B}}$  and  $\delta = \beta_0 \left[ \frac{Be}{\hbar^2} \right]^{1/4}$ . In the region  $\delta > 2,5$  the excitation spectrum can be represented as the system of rotational vibrational bands. In the region  $\delta < 2,5$  the excitation energy can not be separated into rotational and vibrational components. In the region  $\delta < 0,4$  the appearance of some special excitations is possible, in consequence of the negative quadrupole moments of the excited states.

A comparison with experiment is carried out.



# О $\gamma p$ -РЕАКЦИЯХ С ОБРАЗОВАНИЕМ ОСНОВНЫХ СОСТОЯНИЙ ЯДЕР\*

В. И. ГОЛЬДАНСКИЙ

ФИЗИЧЕСКИЙ ИНСТИТУТ ИМ. П. Н. ЛЕБЕДЕВА АН СССР

(Представлено: Z. Gyulai — Поступило: 23 декабря 1957 г.)

Дана оценка вклада отдельных уровней в фотоядерные реакции ( $\gamma p$ ) пяти легких ядер ( $B^{10}$ ,  $C^{12}$ ,  $N^{14}$ ,  $O^{16}$ ,  $S^{32}$ ), полученных по теореме детального равновесия из обратных ( $p\gamma$ ) реакций. Максимальные сечения  $\gamma p$ -реакций с образованием конечного ядра в основном состоянии иногда на много раз превышают максимальные сечения при «гигантском» резонансе. Интегральные сечения составляют приблизительно 10% интегральных сечений в «гигантском» резонансе. При сравнении спектра и углового распределения фотонуклонов с расчетами статистической теории, нужно иметь в виду значительный вклад отдельных уровней.

За последние годы на очень большом числе примеров подтверждено существование так называемого «гигантского» резонанса фотоядерных (например,  $\gamma p$ - и  $\gamma p$ -реакций).

Полуширина этого «гигантского» резонанса составляет несколько Мэв, а максимум сечений располагается при энергии  $\gamma$  — квантов 15—25 Мэв. При таких энергиях возбуждения даже для самых легких ядер расстояние между уровнями не превышает нескольких Кэв, или десятков Кэв, а для более тяжелых ядер отдельные уровни, несомненно, перекрываются. Поэтому положение и форма «гигантского» резонанса обычно связываются с наличием в соответствующей области энергий центра тяжести электрических дипольных уровней (1), возбуждаемых при поглощении ядром  $\gamma$ -квантов.

Однако, для того чтобы однозначно подтвердить дипольный ( $E1$ ) характер поглощения  $\gamma$ -квантов в области гигантского резонанса следовало бы установить природу конечных состояний ядер, а также исследовать угловое распределение испускаемых фотонуклонов. Между тем, в работах, посвященных фотоядерным реакциям, такие наблюдения, как правило, отсутствуют.

Измеряя выход фотопротонов и фотонейтронов или регистрируя активность радиоактивных продуктов фотоядерных реакций, естественно нельзя установить, образуется ли конечное ядро в основном или каком-либо возбужденном состоянии, т. е. не испускаются ли наряду с фотонуклонами еще и  $\gamma$ -кванты. Поскольку исследования фотоядерных реакций проводятся обычно с непрерывным спектром тормозного излучения, то даже и такие

\* Доложено 3 декабря 1957 г. на симпозиуме по ядерной физике в Матрахазе организованном Физическим Обществом им. Лоранд Этвеш.

важные дополнительные источники информации, как угловое и энергетическое распределение фотонуклонов все еще оказывается недостаточными для разграничения случаев образования конечных ядер в различных состояниях.

В настоящее время вопрос о характере поглощения  $\gamma$ -квантов при испускании фотонуклонов приобрел еще дополнительный интерес в связи с обсуждением механизма прямого ядерного фотозффекта, т. е. прямого взаимодействия  $\gamma$ -квантов с ядерными нуклонами, не связанного с образованием составного ядра. При таком обсуждении широко используется сопоставление углового и энергетического распределения фотонуклонов с результатами, предсказываемыми статистической теорией, т. е. без учета индивидуальных свойств отдельных уровней и их вклада в общую картину фотоядерного взаимодействия.

Между тем, начиная с 1952 г. группе канадских физиков (2, 3, 4) благодаря высокой стабилизации энергии ускоряемых в бетатроне электронов удалось выделить в «гигантском» резонансе  $\gamma p$ -реакций для нескольких легких ядер ( $Li^7$ ,  $C^{12}$ ,  $O^{16}$  и  $F^{19}$ ) целый ряд отдельных резонансных уровней. Так например, в реакции  $O^{16}(\gamma p) O^{16}$  (порог 15,6 Мэв) при  $h\nu = 15,9—21,9$  Мэв наблюдается (3) девять отдельных резонансов с интегральными сечениями от 0,06 до 7,5 Мэв миллибарн, дающих в сумме  $\sigma_{\text{инт.}} = 14$  Мэв мбарн.

При всем интересе уточненных исследований надо, однако отметить, что и при изучении отдельных резонансов фотоядерных реакций вопрос о конечных состояниях образующихся ядер остался открытым. Поэтому осталось невыясненным, какова мультипольность поглощаемых в отдельных резонансах  $\gamma$ -квантов и каким, собственно, должно быть угловое распределение испускаемых фотонуклонов.

В настоящем сообщении мы хотим отметить, что ряд сведений, интересных для понимания фотоядерных —  $\gamma p$ -реакций, но до сих пор не полученных из непосредственного их наблюдения (в значительной степени — из-за скудности источников монохроматических  $\gamma$ -квантов) можно заимствовать из экспериментальных данных о сечениях обратных —  $p\gamma$ -реакций, идущих без каскадного испускания  $\gamma$ -квантов.

Сечения  $\gamma p$ -реакций с образованием основных состояний конечных ядер —  $\sigma_{\gamma p}$  связаны с сечениями  $p\gamma$  — реакций простыми соотношениями детального баланса, например, для реакции  $O^{16}(\gamma p)N^{15}$  имеем:

$$\sigma_{\gamma_0} = \sigma_{pN} \cdot 2 \cdot \frac{16}{15} \cdot \frac{mc^2(h\nu - Q)}{(h\nu)^2} \cdot \frac{2I_N + 1}{2I_0 + 1}$$

Здесь:

$I_N (= 1/2)$  и  $I_0 (= 0)$  — спины ядер  $N^{15}$  и  $O^{16}$ ,  $m$  — масса протона,  $Q (= 12,11$  Мэв) — тепловой эффект реакции,  $h\nu$  — энергия  $\gamma$ -кванта, связан-

ная с энергией протона в  $p\gamma$ -реакции ( $E_p$ ) соотношением:  $h\nu = Q + \frac{15}{16} E_p$ .

Из анализа имеющихся в литературе данных можно получить ряд сведений о  $\gamma p$ -реакциях с образованием основных состояний конечных ядер для пяти легких ядер:  $B^{10}$ ,  $C^{12}$ ,  $N^{14}$ ,  $O^{16}$  и  $S^{32}$ .

Сводка результатов приводится в таблице 1 и на рис. 1—6.

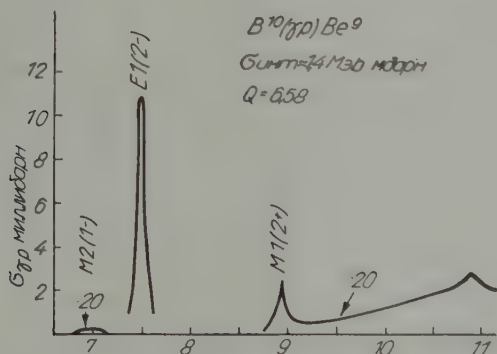


Рис. 1

Сечение реакции  $Be^9(p\gamma)B^{10}$  в первом максимуме дано в (5), а значения  $\sigma$  для других уровней получены пересчетом выходов из толстой мишени (7, 8). Сечения реакции  $B^{11}(p\gamma)C^{12}$  при  $E_p < 2,8$  Мэв заимствованы из (5, 9), абсолютизация сечений при более высоких энергиях получена сопоставлением результатов (9) и (10) при  $E_p = 2—2,8$  Мэв.

Сечения в резонансных максимумах реакции  $C^{13}(p\gamma)N^{14}$  взяты из (5), а для интерполяции функции возбуждения между пиками резонансов использовались данные (11). Наконец, абсолютизация функции возбуждения реакции  $P^{31}(p\gamma)S^{32}$ , данной в (14), производилась по данным работы (16), в которой приводится сечение радиационного захвата  $P^{31}$  протонов с энергией 1,265 Мэв.

Данные приводимые в таблице, не требуют особых пояснений. Заметим лишь, что среди возможных значений орбитальных моментов фотопротонов с связи с малостью энергии указаны лишь  $l = 0, 1, 2$ .

Рис. 1—5 непосредственно иллюстрируют сведения, приведенные в табл. 1. На рис. 6 расчетные данные о тонкой структуре  $\gamma p$ -реакций сопоставляются с результатами наблюдений «гигантского» резонанса.

Как явствует из таблицы и рисунков, максимальные сечения  $\gamma p$ -реакций с образованием основных состояний конечных ядер, связанных с отдельными уровнями, подчас во много раз превосходят максимальные

сечения в «гигантском» резонансе. Интегральные сечения таких реакций, обусловленные отдельными уровнями, достигают примерно 10% от инте-

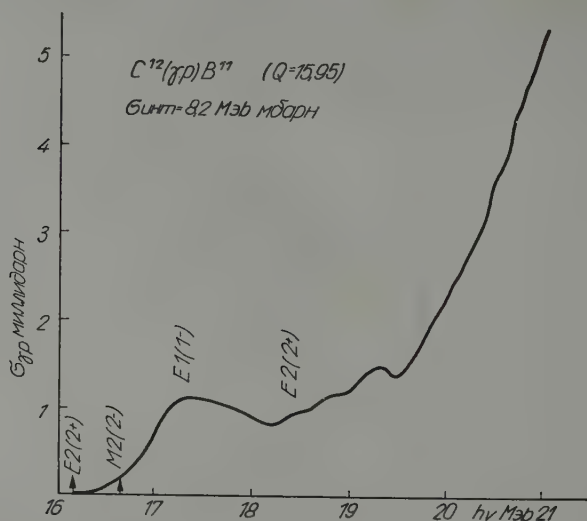


Рис. 2

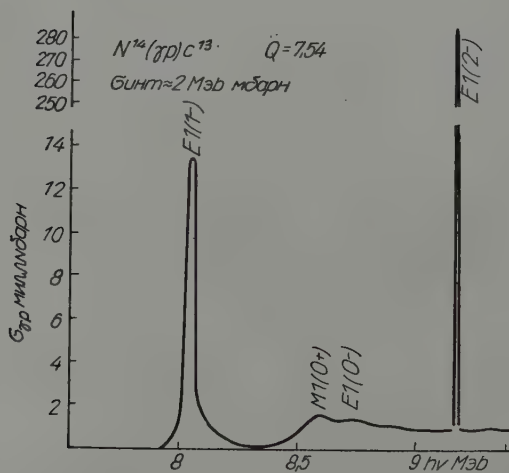
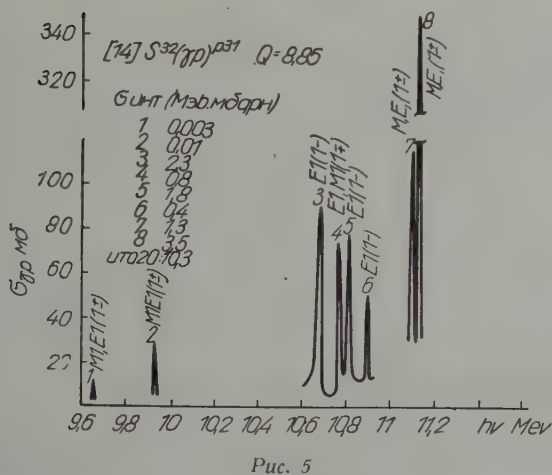
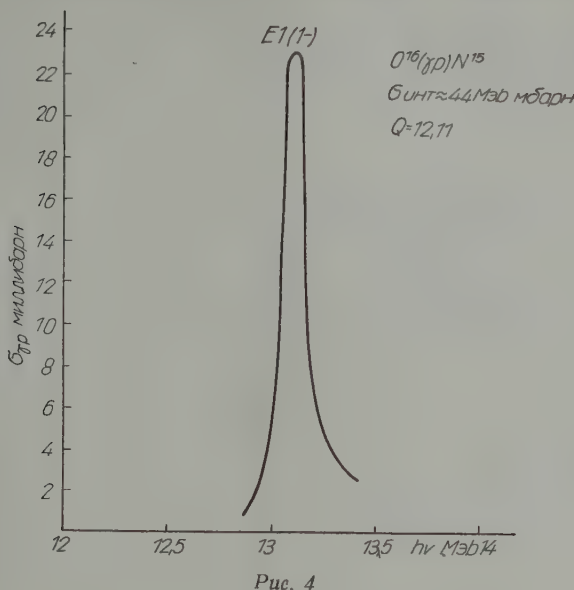


Рис. 3

гральных сечений «гигантского» резонанса, охватывающих всевозможные состояния конечных ядер. Как правило, измерения сечений «гигантского» резонанса  $\gamma p$ -реакций производятся лишь начиная с энергий  $\gamma$ -кван-

тов, превышающих порог на несколько Мэв (см., например, рис. 6). Поэтому приведенные здесь результаты дают не вклад  $\gamma$ -реакций с образованием



основного состояния конечных ядер в гигантский резонанс, а дополнение к этому резонансу. Таким образом анализ сведений о  $\gamma$ -реакциях приводит к некоторому увеличению экспериментальных величин сечений погло-

Реакция	Ссылки	Порог (Мэв)	Интервал энергии $\Delta h\nu$ (Мэв)	Энергия уровня (Мэв)	Момент и четность уровня	Характер поглощения $\gamma$ -кванта	Орбитальный момент протона	$\sigma$ интеграл (Мэв, мбарн)
$B^{10}(\gamma p) Be^9$ $3^+$ $\frac{3}{2}-$	5, 6, 7, 8	6,58	6,58—11	6,89	1—	M2	SD	$\left. \begin{array}{l} \sim 1,1 \\ 0,3 \end{array} \right\} 1,4$
				7,48	2—	E1	SD	
				8,89	2+	M1	P	
				10,83	?	?	?	
$C^{12}(\gamma p) B^{11}$ $O^+$ $\frac{3}{2}-$	5, 9, 10	15,95	15,95—21	16,10	2+	E2	P	$\left. \begin{array}{l} \\ \\ \\ \\ \\ \\ \end{array} \right\} 8,2$
				16,57	2—	M2	SD	
				17,22	1—	E1	SD	
				18,39	2+	E2	P	
				18,86	?	?	?	
				19,25*	?	?	?	
				20,25	?	?	?	
$N^{14}(\gamma p) C^{13}$ $1^+$ $\frac{1}{2}-$	5, 11	7,54	7,54—9,2	8,06	1—	E1	SD	$\left. \begin{array}{l} \\ \\ \\ \end{array} \right\} 2$ $\sim 0,6$
				8,62	0+	M1	P	
				8,70	0—	E1	S	
				9,18	2—	E1	D	
$O^{16}(\gamma p) N^{15}$ $O^+$ $\frac{1}{2}-$	13	12,11	12,11—13,5	13,09**	1—	E1	SD	4,4
$S^{32}(\gamma p) P^{31}$ $O^+$ $\frac{1}{2}+$	14, 16	8,85	8,85—11,2	9,65	1±	M1 (E1)	SD(P)	0,003
				9,932	1±	M1 (E1)	SD(P)	0,01
				10,682	1—	E1	P	2,3
				10,772	1±	E1 (M1)	P(SD)	0,8
				10,812	1—	E1	P	1,8
				10,915	1—	E1	P	0,4
				11,097	1±	M1 (E1)	SD(P)	1,3
				11,115	1±	M1 (E1)	SD(P)	3,5

\* Уровень обнаружен также в реакции  $C^{12}(\gamma n) C^{11}$  [2]

\*\* Уровень обнаружен также в реакции  $N^{15}(p\alpha) C^{12}$  [5]

щения  $\gamma$ -квантов ( $\sigma_\gamma$ ) и к уменьшению различия между теоретическими и экспериментальными значениями ( $\sigma_\gamma$ )<sub>инт.</sub> для легких ядер, отмеченного, например, в 15. Следует широко привлекать экспериментальные данные о  $p\gamma$ - и  $p\gamma$ -реакциях для независимой проверки результатов фотоядерных исследований, проводимых, как правило, с широкими спектрами  $\gamma$



квантов. Было бы, в частности, интересно изучить подобные реакции и в области «гигантского» резонанса. Анализ данных о  $p\gamma$ -реакциях без каскадного испускания  $\gamma$ -квантов позволяет сделать определенный вывод о преобладании (хотя и не исключительном)  $E1$  — поглощения  $\gamma$ -квантов в этой области энергии. В ряде случаев из этих данных можно сделать также заключение о сечениях анизотропного испускания протонов в  $\gamma p$ -реакциях. Например, интегральное сечение для уровней 3, 5 и 6 в реакции

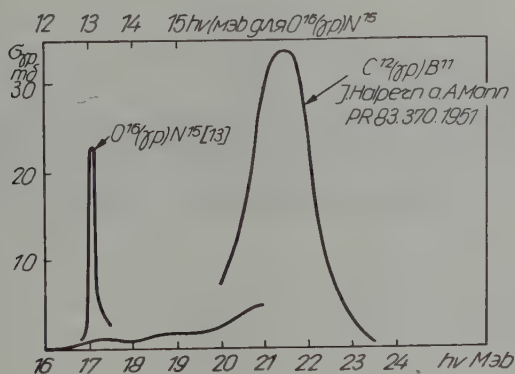


Рис. 6

$S^{32}/\gamma p/P^{31}$ , соответствующих испусканию протонов в  $p$ -состоянии:  $\sigma_{\text{инт.}} = 4,5$  Мэв миллибарн. Следует принимать во внимание вклад отдельных уровней в анизотропное испускание фотонуклонов при сопоставлении спектра углового распределения этих нуклонов с расчетами статистической теории

## ЛИТЕРАТУРА

1. А. Б. Мигдал, ЖЭТФ, 15, 81, 1945.
2. R. N. HASLAM, L. KATZ, R. I. HORSLEY, A. G. CAMERON, R. MONTALBETTI, Phys. Rev. 87, 196, 1952.
3. L. KATZ, R. N. HASLAM, R. I. HORSLEY, A. G. CAMERON, R. MONTALBETTI, Phys. Rev. 95, 464, 1954.
4. J. GOLDEMBERG A. L. KATZ, Ph. Rev. 95, 471, 1954.
5. F. AJZENBERG A. T. LAURITSEN, Rev. Mod. Phys. 27, 77, 1955.
6. S. HUNT, Phys. Rev. 87, 902, 1952.
7. W. F. HORNYAK A. T. COOR, Ph. Rev. 92, 675, 1953.
8. T. M. HAHN, C. W. SNYDER, H. W. WILLARD, J. K. BAIR, E. D. KLEMA, J. D. KINGSTON, F. P. GREEN, Phys. Rev. 85, 934, 1952.
9. T. HUUS A. R. B. DAY, Phys. Rev. 91, 599, 1953.
10. J. K. BAIR, J. D. KINGSTON a. H. B. WILLARD, Phys. Rev. 100, 21, 1955.
11. J. SEAGRAVE, Phys. Rev. 85, 197, 1952.
12. A. K. MANN, J. HALPERN, Phys. Rev. 83, 370, 1951.
13. A. SCHARDT, W. A. FOWLER, C. C. LAURITSEN Phys. Rev. 86, 527, 1952:

14. E. B. PAUL, H. E. GOVE, A. E. LITHERLAND, G. A. BARTOLOMEW, Phys. Rev. 99, 1329, 1955.
15. Ю. К. Хохлов, ДАН 97, 239, 1954.
16. G. R. GROVE, J. N. COOPER, Phys. Rev. 82, 505, 1951.

## ON ( $\gamma p$ ) REACTIONS WITH FINAL NUCLEI IN THE GROUND STATE

By

V. I. GOLDANSKIJ

### S u m m a r y

It is estimated the contribution of individual levels to photonuclear ( $p\gamma$ ) reactions on five light nuclei ( $B^{10}$ ,  $C^{12}$ ,  $N^{14}$ ,  $O^{16}$ ,  $S^{32}$ ) which can be obtained by detailed balance method from experimental data regarding reverse ( $p\gamma$ ) reactions.

The maximum cross sections for ( $\gamma p$ ) reactions with the formation of ground state final nuclei sometimes exceed by a very large factor the maximum cross sections in »giant« resonance. The integral cross sections amount to about 10% of the integral cross section in »giant« resonance.

One must keep in mind the marked contribution of individual levels in comparing the spectrum and angular distribution of photonucleons with calculations from statistical theory.

# ФЕНОМЕНОЛОГИЧЕСКОЕ ОБОБЩЕНИЕ УРАВНЕНИЯ ТОМАСА-ФЕРМИ-ДИРАКА (ТФД) В СЛУЧАЕ ТЕОРИИ МЕТАЛЛОВ И ЕГО ПЕРИОДИЧЕСКИЕ РЕШЕНИЯ

Д. Ф. КУРДГЕЛАИДЗЕ

(Представлено : Р. Gombás — Поступило : 23 декабря 1957 г.)

Обменное взаимодействие соседних металлических атомов описано феноменологически уравнением Т. Ф. Д. в виде :  $\Delta\varphi = \bar{a}(\varphi^{1/2} + \tau_0)^3 + \lambda_3$ . Здесь  $\bar{a}$ ,  $\tau_0$  и  $\lambda_3$  являются свободными параметрами, которые могут быть подобраны к следующим свойствам металла : константа решетки, работа выхода или минимальный потенциал Ферми и средняя или граничная плотность электронов проводимости. Вышенаписанное уравнение обладает периодическими решениями, свойства которых в статье обсуждаются. Случай натрия, как показательный пример, трактуется в подробности.

Согласно электронной теории металлов уравнение (ТФД) с соответствующими граничными условиями — применимо и к металлу [1]. Если в случае изолированного иона граничные условия имеют вид :

$$\lim_{r \rightarrow 0} r S(r) = Z, \quad \varphi(r_0) = \varphi_0 \quad (1)$$

где  $\varphi(r)$  — решение уравнения (ТФД),

$Z$  — заряд иона,

$\varphi_0$  — потенциал ионизации,

то в случае металла условия (1) следует дополнить еще требованием периодичности решения с заданным периодом  $\Omega$ .

Подобная, но двухмерная задача, когда нелинейное уравнение (ТФД) вырождается в линейное уравнение, была с успехом решена Ленардом—Джонсом [2]. Однако, если в случае линейных уравнений граничные условия удастся удовлетворить при помощи наложения различных решений уравнения, то в случае нелинейных уравнений, ввиду отсутствия принципа суперпозиции, решение граничной задачи становится весьма затруднительным.

Указанное обстоятельство заставляет отказаться от одного из граничных условий в случае применения уравнения (ТФД) к металлу. Так например : обычно металл рассматривается как совокупность изолированных ионов, а периодичность вводится искусственным путем, как простое механическое повторение картины [1], [3], [4]. Но можно сделать ударение и на вторую крайность : решить граничную задачу с требованием периодичности и отказаться от решения уравнения в начале координат.

Ясно, что первый подход может дать ответ только на те свойства металла, которые определяются в основном свойствами иона и не применим для решения задач связанных с электронами проводимости, а второй подход — наоборот.

В последнем случае, который нас интересует, уравнение (ТФД) следует однако обобщить. Дело в том, что при выводе уравнения (ТФД) не учитывается сложное обменное взаимодействие соседних атомов металла. Это взаимодействие слабо влияет на связанные электроны и вносит существенный вклад

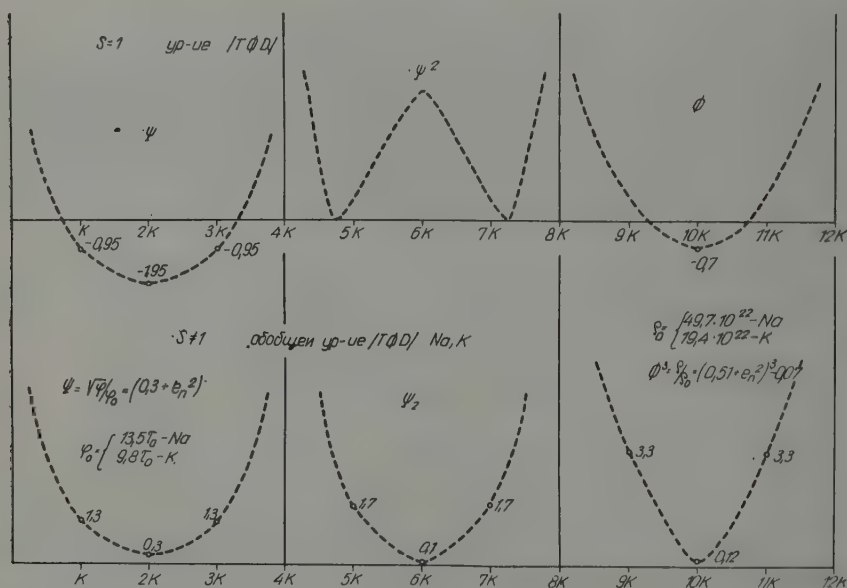


Рис. 1

в поведение электронов проводимости [1]. Прямой учет указанного взаимодействия в уравнении (ТФД) обычным путем представляется довольно трудным и, следовательно, имеет смысл искать феноменологическое обобщение уравнения.

При этом можно исходить из того, что учет обменного взаимодействия Дирака в уравнении (ТФД), приводит только к появлению постоянного слагаемого  $\tau_0$ , при  $\varphi^{1/2}$  в правой стороне уравнения, а учет корреляционной поправки Гомбаша в конечном счете сводится только к замене численного значения постоянного параметра уравнения (ТФД) —  $\tau_0$  [3].

Тогда обобщенное уравнение (ТФД) через варьируемые постоянные коэффициенты в виде:

$$\Delta \varphi = \bar{a} (\varphi^{1/2} + \bar{\tau}_0)^3 + \bar{\lambda}_3 \quad (1)$$

представляется нам довольно общим.

— В уравнении (1).

$$\bar{a} = \lambda_1 a^1, \quad \bar{\tau}_0 = \lambda_2 \tau_0$$

$$\lambda_1, \lambda_2, \lambda_3 = \text{const}$$

$\lambda_1, \lambda_2, \lambda_3$  новые параметры, остальные обозначения те же самые, что и в случае обычного уравнения (ТФД) [3]:

$$\begin{aligned} a' &= 4\pi\sigma_0, \quad \sigma_0 = 0,0955 (1/er_0)^{3/2} \simeq 0,1 (1/er_0)^{3/2} \\ \tau_0 &= 0,254 (e/c_0)^{1/2} \simeq 1/4 (e/c_0)^{1/2}, \quad c_0 = \hbar^2/me^2 \\ \varphi &= V - V_0 + \bar{\tau}_0, \quad V = V_k + Ve \end{aligned} \quad (2)$$

$V_0$  — постоянная,

$V_k$  — потенциал внешнего поля,

$V_e$  — потенциал электронного газа,

$V$  — полный потенциал в данной точке,

$$\varrho = \lambda_1 \sigma_0 (\varphi^{1/2} + \bar{\tau}_0)^3 + \lambda_3/4\pi \quad (3)$$

плотность электронного газа, — действительно: при  $\lambda_3 = \lambda_2 = 0, \lambda_1 = 1$  имеем уравнение (ТФД), при  $\lambda_3 = 0, \lambda_2 = 0,88, \lambda_1 = 1$  уравнение (ТФД) и при  $\lambda_3 = 0, \lambda_2 = 1, \lambda_1 = 1$ , уравнение (ТФД) с учетом поправки Гомбаша.

Введение трех свободных параметров дает возможность согласовать с экспериментом три основные параметры металла, длину кристаллической решетки, работу выхода или минимальный потенциал Ферми, и среднюю или граничную плотность электронов проводимости. Поскольку уравнение (1), как показывается ниже, имеет замкнутые периодические решения, указанную выше программу можно осуществить математически строго.

Будем считать металл бесконечным по всем трем направлениям и будем искать периодические решения уравнения (1), удовлетворяющие условию

$$\varphi > 0, \quad \varrho > 0 \quad (4)$$

везде.

Так как предполагается я представить периодичность кристаллической решетки через периоды решения уравнения (1), то следует ограничиться простой кубической решеткой.

Кроме того, ищется решение формально справедливое для всего пространства, но по сути дела оно справедливо только в области электронов проводимости. Потенциал внутри ионного остова следует находить обычным путем, как сферически симметричное решение обычного уравнения (ТФД) с соответствующими граничными условиями [3].

В связи с этим — поскольку не известна точная граница между двумя областями — возникает затруднение в нормировке решения уравнения. Невыполнима и задача сшивания двух указанных решений на границе. Однако, так как задача нормировки в конечном счете сводится к определению одного из свободных параметров, то ее можно решить косвенным путем.

Решение уравнения (1) удобнее искать в виде :

$$\varphi = \alpha^2 (\beta + e_n^2(\sigma))^2 \quad (5)$$

где  $\alpha, \beta$  — действительные постоянные числа.

$$\sigma = \vec{\omega} \vec{r} + c$$

$$e_{ni}(\sigma) = \operatorname{cn} \sigma + i \operatorname{sn} \sigma \quad (6)$$

$\operatorname{cn} \sigma$  и  $\operatorname{sn} \sigma$  — эллиптические функции.

Ввиду того, что  $e_n(\sigma)$  в некотором смысле является обобщением плоской волны на случай эллиптических функций и обладает во многом сходными с ними свойствами, то некоторые из этих свойств мы здесь укажем :

$$e_n(\sigma) e_n^*(\sigma) = 1$$

$$\operatorname{cn} \sigma = \frac{1}{2} (e_n(\sigma) + e_n^*(\sigma)), \quad \operatorname{sn} \sigma = \frac{1}{2i} (e_n(\sigma) - e_n^*(\sigma))$$

$$e_n(u+v) = e_n^{(1)}(u, v) e_n^{(1)}(v, u); \quad e_n^{(1)}(u, v) = \frac{\operatorname{cn} u + i \operatorname{sn} u \operatorname{dn} v}{\sqrt{1 - k_1^2 \operatorname{sn}^2 u \operatorname{sn}^2 v}} \quad (7)$$

$$\frac{d e_n(\omega x)}{d x} = (i \omega) e_n(\omega x) \operatorname{dn}(\omega x)$$

$$\frac{d^2 e_n(\omega x)}{d x^2} = (i \omega)^2 \{ (1 - k_1^2/2) e_n(\omega x) + k_1^2/2 e_n^3(\omega x) \}$$

$$\left( \frac{d e_n(\omega x)}{d x} \right)^2 = (i \omega)^2 \{ k_1^2/4 + (1 - k_1^2/4) e_n^2(\omega x) + k_1^2/4 e_n^4(\omega x) \}$$

где  $k_1$  — главный модуль эллиптических функций.

При предельном переходе имеем :

$$\begin{aligned} \omega^2 > 0, \quad 1 > k_1^2 \geq 0 \quad e_n(\sigma) &\rightarrow e^{i\sigma} \\ \omega^2 > 0 \quad 1 \geq k_1^2 > 0 \quad e_n(\sigma) &\rightarrow \frac{1 + \sin \sigma}{\operatorname{ch} \sigma} \end{aligned} \quad (8)$$

Подставляя выражение (5) в (3), для плотности электронного газа находим :



$$4 \pi \varrho = \bar{a} \alpha^3 (\gamma + e_n^2(\sigma))^3 + \lambda_3 \quad (9)$$

где

$$\gamma = \beta + \bar{\tau}_0/\alpha \quad (10)$$

После подстановки в (1) выражении (5) и (9), получим уравнение относительно  $e_n(\sigma)$  в виде:

$$e_n^3 e_n'' + \beta e_n e_n'' + 3 e_n'^2 e_n^2 + \beta e_n'^2 + \frac{a}{4} (s \gamma^3 + 3 \gamma^2 e_n^2 + 3 \gamma e_n^4 + e_n^6) = 0 \quad (11)$$

где

$$e_n \equiv e_n(\sigma), \quad e_n' \equiv \frac{d}{d\sigma} e_n(\sigma), \quad (12)$$

$$a = -\bar{a} \alpha / \omega^2$$

новый параметр  $s$  связан с  $\lambda_3$  соотношением:

$$\begin{aligned} \lambda_3 = (s-1) \bar{a} (\alpha \gamma)^3 &= \frac{s-1}{s} [s \bar{a} (\alpha \gamma)^3] = \frac{s-1}{s} [4 \pi \varrho_{\min}] = \\ &= \frac{s-1}{s} [4 \pi \varrho_1^*] \lambda_1 \lambda_3^2 \end{aligned} \quad (13)$$

Используя теперь свойство  $e_n(\sigma)$  по (7) для параметров решения  $\alpha$ ,  $\beta$ ,  $k_1^2$ ,  $\omega^2$  получим систему алгебраических уравнений, решение которых дает:

$$\begin{aligned} a &= \frac{\bar{\tau}_0}{\gamma - \beta} = \frac{\bar{\tau}_0}{\gamma (1 - 5 s \gamma^2)}, \quad \beta = 5 s \gamma^3 \\ k_1^2 &= a/5, \quad \omega^2 = -a \bar{a}/a \end{aligned} \quad (14)$$

$$a = [0,1 + 3/16 (1-s \gamma^2) \gamma]^{-1}$$

$$\gamma^2 = \eta/s, \quad \mu = x/s$$

$$s = x + 0,1 x^3 - \frac{1}{2} x^2 \quad (15)$$

Для того чтобы выяснить характер решения рассмотрим случай обыкновенного уравнения (ТФД). Тогда, как уже было сказано выше, имеем:  $\lambda_1 = \lambda_2 = 1$ ,  $\lambda_3 = 0$  ( $s = 1$ ) и находим:

$$\begin{aligned} \gamma &= \pm 0,731, \quad \beta = \pm 1,950, \quad a = \mp 0,82 \tau_0 \\ a &= \begin{pmatrix} 6,085 \\ 28,00 \end{pmatrix}, \quad k_1^2 = \begin{pmatrix} 1,22 \\ 5,6 \end{pmatrix}, \quad \omega^2 = \begin{pmatrix} 0,04 \\ -0,009 \end{pmatrix} \frac{1}{\epsilon_0^2} \end{aligned} \quad (16)$$

Ввиду двухзначности решения алгебраической системы уравнения для параметров, для решения (1) получим два независимые периодические решения. Одно из них комплексное и без особенности, а второе действительное и с особенностями.

Первое решение комплексное и без особенности дается через :

$$\begin{aligned}\varphi_1(\sigma) &= 0,67 \tau_0^2 \{1,95 + e_n^2(\sigma)\}^2 \\ \varrho_1(\sigma) &= 0,55 (\sigma_0 \tau_0^3) \{0,73 + e_n^2(\sigma)\}^3\end{aligned}\quad (17)$$

с периодом

$$\Omega = 4 K(k_1) = 9,20$$

где теперь

$$\begin{aligned}e_n(\sigma) &= \operatorname{dn} \sigma + i \bar{k}_1 \operatorname{sn} \sigma \\ \sigma &= \bar{\omega} \vec{r} + c, \quad \bar{\omega}^2 = 0,05 1/a_0^2, \quad \bar{k}_1^2 = 0,82\end{aligned}\quad (18)$$

$K(k_1)$  — полный эллиптический интеграл 1-го рода.

Второе периодическое решение, действительное и с особенностью дается через :

$$\begin{aligned}\varphi_2(\sigma) &= 0,67 \tau_0^2 (-1,95 + e_n^2(\sigma))^2 \\ \varrho_2(\sigma) &= 0,55 (\sigma_0 \tau_0^3) (-0,73 + e_n^2(\tau))^3\end{aligned}\quad (19)$$

с периодом

$$\Omega = 4 K(\bar{k}_1) = 9,20$$

где теперь

$$\begin{aligned}e_n(\sigma) &= \frac{1 + \operatorname{cn} \sigma}{\operatorname{sn} \sigma} \\ \sigma &= \bar{\omega} \vec{r}, \quad \bar{\omega}^2 = 0,05 1/a_0^2, \quad \bar{k}_1^2 = 0,82\end{aligned}\quad (20)$$

Выражение  $e_n(\sigma)$  приведенное выше получено из исходного  $e_n(\sigma)$  через формулы преобразования эллиптических функций. Фаза решения подобрана так, что особенность находится в начале координат.

Ниже рассмотрим в основном только второе решение.

Для графического представления функции (19) их лучше переписать в виде :

$$\begin{aligned}\varphi/\varphi_0 &= \Psi^2, \quad \Psi = -1,95 + e_n^2(\sigma), \quad \varphi_0 = 0,67 \tau_0^2 \\ \varrho/\varrho_0 &= \Phi^3, \quad \Phi = \Psi + 1,22 \quad \varrho_0 = 0,55 (\sigma_0 \tau_0^3)\end{aligned}\quad (21)$$

Как видим, оба решения имеют одни и те же  $\bar{\omega}$ ,  $k_1$  и, следовательно, одни и те же периоды  $\Omega$  и длина кристаллической решетки, которая в данном случае определяется по формуле :

$$L_x = L_y = L_z = \frac{\Omega}{\sqrt{3} \bar{\omega}} \simeq 24 a_0 \quad (22)$$

Для последовательного решения вопроса о работе выхода следовало бы решить уравнение Шредингера с найденным выше потенциалом. Однако ввиду трудности получения такого решения можно ограничиться приближенным представлением работы выхода по формуле [5]  $W \simeq \varphi_{\text{ср.д.}}$  или, что удобнее в данном случае, и кроме того ближе к действительности [1] в виде :\*

$$W \simeq \varphi_{\min} \quad (23)$$

тогда учитывая  $e_n^2(\sigma)/\min = 0$  находим :

$$W \simeq \varphi_{\min} = 0,67 \tau_0^2 (1,95)^2 \simeq 1,13 \text{ eV} \quad (24)$$

Из графика № 1, где представлены функции (21), видим, что условие  $\varrho > 0$  не выполняется везде. Атомы как бы являются изолированными друг от друга. Указанное обстоятельство и подсказывает необходимость дополнения плотности постоянным членом обеспечивающим требование :  $\varrho > 0$  везде.

Рассмотрим теперь случай  $\lambda_3 \neq 0$  ( $s \neq 1$ ), тогда, ограничиваясь значениями  $\lambda_1 > 0$ ,  $\lambda_2 > 0$ , условие  $\varrho_{\min} > 0$  дает :

$$4 \pi \varphi_{\min} = \bar{a} s (a \gamma)^3 = \bar{a} \bar{\tau}_0^3 \left( \frac{s^{1/3}}{1 - 5 s \gamma^2} \right)^3 > 0 \quad (25)$$

значение  $s < 0$  отпадает (т. к.  $\gamma^2 > 0$ ) и, учитывая (15), находим :

$$0 \leq s \leq 0,60 \quad (26)$$

Значения параметров решения уравнения (1) соответствующих изменению  $s$  в интервале (26) приведены в таблице № 1.

Как видно из таблицы решения имеют тот же вид, что и в случае  $\lambda_3 = 0$   $\lambda_2 = \lambda_1 = 1$  но для других значений параметров  $\bar{k}_1, \bar{\omega}, \alpha, \beta$

Особо следует указать на то обстоятельство, что свободные параметры  $\lambda_1, \lambda_2$  входят только в масштаб для  $L_x, \varphi, \varrho$  и, следовательно, простым изменением масштаба можем согласовать их значения с экспериментом.

Действительно, зависимость  $L_x, \varphi, \varrho$  от  $\lambda_1, \lambda_2$  имеет вид :

$$L_x = L_x^* \frac{1}{\sqrt{\lambda_1 \lambda_2}}, \quad \varphi = \varphi^* \lambda_2^2, \quad \varrho = \varrho^* s \cdot \lambda_1 \lambda_2 \cdot \lambda_2^2 \quad (27)$$

где теперь  $L_x^*, \varphi^*, \varrho^*$  уже не содержат  $\lambda_1, \lambda_2, s$ . Если заданы экспериментальные значения  $L_x^{\text{эксп}}, \varphi_{\min}^{\text{эксп}}, \varrho_{\min}^{\text{эксп}}$  то  $\lambda_1, \lambda_2, s$  можем определить из уравнений :

\* Указанное приближение относится к приближенному заданию экспериментального значения  $\varphi_{\min}$ , а не математическую сторону вопроса.

$$L_x^* \frac{1}{\sqrt{\lambda_1 \lambda_2}} = L_x^{\text{эксп}}, \quad \varphi_{\min}^* \lambda_2^2 = \varphi_{\min}^{\text{эксп}} \quad (27)$$

$$\varrho_{\min}^* \cdot s \cdot \lambda_1 \lambda_2 \cdot \lambda_2^2 = \varrho_{\min}^{\text{эксп}} \quad (28)$$

Действительно, исключая  $\lambda_1$ ,  $\lambda_2$  из первых двух уравнений (28) находим

$$\left( \frac{L_x^2 \varrho_{\min}^*}{\varphi_{\min}^*} \right)_{\text{эксп}} = \left[ \left( \frac{L_x \varrho_{\min}^*}{\varphi_{\min}^*} \right) s \right]_{\text{Таблиц.}} \quad (29)$$

Уравнение (29) определяет значение  $s$  (см. таблицу № 1) и, следовательно,  $L_x^*$ ,  $\varphi_{\min}^*$ ,  $\varrho_{\min}^*$ . Далее, используя полученные значения  $L_x^*$ ,  $\varphi_{\min}^*$  из первых двух уравнений (28), находим  $\lambda_1$ ,  $\lambda_2$ .

В качестве примера рассмотрим натрий Na и калий K.

Как известно Na и K имеют гранецентрированные кубические решетки, и они ближе всех к простой кубической решетке (так же как и другие щелочные металлы).

Имеем в случае\*\* Na

$$L_x^{\text{эксп}} = 8,36 a_0, \quad \varphi_{\min}^{\text{эксп}} \cong W = 1,80 \text{ eV}, \quad \varrho_{\min}^{\text{эксп}} \cong \varrho_{\text{сред}}^{\text{эксп}} = 2,4 \cdot 10^{22} * \quad (30)$$

Тогда

$$\left( \frac{L_x^2 \varrho_{\min}}{\varphi_{\min}} \right)_{\text{экспер}} = 0,94 \cdot 10^{24} \quad (31)$$

из таблицы № 1 находим:

$$x = 0,55, \quad L_x^* = 7,184 a_0, \quad \varphi_{\min}^* = 2,53 \text{ eV} \quad (32)$$

$$s = 0,41 \quad \varrho_0^* = s \varrho_{\min}^* = 4,56 \cdot 10^{22}$$

Из уравнений

$$8,36 = 7,184 \frac{1}{\sqrt{\lambda_1 \lambda_2}}, \quad 1,80 = 2,53 \cdot \lambda_2^2 \quad (33)$$

получаем:

$$\lambda_1 = 0,95, \quad \lambda_2 = 0,85 \quad (34)$$

$\lambda_3$  и  $\varrho'$  определяются из уравнения (13)

$$\lambda_3 = \bar{a}' [(s-1) \tau_0^3 \lambda_2^3 (a' \gamma)^3] = \frac{s-1}{s} \lambda_1 \lambda_2^3 4\pi \cdot \varrho_0^* = -3,96 (a' \tau_0)^3 \quad (35)$$

\* Задание  $\varrho_{\min}^{\text{эксп}}$  эквивалентно нормировке искомой функции. В данном случае  $\varrho_{\min}^{\text{эксп}} \cong \varrho_{\text{сред}}^{\text{эксп}}$  равносильно приближенной нормировке решения.

\*\* Численные данные взяты из [1]; они расходятся с более поздними данными. Поэтому примеры носят только иллюстративный характер.

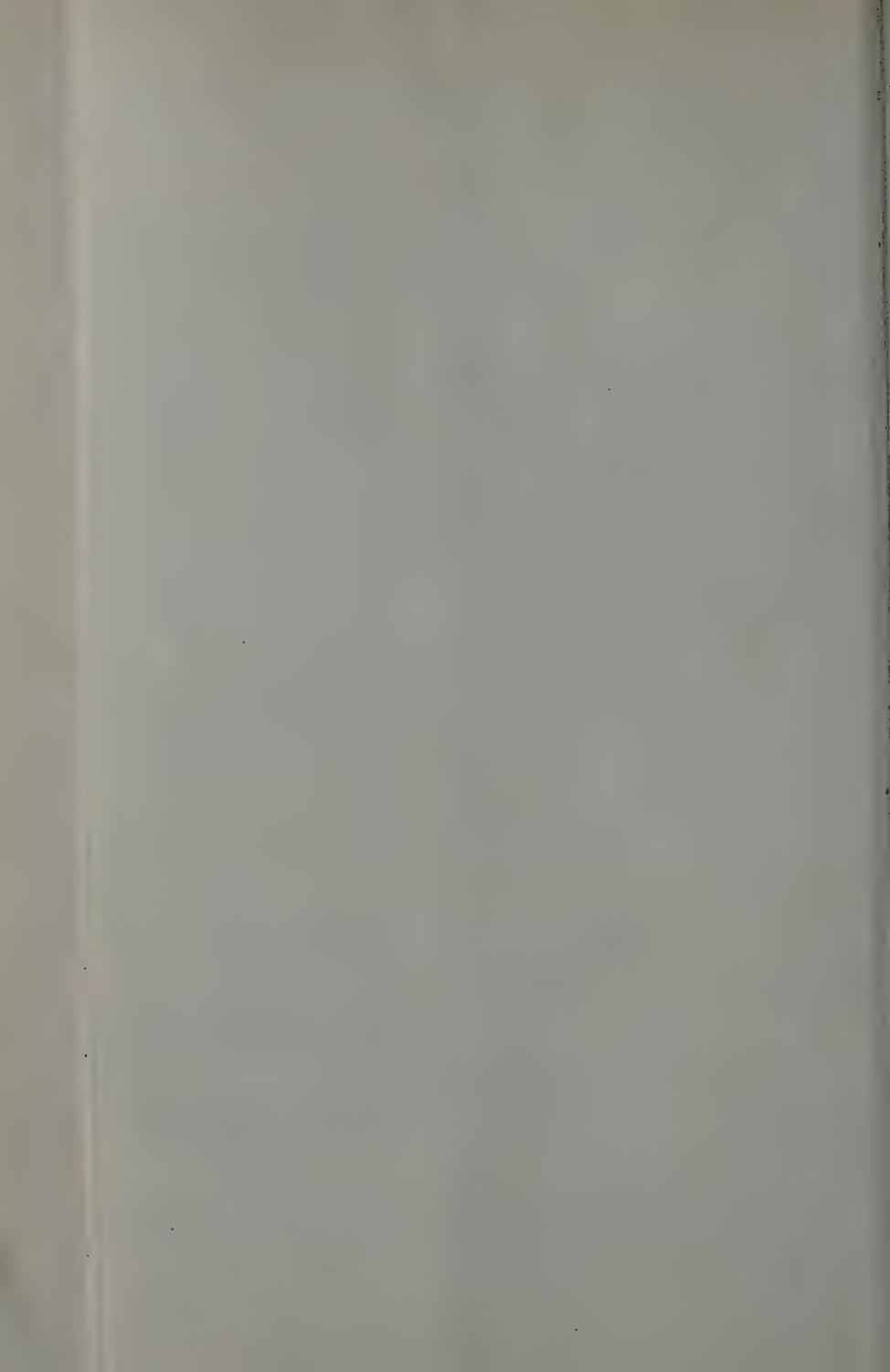
Таб. № 1.

$x =$	$s =$	$\gamma \pm$	$\beta \pm$	$\alpha' \pm$	$k_1^2 = +$	$k_2^2 = +$	$k_1^2 = -$ $k_2^2 = -$	$\frac{\omega_1 - \omega_2}{a_0} \omega$ $\lambda_1 \lambda_2$	$\frac{a_0^2}{\lambda_1 \lambda_2} \dots \frac{a_0^2}{\lambda_1 \lambda_2}$	$a_0 L_z$	$v_{\min} = (a' \beta)^2$ $\times 1,7 \text{ eV}$	$\frac{a_0^2}{\lambda_1 \lambda_2} = s (a' \gamma)^2$ $\times (10^{12} \text{ cm}^{-2})$	$\left( \frac{L_z \rho_0^*}{v_{\min}} \right) \cdot 10^{-2}$ Таб	$(a' \gamma)^2$	$x$	
1	0,600	0,5773	0,5763	974,8	1,108	14,96	0,066	59,0	54,583	3,909	0,476	53650,46	—	—	1782178188,9	1
0,98	0,5939	0,5745	0,5616	77,49	1,108	14,98	0,066	4,70	4,399	0,310	1,167	3218,97	52372,187	2,16	83180,541	1,98
0,95	0,5845	0,5699	0,5375	34,25	1,108	15,04	0,066	2,05	1,928	0,136	2,545	576,203	4346,608	1,96	7436,583	0,95
0,90	0,5679	0,5630	0,5069	17,52	1,108	14,87	0,066	1,06	0,980	0,070	3,590	134,045	544,389	5,23	958,6	0,90
0,85	0,5502	0,5559	0,4731	12,11	1,108	14,79	0,066	0,73	0,677	0,049	4,273	55,8076	167,414	5,44	304,3	0,85
0,80	0,5312	0,5486	0,4396	9,135	1,108	14,73	0,066	0,55	0,511	0,037	4,933	27,404	66,506	5,92	125,20	0,80
0,75	0,5109	0,5418	0,4067	7,403	1,108	14,89	0,066	0,46	0,414	0,031	5,442	15,402	32,725	6,24	64,05	0,75
0,70	0,4893	0,5343	0,3726	6,184	1,108	14,52	0,066	0,37	0,335	0,025	6,065	9,027	17,585	7,04	35,14	0,70
0,65	0,4662	0,5280	0,3431	5,405	1,108	14,51	0,066	0,33	0,309	0,022	6,38	5,450	10,965	7,60	23,25	0,65
0,60	0,4416	0,5215	0,3113	4,776		13,77	0,070	0,29	0,266	0,021	6,852	3,751	6,8183	8,53	15,44	0,60
0,55	0,4154	0,5148	0,2825	4,317		14,22	0,070	0,26	0,241	0,018	7,184	2,530	4,565	9,36	10,94	0,55
0,50	0,3875	0,5119	0,2800	3,968		14,52	0,070	0,24	0,222	0,0164	7,475	1,802	3,243	10,00	8,37	0,50
0,40	0,3264	0,4960	0,1991	3,367	1,109	13,83	0,072	0,20	0,187	0,0150	8,132	0,770	1,518	13,00	4,65	0,40
0,30	0,2577	0,4817	0,1443	2,971	1,109	13,25	0,075	0,18	0,165	0,0134	8,809	0,311	0,755	18,80	2,93	0,30
0,20	0,1808	0,4701	0,0938	2,663	1,109	13,01	0,077	0,16	0,147	0,0123	9,250	0,106	0,354	28,40	1,956	0,20
0,10	0,0951	0,4583	0,0457	2,430	1,109	12,67	0,079	0,145	0,134	0,0115	9,737	0,00187	0,130	66,40	—	0,10
0,01	—	—	—	—	—	—	—	—	—	—	—	—	—	—	1,37	0,01
0	0	0,4472	0	2,236	1,109	12,46	0,081	0,135	0,123	0,0108	10	0	0	—	1	0

$$\alpha = \bar{\tau}^0 \alpha', \quad \tau_0^2 = 1/4 (e/a_0) \simeq 1,7 \text{ eV}, \quad \varrho_0^* = \varrho_{\min} (\lambda_1 = \lambda_2 = 1)$$

Формулы преобразования.

$$\begin{aligned}
 1) \omega^2 = \omega_2^2 > 0, \quad k^2 = k_2^2 > 1 \quad e_n(\omega_2, k_2) &= \text{cn}(\omega_2, k_2) + i \text{sn}(\omega_2, k_2) = \text{dn}(\bar{\omega}_2, \bar{k}_2) + i \bar{k}_2 \text{sn}(\omega_2, \bar{k}_2) \quad \bar{\omega}_2 = k_2 \omega_2, \quad \bar{k}_2 = 1/k_2 \\
 2) \omega^2 = \omega_1^2 < 0, \quad k^2 = k_1^2 > 1 \\
 e_n(\omega_1, k_1) &= \text{cn}(\omega_2, k_1) + i \text{sn}(\omega_2, k_1) = \text{cn}(i \omega_1', k_1) + i \text{sn}(i \omega_1', k_1) = \text{dn}(i \omega_1' k_1, 1/k_1) + i 1/k_1 \text{sn}(i \omega_1' k_1, 1/k_1) = \\
 &= \frac{d(k_1 \omega_1', \sqrt{1-1/k_1^2}) + i(1/k_1) \text{sn}(k_1 \omega_2', \sqrt{1-1/k_1^2})}{\text{cn}(k_2 \omega_2', \sqrt{1-1/k_1^2})} = \frac{\text{dn}(\bar{\omega}_1, k_1) - \bar{k}_1' \text{sn}(\bar{\omega}_2, \bar{k}_1')}{\text{cn}(\bar{\omega}_1, \bar{k}_1')} \quad \bar{\omega}_1 = \bar{\omega} = k_1 \omega_2', \quad \bar{k}_1' = \sqrt{1-1/k_1^2}, \quad \bar{k}_2' = 1/k_1, \quad \omega_1' = i \omega_1' \\
 e_n(\sigma + c)/c = K + e_n(\sigma + K) &= \frac{\text{dn}(\sigma + K) - \bar{k}_1' \text{sn}(\sigma + K)}{\text{cn}(\sigma + K)} = \frac{\bar{k}_1' 1/\text{dn} \sigma - \bar{k}_1' \text{en} \sigma / \text{dn} \sigma}{- \bar{k}_1' \text{sn} \sigma / \text{dn} \sigma} = - \frac{1 - \text{cn} \sigma}{\text{dn} \sigma}
 \end{aligned}$$





$$\varrho' = \lambda_3/4 \pi = -3,96 (\sigma_0^1 \tau_0^3) \simeq -3,96 \cdot 10^{22}$$

Обобщенное уравнение (ТФД) примет вид:

$$\Delta \varphi = a' \{0,95 [\varphi^{1/2} + 0,85 \tau]^3 - 3,96 \tau_0^3\} \quad (36)$$

а периодическое решение данного уравнения будет:

$$\varphi = a^2 (\beta + e_n^2(\sigma))^2 = 13,55 \tau_0^2 \left[ 0,283 + \left( \frac{1 + \operatorname{cn} \sigma}{\operatorname{sn} \sigma} \right)^2 \right]^2 \quad (37)$$

$$\varrho/\varrho_0 = (\gamma + e_n^2(\sigma))^3 + (s-1)\gamma^3 = (0,51 + e_n^2(\sigma))^3 - 0,08$$

$$\varrho_0 = (\sigma_0 \tau_0^3) \lambda_1 \lambda_2^3 \cdot a'^3 = 49,8 \cdot 10^{22}$$

где

$$\sigma = \vec{\omega} \vec{r}, \quad \vec{\omega}^2 = 0,26 \cdot 0,808 \cdot 1/\epsilon_0^2 = 0,021 \frac{1}{\epsilon_0^2} \quad (38)$$

$$\vec{k}_1^2 = 0,066$$

Решение имеет период  $\Omega = 4K = 6,40$  длина периода  $L_x = 8,3a_0$  минимальный потенциал Ферми и минимальная плотность  $\varphi_{\min} = 1,8 \text{ eV}$ ,  $\varrho_{\min} = 2,4 \cdot 10^{22}$  соответственно.

Аналогично в случае К имеем

$$L_x^{\text{эксп}} = 10,3 a_0, \quad \varphi_{\min}^{\text{эксп}} \simeq W = 1,60 \text{ eV}, \quad \varrho_{\min}^{\text{эксп}} = 1,3 \cdot 10^{22} \quad (39)$$

$$\left( \frac{L_x^2 \varrho_{\min}}{\varphi_{\min}^{\text{эксп}}} \right) = 0,85 \cdot 10^{24}$$

из таблицы № 1 находим:

$$x = 0,60, \quad s = 0,44, \quad L_x^1 = 6,85 a_0, \quad \varphi_{\min}^* = 3,75 \text{ eV} \quad (40)$$

$$\varrho_0^* = s \varrho_{\min}^* = 6,82 \cdot 10^{22} \text{ cm}^{-3}$$

Из уравнения

$$10,30 = \frac{6,85}{\sqrt{\lambda_1 \lambda_2}}, \quad 1,60 = 3,75 \cdot \lambda_2^2 \quad (41)$$

получаем:

$$\lambda_1 = 0,65 \quad \lambda_2 = 0,65 \quad (42)$$

Следовательно

$$\lambda_3 = \frac{s-1}{s} \lambda_1 \lambda_2^3 4 \pi \cdot \varrho_0^* = -1,49 (a' \tau_0^3) \quad (43)$$

$$\varrho = \lambda_3/4 \pi = -1,49 (\sigma_0 \tau_0^3) = -1,49 \cdot 10^{22} \text{ cm}^{-3}$$

а обобщенное уравнение примет вид:

$$\Delta \varphi = a' \{0,65 [\varphi^{1/2} + 0,65 \tau_0]^3 - 1,49 \tau_0^3\} \quad (44)$$

и периодическое решение данного уравнения будет:

$$\varphi = 9,79 \tau_0^2 \left\{ 0,31 + \left( \frac{1 + \operatorname{cn} \sigma}{\operatorname{sn} \sigma} \right)^2 \right\} \quad (45)$$

$$\begin{aligned} \varrho/\varrho_0 &= (0,52 + e_n^2(\sigma))^3 - 0,07 \\ \varrho_0 &= 19,4 \cdot 10^{22} \end{aligned} \quad (46)$$

$$\sigma = \bar{\omega} \bar{r}, \quad \bar{\omega}^2 = 0,124, \quad 1/a_0^2, \quad \bar{k}_1^2 = 0,07$$

$$L_x \simeq 10,3 a_0, \quad \varphi_{\min} \simeq 1,6 \text{ eV}, \quad \varrho_{\min} \simeq 1,3 \cdot 10^{22} \text{ cm}^{-3}$$

$$\Omega = 6,40$$

Достоен внимания и тот не тривиальный результат, что согласно таблицы № 1 при увеличении длины кристаллической решетки работа выхода (точнее  $\varphi_{\min}$ ) уменьшается. Указанная закономерность действительно наблюдается у щелочных металлов.

Тот факт, что уравнение (ТФД) имеет два независимых периодических решения при одних и тех же значениях параметров, один из которых с особенностью, а второе без особенности на наш взгляд заслуживает особого внимания.

Для большей наглядности характера полученных решений, можно использовать малость главного модуля эллиптических функций  $\bar{k}_1^2 = 0,07$  и в решениях заменить эллиптические функции тригонометрическими, при этом погрешности будут порядка  $k_1^2$  и следовательно, малы.

## ЛИТЕРАТУРА

1. Бете и Зомерфельд, «Электронная теория металлов».
2. I. E. LENARD—JONES, H. I. Woods Proc. Roy. Soc. Lond. 120 727. 1928.
3. П. Гомбаш «Статистическая теория атома».
4. R. D. COWAN, I. ASHKIN Phys. Rev. 1957. 105 144.
5. И. ТАММ, D. BLOCHINZEV, Zs. f. Phys. 77 774. 1932.

## PHENOMENOLOGICAL GENERALIZATION OF THE THOMAS-FERMI-DIRAC (TFD) EQUATION IN CASE OF THE THEORY OF METALS AND ITS PERIODIC SOLUTIONS

By

D. F. KURDGELAIDZE

### Summary

The exchange interaction between metal atoms is taken into account phenomenologically by writing the TFD equation in the form:  $\Delta\varphi = \bar{a}(\varphi^{1/2} + \tau_0)^3 + \lambda_3$ . Here  $\bar{a}\varrho\tau_0$  and  $\lambda_3$  are treated as *free parameters* to be adjusted to the following properties of the metal: lattice constant, work function or minimal Fermi-potential and average or boundary density of conducting electrons. The equation possesses periodic solutions and the properties of the latter are discussed. As an illustrative example, the case of sodium is investigated in detail.

# ON THE CRYSTAL STRUCTURE OF $\text{AlCl}_3$

By

K. SASVÁRI

CENTRAL CHEMICAL RESEARCH INSTITUTE OF THE HUNGARIAN ACADEMY OF SCIENCES, BUDAPEST

(Presented by Z. Gyulay — Received: XII. 18. 1957)

The crystal lattice of  $\text{AlCl}_3$  has been derived on the basis of crystal-geometrical considerations starting from the dimension of the unit cell and from the fact that in the crystal lattice, according to the electric conductivity measurement of BILTZ and VOIGT, there should be ionic bonds. The crystal lattice derived in this way proved to be the same as that given by KETELAAR and his collaborators in 1947. Therefore the statement seems to be justified that there cannot be  $\text{Al}_2\text{Cl}_6$  molecules in the solid phase of  $\text{AlCl}_3$ , as has been suggested by GERDING and SMIT on the basis of investigations of Raman spectra. In the lattice a graphic picture is given for the mechanism of transition of the crystal lattice to the  $\text{Al}_2\text{Cl}_6$  molecules of the liquid or vapour phase, and also for the mechanism of transition in the reversed direction.

KETELAAR [1] in 1935 was the first to determine the crystal structure of  $\text{AlCl}_3$ . In this the cubic close-packed arrangement of the Cl atoms proved later to be correct. The hexagonal cell assignable in the anion frame is

$$\begin{aligned}a_H &= 5,92 \text{ \AA}, \\c_H &= 18,22 \text{ \AA}.\end{aligned}\tag{1}$$

The Al ions are placed in the holes of the given frame so that a monoclinic symmetry should take place. The axis  $c$  of the monoclinic unit cell is one third of the smaller body diagonal of the hexagonal cell, therefore data of this are

$$\begin{aligned}a &= 5,92 \text{ \AA}, \\b &= 10,22 \text{ \AA}, \beta = 180^\circ - \arctg \left( \frac{c_H}{a_H} \right) = 108^\circ, \\c &= 6,16 \text{ \AA}.\end{aligned}\tag{2}$$

KETELAAR placed the Al ions originally in pairs into each octahedron, in which case the distance between such two Al ions would be 0,64 Å. Such a close arrangement of the Al ions is entirely impossible this, however, cannot be discovered in the X-ray diagram, since the scattering of the Al ions makes only a small contribution to the intensity of the reflexions.

In the first structure given by KETELAAR  $\text{Al}_2\text{Cl}_6$  molecules were present. PALMER and ELLIOT [2] showed by the electron diffraction method, that in the saturated steam of  $\text{AlCl}_3$  such molecules are present which consist struc-

turally of two  $\text{AlCl}_4$  tetrahedra with a common edge. GERDING and SMIT [3] also give an account of the existence of  $\text{Al}_2\text{Cl}_6$  molecules on the basis of Raman-spectroscopical investigations carried out with liquid and solid  $\text{AlCl}_3$ .

KETELAAR and coworkers [4] in 1947 have shown that the measured intensities of the X-ray reflexions can be approached much better by calculation if, in place of the tetrahedral molecule arrangement, the Al ions are placed in individual octahedral cavities. They abandoned existence of the  $\text{Al}_2\text{Cl}_6$  molecule in the solid phase and attained the layer lattice given by them recently which is in contradiction to the statement of GERDING and SMIT. Partly, however, owing to the better agreement of the intensities and partly because of the fact that the Raman spectra obtained in solid and liquid phase do not agree as well as those obtained in the case of  $\text{AlBr}_3$  and  $\text{AlI}_3$  (GERDING and SMIT) the conclusion may be drawn that the existence of  $\text{Al}_2\text{Cl}_6$  molecules in the solid state may not be considered as established. Therefore KETELAAR's newest structure must be taken as correct.

In the present paper the author wants to show that the structure, given recently by KETELAAR, can be attained on the basis of the close packing in the ionic crystals, which has been treated elsewhere [5, 6].

Let us start from the data of the unit cell, considering that the conductivity measurements of BILTZ and VOIGT [7] indicate the presence of an ionic bond in the crystal.

From the data of the unit cell the volume  $v_{\text{Cl}} = 29,7 \text{ \AA}^3$  for one Cl ion is essentially smaller than that of Cl ions with radii of  $1,81 \text{ \AA}$  in closest packing ( $35,5 \text{ \AA}$ ). KETELAAR therefore was led to the statement that the structure is based on the closest packing of the Cl ions.

In a regular close-packed anionic plane the two axes of the assignable orthorhombic cell are

$$\begin{aligned} a &= a' \cdot \sqrt{3}, \\ b &= 3 \cdot a', \end{aligned}$$

if  $a'$  is the distance between two adjacent ions. If these two axes are identified with those of the monoclinic cell  $a$  and  $b$  given by KETELAAR [2] we obtain from both equations similarly

$$a' = 3,42 \text{ \AA}. \quad (3)$$

This does evidently mean that in the anionic planes the Cl ions are arranged regularly but are closer to each other than the distance ( $3,62 \text{ \AA}$ ) calculated from the ionic radius of the Cl ion.

The cations are placed in the spatial cavities of the close-packed anionic frame in such an arrangement that the monoclinic symmetry should be obtained.

For the tetrahedral cavities of a regular close-packed anionic frame

$$r_A + r_X = a' \sqrt{\frac{3}{8}} = 2,22 \text{ \AA}, \quad (4)$$

if  $a' = 3,62 \text{ \AA}$ . This is small compared with  $r_{\text{Cl}} + r_{\text{Al}} = 1,81 + 0,57 = 2,38 \text{ \AA}$ , thus the lattice has to be extended if the Al ions should find room in the tetrahedral cavities. On the other hand, however, the lattice is contracted according to the value  $a' = 3,42 \text{ \AA}$ . This is the reason why the tetrahedral arrangement of the Al ions has to be rejected.

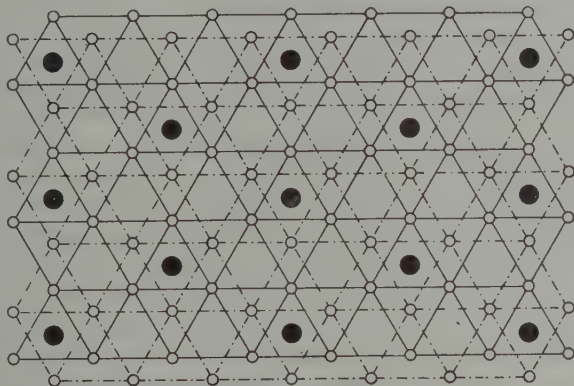


Fig. 1. Hexagonal close-packed anion frame perpendicular to the close-packed planes. One third of the octahedral cavities are filled with Al ions and build columns perpendicular to the planes

We can assume that the Al ions occupy octahedral cavities. The number of the octahedral cavities in the close-packed anionic frame is here thrice the number of the Al ions. If we want to place the Al ions in these, considering Pauling's coordination principle, then every corner of the octahedra filled by Al ions has to be common with another octahedron.

Assuming a hexagonal close packing of the anions, a realization of this could be obtained in such a way that a third of the octahedral columns with common sides are filled up by Al ions (Fig. 1). This cation distribution is unrealizable because the identity in the direction  $c$  would then be a sixth of the value found. Since, however, the identity  $c$  is equal to the distance of seven successive close-packed anionic planes we must reject the possibility of a hexagonal close packing of anions. There remains for the anions the possibility of a cubic close packing. In this the octahedra are connected to each other only by edges or corners and Pauling's coordination principle can only be satisfied when  $2/3$  of the octahedral cavities within the plane intervals are

filled up by Al ions. In this way only every second plane interval can be occupied by Al ions and in the direction of the axis  $c_H$  merely every fourth of these occupied layers will be identical with the first which is just in accordance with the identity measured in the direction  $c_H$ .

Accordingly, the  $\text{AlCl}_3$  can only be a layer lattice with layers known in  $\text{CrCl}_3$  and  $\text{Al}(\text{OH})_3$ . All subsequent layers can be only geometrically identical, but considering their relative position, two different cases can be distinguished.

Placing the cation arrangement, as above described, in every second plane interval of the cubic close-packed anion frame layers are obtained between which every two adjacent layers can be transferred into each other by a parallel displacement. This displacement of the given cationic arrangement, is always parallel to the smaller body diagonal of one of the hexagonal unit cells, which can be set up in the cubic close-packed anionic frame. As this hexagonal unit cell can be chosen in three different ways, differing by  $120^\circ$ , the position of the adjacent layers can also be of three different kinds. The cationic arrangement of the subsequent layers within a crystal lattice can be selected so that either each of the three directions of the displacement is playing a part or, throughout the whole lattice the neighbouring layers are transferred one into the other by a shift in the identical direction. By these two possibilities two different crystal lattices can be obtained.

Carrying on in the cubic close-packed anionic frame the cationic arrangement of a starting layer in the subsequent layers so that each of the three kinds of displacements takes place in some order, the subsequent layers, dependent upon the order of the displacement, can be transferred into each other by a right- or left-handed threefold screw axis ( $3_1$  or  $3_2$ ). Fig. 2 represents schematically the sequence of layers. The cation distribution of layers is easily recognizable on the right in the Fig. Here the horizontal lines signify the close-packed anionic planes in a projection parallel to the layers — the three different positions of the close-packed anionic planes succeeding each other in the manner of cubic close-packing are represented by three different notations — the circles show the notation of the three cation distributions following one another between the anionic plane-pairs. In Fig. 2 the basis of the three different hexagonal cells is marked and the numbered arrows signify the projection perpendicularly to the layers, of the threefold sliding direction. The order of slidings is given by the numbers beside the arrows. The displacements of the starting layer given here result in a crystal lattice of hexagonal symmetry the unit cell of which is identical with that mentioned above. This case is found in the structure of  $\text{CrCl}_3$ .

If the subsequent layers are shifted into each other throughout the whole crystal lattice, always in one direction (Fig. 3), and it is taken into consideration that the mentioned displacement of the cationic arrangement



leads always to an anionic environment identical with the former, then  $1/3$  of the body diagonal of the hexagonal cell — the length of one displacement —

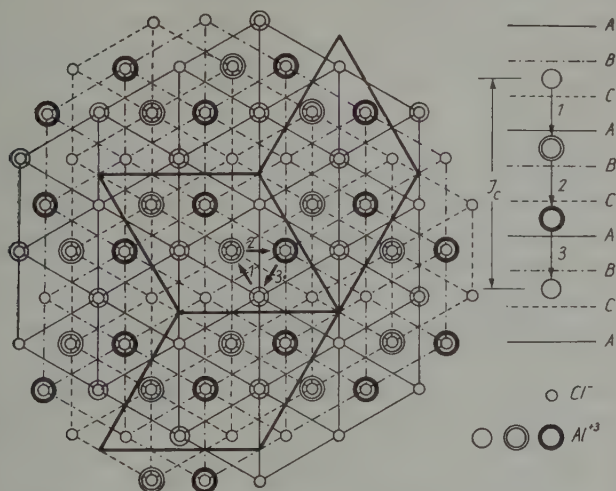


Fig. 2. Ionic arrangement of  $\text{CrCl}_3$ . The right side of Fig. 2 shows the sequence of the anion planes and cation arrangement

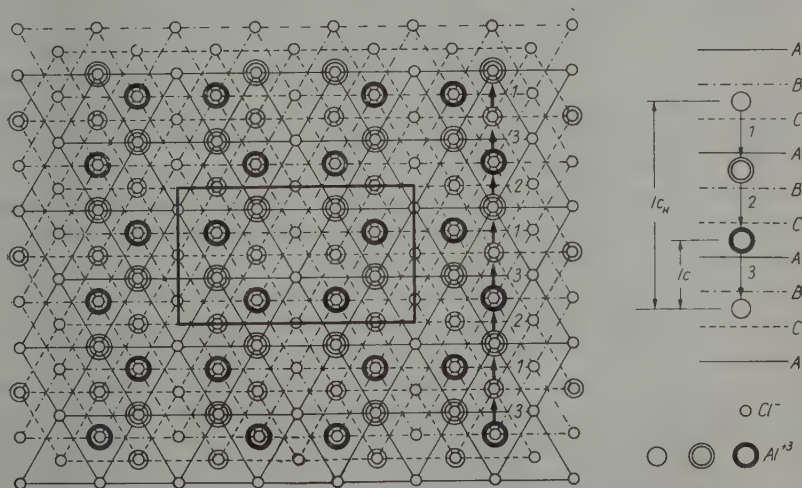


Fig. 3. Ionic arrangement of  $\text{AlCl}_3$  perpendicular to the close-packed anion planes. The right side of Fig. 3 shows the sequence of the anion planes and cation arrangement

is the identity. This will be the real axis  $c$  of the unit cell and instead of the hexagonal cell we attain a monoclinic cell. This is the case with  $\text{AlCl}_3$ .

The dimension of the unit cell and the ion coordinates in the lattice deduced in such a way can only be given approximately. Exact numerical values of the coordinates have to be determined from reflexion intensities, but this causes no essential change in the lattice structure.

Mere geometrical considerations lead therefore to the structure of  $\text{AlCl}_3$  which -- as has been mentioned -- has recently been determined by KETELAAR [1] on the basis of X-ray diffractions. Accordingly,  $\text{Al}_2\text{Cl}_6$  molecules do not exist in the solid phase and this is the reason why it has not been possible to give a convincing proof of the existence of molecules in the solid phase even by Raman spectra [3].

We are able now to picture the mechanism of the  $\text{Al}_2\text{Cl}_6$  molecule formation which follows when the solid phase ceases to exist.

When by an increase of temperature solid  $\text{AlCl}_3$  melts, breakdown of the crystal lattice can be imagined in the following way: first the loose bonds between the layers are interrupted and afterwards the layers fall apart owing to a re-arrangement of the Al ions which takes place within the loosened layers from octahedral to tetrahedral cavities and so  $\text{Al}_2\text{Cl}_6$  molecules are formed. The mechanism of this re-arrangement of cations and the formation of molecules is shown in Fig. 4 in which one layer of the  $\text{AlCl}_3$  crystal lattice is represented schematically in the projection perpendicularly to the layer. The Al ions are shifted during the re-arrangement in the direction of the arrows into the adjacent tetrahedral cavities and the formation of  $\text{Al}_2\text{Cl}_6$  molecules given by PALMER and ELLIOT [2] occurs practically without a change of the position of the anions in the layer. The  $\text{Al}_2\text{Cl}_6$  molecules formed in the layers in this way are in the Fig. separated from each other by dotted lines. It may be imagined that the layers cease to exist only after the formation of the molecules, as soon as the bonding force between them ceases to exist.

From the fact that  $\text{AlCl}_3$  is easily sublimable and at a slow precipitation small crystal plates appear the conclusion may be drawn that some insignificant bonding force between the molecules must be present, and the layer only falls apart when the bonding energy is outbalanced by the heat motion. On the other hand, at precipitation with diminuation of the heat motion the small forces between the molecules are prevailing and the molecules will occupy their places beside each other corresponding to the former layers. And, by the inversion of the above mechanism the layers will be formed during the temperature decreasing when the Al ions are transferred again to octahedral cavities. This kind of layers placed one under another leads to macroscopic crystalline plates.

The mechanism given in Fig. 4 is a reversible one, which means that the mostly ionic bonding of the solid phase occurs prevalently in covalent bonds when during the increase of temperature  $\text{Al}_2\text{Cl}_6$  molecules are formed and, on the other hand, the prevalently ionic bond returns during the decrease

of temperature, when the Al ions occupy again the octahedral cavities. This phenomenon is only then comprehensible, if we assume that the interaction which Al and Cl atoms produce upon each other becomes apparent in the alteration of the electron configuration, but this effect changes with the influence of temperature so that the partial atomic bond turns into a poor

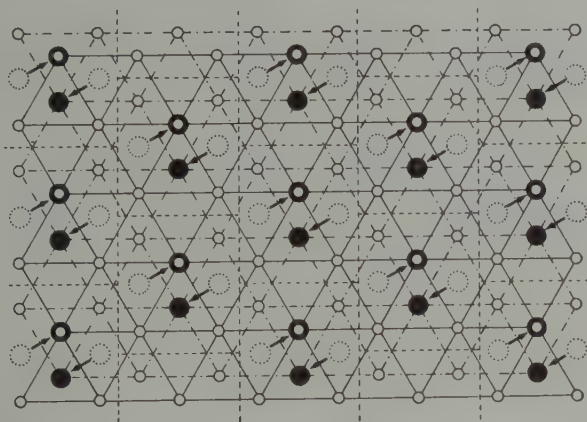


Fig. 4. A layer of the crystal lattice of  $\text{AlCl}_3$ . The dotted circles represent the cation arrangement in the crystal lattice; the circles in full line give the re-arranged cation distribution after building  $\text{Al}_2\text{Cl}_6$  molecules at the temperature of sublimation. The manner of cation re-arrangement is outlined by arrows

atomic bond and vice versa. Unfortunately we are not yet sure of the existence of such an effect, however, by lattice-structural considerations it becomes obvious that factors of this kind are playing a role in the formation of lattice geometry and its alteration.

#### REFERENCES

1. J. A. A. KETELAAR, *Z. Krist.*, **90**, 237, 1935.
2. K. J. PALMER and N. ELLIOT, *J. Amer. Chem. Soc.*, **60**, 1852, 1938.
3. H. GERDING and E. SMIT, *Z. phys. Chem.*, B, **50**, 171, 1941.
4. J. A. A. KETELAAR, C. H. MAC GILLAVRY and P. A. RENES, *Rec. trav. chim.*, **66**, 501, 1947.
5. K. SASVÁRI and A. ZALAI, *Acta Geol. Acad. Sci. Hung.*, **4**, 415, 1957.
6. K. SASVÁRI, *Acta Physica Hung.*, **8**, 245, 1957.
7. W. BILTZ and A. VOIGT, *Z. anorg. allg. Chem.*, **126**, 39, 1923.

О КРИСТАЛЛИЧЕСКОЙ СТРУКТУРЕ  $AlCl_3$ 

К. ШАШВАРИ

## Резюме

Решетка  $AlCl_3$  выведена на основе кристалло-геометрических соображений, исходя из размеров элементарной ячейки и из факта, что согласно измерениям электрической проводимости, произведенным Бильцем и Фойгтом, имеется и ионная связь. Решетка, выведенная этим способом, оказалась идентичной с выведенной Кетэллар и сотр. решеткой в 1947 году. Это, кажется подтверждает, что в твердой фазе  $AlCl_3$  нет молекул  $Al_2Cl_6$ , как предлагали Гердинг и Смит, на основе исследований спектров комбинационного рассеяния. Дана наглядная картина механизма перехода решетки в молекулы  $Al_2Cl_6$ , характеризующие жидкую и паровую фазы.

# ON THE STATISTICAL TREATMENT OF THE FERMION GAS I

By

P. SZÉPFALUSY

PHYSICAL INSTITUTE OF THE UNIVERSITY FOR TECHNICAL SCIENCES, BUDAPEST

(Presented by P. Gombás. — Received: I. 5. 1958)

A new statistical method, very similar to the one generalized to contain the Weizsäcker inhomogeneity correction modified by Gombás, is derived. With regard to the approximations introduced the summation over quantum states need not be approximated by integration but can be carried out exactly. In addition to the determination of the density from the variation principle more accurate methods are described. It is shown that from Plaskett's equation the density can only be determined within the classical „allowed zone” and the proper equation for the „forbidden zone” is given.

## 1. Introduction

For the interpretation of the bound state of systems consisting of particles with spin  $1/2$  the statistical method was first developed by THOMAS [1] and FERMI [2], who worked independently of each other. Later on the statistical method was improved in two main fields. On the one hand in order to calculate the energy due to the interaction of particles more accurately, the theory was generalized by DIRAC [3] to contain the exchange interaction and by GOMBÁS [4] to contain the correlation correction. These attempts, however, failed to eliminate the essential shortcomings of the density calculated on the basis of the Thomas-Fermi method. It is a common characteristic of all the investigations aiming at the correction of these defects that they are essentially independent of the interaction of the particles. In this connection I would like to refer to the papers of WEIZSÄCKER [5], GOMBÁS [6] and PLASKETT [7], which are the papers most closely related to the present one. It will be shown that the Weizsäcker inhomogeneity correction modified by GOMBÁS and the generalization of the Thomas-Fermi method suggested by PLASKETT can be traced back to a common basis further that the method described here can be regarded as an improved version of these methods.

In connection with the statistical energy expression obtained here it is suitable to make the following preliminary comment. In deriving the Thomas-Fermi statistical energy expression with the aid of the Wentzel-Kramers-Brillouin (WKB) method MARCH and PLASKETT [8] have shown that the statistical method involves two essential approximations as compared with the exact wave mechanical calculation. On the one hand it is based on the results

of the WKB method and on the other it approximates the summation over the quantum states by integration. To correct the latter error MARCH and PLASKETT apply the Euler-Maclaurin formula which makes a more accurate evaluation of the summation possible. In a former paper [9] we have shown that with a certain approximating assumption the summation over the quantum states can be carried out exactly. In the present paper this approximating assumption is necessarily involved thus the exact summation of the quantum states becomes possible.

We begin our investigation with wave mechanical considerations. Starting from the Schrödinger equation of  $n$  fermions we consider the form the one-particle state equations take if one-particle wave functions not orthogonal to each other are chosen. The equations thus obtained underlie the derivation of a new statistical model.

We now disregard the interaction of particles and restrict ourselves to the one-dimensional problem.

## 2. Non-orthogonal one-particle wave function system

The Schrödinger equation of  $n$  particles in the potential field  $V(x)$  is

$$\sum_{i=1}^n H(x_i) \Phi = \mathcal{E} \Phi, \quad (1)$$

where

$$H(x) = -\frac{\hbar^2}{2m} \frac{d^2}{dx^2} + V(x) \quad (1')$$

is the one-particle Hamiltonian.

Apart from the normalization constant a proper antisymmetrical solution of this equation is

$$\Phi = \begin{vmatrix} \varphi_1^0(x_1) \chi_-(\sigma_1) & \dots & \varphi_1^0(x_n) \chi_-(\sigma_n) \\ \varphi_1^0(x_1) \chi_-(\sigma_1) & \dots & \varphi_1^0(x_n) \chi_-(\sigma_n) \\ \dots & \dots & \dots \\ \dots & \dots & \dots \\ \varphi_f^0(x_1) \chi_+(\sigma_1) & \dots & \varphi_f^0(x_n) \chi_-(\sigma_n) \\ \varphi_f^0(x_1) \chi_-(\sigma_1) & \dots & \varphi_f^0(x_n) \chi_-(\sigma_n) \\ \dots & \dots & \dots \\ \varphi_g^0(x_1) \chi_+(\sigma_1) & \dots & \varphi_g^0(x_n) \chi_+(\sigma_n) \end{vmatrix}, \quad (2)$$

if the one-particle wave functions satisfy the equation



$$H \varphi^0(x) = \varphi^0(x) E. \quad (3)$$

Here  $\varphi^0(x)$  is the row vector formed from the wave functions  $\varphi_i^0(x)$

$$\varphi^0 = (\varphi_1^0, \varphi_2^0, \dots, \varphi_g^0), \quad (3')$$

$E$  is a diagonal matrix

$$E = \begin{bmatrix} E_1 & & & \\ & E_2 & & \\ & & \ddots & \\ & & & E_r \end{bmatrix}. \quad (3'')$$

The spin variable has been denoted by  $\sigma$  and the spin functions corresponding to the two possible spin states by  $\chi_+$  and  $\chi_-$  respectively.  $f$  and  $g$  are defined in the following manner

$$f = \frac{n - q}{2}, \quad g = \frac{n + q}{2},$$

where  $q = 0$  if  $n$  is even and  $q = 1$  if  $n$  is odd. If  $n$  is even  $f = g$  and the term with index  $g$  in wave function (2) should of course be omitted. The spin function of the  $g$ -th state may be either  $\chi_+$  or  $\chi_-$ , this being indicated by the index  $\pm$  of the spin function.

Substituting the wave function  $\Phi$  in (2) into equation (1) the energy eigenvalue of the system is

$$\mathcal{E} = 2 \sum_{i=1}^g E_i - q E_g. \quad (4)$$

The wave functions  $\varphi_i^0$  are orthogonal as they are the eigenfunctions belonging to various eigenvalues of the same operator. This is indicated by the index 0.

By direct substitution we find that equation (1) can also be satisfied by such a wave function

[illegible]

the elements of which satisfy the equation

$$H \varphi(x) = \varphi(x) \epsilon, \quad (6)$$

where

$$\varphi = (\varphi_1, \varphi_2, \dots, \varphi_g) \quad (6')$$

and

$$\epsilon = \begin{pmatrix} \epsilon_{11} & \dots & \epsilon_{1g} \\ \dots & \dots & \dots \\ \epsilon_{g1} & \dots & \epsilon_{gg} \end{pmatrix}. \quad (6'')$$

Equations (3), (3'), (3'') correspond to the special case of equations (6), (6'), (6'') where the matrix  $\epsilon$  is diagonal, i. e. the one-particle wave functions are orthogonal to one another.

The eigenvalue now is

$$\mathcal{E} = 2 \sum_{i=1}^g \epsilon_{ii} - q \epsilon_{gg}. \quad (4')$$

At the same time it is obvious that the wave functions (2) and (5) can differ but by a proportionality factor. From this follows that between the one-particle wave function systems  $\varphi^0$  and  $\varphi$  the following linear relation must exist

$$\begin{aligned} \varphi^0 &= \varphi C, \\ \varphi_i^0 &= \sum_{k=1}^g \varphi_k C_{ki}. \end{aligned}$$

As the components of both the vectors  $\varphi^0$  and  $\varphi$  are linearly independent,  $C$  cannot be singular, i. e. there also exists the inverse transformation

$$\begin{aligned} \varphi &= \varphi^0 C^0, \\ \varphi_i &= \sum_{k=1}^g \varphi_k^0 C_{ki}^0. \end{aligned} \quad (7)$$

$C^0$  denotes the reciprocal of the matrix  $C$ .

It is suitable to take the wave functions  $\varphi_i^0$  and  $\varphi_i$  as normalized to 1. Further, as is known, in the case of a bound state the wave functions  $\varphi_i^0$  and  $\varphi_i$  can be regarded as real without restricting the generality. Thus

$$\int \varphi_i^0 \varphi_k^0 dx = \delta_{ik}$$

and

$$\int \varphi_i^2 dx = 1.$$

Now equation (7) immediately gives

$$\sum_{k=1}^g C_{ki}^0 = 1$$

and

$$C_{ki}^0 = \int \varphi_k^0(x') \varphi_i(x') dx'.$$

Apply transformation (7) to equation (3):

$$H \varphi(x) = \varphi(x) C E C^0.$$

Comparing this equation with equation (6) we obtain:

$$\epsilon = C E C^0.$$

Using this transformation equation (6) takes the following form

$$(H + O_i) \varphi_i(x) = E_i \varphi_i(x). \quad (8)$$

$O_i$  may appear in the concrete form of e. g. an integral operator

$$O_i \varphi_i(x) = \int \sum_{k=1}^g (E_i - E_k) \varphi_k^0(x') \varphi_k^0(x) \varphi_i(x') dx',$$

or, what is essential for our considerations below, it can also be written in the form

$$O_i = \frac{1}{2m} (p_i^2 - \pi_i^2), \quad (9)$$

where  $p_i^2$  and  $\pi_i^2$  are the quantities defined by equations

$$-\hbar^2 \frac{d^2 \varphi_i^1(x)}{dx^2} = p_i^2(x) \varphi_i^1(x) \quad (9')$$

and

$$-\hbar^2 \frac{d^2 \varphi_i(x)}{dx^2} = \pi_i^2(x) \varphi_i(x) \quad (9'')$$

respectively.

Substituting the form (9) of  $O_i$  into equation (8) after rearrangement we may cancel by  $\varphi_i(x)$  and obtain for wave functions  $\varphi_i^0(x)$  the equation (3). Thus if  $O_i$  is expressed in the form (9) equation (8) is a trivial transformation of (3). However, as we shall see later, with some further conditions on the wave functions  $\varphi_k$   $(p_i^2 - \pi_i^2)/2m$  can be expressed in a semi-classical approximation by the wave functions  $\varphi_k$ , i. e. in such an approximation equations (8) and (9) can still be used for the determination of a non-orthogonal one-particle wave function system  $\varphi$ .

For the following we shall need the expression of the density. The density of the  $i$ -th particle is by definition

$$\nu(x) = \frac{\int \Phi(x_1, \dots, x_{i-1}, x, x_{i+1}, \dots, x_n)^2 dx_1 \dots dx_{i-1} dx_{i+1} \dots dx_n}{\int |\Phi|^2 dx_1 \dots dx_n}$$

and, as  $\Phi$  is antisymmetrical,  $\nu(x)$  is the same for any particle, the total density thus being

$$\varrho(x) = n \nu(x). \quad (10)$$

In the case of orthogonal one-particle wave functions the integration can readily be carried out and the following result is obtained

$$\varrho(x) = 2 \sum_{i=1}^g \varphi_i^{02}(x) - q \varphi_g^{02}(x). \quad (10')$$

To the energy expression (4) and the density expressions (10') the following meaning can be attributed. We may imagine the particles of the system to fill the one-particle states characterized by the wave functions  $\varphi_i^n$  and the energy eigenvalues  $E_i$  and the respective sums of the densities and energies of the particles thus distributed give the density and energy of the system. It must be emphasized that this is only to illustrate the situation as in reality the densities of the individual particles are identical and according to (10) they are equal to the  $n$ -th part of the total density.

Let us investigate the situation from this standpoint, in the case of non-orthogonal one-particle wave functions. The expression (10') of the density remains unchanged if

$$2 \sum_{i=1}^g \varphi_i^{02}(x) - q \varphi_g^{02}(x) = 2 \sum_{i=1}^g \varphi_i^2(x) - q \varphi_g^2(x).$$

Then, provided that  $n$  is even, the transformation the matrix of which is  $C$  or  $C^0$  is orthogonal. This means, however, that wave functions  $\varphi_i$  also form an orthonormalized system of functions which contradicts our assumption. If  $n$  is odd, but sufficiently large, the wave-functions  $\varphi_i$  become quasi-orthogonal, which is also incompatible with the following.

This problem can be solved if the wave functions satisfy the following conditions

a) the wave functions  $\varphi_i$  should be everywhere positiv nodeless wave-functions.

b) the densities  $\nu_i = \varphi_i^2$  should average the densities  $\nu_i^0 = \varphi_i^{02}$  as well as possible. (Thus e. g.  $\nu_1 = \nu_1^0$ ) Between the wave functions  $\varphi_i$  and  $\varphi_i^0$  the linear transformation (7) must exist. The matrix components of  $C^0$  should be chosen so that, in addition to satisfying condition a), the values of the

integrals of  $v_i$  and  $v_i^0$  agree for the subsequent intervals. (These intervals are first of all determined by the nodes of wave-function  $q_i^0$ . If  $i \rightarrow g$  limits for these intervals can also be designated between these nodes which are suitable to assume where the two neighbouring nodes are far from each other.)

Thus the function

$$N(x) = 2 \sum_{i=1}^g v_i - q v_g \quad (10'')$$

averages the density  $q$  well and in the following can also be regarded as a density. Thus, with regard to equation (8) the visualizing idea that the energy and the density of one-particle states can be regarded as the energy and density, respectively of the individual particles can be maintained in the case of the non-orthogonal one-particle wave function system  $q$ .

The necessity of condition *a*) will be shown below.

### 3. Semiclassical approximation

Consider what the semi-classical analogue of the expression (9) of  $O_i$  is. Applying the first approximation of the WKB method  $p_{i,2m}^2$  is the kinetic energy of the particle in the *i*-th state thus

$$2 \int_{x_1(E_i)}^{x_2(E_i)} p_i dx = (i - 1/2) h, \quad (11)$$

where

$$p_i = [2m(E_i - V(x))]^{1/2} \quad (11')$$

and  $x_1(E_i)$  and  $x_2(E_i)$  are the classical turning points.<sup>1</sup>

Introduce the notation

$$P_i = (p_i + p_{i+1})/2. \quad (12)$$

$P_i$  can be regarded as the maximum momentum of the particles occupying the quantum states of energy lower than that of the  $(i + 1)$ -th quantum state. The density of these particles be denoted by

$$N_i = 2 \sum_{k=1}^i v_k. \quad (12')$$

<sup>1</sup> Here  $E_i$  means the eigenvalue obtained in the WKB approximation, whereas in the preceding chapter  $E_i$  denoted the exact eigenvalue. In the following the exact eigenvalue as well as the eigenvalues obtained in the various approximations will be denoted by  $E_i$ . In the case where this might lead misunderstanding special reference will be made.

As a first approximation of the WKB method the well-known statistical relation can be derived:

$$P_i = \frac{h}{4} N_i. \quad (13)$$

We note that in a former paper [9] this relation was improved to distinguish between systems consisting of an even or odd number of particles. Thus for the  $g$ -th state:

$$P = \frac{h}{2n} N. \quad (13')$$

Here the notation  $P_g = P$  has been introduced. If  $n$  is even (13') goes over into (13). (Then  $N = Ng$ .)

$v_i$  can be written in the form

$$v_i = \frac{1}{2} (N_i - N_{i-1}) = \frac{2}{h} (P_i - P_{i-1}) \quad (14)$$

By relation (11')

$$p_{i+1}^2 - p_{i-1}^2 = 2m(E_{i+1} - E_{i-1}), \\ (i \geq 2)$$

based on which and using (12), (13) and (14) we obtain

$$v_i = \frac{m(E_{i+1} - E_{i-1})}{h} \frac{1}{p_i'}, \\ (i \geq 2) \quad (14')$$

where

$$p_i' = (p_{i+1} + p_{i-1})/2.$$

With this, according to equation (9'') taking the condition  $a)$  at the end of the previous chapter into account

$$\frac{1}{2m} \pi_i^2 = - \frac{\hbar^2}{2m} p_i'^{1/2} \frac{d^2 p_i'^{1/2}}{dx^2}, \\ (i \geq 2)$$

which in the region  $V < E_i$

$$O_i = \frac{1}{2m} p_i^2 + \frac{\hbar^2}{2m} p_i'^{1/2} \frac{d^2 p_i'^{1/2}}{dx^2}, \\ (i \geq 2) \quad (15)$$

$$O_1 \equiv 0, \text{ as } p_1^2 \equiv \pi_1^2.$$



To evaluate this let us consider the following.

MILNE [10] suggests the following way to determine the eigenvalues

$$2 \int_{-\infty}^{\infty} P'_i dx = i h, \quad (16)$$

where  $P'_i$  satisfies the following second order differential equation

$$\frac{1}{2m} P_i'^2 - \frac{\hbar^2}{2m} P_i'^{1/2} \frac{d^2 P_i'^{-1/2}}{dx^2} + V(x) = E_i. \quad (16')$$

The similarity between the equations of Milne's method and those of the WKB method is striking, an essential difference, however, is that MILNE's method is exact ( $E_i$  is the exact eigenvalue). Comparing equation (16') with (11') we see that in the WKB approximation, in which case the eigenvalues  $E_i$  in the equations (16') and (11') agree,  $p_i$  and  $P'_i$  must be related in the region  $V < E_i$  in the following manner

$$\frac{1}{2m} p_i^2 = \frac{1}{2m} P_i'^2 - \frac{\hbar^2}{2m} P_i'^{1/2} \frac{d^2 P_i'^{-1/2}}{dx^2}. \quad (17)$$

Assumption (16) makes very plausible that the function  $P'_i$  and the momentum  $P_i$  in (13) may be taken as approximately equal. This relation has been shown by Plaskett [7].

Assuming further that

$$P_i'^{1/2} \frac{d^2 P_i'^{-1/2}}{dx^2} = p_i'^{1/2} \frac{d^2 p_i'^{-1/2}}{dx^2} = p_i'^{1/2} \frac{d^2 p_i'^{-1/2}}{dx^2}, \quad (17')$$

we obtain from (17) and (15) that in the region  $V < E_i$

$$\begin{aligned} O_i &= \frac{1}{2m} P_i'^2 = \frac{\hbar^2}{32m} N_i^2, \\ (i \geq 2) \\ O_1 &\equiv 0 \end{aligned} \quad (15')$$

In the region  $V > E_i$   $O_i = 0$  as here the wave functions  $\varphi_i^0$  and  $\varphi_i$  can be taken as approximately equal by conditions *b*) of the previous chapter, since in this region the function  $\varphi_i^0$  has no node.

By substituting this form of  $O_i$  into equation (8) we obtain a system of equations from which the wave-functions  $\varphi_i$  and the eigenvalues  $E_i$  can actually be determined :

$$-\frac{\hbar^2}{2m} \frac{1}{v_i^{1/2}} \frac{d^2 v_i^{1/2}}{dx^2} + \frac{1}{2m} P_i^2 + V = E_i, (V < E_i), \quad (8')$$

$$-\frac{\hbar^2}{2m} \frac{1}{v_i^{1/2}} \frac{d^2 v_i^{1/2}}{dx^2} + V = E_i, (V > E_i), \quad (8'')$$

$$(i \geq 2)$$

$$-\frac{\hbar^2}{2m} \frac{1}{v_1^{1/2}} \frac{d^2 v_1^{1/2}}{dx^2} + V = E_1.$$

For the following the relation of equation (8') to PLASKETT's equation is essential. Substituting in equation (8') the approximation (14') of  $v_i$  valid for the region  $V < E_i$  and using (17')

$$-\frac{\hbar^2}{2m} N_i^{1/2} \frac{d^2 N_i^{-1/2}}{dx^2} + \frac{1}{2m} P_i^2 + V = E_i, (V < E_i). \quad (16'')$$

$$(i \geq 2)$$

However, in the region  $V > E_i$  the assumption can be allowed that  $v_i$  is proportional to  $N_i$  as, if  $V \gg E_i$   $v_i$  is practically identical with  $N_i$ . Thus according to equation (8''),

$$-\frac{\hbar^2}{2m} N_i^{1/2} \frac{d^2 N_i^{-1/2}}{dx^2} + V = E_i, (V > E_i). \quad (16''')$$

Plaskett's equation is obtained by replacing  $P'_i$  in equation (16') by  $P_i$  in (13). The equation thus obtained agrees with (16'') it does not, however, involve the restriction that the equation is valid only for the region  $V < E_i$ . In deriving form (15') of  $O_i$  Plaskett's equation has been used and the first approximation of the WKB method has been applied. Thus one term of equation (8') also contains these approximations. Equation (8'') is free of them as it can be regarded as the direct consequence of the fact that in the region  $V > E_i$  the wave functions  $\varphi_i^0$  and  $\varphi_i$  are approximately equal. Equation (16''), which is the approximation of equation (8') is identical with Plaskett's while equation (16''') is, according to above, certainly more accurate in the region  $V > E_i$  than Plaskett's equation. We may thus conclude that equations (16'') and (16''') are the improved versions of Plaskett's equation.

BALLINGER and MARCH [11] investigated the solution of Plaskett's equation in the case of an oscillator potential and found that the solution is not unique. According to the above, however, we must proceed in such a manner that the solution of equation (16'') obtained in the region  $V < E_i$  must be fitted to the solution of equation (16''') obtained in the region  $V > E_i$ . The fitting is a new condition for the solution of equation (16'') whereby the solution is likely to become unique.

The question arises whether an equation could be found from which the density could be determined for the whole space. Assume that in the region  $V < E_i$  the density is large as compared to the variation of the density. Then we have

$$N_i^{-1/2} \frac{d^2 N_i^{1/2}}{dx^2} = - N_i^{1/2} \frac{d^2 N_i^{-1/2}}{dx^2}$$

and equation (16'') can be written in the form

$$-\frac{\hbar^2}{2m} N_i^{-1/2} \frac{d^2 N_i^{1/2}}{dx^2} + \frac{1}{2m} P_i^2 - \frac{\hbar^2}{m} P_i^{1/2} \frac{d^2 P_i^{-1/2}}{dx^2} + V = E_i.$$

Applying (17) and (17')

$$\frac{1}{2m} P_i^2 - \frac{\hbar^2}{m} P_i^{1/2} \frac{d^2 P_i^{-1/2}}{dx^2} = \frac{1}{2m} p_i^2 - \frac{\hbar^2}{2m} p_i^{1/2} \frac{d^2 p_i^{-1/2}}{dx^2},$$

further, by generalizing relation (17) to some extent

$$\frac{1}{2m} p_i^2 - \frac{\hbar^2}{2m} p_i^{1/2} \frac{d^2 p_i^{-1/2}}{dx^2} = \frac{1}{2m} P_{i-1}^2.$$

Thus

$$-\frac{\hbar^2}{2m} N_i^{-1/2} \frac{d^2 N_i^{1/2}}{dx^2} + \frac{1}{2m} P_{i-1}^2 + V = E_i. \quad (18)$$

If  $i = 1$  this equation goes over into the exact wave mechanical equation, further, if  $V > E_i$  into equation (16''), since, in this case,  $P_{i-1}^2/2m$  can be neglected. Thus equation (18) can be regarded as valid for all states and the whole space.

#### 4. The statistical energy expression

Starting from equation (18) a further approximation makes it possible to express the energy of the system with the aid of the particle density of the system. The energy value  $E_i$  is obtained by multiplying equations (18) by  $N_i/2i$  and by integrating over the whole space. The total energy is obtained by summation according to (4)

$$\mathcal{E} = \sum_{i=1}^g \frac{1}{i} \left\{ -\frac{\hbar^2}{2m} \int N_i^{1/2} \frac{d^2 N_i^{1/2}}{dx^2} dx + \frac{\hbar^2}{32m} \int N_{i-1}^2 N_i dx + \int N_i V dx \right\} - \\ - \frac{1}{2g} \left\{ -\frac{\hbar^2}{2m} \int N_g^{1/2} \frac{d^2 N_g^{1/2}}{dx^2} dx + \frac{\hbar^2}{32m} \int N_{g-1}^2 N_g dx + \int N_g V dx \right\}.$$

Introduce the approximation that  $N_i = \frac{2i}{n} N$ . Then the energy expression is

$$\mathcal{E} = \mathcal{E}_W + \mathcal{E}_K + \mathcal{E}_P \quad (19)$$

where

$$\begin{aligned} \mathcal{E}_W &= -\frac{\hbar^2}{2m} \int N^{1/2} \frac{d^2 N^{1/2}}{dx^2} dx = \frac{\hbar^2}{8m} \int \frac{1}{N} \left( \frac{dN}{dx} \right)^2 dx, \\ \mathcal{E}_K &= \frac{\hbar^2}{8m} \frac{1}{n^3} \left[ \frac{(g-1)g(2g-1)}{3} - q(g-1)^2 \right] \int N^3 dx, \\ \mathcal{E}_P &= \int V N dx. \end{aligned}$$

Obviously  $\mathcal{E}_W$  is just the energy which is generally called the Weizsäcker inhomogeneity correction. It is suitable to compare the kinetic energy  $\mathcal{E}_K$  with the Fermi zero point kinetic energy. The expression for the zero point kinetic energy has been improved upon in a previous paper [9] in such a manner that — under condition similar to those of the present paper — instead of integrating over the momentum space we summed over the states exactly

$$\mathcal{E}_0 = \frac{\hbar^2}{8m} \frac{1}{n^3} \left[ \frac{g(4g^2-1)}{6} - q(g-1/2)^2 \right] \int N^3 dx.$$

Comparing the expressions of  $\mathcal{E}_K$  and  $\mathcal{E}_0$  we have

$$E_K = t \mathcal{E}_0$$

where

$$t = \frac{2(g-1)g(2g-1) - 6q(g-1)^2}{g(4g^2-1) - 6q(g-1/2)^2}$$

or in a different manner

$$\begin{aligned} t &= \frac{n-2}{n+1} \quad \text{if } n \text{ is even,} \\ t &= \frac{(n-1)[(n-1)^2+2]}{n[n^2+2]} \quad \text{if } n \text{ is odd.} \end{aligned}$$

If the number of particles is 1 or 2,  $\mathcal{E}_K = 0$  thus here the total kinetic energy is represented by the Weizsäcker correction only and the relations go over into the exact wave mechanical expressions.

The fact that in the statistical theory the zero point kinetic energy should be decreased when the Weizsäcker correction is incorporated in the theory was first pointed out by GOMBÁS [6]. His method was confirmed by his calculations for atoms.

### 5. Determination of the density

The statistical equation determining the density can be obtained by searching for the density for which  $\mathcal{E}$  is a minimum. Elementary calculation yields

$$-\frac{\hbar^2}{2m} \frac{1}{N^{1/2}} \frac{d^2 N^{1/2}}{dx^2} + \frac{1}{2m} \frac{1}{ng^2} [(g-1)g(2g-1) - 3q(g-1)^2] P^2 + V = V_0, \quad (19')$$

where  $V_0$  is the Lagrange multiplier.

The determination of the density is more accurate if the following procedure is applied. Let us write equations (16'') and (16''') for the  $g$ -th state. Take into account that  $P_g = P$  and if  $n$  is even  $N_g = N$  and if  $n$  is odd, we may use the approximation  $N_g = \frac{2g}{n} N$ ,

$$-\frac{\hbar^2}{2m} N^{1/2} \frac{d^2 N^{-1/2}}{dx^2} + \frac{1}{2m} P^2 + V = E_g, \quad (V < E_g), \quad (20)$$

$$-\frac{\hbar^2}{2m} N^{-1/2} \frac{d^2 N^{1/2}}{dx^2} + V = E_g, \quad (V > E_g). \quad (20')$$

Instead of using equation (20) of Plaskett we may also proceed in the following manner. Equation (8') for the  $g$ -th state is

$$-\frac{\hbar^2}{2m} \frac{1}{v_g^{1/2}} \frac{d^2 v_g^{1/2}}{dx^2} + \frac{1}{2m} P^2 + V = E_g, \quad (V < E_g). \quad (21)$$

Calculate the density from equation (19') for the case when the number of particles of the system is  $n$  and  $n-1$  resp. The difference between these two will yield approximately  $v_g$ . Knowing  $v_g$  and using (13') from equation (21) we may express  $N$

$$N = \frac{2}{h} \frac{n}{g} \left\{ 2m \left[ E_g - V + \frac{\hbar^2}{2m} \frac{1}{v_g^{1/2}} \frac{d^2 v_g^{1/2}}{dx^2} \right] \right\}^{1/2}, \quad (V < E_g). \quad (21')$$

Equation (20) and (21') are both approximations of equation (21).

In conclusion it should be mentioned that for a large number of particles we may obtain from (21) a partial differential equation for  $N$  as the continuous function of the number of particles. Regarding  $N$  as the derivable function

of the number of particles, then  $v_g = \int_{n-1}^n \frac{\partial N}{\partial k} dk$  and if  $n$  is large  $v_g = \frac{\partial N}{\partial n}$  which

substituted into equation (21) yields that

$$-\frac{\hbar^2}{4m} \frac{\partial N}{\partial n} \frac{\partial^3 N}{\partial x^2 \partial n} + \frac{\hbar^2}{8m} \left( \frac{\partial^2 N}{\partial x \partial n} \right)^2 + \frac{\hbar^2 g^2}{8m n^2} N^2 \left( \frac{\partial N}{\partial n} \right)^2 + \\ + V \left( \frac{\partial N}{\partial n} \right)^2 = E_g \left( \frac{\partial N}{\partial n} \right)^2, \quad (V < E_g).$$

Similarly, starting from equation (8'') assumed for the  $g$ -th state

$$-\frac{\hbar^2}{4m} \frac{\partial N}{\partial n} \frac{\partial^3 N}{\partial x^2 \partial n} + \frac{\hbar^2}{8m} \left( \frac{\partial^2 N}{\partial x \partial n} \right)^2 + V \left( \frac{\partial N}{\partial n} \right)^2 = E_g \left( \frac{\partial N}{\partial n} \right)^2, \\ (V > E_g).$$

### Acknowledgement

Thanks are due to Professor P. GOMBÁS for continuous interest in this work.

### REFERENCES

1. L. H. THOMAS, Proc. Camb. Phil. Soc., **23**, 542, 1927.
2. E. FERMI, Z. Phys., **48**, 73, 1928.
3. P. A. M. DIRAC, Proc. Camb. Phil. Soc., **26**, 376, 1930.
4. P. GOMBÁS, Z. Phys., **121**, 523, 1943.
5. C. F. WEIZSÄCKER, Z. f. Phys., **96**, 431, 1935.
6. P. GOMBÁS, Acta Phys. Hung., **3**, 105 and 127, 1953; Acta Phys. Hung., **5**, 483, 1956; Ann. d. Phys., **18**, 1, 1956.
7. J. S. PLASKETT, Proc. Phys. Soc., A, **66**, 178, 1953.
8. N. H. MARCH and J. S. PLASKETT, Proc. Roy. Soc., **235**, 419, 1956.
9. P. SZÉPFALUSY, Acta Phys. Hung., **7**, 433, 1957.
10. W. E. MILNE, Phys. Rev., **35**, 863, 1930.
11. R. A. BALLINGER and N. H. MARCH, Proc. Phys. Soc., A, **67**, 378, 1954.

### О СТАТИСТИЧЕСКОЙ ТРАКТОВКЕ ФЕРМИОН-ГАЗА

П. СЕПФАЛУШИ

### Резюме

Выводится новая статистическая модель, которая в большой мере подобна видоизмененной Гомбашем модели Вайцсеккера, дополненной поправкой на неоднородность. При введенных приближениях суммирование по квантовым состояниям не надо аппроксимировать интегрированием, а можно произвести точно. Кроме определения плотности из вариационного принципа, показаны и более точные методы расчета. Доказывается, что плотность из уравнений Пласскета можно определить только в рамках «классической допустимой области» и выводятся соответствующие уравнение на «запрещенную область».



# НЕКОТОРЫЕ ВОПРОСЫ, ОТНОСЯЩИЕСЯ К ВЫРАЩИВАНИЮ МОНОКРИСТАЛЛОВ ПОЛУПРОВОД- НИКОВ, ИХ СТРУКТУРЕ И СВОЙСТВАМ

(Изложение материалов лекций)

Д. А. ПЕТРОВ

ИНСТИТУТ МЕТАЛЛУРГИИ АКАДЕМИИ НАУК, МОСКВА, СССР

(Представлено Z. Gyulai — Поступило 10 января 1958 г.)

Была исследована термическая устойчивость некоторых полупроводников типа  $A^{III}B^V$  —  $AlSb$ ,  $GaSb$ ,  $InSb$  — и  $Ge$  измерением вязкости их расплава. Соответствующие кривые свободной энергии обладают минимумом, который — повидимому свидетельствует об изменении координационного числа, приближаясь таким образом к структуре кристаллической фазы. Даны важнейшие условия монокристаллического роста, на основе которых описан модифицированный вариант метода Чохральского. В конце изложена связь между некоторыми структурно-чувствительными свойствами и структурой монокристаллов.

Получение монокристаллов германия и кремния давно вышло из стен лабораторий и стало массовым производством в цехах заводов. Сотни монокристаллов этих материалов выпускаются ежедневно для удовлетворения нужд радио- и электротехнической промышленности, транспорта и энергетики. Обеспечение массового производства монокристаллов требует самого тщательного и детального изучения всех сторон этого процесса.

Наиболее распространенным методом получения монокристаллов из этих материалов является метод *Чохральского*.

Этим методом монокристаллы получаются кристаллизацией из расплава.

Изучая процесс формирования кристалла и изменения, которые могут наступать в нем при охлаждении его от температуры образования, кристаллофизик или металлург не может ограничиваться изучением структуры и свойств самого кристалла и их изменениями под влиянием внутренних и внешних факторов. В исследование неизбежно вовлекается также расплав, из которого формируется кристалл. От структуры и свойств расплава существенным образом зависят свойства и структура кристалла.

Еще более это относится к области исследования монокристаллов химических соединений — полупроводников, в первую очередь класса  $A^{III}B^V$ , которые в ближайшем будущем будут играть неменьшую роль в полупроводниковой технике, чем сегодня монокристаллы германия и кремния.

Вопросы термической устойчивости химических соединений — полупроводников — в расплавленном состоянии оказываются существенными для ряда соединений при решении проблемы получения их монокристаллов. Как раз, повидимому, один из наиболее интересных соединений этого класса

— GaAs и InP сильно диссоциируют с образованием элементарных веществ еще до перехода в жидкое состояние. С синтезом соединений из элементов также связан ряд вопросов, которые подлежат изучению.

Занимаясь исследованием процессов получения монокристаллов полупроводников, мы уделяем некоторое внимание исследованию также этих вопросов, и я хотел бы вначале изложить кратко результаты этих исследований.

### Исследование термической устойчивости некоторых соединений класса $A^{III}B^V$ и германия и некоторые замечания по поводу поведения расплавленных полупроводников в предкристаллизационный период

Термическая устойчивость соединений определялась на основании измерения вязкости их в температурном интервале от точки плавления и выше. Результаты измерений для AlSb, GaSb, InSb и Ge показаны на рис. 1. Легко видеть, что для всех трех соединений, в отличие от германия, кривые вязкости с некоторых температур, разных для каждого из исследованных

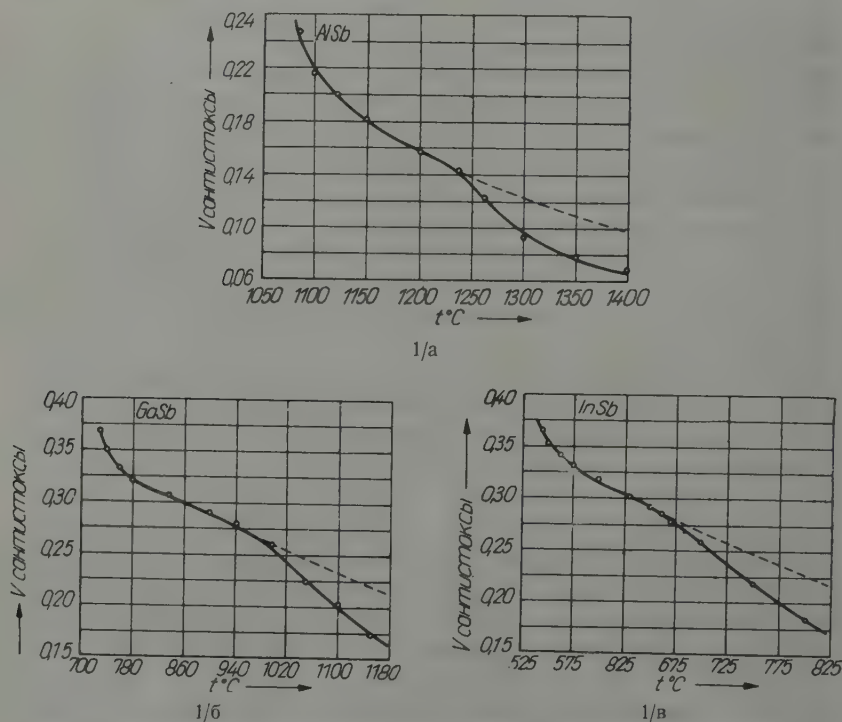


Рис. 1. Вязкость соединений AlSb, GaSb, InSb и Ge выше точки плавления

соединений, начинают значительно уклоняться от первоначального плавного хода. Эти результаты несомненно свидетельствуют о начинающейся при этих температурах значительной диссоциации соединений на составные элементы. Заметим для дальнейшего, что для InSb температура начала диссоциации лежит значительно ниже температуры плавления германия, для двух других соединений она — выше этой температуры, однако, незначительно.

Обратим далее внимание на то, что при температурах близких к точкам плавления соединений, т. е. в предкристаллизационный период, вязкость соединений и германия при охлаждении нарастает более резко, чем в области более высоких температур. Из хода кривых вязкости, используя уравнение свободной энергии вязкого течения :

$$F_{\text{вязк}} = RT \ln \frac{M \nu}{Nh}$$

можно построить кривые изменения свободной энергии процесса от температуры. Результаты показаны на рис. 2.

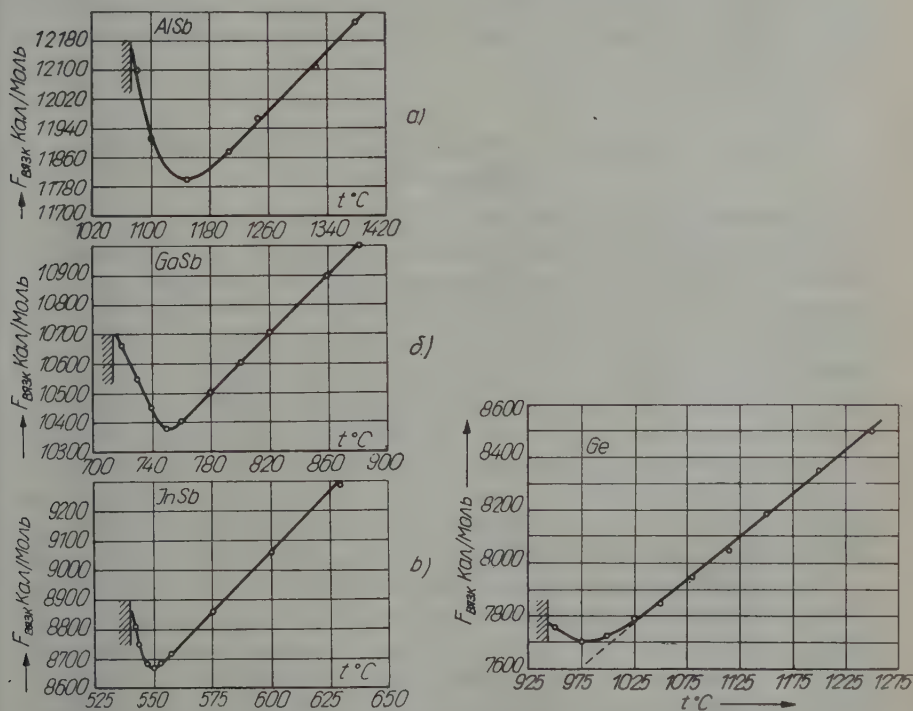


Рис. 2. Изменение свободной энергии вязкого течения с температурой

Обращает на себя внимание наличие минимума на этих кривых, за которым при понижении температуры свободная энергия возрастает. Минимум совпадает приблизительно с изломом на кривых вязкости. Это свидетельствует, как нам представляется, об определенном разрыхлении (расширении) жидкости, в связи с переходом ее в предкристаллизационную область и приближением элементов ее структуры к структуре будущего кристалла. Координационное число у жидких германия и кремния, и, вероятно, у жидких соединений класса  $A^{III}B^V$  близко к восьми, тогда как в кристаллическом состоянии составляет четыре.

Интересно отметить, что при переохлаждениях расплавов этих веществ подобных изменений не наблюдается.

Эти факты, как нам представляется, имеют непосредственное отношение к формированию структуры кристалла, образующегося из расплава, к кинетике процесса кристаллизации, и, возможно, могут явиться одним из объяснений возникновения дислокаций в процессе роста кристалла.

Если ход кривых изменения свободной энергии действительно связан с изменением координационного числа, то в предкристаллизационный период у исследованных полупроводников должна аномально изменяться также плотность. Измерения плотности этих веществ в интересующем нас температурном интервале позволили бы окончательно решить этот вопрос.

### **Условия и техника получения совершенных монокристаллов полупроводников**

Совершенный монокристалл является термодинамически наиболее устойчивой структурой твердого тела. Всякие отступления от совершенства связаны с увеличением свободной энергии кристалла, и означают нарушение нормальных расстояний и следовательно связей между атомами в решетке. Всякое нарушение связи между атомами означает возникновение частично свободных или полусвободных связей, а т. е. связь осуществляется электронами, то следовательно возникновение частично свободных или полусвободных электронов. Так как кристалл полупроводника осуществляет среду, в которой протекают электронные процессы, подобные происходящим в высоком вакууме электронной лампы, то всякое нарушение совершенства кристалла связано с возникновением помех протеканию этих процессов и следовательно с ухудшением работы материала в приборе.

Совершенный монокристалл является системой наиболее приближающейся к равновесной. Естественно, что условия роста такого кристалла должны быть соответствующими. Идеальный кристалл может вырастать, очевидно, только в условиях крайне медленного формирования. Отступления от равновесных условий роста будут тем больше, чем быстрее растет кристалл. Отступления от медленных скоростей роста должны приводить

к возникновению всякого рода структурных несовершенств в монокристалле в виде дислокаций, двойников и др., и в конечном счете к поликристалличности выращиваемого слитка.

Весьма совершенные по структуре кристаллы в настоящее время выращиваются в парообразной фазе в виде очень тонких нитей, сечения которых не превышают, правда, порядка нескольких микрон. Механическая прочность таких нитей, несущих только единичную дислокацию, приближается к теоретическому пределу. Для кремния были получены нити с прочностью  $400 \text{ кг/мм}^2$ , превышающей в несколько раз прочность хорошей стали.

Так как выращиваемый кристалл обладает геометрическим объемом, возникает вопрос об его однородности во всех точках объема. Неоднородность кристалла может быть вызвана, как неоднородностью распределения в нем примесей, так и неоднородностью распределения структурных нарушений. Локальное скопление примесей или структурных несовершенств в объеме монокристалла вызывает соответственные локальные нарушения происходящих в кристалле электронных процессов.

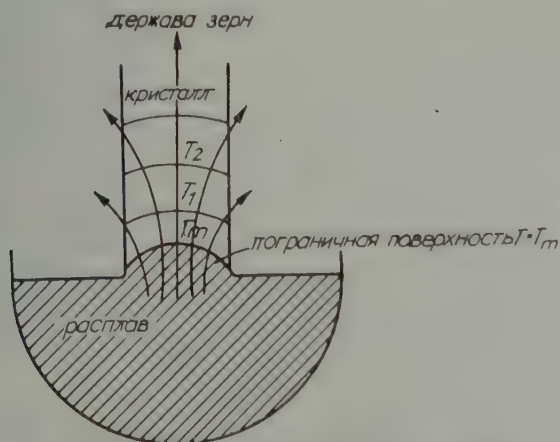


Рис. 3. Иллюстрация к форме границы раздела между кристаллом и расплавом

Одним из мероприятий, направленных на создание условий получения однородного монокристалла, является обеспечение плоской границы раздела между растущим кристаллом и расплавом.

В обычных условиях выращивания кристалла это условие, как правило, не выполняется.

Вследствие значительного отвода тепла в стороны (рис. 3), температура на поверхности кристалла в каком-нибудь горизонтальном сечении ниже, чем в центре кристалла (рис. 3). При остывании поверхностные слои



с меньшей температурой претерпевают меньшее сжатие, чем центральные части слитка. В слитке возникают термические напряжения. Пока кристалл находится в области температур, при которых возможны пластические деформации, это стремление проявляется в возникновении локальных

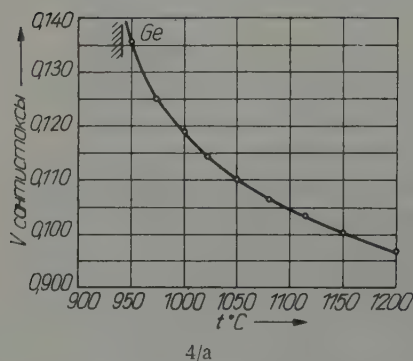


Рис. 4. Макрофотография слитка германия, иллюстрирующая неравномерное распределение дислокаций

пластических сдвигов. Последние вызывают возникновение дополнительных локальных нарушений (дислокаций) в кристалле. Эти нарушения распределяются неравномерно в кристалле, как указывает рис. 4. Средняя по высоте часть кристалла растет, по-видимому, в наиболее благоприятных условиях в смысле формы границы раздела расплав-кристалл, и она меньше всего поражена дефектами. Наиболее поражена дефектами верхняя и нижняя части кристалла, для которых граница раздела неблагоприятна. Особенно поражена дефектами поверхностная корка кристалла.



В современных установках стремятся создать условия, при которых наличие плоской границы обеспечивается автоматически в процессе роста кристалла в любом сечении. Это достигается созданием соответствующего температурного поля в области границы раздела и перемещением нагревателя и тигля относительно друг друга.

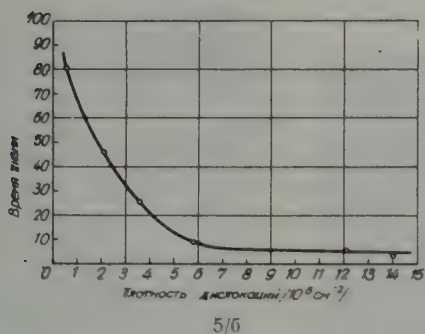
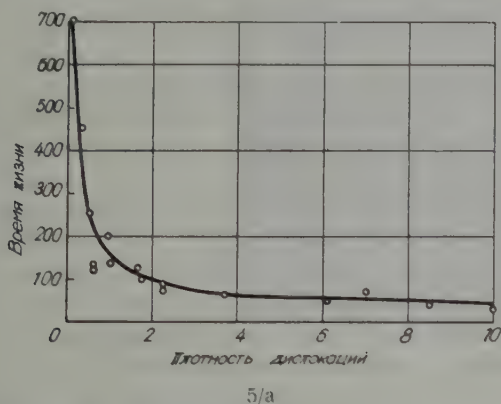


Рис. 5. Зависимость времени жизни неосновных носителей тока от плотности дислокаций в монокристаллах германия и кремния

Наличие плоской границы раздела полностью разрешает также проблему однородности кристалла по распределению примесей.

Крайне нежелательным являются всякие более или менее резкие нарушения скорости выращивания кристалла и температуры расплава. Результатом подобных нарушений является возникновение множества местных структурных несовершенств кристалла.

Поддержание постоянства скорости выращивания и температуры расплава является одним из важнейших условий в современных установках.

Одним из существенных недостатков, свойственных методу Чохраль-

ского, является неравномерность распределения примесей вдоль длины слитка. Слиток получается более чистым от примесей в верхней части и более загрязненным примесями в нижней части.

Исправление этого недостатка может быть осуществлено двумя путями. В американском варианте это достигается программным изменением скорости выращивания. Вначале, когда кристалл растет более чистым, скорость увеличивают, создавая благоприятные условия для механического захвата оттесняемой кристаллом примеси. К концу выращивания скорость уменьшают, компенсируя тем самым больший захват примеси к концу процесса.

В нашем варианте создание однородности по длине слитка достигается непрерывным питанием расплава материалом того же состава, какой задан для выращивания монокристалла (4). В этом варианте отсутствует вынужденное изменение скорости выращивания, нежелательность которого обсуждалась выше.

Я рассмотрел только основные стороны современной техники выращивания совершенных монокристаллов полупроводников. Эта техника требует создания весьма совершенных металлургических установок с весьма точно работающими механизмами, обеспечивающими высокое постоянство скоростных и температурных факторов выращивания кристалла.

### **Структура и свойства монокристаллов**

Электрические свойства кристалла крайне чувствительны к содержанию в нём примесей. Поэтому неравномерное распределение или общее избыточное содержание примеси неблагоприятно для всех электрических свойств кристалла.

На структурные несовершенства реагируют не все, а только так называемые структурно-чувствительные характеристики кристалла. Особенно структурно-чувствительным свойством является время жизни неосновных носителей тока. Поэтому борьба за высокое время жизни неосновных носителей во всем объеме кристалла есть борьба за высокое совершенство кристалла. Структурно-чувствительными свойствами являются далее подвижность основных носителей, обратное напряжение, коэффициент усиления и некоторые другие.

Имеется достаточно большой экспериментальный материал, посвященный вопросу связи структурных дефектов и электрических свойств монокристаллов.

Общая закономерность такова, что с повышением плотности нарушений (дислокаций) ухудшаются структурно-чувствительные характеристики кристалла. В особенности резко, как уже было отмечено, ухудшается время жизни. Это иллюстрируется рис. 5 из (5), на котором показано изме-

нение времени жизни для германия с высоким удельным сопротивлением, близким к собственному (30—40 омсм) и кремния с удельным сопротивлением порядка 40 омсм.

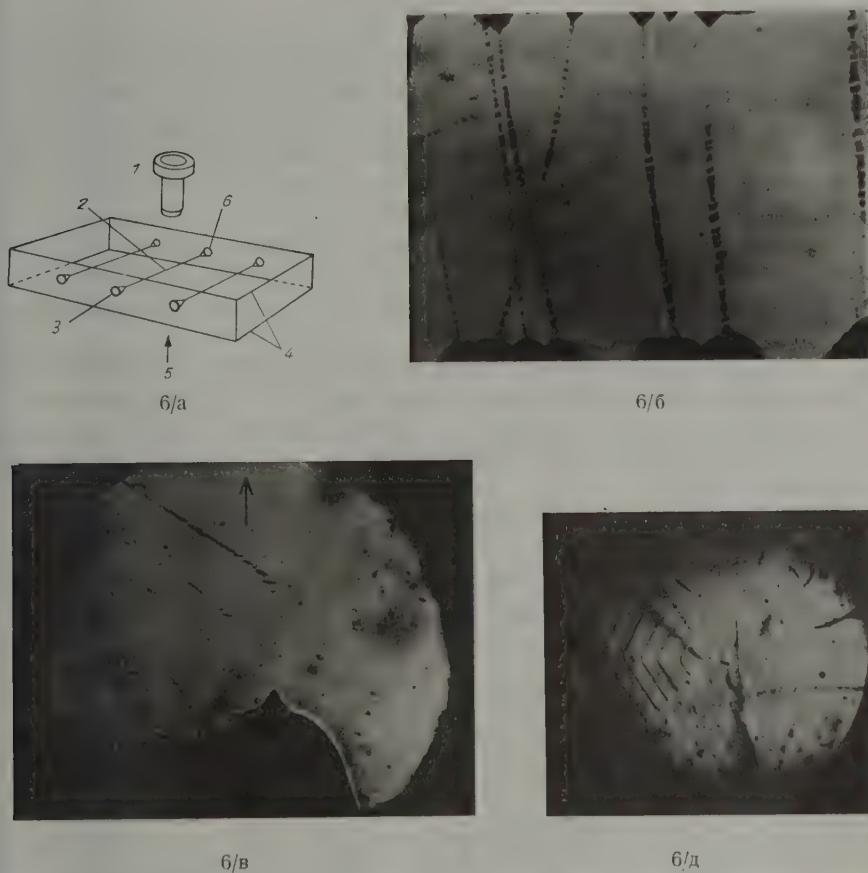


Рис. 6. Микрофотографии кремния, снятые в микроскопе с инфракрасным источником света

При плотности дислокаций порядка  $10^7/\text{см}^3$  время жизни для германия составляет 10 мксек, для  $5 \cdot 10^4/\text{см}^3$  соответственно  $\sim 2000$  мксек. Для кремния при плотности  $10^7/\text{см}^3 \sim 4\text{—}5$  мксек, для  $5 \cdot 10^5 \sim 80$  мксек.

Плотность дефектов в кристаллах кремния обычно больше чем в кристаллах германия. Это объясняется в первую очередь тем, что термические напряжения в кремнии должны быть значительно большими, чем в германии, из-за значительно большей теплоотдачи с поверхности.

Крайне интересной проблемой является взаимодействие примесей и структурных дефектов. Представляя области с избыточным электрическим зарядом, структурные дефекты являются местами, на которых легко могут собираться и по которым наиболее легко могут диффундировать ионизированные примеси.

Применяя исследование монокристаллов полупроводников в микроскопе с инфракрасным источником света, можно наблюдать, как это впервые удалось Дешу (6), распределение и форму дислокаций возникших в процессе роста кристалла или вызванных приложением внешних воздействий.

На микрофотографиях Деша отчетливо просматриваются линии, по которым диффундировала медь. Дислокации в общем следуют вдоль оси роста. Они берут начало на ямках травления на обеих поверхностях образца. Часто дислокации распространяются на всю длину кристалла.

Применение инфракрасного микроскопа в сочетании с другими методами исследования весьма целесообразно при изучении взаимодействия примесей с дислокациями.

Не следует ограничиваться при изучении структурных несовершенств в монокристаллах полупроводников объектами только этой специальной области. Крайне важные результаты приносят работы также с другими веществами, на первый взгляд имеющими только отдаленное отношение к полупроводникам.

Следует указать в этом отношении хотя бы на работу Джильмана и Джонсона (7), в которой были исследованы дислокации в кристаллах литий-фтор. Авторам удалось показать наличие как краевых, так и винтовых дислокаций в этих кристаллах, наблюдать перемещение дислокаций в процессе травления вследствие релаксации, различные формы ямок травления.

Эта область изучена далеко недостаточно и требует самого пристального внимания исследователя.

#### ЛИТЕРАТУРА

1. Д. А. Петров, В. М. Глазов (сдана в печать в Известия АН СССР).
2. Д. А. Петров, В. М. Глазов (сдана в печать в Доклады АН СССР).
3. Д. А. Петров, ЖФХ, 1956, № 1.
4. BILLIG: Some defects in crystals grown from the melt. I. Defects caused by thermal stresses. Proc. Roy. Soc. A. Vol. 235, p. 37. (1956).
5. DASH: Bull. Amer. Phys. Soc. Vol. 30—11. 1955.
6. GILMAN: Observations of Dislocation Glide and Climb in Lithium Fluoride Crystals. Journ. of Appl. Phys. Vol. 27. p. 1018—1022. (1956).

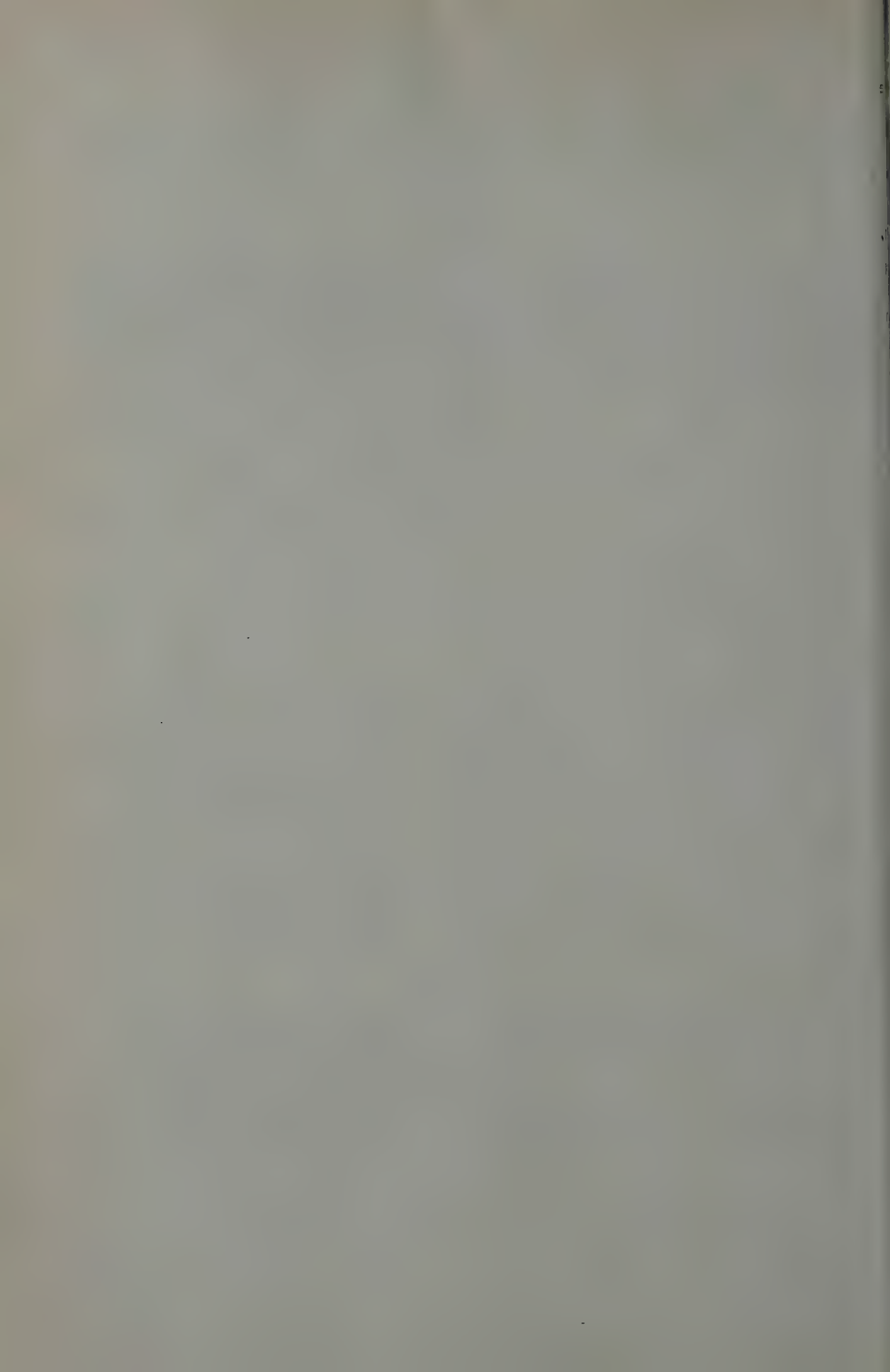
# SOME PROBLEMS OF GROWTH, STRUCTURE AND PROPERTIES OF SEMICONDUCTOR MONOCRYSTALS

By

D. A. PETROV

## Summary

Thermal stability of some  $A^{III}B^V$  type semiconducting alloys—AlSb, GaSb, InSb and Ge — is investigated by viscosity measurements in their molten phase. The corresponding free-energy-curves possess a minimum possibly indicating a change in the coordination-number, approaching in this manner the structure of the crystallized phase. Conditions of monocrystalline growth are given and based on it, a modified version of the Czochralski method is described. Finally the connection between some structure-sensitive properties of crystals and their homogeneity is discussed.





# DIE LAGE DER ABSORPTIONSBANDEN VON STÖRSTELLENELEKTRONEN IN IONENGITTERN

Von

O. STASIW

INSTITUT FÜR KRISTALLPHYSIK DER DEUTSCHEN AKADEMIE DER WISSENSCHAFTEN, BERLIN

(Vorgelegt von Z. Gyulai — Eingegangen: 20. II. 1958)

Die Lage der langwelligsten Absorptionsbande in Silberhalogeniden mit Fremddionen-zusätzen  $O^-$ ,  $S^-$ ,  $Se^-$  und  $Te^-$ , und der Farbzentrenbanden läßt sich durch eine empirisch gefundene Beziehung darstellen. Es resultiert ein Zusammenhang für die Bindung der Elektronen an Fremddionen und Farbzentren. Es läßt sich weiter zeigen, daß für die Absorption der gebildeten photochemischen Reaktionsprodukte nach der Bestrahlung die Polarisierbarkeiten der Fremddionen eine wesentliche Rolle spielt.

## 1. Einleitung

Seit einigen Jahren wird versucht, die Absorptionsspektren der Farbzentren in den Alkalihalogeniden theoretisch zu erfassen. Nach MOLLWO<sup>1</sup> gilt in guter Näherung die Beziehung.

$$\nu_{\max} d^2 = \text{const} \quad (1)$$

( $d$  = Gitterkonstante\*). Später wurde von MOTT und GURNEY<sup>2</sup>, TIBBS<sup>3</sup>, SIMPSON<sup>5</sup>, PINCHERLE<sup>4</sup> u. a. ein vereinfachtes Modell des Farbzentrum untersucht. Als Potential wird ein Coulombpotential  $\frac{e}{\kappa \cdot r}$  angesetzt, wobei  $\kappa$  die makroskopische Dielektrizitätskonstante bedeutet. Zu diesem Potential gehören wasserstoffähnliche Energiezustände und Eigenfunktionen. PEKAR<sup>6</sup> behandelt die Farbzentren wie ruhende Polaronen in einem durch die statische und optische Dielektrizitätskonstante bestimmten Coulombfeld.

Die Abschätzung der Energieeigenwerte eines im Gitter eingefangenen Elektrons ergibt bei fast sämtlichen Modellen, daß die Eigenfrequenzen um-

\* Abweichend von der üblichen Bezeichnung soll hier unter Gitterkonstante der kürzeste Abstand zweier Ionen im Kristall verstanden werden.

<sup>1</sup> E. MOLLWO, Gött. Nachr. Math.-Phys., Klasse 97, 1931.

<sup>2</sup> Vgl. MOTT u. GURNEY, Electronic Processes in Ionic Crystals, Oxford (1948).

<sup>3</sup> S. R. TIBBS, Trans. Faraday Soc., **35**, 1471, 1939.

<sup>4</sup> J. H. SIMPSON, Proc. Soc. (London), A **197**, 269, 1949.

<sup>5</sup> L. PINCHERLE, Proc. Phys. Soc., (London), A **64**, 248 1951.

<sup>6</sup> S. I. PEKAR, J. Exp. Theor. Phys., **16**, 335, 1946; **17**, 868, 1947; **19**, 746, 1949; **20**, 510, 1950.

gekehrt proportional dem Quadrat der Gitterkonstanten sind, also eine der Mollwo-Formel entsprechende Beziehung jedoch mit abweichender Konstanten. Allerdings sind noch die Energieterme von der makroskopischen Dielektrizitätskonstanten des Alkalihalogenids abhängig. Der geringe Unterschied der Dielektrizitätskonstanten der Alkalihalogenide läßt eine Entscheidung über den Einfluß von  $\kappa$  auf  $\nu_{\max}$  nicht zu. Damit bleibt von dieser Seite offen, ob das für das Farbzentrum zu Grunde gelegte Modell eine ausreichende Näherung darstellt.

## 2. Neue Ergebnisse der Untersuchung der Absorption von Störstellenelektronen

In der letzten Zeit ist es gelungen,<sup>7</sup> für die ersten Absorptionsbanden, die in den Silberhalogeniden mit  $O^{2-}$ -,  $S^{2-}$ -,  $Se^{2-}$ - und  $Te^{2-}$ -Zusatz bei tiefen Temperaturen beobachtet werden, eine einfache empirische Beziehung anzugeben. Es gilt

$$h\nu d^2 = aR - bR^2$$

oder umgeschrieben

$$h\nu d^2 = \frac{a^2}{4b} - b \left( R - \frac{a}{2b} \right)^2. \quad (2)$$

Dabei bedeuten:  $h\nu$  die absorbierte Energie im Maximum der Absorptionsbande,  $d$  die Gitterkonstante des Grundgitters und  $R$  der Ionenradius des eingebauten zweiwertigen Fremdanions. Die Konstanten  $a$  und  $b$  können aus den gemessenen Werten für die Maxima der Absorptionsbanden und den zugehörigen Ionenradien ermittelt werden. In der durch (2) gegebenen Darstellung sind die Konstanten  $a$  und  $b$  weder vom Grundgitter noch von den eingebauten Fremdanionen abhängig.

Abb. 1 und Abb. 2 zeigen die Abhängigkeit der absorbierten Energie im Bandenmaximum vom Ionenradius. In der Abb. 1 wurde, um die Konstanten  $a$  und  $b$  empirisch zu ermitteln, als Ordinate  $\frac{h\nu d^2}{R}$  über  $R$  aufgetragen. Es ergibt sich im Bereich der vorgegebenen Ionenradien eine Gerade.

Diese Darstellung, Abb. (2), führt zu dem Ergebnis: Für einen bestimmten Ionenradius, der dem Wert  $\frac{a}{2b}$  entspricht, gibt es einen Grenzwert in der absorbierten Energie. Dieser Wert wird durch das Maximum der Parabel festgelegt. Es kann auch gezeigt werden,<sup>8</sup> daß, falls man dem Farbzentrum einen fiktiven Ionenradius  $\frac{a}{2b}$  zuordnet, sich dann die von MOLLWO<sup>1</sup> auf-

<sup>7</sup> H. D. KOSWIG, Z. Physik, **149**, 204, 1957.

<sup>8</sup> H. D. KOSWIG u. O. STASIW, Z. Physik, **149**, 210, 1957.

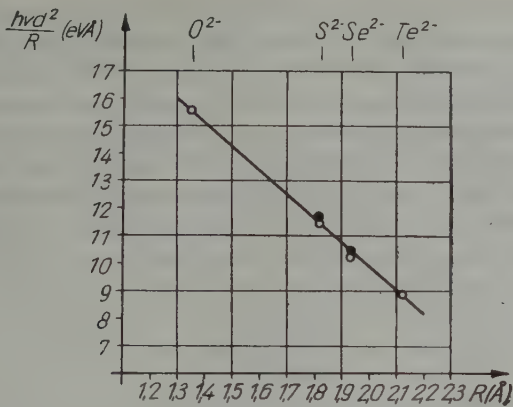


Abb. 1

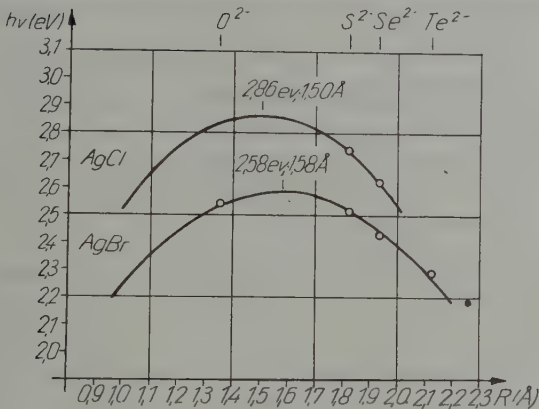


Abb. 2

gestellte Beziehung (1) ergibt, wobei die Konstante der Gl. (1) sich zu  $\frac{a^2}{4b}$  erhält (Gl. 2).

3. Diskussion der Gln. (1) und (2)

Die Möglichkeit der Beschreibung der Absorption der Farbzentren in den Alkalihalogeniden mit der für die Absorption der zweiwertigen Fremdionen in Ag-Halogeniden gültigen Beziehung (2) läßt einige Folgerungen über die Natur der Störstellen zu. Die Konstanten  $a$  und  $b$  sind weder vom Fremdanion noch vom Grundgitter abhängig. Für den Absorptionsvorgang der Fremd-

ionen in den Silberhalogeniden spielt z. B. die Elektronenaffinität keine Rolle, wie man es zunächst erwarten würde. Die Konstanten  $a$  und  $b$  können also nur durch die Störstelle selbst bestimmt sein. Berücksichtigt man weiter, daß mit der Gl. (2) auch die Farbzentren beschrieben werden, dann bedeutet das, daß die Überschußelektronen der zweiwertigen Anionen in gleicher Weise an die Störstelle gebunden werden wie das Elektron im Farbzentrum. Ein derartiger Bindungszustand des Überschußelektrons würde auch verständlich machen, warum z. B. die Elektronenaffinität keine Rolle bei der Absorption der Anionen spielt.

Damit erscheint die von MOLLWO<sup>1</sup> gefundene Beziehung (1) als ein Sonderfall der allgemeineren Gleichung<sup>7</sup>

$$h\nu d^2 = F(R), \quad (3)$$

$F(R)$  ist dabei eine Funktion des Ionenradius der eingebauten Störstelle. Die von MOLLWO<sup>1</sup> ermittelte Konstante ergibt sich dann, wenn für das Farbzentrum ein fiktiver Ionenradius  $\frac{a}{2b}$  in (3) eingeführt wird. Für das Farbzentrum, das als ein in eine Halogenlücke eingefangenes Elektron betrachtet wird, bedeutet dies, daß das eingefangene Elektron sich einen günstigen Ionenradius selbst schafft. Dieser Radius entspricht einem Gleichgewichtszustand mit größter Bindung des Elektrons, wie es auch durch das Maximum der Parabel beschrieben wird.

Die Konstante  $\frac{a^2}{4b}$  der Gl. (1), ist eine vom Gitter unabhängige Größe, da sie sowohl für die Alkali- als auch für die Silberhalogenide gilt.

Für die Lage der Absorptionsbanden des Farbzentrons und der Fremdanionen kann also in dieser Näherung nicht die makroskopische Dielektrizitätskonstante zur Beschreibung herangezogen werden. Nur die Gitterkonstante und der Raumbedarf der Störstelle, der beschrieben wird durch den Ionenradius, bestimmen die spektrale Lage der Absorptionsbande.

Eine genaue Diskussion der Konstanten  $a$  und  $b$  zeigt, daß eine Abhängigkeit von den Eigenschaften des Grundgitters, in das die Störstelle eingebettet ist, zwar noch vorhanden sein kann. Jedoch müßten  $a$  und  $b$  dann so von dieser Gittereigenschaft abhängen, daß sich für alle Kristalle  $\frac{a^2}{4b} = \text{const.}$  ergibt.

Interessant ist noch das Verhalten der Silberhalogenide. Aus der Gl. (3) errechnet man die Lage der Farbzentrenabsorption für AgBr zu 2,59 eV. Bisher konnten die Farbzentren in Silberhalogeniden experimentell noch nicht nachgewiesen werden. Eine genaue Betrachtung der Absorptionsmessungen an

Ag-Halogenid-Mischkristallen von VOLKE<sup>9</sup> zeigt insbesondere bei den Se- und Te-haltigen Kristallen an dieser Stelle einen durchaus anormalen Verlauf der Absorption. Bei den O- und S-haltigen Silberhalogenidkristallen dürfte diese Betrachtung kaum durchzuführen sein, da die Absorption der Fremdionen nahe an der Grenzenergie liegt. Die Absorptionsenergien in den letztgenannten Mischsystemen im AgBr weichen nur geringfügig von dem berechneten Wert der Farbzentrenbande ab. Genaue Untersuchungen über den anormalen Verlauf der Absorption, insbesondere in Se- und Te-haltigen Kristallen, sind im Gange, da die Existenz von Farbzentren in AgBr durchaus wahrscheinlich ist.

#### 4. Zur Absorption der photochemischen Reaktionsprodukte

Wird der Kristall mit Anionenzusätzen bestrahlt, dann bilden sich im langwelligen Bereich, wie die Abb. 3 zeigt, photochemische Reaktionsprodukte. Das langwellige Hauptmaximum der gebildeten photochemische Reaktions-

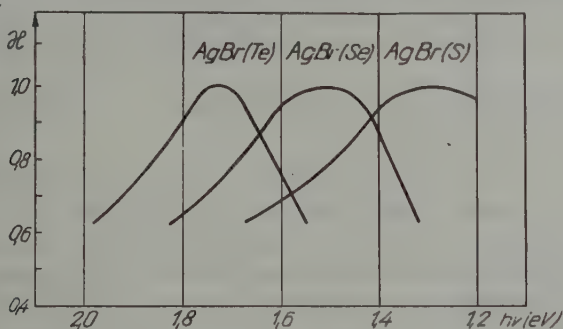


Abb. 3

produkte nach der Einstrahlung in das durch Sensibilisierung hervorgerufene Spektrum bei  $Ag_2S$ -haltigen Silberbromidkristallen liegt langwelliger als dasjenige bei  $Ag_2Se$ -Zusatz. Das durch Sensibilisierung hervorgerufene Spektrum selbst zeigt dagegen ein entgegengesetztes Verhalten; und zwar liegt das Maximum der ersten Bande der Ausläuferabsorption in  $Ag_2S$ -haltigen Silberbromidkristallen bei  $490\text{ m}\mu$  und in  $Ag_2Se$ -haltigen bei  $514\text{ m}\mu$ .

Dieses an sich merkwürdige Verhalten der durch Sensibilisierung hervorgerufenen Absorption und der Absorption der photochemischen Reaktionsprodukte kann leicht durch Bildung der einfachsten Zentren  $Ag[S'_G Br_\square]$  und  $Ag[Seg'_G Br_\square]$  qualitativ erklärt werden. Ein  $Ag[S'_G Br]$ -Zentrum ist gleich-



bedeutend mit einem Farbzentrum, das an einen Frenkelschen Komplex  $\text{Ag}_2\text{S}_G$  angelagert ist.

Die Energie, die bei Lichtabsorption an einem  $\text{Ag}_0[\text{S}'_G\text{Br}_\square]$ -oder  $\text{Ag}_0[\text{Se}'_G\text{Br}_\square]$ -Komplex aufgenommen wird, kann durch folgenden Kreisprozeß berechnet werden: Man entfernt zunächst das angelagerte Farbzentrum vom  $\text{Ag}_0\text{S}'_G$ -Komplex. Die dazu notwendige Arbeit hat den Betrag  $A_1$ . Zur Ionisierung des im Gitter auf diese Weise entstandenen isolierten Farbzentrums (unter Bildung eines freien Elektrons und einer Bromlücke) ist anschließend noch der Energiebetrag  $\Delta E$  aufzuwenden. Bei der Anlagerung der Bromlücke an den Frenkelschen Komplex  $\text{Ag}_0\text{S}'_G$ , (wo zuvor das Farbzentrum abgetrennt wurde), wird ein Energiebetrag  $A_2$  gewonnen. Die absorbierte Energie ist demnach

$$h\nu = A_1 + \Delta E - A_2.$$

Der Energiebetrag  $\Delta E$  ist für  $\text{Ag}_0[\text{S}'_G\text{Br}_\square]$ - und  $\text{Ag}_0[\text{Se}'_G\text{Br}_\square]$ -Komplexe gleich. Dagegen unterscheiden sich die Energiebeträge  $A_1$  und  $A_2$  wesentlich.  $A_2$  besteht aus zwei Anteilen: Aus einem Coulombanteil  $\frac{e^2}{d}$  und dem Anteil der Polarisationsenergie  $\frac{e\mu}{d^2}$ , in der  $\mu$  das Dipolmoment des Fremdions bedeutet.

Es ist also  $A_2 = \frac{e^2}{d} \left( 1 - \frac{\mu}{ed} \right)$ . Das Dipolmoment  $\mu$  wird von dem Silberion auf Zwischengitterplatz erzeugt, das sich in unmittelbarer Nachbarschaft des Fremdions befindet. Bei der Anlagerung der Bromionenlücke an einen  $\text{Ag}_0\text{S}'_G$ - oder  $\text{Ag}_0\text{Se}'_G$ -Komplex wirkt dieser Anteil im entgegengesetzten Sinne wie die Coulombanziehung, also abstoßend. Infolge der größeren Polarisierbarkeit der Selenionen ist der Betrag  $A_2$  beim  $\text{Ag}_0[\text{S}'_G\text{Br}_\square]$ -Komplex kleiner als beim  $\text{Ag}_0[\text{Se}'_G\text{Br}_\square]$ -Komplex. Dieser Unterschied bewirkt, daß das Absorptionsspektrum der schwefelhaltigen Komplexe entsprechend der letzten Formel, die aus dem Kreisprozeß gewonnen wurde, langwelliger als bei den selenhaltigen liegt.

Etwas problematischer ist die Abschätzung des Energieanteiles  $A_1$ . Sicher ist jedoch, daß die Elektronenbahnen des Farbzentrums die des Schwefelions infolge geringerer Polarisierbarkeit der Schwefelionen durch die angelagerten Silberionen auf Zwischengitterplätzen stärker überlappen als die der Selenionen.  $A_1$  bewirkt, daß die Bindung des Elektrons des Farbzentrums an dem  $\text{Ag}_0\text{S}'_G$ -Komplex lockerer ist als die an  $\text{Ag}_0\text{Se}'_G$ .

Ein ähnliches Verhalten zeigen auch  $\text{Ag}_0[\text{Te}'_G\text{Br}_\square]$ -Komplexe. Das Absorptionsspektrum dieser photochemischen Reaktionsprodukte ist noch kurzwelliger als dasjenige von  $\text{Ag}_0[\text{Se}'_G\text{Br}_\square]$ . Andere Zentren, z. B., die einfachen Zentren  $\text{S}'_G\text{Br}_\square$  oder  $\text{Se}'_G\text{Br}_\square$ , werden ein solches umgekehrtes Verhalten gegen-



über der sensibilisierenden Absorption nicht zeigen. Nur wenn gleichzeitig ein Silberion auf Zwischengitterplatz an  $S'_G\text{Br}_\square$  angelagert ist, was eine zusätzliche Polarisierung hervorruft, ist ein solches umgekehrtes Verhalten zu erwarten.

Gleiches Verhalten zeigen die Absorptionsspektren der photochemischen Reaktionsprodukte und das durch Sensibilisierung erzeugte Spektrum der  $\text{Ag}_2\text{S}$ - oder  $\text{Ag}_2\text{Se}$ -haltigen Silberchloridkristalle.

## ПОЛОЖЕНИЕ АБСОРБЦИОННЫХ ПОЛОС ДЕФЕКТНЫХ ЭЛЕКТРОНОВ В ИОННЫХ РЕШЕТКАХ

О. СТАСИВ

Р е з ю м е

Положения длинноволновых абсорбционных полос в галогенидах серебра с примесями ионов  $\text{O}^-$ ,  $\text{S}^-$ ,  $\text{Se}^-$  и  $\text{Te}^-$ , и полос центров, окрашивания могут быть представлены найденным экспериментально соотношением. Получается соотношение для связи электронов в центрах окрашивания. Может быть также показано, что в абсорбции образующихся после облучения продуктов фотохимической реакции, поляризуемость примесных ионов играет важную роль.



## LETTER TO THE EDITOR

### CALCULATION OF THE ENERGY EXPRESSION IN CASE OF A WAVE FUNCTION BUILT UP FROM TWO ELECTRON ORBITS

(Received : IV. 29. 1958)

The wave function of a system is built up by the HLSP and LCAO methods from one electron orbitals. In principle, however, also many electron orbitals may be used as building units. The use of two-electron orbitals has been primarily suggested by FOK [1]. In the case examined by him, two electron orbitals are symmetric in the space coordinates. Then the whole wave function can be written as the linear combination of determinants. The energy expression for a wave function of this type has been derived by HURLEY LENNARD-JONES and POPLÉ [2].

By us the wave function of the system is built up from antisymmetric two electron orbitals  $\psi(1|2)$  i. e.

$$\psi(1|2) = -\psi(2|1).$$

Here also the spin coordinates are included in the arguments. Let us assume that :

1. the number  $N$  of the electrons of the system is even ;
2. The wave function of the system can be approximated as the product of  $\frac{N}{2}$  two electron functions :

$$\psi_1(1|2) \psi_2(3|4) \psi_3(5|6) \dots \psi_{\frac{N}{2}}(N-1|N).$$

By the Pauli principle it is required to antisymmetrize this product :

$$\Phi = C \sum_P (-1)^P P \psi_1(1|2) \dots \psi_i(\kappa|\lambda) \dots \psi_j(\mu|\nu) \dots \psi_{\frac{N}{2}}(N-1|N). \quad (1)$$

Here  $C$  is the normalization factor, whereas  $P$  signifies those permutations by which electrons are interchanged between the individual two electron orbitals. We have to sum over these. (Permutations by which electrons are interchanged within the individual two electron orbitals should not be con-

sidered, since two electron orbitals are already antisymmetrical in themselves.)

In our case  $\frac{N!}{2^{\frac{N}{2}}}$  different permutations exist.

For the sake of further simplification of computations let us assume that the two electron orbitals are orthonormalized, i. e.

$$\begin{aligned} \int \psi_i^* (1|2) \psi_i (1|2) d\tau_1 d\tau_2 &= 1, \\ \int \psi_i^* (1|\kappa) \psi_i (1|\lambda) d\tau_1 &= 0, \quad \text{if } i \neq j. \end{aligned} \quad (2)$$

Considering these, we obtain from the condition  $\int \Phi^* \Phi d\tau = 1$ , that

$$C = \frac{2^{\frac{N}{4}}}{\sqrt{N!}}. \quad (3)$$

If mean values of physical quantities (energy, dipolmomentum, diamagnetic susceptibility etc.) should be determined, then it is advisable to produce the density matrices  $\Gamma^\nu$  of  $\Phi$ :

$$\begin{aligned} \Gamma^\nu (1' 2' \dots \nu' | 12 \dots \nu) &= \binom{N}{\nu} \int \Phi^* (1' 2' \dots \nu' \nu + 1 \dots N) \Phi (12 \dots \nu \dots \\ &\dots N) d\tau_{\nu+1} \dots d\tau_N. \end{aligned} \quad (4)$$

By using these, the physical quantities can be easily computed. If our aim set is the calculation of the energy, then it is sufficient to compute the first and second order density matrices (if we confine ourselves to two-body forces).

Considering formulae (1), (2), (3) and (4) as well as the fact, that operator  $H$  is symmetric in the electron coordinates, the first order density matrix will be the following:

$$\Gamma (1'|1) = 2 \sum_{i=1}^{\frac{N}{2}} \int \psi_i^* (1'|2) \psi_i (1|2) d\tau_2,$$

whereas the second order density matrix:

$$\begin{aligned} \Gamma^2 (1' 2' | 12) &= \sum_{i=1}^{\frac{N}{2}} \psi_i^* (1'|2') \psi_i (1|2) + 4 \sum_{1=i < j}^{\frac{N}{2}} \int \{ \psi_i^* (1'|3) \psi_j^* (2'|4) \psi_i (1|3) \psi_j (2|4) - \\ &- \psi_i^* (1'|3) \psi_j^* (2'|4) \psi_i (2|3) \psi_j (1|4) \} d\tau_3 d\tau_4, \end{aligned}$$

and the energy can be written :

$$E = H(0) + \int H(1) \Gamma(1' | 1) d\tau_1 + \int H(12) \Gamma^2(1' 2' | 12) d\tau_1 d\tau_2.$$

Here  $H(0)$  signifies the part of the Hamilton operator not depending on electron coordinates,  $H(1)$  that one depending only on the coordinates of one electron, whereas  $H(12)$  the part which depends on the coordinates of two electrons.

Let us introduce the following denotations :

$$E_i = 2 \int \psi_i^*(1|2) \left[ H(1) + \frac{1}{2} H(12) \right] \psi_i(1|2) d\tau_1 d\tau_2,$$

$$C_i = \sum_j' \int \psi_i^*(1|3) \psi_j^*(2|4) H(12) \psi_i(1|3) \psi_j(2|4) d\tau_1 d\tau_2 d\tau_3 d\tau_4,$$

$$A_i = \sum_j' \int \psi_i^*(1|3) \psi_j^*(2|4) H(12) \psi_i(2|3) \psi_j(1|4) d\tau_1 d\tau_2 d\tau_3 d\tau_4.$$

( $\sum_j'$  means that the term  $j = i$  should be omitted from the summation).  
As a final result we obtain the following simple formula

$$E = H(0) + \sum_i (E_i + 2C_i - 2A_i).$$

The descriptive meaning of the individual terms is the following :  $E_i$  is the energy of an electron pair being on the  $i$ -th orbit,  $C_i$  is the Coulomb-like interaction energy of one of the electrons on the  $i$ -th orbit with electrons being on other orbits. Whereas  $A_i$  is the exchange energy of one of the electrons on the  $i$ -th orbit with electrons on other orbits.

E. KAPUY

Research Group for Theoretical Physics of the  
Hungarian Academy of Sciences, Budapest

#### LITERATURE

1. F. A. FOК, Dokl. Akad. Nauk U.R. S. S., **73**, 735, 1950.
2. A. C. HURLEY, J. LENNARD-JONES and J. A. POPLE, Proc. Roy Soc., **A**, **320**, 446, 1953.





**E. L. NIKOLAI: Theoretische Mechanik. Band I. Deutscher Verlag der Wissenschaften, Berlin, 1956, 282 Seiten**

In der Ausgabe des »Deutscher Verlag der Wissenschaften« zu Berlin erschien in deutscher Übersetzung das russische Lehrbuch »Theoretische Mechanik« von E. L. NIKOLAI. Das Werk besteht aus zwei Teilen; der erste ist der Statik und Kinematik, der zweite der Dynamik gewidmet. Vorläufig gelangte nur der erste Teil zur Ausgabe. Das Werk erreichte im russischen Original 15 Auflagen. Mit Hinsicht auf die Fruchtbarkeit der russischen Lehrbuchproduktion verleiht diese Tatsache dem Lehrbuch schon im vorhinein ein gewisses Ansehen und erweckt im Leser berechnete Erwartungen. Eines ähnlichen zeitbeständigen Charakters kann sich vielleicht nur die Abraham-Beckersche Elektrodynamik rühmen.

Bei der Beurteilung des Werkes ist in Betracht zu ziehen, dass es ausgesprochen als einleitendes Werk für Anfänger verfasst wurde. Die Beurteilung hat sich also in erster Linie auf die Anordnung des Stoffes sowie auf die angewandten Methoden zu richten. Der an den technischen Hochschulen allgemein üblichen Gewohnheit entsprechend bevorzugt das Werk die graphostatische Behandlungsmethode. Die auf das Koordinatensystem bezügliche Komponentenmethode ist im Werk nicht grundsätzlich ausgeschlossen wird aber nur der Einfachheit und Vollständigkeit halber angewendet.

Die vorsichtige Einführung des Vektorenbegriffes gilt als Musterbeispiel für die didaktische Sorgfalt des Autors. Es muss jedoch bemerkt werden, dass es vorteilhafter gewesen wäre, die Vektorenaddition der Definition der Vektoren anzuschliessen, um so darauf hinweisen zu können, dass der endliche Drehwinkel — der ebenfalls durch

eine orientierte Länge dargestellt werden kann — aus dem Gebiet des Vektorenbegriffes auszuschliessen ist. Auch ist es nicht überflüssig, darauf hinzuweisen, dass der Einheitsvektor als dimensionlos zu betrachten sei. Hingegen offenbart sich didaktisches Taktgefühl darin, dass die Unabhängigkeitsbeweise der sechs auf das Gleichgewicht der starren Körper bezüglichen Axiome auf dieser Anfängerstufe nicht Gegenstand einer besonderen Untersuchung bilden. Den Axiomen folgen mit Euklidischer Strenge jene Theoreme, welche die genügenden und hinreichenden Bedingungen des Gleichgewichtes der starren Körper enthalten. Das Prinzip des stufenweisen Fortschrittes gelangt hier voll zur Geltung. Zuerst wird die Bestimmung der Resultierenden der in einem Punkte angreifenden Kräfte gemäss der Polygon- so wie der Komponentenmethode behandelt. Dem schliesst sich der Fall der verschiedenen Angriffspunkte an, wodurch die Einführung des Kräftepaars benötigt wird. Die Herleitung der Gleichgewichts-äquivalenz der Kräftepaare sowie im Zusammenhang damit die Addition der in einer Ebene liegenden und dann der in verschiedenen Ebenen liegenden Kräftepaare erfolgt in instruktiver Art und Weise. In diesen Ableitungen bewahrt der Autor die methodische Reinheit und benutzt überall das graphische Verfahren.

Die Konstruktion des Angriffspunktes der resultierenden Kraft erfolgt wie üblich mit Hilfe des Seilpolygons. Die Darlegung ist so klar und übersichtlich, dass auch ein mittelmässiger Anfänger keine Schwierigkeiten begegnen wird. Er wird wahrscheinlich nur bei der Lösung der am Ende der einzelnen Kapitel vorkommenden sehr praktischen

Aufgaben verblüfft sein. Die meisten Aufgaben sind mit richtigem Gefühl so ausgewählt, dass sie an die Abstraktionsfähigkeit des Lesers ziemliche Anforderungen stellen. Das Gerüst der mechanischen Kräfteverhältnisse muss erst herausgeschält werden, um unter den anzuwendenden Theoremen die entsprechenden herausfinden zu können.

Das zweite Kapitel ist dem Begriff und der Bestimmung des Schwerpunktes gewidmet. Es wird nachgewiesen, dass in Falle homogener Körper der Schwerpunkt in einer Symmetrieebene liegt, falls eine solche existiert. Im Werke sind die beiden Guldinschen Regeln, die sich auf den Schwerpunkt von Drehkörpern und Drehflächen beziehen, ebenfalls dargestellt. Einige lehrreiche Beispiele heben den Reiz des Kapitels bedeutend.

Die Richtlinie der Kinematik ist natürlich bestimmt. Die zu behandelnden Quantitäten sind die Verrückung, die Geschwindigkeit und die Beschleunigung. Die Einführung dieser Begriffe erfolgt mit bis ins kleinste gehenden Sorgfalt. Die Beschreibung der Bewegung eines Punktes erfolgt zuerst durch Angabe der Bahn und der Zeitabhängigkeit der durchlaufenden Weglänge und dann weiter mit Hilfe von zeitabhängigen Funktionen der Koordinaten in verschiedenen Koordinatensystemen. So wird stufenweise aus dem Geschwindigkeitsskalar der Geschwindigkeitsvektor entwickelt, und so ändert sich auch seine Definition zum zeitlichen Differentialquotienten des Vektors der Verrückung anstatt jenes des Weges. Hier taucht im Leser die berechnete Frage auf, ob vom didaktischen Gesichtspunkt eine allzu eingehende Behandlung sozusagen offensichtlicher Tatsachen richtig ist. Zweifellos kann ein für Anfänger bestimmtes Lehrbuch die Evidenz nicht missbrauchen, der richtige Weg ist jedoch nicht das entgegengesetzte Extrem.

In denselben zwei Schritten erfolgt die Einführung der Beschleunigung. Die für die Schmiegungsfläche angewandten zwei Benennungen: Tangentialebene bzw. Krümmungsebene klingen ungewohnt. Die Bestimmung der tangentialen und normalen Beschleunigungskomponenten erfolgt traditions-

gemäss durch die Einführung des tangentialen Einheitsvektors.

Die Anwendung auf die gleichförmige Kreisbewegung wird auf später verschoben, weil der Autor die Behandlung der fortschreitenden Bewegung und Rotation der starren Körper dazwischenschaltet. Die letztere bietet Gelegenheit zur Einführung der Winkelgeschwindigkeit und Winkelbeschleunigung.

In den folgenden zwei Kapiteln ist die Frage erörtert, wie die Verrückung, die Geschwindigkeit und die Beschleunigung eines sich bewegenden Punktes in irgendeinem Inertialsystem bestimmt werden kann, wenn diese in einem sich relativ zu dem Inertialsystem bewegenden Koordinatensystem gegeben sind.

Das Problem wird für zwei besondere Fälle gelöst. Das zweite Koordinatensystem führt im Verhältnis zu dem Inertialsystem eine fortschreitende Bewegung aus, bezw. rotiert um eine feste Achse. Die hier angewandte geometrische Methode ist unbedingt anschaulicher, als die allbekannte analytische, die zum Beispiel in der Sommerfeld'schen Mechanik benutzt wird. Verwunderlich erscheint es jedoch, dass in der in Rede stehenden 15-ten Auflage das Attribut »inertial« noch immer nicht gebraucht ist, hingegen statt dessen der vollkommen veraltete Ausdruck »absolut fest« steht. Es stand dem Übersetzer allerdings frei, den modernen Ausdruck zu gebrauchen. Als Anwendung der Ergebnisse finden wir die Ableitung der expliziten Form der Beschleunigungskomponenten in ebenen Polarkoordinaten. Bekanntlich werden dieselben bei der Behandlung der Planetenbewegung benötigt. Die Anwendung ist geistreich, die beiden Probleme sind jedoch so fernliegend, dass auch die direkte Ableitung der Polarkomponenten ratsam gewesen wäre.

Dem Geiste des Werkes entsprechend geht der allgemeinen Bewegung der starren Körper die einfachere ebene Bewegung voran bei der auch jeder seiner Schnitte in einer Ebene bleibt.

Das weiteren werden der Geschwindigkeits- und Beschleunigungsplan, das Schal-

sche Theorem sowie das Geschwindigkeitszentrum besprochen. Das Anwendungsgebiet besteht in diesem Falle in der Bestimmung der sich auf die einzelnen ebenen Teile irgendeines Mechanismus beziehenden momentanen Geschwindigkeitszentren.

Im letzten Kapitel wird die Rotation eines starren Körpers um einen festen Punkt behandelt. Die lineare Geschwindigkeit und Beschleunigung eines Punktes des starren Körpers wird durch den Author mit ausserordentlicher Ausführlichkeit hergeleitet. Die Berechnung wiederholt sich bei der allgemeinsten Bewegung des starren Körpers, die auf die Schraubenbewegung zurückgeführt werden kann.

Die Ansprüche des Anfängers werden durch das Nikolaische Lehrbuch weitgehend

zufriedengestellt. Zum Privatstudium kann ein geeigneteres Lehrbuch kaum empfohlen werden. In dem sich auf 17 Bogen erstreckenden Werk ist sozusagen auf jeder Seite eine Abbildung vorzufinden, die den Text vorzüglich illustriert. Das Prinzip des vorsichtigen Fortschreitens vom Einfachen zum Komplizierten kommt überall zur Geltung.

Die Anzahl der Druckfehler ist viel höher, als aus der beigelegten Druckfehlerberichtigung ersichtlich ist.

In der von X. EDER und R. ROMPE herausgegebenen Lehrbuchserie ist die Mechanik von NIKOLAI zweifellos ein willkommenes Werk.

Professor A. NOVOBÁTZKY

Physikalisches Institut der Roland Eötvös  
Universität, Budapest

A kiadásért felel az Akadémiai Kiadó igazgatója

Műszaki felelős: Farkas Sándor

A kézirat nyomdába érkezett: 1958. V. 16. — Terjedeleme: 21,25 (A/5) ív, 60 ábra, 2 melléklet

---

Akadémiai Nyomda, Budapest, Gerlóczy u. 2. — 45805/58 — Felelős vezető: Bernát György

# I N D E X

<i>G. Schmidt</i> : Electrical Discharges in High Vacuum — <i>Г. Шмит</i> : Электрические разряды в высоком вакууме .....	1
<i>I. Berkes</i> : Effect of Magnetic Stray Field on the Location of Image in Nuclear Spectrometers — <i>М. Бёркеи</i> : Влияние рассеяния магнитного поля на изображение в ядерных спектрометрах .....	13
<i>K. L. Nagy</i> : Tomonaga's Intermediate Coupling Theory Using Configuration Space Methods — <i>К. Л. Надь</i> : Метод средней связи Томонага, при использовании конфигурационно-пространственных методов .....	23
<i>G. Domokos</i> : Production of Heavy Unstable Particles in Extremely Energetic Nucleon-Nucleon Collisions — <i>Г. Домокош</i> : Рождение тяжелых нестабильных частиц соударениях нуклонов большой энергии .....	49
<i>L. Nagy</i> : Shower Production at Small Thicknesses of Absorber — <i>Л. Надь</i> : Рождение ливней при малых толщинах Al, Fe, Cu, Pb .....	63
<i>T. Tietz</i> : Eine analytische Formel für die Theorie der Bildung der Elektronengruppen im periodischen System der Elemente — <i>Т. Тимц</i> : Аналитическое выражение для теории возникновения электронных групп в периодической системе элементов .....	73
<i>R. Gáspár</i> : Plane Wave Method with a Modified Potential Field — <i>Р. Гашнап</i> : Определение зонного энергетического спектра электронов в металлах .....	79
<i>I. Dohán, T. Gémesy, T. Sándor</i> und <i>A. Somogyi</i> : Bestimmung des Verhältnisses zwischen der Zahl der Photonen und der Zahl der Elektronen in den ausgedehnten Luftschauern der kosmischen Strahlung mittels einer Wilsonkammer — <i>И. Доган, Т. Гемеш, Т. Шандор</i> и <i>А. Шомоди</i> : Определение отношения числа фотонов и электронов в широких атмосферных ливнях космического излучения камерой Вильсона .....	97
<i>R. Gáspár</i> and <i>I. Tamáßy-Lentei</i> : The United Atom Model of the HF Molecule — <i>Р. Гашнап</i> и <i>И. Тамаш-Лентси</i> : Объединенная атомная модель молекулы HF .....	105
<i>K. Ladányi</i> : Variational Method for the Solution of the Quantummechanical Many-body Problem — <i>К. Ладани</i> : Вариационный метод для решения проблем у многих тел в квантовой механике .....	115
<i>I. Deézi</i> : A Recent Rotational Analysis of the $\gamma$ Bands of the NO Molecule — <i>И. Дежи</i> : Новый вращательный анализ $\gamma$ -полос NO молекулы .....	125
<i>I. Náray-Szabó</i> : Zusammenhang zwischen der Struktur und den physikalischen Eigenschaften des Glases — <i>И. Нарай-Сабо</i> : Соотношение между структурой и физическими свойствами стекла .....	151
<i>T. Tietz</i> : The Scattering of Electrons by Free Neutral Atoms in the Thomas-Fermi Model — <i>Т. Тимц</i> : Рассеяние электронов свободными нейтральными атомами по модели Томас—Ферми .....	163
<i>A. С. Давыдов</i> и <i>Г. Ф. Филиппов</i> : Коллективные возбужденные состояния метнотметных атомных ядер — <i>A. S. Davydov</i> and <i>G. F. Filippov</i> : Collective Excitations of the Even-even Atomic Nuclei. ....	169

<i>В. И. Гольданский</i> : О $\gamma$ р-реакциях с образованием основных состояний ядер — <i>V. I. Goldanskij</i> : On ( $\gamma$ R) Reactions with Final Nuclei in the Ground State	177
<i>Д. Ф. Курдгеладзе</i> : Феноменологическое обобщение уравнения Томаса—Ферми— Дирака (ТФД) в случае теории металлов и его периодические решения — <i>D. F. Kurdgeladze</i> : Phenomenological Generalization of the Thomas—Fermi— Dirac (TFD) Equation in Case of the Theory of Metals and its Periodic Solutions	185
<i>К. Sasvári</i> : On the Crystal Structure of $\text{AlCl}_3$ — <i>К. Шашиари</i> : О кристаллической структуре $\text{AlCl}_3$	195
<i>P. Szépfalussy</i> : On the Statistical Treatment of the Fermion Gas — <i>П. Сепф луши</i> : О статистической трактовке фермион-газа	203
<i>Д. А. Петров</i> : Некоторые вопросы, относящиеся к выращиванию монокристаллов полупроводников, их структуре и свойствам — <i>D. A. Petrov</i> : Some Problems of Growth, Structure and Properties of Semiconductor Monocrystals	217
<i>O. Stasiw</i> : Die Lage der Absorptionsbanden von Störstellenelektronen in Ionengittern — <i>О. Стасив</i> : Положение абсорбционных полос дефектных электронов в ионных решетках	229

#### *Letter to the Editor*

<i>E. Kapuy</i> : Calculation of the Energy Expression in Case of Wave Function Built up from two Electron Orbits	237
--	-----

#### *Buchbesprechung — Book Review — Обзор книг*

<i>E. L. Nikolai</i> : Theoretische Mechanik. Band I.	241
---	-----



# ÜBER DAS VERHÄLTNISS DES WELLENMECHANISCHEN ENERGIEEIGENWERTPROBLEMS ZUR KLASSISCHEN MECHANIK

Von

I. FÉNYES

INSTITUT FÜR THEORETISCHE PHYSIK DER ROLAND EÖTVÖS UNIVERSITÄT, BUDAPEST

(Vorgelegt von K. F. Novobátzky. — Eingegangen: 3. VIII. 1957)

Das Hauptziel dieser Arbeit ist es, den mathematischen Zusammenhang zwischen zwei Theorien aufzuklären und die theoretische Begründung der von klassischen Grundlagen ausgehenden wellenmechanischen Näherungsmethoden zu geben. Es werden weiterhin noch einige prinzipielle Probleme der klassischen Begründung der Quantenmechanik berührt: 1. Im allgemeinen haben die Eigenwertprobleme keine klassisch mechanischen Grenzfälle. 2. Die Abbildung des Problems des Energieeigenwertes auf ein Modell von klassischem Charakter. Die Schwierigkeiten der klassischen Interpretation der Energieeigenzustände, die durch reelle Eigenfunktionen charakterisiert sind. Die formale Lösung der Schwierigkeiten. 3. Gegenseitige Eindeutigkeit der Abbildung. Die Wellenmechanik als Verallgemeinerung der Bohrschen Theorie. 5. Einige charakteristische Eigenschaften des »Impulses«  $u$  und der »Wirkungsfunktion«  $S$ . Die Gültigkeitsgrenzen des klassischen Modells: Analogie zur statistischen Interpretation der Hydrodynamik.

1. Es wird allgemein anerkannt, dass ebenso wie die klassische Mechanik aus der relativistischen Mechanik durch den Grenzübergang  $c \rightarrow \infty$  erhalten wird, so wird sie auch aus der Wellenmechanik durch den Grenzübergang  $\hbar \rightarrow 0$  erhalten. In einer früheren Arbeit [1], in welcher sich der Verfasser mit dem Divergenzproblem der W. K. B. Methode befasste, unterwarf er den in der Wellenmechanik angewandten Grenzübergang  $\hbar \rightarrow 0$  einer eingehenden Untersuchung. Das dort erhaltene Resultat war, dass jene wellenmechanischen Grössen, die als Analogen bestimmter klassisch mechanischer Grössen betrachtet werden können, im Falle von Eigenwertproblemen im allgemeinen an der Stelle  $\hbar = 0$  eine wesentliche Singularität aufweisen. Auf diese Weise haben die wellenmechanischen Eigenwertprobleme im allgemeinen keine klassisch mechanischen Grenzfälle. Diese Eigenschaft der Wellenmechanik ist nicht alleinstehend. Auch die Elektrodynamik hat als notwendig relativistische Disziplin gewöhnlich keinen klassischen (nicht-relativistischen) Grenzfall. Wir können also behaupten, dass das wellenmechanische Eigenwertproblem als eine notwendigerweise nichtklassische mechanische Disziplin keinen klassisch mechanischen Grenzfall hat.

Das Gesagte ist ebenso vom prinzipiellen wie auch vom praktischen Standpunkt (Näherungsmethoden) aus von grossem Interesse. Was die prinzipielle Frage der Quantenmechanik anbelangt, so bezweifelt die obige Behauptung nicht die Berechtigung jener Bestrebungen, deren Ziel die deterministische Erklärung der Wellenmechanik ist. Der Verfasser ist der Meinung, dass die

erwähnten Schwierigkeiten von solcher Natur sind, dass sie die Möglichkeit, den wellenmechanischen Vorgängen einen kausalen Hintergrund zuzuschreiben, nicht eindeutig ausschliesst. Soviel ist allerdings auch aus dem Obenerwähnten ersichtlich, dass das Grundprinzip der Quantenmechanik — nämlich dass die Messung das System immer im Eigenzustand findet — der Möglichkeit einer deterministischen Erklärung widerspricht. Infolgendessen kann die Quantenmechanik nur dann auf eine — die Existenz der verborgenen Parameter annehmende — Theorie zurückgeführt werden, wenn das erwähnte Grundprinzip durch ein anderes ersetzt wird. Es bleibt eine offene Frage, auf welcher Art dies realisiert werden könnte. Die prinzipiellen Aspekte dieser Frage werden hier nicht eingehend behandelt. Das Verhältnis zwischen Wellenmechanik und klassischer Mechanik soll hier überwiegend von dem Gesichtspunkt der sich auf klassische Grundlagen aufbauenden wellenmechanischen Näherungsmethoden untersucht werden.

Die Ansicht, dass die klassische Mechanik als der Grenzfall der Wellenmechanik betrachtet werden kann, beruht auf zwei wohlbekannten Tatsachen:

a) Werden die klassischen Grössen durch die entsprechenden wellenmechanischen Operatoren ersetzt, so gelangt man zu gültigen wellenmechanischen Beziehungen.

b) In den aus der Schrödinger-Gleichung

$$\hbar^2 \Delta \varphi + p^2 \varphi = 0 \quad (1)$$

durch die Transformation

$$\varphi = \exp \frac{i}{\hbar} W, \quad (2)$$

$$y = \nabla W = \frac{\hbar}{i} \frac{\nabla \varphi}{\varphi} \quad (3)$$

gewonnenen Gleichungen

$$\frac{\hbar}{i} \Delta w + (\nabla W)^2 - p^2 = 0 \quad (4)$$

bzw.

$$\frac{\hbar}{i} \operatorname{div} y + y^2 - p^2 = 0 \quad (5)$$

hat  $y$  eine dem klassischen Impuls,  $W$  hingegen eine der klassischen Wirkungs-funktion analoge Bedeutung. Wird der Übergang  $\hbar \rightarrow 0$  formal durchgeführt, so werden für  $y$  und  $W$  wirklich die klassischen punktmechanischen Gleichungen erhalten.

Beide oben erwähnte Gesichtspunkte sind aber vollkommen formal, sowohl hinsichtlich ihres physikalischen Inhaltes wie auch betreffs ihrer mathematischen Beziehungen. Der Begriff des Grenzfalls hat nämlich nur dann einen

Sinn wenn er das Ergebnis eines gut definierten Grenzüberganges darstellt. Der Grenzübergang hingegen bedeutet einen stufenweisen Prozess, also ist die Interpretation des Grenzfalles dann nicht formal, wenn diese gleichzeitig eine stufenweise Überbrückung der exakten Theorie und jener, die den Grenzfall bildet, ist. Es ist offensichtlich, dass dieses Kriterium weder von a) noch von b) befriedigt wird. In diesen Fällen handelt es sich nicht um Grenzübergänge, sondern bloss um formale Analogien, die vom mnemotechnischen Gesichtspunkt aus sehr nützlich sind. Hingegen können sie nicht die theoretische Basis jener Untersuchungen bilden, die sich entweder auf die prinzipiellen Fragen der Quantenmechanik oder auf die von der klassischen Theorie ausgehenden Näherungsmethoden beziehen. Werden zum Beispiel in den Gleichungen (4) und (5) die Glieder die  $\hbar$  explizit enthalten, vernachlässigt so wird nicht der Grenzübergang  $\hbar \rightarrow 0$  durchgeführt, dazu müsste nämlich die Abhängigkeit von  $\hbar$  von  $y$  bzw.  $W$  in Betracht gezogen werden. Wird diese Frage untersucht [1], so stellt sich heraus, dass  $y$  bzw.  $W$  an der Stelle  $\hbar = 0$  wesentliche Singularitäten haben, infolgedessen existiert der gesuchte Grenzwert nicht. Demgegenüber charakterisiert die Aussage, dass die relativistische Mechanik mittels des Übergangs  $c \rightarrow \infty$  in die klassische Mechanik übergeht, einen gut definierten und sinnvollen Prozess. Die klassische Mechanik nähert sich nämlich umso mehr der relativistischen Mechanik, je kleiner die in Rede stehenden Geschwindigkeiten im Verhältnis zu  $c$  sind. Weiterhin können die relativistischen Gleichungen wirklich nach Potenzen von  $\frac{v}{c}$  in Reihen entwickelt werden.

Das obige Problem behandelten wir deshalb so eingehend, weil es die prinzipielle Basis unserer weiteren Gedanken bildet.

2. Dem früher Gesagten scheinen jene Tatsachen zu widersprechen, die darauf hinweisen, dass Näherungsmethoden existieren, die von klassischen Überlegungen Gebrauch machen und die häufig die Ergebnisse der exakten wellenmechanischen Berechnungen zufriedenstellend zu reproduzieren fähig sind. Solche Näherungsmethoden sind die folgenden: die Bohrsche Theorie die W. K. B. Methode und das statistische Atommodell. Im der erwähnten Arbeit [1] des Verfassers wurde zum Teil schon darauf hingewiesen, dass diese Näherungsmethoden von den mit dem Übergang  $\hbar \rightarrow 0$  verbundenen Erklärungen unabhängig gemacht werden können. Diesbezüglich wurde dort ein ebenfalls klassisches Modell der Wellenmechanik angewandt, dessen Grundgedanken aus den früheren Arbeiten von L. DE BROGLIE [2] und L. A. YOUNG [3] genommen wurden. Das Modell hingegen wurde keiner eingehenden Untersuchung unterworfen, infolgedessen blieben mehrere Fragen unbeantwortet. Auch wurden die Anwendungsmöglichkeiten nicht vollkommen ausbeutet. Im weiteren soll versucht werden, gerade die obigen Lücken auszufüllen.

Es ist wohlbekannt, dass L. DE BROGLIE [2] bei der Untersuchung der Möglichkeiten der kausalen Interpretation der Wellenmechanik das Verhältnis zwischen der Schrödinger-Gleichung und der klassischen Mechanik in folgender Form angegeben hat: Es werde die Schrödinger Gleichung

$$\frac{\hbar}{i} \frac{\partial \Phi}{\partial t} - \frac{\hbar^2}{2m} \Delta \Phi + U\Phi = 0 \quad (6)$$

betrachtet und es werde geprüft welche Beziehungen hinsichtlich der Amplituden ( $\psi$ ) der komplexen Wellenfunktion  $\Phi$  und der Phase ( $S$ ) gültig sind. Da

$$\Phi = \psi \exp \frac{i}{\hbar} S, \quad (7)$$

so werden aus (6) die folgenden zwei reellen Gleichungen erhalten:

$$\frac{\partial S}{\partial t} + \frac{1}{2m} (\nabla S)^2 + U - \frac{\hbar^2}{2m} \frac{\Delta \psi}{\psi} = 0, \quad (8)$$

$$\frac{\partial \psi^2}{\partial t} + \frac{1}{m} \operatorname{div} (\psi^2 \nabla S) = 0, \quad (9)$$

wo laut der Bornschen Hypothese

$$\psi^2 = \rho \quad (10)$$

die Wahrscheinlichkeitsdichte und  $\nabla \frac{S}{m}$  die Geschwindigkeit der Wahrscheinlichkeitsströmung ist.

Die Gleichung (8) entspricht hinsichtlich ihrer Form der Hamilton—Jacobischen Gleichung der Punktmechanik mit dem Unterschied, dass in ihr auch das »Quantenpotential«

$$U_{qu} = -\frac{\hbar^2}{2m} \frac{\Delta \psi}{\psi} \quad (11)$$

auftritt. Gleichzeitig ist (9) die durch (10) definierte Kontinuitätsgleichung der Dichteverteilung. Sieht man davon ab, welche prinzipiellen Interpretationen den Gleichungen (6)—(11) gegeben werden können und ohne irgendeine Anschauung hinsichtlich der Richtigkeit einer derselben zu vertreten, so kann die mit den Gleichungen in Verbindung bringbare Betrachtung klassischen Charakters doch in jedem Fall angewandt werden, in dem es sich um eine auf klassischen Grundlagen aufgebaute Näherung (also nicht um eine Interpreta-

tion) der Wellenmechanik handelt. Wird nun versucht, den bekanntgegebenen Formalismus auf das Energie-Eigenwertproblem anzuwenden, so stösst man auf folgende Schwierigkeiten:

Die Eigenfunktion, die zu einfachen Energieeigenwerten gehören, sind immer reell, wäre die Eigenfunktion nämlich komplex, dann wäre notwendigerweise zugleich auch ihre Konjugierte eine Eigenfunktion (von der sie linear unabhängig ist, im Gegensatz zu der Voraussetzung).

Im Falle von entarteten Problemen, wenn zu dem Eigenwert Eigenfunktionen ungerader Zahl gehören, ist von diesen mindestens eine aus ähnlichen Gründen unbedingt reell. Weiterhin ist es auch offensichtlich, dass die komplexen Eigenfunktionen konjugierte Paare bilden, aus denen reelle Eigenfunktionspaare konstruiert werden können. Ohne die Allgemeinheit zu beeinträchtigen, kann deswegen behauptet werden, dass die Eigenfunktionen immer reell sind. Um dies auch in der Bezeichnung zum Ausdruck zu bringen, seien die reellen Eigenfunktionen mit  $f$  bezeichnet. Dementsprechend ist die Schrödinger-Gleichung der Eigenwertprobleme die folgende:

$$\hbar^2 \Delta f + p^2 f = 0, \quad (12)$$

wo  $p$  der klassische Impuls ist. Die Schwierigkeit besteht darin, dass in Verbindung mit (12) die Substitution (7) keinen Sinn hat. Es ist gar kein prinzipiell begründbarer und in der Quantenmechanik verwurzelter Grund dazu vorhanden, die reelle Funktion  $f$  durch eine komplexe Funktion  $\Phi$  zu substituieren<sup>1</sup>. Von dem Gesichtspunkt der mit den Gleichungen (8) und (9) verbundenen dynamischen Anschauung bedeutet die Tatsache, dass  $f$  reell ist, soviel, dass das in Rede stehende Problem statischen Charakters ist. In diesem Fall ist nämlich die Wirkungsfunktion  $S$  vom Ort unabhängig, und der Wert des Impulses  $\nabla S$  ist gleich Null. Dementsprechend, da in der Gleichung (12)  $p^2 = 2m(E - U)$ , ist

$$E = U - \frac{\hbar^2}{2m} \frac{\Delta f}{f}, \quad (13)$$

d. h. die Energie besteht nur aus den zwei potentiellen Energien und enthält die kinetische Energie  $(\nabla S)^2/2m$  nicht. Dies hingegen entspricht weder der Bohrschen Theorie, noch der W. K. B. Methode oder der anschaulichen Auffassung des statistischen Atommodells. Diese Näherungsmethoden wenden nämlich ausdrücklich dynamische Anschauung an. Obzwar wir unser Verfahren auf diese Art prinzipiell nicht begründen können, wird die Abbildung auf ein

<sup>1</sup> Wir erhalten (12) aus (6) durch die Substitution

$$\Phi = f \exp \frac{i}{\hbar} (Et + \alpha),$$

welche die stationären Probleme charakterisiert, sodass also in (12) der exponentielle Faktor von  $\Phi$  nicht mehr vorkommt.



Problem von klassisch dynamischem Charakter der Gleichung (12) benötigt. Es kann nämlich nur auf diese Weise ein konsequentes (mathematisches) Verhältnis zwischen Wellenmechanik und Bohrscher Theorie aufgefunden werden. Es ist der Standpunkt der Zweckmässigkeit, der die Anwendung der Substitution (7) in Verbindung mit der Gleichung (12) begründet. Andererseits wäre es genau so berechtigt, nicht durch die komplexe Quantität (7) sondern zum Beispiel durch ein Quaternion oder auch durch hyperkomplexe Quantitäten von höherer Ordnung zu ersetzen. Im letzteren Fall würde man anstatt (12) nicht zwei, sondern vier, bzw. noch mehr reelle Gleichungen erhalten. Es bedarf keiner eingehenden Begründung, dass der physikalischen Realität solcher Abbildungen von dem Gesichtspunkt der konventionellen Mechanik jede Grundlage fehlt, jedoch kann das Verfahren vom praktischen Gesichtspunkt aus begründet sein, vorausgesetzt, dass man dadurch in den Besitz einer leicht handhabbaren Näherungsmethode gelangt.

Es sei der Energieausdruck (13), der zu dem Eigenwertproblem (12) gehört, in Betracht gezogen und der Ausdruck des hier vorkommenden »Quantenpotentials« so formal in zwei Teile zerlegt, dass der eine Teil formal als klassische kinetische Energie betrachtet werden kann. Es sei also

$$-\frac{\hbar^2}{2m} \frac{\Delta f}{f} = \frac{1}{2m} (\nabla S)^2 - \frac{\hbar^2}{2m} \frac{\Delta \psi}{\psi}, \quad (14)$$

wo  $\nabla S$  der »Impuls« ist, also

$$\frac{1}{2m} (\nabla S)^2 \quad (15)$$

die klassische kinetische Energie und

$$-\frac{\hbar^2}{2m} \frac{\Delta \psi}{\psi} \quad (16)$$

das »Quantenpotential« des zu interpretierenden dynamischen Modells. Da die Gleichung (14) das Verhältnis von  $S$  und  $\psi$  unbestimmt lässt, besteht die Möglichkeit der willkürlichen Hinzunahme noch eines Zusammenhanges. Es ist am zweckmässigsten,  $\psi^2$  auch jetzt als Dichte zu betrachten, so dass der fehlende Zusammenhang eben die Kontinuitätsgleichung

$$\operatorname{div} \psi^2 \nabla S = 0 \quad (17)$$

wird. Letzten Endes bedeutet dieses Verfahren, dass die statischen Eigen-



zustände, die durch reelle  $f$  charakterisiert sind<sup>2</sup>, durch Anwendung der Substitution

$$f \rightarrow \varphi = \psi \exp \frac{i}{\hbar} S \quad (18)$$

auf die »zugeordneten«, stationären Zustände, die durch die komplexe Wellenfunktion  $\varphi$  charakterisiert sind, abgebildet werden. Es sei nämlich in (12) an Stelle von  $f$  aus (18)  $\varphi$  substituiert, dann erhält man die Kontinuitätsgleichung (17) und die folgende dynamische Gleichung

$$E = U + \frac{1}{2m} (\nabla S)^2 - \frac{\hbar^2}{2m} \frac{\Delta \psi}{\psi}. \quad (19)$$

Das ist eigentlich eine Energiegleichung, deren Gradient die dynamische Gleichung ist.

Es ist sofort ersichtlich, dass die Abbildung von (12) auf die Gleichungen (17) und (19) nicht ein-eindeutig ist. Mit der Anwendung von weiteren Beschränkungen kann hingegen die Ein-Eindeutigkeit der Abbildung auch gesichert werden.

Die Gleichungen (17) und (19) sind formal die Gleichungen einer potentiellen Strömung, in welcher das in (16) hervorgehobene Energieglied die von der inneren Spannung herrührende Energie bedeutet. Die Dichte des »Mediums« ist

$$\rho = \varphi^* \varphi = \psi^2, \quad (20)$$

die sich offensichtlich stark von der Wahrscheinlichkeitsdichte des entsprechenden Eigenzustandes

$$v = f^2 \quad (21)$$

unterscheidet. Die Verallgemeinerung der Abbildung (18) auf einen nicht stationären Fall, wird so erhalten, dass die reelle Funktion die in (8) und (9) vorkommt, wieder durch eine komplexe Funktion substituiert wird. Wäre die gestellte Aufgabe, die Bohrsche Theorie, die W. K. B. Methode und das statistische Atommodell auf einen nicht-stationären Fall zu verallgemeinern, so müsste wirklich dieser Weg befolgt werden.

3. Es sei angenommen, dass im gegebenen Fall alle Lösungen von (17) und (19) bekannt sind. Die Frage ist, auf Grund welcher Kriterien werden

<sup>2</sup> In den Fällen, in denen die Eigenfunktionen auch komplex sein können, dürfte die hier erwähnte Schwierigkeit dadurch vermieden werden, dass von der Erzeugungsmöglichkeit der Eigenfunktionen in reelle Form abgesehen wird. Jedoch in allen Fällen, wenn zu dem Energieeigenwert eine ungleiche Zahl von Eigenfunktionen gehört, ist der Auftritt bestimmter reellen Eigenzustände notwendig. Die reellen Eigenzustände haben also immer einen Sinn; ohne Beeinträchtigung der Allgemeinheit kann deswegen behauptet werden, dass die Energieeigenfunktionen  $f$  reell sind. Die reellen Eigenzustände entsprechen stehenden Wellen.

unter den Lösungen jene  $\psi$  und  $S$  ausgewählt, aus welchen die Eigenfunktionen konstruiert werden können. Weiter muss auch auf die Frage geantwortet werden, auf welche Weise die Eigenfunktion  $\psi$  und  $S$  konstruiert werden kann. Diese letztere Frage kann sogleich beantwortet werden. Da  $\varphi$  und  $\varphi^*$  gleichfalls Lösungen von (12) sind, ist die reelle  $f$  Funktion

$$f = \frac{1}{2}(\varphi + \varphi^*) = \psi \cos \frac{1}{\hbar} S \quad (22)$$

ebenfalls eine Lösung, die bei geeigneten  $S$  und  $\psi$  eindeutig normierbar und zweimal differenzierbar ist und im Inneren des Bereiches über eine vorgeschriebene Anzahl von Nullstellen verfügt. Wenn wir wirklich solche  $\psi$  und  $S$  finden können, dann sind die  $f$  Eigenfunktionen. Da die Gleichung (17) zwischen  $\psi$  und  $S$  ein bestimmtes Verhältnis vorschreibt, kann  $f$  gemäss (22) schon auf Grund einer geeigneten  $S$  auferlegten Forderung zur Eigenfunktion erklärt werden. Die allgemeine Behandlung der Frage im Falle von mehrdimensionalen Problemen ist aus mathematischen Gründen zu kompliziert, deswegen wird hier eingehend nur das eindimensionale Problem behandelt. Aus (17) erhält man

$$u = \frac{dS}{dx} = \frac{a^2}{\psi^2}, \quad \psi^2 \frac{dS}{dx} = a^2 = \text{konst.}, \quad \psi = \frac{a}{u^{1/2}}, \quad (23)$$

also

$$f = \frac{a}{u^{1/2}} \cos \frac{1}{\hbar} \left( \int u dx + \delta \right), \quad (24)$$

$$f = \frac{a}{S^{1/2}} \cos \frac{1}{\hbar} (S + \delta).$$

Falls  $S$  die Lösung der Gleichungen (17) und (19) ist, dann ist  $S$  einwertig und dreimal differenzierbar, falls  $f$  ebenfalls einwertig und zweimal differenzierbar ist. Die Normierbarkeit von  $f$  und die Forderung, dass es im inneren des Bereiches über eine gegebene Anzahl von Nullstellen verfüge ( $k$ -te Lösung mit  $k-1$  Nullstellen), kann dadurch befriedigt werden, dass laut L. A. YOUNG [3] die folgende Quantenbedingung auferlegt wird:

$$\int u dx = k\hbar\pi. \quad (25)$$

Diese Quantenbedingung bedarf in bestimmten Fällen einer Modifizierung. (Die Korrektur und die wellenmechanische Begründung von (25) wird an einer anderen Stelle behandelt.)

4. Man sieht, dass die Gleichungen (17)–(19) in sich zur Charakterisierung des quantenmechanischen Eigenwertproblems noch nicht geeignet sind. Hingegen sind die Gleichungen, die durch dieses klassische Modell charakterisiert werden, entsprechend gequantelt zur Beschreibung der Energieeigen-

wertprobleme geeignet. Es ist offensichtlich, dass dies die Verallgemeinerung der Bohrschen Theorie ist. Gemäss dieser Auffassung ergibt sich also das durch die Gleichung (12) charakterisierte Eigenwertproblem als die Verallgemeinerung der Bohrschen Theorie. Das bedeutet hingegen, dass die Wellenmechanik näher nicht durch die Gleichungen (17)–(19), sondern durch die von diesen nicht herrührenden und separat zu postulierenden Quantelungsregeln charakterisiert ist.

Der Übergang von der klassischen Mechanik zu der Wellenmechanik besteht also aus den folgenden Schritten :

a)

$$E = \frac{1}{2m} (\nabla S)^2 + U. \quad (19')$$

Die obige Hamilton—Jacobi-Gleichung wird durch das Quantenpotential (16) ergänzt zu

$$E = \frac{1}{2m} (\nabla S)^2 + U - \frac{\hbar^2}{2m} \frac{\Delta \psi}{\psi}. \quad (19)$$

b)  $\psi^2$  werde in (19) als eine Dichtefunktion betrachtet und zu (19) die Kontinuitätsgleichung (17) hinzugefügt :

$$\operatorname{div} (\psi^2 \nabla S) = 0. \quad (17)$$

c) Die Gleichungen (17) und (19) können mit der Ableitung der komplexen Funktion

$$\varphi = \psi \exp \frac{i}{\hbar} S \quad (18)$$

zu einer Wellengleichung zusammengefasst werden :

$$\hbar^2 \Delta \varphi + p^2 \varphi = 0. \quad (26)$$

d) Der erste Schritt der Quantelung besteht darin, dass die Wellen  $\varphi$  und  $\varphi^*$  miteinander interferieren und so entsteht die stehende Welle :

$$f = \psi \cos \frac{1}{\hbar} (S + \delta).$$

e) Der zweite Schritt der Quantelung schreibt die Anwendung der Quantenbedingung (25) vor.

Die Wellenmechanik unterscheidet sich also in drei charakteristischen Punkten von der klassischen Statistik : in der Anwendung des Quantenpoten-

tials, in der Interferenz und in der Phasenquantelung. Der Umstand, dass in der Wellenmechanik das Quantenpotential (16) am wenigsten charakteristisch ist, wird durch folgende Tatsache nachgewiesen. Es gibt solche Potentiale  $U$ , zu denen Quantenpotentiale von konstanten Werten gehören

$$-\frac{\hbar^2}{2m} \frac{\Delta\psi}{\psi} = E_0 = \text{konst.} \quad (27)$$

In diesem Falle charakterisieren die Gleichungen (17)–(19) ein vollkommen klassisches Problem, aus welchem durch die Anwendung der zwei Quantenbedingungen (die Interferenz und die Phasenquantelung) die exakte Lösung des betreffenden wellenmechanischen Eigenwertproblems erhalten wird. Mit dem Fallenlassen der Quantenbedingungen lassen wir hingegen das Eigenwertproblem selbst fallen.

Es seien alle möglichen Lösungen von (27) in Betracht gezogen und es seien die als Lösung erhaltenen  $\varphi$  in die Gleichung (17) substituiert und die zu den einzelnen  $\varphi$  gehörenden  $S$  bestimmt.

Die erhaltenen Lösungen  $S$  seien in (19) substituiert, dann gibt das auf diese Art erhaltene Verhältnis von  $U$  und  $E$  darüber Auskunft, welche Probleme bei Behandlung gemäss der Bohrschen Theorie und der Wellenmechanik zu analogen Ergebnissen führen.

5. Es seien einige charakteristische Eigenschaften des »Impulses«  $u$  und der »Wirkungsfunktion«  $S$  untersucht.  $u$  kann mit Hilfe von  $f$  folgendermassen ausgedrückt werden.

Es werde die Variable

$$Z = \cos \frac{1}{\hbar} \left( \int u dx + \delta \right) \quad (28)$$

eingeführt. Dann erhält man einerseits aus (24)

$$u = \frac{a^2}{f^2} Z^2, \quad (29)$$

andererseits aus (29)

$$\frac{1}{\hbar} \left( \int u dx + \delta \right) = \arccos Z, \quad (30)$$

$$u = -\hbar \frac{Z'}{\sqrt{1-Z^2}}.$$

Wird  $u$  aus (29) und (30) eliminiert, so bekommt man bezüglich die folgende Differentialgleichung

$$\frac{a^2}{f^2} = -\hbar \frac{Z'}{\sqrt{1-Z^2}}, \quad (31)$$

welche durch Separierung der Variablen einfach integriert werden kann

$$\int \frac{a^2}{f^2} dx = \hbar \frac{\sqrt{1-Z^2}}{Z},$$

$$Z^2 = \frac{1}{1 + \left( \frac{1}{\hbar} \int \frac{a^2}{f^2} dx \right)^2}, \quad (32)$$

und so aus (29)<sup>3</sup>

$$u = \hbar \frac{\frac{c^2}{f^2}}{1 + \left( \int_{x_0} \frac{c^2}{f^2} dx \right)^2}, \quad c^2 = \frac{a^2}{\hbar} \quad (33)$$

weiterhin

$$S = \hbar \arctg \int_{x_0} \frac{c^2}{f^2} dx + S_0. \quad (34)$$

In erster Linie ist es auffallend, dass  $c$  und  $x_0$  vollkommen willkürliche Konstanten sind, d. h. die Gültigkeit der Quantenbedingungen (25) hängt nur davon ab, welche Werte  $f$  an den Grenzen annimmt und wie oft es im Inneren des Bereiches zu Null wird. Die Quantenbedingung (25) ist für unendlich viele Wertepaare  $x_0, c$  erfüllt, so dass unendlich viele  $S$  bzw.  $u$  existieren, von welchen ein jedes dieselbe Eigenfunktion  $f$  erzeugt. Dementsprechend können zu einem gegebenen  $p^2$  unendlich viele  $u^2$  zugeordnet werden. In dem Bereich, in welchem  $p^2 > 0$ , gehört zu jedem  $x$  ein solches  $u$ , dass an dieser Stelle

$$u(\bar{x}) = p(\bar{x}). \quad (35)$$

Ein anderer wichtiger Umstand ist, dass  $u$  laut der Gleichung (33) eine definite Funktion ist. (Sie kann hingegen an den Endepunkten auch Null sein, falls aber die Endpunkte unendlich entfernte Punkte sind, dann ist sie dort notwendigerweise Null.) Hingegen ist  $p$  nicht einmal überall reell. Eben deshalb ist es zweckmässiger,  $u^2$  und  $p^2$  zu vergleichen. Solange  $u^2$  überall positiv ist, ist  $p^2$  ausserhalb des klassischen Bahngebietes negativ. Dieser Umstand weist darauf hin, dass es nicht am vorteilhaftesten ist  $u$  durch  $p$  anzunähern. Es ist viel nützlicher  $u$  durch eine solche Funktion  $P$  anzunähern, die gequantelt werden kann und im allgemeinen über dieselben qualitativen Eigenschaften verfügt wie  $u$  [5].

<sup>3</sup> Bezüglich einiger speziellen Fälle hat auch I. LENTEI [4] den Zusammenhang (33) abgeleitet.

Betreffend die Zahl der Integrationskonstanten unterscheiden sich der quantenmechanische »Impuls«  $u$  und die »Wirkungsfunktion«  $S$  in bedeutendem Masse von ihrem klassischen Analogen.  $S$  enthält drei Integrationskonstanten von denen eine additiv ist, die anderen zwei hingegen sind  $x_0$  und  $c$ .  $u$  enthält zwei Integrationskonstanten  $x_0$  und  $c$ . Das ist selbstverständlich, da  $S$  durch die Gleichung dritter Ordnung

$$\hbar^2 \left[ \frac{3}{4} \left( \frac{S''}{S'} \right)^2 - \frac{1}{2} \cdot \frac{S'''}{S'} \right] + p^2 - S'^2 = 0, \quad (36)$$

$u$  hingegen durch die Gleichung zweiter Ordnung

$$\hbar^2 \left[ \frac{3}{4} \left( \frac{u'}{u} \right)^2 - \frac{1}{2} \frac{u''}{u} \right] + p^2 - u^2 = 0 \quad (37)$$

bestimmt ist. Dieser Umstand bedeutet eine unüberwindliche Diskrepanz zwischen der klassischen Punktmechanik und der Wellenmechanik. Man verfährt viel konsequenter, wenn  $\varphi$  als Potentialfunktion und (19) als die Gleichung einer potentiellen Strömung betrachtet wird. (Von diesem Gesichtspunkt ist es aber gleich, ob  $\varphi^2$  als eine Wahrscheinlichkeitsdichte oder als die Dichte eines imaginären »Mediums« betrachtet wird.)

Im ersten Augenblick erscheint der Gedanke, dass die erwähnten, unbestimmten Konstanten mit den verborgenen Parametern in Verbindung gebracht werden können, als gewinnend. Die zwei Dinge haben jedoch nichts miteinander zu tun. Nicht weil die vom Gesichtspunkt der Punktmechanik überflüssige Anzahl von Konstanten nicht durch ein klassisch mechanisches Modell interpretiert werden könnte, dies würde nämlich eben den Überschuss bedeuten um den die Quantenmechanik vom physikalischen Gesichtspunkt aus komplizierter ist als die klassische Mechanik. Der Umstand, dass in der Quantenmechanik die Messangaben und die Eigenwerte zusammenfallen, zieht notwendigerweise (wie es von NEUMANN bewiesen wurde) die Unmöglichkeit der verborgenen Parameter nach sich. Solange also die mathematische Modellierung des quantenmechanischen Messbegriffes sich nicht entsprechend ändert, ist es ein Unsinn, den Gedanken der Möglichkeit der verborgenen Parameter aufzuwerfen.

6. Die laut (22) und (25) quantelten Lösungen der Gleichungen (17) und (19) liefern die Lösung der Eigenwertprobleme (12). Es ist also gelungen, durch Anwendung der erwähnten Gleichungen und Quantenbedingungen dem wellenmechanischen Energieeigenwertproblem ein anschauliches Modell zuzuordnen. Es besteht aber die Frage, ob dieses Bild klassischen Charakters für alle quantenmechanischen Probleme angenommen werden kann. Offensicht-



lich ist die Antwort verneinend. Es ist nämlich auffallend, dass hier das Äquivalent des klassischen Impulses  $p \setminus S$  ist, das formal auch ein klassischen Charakters ist, obzwar in der Wellenmechanik in Wirklichkeit dem klassischen Impuls der Operator

$$\frac{\hbar}{i} \frac{\partial}{\partial q}$$

entspricht; dies hingegen ist der klassischen Anschauung vollkommen fremd. Eben deshalb ist es bedenklich, die Operatoren und die bezüglichen Kommutationsverhältnisse ohne Kritik in den Hintergrund zu schieben.

Es wird sofort ersichtlich, dass bei den Energieeigenwertproblemen die Schwierigkeit durch die Anwendung des Quantenpotentials eliminiert wird, hingegen ist dies bei anderen Eigenwertproblemen nicht der Fall (bzw. wird sie durch andere Quantenpotentiale behoben). Es sei zum Beispiel der Erwartungswert des zu  $x$  gehörenden Impulsoperators gebildet; dann erhält man die folgende Gleichung

$$\frac{\hbar}{i} \int \varphi^* \frac{\partial \varphi}{\partial x} dv = \frac{\partial S}{\partial x}. \quad (38)$$

Weiterehin ergibt sich der Erwartungswert des Operators der kinetischen Energie zu

$$-\frac{\hbar^2}{2m} \int \varphi^* \Delta \varphi dv = -\frac{\hbar^2}{2m} \left( \frac{\Delta f}{f} \right) = -\frac{\hbar^2}{2m} \left( \frac{\Delta \psi}{\psi} \right) + \frac{1}{2m} (\nabla S)^2. \quad (39)$$

Im Falle der Anwendung der Operatoren wird also das Quantenpotential formal als eine kinetische Energie betrachtet. Die einheitliche Behandlung der zwei Energieglieder kann jedoch nur durch Einführung des Impulsoperators durch die angewandte spezielle quantenmechanische Mitteilung realisiert werden. Dadurch, dass in der Gleichung (19) dreierlei Energien eine Rolle spielen, wird die Darstellung der Operatoren formal vermeidbar, hingegen kann bei anderen Problemen keine Äquivalenz zwischen den beiden Behandlungen bestehen. Je nach dem, um welches Eigenwertproblem und um welche Grösse es sich handelt, müssen verschiedene (aufeinander nicht zurückführbare) physikalische Grössen zur Aushilfe eingeführt werden. Ein Modell klassischen Charakters kann also dem Eigenwertproblem einer jeden Grösse zugeordnet werden. Diese Modelle ändern sich hingegen von Grösse zu Grösse und folgen nicht auseinander.

Der folgende Vergleich beleuchtet das Gesagte noch besser. Es ist bekannt, dass die Gleichungen der klassischen Hydrodynamik auch statistisch interpretiert werden können. In diesem Falle bedeutet die Flüssigkeitsdichte

(entsprechend normiert) die Wahrscheinlichkeitsdichte eines auserwählten Moleküls, die Geschwindigkeit der Flüssigkeit hingegen der Erwartungswert der Geschwindigkeit des Moleküls (an gegebenem Ort und zu gegebener Zeit). Im einfachsten Fall, dem Fall einer potentiellen Strömung ohne innere Reibung, ist das Wahrscheinlichkeitsverhalten des auserwählten Moleküls durch die folgenden Gleichungen charakterisiert:

$$U + P(\varrho) + \frac{1}{2m} (\nabla S)^2 = E, \quad (40)$$

$$\operatorname{div}(\varrho \nabla S) = 0. \quad (41)$$

Auch hier kommen dreierlei Energien vor, jedoch kann durch die Einführung eines Operators  $\bar{p}$  formal erzielt werden, dass nur kinetische und potentielle Energien zu behandeln sind. Der Operator muss so bestimmt und eine spezielle Mittelungsmethode so interpretiert werden, dass

$$\bar{p} = \overline{\nabla S} \quad (42)$$

und

$$\frac{1}{2m} \bar{p}^2 = \overline{P(\varrho)} + \frac{1}{2m} \overline{(\nabla S)^2} \quad (43)$$

wird. Von dem Gesichtspunkt der angewandten Anschauung klassischen Charakters geschieht in der Wellenmechanik bei der Einführung der Schreibweise der Operatoren genau dasselbe. Vom Gesichtspunkt der Hydrodynamik ist die Darstellung der Operatoren nur ein leerer Formalismus. In Fällen, wenn zur praktischen Lösung der hydrodynamischen Probleme die wellenmechanischen Analogien eine Hilfe gewährleisten können (z. B. die Erweiterung von wellenmechanischen Näherungsmethoden in die Hydrodynamik) kann das Verfahren unbedingt auch annehmbar und von Nutzen sein.

Es sei zum Schluss bemerkt, dass sowohl die in der Wellenmechanik anwendbaren Bilder klassischen Charakters und auch die in der Hydrodynamik anwendbaren Bilder quantenmechanischen Charakters nur auf je einen Problembereich angewandt werden können. Das ist eine natürliche Folge davon, dass sich die Erwartungswerte der Potenzen von

$$\frac{\hbar}{i} \frac{\partial}{\partial q} \quad \text{und} \quad \frac{\partial S}{\partial q}$$

und

$$\dagger \quad \text{und} \quad \nabla S$$

notwendigerweise voneinander unterscheiden.

Durch das Gesagte wird die Gültigkeitsgrenze des Modells klassischen Charakters, das durch die Gleichungen (17) und (19) charakterisiert ist, sowie jene der Näherungsmethoden, die auf dieses Modell aufgebaut sind, klar bestimmt. Die Bohrsche Theorie, die W. K. B. Methode und das statistische Atommodell sind nur zur annähernden Lösung der wellenmechanischen Energieeigenwertprobleme und der damit lösbaren anderen Probleme geeignet. Wenn also das Ziel die annähernde Behandlung eines sich auf eine andere physikalische Grösse beziehenden Problemenkreises wäre, dann müssten wir die erwähnten Näherungsmethoden entsprechend modifizieren.

### LITERATUR

1. I. FÉNYES, Acta Phys. Hung., **4**, 133, 1954.
2. L. DE BROGLIE, Einführung in die Wellenmechanik, Leipzig AVG. 1929.
3. L. A. YOUNG, Phys. Rev., **38**, 1612, 1931.
4. I. LENTEI, Acta Phys. Hung., **5**, 353, 1955.
5. I. FÉNYES, Acta Phys. Hung., **5**, 229, 1955.

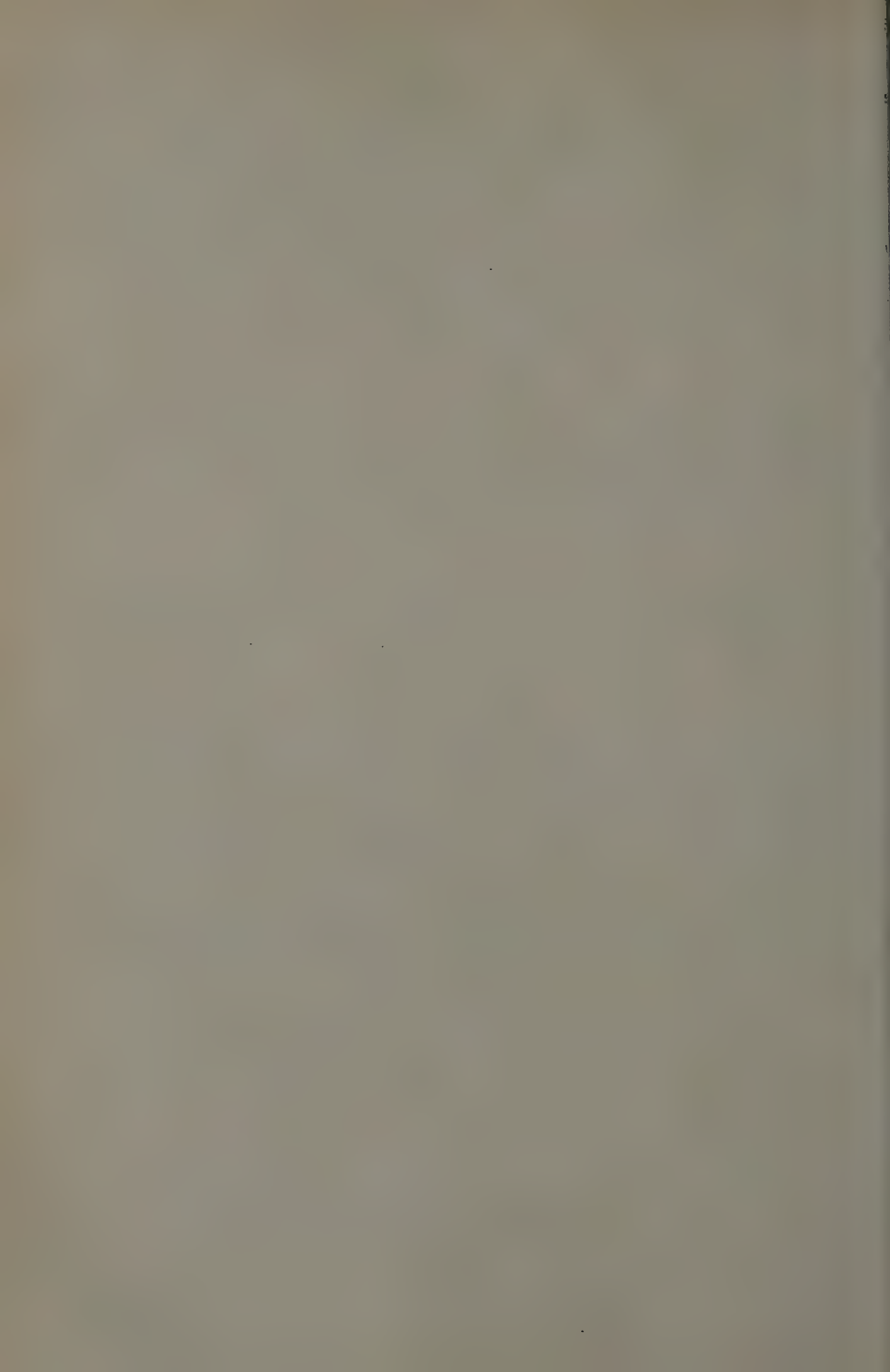
### О СООТНОШЕНИИ МЕЖДУ КВАНТОМЕХАНИЧЕСКОЙ ПРОБЛЕМОЙ СОБСТВЕННЫХ ЗНАЧЕНИЙ ЭНЕРГИИ И КЛАССИЧЕСКОЙ МЕХАНИКОЙ

И. ФЕНЕШ

#### Резюме

Главной целью работы является выяснение математических соотношений между двумя теориями и принципиальное обоснование квантовомеханических методов приближения, исходящих из классических основ. При этом, однако, касаются некоторых принципиальных вопросов классического обоснования квантовой механики.

1. Проблема собственных значений энергии вообще не имеет классического предельного случая.
2. Преобразование проблемы собственных значений энергии в модель классического характера. Трудности классической интерпретации состояний с реальными собственными функциями. Формальное решение трудностей.
3. Взаимная однозначность преобразований.
4. Квантовая механика, как обобщение теории Бора.
5. Некоторые характеристические свойства «импульса» и «функции действия»  $S$ .
6. Пределы модели классического характера; аналогия со статистической интерпретацией гидродинамики.



# $\hbar$ -QUANTIZATION OF THE FREE, BILOCAL BOZON FIELD

By

G. PÓCSIK

INSTITUTE FOR THEORETICAL PHYSICS, SZEGED

(Presented by K. F. Novobátzky. — Received: VIII. 9. 1957)

The relation of RAYSKI's systematization theory of elementary particles with the higher-spin theory of FIERZ offers a possibility for the  $\hbar$ -quantization of the free, bilocal bozon field. We introduce a relativistic invariant  $D$ -function, the properties of which are also dealt with. Finally the problems arising when taking into consideration isospaces are discussed.

## § 1. Introduction

In the quantized field theory of non-local and bilocal fields — similar to the case of local quantum field theory — the fields are characterized by field quantities, which satisfy certain commutation relations.

In the non-local field theory such commutation relations may be obtained also with the quantization method [1] used by SCHWINGER. This method serves as a basis in non-local field theory for the working out [2] of a quasi-canonical quantization procedure. Thus we succeed in ensuring validity of the usual canonical commutation relations at least on the space-like hypersurface limiting the region (in which the form factor is interpreted).

The problem is even more complicated in the bilocal field theory i. e. we have to go over already from the local field theory into the bilocal field theory by quantization. The reason for this so-called  $l$ -quantization is to be found in the fact that the field quantities depend also on the displacement operator [3]. In the bilocal quantum theory of fields the field quantities will be double operators, i. e.  $l$ -quantized field operators and quantities which are subject to the Bose-Einstein resp. Fermi-Dirac quantization.

Since the canonical quantization procedure cannot be directly applied, it seems advisable to search for direct methods.

The quantization rules of the YUKAWA theory were given by BLOCH [4] so as to obtain, after carrying out the usual integrations, the corresponding commutation relations of the local field theory.

RAYSKI proceeded in an essentially similar way [5] in the case of the bilocal particle of spin  $1/2$  starting from an equation [6] type YUKAWA.

The quantization of RAYSKI's theory can be given on the basis of the relation [3] with the higher-spin theory of FIERZ.

Owing to the fact that also YUKAWA's theory is connected with that of FIERZ [7] the computations can be repeated also in this case with due modification. Further on we deal with free particles of integer spin. As a matter of course the method can be applied also to particles of half integer spin. In § 2 the commutation relations will be deduced and the results obtained discussed, whereas in § 3 the iso-field will be dealt with.

## § 2. The $\hbar$ -quantization of the bilocal bozon field

Let us denote by  $\varphi(x, r)$  the wave function of the free, bilocal bozon field.  $\varphi(x, r)$  satisfies the generalized Schrödinger-Gordon equation completed by the reaction force [3]

$$\left\{ \nabla_{\mu\mu} + 4a^4 (\bar{\nabla}_{\mu\mu} + \frac{l^4}{r_0^2} \nabla_{\mu} \bar{\nabla}_{\mu} - L^2(r) \right\} \varphi(x, r) = 0, \quad (1)$$

where  $a$  is the constant characterizing the family;

$$L^2(r) = \frac{1}{r_0^2} (r_{\mu} r_{\nu} \bar{\nabla}_{\mu} \bar{\nabla}_{\nu} + 2 r_{\mu} \bar{\nabla}_{\mu})$$

is the invariant generalization of the Laplace-operator's radial part and

$$\nabla_{\mu \dots \nu} = \nabla_{\mu} \dots \nabla_{\nu}, \quad \nabla_{\mu} = \frac{\partial}{\partial x_{\mu}}; \quad \bar{\nabla}_{\mu \dots \nu} = \bar{\nabla}_{\mu} \dots \bar{\nabla}_{\nu}, \quad \bar{\nabla}_{\mu} = \frac{\partial}{\partial r_{\mu}}.$$

Let us consider the infinite series of the local (tensor or pseudo-tensor) FIERZ fields  $\varphi(x)$ ,  $\varphi_{\mu_1}(x)$ , ... The tensor or pseudotensor  $\varphi_{\mu_1 \dots \mu_n}(x)$  with index  $n$  describes the particle of integer spin  $n$  and has the following properties

$$\begin{aligned} a) \quad & \varphi_{\dots \mu \dots \nu \dots}(x) = \varphi_{\dots \nu \dots \mu \dots}(x), \\ b) \quad & \nabla_{\mu} \varphi_{\dots \mu \dots}(x) = 0, \\ c) \quad & \varphi_{\dots \mu \dots \mu}(x) = 0, \\ d) \quad & (\nabla_{\mu\mu} - M_n^2) \varphi_{\mu_1 \dots \mu_n}(x) = 0, \end{aligned} \quad (2)$$

where  $M_n$  is the mass of the particle of spin  $n$ .

The relation with the FIERZ theory manifests itself in that the wave function

$$\varphi(x, r) = \varphi(x) + \sum_{n=1}^{\infty} \varphi_{\mu_1 \dots \mu_n}(x) r_{\mu_1} \dots r_{\mu_n} \quad (3)$$



satisfies equation (1) and that we obtain for the mass of the particle with spin  $n$

$$M_n = a l^{-1} (4n(n+1))^{1/4} = M_1 \left( \frac{n(n+1)}{2} \right)^{1/4}. \quad (4)$$

It can be shown that also equations

$$\begin{aligned} a) \quad & \bar{\nabla}_{\mu\mu} \varphi(x, r) = 0, \\ b) \quad & \nabla_\mu \bar{\nabla}_\mu \varphi(x, r) = 0, \\ c) \quad & (\nabla_{\mu\mu} - 4a^4 L^2(r)) \varphi(x, r) = 0 \end{aligned} \quad (5)$$

are satisfied by (3).

It should be noted here that the individual FIERZ fields are unambiguously determined by  $\varphi(x, r)$ :

$$\begin{aligned} \varphi(x) &= \lim_{r_\mu \rightarrow 0} \varphi(x, r), \\ \varphi_{\mu_1 \dots \mu_n}(x) &= \frac{1}{n!} \lim_{r_\mu \rightarrow 0} \bar{\nabla}_{\mu_1 \dots \mu_n} \varphi(x, r). \end{aligned}$$

Corresponding formulae hold spinor fields.

In the quantized theory of fields  $\varphi(x)$ ,  $\varphi_\mu(x)$ , ... will be field operators, consequently also  $\varphi(x, r)$  will be one. Our task is to determine the commutation relations, i. e. the commutators  $[\varphi(x, r), \varphi(x', s)]$  and  $[\varphi(x, r), \varphi^*(x', s)]$  ( $s_\mu$  is not necessarily the same as  $r_\mu$ ).

First of all we show that

$$[\varphi(x, r), \varphi(x', s)] = [\varphi^*(x, r), \varphi^*(x', s)] = 0,$$

in complete accordance with the local field theory. I. e. owing to (3) for instance

$$\begin{aligned} & [\varphi(x, r), \varphi(x', s)] - [\varphi(x), \varphi(x')] + \sum_{n=1}^{\infty} \{ [\varphi(x), \varphi_{\mu_1 \dots \mu_n}(x')] s_{\mu_1} \dots s_{\mu_n} + \\ & + [\varphi_{\mu_1 \dots \mu_n}(x), \varphi(x')] r_{\mu_1} \dots r_{\mu_n} \} + \sum_{m,n=1}^{\infty} [\varphi_{\mu_1 \dots \mu_n}(x), \varphi_{\nu_1 \dots \nu_m}(x')] \cdot \\ & \cdot r_{\mu_1} \dots r_{\mu_n} s_{\nu_1} \dots s_{\nu_m}. \end{aligned}$$

Because every commutator should vanish in which field operators belonging to particles of different spins occur only the sum

$$\sum_{n=1}^{\infty} [\varphi_{\mu_1 \dots \mu_n}(x), \varphi_{\nu_1 \dots \nu_n}(x')] r_{\mu_1} \dots r_{\mu_n} s_{\nu_1} \dots s_{\nu_n}$$

remains. The commutators occurring in this, however, yield zero according to FIERZ.

We obtain in a quite similar way the equation

$$[\varphi(x, r), \varphi^*(x', s)] = [\varphi(x), \varphi^*(x')] + \sum_{n=1}^{\infty} [\varphi_{\mu_1 \dots \mu_n}(x), \varphi_{\nu_1 \dots \nu_n}^*(x')] r_{\mu_1} \dots r_{\mu_n} s_{\nu_1} \dots s_{\nu_n}. \quad (7)$$

The value of the commutators occurring in  $\Sigma$  are according to FIERZ [7] in the unit system  $\hbar = c = 1$ :

$$[\varphi_{\mu_1 \dots \mu_n}(x), \varphi_{\nu_1 \dots \nu_n}^*(x')] = -i D_{\mu_1 \dots \mu_n; \nu_1 \dots \nu_n} D^{(n)}(x - x'). \quad (8)$$

$D^{(n)}(x - x')$  is the relativistic invariant  $D$ -function of the particle of spin  $n$ . Whereas  $D_{\mu_1 \dots \mu_n}$  is a differential operator containing  $2k$ -times ( $k = n, \dots, 1$ ) differentiations.  $D_{\mu_1 \dots \mu_n}$  can be expressed by the operator

$$d_{\mu\nu}^{(n)} = \delta_{\mu\nu} - M_n^{-2} \nabla_{\mu\nu}, \quad (n = 1, \dots)$$

using the relation

$$D_{\mu_1 \dots \mu_n; \nu_1 \dots \nu_n} = \sum_{l=0}^{\left[\frac{n}{2}\right]} \sum_{(\mu\nu)} (-1)^l \frac{(2n-2l)!}{(2n)! l! (n-l)! (n-2l)!} \cdot d_{\mu_1 \mu_2}^{(n)} \dots d_{\mu_{2l-1} \mu_{2l}}^{(n)} d_{\nu_1 \nu_2}^{(n)} \dots d_{\nu_{2l-1} \nu_{2l}}^{(n)} \cdot d_{\mu_{2l+1} \nu_{2l+1}}^{(n)} \dots d_{\mu_n \nu_n}^{(n)}, \quad (9)$$

where  $\left[\frac{n}{2}\right]$  is the next integer number  $< \frac{n}{2}$  and  $(\mu, \nu)$  signifies the summation over all the permutatins of the indices  $\mu$  and  $\nu$ . Substituting (8) into (7) we obtain

$$[\varphi(x, r), \varphi^*(x', s)] = -i \left( D^{(0)}(x - x') + \sum_{n=1}^{\infty} D_{\mu_1 \dots \mu_n} D^{(n)}(x - x') r_{\mu_1} \dots r_{\mu_n} s_{\nu_1} \dots s_{\nu_n} \right). \quad (10)$$

The right hand side of (10) defines the relativistic invariant function  $D$

$$D(x - x', r, s) = D^{(0)}(x - x') + \sum_{n=1}^{\infty} D_{\mu_1 \dots \mu_n; \nu_1 \dots \nu_n} D^{(n)}(x - x') r_{\mu_1} \dots r_{\mu_n} s_{\nu_1} \dots s_{\nu_n} \quad (11)$$

of the bilocal particle family. The series (11) is convergent in the region where  $\varphi(x, r)$ ,  $\varphi^*(x', s)$  are defined.

The fundamental relativistic invariant commutation relations are given by (6) resp. (10) (11)

$$\begin{aligned} [\varphi(x, r), \varphi(x', s)] &= [\varphi^*(x, r), \varphi^*(x', s)] = 0, \\ [\varphi(x, r), \varphi^*(x', s)] &= -i D(x - x', r, s). \end{aligned} \quad (12)$$

By equation (12) the quantization rules of some higher spin fields are determined

$$\begin{aligned} D^{(0)}(x - x') &= \lim_{r_\mu \rightarrow 0} D(x - x', r, s) = \lim_{s_\mu \rightarrow 0} \dots = \\ &= \lim_{\substack{r_\mu \rightarrow 0 \\ s_\mu \rightarrow 0}} \dots \end{aligned}$$

$$\begin{aligned} D_{\mu_1 \dots \mu_n; \nu_1 \dots \nu_n} D^{(n)}(x - x') &= \lim_{r_\mu \rightarrow 0} (n!)^{-2} \bar{\nabla}_{\mu_1}^{(r)} \dots \bar{\nabla}_{\mu_n}^{(r)} \bar{\nabla}_{\nu_1}^{(s)} \dots \bar{\nabla}_{\nu_n}^{(s)} D(x - x', r, s) = \\ &= \lim_{s_\mu \rightarrow 0} \dots = \lim_{\substack{r_\mu \rightarrow 0 \\ s_\mu \rightarrow 0}} \dots \quad (n = 1, \dots) \end{aligned}$$

In the local field theory the commutation function satisfies the Schrödinger—Gordon equation. From (12) it can be seen but it is obtained also by calculation that for the commutation function must satisfy the equations (1) (5) written for variable pairs  $(x, r)$  and  $(x', s)$ .

The symmetry properties of the commutation function can be read off from (11). — The properties assumed by RAYSKI are in general satisfied,  $D(x, r, s)$  is however not symmetrical under the inversions  $r_\mu \rightarrow -r_\mu$  or  $s_\mu \rightarrow -s_\mu$ , but only under  $r_\mu \rightarrow -r_\mu$  and  $s_\mu \rightarrow -s_\mu$ .

It is evident that  $D(x, r, s) = 0$  is fulfilled for  $x_0 = 0$  only in an inertial system. Neither is  $(\nabla_0 D(x))_{x_0=0} = \delta(x)$  valid, but in an inertial system

$$\begin{aligned} (\nabla_0 D(x, r, s))_{x_0=0} &= (1 + A^{(1)}(r, s) + (A^{(2)}(r, s))^2 - \frac{1}{3} A^{(2)}(r, r) A^{(2)}(s, s) + \\ &+ \dots) \delta(x), \end{aligned}$$

where

$$A^{(n)}(r, s) = d_{\mu\nu}^{(n)} r_\mu s_\nu \quad (n = 1, \dots).$$

### § 3. Considering the isobar spin field

PAIS was the first, who in 1953 called attention to an other variant of the "bilocal" field theory [8], which applies the isobar spin field ( $u$ -field) instead of the  $r$ -field. The theory in its present form [9] further developed PAIS'ideas.

In a more complete theory the spin and isospin dependences have to be considered simultaneously, i. e. in the above expressions also the  $u$ -field should be taken into account.

The Bose-Einstein quantization of a theory of such two auxiliary fields can be given by the rule

$$[\varphi(x, r, u) \varphi^*(x', s, u')] = -i \delta(u - u') D(x - x', r, s). \quad (13)$$

All the other commutators vanish.

The general characteristics of such a general field theory are the following.

1. The spin rotator and isotor character of an elementary particle are considered simultaneously.

2. The total angular momentum is composed of three parts: I. orbital momentum in the  $x$ -field+spin momentum, II. orbital momentum in the  $r$ -field [10], III. orbital momentum in the  $u$ -field+isospin.

3. The total mechanical mass of the particle is quantized together by the orbital momenta of the  $r$ - and  $u$ -spaces.

4. Different values  $r$  and  $u$  are belonging to the spin rotator and to the isotor. It is a plausible assumption that  $r$  depends on the total mechanical mass, whereas  $u$  on its part depending on the isospace.

5. The spectrum of the total mechanical mass is denoted by two indices  $(a, n)$ . Both may be either integer or half-odd integer. By the first the spin  $(n)$ , whereas by the other  $(a)$  — with the 3-rd component of the isospin — the individual charge states are determined.

For a given  $n$  more  $a$ -s are possible and vice versa. The mass spectrum of the individual families is determined by an entity being at the lowest level.

6. For the determination of the number of particle families, families obtained in case of use of an  $r$ -resp.  $u$ -space have to be combined. There exist families 4 bib, 4 bif, 6 fif, 6 fibI., 6 fibII. (Hence there exist 8 bozon, 18 fermion families.) These are systematized by the order of field equations, the parity and by the attributum.

7. Refinement of the model is attained by the introduction of the field mass. Assuming that the field mass varies only per family the problem may be solved by introducing the field mass into the field equation.

It can be expected that in the elementary particle theory described in points 1—7 in case of interactions the strength of the effective coupling is in essential determined by that part of the field functions which depends on the auxiliary fields. The latter possibility has been pointed out by TANAKA [11], assuming a Fermi-type interaction.

I am indebted to Professors J. RAYSKI and J. I. HORVÁTH for their remarks.

## REFERENCES

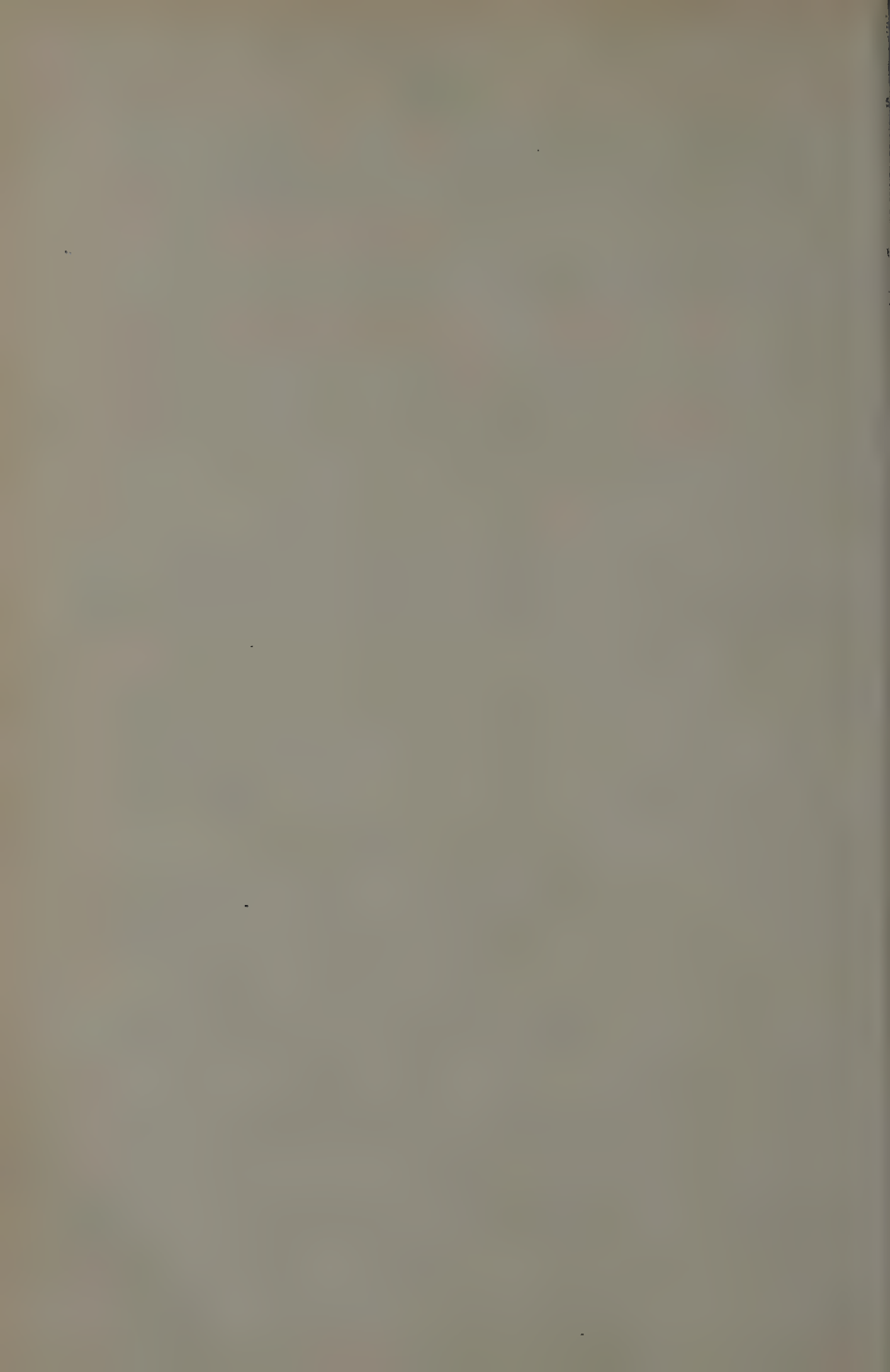
1. J. SCHWINGER, Phys. Rev., **82**, 914, 1951.
2. J. RAYSKI, Acta Phys. Pol., **13**, 15, 1954.
3. J. RAYSKI, Acta Phys. Pol., **14**, 337, 1955.
4. C. BLOCH, Mat.-Fys. Medd at Det. Kgl. Danske Videns. Sels., **26**, 5, 1950.
5. J. RAYSKI, Acta Phys. Pol., **11**, 109, 1952.
6. H. YUKAWA, Phys. Rev., **77**, 219, 1950.
7. M. FIERZ, Helv. Phys. Acta, **23**, 419, 1952.
8. A. PAIS, Physica, **19**, 869, 1953.
9. J. RAYSKI, Nuovo Cimento, **4**, 1231, 1956 ; **5**, 872, 1957 ; Acta Phys. Pol., **16**, 279, 1957.
10. G. PÓCSIK, Acta Phys. Hung., **8**, 277, 1958.
11. S. TANAKA, Nuovo Cimento, **5**, 1364, 1957.

 $\hbar$ -КВАНТОВАНИЕ СВОБОДНОГО, БИЛОКАЛЬНОГО ПОЛЯ  
ЧАСТИЦ БОЗЕ

дъ. почик

## Резюме

Связь между теорией систематики элементарных частиц Райского и теорией частиц с большим числом спинов Фирца, даем возможность  $\hbar$ -квантования свободного биллокального поля частиц Бозе. Вводится релятивистически инвариантная  $D$ -функция, и исследуются ее свойства. В конце работы, рассматриваются некоторые вопросы, связанные с учетом изо-пространства.





# FREE FIELD OPERATORS AND THE YANG-FELDMAN FORMALISM

By

K. L. NAGY

INSTITUTE OF THEORETICAL PHYSICS, ROLAND EÖTVÖS UNIVERSITY, BUDAPEST

(Presented by K. F. Novobátzky. — Received: XII. 30. 1957)

SCHWEBER's and POLKINGHORNE's calculations on the subject are simplified and to some extent generalized. Free fields having commutation relations in which the interaction effect is contained are defined. These fields are connected with the matrix elements of  $U[\sigma', \sigma]$ .

## Introduction

Many results of the recent developments of quantum field theory are due to the extensive use of the Heisenberg picture. YANG, FELDMAN [1] and KÄLLÉN [2] first formulated the relativistic field theoretical scattering theory in the Heisenberg picture. Starting from their formalism and especially from the results and methods developed by SCHWEBER [3], POLKINGHORNE [4] defined other free fields connected with the  $S$ -matrix having non-trivial commutation relations and thus containing the effects of the interaction.

Here we shall simplify and generalise these results. Commutation rules are derived between the fields  $\varphi_\sigma$  and  $\varphi_{\sigma'}$ , without using the interaction picture and free fields are defined which in special cases agree with those of POLKINGHORNE. These fields are connected with the matrix elements of  $U[\sigma', \sigma]$ . Keeping throughout to the Heisenberg picture in addition one gets simply the equation for the Heisenberg current operator obtained by CINI and FUBINI [5].

## The Yang-Feldman formalism

Consider for the sake of simplicity a neutral scalar field  $\varphi(x)$  interacting with a Dirac-field  $\psi(x)$ . The equation of motion and the commutation relations are in this case in the Heisenberg picture

$$(\square - \mu^2)\varphi(x) = j(x), \quad (1)$$

$$\left. \begin{aligned} [\varphi(x), \varphi(x')] &= i\hbar c \Delta(x - x'), \\ [\varphi(x), \psi(x')] &= \dots = 0, \end{aligned} \right\} (x - x')^2 > 0. \quad (2)$$

The general solution of (1) is the sum of the general solution of the homogeneous equation

$$(\square - \mu^2) \Phi(x) = 0 \quad (3)$$

and a particular solution of (1):

$$\varphi(x) = \int_{\sigma} \Delta(x-x') d_{\nu} \Phi(x') d\sigma_{\nu}(x') + \int_{-\infty}^{+\infty} \Delta^{(i)}(x-x') j(x') dx', \quad (4)$$

where

$$d_{\nu} = \left( \frac{\vec{\partial}}{\partial x_{\nu}} - \frac{\overleftarrow{\partial}}{\partial x_{\nu}} \right),$$

and  $\Delta^{(i)}(x)$  is any of the Green's functions satisfying

$$(\square - \mu^2) \Delta^{(i)}(x) = \delta(x). \quad (5)$$

In order to give meaning to the improper integrals we suppose the interaction adiabatically switched on and off at infinity. Demanding  $\varphi(x)$  to be equal on the arbitrary surface  $\sigma$  with a given  $\varphi(x)$  we obtain from (4)

$$\begin{aligned} \varphi(x) &= \int_{\sigma} \Delta(x-x') d_{\nu} \varphi(x') d\sigma_{\nu}(x') + \int_{-\infty}^{+\infty} \Delta_{\sigma}(x-x') j(x') dx' = \\ &= \varphi_{\sigma}(x) + \int_{-\infty}^{+\infty} \Delta_{\sigma}(x-x') j(x') dx', \end{aligned} \quad (6)$$

where

$$\Delta_{\sigma}(x-x') = \Delta^{(i)}(x-x') - \int_{\sigma} \Delta(x-x'') d_{\nu} \Delta^{(i)}(x''-x') d\sigma_{\nu}(x'') \quad (7)$$

is the YANG-FELDMAN Green function which is independent of the index  $i$  because  $\Delta^{(i)} - \Delta^{(j)}$  satisfies the free field equation. In consequence of (2) and (6)

$$\begin{aligned} (\square - \mu^2) \varphi_{\sigma}(x) &= 0, \\ [\varphi_{\sigma}(x), \varphi_{\sigma'}(x')] &= i\hbar c \Delta(x-x'), \\ \varphi_{\sigma}(x) &= u^{-1}[\sigma, \sigma'] \varphi_{\sigma'}(x) u[\sigma, \sigma']. \end{aligned} \quad (8)$$

$u$  is unitary and  $u[\sigma, \sigma] = 1$ . Denote  $\varphi_{in}(x) = \varphi_{-\infty}(x)$ ,  $\varphi_{out}(x) = \varphi_{+\infty}(x)$ .  $u[+\infty, -\infty] = S$ ,  $S$  is the  $S$ -matrix. Equation (6) gives

$$\varphi_{\sigma}(x) = \varphi_{\sigma'}(x) + \int_{-\infty}^{+\infty} \Delta_{\sigma\sigma'}(x-x') j(x') dx', \quad (9)$$

where

$$\begin{aligned} \Delta_{\sigma\sigma'}(x-x') &= \Delta_{\sigma'}(x-x') - \Delta_{\sigma}(x-x') = \left( \int_{\sigma} - \int_{\sigma'} \right) \Delta(x-x'') d_v'' \Delta^{(i)}(x''-x') d\sigma_v(x'') = \\ &= \begin{cases} = 0 & \text{if } x \notin (\sigma, \sigma'), \\ = \Delta(x-x') & \text{if } x \in (\sigma, \sigma'), \sigma \text{ is later than } \sigma', \\ = -\Delta(x-x') & \text{if } x \in (\sigma, \sigma'), \sigma \text{ is earlier than } \sigma'. \end{cases} \quad (10) \end{aligned}$$

In order to obtain commutation relations we determine first  $[j(x), \varphi(y)]$ . From (6) we obtain

$$\begin{aligned} [j(x), \varphi(y)] &= \int_{\sigma} \Delta(y-x') d_v' [j(x), \varphi(x')] d\sigma_v(x') + \\ &+ \int_{-\infty}^{+\infty} \Delta_{\sigma}(y-x') [j(x), j(x')] dx'. \end{aligned} \quad (11)$$

The commutator  $[j(x), \varphi(x')]$  is known from (2) if we choose such a surface  $\sigma$  which contains the point  $x$ , thus e. g. dropping the renormalization counter terms  $[j(x), \varphi(x')] = 0$ , retaining them

$$\int_{\sigma} \Delta(y-x') d_v' [j(x), \varphi(x')] d\sigma_v(x') = i\hbar c \Delta(y-x) (\delta\mu^2 + 3\lambda\varphi^2(x)).$$

In the following we neglect these trivial terms. Thus

$$[j(x), \varphi(y)] = \int_{-\infty}^{+\infty} \Delta_{\sigma}(y-x') [j(x), j(x')] dx', \quad x \in \sigma. \quad (12)$$

From (6), (12) and (10) we obtain

$$\begin{aligned} [j(x), \varphi_{\sigma'}(y)] &= \int_{-\infty}^{+\infty} \Delta_{\sigma'\sigma}(y-x') [j(x), j(x')] dx' = \\ &= \int_{\sigma'}^{\infty} \Delta(y-x') j(x') j(x) dx' + \int_{-\infty}^{\sigma} \Delta(y-x') j(x) j(x') dx' - \\ &- \int_{-\infty}^{+\infty} \Delta(y-x') P(j(x) j(x')) dx'. \end{aligned} \quad (13)$$

If  $\sigma' \rightarrow -\infty$ , (13) is the equation for the current operator obtained by CINI and FUBINI [5]. Now (8), (9) and (13) give

$$\begin{aligned} [\varphi_{\sigma''}(x), \varphi_{\sigma'}(y)] &= i\hbar c \Delta(x-y) + \\ &+ \int_{-\infty}^{+\infty} \int_{-\infty}^{+\infty} \Delta_{\sigma''\sigma'}(x-x') \Delta_{\sigma'\sigma}(y-x'') [j(x'), j(x'')] dx' dx'', \quad x' \in \sigma. \end{aligned} \quad (14)$$

We note that these commutation relations are derived without mentioning the interaction picture.

## Other free fields

We can define beside the YANG-FELDMAN fields  $\varphi_\sigma(x)$  other free fields which might be of some importance. The simplest ones are the superpositions of the  $\varphi_\sigma(x)$ -s with different indices. Thus we might define e. g.:

$$\varphi_{sym} = \frac{1}{2}(\varphi_{out} + \varphi_{in}),$$

$$\varphi_{rad} = \varphi_{out} - \varphi_{in}.$$

The commutation relations of these fields can be easily determined from (14)

$$\begin{aligned} [\varphi_{sym}(x), \varphi_{sym}(y)] &= i\hbar c \Delta(x-y) - \\ &- \frac{1}{4} \int_{-\infty}^{+\infty} \Delta(x-x') \Delta(y-x'') [j(x'), j(x'')] dx' dx'', \\ [\varphi_{rad}(x), \varphi_{rad}(y)] &= \int_{-\infty}^{+\infty} \Delta(x-x') \Delta(y-x'') [j(x'), j(x'')] dx' dx''. \end{aligned}$$

Beside these trivial fields we define field  $\varphi_{\sigma''\sigma'}(x)$ :

$$\begin{aligned} \varphi_{\sigma''\sigma'}(x) &= \varphi_{\sigma''}^{(+)}(x) + \varphi_{\sigma'}^{(-)}(x) = \\ &= \varphi_{\sigma'}(x) + \int_{-\infty}^{+\infty} \Delta_{\sigma''\sigma'}^{(+)}(x-x') j(x') dx' = \\ &= \varphi_{\sigma''}(x) + \int_{-\infty}^{+\infty} \Delta_{\sigma'\sigma''}^{(-)}(x-x') j(x') dx'. \end{aligned} \quad (15)$$

From (6) we obtain

$$\begin{aligned} \varphi(x) &= \varphi_{\sigma''\sigma'}(x) + \int_{-\infty}^{+\infty} \{\Delta_{\sigma'}(x-x') - \Delta_{\sigma''\sigma'}^{(+)}(x-x')\} j(x') dx' = \\ &= \varphi_{\sigma''\sigma'}(x) + \int_{-\infty}^{+\infty} \{\Delta_{\sigma''}(x-x') - \Delta_{\sigma'\sigma''}^{(-)}(x-x')\} j(x') dx'. \end{aligned} \quad (16)$$

The field  $\varphi_{\sigma''\sigma'}$  agrees with the  $\Phi^{F'}$ , the  $\varphi_{-\infty, +\infty}$  with the  $\Phi^F$  field of POLKINGHORNE [4]. From (14) and (15) we get

$$\begin{aligned} [\varphi_{\sigma''\sigma'}(x), \varphi_{\sigma'\sigma''}(y)] &= i\hbar c \Delta(x-y) + \\ &+ \int_{-\infty}^{+\infty} \int_{-\infty}^{+\infty} \{(\Delta_{\sigma''\sigma'}^{(+)}(x-x') + \Delta_{\sigma'\sigma''}^{(-)}(x-x')) \Delta_{\sigma'\sigma''}^{(+)}(y-x'') + \\ &+ (\Delta_{\sigma''\sigma'}^{(-)}(x-x') + \Delta_{\sigma'\sigma''}^{(+)}(x-x')) \Delta_{\sigma''\sigma'}^{(-)}(y-x'')\} [j(x'), j(x'')] dx' dx''. \end{aligned} \quad (17)$$

### Scattering theory

Before starting to study the scattering matrix elements we want to establish the connection between the interaction picture field and the fields  $\varphi_\sigma(x)$ . Operators in the interaction picture which agree with Heisenberg operators at the surface  $\sigma_0$  are defined as follows :

$$\begin{aligned}\Omega(x) &= U^{-1}[\sigma, \sigma_0] \Omega_i(x) U[\sigma, \sigma_0], & x \in \sigma, \\ U[\sigma, \sigma_0] &= P \exp \left( -\frac{i}{\hbar c} \int_{\sigma_0}^{\sigma} H_i(x) dx \right).\end{aligned}\quad (18)$$

These give in particular  $(\square - \mu^2) \varphi_i(x) = 0$ , thus

$$\varphi_i(x) = \varphi_{\sigma_0}(x). \quad (19)$$

Comparing (8) and (18), noting that  $\varphi(x) = \varphi_\sigma(x)$  if  $x \in \sigma$  and that  $u$  transforms also the  $\psi$  field in form (8), we conclude that  $u$  apart from an irrelevant number phase factor  $c$  equals  $U$ . Equations (8), (9), (18) and (19) lead to

$$\begin{aligned}\varphi_\sigma(x) &= \varphi_i(x) + \int_{-\infty}^{+\infty} \Delta_{\sigma\sigma_0}(x-x') j(x') dx' = \\ &= U^{-1}[\sigma, \sigma_0] \varphi_i(x) U[\sigma, \sigma_0],\end{aligned}\quad (20)$$

where  $x$  is arbitrary. Specialising  $\sigma_0 = 0$ ,  $\sigma = \pm \infty$  we have rederived SCHWEBER's formulae without having used detailed properties of  $U$ . From (20) it follows that  $\varphi_\sigma^{(+)}(x) U^{-1}[\sigma, \sigma_0] \Psi = 0$ , if  $\varphi^{(+)}(x) \Psi = 0$ .

From the above formalism we can write down the  $S$ -matrix elements in different closed forms. Now we study for the sake of simplicity the meson-nucleon scattering. Consider the matrix element of  $U[\sigma', \sigma]$  between the states  $\varphi_i^{(-)}(x) U[\sigma', \sigma] \Psi_a$  and  $\varphi_i^{(-)}(y) \Psi_b$  where  $\Psi$  describes a bare nucleon in the state  $a$  or  $b$ :  $\Psi_b = \psi^{(-)}(b) \Phi_0$ ,  $\Phi_0$  the bare vacuum thus  $\varphi_i^{(-)} \Psi_a = \varphi_i^{(-)} \Psi_b = 0$ . From (20)

$$\begin{aligned}U[\sigma', \sigma]_{ab} &= (U[\sigma', \sigma] \Psi_a, \varphi_i^{(+)}(x) U[\sigma', \sigma] \varphi_i^{(-)}(y) \Psi_b) = \\ &= (U[\sigma_0, \sigma] \Psi_a, \varphi_{\sigma'}^{(+)}(x) \varphi_{\sigma}^{(-)}(y) U[\sigma_0, \sigma] \Psi_b) = \\ &= (U[\sigma_0, \sigma] \Psi_a, [\varphi_{\sigma'}^{(+)}(x), \varphi_{\sigma}^{(-)}(y)] U[\sigma_0, \sigma] \Psi_b).\end{aligned}\quad (21)$$

Applying the commutation relation (14) we can explicitly write down this matrix element containing only  $j$ -s. Using instead of  $\varphi_\sigma$  and  $\varphi_{\sigma'}$  fields the  $\varphi_{\sigma, \sigma}$  field

$$U[\sigma', \sigma]_{ab} = (U[\sigma_0, \sigma] \Psi_a, [\varphi_{\sigma'}^{(+)}(x) \varphi_{\sigma}^{(-)}(y)] U[\sigma_0, \sigma] \Psi_b). \quad (22)$$

Relation (17) gives naturally just the same value for the commutator as (14) in (21). The state functions depend now on the choice of  $\sigma_0$ . We obtain the simplest matrix element if we choose  $\sigma_0 = \sigma$ . If  $\sigma \rightarrow -\infty$  the choice  $\sigma_0 = 0$  has also some advantages, for then

$$U[0, -\infty] \Psi_b = U^{-1}[-\infty, 0] \bar{\psi}_i^{(-)}(b) U[-\infty, 0] U[0, -\infty] \Phi_0 = \\ = \bar{\Psi}_{in}^{(-)}(b) \Psi_0,$$

where according to the results of GELL-MANN and Low [6]  $\Psi_0$  is apart from a (infinite) phase factor the state function describing the true vacuum. The single nucleon states are steady states, that is to say eigenstates of the  $S$ -matrix, therefore  $\varphi_i^{(+)}(x) U[+\infty, -\infty] \Psi_a \sim \varphi_i^{(+)}(x) \Psi_a$  and thus  $S_{ab}$  obtained from (21) or (22) agrees with the scattering matrix element obtained by POLKINGHORNE:

$$S_{ab} = i\hbar c \Delta^{(+)}(x-y) \delta_{ab} - \\ - \iint_{-\infty}^{+\infty} \Delta^{(+)}(x-x') \Delta^{(+)}(y-x'') \Theta(x'-x'') [j(x'), j(x'')] dx' dx''.$$

Similarly

$$(S-1)_{ab} = T_{ab} = (\Psi_a, [\varphi_{ad}^{(+)}(x), \varphi_{in}^{(-)}(y)] \Psi_b).$$

#### REFERENCES

1. C. N. YANG, and D. FELDMAN, Phys. Rev., **79**, 927, 1950.
2. G. KALLÉN, Arkiv för Fys., **2**, 371, 1950.
3. S. S. SCHWEBER, Nuovo Cimento, **2**, 397, 1955.
4. J. C. POLKINGHORNE, Proc. Cambr. Phil. Soc., **53**, 843, 1957.
5. M. CINI and S. FUBINI, Nuovo Cimento, **2**, 192, 860, 1955.
6. M. GELL-MANN and F. Low, Phys. Rev., **84**, 350, 1951.

#### ОПЕРАТОРЫ СВОБОДНОГО ПОЛЯ И ФОРМАЛИЗМ ЯНГА-ФЕЛЬДМАНА

К. Л. НАДЬ

#### Резюме

Расчеты Швебера и Полкингорна были упрощены и обобщены. Определены свободные поля, переставочные соотношения которых содержат эффекты взаимодействия. Эти поля связаны с матричными элементами оператора  $S$ .



# ELEMENTARY METHOD FOR THE CALCULATION OF THE LATTICE ENERGIES OF THE NaCl CRYSTAL II

By

F. FÁTHY and F. BUKOVSKY

INSTITUTE FOR EXPERIMENTAL PHYSICS OF THE UNIVERSITY OF BUILDING SCIENCES, BUDAPEST

(Presented by Z. Gyulai. — Received: 24. II. 1958)

In a preceding paper a simple method was given by the authors for the calculation of the lattice energies of NaCl-type crystals using elementary mathematical methods [1]. In the present paper the method is further developed. The binding energy is given of an ion situated sideways at the end of the (half) ion chain infinite in one direction, and that infinite in two directions. By the method given the numerical calculation is simplified further.

## § 1

For crystals of NaCl-type — considering Coulomb forces only — the binding energy of a further ion which is being built into an already existing crystal body is [2]

$$U = \Phi \cdot \frac{e^2}{d},$$

where  $e$  is the ion charge,  $d$  the smallest ion-ion distance. The dimensionless proportionality factor  $\Phi$  gives the binding energy numerically in  $e^2/d$  units. Our task is the determination of this proportionality factor. In the following we shall for simplicity's sake speak of binding energy, when meaning determination of this proportionality factor. For NaCl the stated energy unit is  $e^2/d = 5,1$  electronvolts.

In carrying out computations the individual ion chains are of particular importance, therefore the proportionality factor related to ion chains will be denoted for distinction by  $\varphi$ . If the ion which is being built in is imagined, as is usual, to be a small cube and the crystal body is broken up into ion chains, — the built-in ion being situated on the lattice plane formed by its ends (Fig. 1a) — then the binding energy is given by the formula

$$\varphi(a) = \sum_{n=1}^{\infty} (-1)^{n+a-1} \frac{1}{\sqrt{n^2 + a}}, \quad (1)$$

where  $\sqrt{a}$  signifies the length in  $d$  units of the straight line between the built-in

ion and the ion chain considered<sup>1</sup>. For accuracy of up to seven decimals in case of higher values of  $a$  the simple asymptotic formula has been used.

$$\varphi(a > 25) \sim (-1)^a \frac{1}{2\sqrt{a}}. \quad (2)$$

The values  $\varphi$  thus computed and included in a table ([1], Table I) give the possibility to determine the binding energy for an ion built into crystal

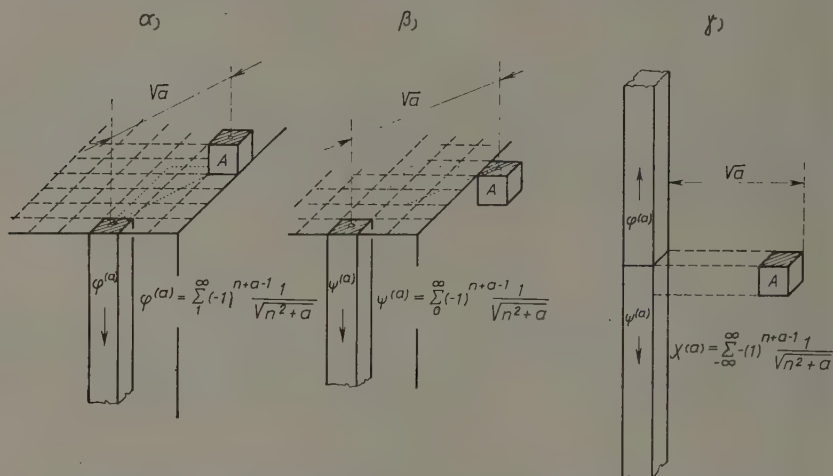


Fig. 1. Binding energies of ion chains in different positions:  $\varphi(a)$ ,  $\psi(a)$ ,  $\chi(a)$

bodies of different forms and sizes. In several cases, however, we attain our aim in a much simpler way if we know the binding energies also in the positions corresponding to the figures  $\beta$  or  $\gamma$  of Figure 1, hence when the built-in ion falls in one plane with the ends of the half chains or the chain is infinite in both directions. In these cases the proportionality factors will be denoted by  $\psi(a)$  and  $\chi(a)$ , respectively.

## § 2

Let us separate the first element of the half chain in the case corresponding to figure  $\beta$ . Its binding energy is (Fig. 2)

$$\psi_1(a) = (-1)^{a-1} \frac{1}{\sqrt{a}},$$

<sup>1</sup> It seemed advisable to change to a slight extent the denotations of the first paper [1]. The quantity given by equation (1) was earlier denoted by  $\varphi_{\infty}^{(a)}$ .

whereas the binding energy of the remaining half chain will be

$$\varphi(a),$$

thus we obtain for the original half chain

$$\begin{aligned} \psi(a) &= (-1)^{a-1} \frac{1}{\sqrt{a}} + \varphi(a) = \\ &= \sum_{n=0}^{\infty} (-1)^{n+a-1} \frac{1}{\sqrt{n^2+a}}. \end{aligned} \quad (3)$$

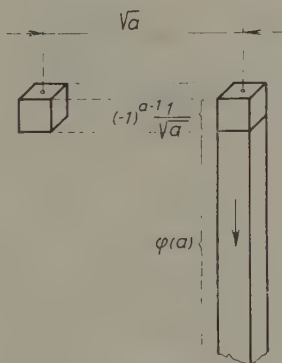


Fig. 2. For the calculation of  $\psi(a)$

From equation (2) it follows that from the point of view of our calculations for high values of  $a$

$$\psi(a > 25) \cong (-1)^{a-1} \frac{2}{2\sqrt{a}} + (-1)^a \frac{1}{2\sqrt{a}} \cong -\varphi(a), \quad (4)$$

i.e. it is sufficient to determine the value of  $\psi(a)$  only up to  $a = 25$  (Table I).

Finally, the binding energy may be calculated also for cases when the chain is infinite in both directions (Fig. 1  $\gamma$ ). For this we find according to equations (1) and (3)

$$\chi(a) = \varphi(a) + \psi(a) = \sum_{n=-\infty}^{+\infty} (-1)^{n+a-1} \frac{1}{\sqrt{n^2+a}}. \quad (5)$$

For growing crystals the bulk of the building-in takes place far from edges and peaks, where we may compute using values  $\chi$ . We obtain owing to (4)

$$\chi(a > 25) = 0, \quad (6)$$

Table I

$a$	$\varphi(a)$	$\psi(a)$	$\chi(a)$
0	0,6931472	—	—
1	—,4409176	0,5590824	0,1181648
2	,3399177	—,3671891	—,0272715
4	,2481668	—,2518333	—,0036665
5	—,2227796	,2244341	,0016545
8	,1766618	—,1768917	—,0002299
9	—,1666015	,1667318	,0001304
10	,1580759	—,1581518	—,0000759
13	—,1386660	,1386841	,0000181
16	,1249975	—,1250025	—,0000050
17	—,1212662	,1212694	,0000032
18	,1178499	—,1178524	—,0000025
20	,1118030	—,1118039	—,0000009
25	—,1000000	,1000000	,0000000

which means that ion chains being 5 or more lattice constants distant from the built-in ion already do not contribute to the binding energy<sup>2</sup>. In Table I numerical values of functions  $\varphi(a)$ ,  $\psi(a)$  and  $\chi(a)$  are contained up to  $a = 25$ . Further values for  $\varphi$  and  $\psi$  (owing to (4)) can be taken from Table I of paper [1].

So as to be able to use the introduced three functions, the values of  $a$  belonging to the individual ion chain are needed. These are given by the "map" illustrated in Figure 3. The plane of the map is normal to the direction of the parallel ion chains,  $O$  is the place of the built-in ion. It follows from (6) that in case of the function  $\chi$  only fields within the thick line have to be taken into consideration.

A geometrical meaning may be given to the results obtained up to now. Let us consider all the ion chains of infinite length in both directions, for which the value of  $a$  is the same. These constitute a cylinder, the axis of which may be taken to be the  $z$  axis of the coordinate system, the equation of its basic circle is then given by

$$x^2 + y^2 = a.$$

The reciprocal of the cylinder diameter appears in the right-hand side of the asymptotical formula (2).

It follows from (6) that the binding energy of an ion inside the crystal trunk is the same as if the crystal trunk were constituted only of ions within the cylinder.

<sup>2</sup> For the very quick convergence of  $\chi(a) \rightarrow 0$  see KOSSEL [2], Fig. 5.

We may call this cylinder the efficiency cylinder in analogy with the efficiency sphere used for the interpretation of surface phenomena of fluids. The

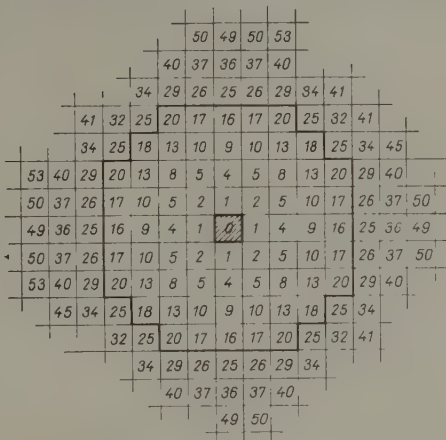


Fig. 3. The "map"

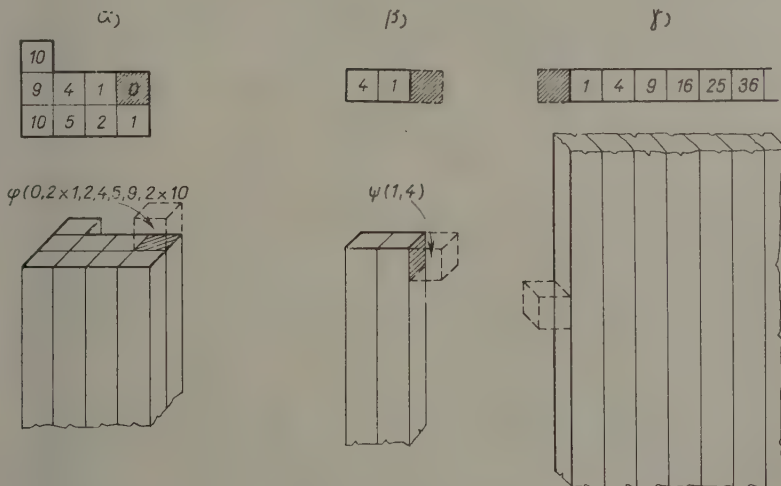


Fig. 4. Binding energies

middle part of the map which is framed by a thick line corresponds to the inside of the basic circle of the efficiency cylinder. The inner energy content of the efficiency cylinder is the Madelung constant<sup>3</sup>.

<sup>3</sup> One of the authors (BUKOVSKY) succeeded in determining in a relatively simple way, summing over the coaxial cylinder shells, the value of the Madelung constant also for CsCl. A respective publication is in the press.

## § 3

Some instances are given for the use of the map and Table I<sup>4</sup>. The individual figures of our Figure 4 require application of functions  $\varphi$ ,  $\psi$  and  $\chi$  for the computation of the binding energies. In Figure 4a the binding energy is given by

$$\begin{aligned}\Phi &= \varphi(0) + 2\varphi(1) + \varphi(2) + \varphi(4) + \varphi(5) + \\ &+ \varphi(9) + 2\varphi(10) = +0,3261672,\end{aligned}$$

which may for short be written as follows :

$$\varphi(0, 2 \cdot 1, 2, 4, 5, 9, 2 \cdot 10) = 0,3261672.$$

In Figure 4 $\beta$  the ion laterally joins the end of the band consisting of two chains and the binding energy is then obtained as

$$\psi(1,4) = +0,3072492.$$

Finally in Figure 4 $\gamma$  the energy is

$$\chi(1, 4, 9, 16) = +0,1146236.$$

Our latter result corresponds to the value obtained in [1]

$$\Phi_{\infty}^{(0)} = +0,114624$$

and shows that the use of the functions introduced here means a further considerable abbreviation in the numerical calculations.

The advantage gained by their use will be even more striking when determining the value of the Madelung constant<sup>5</sup>. This requires — when

<sup>4</sup> Calculations have been carried out anew for 8 decimals. Results are published for seven decimals.

<sup>5</sup> In the meantime one of the authors had occasion (September 7, 1958, BUKOVSKÝ) to meet Professor EMERSLEBEN. From the discussions we report the following :

The value of the Madelung constant has been repeatedly and with great accuracy determined by EMERSLEBEN for NaCl. See: EMERSLEBEN: Der Wert der Madelungkonstanten des Steinsalzgitters, Kritische Zusammenfassung, Wissenschaftliche Zeitschrift der Universität Greifswald, III. 607—617, 1953/54. In this review a critical description with detailed literature of the methods known for the determination of the Madelung constant may be found. The following quotation is taken from page 609 of that paper "the methods of calculation usually make extensive use of complicated mathematics, so that not every user can be expected to be able to check these numerical values". Later on page 612 we read: "The series may indeed be summed. However, this way does not yet seem to have been followed directly." This refers to the non-convergent EMERSLEBEN formula quoted on page 101 in the first part of our present paper [1].

The two sentences quoted may justify the present paper. Namely the elementary method described in it follows the path mentioned in the second sentence and by it anybody, who is interested, is enabled to check the published calculations, a procedure which is always highly desirable.



using our Tables and our short way of writing — a few summations only :

$$\begin{aligned}\Phi(M) &= 2\varphi(0) + 4\chi(1, 2, 4, 8, 9, 16, 18) + \\ &+ 8\chi(5, 10, 13, 17, 20) = 1,7475652.\end{aligned}$$

## § 4

It was only after part I [1] of our present paper had been written that we became acquainted with FRANK's approximative method [3] which set itself aims similar to ours : "The most important of lattice sums have by now been evaluated at the cost of considerable labour : but there are still many which one often needs or would like to know especially for bounded lattices of for off-lattice points. It is not too late to welcome an improved method." Let us consider briefly this method and compare it with the one described here.

FRANK decomposed the crystal body into cubes of edge length  $d$ , the ions being situated in the centres of these cubes. The system of ions considered as point charges is equivalent to the sum of the following two charge groups :

1. 8 point charges each of a magnitude  $e/8$  placed in the corners of the cell.

2. one charge  $e$  in the centre and 8 charges of magnitude  $-e/8$  each in the corners.

Potentials of the individual charge groups are considered separately and unified subsequently.

The summation is simple for crystals of NaCl type. In order to check the method FRANK computes the same two cases as we, namely — in our denotation — the values of  $\varphi(a)$  and  $\Phi(M)$ . The formula valid for the first case

$$\varphi(0) \simeq \varphi_n(0) + (-1)^n \frac{1}{\sqrt{(2n+1)^2 + 2}} = \varphi_n(0) + R_n$$

attains within a strikingly short time the value of  $\ln 2$  if for  $n = 14$   $\varphi_n$  is correct up to 6 decimals. The convergence is improved to a great extent by the residual term  $R_n$ . As regards the computation of the Madelung constant FRANK's considerations are similar to EVJEN's [5] summing over the cube shells and placing into the external 8 corners of the external cube shell point charges of magnitude  $\pm e/8$ , the sign of which is opposite to the sign of the extreme lattice ion. Thus, however, we obtain already for the first narrow surroundings very cumbersome sums ; for a surrounding of side edge  $5d$  10 terms are obtained, whereas for the side edge  $7d$  19 terms have to be summed,

and as, when forming the terms, no regularity appears, the summation is not quite simple. This method is used and described in the interesting paper of LÜDEMANN [4].

The efficiency of FRANK's method corresponds approximately to ours, described in part I of this paper [1], it is, however, disregarding the single computation of  $\varphi(0)$ , more complicated. LÜDEMANN also mentions time-vasting computations. The method could of course be further developed. Thus for instance in FRANK's formula for the approximative calculation of  $\varphi(a)$  the general remainder term

$$R_n = (-1)^{n+a} \frac{1}{\sqrt{(2n+1)^2 + (2a+1)^2 + 1}}$$

may be used. The convergence, however, deteriorates with increasing  $a$ . Thus for instance already in case of  $\varphi(2)$  for  $n = 20$  only the first three decimals are obtained correctly.

The extension of our method presented here makes possible — using the energy values published in our Tables — to write down directly the binding energy of the ion at an arbitrary point of the crystal trunk. This was primarily necessary for the interpretation of particular crystal forms, observed by GYULAI, namely for the interpretation of needles and plates precipitating from a saturated solution [6]. A further advantage of our method consists in that the natural system given by the ions of aequidistant point charges of alternating signs and equal magnitude is not broken up and the known difficulties are overcome by applying an adequate mathematical apparatus by which calculations are not only abbreviated but lead quickly to more correct results. In practical applications our method proved to be good [7].

The authors are greatly indebted to Prof. ZOLTÁN GYULAI for his interest and assistance.

#### REFERENCES

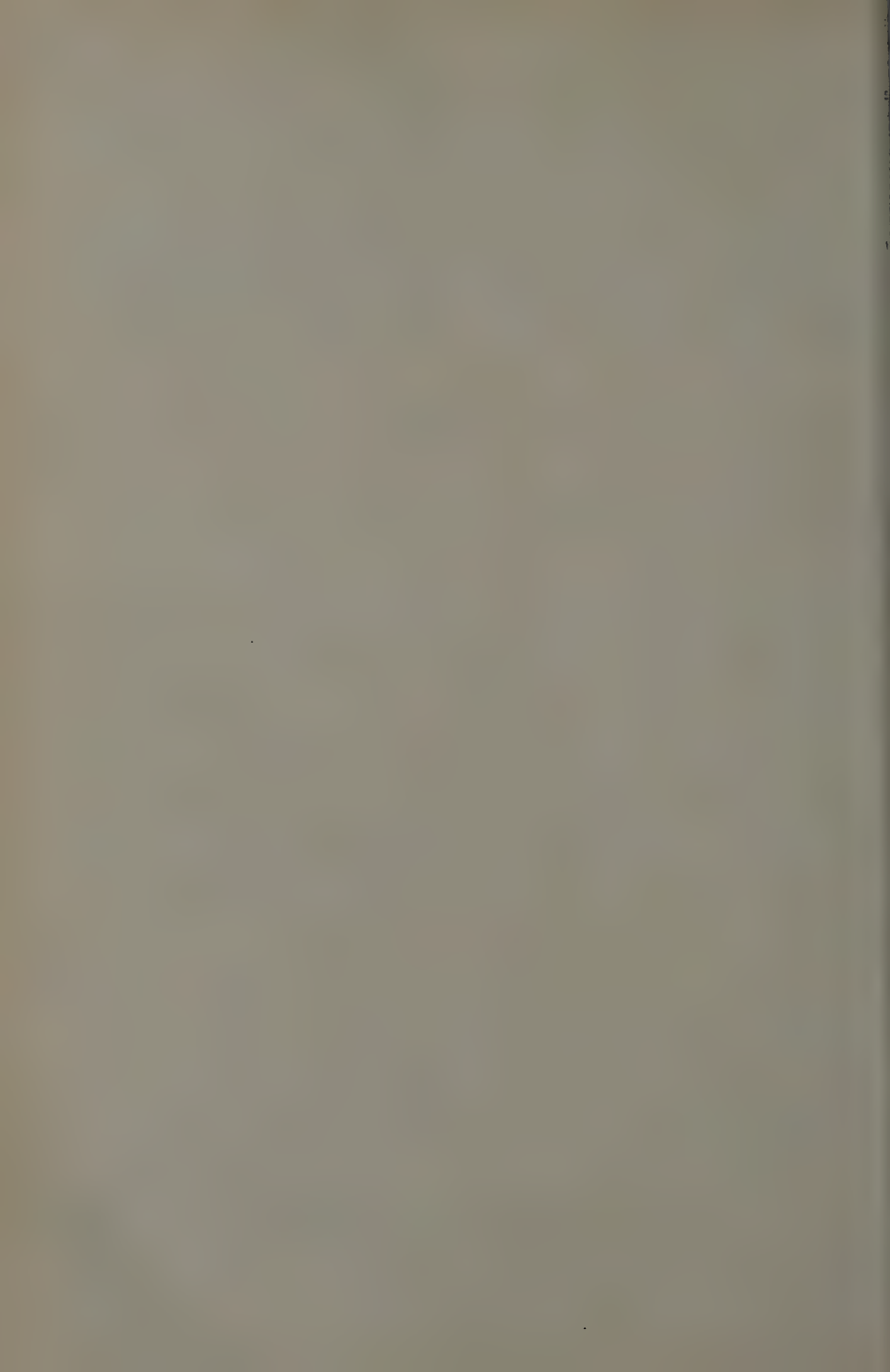
1. F. FÁTHY and F. BUKOVSKY, *Acta Phys. Hung.*, **3**, 89, 1957. (See there for further references.)
2. W. KOSSEL, *Die molekularen Vorgänge beim Kristallwachstum*. Leipziger Vorträge, Hirzel, Leipzig, 1928.
3. F. C. FRANK, *Phil. Mag.*, **41**, 1287, 1950.
4. H. LÜDEMANN, *Zs. f. Krist.*, **108**, 377, 1957.
5. H. M. EVJEN, *Phys. Rev.*, **39**, 675, 1932.
6. Z. GYULAI, *Acta Phys. Hung.*, to be published.
7. F. BUKOVSKY, *Acta Phys. Hung.*, **3**, 109, 1957. (See also footnote 3.)

ЭЛЕМЕНТАРНЫЙ МЕТОД ВЫЧИСЛЕНИЯ ЭНЕРГИИ РЕШЕТКИ КРИСТАЛЛА  
NaCl

Ф. ФАТИ и Ф. БУКОВСКИ

## Резюме

В предыдущей работе авторы дали простой метод с элементарным математическим аппаратом для вычисления энергии решетки кристаллов типа NaCl. В настоящей работе они продолжают в развитии метода. Они определяют энергию связи бокового иона на конце цепочки ионов, полубесконечной в одном направлении, и энергию связи ионов на обеих сторонах цепочки, бесконечной в обоих направлениях. Эта модификация далее упростит численную работу.



# ON THE CALCULATION OF INTENSITY SCATTERED BY FINE-CRYSTALLINE COALS

By

P. SZABÓ

CENTRAL RESEARCH INSTITUTE OF PHYSICS, DEPARTMENT FOR NEUTRONPHYSICS, BUDAPEST

(Presented by L. Jánossy. — Received: 25. II. 1958)

Intensity scattered from fine-crystalline coals is dealt with as a function of crystallite dimensions for disorders of different extent. It turns out from the discussion that types and extents of the disorder are not correctly taken into consideration by intensity relations used generally for the determination of crystallite dimensions. Owing to this fact the crystallite dimensions determined in the usual way are not quite correct. Disorder is taken into account in a suitable manner in our treatment, thus making possible experimental determination of the disorder and — in addition to a more correct determination of crystallite dimensions — helping to a better knowledge of the structure of fine-crystalline coals. We outline the kind of neutron diffraction measurements which should be carried out in order to exploit this possibility.

## I. Former work

Already before 1941 many authors have been concerned [1] with the determination of the crystallite dimensions of fine-crystalline coals (active coals, carbon blacks) from Debye-Scherrer line widths. These measurements greatly contributed to the formulation of the idea which we have about the structure of these coals, which are also important from technical viewpoints.

With the decrease of crystallite dimensions, intensity ratios characteristically vary in the interference pattern. According to ARNFELT [2] the features of the interference pattern can be explained briefly in the following way. As the crystallite dimensions of the graphite are diminishing, disorders of ever greater extent appear in the structure of crystallites. This disorder consists in that the grating planes normal to the hexagonal crystallographic axis  $\bar{a}_3$  — remaining parallel and equidistant — are irregularly shifted and rotated with respect to their positions given by the graphite structure. The extent of disorder is the greater the smaller the crystallites.

For the determination of crystallite dimensions of such types of graphites from Debye-Scherrer line widths the same calculations are currently used as for the determination of dimensions of disorder-free crystallites and thus this method would certainly have had to be justified.

## II. Warren's method

In 1941 calculations were published [3] by WARREN which seem to justify this method — if the latter is modified to a certain extent. Since then the

determination of crystallite dimensions of fine-crystalline coals from Debye-Scherrer line widths has been carried out on the basis of WARREN's calculations [4].

The X-ray scattering of crystallites consisting of  $N_3$  uniform grating planes parallel to each other and at a distance  $a_3$  from one another with edge vectors  $N_1\bar{a}_1$  and  $N_2\bar{a}_2$  is dealt with by WARREN under the assumption that these planes occur in the individual crystallites shifted parallel to  $\bar{a}_1$  and  $\bar{a}_2$  completely irregularly with respect to their positions determined by the graphite structure. ( $\bar{a}_1, \bar{a}_2, \bar{a}_3$  are edge vectors of the orthohexagonal elementary cell of the graphite,  $N_1, N_2$  and  $N_3$  are whole numbers.)

We obtain the intensity scattered by random crystallite agglomerations in a certain direction by integrating the intensity scattered by one crystallite over all the possible positions in space of the crystallite. This integration should be carried out over the rectangular reciprocal grating coordinates  $A_1, A_2, A_3$  as variables over the surface satisfying the condition

$$\left(\frac{A_1}{a_1}\right)^2 + \left(\frac{A_2}{a_2}\right)^2 + \left(\frac{A_3}{a_3}\right)^2 = \left(\frac{2 \sin \vartheta}{\lambda}\right)^2,$$

where  $\vartheta$  is the so-called angle of reflection and  $\lambda$  the wave length of the X-rays. In the following such integrals will be called briefly "integrals".

WARREN's calculations start from the following statements:

1. From among the reflections of graphite in case of fine-crystalline coals only reflections of two types occur. a) The first one is of such a type which may be expected from completely disordered agglomerations of the above-mentioned grating planes. Hence these reflections can be characterized by two indices ( $hk$ ) and their intensity is given by the integral of the function

$$|F|^2 \frac{\sin^2 \pi N_1 A_1}{\sin^2 \pi A_1} \cdot \frac{\sin^2 \pi N_2 A_2}{\sin^2 \pi A_2}, \quad (\text{x})$$

where  $|F|^2$  is the structure factor of the space lattice of graphite. b) The other type corresponds to the (00l) type reflections of graphite and the intensity of such reflections is given by the integral of the function

$$|F|^2 \frac{\sin^2 \pi N_1 A_1}{\sin^2 \pi A_1} \cdot \frac{\sin^2 \pi N_2 A_2}{\sin^2 \pi A_2} \cdot \frac{\sin^2 \pi N_3 A_3}{\sin^2 \pi A_3}, \quad (\text{xx})$$

where  $|F|^2$  means the same as before.

2. In case the grating planes — apart from the abovementioned shift-ings — are in addition rotated irregularly, this no longer changes the occurring reflections.



### III. Shortcomings of Warren's calculations

From the following considerations we shall see that in spite of WARREN's statement (see loc. cit. equation (40)) we have to put in the place of  $|F|^2$ , not the crystal structure factor of the graphite lattice, but the structure factor of the grating plane belonging to the planes in question; the statement  $1/a$  is even so only correct when very great irregular shiftings may occur, which are much greater than  $a_1$  and  $a_2$ , respectively; neither in this case is statement 2) exact; statement  $1/b$  is just the less exact the greater the shiftings.

The assumption of very great shiftings seems in itself physically not permissible. We obtain for  $N_1, N_2, N_3$  determined on the basis of WARREN's calculations very often (for instance for certain carbon blacks) very small whole numbers and the result that the crystallites are very small is in accordance with other (for instance adsorption) experiments. The assumption of great shiftings of small grating planes is, however, evidently in contrast with the assumption of parallelity of the grating planes and of their having a fixed distance from each other of which use is made in the calculations.

Therefore in the following — in addition to confirmation of the above statements — we endeavour to establish what kind of deviations from WARREN's formulae are obtained if instead of assuming possibility of very great shiftings smaller, plausible shiftings are taken into account, for instance shiftings of sizes up to  $a_1$  and  $a_2$ , respectively, in directions  $\bar{a}_1$  and  $\bar{a}_2$ , respectively.

### IV. Computations

Let us denote by

$$\bar{r}_c = x_1 \bar{a}_1 + x_2 \bar{a}_2 + x_3 \bar{a}_3 \quad (1)$$

the place vector of the individual elementary cells. Omitting simply the factors which may be practically considered as constant in the above-mentioned integration (which were considered so also by WARREN) the intensity is given by the integral of the average value of the sum

$$\left| \sum e^{2\pi i(x_1 A_1 + x_2 A_2 + x_3 A_3)} \right|^2 \quad (2)$$

( $i$  is the imaginary unit). The summation refers to all the elementary cells of the crystallite, whereas the averaging is to be carried out over all possible values of  $x_1, x_2, x_3$ .

### 1. Possibility of small shiftings

Let us denote the shiftings of the grating planes in question of the crystallite (distinguished from one another by the index  $n_3$ ) by  $\delta_{n_3} \bar{a}_1$  and  $\varepsilon_{n_3} \bar{a}_2$ , respectively. Then the average of expression (2) can evidently be written

$$\begin{aligned}
 & \left| \sum_{n_1=1}^{N_1} \sum_{n_2=1}^{N_2} \sum_{n_3=1}^{N_3} e^{2\pi i [(n_1 + \delta_{n_3}) A_1 + (n_2 + \varepsilon_{n_3}) A_2 + n_3 A_3]} \right|_{\text{average}}^2 = \\
 & \frac{\sin^2 \pi N_1 A_1}{\sin^2 \pi A_1} \cdot \frac{\sin^2 \pi N_2 A_2}{\sin^2 \pi A_2} \left| \sum_{n_3=1}^{N_3} e^{2\pi i (n_3 A_3 + \delta_{n_3} A_1 + \varepsilon_{n_3} A_2)} \right|_{\text{average}}^2 = \\
 & = \frac{\sin^2 \pi N_1 A_1}{\sin^2 \pi A_1} \cdot \frac{\sin^2 \pi N_2 A_2}{\sin^2 \pi A_2} \times \\
 & \times \left\{ N_3 + \sum_{n_3=1}^{N_3} \sum_{n'_3=1}^{N_3} e^{2\pi i [(n_3 - n'_3) A_3 + (\delta_{n_3} - \delta_{n'_3}) A_1 + (\varepsilon_{n_3} - \varepsilon_{n'_3}) A_2]} \right\}_{\text{average}} = \\
 & = \frac{\sin^2 \pi N_1 A_1}{\sin^2 \pi A_1} \cdot \frac{\sin^2 \pi N_2 A_2}{\sin^2 \pi A_2} \cdot \overline{f(A_3)}.
 \end{aligned} \tag{3}$$

Assuming now for instance that  $0 \leq \delta_{n_3} \leq 1$ , as well as  $0 \leq \varepsilon_{n_3} \leq 1$ , the average of the general term of the double sum occurring in  $f(A_3)$  will be

$$\begin{aligned}
 & \int_0^1 \int_0^1 \int_0^1 e^{2\pi i [(n_3 - n'_3) A_3 + (\delta_{n_3} - \delta_{n'_3}) A_1 + (\varepsilon_{n_3} - \varepsilon_{n'_3}) A_2]} d\delta_{n_3} d\delta_{n'_3} d\varepsilon_{n_3} d\varepsilon_{n'_3} = \\
 & \frac{1}{\pi^4 A_1^2 A_2^2} e^{2\pi i (n_3 - n'_3) A_3} \sin^2 \pi A_1 \sin^2 \pi A_2.
 \end{aligned} \tag{4}$$

Hence the average value of  $f(A_3)$  becomes

$$\overline{f(A_3)} = N_3 + \frac{1}{\pi^4 A_1^2 A_2^2} \sin^2 \pi A_1 \cdot \sin^2 \pi A_2 \sum_{n_3=1}^{N_3} \sum_{\substack{n'_3=1 \\ n_3 \neq n'_3}}^{N_3} e^{2\pi i (n_3 - n'_3) A_3} = \tag{5}$$

$$= N_3 - \frac{N_3}{\pi^4 A_1^2 A_2^2} \sin^2 \pi A_1 \cdot \sin^2 \pi A_2 + \frac{1}{\pi^4 A_1^2 A_2^2} \sin^2 \pi A_1 \sin^2 \pi A_2 \frac{\sin^2 \pi N_3 A_3}{\sin^2 \pi A_3}.$$

Substituting  $\overline{f(A_3)}$  from (5) into (3) we obtain

$$N_3 \frac{\sin^2 \pi N_1 A_1}{\sin^2 \pi A_1} \cdot \frac{\sin^2 \pi N_2 A_2}{\sin^2 \pi A_2} - \frac{N_3}{\pi^4} \cdot \frac{\sin^2 \pi N_1 A_1}{A_1^2} \cdot \frac{\sin^2 \pi N_2 A_2}{A_2^2} + \\ + \frac{1}{\pi^4} \cdot \frac{\sin^2 \pi N_1 A_1}{A_1^2} \cdot \frac{\sin^2 \pi N_2 A_2}{A_2^2} \cdot \frac{\sin^2 \pi N_3 A_3}{\sin^2 \pi A_3} \quad (6)$$

The intensity is therefore given by the integral of the last expression and it can easily be seen that it will differ from the integral of (x) as well as from that of (xx) (both deprived from the factor  $|F|^2$ , which is considered here as constant).

In complete analogy with the above derivation the intensity can be dealt with in case of any other condition referring to the region of  $\delta_{n_3}$  and  $\varepsilon_{n_3}$ , resp. The different conditions lead to different expressions analogous with (6).

In the limiting case when the extension of these regions is 0, which corresponds to the completely regular space lattice of the graphite, as a matter of course (6) goes over into the formula (xx) referring to space lattices (if we omit there the factor  $|F|^2$ ).

## 2. Possibility of very great shiftings

If we allow for a variation of  $\delta_{n_3}$  and  $\varepsilon_{n_3}$  not from 0 to 1, but in a much greater range, then averaging carried out in analogy with the above will lead in cases  $A_1 \neq 0$  and  $A_2 \neq 0$ , hence for reflections of type  $(hk)$ , indeed to (x) (if we omit there the factor  $|F|^2$ ).

The expression (xx) given for reflections of type  $(00l)$ , however, can be least applied just in cases when very great shiftings are possible. In the case namely, if  $A_1$  and  $A_2$  do not differ too little from 0, the phase shiftings  $\delta_{n_3} A_1$  and  $\varepsilon_{n_3} A_2$  become quite uncertain. Thus in such cases the averaging denoted in (3) leads not to (xx) but to (x). On the other hand, in a very small surrounding of  $A_1 = 0$  and  $A_2 = 0$  the averaging carried out in an analogous manner to that in point IV. 1. does not lead either to (x) or to (xx). Finally, if  $A_1$  and  $A_2$  are exactly 0, then the averaging leads to (xx).

Accordingly in case of reflections of type  $(00l)$  formula (xx) has to be replaced by formula (x) for all values of  $|A_1|$  and  $|A_2|$ , respectively, bigger than a certain value. This value depends on the size of shiftings considered; i. e. the greater the shiftings taken into account the smaller is this value. As a matter of course, with the decrease of the extent of permissible shiftings (xx) means an ever better approximation in case of the  $(00l)$  interferences. This

may be guessed also in advance: if the permissible shiftings decrease to 0, then we come back to the case of the exact graphite space lattice for which (xx) is exactly valid.

### 3. Joint effect of shiftings and rotations

When in the graphite space lattice the grating planes are rotated through different angles  $\beta_{n_1}$  around a selected axis  $\bar{a}_3$ , then instead of (1) evidently

$$\begin{aligned} \bar{r}_c = & \left( n_1 \cos \beta_{n_3} - n_2 \frac{a_2}{a_1} \sin \beta_{n_3} \right) \bar{a}_1 + \\ & + \left( n_1 \frac{a_1}{a_2} \sin \beta_{n_3} + n_2 \cos \beta_{n_3} \right) \bar{a}_2 + n_3 \bar{a}_3 \end{aligned} \quad (1')$$

should be written. Whereas if apart from this also shiftings occur, then

$$\begin{aligned} \bar{r}_c = & \left( n_1 \cos \beta_{n_3} - n_2 \frac{a_2}{a_1} \sin \beta_{n_3} + \delta_{n_3} \right) \bar{a}_1 + \\ & + \left( n_1 \frac{a_1}{a_2} \sin \beta_{n_3} + n_2 \cos \beta_{n_3} + \varepsilon_{n_3} \right) \bar{a}_2 + n_3 \bar{a}_3. \end{aligned} \quad (1'')$$

Thus now expr. (2) will become

$$\begin{aligned} & \left| \sum_{n_1=1}^{N_1} \sum_{n_2=1}^{N_2} \sum_{n_3=1}^{N_3} \exp \left\{ 2\pi i \left[ \left( n_1 \cos \beta_{n_3} - n_2 \frac{a_2}{a_1} \sin \beta_{n_3} + \delta_{n_3} \right) A_1 + \right. \right. \right. \\ & \left. \left. \left. + \left( n_1 \frac{a_1}{a_2} \sin \beta_{n_3} + n_2 \cos \beta_{n_3} + \varepsilon_{n_3} \right) A_2 + n_3 A_3 \right] \right\} \right|_{\text{average}}^2. \end{aligned} \quad (7)$$

If the angles  $\beta_{n_1}$  with equal probability take up each value between 0 and  $2\pi$  then (7) can be written

$$\begin{aligned} & \frac{1}{4\pi^2} \int_0^{2\pi} \int_0^{2\pi} \sum_{n_1=1}^{N_1} \sum_{n_2=1}^{N_2} \exp \left\{ 2\pi i \left[ \left( n_1 \cos \beta_{n_3} - n'_1 \cos \beta'_{n_3} - n_2 \frac{a_2}{a_1} \sin \beta_{n_3} + \right. \right. \right. \\ & \left. \left. \left. + n'_2 \frac{a_2}{a_1} \sin \beta'_{n_3} \right) A_1 + \left( n_1 \frac{a_1}{a_2} \sin \beta_{n_3} - n'_1 \frac{a_1}{a_2} \sin \beta'_{n_3} + \right. \right. \right. \\ & \left. \left. \left. + n_2 \cos \beta_{n_3} - n'_2 \cos \beta'_{n_3} \right) A_2 \right] \right\} d\beta_{n_3} d\beta'_{n_3} \cdot \\ & \cdot \left| \sum_{n_3=1}^{N_3} \exp \left\{ 2\pi i (n_3 A_3 + \delta_{n_3} A_1 + \varepsilon_{n_3} A_2) \right\} \right|_{\text{av rag.}}^2. \end{aligned} \quad (8)$$

The second factor of (8) agrees with  $f(\bar{A}_3)$  in (3). The first factor of (8), however, evidently does not lead to the expression (x) deprived of its factor  $|F|^2$  which forms the first two factors of (3). Hence (8) differs from (3) and thus the effect of irregular rotations does not agree with that of irregular shiftings indeed, in contrast to WARREN's assumption.

#### 4. Crystal structure factor

Hitherto only the intensity arising from the points indicating the elementary cells has been dealt with. The effect upon the intensity of atoms the position of which inside the cells is determined with respect to the points indicating the elementary cells can be taken into account by the structure factor  $|F|^2$ . Its relatively slow variation with the scattering angle practically does not affect the calculation of crystallite size, but evidently influences considerably the absolute intensity of the different reflections.

WARREN in his calculations applies the  $|F|^2$  referring to the graphite space lattice. (See WARREN, loc. cit., equation (40).) Owing, however, to the shiftings, whether great or small, assumed in his calculations, the condition according to which the positions of all the atoms in the elementary cells of the graphite are fixed with respect to the points indicating the cells, is no longer fulfilled. The graphite structure is namely such that between two grating planes lying at a distance  $a_3$  from each other there can be found an identical grating plane at a distance  $\frac{1}{2} a_3$  from them, but shifted in a given manner parallel with these two planes. There is no reason to assume that in case of disorder each such "intermediate" grating plane will be shifted, respectively rotated, exactly together with — say — the grating plane lying below it, in which case we would have to deal not with shiftings of individual grating planes but of pairs of grating planes. (In this case in spite of the disorder, an  $|F|^2$  identical with that belonging to the original space lattice would have to be used.)

Owing to the equivalence of neighbouring grating planes only the assumption seems to be justified that the above-mentioned possibility of irregular shifting and rotation holds for all the grating planes being at a distance  $\frac{1}{2} a_3$  from each other and normal to  $\bar{a}_3$ .

Accordingly, in the above expressions the following modifications have to be performed. 1. We have to put  $\frac{1}{2} \bar{a}_3$  instead of  $\bar{a}_3$ , and  $N_3$  is to be understood as the number of such grating planes to be found in one crystallite. This modification does not affect the integral of (x) which has to be used in case of very large shiftings and for  $A_1 \neq 0$ ,  $A_2 \neq 0$ . As against this the integral of (6) (respectively the integral of other analogous expressions referring to other possible sizes of shiftings) will evidently be affected by this modifica-

tion. 2. Instead of the crystal structure factor of the graphite now the structure factor of the plane lattice formed by the atoms of the two dimensional cell of edge vectors  $\bar{a}_1, \bar{a}_2$  has to be used. This is valid even for very great shiftings, hence in the case when the expression (x) applies and changes considerably the total intensity computed for the individual reflections, a fact immediately obvious when forming the two types of  $|F|^2$ .

## V. Conclusions

In the foregoing the following statements were made :

a) The expression (x) used by WARREN is exactly valid only for the case when very great shiftings may occur, whereas formula (xx) only in case of no shifting. The usual simultaneous use of both can by no means be exact.

b) In the case of the particular assumption of certain small shiftings expression (6) (multiplied by  $|F|^2$ ) has to be applied instead of expressions (x) and (xx). On the basis of our derivation the adequate expression for the case of shiftings of different magnitude can be easily given.

c) If in addition to the possibility of shifting also the possibility of rotation is taken into account, then — in contrast to WARREN's statement — the intensity formula has to be modified.

d) In the case of the disorder dealt with (whether very great shiftings and rotations or only smaller ones may occur) it is not the structure factor of the graphite space lattice which has to be used for the calculation of the intensity but that of the plane lattice normal to  $\bar{a}_3$ , again in contrast to WARREN's statement. Though this changes the intensity within a reflection only by a practically constant factor, it causes, however, a considerable difference in the total coherent intensity distribution.

### 1. Calculation of crystallite dimensions considering the extent of shiftings

The problem arises what kind of difference is caused in the values of crystallite dimensions calculated from the width of the Debye-Scherrer lines when using expressions (x) and (xx) or expression (6), or rather one of the expressions analogous with it which consider correctly the extent of shiftings. Concerning this, we may give the following estimate.

The integration (xx) was carried out by LAUE in an approximate manner [5], whereas (x) was integrated by WARREN (loc. cit.) in an approximation essentially going back to LAUE.

The relations of crystallite size and line width determined from these calculations cannot be compared directly with each other because LAUE gave this relation for the so called integral, and WARREN for the half-value width.



The comparison, however, can be made by transforming LAUE's relation so as to refer also to the half value width. In this way it can be easily shown that, computing the crystallite size from a given line width on the basis of expression (x), its value will be about twice that resulting from the computation on the basis of expression (xx).

We have seen in points IV. 1 and IV. 2 that expression (6) and those analogous with it are going over into expression (xx) and (x), respectively, as limiting cases for very small, resp. for very great shiftings. Considering the character of the calculation leading to crystallite dimensions from these expressions the conclusion may be drawn that if we compute on the basis of expression (x) and (xx) instead of expression (6) resp. of any expression analogous with it, corresponding to the actual disorder, then the computed crystallite dimensions will be correct only within a factor of 2.

It should be noted that the crystallite dimensions calculated on the basis of WARREN's method cannot be exact for any shifting. Namely, according to this method — as has already been mentioned — expressions (x) and (xx) are simultaneously used: for reflections of type  $(hk)$  expression (x), and expression (xx) for reflections of type  $(00l)$ . Further,  $N_1$  and  $N_2$  are calculated from reflections of type  $(hk)$ , i. e. on the basis of (x) whereas  $N_3$  from reflections of type  $(00l)$ , i. e. on the basis of (xx). Thus the better the values obtained for  $N_1$  and  $N_2$  (in case of great shiftings), the worse the values obtained for  $N_3$ ; and (in case of small shiftings) vice versa.

## 2. Determination of the extent of shiftings

The extent of the shiftings dealt with can scarcely be established with a satisfactory precision by X-ray diffraction. So, from among the expressions discussed by us the correct one for a given case cannot be chosen on the basis of X-ray diffraction measurements. Thus remaining within the possibilities given by X-ray diffraction we should have to content ourselves with theoretical criticism of the usual method of calculation (apart from our remark made concerning the factor  $|F|^2$ ).

The application of neutron diffraction, however, offers the possibility to choose from among the different expressions dealt with the most convenient for a given case, i. e. to establish the type and extent of the disorder. If these are known the above-mentioned uncertainty prevailing in the determination of crystallite dimensions can be eliminated.

Neutron diffraction is rendered suitable for such investigations by the following features. The absorption of slow neutron radiation is very small in coals as compared with X-ray radiation. The neutron scattering of coal is practically completely coherent while for X-ray scattering the coherent

part can be obtained only by subtracting by computation the incoherent part from the measured scattering. This of course gives rise to a further uncertainty. Finally, in case of X-ray diffraction the intensity strongly decreases towards the larger scattering angles, due to the decrease of the atomic form factor, whereas for neutron diffraction this effect is lacking, which in the case of the weak reflections of fine-crystalline coals is of great advantage. Owing to all these properties the coherent intensity distribution, free from disturbing effects (absorption, incoherent scattering) can be obtained much easier and more exactly from neutron diffraction than from X-ray diffraction, by an adequate correction of the measured intensities.

In addition to the expected differences in the width of the reflections caused by using expressions (x) and (xx) instead of expression (6), respectively of its analogons, evidently considerable differences can be expected in the total intensity distribution, particularly in its diffuse part.

Thus it can be expected that from neutron diffraction measurements on fine-crystalline coals the extent of disorder may be established by determining which expression ((6) or one of its analogous expressions) fits best the experimental curve. Here it is of course important to use the correct structure factor (namely that of the plane lattice), otherwise certainly intensity distributions differing from the experimental one will be obtained.

It may not be necessary to measure and compute the total intensity curve in order to determine the extent of disorder. Namely not only can the coherent intensity distribution be determined much more exactly by neutron diffraction than by X-ray diffraction due to the properties of the former mentioned above but absolute intensity measurements can also be carried out on crystalline powders. At the intensity maxima of the individual reflections the ratio of the absolute diffuse intensity to the reflection width is evidently obtained essentially different from the various expressions dealt with here. Thus, also from this ratio conclusions may be drawn concerning the extent of disorder. (In principle conclusions concerning the disorder could be also drawn from the ratio of diffuse and reflection intensities at the place of intensity maxima. However, the reflection width can be measured with higher precision than the maxima of reflection intensity and the difference in accuracy will be particularly great for the very weak reflections which are to be expected in the case of more or less disordered coal-crystallites of small size in which we have here been interested.)

Thus it may be hoped that the application of the method outlined here may contribute to a better knowledge of the structure of fine-crystalline coals.

## REFERENCES

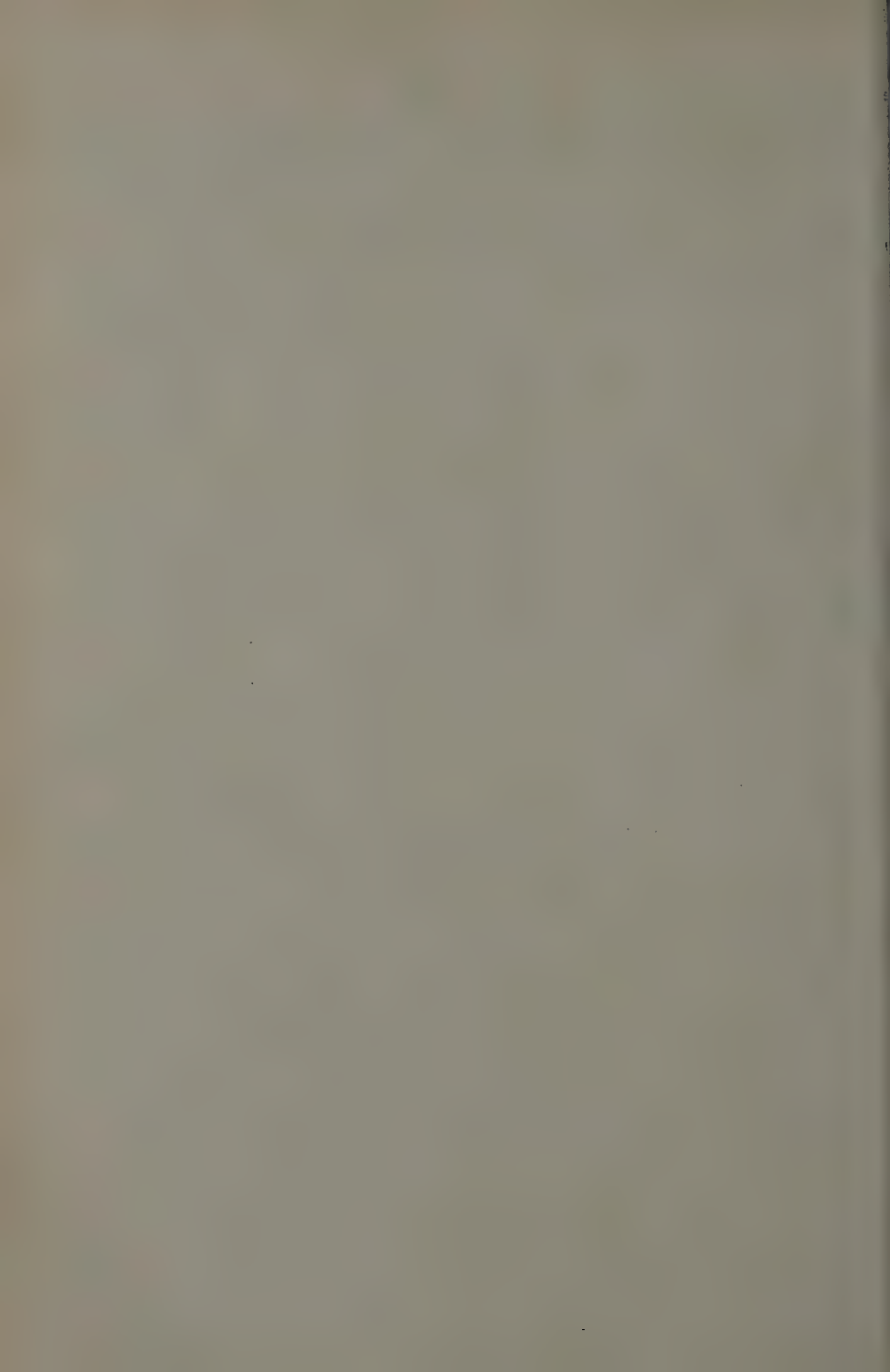
1. U. HOFMANN and D. WILM, *Z. für phys. Chemie*, B **18**, 401, 1932 ; *Koll. Z.* **70**, 21, 1935 ; *Z. für Elektrochemie*, **42**, 504, 1936 ; G. CLARK and H. RHODES, *Ind. Eng. Chem. Anal. Ed.*, **12**, 66, 1940 ; K. BIASTOCH and U. HOFMANN, *Angew. Chemie*, **53**, 327, 1940 ; etc.
2. H. ARNFELT, *Arkiv f. Mat., Astron., Fys.*, **23**, B 1, 1932.
3. B. E. WARREN, *Phys. Rev.*, **59**, 693, 1941.
4. J. BISCOE and B. E. WARREN, *J. Appl. Phys.*, **13**, 364, 1942 ; R. E. FRANKLIN, *Proc. Roy. Soc. A*, **209**, 196, 1951 ; etc.
5. M. v. LAUE, *Z. für Krist.*, **64**, 115, 1926.

## О ВЫЧИСЛЕНИИ ИНТЕНСИВНОСТИ, РАССЕЯННОЙ МЕЛКОКРИСТАЛЛИЧЕСКИМИ УГЛЯМИ

П. САБО

## Резюме

Исследуется интенсивность рассеяния мелкокристаллическими углями при разных степенях упорядоченности. Обнаружено, что формулы интенсивности, общепринятые для определения размеров кристаллов, не отражают правильно тип и степень упорядоченности. Из-за этого, размеры кристаллитов, определенные обычным способом, не вполне верны. Учитывая надлежащим образом неупорядоченность, наши формулы дают возможность определить ее степень экспериментально ; этим способом — кроме более точного определения размеров кристаллитов — возможно более точно изучить структуру мелкокристаллических углей. Описано тип нейтроно-дифракционных измерений, необходимых для использования этой возможности.



# МЕТОДЫ ОПРЕДЕЛЕНИЯ ФЛУКТУАЦИИ ЭНЕРГИИ И УГЛОВОГО РАССЕЯНИЯ БЫСТРЫХ ИОНИЗУЮЩИХ ЧАСТИЦ

А. БЕКЕШИ, Л. ПАЛ и Л. ЯНОШИ

ЦЕНТРАЛЬНЫЙ ФИЗИЧЕСКИЙ НАУЧНО-ИССЛЕДОВАТЕЛЬСКИЙ ИНСТИТУТ ВЕНГЕРСКОЙ  
АКАДЕМИИ НАУК, БУДАПЕШТ

(Поступило : 28. II. 1958)

В работе излагаются и критически сравниваются методы определения флуктуации энергии и углового рассеяния быстрых ионизирующих частиц. Особое внимание уделялось изложению физического содержания перечисленных приближенных методов. Даются общие указания на улучшение приближений.

## § 1. Введение

Быстрые заряженные частицы космического излучения при прохождении через поглощающее вещество теряют свою энергию и отклоняются от первоначального направления. Потери по энергии и угловое рассеяние возникают вследствие столкновений с атомами поглощающего вещества. Эти столкновения носят вероятный характер. Таким образом, можно определить только вероятность того, что после столкновения энергия частицы находится в интервале  $(E, E + dE)$ , а ее траектория отклонится от некоторого заданного направления на угол, попадающий в интервал  $(A, A + dA)$ . В абсорбенте происходит не одно столкновение, а весьма много и с точки зрения измерения важен как раз суммарный результат этих столкновений.

Вычислением флуктуации энергии и углового рассеяния быстрых частиц занимался целый ряд авторов, но из различных точек зрения.

Если известно, например, эффективное сечение тормозного излучения, т. е. статистическое распределение потери энергии при одном столкновении, то легко можно вычислить среднюю потерю для одного столкновения или — что является более важным, — получить потерю на единичную длину.

Известно, что вследствие тормозного излучения частица может потерять значительную часть своей энергии при одном столкновении. Кроме того, различные потери по энергии могут встречаться примерно с одинаковой вероятностью. Вследствие этого, результаты столкновений, последующих друг за другом, могут сильно отличаться, т. е. флуктуация энергии может быть значительна.

Для определения средней потери энергии на единичную длину достаточно знать величину средней потери энергии при одном столкновении, но

для определения флуктуации уже необходимо проанализировать весь стохастический процесс. Потеря энергии частиц в тормозном излучении была определена впервые Гейтлером и Бете [1], ими же была определена флуктуация энергетических потерь специальной функцией, хорошо приближающей эффективное сечение тормозного излучения. Для решения данной проблемы ими был использован специальный метод, применяемый лишь к данной функции.

В противоположность тормозного излучения ионизационные потери в одном акте приводят лишь к незначительным изменениям энергии. Большая потеря энергии в одном акте возможна, но вероятность ее очень мала. Флуктуация потери тоже мала, поэтому в первом приближении достаточно определить лишь ее среднее значение. Блох [2], Бете [3] и другие определили среднее значение ионизационных потерь при разных условиях и в разных приближениях.

В последнее время в связи с определением массы и скорости на основе ионизации стало необходимым проанализировать флуктуацию ионизационных потерь, ибо она может ограничивать точность определения этих величин. Эта проблема была решена впервые Ландау [4] для случая тонкого абсорбента. Потом Бланк [5], Померанчук [6], Шульц [7], Саймон\* [8], Пал [9] и Мойал [10] занимались этим вопросом. В решении Ландау играет роль не столько толщина абсорбента, сколько энергия частицы. По его предположению потеря энергии в одном акте не зависит от мгновенной энергии частицы. Это условие, конечно, находится в тесной связи с толщиной абсорбента, но в то время как свинец толщиной в один метр является тонким для мезонов с экстремальной большой энергией, фотоэмульсия для медленных частиц уже является толстой. В цитированной статье Пала [9] дается уточнение решения Ландау и одновременно указывается на возможность другого решения, к которому мы вернемся еще в данной работе.

Среднее значение углового рассеяния из-за симметрии равно нулю, но флуктуация может быть значительна. Определение флуктуации имеет, например, большое значение в таких случаях, когда по отклонению в магнитном поле стараемся найти импульс или знак заряда мезонов. Впервые эта задача была решена Ферми [12], но он предполагает в своем решении, что энергия частицы постоянна. Яноши [13] и Эйджс [13а] обобщили метод Ферми для случая переменной энергии. В обоих случаях пренебрегаются столкновения под большими углами, имеющими малую вероятность.

Все эти стохастические процессы в самом общем виде детально были изучены в работах Колмогорова [14] и Феллера [15]. Предметом данной работы является принципиальное сравнение методов, примененных разными авторами.

\* Результаты Саймона не были нами известны, узнали о них лишь из книги Росси [11].



## § 2. Постановка вопроса

Пусть характеризуют состояние частицы в момент времени  $t$  некоторые параметры  $A_1, A_2, \dots, A_k$ . Эти параметры меняются во времени. В момент времени  $t = t'$  параметры  $A_1, A_2, \dots, A_k$  принимают значения

$$A'_1, A'_2, \dots, A'_k.$$

Кроме того, пусть  $S_1, S_2, \dots, S_k$  некоторые интервалы, выбранные таким образом, что

$$A'_1 \subset S_1, A'_2 \subset S_2, \dots, A'_k \subset S_k.$$

Можно описать движение частицы, если задать функцию распределения

$$\varphi(\mathbf{A}, t; \mathbf{S}, t'), \quad (1)$$

выражающую вероятность того, что частица в момент времени  $t$ , исходя из состояния  $\mathbf{A} = A_1, A_2, \dots, A_k$  в промежутке времени  $(t', t)$  переходит в какое-то другое состояние, характеризуемое величинами  $A'_1, A'_2, \dots, A'_k$ , находящимися в интервале  $\mathbf{S}$  т. е.

$$\mathbf{A}' \subset \mathbf{S}. \quad (2)$$

Таким образом, можно предполагать, что

$$\varphi(\mathbf{A}, t; \mathbf{S}, t) = \Delta(\mathbf{A}, \mathbf{S}), \quad (3)$$

где функция  $\Delta(\mathbf{A}, \mathbf{S})$  определяется следующим образом:

$$\Delta(\mathbf{A}, \mathbf{S}) = \begin{cases} 1, & \text{если } \mathbf{A} \subset \mathbf{S} \\ 0, & \text{вне интервала.} \end{cases}$$

В случае общей постановки вопроса предположим, что независимой переменной является время. Такое предположение вообще не принято; обычно рассматривают значение одной из координат частицы как независимую переменную.

Как ниже покажем, этот последний метод рассмотрения уже означает некоторое пренебрежение.

При рассмотрении прохождения частицы через поглощающее вещество можно предполагать, что в начальный момент направление движения частицы параллельно с осью  $X$  прямоугольной системы координат  $XYZ$ . Если еще предполагать, что состояние частицы не флуктуирует слишком

сильно, то можно взять координату  $x$  в качестве независимого параметра. В этом случае состояние частицы характеризуется функцией

$$\varphi(\mathbf{A}, x; \mathbf{S}, x'). \quad (4)$$

Однако, строго говоря, на эту функцию не применимо начальное условие

$$\varphi(\mathbf{A}, x; \mathbf{S}, x) = \Delta(\mathbf{A}, \mathbf{S}).$$

Это легко может быть наглядно показано.

Вероятность того, что в момент времени  $t$  частица исходит из состояния  $x$ ,  $\mathbf{A}$  и переходит в промежутке времени  $(t', t)$  в состояние  $x$ ,  $\mathbf{A}' \supset \mathbf{S}$ , в общем случае не равна нулю и поэтому

$$\varphi(\mathbf{A}, x; \mathbf{S}, x) \neq 0 \quad (4')$$

независимо оттого, что  $\mathbf{S}$  включает ли в себе  $\mathbf{A}$  или нет.

Отсюда следует, что можно выбрать  $x$  за независимую переменную только в том случае, если можно пренебречь эффектами, связанными с возвратом частицы.

Если взять за независимую переменную, например, длину дуги вместо координаты  $x$ , то возможно более точное решение вопроса. Так как длина дуги является величиной, монотонно возрастающей, о возврате здесь речь не может идти. Выбор длины дуги за независимую переменную включает в себе некоторую трудность. Дело в том, что необходимо учитывать и те случаи, когда частица останавливается. Это приводит к сингулярному состоянию. Одним из нас [16] эти вопросы были подробно рассмотрены.\*

Обычным выбором параметров является следующая схема:

$x$  — независимая переменная,

$A$  — угол между проекцией траектории частицы на плоскость  $(X, Z)$  и осью  $X$ ,

$Z$  — расстояние частицы от первоначального направления  $OX$  на глубине  $x$  в плоскости  $(X, Z)$ ,

$E$  — энергия частицы.

Ради простоты обозначаем величины  $A, Z, E$  через  $\mathbf{A}$ , а интервал  $\mathbf{S}$  обычно берется бесконечно узким. Итак

$$\varphi(E, A, Z, x; E', A', Z', x') dA' dE' dZ' \quad (5)$$

\* Дальнейшее обобщение стохастических процессов космического излучения было дано Л. Палом [17].

вероятность того, что на глубине  $x$  частица исходит из состояния  $\mathbf{A}$ , и пройдя некоторый путь, до глубины  $x'$  она переходит в состояние  $\mathbf{A}'$ , находящееся в интервале  $\mathbf{S}$ . Для простоты обозначим через  $\varepsilon$  энергию  $E$  и угол рассеяния  $A$ , играющие подобную роль в обобщенном рассмотрении. Для определения функции (5) необходимо знать эффективное сечение :

$$q(\varepsilon, \varepsilon') d\varepsilon' \quad (6)$$

являющееся вероятностью того, что после столкновения частица имеет энергию, находящуюся в интервале  $(E', E' + dE')$  и в процессе столкновения ее траектория отклонится от направления оси  $OX$  на угол, попадающий в интервал  $(A', A' + dA')$  при условии, что до столкновения эти же величины имели значения  $E$  и  $A$ .

Сейчас определим вероятность того, что величина  $\varepsilon$  на пути  $\Delta x$  изменится и примет значение, находящееся в интервале  $(\varepsilon', \varepsilon' + d\varepsilon')$ . Пусть эта вероятность имеет вид :

$$\varphi(x, \varepsilon; x + \Delta x, \varepsilon') d\varepsilon.$$

Если  $\Delta x$  очень мало, то можно предполагать, что вдоль участка  $\Delta x$  происходит не больше одного столкновения. В этом случае :

$$\begin{aligned} \varphi(x, \varepsilon; x + \Delta x, \varepsilon') &= Nq \Delta x + \left\{ 1 - N \int q(\varepsilon, \varepsilon') d\varepsilon' \Delta x \right\} \delta(\varepsilon - \varepsilon') = \\ &= w(\varepsilon, \varepsilon') \Delta x + \left\{ 1 - \int w(\varepsilon, \varepsilon') d\varepsilon' \Delta x \right\} \delta(\varepsilon - \varepsilon'), \end{aligned} \quad (7)$$

где  $\delta(\varepsilon - \varepsilon')$  — функция Дирака, а  $w(\varepsilon, \varepsilon') = Nq(\varepsilon, \varepsilon')$ ,  $N$  — число атомов в одном кубическом сантиметре и  $\Delta x$  — толщина абсорбента в сантиметрах, или же  $N$  — число атомов в одной грамме, и  $\Delta x$  — толщина абсорбента в гр. см<sup>-2</sup>. Так как  $N\Delta x$  — вероятность того, что на пути  $\Delta x$  частица претерпевает одно столкновение, то вероятность столкновения с двумя атомами на этом же пути пропорциональна  $\Delta x^2$ . Однако, если  $\Delta x$  достаточно мало, то вероятность столкновения почти равна нулю, итак направление движения и энергия частицы меняются лишь незначительно. Для этого рассмотрения можно применять интегро-дифференциальные уравнения Феллера [15].

Можно, однако, исходить из «непрерывной» модели, по которой невозможно выбрать  $\Delta x$  настолько малым, чтобы функция  $\varphi(x, \varepsilon; x + \Delta x, \varepsilon')$  была пропорциональна  $\Delta x$ ; а наоборот, пусть  $\Delta x$  сколь угодно малая величина, все-таки частица претерпевает столкновения со многими атомами. Эффект отдельных столкновений, однако, настолько мал, что средняя потеря энергии

$$O(E) = \int_{E'} \int_{A'} (E - E') w(\varepsilon, \varepsilon') dE' dA' \quad (8)$$

и дисперсия

$$P^2(E) = \iint_{E'A'} (E - E')^2 w(\varepsilon, \varepsilon') dE' dA' \quad (9)$$

остаются конечными, но моменты высшего порядка уже исчезают. Среднее значение и дисперсия углового рассеяния частицы также конечны, а моменты высшего порядка также исчезают. Для этой модели можно применять дифференциальные уравнения Колмогорова [14] (§ 4). Эти уравнения хорошо описывают, например, броуновское движение. При данной проблеме они являются хорошим приближением лишь в том случае, если число столкновений велико даже при малом  $\Delta x$ , но отдельные эффекты столкновений можно считать незначительными.

Целесообразно отделить столкновения с резким изменением энергии от столкновений с незначительным изменением. Столкновения с резким изменением учитываются таким образом, что расчёты введутся так, как будто бы частица исчезла после такого столкновения. Это разделение столкновений было необходимо при построении каскадного уравнения Яноши [13].

Таким образом, все явления, не интересующие нас, (например распад мезонов при их диффузии, тормозное излучение и т. д.) можно рассматривать как столкновения с резким изменением энергии.

Из обычных столкновений также можно исключить столкновения, приводящие к изменению энергии и направления движения, превышающие некоторый предел. Это можно осуществить срезанием эффективного сечения при некоторой энергии и направлении. Столкновения, не рассматриваемые из-за срезания эффективного сечения, включаются в класс столкновений с резким изменением.

Результаты расчетов со срезанными эффективными сечениями являются более-менее хорошим приближением, но можно их считать совершенно точным ответом на следующий вопрос: каково будет распределение частиц по энергии и по направлению, не претерпевающих столкновения с резким изменением.

Соответственно выше изложенным, кроме функции  $w(\varepsilon, \varepsilon')$  характеризующей столкновения с умеренным изменением, вводим еще эффективное сечение  $\alpha(\varepsilon)$  описывающее столкновения с резким изменением.  $\alpha(\varepsilon)$  равняется срезанной части эффективного сечения, т. е.:

$$\alpha(\varepsilon) = \int_{E'=0}^{E_k} \int_{A'} w(\varepsilon, \varepsilon') d\varepsilon' dA', \quad (10)$$

где  $E_k$  — критическая энергия. Если не учитывать столкновений с резким изменением, то

$$\int \varphi(x, \varepsilon; x', \varepsilon') d\varepsilon' = 1 \quad (11)$$

не будет справедливо. Этот интеграл дает вероятность того, что частица не претерпевает столкновения с резким изменением.

### § 3. Определение кинетических уравнений

Для определения функции  $q(\varepsilon, x; \varepsilon', x')$  можно написать два интегро-дифференциальных уравнения. В первом уравнении на глубине  $x'$  величины  $E', A', Z'$  являются простыми параметрами, а значения  $E, A, Z$  на глубине  $x$  — существенными переменными, во втором уравнении наоборот. Хотя второе уравнение на первый взгляд оказывается более естественным и соответственно этому используется чаще первого, все-таки оба равноценны, даже для некоторых целей, например, для построения уравнений каскадной теории первое уравнение является более подходящим.

Первое и второе уравнения по сути дела тождественны уравнениям Феллера [15]. Феллер пользуется функциями распределения для сохранения математического единства, но физически более наглядной является функция плотности вероятности  $\varphi$ . Конечно, в этом случае необходимо применять  $\delta$  — функцию Дирака.

Вместо  $\delta$  — функции часто можно использовать  $\delta^*$  — функцию, регулярную, дифференцируемую, напр. функцию:

$$\delta^*(x) = \frac{1}{\sqrt{\pi\kappa}} \exp(-x^2/\kappa). \quad (12)$$

Если  $\kappa$  достаточно мало, то выбор (12) значительно не изменяет конечного результата, и тогда без всяких предельных переходов можно применять функцию  $\delta^*$  вместо  $\delta$  — функции. В качестве примера можно привести следующее рассмотрение: если в поперечное сечение хотим включить координату  $Z$ , то вместо

$$q(\varepsilon, Z; \varepsilon', Z') = q(\varepsilon, \varepsilon') \delta(Z, Z')$$

хорошим приближением можно писать, что

$$q(\varepsilon, Z; \varepsilon', Z') = q(\varepsilon, \varepsilon') \delta^*(Z, Z'). \quad (13)$$

Если поставим в (13) выше определенную функцию (12) и предположим, что

$$\kappa \sim 10^{-100} \text{ см},$$

то конечное выражение соответствует предположению, что частица после каждого столкновения смещается на расстояние около  $10^{-100}$  см.



Однако, эти смещения не могут привести ни к какому действию, так как число атомов в абсорбенте по порядку величины примерно  $10^{24}$ , поэтому если бы частицы претерпевали столкновения даже с каждым атомом, то и в этом случае не было бы никакого измеряемого эффекта от предположенных смещений. Отсюда следует, что предположение таких смещений с одной стороны не ограничивает общности физического рассмотрения, а с другой стороны делает возможным заменить разрывную  $\delta$  — функцию дифференцируемой функцией.

Замен  $\delta$  — функции функцией  $\delta^*$  математически может привести к ошибке, если поперечное сечение разрывно и число столкновений неограничено, но физически число столкновений во всех случаях должно быть ограничено хотя и потому, что в абсорбенте имеется конечное число атомов. Поэтому всегда можно заменить поперечное сечение функцией, соответствующей ограниченному числу столкновений.

Вывод первого уравнения возможен на основе рассуждений, применяемых Яноши [13], [18] в теории каскадных процессов.

Предположим, что частица при прохождении пути  $\xi$  в абсорбенте не претерпевает ни одного столкновения. Вероятность этого можно написать в следующем виде:

$$\exp \left\{ - \xi [a(\varepsilon) + \int_{\varepsilon''} w(\varepsilon, \varepsilon'') d\varepsilon''] \right\}$$

при этом координата  $Z$  частицы принимает значение  $Z + A\xi$ .

Строго говоря, вместо  $Z + A\xi$  нужно писать  $Z + \xi \operatorname{tg} A$ , однако предполагается, что  $A$  достаточно мало, так что данное приближение законно. (Столкновения же с большими углами принадлежат в класс столкновений с резким изменением, так что они учитываются с введением эффективного сечения  $a(\varepsilon)$ .) Далее, предположим, что первое столкновение происходит в интервале  $(\xi, \xi + d\xi)$  с умеренным изменением. Вследствие этого столкновения энергия частицы уменьшается на  $E''$ , а направление ее движения изменяется на  $A''$ .

Вероятность такого столкновения в приближении  $A \ll 1$  есть

$$w(\varepsilon, \varepsilon'') d\varepsilon'' d\xi.$$

На остальном пути  $x' - x - \xi$  вследствие многих столкновений энергия частицы уменьшается на  $E'$ , а угол  $A''$  и горизонтальное отклонение  $Z + A\xi$  принимают значения  $A'$  и  $Z'$ .

Вероятность этого события:

$$\varphi(x + \xi, \varepsilon'', Z + A\xi; x', \varepsilon', Z') d\varepsilon' dZ'. \quad (14)$$



Изложенный здесь метод является одним из возможных изложений теории кинетического уравнения, описывающего стохастический процесс с умеренным изменением параметров.

Для того, чтобы принять во внимание все возможные осуществления данного события, исключающие друг друга, необходимо проинтегрировать все эти выражения по всем возможным значениям переменной  $\xi$ .

Кроме того, возможно еще, что в абсорбенте ни одного столкновения не происходит, что имеет вероятность

$$\exp \left\{ (x' - x) \left[ -\alpha(\varepsilon) - \int_{\varepsilon''} w(\varepsilon, \varepsilon'') d\varepsilon'' \right] \right\}, \quad (15)$$

Обозначим для краткости величину  $\int_{\varepsilon''} w(\varepsilon, \varepsilon'') d\varepsilon'' + \alpha(\varepsilon)$  через  $\beta(\varepsilon)$ .

В этом случае :

$$\begin{aligned} \varphi(x, \varepsilon, Z; x', \varepsilon', Z') = & \exp \left\{ -(x' - x) \beta(\varepsilon) \right\} \delta(\varepsilon' - \varepsilon) \delta[Z' - Z - A(x' - x)] + \\ & + \int_{\xi=0}^{x'-x} d\xi \int_{\varepsilon''} \exp \left\{ -\xi \beta(\varepsilon) \right\} w(\varepsilon, \varepsilon'') \varphi(x + \xi, \varepsilon'', Z + A\xi; x', \varepsilon, Z') d\varepsilon''. \end{aligned} \quad (16)$$

Если умножим это уравнение на  $\exp \left\{ (x' - x) \beta(\varepsilon) \right\}$  и вместо  $\xi$  вводим новое переменное  $\eta = x' - x - \xi$  и продифференцируем его по  $x$ , то после сокращений получим следующее интегро-дифференциальное уравнение :

$$\begin{aligned} \frac{\partial \varphi}{\partial x} = & -A \frac{\partial \varphi}{\partial Z} + \alpha(\varepsilon) \varphi + \int_{\varepsilon''} w(\varepsilon, \varepsilon'') \left\{ \varphi(x, \varepsilon, Z; x', \varepsilon', Z') - \right. \\ & \left. - \varphi(x, \varepsilon'', Z; x', \varepsilon', Z') \right\} d\varepsilon''. \end{aligned} \quad (17)$$

При начальном условии

$$\varphi(x = x', \varepsilon, Z; x', \varepsilon', Z') = \delta(\varepsilon - \varepsilon') \delta(Z - Z') \quad (18)$$

Вывод второго уравнения может быть осуществлен, например, следующим образом :

Вероятность

$$\varphi(x, \varepsilon, Z; x' + dx', \varepsilon', Z')$$

складывается из вероятностей двух взаимно не совместимых событий, именно :

1°. Либо уже на глубине  $x'$  состояние частицы характеризуется параметрами,  $\varepsilon'$  и  $Z'$  —  $A dx'$  и на пути  $dx'$  столкновения не происходит.

2°. Либо на глубине  $x'$  состояние частицы характеризуется параметром  $\varepsilon''$  и на пути  $dx'$  происходит столкновение, которое перенесет ее в состояние  $\varepsilon'$ . Так как  $Z$  не может измениться скачкообразно, оно может отличаться от  $Z'$  лишь членом порядка величины  $dx'$ .

Таким образом, можем написать, что :

$$\varphi(x, \varepsilon, Z; x' + dx', \varepsilon', Z') = \varphi(x, \varepsilon, Z; x', \varepsilon', Z - A' dx') \{1 - \beta(\varepsilon') dx'\} + \\ + \int_{\varepsilon''} w(\varepsilon', \varepsilon') \varphi(x, \varepsilon, Z; x', \varepsilon'', Z') d\varepsilon'' dx'. \quad (19)$$

После элементарных вычислений получим :

$$\frac{\partial \varphi}{\partial x'} = -\alpha(\varepsilon') \varphi - A' \frac{\partial \varphi}{\partial Z'} - \int_{\varepsilon''} w(\varepsilon', \varepsilon'') \varphi(x, \varepsilon, Z; x', \varepsilon', Z') d\varepsilon'' + \\ + \int_{\varepsilon''} w(\varepsilon'', \varepsilon') \varphi(x, \varepsilon, Z; x', \varepsilon'', Z') d\varepsilon'' \quad (20)$$

при начальном условии :

$$\varphi(x, \varepsilon, Z; x' = x, \varepsilon', Z') = \delta(\varepsilon - \varepsilon') \delta(Z - Z').$$

Интересно, что в первом уравнении первое, а во втором — последнее столкновение играет основную роль. Наверно, это обстоятельство является причиной того, что в каскадной теории легче всего вывести первое уравнение ( $G$  — уравнение Яноши), а вывод соответствующего второго уравнения (Мессел [19]) является более сложной задачей. Дело в том, что при первом столкновении имеется всего одна частица, а при последнем столкновении число различных частиц весьма большое, так что трудно учесть все возможные события.

Принято вместо  $E'$  и  $A'$  использовать другие параметры, например  $\Delta = E - E'$  и  $\alpha = A - A'$ . Не трудно привести уравнения (17) и (20) к виду, соответствующему новым переменным.

Уравнения (17) и (20) описывают процесс уменьшения энергии и изменения направления и места частицы при прохождении через поглощающее вещество. Каждому столкновению соответствует одно скачкообразное изменение параметров. Феллер [15] в своей цитированной работе приводит весьма интересный метод постепенного приближения для решения уравнений типа (17), (20).

Пусть будет начальное условие  $\delta(\varepsilon - \varepsilon')$  нулевым приближением. Подставляя  $\delta(\varepsilon - \varepsilon')$  в правую часть уравнения (20), получим производную по  $x'$  первого приближения. Подставляя первое приближение в правую часть уравнения (20), получим производную по  $x'$  второго приближения и. т. д. Таким образом получим  $\varphi$  в виде степенного ряда :

$$\varphi(x, \varepsilon; x', \varepsilon') = \sum_{k=0}^{\infty} \varphi_k(x, \varepsilon; x', \varepsilon') \frac{(x'' - x)^k}{k!}.$$

Для определения отдельных членов  $q_k$  имеет место следующая система уравнений:

$$\begin{aligned} \varphi'_{k+1}(x, \varepsilon; x', \varepsilon') = & -\varphi_k(x, \varepsilon; x', \varepsilon') \int_{\varepsilon''} w(\varepsilon, \varepsilon'') d\varepsilon'' + \\ & + \int_{\varepsilon''} \varphi_k(x, \varepsilon; x', \varepsilon'') w(\varepsilon'', \varepsilon') d\varepsilon'', \end{aligned} \quad (21)$$

если в уравнении (20) пренебрегаем столкновениями с резким изменением и зависимостью от  $Z$ . Феллер доказал сходимость данного метода в случае функции распределения, и показал, что это решение в то же время удовлетворяет и уравнению (17).

Однако, этот метод, по сути дела, означает то, что каждое столкновение учитывается отдельно. Вследствие этого, метод Феллера мало эффективен для численных вычислений таких процессов, для которых характерны многочисленные столкновения с малыми потерями энергии. Нулевое приближение соответствует случаю, когда столкновения не учитываются. Если  $\varphi_k$  означает учет эффекта  $k$ -ого возможного столкновения, то в выражении (21)  $\int_{\varepsilon''} \varphi_k(x, \varepsilon; x', \varepsilon'') w(\varepsilon'', \varepsilon') d\varepsilon''$  является коррекцией, соответствующей следующему  $k+1$ -ому столкновению, а  $\int_{\varepsilon''} w(\varepsilon, \varepsilon'') \varphi_k(x, \varepsilon; x', \varepsilon') d\varepsilon''$  соответствует тому случаю, когда  $k+1$ -ое столкновение не осуществилось; одним словом, член  $\varphi_{k+1}$  является коррекцией  $k+1$ -ого столкновения.

Метод Феллера во всяком случае доказывает, что постановка вопроса математически правильна и уравнения (17), (20) имеют однозначные решения.

Функция  $w(\varepsilon, \varepsilon')$  может стремиться к бесконечности при  $\varepsilon \rightarrow \varepsilon'$ . Это выражает физическую сущность процесса, именно, что в нем очень существенны малоэффективные столкновения.

Если  $w$  становится бесконечным так, что  $\int_{\varepsilon''} w(\varepsilon, \varepsilon'') d\varepsilon''$  даже как собственный интеграл не существует, то необходимо привести некоторое изменение. Если срезать эффективное сечение при некотором  $\varepsilon'' = \bar{\varepsilon}$  так, чтобы  $\int_{\varepsilon''} w(\varepsilon, \varepsilon'') d\varepsilon''$  существовал, то вместо (17) получим:

$$\begin{aligned} \frac{\partial \varphi}{\partial x} = & -A \frac{\partial \varphi}{\partial Z} + \alpha(\varepsilon) \varphi + \\ & + \int_{\varepsilon''} w(\varepsilon, \varepsilon'') \{ \varphi(x, \varepsilon, Z; x', \varepsilon', Z') - \varphi(x, \varepsilon'', Z; x', \varepsilon', Z') \} d\varepsilon''. \end{aligned} \quad (22)$$

Если теперь попытаемся совершить переход к пределу  $\varepsilon \rightarrow \varepsilon'$  то может быть, что уравнение (22) теряет смысл. Этот случай отражает, что описание физического процесса с эффективным сечением  $w(\varepsilon, \varepsilon')$  не является удовлетворительным. Улучшение, конечно, является физическим вопросом, а не

математическим. При расчете флуктуации ионизационных потерь полное эффективное сечение не дает удовлетворительного результата.

Однако возможно, что после формального совершения перехода  $\bar{\varepsilon} \rightarrow \varepsilon$  получается математически удовлетворительный результат. В этом случае эффективное сечение довольно хорошо описывает физическое содержание процесса. Хотя принципиально возможно определить конечное эффективное сечение на основе более точной физической теории, все-таки можно ожидать, что результат этим существенно не изменится, только вычисление становится более сложным. Примером для этого случая является вычисление флуктуации тормозного излучения при эффективном сечении

$$w(E, E') = \left\{ C E \ln \frac{E}{E'} \right\}^{-1} \quad C = \text{постоянная}$$

используемом Бете и Гейтлером.

Не учитывая зависимости от  $A$ , уравнения (17) и (20) легко решаются, если эффективное сечение однородно, т. е.  $w$  имеет вид:

$$w(E, E') = v \left( \frac{E'}{E} \right) \frac{1}{E}.$$

Вводя следующие обозначения:

$$y' = \ln \frac{E}{E'} \quad \text{и} \quad \varphi(x, E; x', E') = \frac{1}{E'} \psi(x, E; x', y'),$$

с помощью преобразования Лапласа можем написать, что

$$L\{\psi\} = \exp\{(x' - x) \int (u^\lambda - 1) v(u) du\}. \quad (23)$$

Используя выражение (23), либо с помощью метода перевала, либо аналитически можем определить функцию  $\psi$ .

Например, в специальном случае Бете—Гейтлера

$$v\left(\frac{E'}{E}\right) = \left\{ C \ln \frac{E}{E'} \right\}^{-1}. \quad (24)$$

$L\{\psi\}$  имеет вид

$$L\{\psi\} = \exp\left\{(x' - x) \frac{1}{C} \int_0^1 \frac{u^\lambda - 1}{\ln u} du\right\} = (\lambda + 1)^{-\frac{(x' - x)}{C}}. \quad (25)$$

Если  $x$  измеряется в так называемых каскадных единицах, то  $C = \ln 2$ . Из (25) получаем, что

$$\psi = \frac{e^{-y} y^{\frac{x' - x}{C} - 1}}{\Gamma\left(\frac{x' - x}{C}\right)}, \quad (26)$$

или

$$\varphi = \frac{1}{E} \frac{\ln\left(\frac{E}{E'}\right)^{\frac{x' - x}{C} - 1}}{\Gamma\left(\frac{x' - x}{C}\right)}. \quad (27)$$

Уравнения (17) и (20) можно решать с помощью преобразования Лапласа и в том случае, если эффективное поперечное сечение имеет вид

$$w(E, E') = v(E - E')$$

т. е. если оно зависит только от потери энергии. Необходимо обратить внимание на то, что при строгом рассмотрении  $w(E, E')$  нельзя считать полностью независимым от мгновенной энергии  $E$ , ведь в этом случае при малых  $E$  потеря энергии могла бы быть больше энергии  $E$  с вероятностью, отличающейся от нуля. Все-таки можно получить хорошее приближение, если значение  $v$  при большом значении его аргумента  $\Delta = E - E'$  очень мало или равно нулю, и энергия частицы на пути  $x' - x$  сильно не уменьшается. Метод Ландау [4] для вычисления флуктуации ионизационных потерь справедлив, как раз в этом случае. Действительно, при больших значениях  $E$  эффективное поперечное сечение не зависит от  $E$ , и вероятность большой потери энергии мала. Таким образом, если толщина абсорбента мала, то приближение является хорошим.

#### § 4. Приближение с помощью дифференциальных уравнений

Если характер процесса определяется часто повторяющимися столкновениями, приводящими к незначительному изменению параметров и эффективное поперечное сечение обладает большим значением только при  $\varepsilon' \sim \varepsilon$ , то решение дифференциального уравнения Колмогорова является хорошим приближением уравнений (17) и (20). Вычисления, приведенные ниже, показывают, с каким пренебрежением связано применение уравнений Колмогорова, относящихся к непрерывному процессу, вместо уравнений (17) и (20) чисто разрывного процесса.

Разложим в ряд подинтегральной функции  $\varphi(x, \varepsilon', Z; x', \varepsilon', Z')$  в уравнении (17) по степеням  $\varepsilon - \varepsilon'$ , и закончим разложение членами второго порядка. Учитывая, что

$$\int_{\varepsilon''} (A - A'') w(\varepsilon, \varepsilon'') d\varepsilon'' \quad \text{и} \quad \int_{\varepsilon''} (A - A'') (E - E'') w(\varepsilon, \varepsilon'') d\varepsilon''$$

из-за симметрии исчезают, получим, что

$$\frac{\partial \varphi}{\partial x} = -A \frac{\partial \varphi}{\partial Z} + a(\varepsilon) \varphi + O(E) \frac{\partial \varphi}{\partial E} - \frac{1}{2} P^2(E) \frac{\partial^2 \varphi}{\partial E^2} - \frac{1}{2} \delta^2(E) \frac{\partial^2 \varphi}{\partial A^2}, \quad (28)$$

где

$$O(E) = \int_{\varepsilon''} (E - E'') w(\varepsilon, \varepsilon'') d\varepsilon''$$

средняя потеря энергии на единичном пути, а

$$P^2(E) = \int_{\varepsilon''} (E - E'')^2 w(\varepsilon, \varepsilon'') d\varepsilon'' \quad \text{и} \quad \delta^2(E) = \int_{\varepsilon''} (A - A'')^2 w(\varepsilon, \varepsilon'') d\varepsilon''$$

дисперсии потери энергии и углового рассеяния. Таким образом, если члены третьего порядка являются малыми, то (28) можно считать хорошим приближением. Члены высшего порядка, в окрестности  $\varepsilon \sim \varepsilon'$  дают малую поправку; вопрос только в том, что  $w(\varepsilon', \varepsilon'')$  уменьшается ли достаточно быстро при  $\varepsilon'' \ll \varepsilon$ . Уравнение (28), по сути дела, является первым уравнением Колмогорова.

Второе уравнение (20) в аналогичном приближении дает уравнение Фокера—Планка (второе уравнение Колмогорова). Умножая уравнение (20) произвольной функцией  $R(\varepsilon')$  и интегрируя по  $\varepsilon'$  (учитывая, что порядок интегрирования можно поменять в первом интеграле правой части), получим:

$$\begin{aligned} & \int_{\varepsilon'} R(\varepsilon') \left\{ \frac{\partial \varphi}{\partial x'} + A' \frac{\partial \varphi}{\partial Z'} + a(\varepsilon') \varphi \right\} d\varepsilon' = \\ & = \iint_{\varepsilon' \varepsilon''} w(\varepsilon', \varepsilon'') \varphi(x, \varepsilon, Z; \varepsilon', Z') \{R(\varepsilon'') - R(\varepsilon')\} d\varepsilon'' d\varepsilon'. \end{aligned}$$

Разлагая  $R(\varepsilon'')$  в ряд по степеням  $\varepsilon' - \varepsilon''$  и учитывая только члены второго порядка, находим, что

$$\begin{aligned} & \int_{\varepsilon'} R(\varepsilon') \left\{ \frac{\partial \varphi}{\partial x'} + A' \frac{\partial \varphi}{\partial Z'} + a(\varepsilon') \varphi \right\} d\varepsilon' = \\ & = \int_{\varepsilon'} \varphi O(E') \frac{\partial R}{\partial E'} d\varepsilon' + \frac{1}{2} \int_{\varepsilon'} \varphi \left\{ P^2(E') \frac{\partial^2 R}{\partial E'^2} + \sigma^2(E') \frac{\partial^2 R}{\partial A'^2} \right\} d\varepsilon'. \end{aligned}$$



В правой части интегрированием по частям можно исключить производные функции  $R(\varepsilon')$ . О проинтегрированных членах можно предполагать, что они исчезают, ибо функция  $R(\varepsilon')$  является произвольной. Полученное уравнение справедливо для произвольной  $R(\varepsilon')$  только в том случае, если

$$\begin{aligned} \frac{\partial \varphi}{\partial x'} = & -A' \frac{\partial \varphi}{\partial Z'} - \alpha(\varepsilon') \varphi + \frac{\partial}{\partial E'} \{O(E') \varphi\} + \frac{1}{2} \frac{\partial^2}{\partial E'^2} \{P^2(E') \varphi\} + \\ & + \frac{1}{2} \sigma^2(E') \frac{\partial^2 \varphi}{\partial A'^2}. \end{aligned} \quad (29)$$

Это уравнение сопряжено с уравнением (28) и тождественно второму уравнению Колмогорова.

### § 5. Вычисление флуктуации углового рассеяния при малых углах с учетом потери энергии

Если в уравнениях (28) и (29) пренебречь членом, содержащем  $P^2(E)$ , т. е. пренебречь статистическим характером потери энергии, то в этом случае легко можно написать совместное решение уравнений (28) и (29), удовлетворяющее начальному условию

$$\delta(E' - E) \delta(A' - A) \delta(Z' - Z).$$

Легко убедиться в том, что  $\varphi$  имеет вид:

$$\varphi(x, \varepsilon, Z; x', \varepsilon', Z') = \exp \left\{ - \int_{E'}^E \frac{\alpha(E'')}{O(E'')} dE'' \right\} \frac{\delta \left( x' - x - \int_{E'}^E \frac{dE''}{O(E'')} \right)}{O(E')} \psi(x, \varepsilon, Z; x', \varepsilon', Z'), \quad (30)$$

где  $\psi$  удовлетворяет следующим уравнениям:

$$\begin{aligned} \frac{\partial \psi}{\partial x} = & -A \frac{\partial \psi}{\partial Z} + O(E) \frac{\partial \psi}{\partial E} - \frac{1}{2} \delta^2(E) \frac{\partial^2 \psi}{\partial A^2} \\ \text{и} \quad \frac{\partial \psi}{\partial x'} = & -A' \frac{\partial \psi}{\partial Z'} + O(E') \frac{\partial \psi}{\partial E'} + \frac{1}{2} \delta^2(E') \frac{\partial^2 \psi}{\partial A'^2}. \end{aligned} \quad (31)$$

Из (30) видно, что энергия частицы  $E'$  может иметь только значение, удовлетворяющее условию

$$x' - x - \int_{E'}^E \frac{dE''}{O(E'')} = 0, \quad (32)$$

так как при любом другом значении  $E'$  исчезает. Это означает, что между  $x'$  и  $E'$  существует однозначная связь в следующем виде:

$$x' - x = \int_{E'}^E \frac{dE''}{O(E'')}. \quad (33)$$

Учитывая уравнение (33), достаточно решить уравнения (31) на гиперповерхности, определенной уравнением (33). Другими словами, достаточно удовлетворять дифференциальным уравнениям (31) для тех значений  $x$ ,  $x'$  и  $E$ ,  $E'$ , которые удовлетворяют уравнению (33). С помощью (33) можно исключать  $x$  и  $x'$ . Очевидно, что  $\psi$  зависит только от толщины абсорбента, т. е. от  $x' - x$  при условии, что абсорбент является однородным, (а это предполагается, ибо иначе  $O(E)$  и  $P^2(E)$  в явном виде зависели бы от  $x - x'$ ). Пусть  $x' - x = x''$  тогда

$$x'' = \int_{E'}^E \frac{dE''}{O(E'')}.$$

Таким образом, можем написать, что

$$\psi(x'', \varepsilon, Z; \varepsilon', Z') = \psi \left\{ \int_{E'}^E \frac{dE''}{O(E'')}, \varepsilon, Z; \varepsilon', Z' \right\} \chi(\varepsilon, Z; \varepsilon', Z'). \quad (34)$$

Используя (34), из (31) получим следующие уравнения:

$$\begin{aligned} O(E) \frac{\partial \chi}{\partial E} &= A \frac{\partial \chi}{\partial Z} + \frac{1}{2} \sigma^2(E) \frac{\partial^2 \chi}{\partial A^2}, \\ O(E') \frac{\partial \chi}{\partial E'} &= E' \frac{\partial \chi}{\partial Z'} - \frac{1}{2} \sigma^2(E') \frac{\partial^2 \chi}{\partial A'^2}. \end{aligned} \quad (35)$$

Эти уравнения для  $\chi$  могут быть получены непосредственно, если вместо  $x$  и  $x'$  в качестве стохастического параметра вводим, на основе зависимости (33), величины  $E$  и  $E'$ . Исключением является тот случай, когда энергия постоянна, т. е.  $O(E) = 0$ . Этим случаем [11] занимался Ферми.

Нетрудно найти решение уравнений (35) с помощью преобразования Лапласа. После несложных вычислений получаем:

$$\chi = \frac{1}{4\pi A} \exp \left\{ -\frac{1}{4A} (\beta_1 A'^2 - 2\beta_2 A'' Z'' + \beta_3 Z''^2) \right\}, \quad (36)$$

где

$$\left. \begin{aligned} \Delta &= \beta_1 \beta_3 - \beta_2^2, \quad A'' = A' - A, \quad Z'' = Z' - Z - A \int_{E'}^E \frac{dE''}{O(E'')}, \\ \beta_3 &= \frac{1}{2} \int_{E'}^E \frac{\sigma^2(E'')}{O(E'')} dE'', \quad \beta_2 = \int_{E'}^E \frac{\beta_3(E'')}{O(E'')} dE'', \\ \beta_1 &= 2 \int_{E'}^{E'} \frac{\beta_2(E'')}{O(E'')} dE''. \end{aligned} \right\} \quad (37)$$

С помощью (33) можно снова ввести переменную  $x' - x$  вместо  $E - E'$  в функцию  $\chi$ , что является и более естественным.

Таким образом, полное решение имеет вид:

$$\varphi = \exp \left\{ - \int_{E'}^E \frac{\alpha(E'')}{O(E'')} dE'' \right\} \frac{\delta \left( x' - x - \int_{E'}^E \frac{dE''}{O(E'')} \right)}{O(E')} \chi, \quad (38)$$

где функция  $\chi$  определяется уравнениями (36) и (37). Необходимо заметить, что

$$\iint \chi dA' dZ' = 1,$$

но

$$\iiint \varphi dE' dA' dZ' \neq 1,$$

а

$$\iiint \varphi dE' dA' dZ' = \exp \left\{ - \int_{E'}^E \frac{\alpha(E'')}{O(E'')} dE'' \right\} x - x' \approx \int_{E'}^E \frac{dE''}{O(E'')}, \quad (39)$$

где последнее выражение указывает на то, что в интеграле  $\int_{E'}^E \frac{dE''}{O(E'')}$  нижний предел  $E'$  должен быть выбран таким образом, чтобы условие (33) выполнялось. Величина (39) отражает вероятность того, что частица с энергией  $E$  проходит путь  $x' - x$  без столкновения с резким изменением.

## § 6. Вопрос о флуктуации энергии

Уравнения (28) и (29) являются хорошими приближениями только в том случае, если потеря энергии в одном акте достаточно мала. Если срезать эффективное поперечное сечение настолько, чтобы уравнения (28) и (29) были хорошими приближениями и кроме  $E$  и  $E'$  не учитывать других переменных, то уравнения для  $\varphi$  имеют вид:

$$\left. \begin{aligned} \frac{\partial \varphi}{\partial x''} &= -O(E) \frac{\partial \varphi}{\partial E} + \frac{1}{2} P^2(E) \frac{\partial^2 \varphi}{\partial E^2} - \alpha(E) \varphi, \\ \frac{\partial \varphi}{\partial x''} &= \frac{\partial}{\partial E'} \{O(E') \varphi\} + \frac{1}{2} \frac{\partial^2}{\partial E'^2} \{P^2(E') \varphi\} - \alpha(E) \varphi, \end{aligned} \right\} \quad (40)$$

где

$$x'' = x' - x.$$

Если пренебрегать столкновениями с резким изменением, то для  $\varphi$  получаем следующие уравнения:

$$\left. \begin{aligned} \frac{\partial \varphi}{\partial x''} &= -O(E) \frac{\partial \varphi}{\partial E} + \frac{1}{2} P^2(E) \frac{\partial^2 \varphi}{\partial E^2}, \\ \frac{\partial \varphi}{\partial x''} &= \frac{\partial}{\partial E'} \{O(E') \varphi\} + \frac{1}{2} \frac{\partial^2}{\partial E'^2} \{P^2(E') \varphi\} \end{aligned} \right\} \quad (41)$$

с начальным условием  $\varphi(x'' = 0, E, E') = \delta(E - E')$ . Так как в явном виде невозможно найти общее решение уравнений (41), то при заданных  $O(E)$  и  $P^2(E)$  могут быть применены только численное решение или приближенные методы.

Точное решение уравнений (41) можно найти в том случае, если эффективное поперечное сечение имеет вид  $v \left( \frac{E'}{E} \right) \frac{1}{E}$  (Колмогоров [14]), так как в этом случае  $O(E)$  и  $P^2(E)$  являются пропорциональными  $E$ , и это позволяет переписать уравнения (41) с помощью преобразований  $\ln y = E$  и  $\ln y' = E'$  в виде уравнения теплопроводности. Этот случай не особенно интересен, так как при этих эффективных сечениях сами исходные интегральные уравнения легко решаются.

Если толщина абсорбента мала, то можно считать  $O(E)$  и  $P^2(E)$  примерно постоянными и тогда решение уравнений (41) по Росси [11] имеет вид:

$$\varphi(x'', E, E') = \frac{1}{P\sqrt{2\pi x''}} \exp \left\{ -\frac{(E - E' - O x'')^2}{2P^2 x''} \right\}. \quad (42)$$

Лучшим приближением является приближение Пала [9]. Он исходит из того, что при вычислении флуктуации энергии на глубине  $x'$  можно предполагать, что потеря энергии на пути  $x' - x$  мало отличается от средней потери и поэтому в выражениях  $O(E')$  и  $P^2(E')$  вместо  $E'$  можно подставлять среднюю энергию  $\bar{E}$  на глубине  $x'$ . Определение  $\bar{E}$  дается уравнением (33) в следующем виде:

$$x'' = \int_E^{\bar{E}} \frac{dE''}{O(E'')}.$$

Это приближение является хорошим, если  $E'$  не очень отличается от  $\bar{E}$ . После замены  $E'$  на  $\bar{E}(x'')$  во втором уравнении (41) коэффициенты  $O$  и  $P^2$  зависят только от  $x''$  и тогда можно найти решение (41) в следующем виде:

$$\varphi = \frac{1}{S \sqrt{2\pi}} \exp \left\{ -\frac{1}{2S^2} [\bar{E}(x'') - E']^2 \right\}, \quad (42')$$

$$S^2 = \int_0^{x''} P^2 \{ \bar{E}(x'') \} dx''. \quad (43)$$

Необходимо отметить, что

$$\bar{E}(x'') = E - \int_0^{x''} O \{ \bar{E}(x'') \} dx''. \quad (44)$$

Решение (42) дает вероятность, отличающуюся от нуля и для  $E' < 0$  и для  $E' > E$ , что не имеет физического смысла. Это указывает на то, что решение (42) не может быть применено к очень тонким или к очень толстым абсорбентам.

Необходимо отметить, что в случае малой дисперсии ( $S^2/\bar{E} \ll 1$ ) выражение (42) должно быть справедливо в широком интервале энергий  $E'$ . При  $S \rightarrow 0$  из (42'), получим, что

$$\varphi = \delta \{ \bar{E}(x''), E - E' \}. \quad (45)$$

Выражение (45) точно совпадает с решением, которое легко получается из (30), если предполагать, что  $P^2(E) = S^2(E) = a(E) = 0$  и пренебрегать зависимостью от  $Z$ . Это указывает на физическую правильность решения (42').

Для оценки погрешности приближенного решения (42') при разных значениях  $E'$  может быть применен следующий метод. Во втором уравнении (41) можно отделить некоторую часть, играющую роль малого возмущающего члена, следующим образом

$$\frac{\partial \varphi}{\partial x''} = O(\bar{E}) \frac{\partial \varphi}{\partial E'} + \frac{1}{2} P^2(E') \frac{\partial^2 \varphi}{\partial E'^2} + \psi(x'', E, E'), \quad (46)$$

где

$$\psi(x'', E, E') = -\frac{\partial}{\partial E'} \{ [O(E') - O(\bar{E})] \varphi \} + \frac{1}{2} \frac{\partial^2}{\partial E'^2} \{ [P^2(E') - P^2(\bar{E})] \varphi \}.$$

Как видно,  $\psi = 0$  при  $E' = \bar{E}$  и при небольших отклонениях от  $\bar{E}$  с помощью метода постепенного приближения можно определить погрешность решения (42').

Как видно, проблемы флуктуации энергии и углового рассеяния еще далеко не разрешены. Не имеется решение проблемы флуктуации энергии ни в случае частиц, обладающих малой энергией, ни в случае толстого абсорбента. Нет еще совместного решения флуктуации энергии и углового рассеяния. Кроме того, еще совсем не разработана оценка погрешностей существующих приближений. Нет сомнения, что возможно улучшать приближенные методы и в настоящее время в этом направлении продолжают исследования.

## ЛИТЕРАТУРА

1. H. A. BETHE and W. HEITLER, Proc. Roy. Soc., A **146**, 83, 1934.
2. F. BLOCH, Z. f. Phys., **81**, 363, 1933.
3. H. A. BETHE, Ann. d. Phys., **5**, 325, 1930 ; Z. f. Phys., **76**, 293, 1932.  
M. S. LIVINGSTON and H. A. BETHE, Rev. Mod. Phys., **9**, 245, 1937.
4. L. D. LANDAU, Journ. of Phys. USSR, **8**, 204, 1944.
5. O. BLUNCK, Z. f. Phys., **128**, 500, 1950 ; **130**, 641, 1951.
6. И. ПОМЕРАНЧУК, ЖЭТФ, **18**, 759, 1948.
7. W. SCHULTZ, Z. f. Phys., **129**, 530, 1951.
8. K. R. SYMON, Howard University, Thesis (1948).
9. Л. ПАЛ, Вестник МГУ, **6**, 111, 1953.
10. J. E. MOYAL, Nucl. Phys., **1**, 180, 1956.
11. B. ROSSI, High-Energy Particles, p. 31, Prentice-Hall, Inc. New York (1952).
12. B. ROSSI and K. GREISEN, Rev. Mod. Phys., **13**, 240, 1941.
13. Л. ЯНОШИ, ЖЭТФ, **26**, 386, 1954 ; **26**, 518, 1954. L. JÁNOSSY, Acta Phys. Hung.  
**2**, 289, 1953.
- 13a. L. EYCES, Phys. Rev., **74**, 1534, 1948.
14. A. KOLMOGOROFF, Math. Annalen, **104**, 415, 1931.
15. W. FELLER, Math. Annalen, **113**, 113, 1936.
16. Л. ЯНОШИ, ЖЭТФ, **30**, 351, 1956.
17. Л. ПАЛ, ЖЭТФ, **30**, 362, 1955.
18. L. JÁNOSSY, Proc. Phys. Soc. A, **63**, 241, 1950. L. JÁNOSSY and H. MESSEL, Proc. Phys. Soc. A, **63**, 1101, 1950.
19. H. MESSEL and J. W. GARDNER, Phys. Rev., **84**, 1256, 1951 ; H. MESSEL and R. B. POTTS, Phys. Rev., **86**, 847, 1952.

## METHODS OF DETERMINATION OF THE FLUCTUATION OF THE ENERGY AND THE DISTRIBUTION OF ANGLES OF FAST IONIZING PARTICLES

By

Á. BÉKÉSSY, L. JÁNOSSY and L. PÁL

### Abstract

The methods of determination of the fluctuation of the energy and the distribution of angles of fast ionizing particles are described and critically compared. Special attention is paid to the physical contents of the methods of approximation. A general method is given of how to improve approximation.



# APPLICATION OF ONE-CENTER WAVE FUNCTIONS TO TETRAHEDRAL SYMMETRIC HYDRID MOLECULES

## I. THEORETICAL BASIS OF THE METHOD

By

E. KAPUY

RESEARCH GROUP FOR THEORETICAL PHYSICS OF THE HUNGARIAN ACADEMY OF SCIENCES, BUDAPEST

(Presented by A. Kónya. — Received: VII. 28. 1958)

The quantitative treatment of the polyatomic molecules encounters serious difficulties of mathematical nature. A considerable part of these may be overcome by the use of one-center wave functions. In case of molecules with high degree of symmetry this method seems to be successful. In the present work the application of the method to tetrahedral hydride molecules is examined. It gives methods for the building up of the wave function and the simplification of the computations.

### Introduction

The  $\text{XH}_4$  molecules consist of an atom (ion) X being in the centre of tetrahedron and four hydrogen atoms situated in the peaks of this tetrahedron. (X may be C,  $\text{N}^+$ , Si, Ge, etc.) It is characteristic for them that the four bonds are completely equivalent and to a high extent independent of each other. Their electronic ground term is  $^1A_1$ .

For the calculation of the energy and the eigenfunction the HLSP method [1, 2, 3, 4, 5] as well as the LCAO-MO method [1, 6, 7, 8] may be used, but, owing to the analytical and numerical calculation of the three- and four-center integrals involved, serious difficulties are encountered. (It may be, however, that in the near future these difficulties will be eliminated by the use of fast electronic computers.)

The occurrence of three- and four-center integrals may be avoided by using orbitals having identical centers (in our case the nucleus of the X atom). In this case only one- and two-center integrals occur, which can be easily computed. It has been shown by MULLIKEN [9] that due to the high degree of symmetry of  $\text{CH}_4$ , the problem can be rendered (probably to a good approximation) spherically symmetric, if the charge of the four protons is averaged over a spherical surface. The ground state of  $\text{CH}_4$ ,  $(1a_1)^2 (2a_1)^2 (1f_2)^6 \ ^1A_1$ , is very similar to the ground state of Ne,  $(1s)^2 (2s)^2 (2p)^6 \ ^1S_0$ , hence the methods used for atoms may be applied with a slight modification to such molecules.

With the aid of the Hartree SCF method, calculations were carried out by BUCKINGHAM, MASSEY and TIBBS for  $\text{CH}_4$  [10]. The result was very encouraging: also for the binding energy a strikingly good value was obtained.

Subsequently calculations were carried out by HARTMANN [11] for  $\text{CH}_4$  and  $\text{NH}_4^+$ . He applied hydrogen-like orbitals and neglected the electrons of the 1s shell. Varying the parameter in the exponent, good results were obtained for the energy and the nuclear distance.  $\text{CH}_4$  and  $\text{NH}_4^+$  were dealt with as well by BERNAL who also used hydrogen-like orbitals, but the electrons of the 1s shell were also considered by him. He too varied the parameters in the exponent, however, the results were less satisfactory than in the preceding two cases. The method does not give the binding energy.

The Hartree SCF method has been applied to  $\text{SiH}_4$  by CARTER [13], but he did not obtain a binding energy either.

The results of [10], [11] and those of [12], [13] are apparently contradictory to each other. The aim set in the present work is to examine the application of the method to tetrahedral hydrid molecules and its efficiency in the case of the  $\text{CH}_4$  molecule.

### 1. The Schrödinger equation

The Schrödinger equation of a hydrid molecule of type  $\text{XH}_4$  having a central nucleus of atomic number  $Z$  in the "fixed nuclei" approximation expressed in atomic units is [14, 15]:

$$\left( -\frac{1}{2} \sum_{i=1}^n \Delta_i - \sum_{i=1}^n \frac{Z}{r_i} - \sum_{i=1}^n \sum_{p=1}^4 \frac{1}{r_{ip}} + \sum_{1 \leq i < j}^n \frac{1}{r_{ij}} + \sum_{p=1}^4 \frac{Z}{R_p} + \sum_{1 \leq p < q}^4 \frac{1}{R_{pq}} \right) \Psi_\lambda - E_\lambda \Psi_\lambda. \quad (1)$$

Here  $n$  is the number of electrons, indices  $i, j$  refer to the electrons and indices  $p, q$  to the protons. Hence  $r_i$  is the distance of the  $i$ -th electron from the central nucleus,  $r_{ip}$  the distance of the  $i$ -th electron from the  $p$ -th proton,  $R_p$  the distance of the  $p$ -th proton from the central nucleus and  $R_{pq}$  the distance between the  $p$ -th and  $q$ -th proton. It is best to place the origin of the coordinate system into the central nucleus. The  $\Psi_\lambda$ -s are functions of the  $3n$  electron coordinates, but they also depend on the coordinates  $R_p$  and  $R_{pq}$  of the nuclei. The energy eigenvalues  $E_\lambda$  are also functions of the coordinates of the nuclei. In order to simplify the calculations the four protons are fixed in the peaks of a tetrahedron, their distances from the center of that tetrahedron being  $R$ . Thus the frame formed by the nuclei has the symmetry of the point group  $T_d$ .

### 2. The building up of the wave function. The variation method

Let the  $\varphi_j$ -s be  $N$  normalized, linearly independent one-electron orbitals, having the very same centre. Completing these by the spin functions  $\alpha$  and  $\beta$

we obtain  $2N$  linearly independent  $u_k$  orbitals. From them  $\binom{2N}{n}$  different determinants  $\Phi_i$  of  $n^{\text{th}}$  order may be formed. Separately the  $\Phi_i$ -s and an arbitrary linear combination of them changes sign when the coordinates of any two electrons interchange.

$$\sum_i C_i \Phi_i. \quad (2)$$

The  $C_i$ -s are the variational parameters whereas the  $\Phi_i$ -s are determinants of  $n$ -th order, consisting of the spin-orbitals  $u_k$ . The  $\varphi_j$ -s may include also variational parameters  $c_{j1} c_{j2} c_{j4} \dots$  etc. The task is to determine those parameters  $C_i, c_j$ , by which the energy expression is minimized. The variation of the  $C_i$ -s leads to the well-known secular equation of the form  $\sum_i C_i (H_{ij} - S_{ij}E)$  the lowest root of which gives the approximation of the energy eigenvalue of the ground state [16].

Since  $H_{ij} = \int \Phi_i^* H \Phi_j d\tau$  and  $S_{ij} = \int \Phi_i^* \Phi_j d\tau$  are still functions of the  $c_j$ -s, the energy has to be separately minimized according to these too.

### 3. The factorization of the secular equation

If the system has apart from the operator  $H$  also such hermitian operators  $R, Q, \dots$  which commute with  $H$  and with each other, i. e.

$$\begin{aligned} HP - PH &= 0, & PQ - QP &= 0, \\ HQ - QH &= 0, & & \\ \dots & & & \end{aligned} \quad (3)$$

then the physical quantities represented by the corresponding operators can be measured simultaneously with the energy and have a common eigenfunction system [17]. (It was assumed that operators  $P, Q, \dots$  are functions neither of operator  $H$  nor of each other.) It can be easily seen, that if  $\psi_{ikm}$  belongs to the eigenvalue  $p_k$  of  $P$  and  $q_m$  of  $Q$ , then :

$$\int \Psi_{ikm}^* \Psi_{jln} d\tau = S_{ijklmn} \delta_{kl} \delta_{mn}, \quad (4)$$

$$\int \Psi_{ikm}^* H \Psi_{jln} d\tau = H_{ijklmn} \delta_{kl} \delta_{mn}. \quad (5)$$

For molecules, neglecting the magnetic interactions, the square of the resultant spin momentum ( $S^2$ ) and the projection of the resultant spin momentum on the  $Z$  axis ( $S_z$ ) are such operators. In our case the operator  $H$  is also invariant against the operations of the point group  $T_d$ . Bringing the approximative functions into such a form that they belong to the given rows of the individual

irreducible representations, i. e. to be of given symmetry species then relations (4) and (5) can be applied to them too.

Using these, the secular equation is factorized into equations of lower order. Since in general our aim is to determine the energy and eigenfunction of a given molecular state, the trial functions  $\sum_i C_i \Phi_i$  are taken straightaway in such a form as to belong to the given eigenvalues of operators  $S^2$  and  $S_z$  and to given rows of the irreducible representations.

#### 4. Eigenfunctions of the operators $S_z$ and $S^2$

It can be easily seen that the determinants  $\Phi_i$  are eigenfunctions of the operator  $S_z$ , namely they belong to its eigenvalue  $\frac{1}{2}(n_\alpha + n_\beta)$  (in  $\hbar$  units).  $n_\alpha$  and  $n_\beta$  are the number of the spin functions  $\alpha$  and  $\beta$ , respectively in the determinant  $\Phi_i$  under discussion ( $n_\alpha + n_\beta = n$ ).

Functions belonging to the eigenvalue 0 of the operator  $S^2$  can be constructed as follows [15]. Let us assume that the determinant consists of

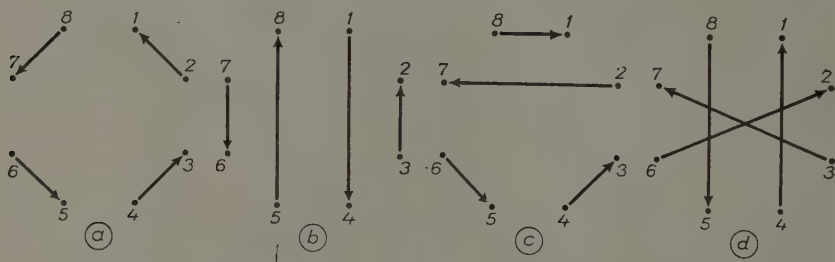


Fig. 1

$n$  given orbitals  $\varphi_j$  ( $n$  has to be an even number). Among these may be identical pairs, but it is then necessary within each pair that one of the orbitals has spin function  $\alpha$  the other one spin function  $\beta$  (doubly occupied orbitals). The  $v \leq n$  free orbitals can occur arbitrarily with spin functions  $\alpha$  or  $\beta$ .

Altogether  $N_0 = \frac{v!}{\left[\frac{v}{2}\right]!^2}$  such determinants  $\Phi_i^0$  can be constructed in case

of  $v$  singly occupied orbitals, which belong to the eigenvalue 0 of  $S_z$ , i. e.  $v_\alpha = v_\beta$ .  $v_\alpha$  and  $v_\beta$  are the number of the free orbitals with spinfunctions  $\alpha$  and  $\beta$ , respectively (for instance if  $v = 8$ ,  $N_0 = 70$ ).

The total spin state will be singlet if the electrons are forming singlets in pairs. Electron pairs, being in the doubly occupied orbitals, always form

singlets in each determinant  $\Phi_i^0$ . From the determinants  $\Phi_i^0$  we form such linear combinations in which the  $\nu$  singly occupied orbitals  $\varphi_j$  form  $\frac{\nu}{2}$  singlet pairs.

From  $\nu$  points  $\frac{\nu}{2}$  pairs can be formed in  $\frac{\nu!}{2^{\frac{\nu}{2}} \left[ \frac{\nu}{2} \right]!}$  variations.

Taking the points on the circumference of a circle the pair creation can be represented by arrows (RUMER's schema). For instance in the case  $\nu = 8$ , four such schemata can be seen in the figure. Altogether 105 such schemata may be formed. These are, however, not linearly independent [18]. Among the  $\frac{\nu!}{2^{\frac{\nu}{2}} \left[ \frac{\nu}{2} \right]!}$  schemata only  $\frac{\nu!}{\left[ \frac{\nu}{2} \right]! \left[ \frac{\nu}{2} + 1 \right]!}$  are linearly independent (i. e.

in case of  $\nu = 8$  only 14), namely those in which the arrows do not cross each other. A linear combination  $\sum_i C_i \Phi_i$  corresponding to such a schema can be obtained as follows [15]:

$${}^1\Psi_{j \rightarrow k, l \rightarrow m, \dots} = \sum_{i=1}^{N_0} \delta_{jk}(i) \delta_{lm}(i) \dots \Phi_1^0. \quad (6)$$

By the left upper index of  ${}^1\Psi$  the multiplicity is denoted ( $M = 2S + 1$ ), the indices connected by an arrow (for instance  $j \rightarrow k$ ) show that in the corresponding schema the arrow is directed from the  $j$ -th orbital towards the  $k$ -th orbital. The meaning of the symbol  $\delta_{jk}(i)$  is the following:

$$\delta_{jk}(i) = \begin{cases} 1, & \text{if the spin function of } \varphi_j \text{ is } \alpha, \text{ and that one of } \varphi_k \text{ is } \beta. \\ -1, & \text{if the spin function of } \varphi_j \text{ is } \beta, \text{ that one of the } \varphi_k \text{ is } \alpha. \\ 0, & \text{in all other cases.} \end{cases}$$

Hitherto the  $n$  orbitals  $\varphi_j$  occurring in the determinants, and the number of equal pairs among these, were considered as given.

Even more singlet functions can be obtained if the occupation number is varied in case of given  $\varphi_j$ -s for the individual  $\varphi_j$ -s, and on the other hand if we exchange among the  $\varphi_j$ -s one or more by new ones. If  $N$  different orbitals  $\varphi_j$  are at our disposal then altogether  $\binom{2N}{n}$  Slater determinants can be formed. Among these

$$\sum_{i=0}^{\frac{n}{2}} \binom{N}{\frac{n}{2} + i} \binom{\frac{n}{2} + i}{2i} \frac{[2i]!}{[i!]^2}$$

belong to the eigenvalue 0 of  $S_z$  and

$$\sum_{i=0}^{\frac{n}{2}} \left( \frac{n}{2} + i \right) \binom{N}{2i} \frac{[2i]!}{i! [i+1]!}$$

to the eigenvalue 0 of  $S^2$ . This method can be easily generalized also for the case of higher multiplets.

### 5. Construction of wave function of given symmetry species

Let us assume that the operator  $H$  commutes with the operations of a point group  $A(i)$  ( $i = 1, 2, \dots, G$ ). Let  $D^j(i)$  and  $D^{j'}(i)$  be the two unitary non-equivalent irreducible representations of the operation  $A(i)$ , with dimensions  $n_j$  and  $n_{j'}$ , respectively. If  $f_1^j, f_2^j, \dots, f_{n_j}^j$  and  $g_1^{j'}, g_2^{j'}, \dots, g_{n_{j'}}^{j'}$  are such functions for which is valid

$$A(i) f_{\kappa}^j = \sum_{\lambda=1}^{n_j} f_{\lambda}^j D_{\lambda\kappa}^j(i), \quad (\kappa = 1, 2, \dots, n_j);$$

$$A(i) g_{\kappa'}^{j'} = \sum_{\lambda'=1}^{n_{j'}} g_{\lambda'}^{j'} D_{\lambda'\kappa'}^{j'}(i), \quad (\kappa' = 1, 2, \dots, n_{j'}),$$

then the function  $f_{\kappa}^j$  belong to the row  $n$  of the irreducible representation  $j$ , and the function  $g_{\kappa'}^{j'}$  to the row  $\kappa'$  of the irreducible representation  $j'$ . In this case the following relations similar to (4) and (5) are valid [19]:

$$\int f_{\kappa}^{j*} g_{\kappa'}^{j'} dv = \frac{G}{n_j} \delta_{j'j} \delta_{\kappa'\kappa} \sum_{\lambda} \left( \int f_{\lambda}^{j*} g_{\lambda}^j dv \right), \quad (7)$$

$$\int f_{\kappa}^{j*} H g_{\kappa'}^{j'} dv = \frac{G}{n_j} \delta_{j'j} \delta_{\kappa'\kappa} \sum_{\lambda} \left( \int f_{\lambda}^{j*} H g_{\lambda}^j dv \right). \quad (8)$$

If  $F$  is such a function (orbital or many-electron wave function), to which the operations  $A(i)$  of the group can be applied, then knowing the matrix elements of the irreducible representations of the group,  $F$  can be decomposed into such parts  $f_{\kappa}^j$ , which belong to certain rows of the individual irreducible representations:

$$f_{\kappa}^j = \frac{n_j}{G} \sum_{i=1}^G D_{\kappa\kappa}^{j*}(i) A(i) F. \quad (9)$$



If only the characters  $\chi^j$  are known, then  $F$  can be decomposed into such parts  $f^j$ , which belong to the individual irreducible representations :

$$f^j = \frac{n_j}{G} \sum_{i=1}^G \chi^{j*}(i) A(i) F. \quad (10)$$

In the molecules similarly to the atoms the orbitals belonging to given rows of irreducible representations are denoted by the small letter of the corresponding irreducible representation, adding to it as right lower index the row number and after this the bracketed sign of the corresponding point group. Before the letter a number is written (1, 2, 3 etc), to express the energetical order of orbitals of identical symmetry species [20]. For instance  $1a_1 (T_d)$  or  $1f_2 (T_d)$ . Hereby the brief denotation of electron configurations is made possible. For instance for the  $\text{CH}_4$  molecule  $(1a_1)^2 (2a_1)^2 (1f_2)^6 {}^1A_1$ .

The denotation of the total electron state is similarly effectuated but then the capital letter symbolizing the corresponding irreducible representation is used and multiplicity is denoted by the left upper index. For instance  ${}^3F_2$ , if more states of identical symmetry species exist a further index has to be introduced in order to express the energetical sequence.

In general the determinant wave functions  $\Phi_i$  do not belong to given rows of the irreducible representations, neither in the case when each of the orbitals  $\varphi_j$  occurring in them is of a given symmetry species. The following two cases are exceptions :

a) If the determinant  $\Phi_i$  consists of such orbitals of given symmetry species that orbitals belonging to each row of the irreducible representations occurring in it are appearing once.

b) If orbitals belonging to each row of the irreducible representations occurring in it are appearing twice (once with spin functions  $\alpha$  and once with  $\beta$ ).

In these cases  $\Phi_i$  belongs to the so-called totally symmetric representation (this is a one-dimensional irreducible representation, each matrix of which is  $+1$ ) [21].

In case b) the molecule has closed shells. (The multiplicity of the electron state is 1.)

\*

The approximative one-center wave functions may be easily built up by the current methods. The MO (Molecular Orbital) method is closer to the nature of the matter, but also the VB (Valence Bond) method can be well applied.

## 6. The MO method

Let us choose a normalized (but not necessarily orthogonal) set  $\varphi_k$ . For this we have nothing else to go by than to attain a good approximation. The problem, which set of functions is the most adequate for the approximation of the orbitals of the valence shells — disregarding some general points of view — can be answered only if experience gained by many computations is at our disposal. Since a considerable part of the energy is given by the closed inner shells, such a set of functions should be chosen that the inner orbitals are well approximated by certain terms of it.

Hydrogen-like, Slater, Morse-Young-Haurwitz orbitals and the solutions obtained by Hartree-Fock's SCF method or their combination are appropriate. Into the radial part of the orbitals variational parameters are built in (the factor of the exponent, the coefficients of the linear combinations, eventually the power index of  $r$ ). After such linear combinations  $\psi_{\kappa i}^j$  are formed of the  $\varphi_k$ -s, which belong to the given rows ( $\kappa$ ) of the given irreducible representations ( $j$ ). Since against the operations of the group the radial parts are invariant, only the angular parts have to be examined. Using (9) and the irreducible representations [22] of the group  $T_d$ , the following table is obtained as a result for  $l$  from  $l = 0$  to  $l = 3$ .

	$A_1$	$E$		$F_1$			$F_2$		
	$a_1$	$e_1$	$e_2$	$f_{11}$	$f_{12}$	$f_{13}$	$f_{21}$	$f_{22}$	$f_{23}$
$s$	1								
$p$							$\xi$	$\eta$	$\zeta$
$d$		$3\xi^2-1$	$\xi^2-\eta^2$				$\eta\zeta$	$\xi\zeta$	$\xi\eta$
$f$	$\xi\eta\zeta$			$\xi(\zeta^2-\eta^2)$	$(\eta\zeta^2-\xi^2)$	$\zeta(\xi^2-\eta^2)$	$\xi(5\xi^2-3)$	$\eta(5\eta^2-3)$	$\zeta(5\zeta^2-3)$

$$\xi = \sin \vartheta \cos \varphi; \quad \eta = \sin \vartheta \sin \varphi; \quad \zeta = \cos \vartheta.$$

An orbital of given symmetry species is formed in such a manner that angular parts in the corresponding column are provided by different radial parts and linear combinations are formed of them with coefficients which are at present undetermined. For instance

$$\begin{aligned}
 1 a_1 &= c_{11} R_{11} + c_{12} R_{12} \xi \eta \zeta + \dots, \\
 2 a_1 &= c_{21} R_{21} + c_{22} R_{22} \xi \eta \zeta + \dots, \\
 1 f_{21} &= c_{31} R_{31} \xi + c_{32} R_{32} \eta \zeta + c_{33} R_{33} \xi (5 \xi^2 - 3) + \dots
 \end{aligned} \tag{12}$$

a) The  $\psi_{ki}^j$ -s thus obtained are completed with the spin functions  $\alpha$  and  $\beta$  and determinants  $\Phi_i$  of  $n$ -th order ( $n$  is the number of the electrons) are built up from them.

b) After this disregarding the spin factors with the aid of (9) such linear combinations  $\Psi_{\kappa}^j$  are formed of the  $\Phi_i$ -s which belong to the row  $\kappa$  of the irreducible representation  $j$ .

c) Then, with the  $\Psi_{\kappa}^j$ -s belonging to the same  $\kappa$  and  $j$  such functions  ${}^M\Psi_{\kappa\sigma}^j$  are constructed which belong to the given eigenvalues of the operators  $S_z$  and  $S^2$  ( $M$  is the multiplicity).

The linear combination formed from the  ${}^M\Psi_{\kappa\sigma}^j$ -s with the coefficients  ${}^MC_{\kappa\sigma i}^j$  is the most general trial function of the given electron state denoted by  $(M, j, \kappa)$ . Computing the energy expression with it and varying the parameters  $C$ ,  $c$  as well as the parameters built in to the  $R$ -s for minimizing the energy, we obtain the energy and wave function of the lowest electron state of given  $M, j, \kappa$ .

The calculation cannot be carried out in such a generality in practice owing to the immense work involved. Therefore application of the following simplifications is advisable:

a) The closed inner shells of the central atom are built up from such orbitals as in the case of the free atom and variational parameters are applied in their radial parts only. (For in stance in case of  $\text{CH}_4$   $1s$  is taken for  $1a_1$ , etc.)

b) The trial function is built up from only one  ${}^M\Psi_{\kappa\sigma}^j$  or from one containing only few terms, similarly the molecular orbitals  $\psi_{\kappa i}^j$  should contain a small number of terms only.

c) If the trial function consists of a single  ${}^M\Psi_{\kappa\sigma}^j$  only two further possibilities of simplification exist:

a) If the radial parts are fixed and only the parameters  $c$  varied, then the calculation can be carried out similarly to the LCAO-SCF method [23].

$\beta$ ) If the orbitals consist only of one term then — similarly as for atoms — the simple variational method, either the Hartree or Hartree-Fock SCF method can be applied for the determination of the radial parts [10].

Let us consider for instance the  ${}^1A_1$  ( $T_d$ ) ground state of the  $\text{CH}_4$  molecule, which can be most simply expressed by the single configuration  $(1a_1)^2 (2a_1)^2 (1f_2)^6$ . As  $1a_1$  orbital the Slater function  $1s$ , whereas as  $2a_1$  orbital the Slater function  $2s$  can be taken eventually completed by the term containing the angular part  $\xi\eta\zeta$  whereas as  $1f_2$  orbitals, Slater orbitals  $2p$  are employed possibly completed by terms containing angular terms  $d$  and  $f$ . This configuration can be expressed by a single determinant. The approximation can be improved by considering the configurational interaction.

## 7. The VB method

First the orbitals of the hydrogen atoms situated on peaks of the tetrahedron are expanded into such a set of functions the center of which is the central atomic nucleus. After this with orbitals thus obtained we proceed in such a manner as is usual in the HLSP method [24, 25].

For instance if one of the hydrogen atoms lies on the Z-axis at a distance  $R$  from the center, then the  $1s$  orbital of it can be approximated for example with the aid of the Slater orbitals as follows :

$$\begin{aligned} \varphi'_H = & c_{1s}R_1 + c_{2s}R_2 + c_{2p}R_2 \cos \vartheta + c_{3s}R_3 + c_{3p}R_3 \cos \vartheta + \\ & + c_{3r}R_3 (3 \cos^2 \vartheta - 1) + c_{4s}R_4 + c_{4p}R_4 \cos \vartheta + \\ & + c_{4d}R_4 (3 \cos^2 \vartheta - 1) + c_{4f}R_4 (5 \cos^3 \vartheta - 3 \cos \vartheta) + \dots \end{aligned} \quad (13)$$

Later the parameters  $c_i$  as well as the parameters in the  $R_i$ -s have to be determined so that the energy of the molecule should be minimal. Since practically only a few terms can be taken into consideration, such a set of functions has to be used that by a few terms already an adequate approximation is obtained. (For instance eigenfunctions of the H atom are not suitable, because they form a complete set only with the inclusion of the states of positive energy.) After that the well-known HLSP method is followed :

a) The orbitals  $\varphi'_H$  of the hydrogen atoms and the orbitals of the central atom are provided with spin functions  $\alpha$  and  $\beta$ , then determinants  $\Phi_i$  of  $n$ -th order are formed from them.

b) From the determinants  $\Phi_i$  such combinations  ${}^M\Psi$  are formed, which belong to the given eigenvalues of the operators  $S_z$  and  $S^2$ . (See 4.)

c) Such combinations  ${}^M\Psi_\kappa^j$  are formed from the  ${}^M\Psi$ -s which belong to the row  $\kappa$  of irreducible representation  $j$ . (See 5.)

The linear combination of functions having identical values  $M, j, \kappa$  is the most general trial function of the electron state characterized by  $(M, j, \kappa)$ .

In order to decrease the extension of the calculation the following simplifications may be used :

a) The closed shells of the central atom are built up from the orbitals of the corresponding free atoms (these are doubly occupied).

b) In the valence shell of the central atom four orbitals are considered only (one orbital  $s$  and three  $p$ ) and the ionic-homopolar resonance is neglected. Thus it remains still a restricted configurational interaction (the central atom appears with  $s^2p^2$ ,  $sp^3$  and  $p^4$  configurations).

c) For the sake of further simplification only a single configuration of the central atom is taken into consideration which consists of the four equivalent hybrid orbitals  $sp^3$  [25] [26]. With the four hybrid and the four  $\varphi'_H$  orbitals 70 determinants  $\Phi_i^0$  can be formed, which belong to the eigenvalue 0 of the operator  $S_z$ .

From these with the aid of (6) 14 linearly independent combinations can be constructed which belong to the eigenvalue 0 of the operator  $S^2$  [3, 4]. With the aid of (10) three combinations can be formed of these which belong to the irreducible representation  $A_1$ .

Among these the simplest can be represented by a single RUMER schema. (See schema *a*) on the Figure.) By numbers 1, 3, 5, 7 the orbitals of the hydrogen atoms are denoted, and by numbers 2, 4, 6, 8 the  $sp^3$  hybrid orbitals of the central atom directed in turn towards them. This schema is a linear combination of 16 determinants.

### 8. Calculation of the energy expansion in case of wave functions formed of determinants

The operator  $H$  of equation (1) can be written in the following form :

$$H = H_0 + \sum_{i=a}^n H_i + \sum_{1=i < j}^n H_{ij}. \quad (14)$$

In  $H_0$  the coordinates of the nucleus only, in  $H_i$  the coordinates of the  $i$ -th electron only, whereas in  $H_{ij}$  the coordinates of the  $i$ -th and  $j$ -th electron are included.

Let us introduce the density matrix of first order  $\Gamma(1' | 1)$ , of second order  $\Gamma^2(1' 2' | 12)$  and in general of  $\nu$ -th order  $\Gamma^\nu(1' 2' \dots \nu' | 12 \dots \nu)$  of the normalized wave function  $\Psi$  of  $n$  electrons [27, 28, 29]:

$$\begin{aligned} \Gamma(1' | 1) &= n \int \Psi^*(1' 2 \dots n) \Psi(1 2 \dots n) d\tau_2 d\tau_3 \dots d\tau_n, \\ \Gamma^2(1' 2' | 12) &= \binom{n}{2} \int \Psi^*(1' 2' 3 \dots n) \Psi(1 2 3 \dots n) d\tau_3 d\tau_4 \dots d\tau_n, \\ \Gamma^\nu(1' 2' \dots \nu' | 12 \dots \nu) &= \binom{n}{\nu} \int \Psi^*(1' \dots \nu' \nu + 1 \dots n) \\ &\quad \Psi(1 \dots \nu \nu + 1 \dots n) d\tau_{\nu+1} \dots d\tau_n. \end{aligned} \quad (15)$$

With their aid the energy can be easily written, considering that  $H$  is symmetrical in the electron coordinates and  $\Psi$  satisfies the Pauli principle

$$E = H_0 + \int H_1 \Gamma(1' | 1) d\tau_1 + \int H_{12} \Gamma^2(1' 2' | 12) d\tau_1 d\tau_2.$$

$H_1$  and  $H_{12}$  act only upon the coordinates not primed. After the effect of the operators, the primed coordinates are equated with the unprimed ones and the integration is performed.

Let  $\Psi$  be a linear combination of the  $n$ -th order determinants

$$\Psi = C_1 \Psi_1 + \dots + C_K \Psi_K + \dots + C_L \Psi_L + \dots$$

of the following form

$$\Psi_K = \frac{1}{\sqrt{D_{KK}} \sqrt{n!}} \det [u_1 u_2, \dots, u_n], \Psi_L = \frac{1}{\sqrt{D_{LL}} \sqrt{n!}} \det [v_1 v_2, \dots, v_n].$$

(The  $u_k$ -s and  $v_l$ -s are normalized spin orbitals.)

Then the energy can be expressed with the aid of the density matrices in the following way :

$$\begin{aligned} E = & \sum_{KL} C_K^* C_L [H_0 \int \Psi_K^* \Psi_L d\tau + \int H_1 \Gamma_{KL} (1' | 1) d\tau_1 + \\ & + \int H_{12} \Gamma_{KL}^2 (1' 2' | 12) d\tau_1 d\tau_2]; \\ \int \Psi_K^* \Psi_L d\tau = & \frac{\det [d_{KL} (k | l)]}{\sqrt{D_{KK}} \sqrt{D_{LL}}} = \frac{D_{KL}}{\sqrt{D_{KK}} \sqrt{D_{LL}}}, \end{aligned} \quad (16)$$

where

$$d_{KL} (k | l) = \int u_k^* (1) v_l (1) d\tau_1, \quad (k, l = 1, 2, \dots, n).$$

The minors of first order  $D_{KL} (k | l)$  and second order  $D_{KL} (k_1 k_2 | l_1 l_2)$  etc. of the determinants  $D_{KL} = \det [d_{KL} (k | l)]$  play an important role in the calculation of the density matrices :

$$\begin{aligned} \Gamma_{KL} (1' | 1) = & \frac{1}{\sqrt{D_{KK}} \sqrt{D_{LL}}} \sum_{kl} u_k^* (1') v_l (1) D_{KL} (k | l), \\ \Gamma_{KL}^2 (1' 2' | 12) = & \frac{1}{\sqrt{D_{KK}} \sqrt{D_{LL}}} \frac{1}{2!} \sum_{\substack{k_1 < k_2 \\ l_1 < l_2}} \begin{vmatrix} u_{k_1}^* (1') u_{k_2}^* (1') \\ u_{k_1}^* (2') u_{k_2}^* (2') \end{vmatrix} \begin{vmatrix} v_{l_1} (1) v_{l_2} (1) \\ v_{l_1} (2) v_{l_2} (2) \end{vmatrix} D_{KL} (k_1 k_2 | l_1 l_2). \end{aligned} \quad (17)$$

If the determinant  $D_{KL}$  is not zero, the density matrices may be obtained even in a simpler way [28]. Let us introduce the following expression

$$\varrho_{KL} (1' | 1) = \sum_{kl} u_k^* (1') v_l (1) d_{KL}^{-1} (l | k). \quad (18)$$

Here  $d_{KL}^{-1} (l | k)$  is the element  $(l | k)$  of the inverse of  $D_{KL}$ , i. e.

$$d_{KL}^{-1} (l | k) = \frac{D_{KL} (k | l)}{D_{KL}}.$$



With the aid of (18) the density matrices (17) can be expressed as

$$\Gamma_{KL}(1'|1) = \frac{D_{KL}}{\sqrt{D_{KK}D_{LL}}} \varrho_{KL}(1'|1), \quad (19)$$

$$\Gamma_{KL}^2(1'2'|12) = \frac{D_{KL}}{\sqrt{D_{KK}D_{LL}}} \frac{1}{2!} \begin{vmatrix} \varrho_{KL}(1'|1) & \varrho_{KL}(1'|2) \\ \varrho_{KL}(2'|1) & \varrho_{KL}(2'|2) \end{vmatrix}.$$

Writing this into the energy expression we obtain

$$E = \sum_{KL} C_K^* C_L \frac{D_{KL}}{\sqrt{D_{KK}D_{LL}}} \left[ H_0 + \int H_1 \varrho_{KL}(1'|1) d\tau_1 + \right. \\ \left. + \frac{1}{2} \int H_{12} \begin{vmatrix} \varrho_{KL}(1'|1) & \varrho_{KL}(1'|2) \\ \varrho_{KL}(2'|1) & \varrho_{KL}(2'|2) \end{vmatrix} d\tau_1 d\tau_2 \right]. \quad (20)$$

If  $\Psi$  consists of  $N$  terms then  $\frac{N(N+1)}{2}$  kinds of  $\varrho_{KL}$  have to be formed.

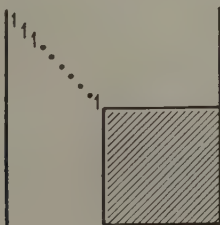
The number of the terms of the individual  $\varrho_{KL}$ -s depends on the orthogonality conditions of the spin orbitals, it is minimally  $n$ , maximally  $n^2$ .

Since the energy contribution of the inner closed shells is orders of magnitude higher than that of the valence shells, it is advisable to separate them. For chemical problems in general the energy conditions of the valence shell are important. In hydrid molecules of type  $\text{XH}_4$  only the central atom has closed shells, therefore the separation can be easily carried out, if the following conditions are satisfied.

a) In each determinant of the trial function  $\Psi$  the orbitals of the inner shells are identical.

b) Each orbital of the valence shells is ortohogonal to each orbital of the inner shell.

If the orbitals of the inner shell are orthogonal also to each other then the determinants  $D_{KL}$ ,  $D_{KK}$ ,  $D_{LL}$  have the following form :



(21)

In the unshaded places (matrix elements between the inner orbitals as well as matrix elements between inner and valence orbitals) each element is zero with the exception of the diagonal elements, whereas in the shaded places (matrix elements between the valence orbitals) the value of the elements depends on the form of the valence orbitals. In this case the  $\varrho_{KL}$ -s can be decomposed into two parts  $\varrho_{KL} = \varrho^i + \varrho_{KL}^v$ . Substitute this form of  $\varrho_{KL}$  into the energy expression (18) and separate the terms depending on  $\varrho^i$  only:

$$E = \sum_{KL} C_K^* C_L \frac{D_{KL}}{\sqrt{D_{KK} D_{LL}}} \left[ H_0 + \int H_1 \varrho_{KL}^v(1' | 1) d\tau_1 + \right. \\ \left. + \frac{1}{2} \int H_{12} \begin{vmatrix} \varrho_{KL}^v(1 | 1) & \varrho_{KL}^v(1 | 2) \\ \varrho_{KL}^v(2 | 1) & \varrho_{KL}^v(2 | 2) \end{vmatrix} d\tau_1 d\tau_2 + \int H_{12} \begin{vmatrix} \varrho_{KL}^v(1 | 1) & \varrho_{KL}^v(1 | 2) \\ \varrho^i(2 | 1) & \varrho^i(2 | 2) \end{vmatrix} d\tau_1 d\tau_2 + \right. \\ \left. + \int H_1 \varrho^i(1' | 1) d\tau_1 + \frac{1}{2} \int H_{12} \begin{vmatrix} \varrho^i(1 | 1) & \varrho^i(1 | 2) \\ \varrho^i(2 | 1) & \varrho^i(2 | 2) \end{vmatrix} d\tau_1 d\tau_2 \right]. \quad (22)$$

Since  $H_{12} = \frac{1}{r_{12}}$  is a multiplying operator it is superfluous to prime the coordinates in the corresponding terms.

In the operator  $H^i$  of the core consisting of the central nucleus and the closed shells  $H_0^i$  is zero and  $H_1^i$  does not contain the potential energy  $V^p(1)$  originating from the four protons.

Considering that  $\Psi$  is normalized, i. e.

$$\sum_{KL} C_K^* C_L \frac{D_{KL}}{\sqrt{D_{KK} D_{LL}}} = 1,$$

and incorporating the fourth term of (22) changing the denotation into the second term we obtain

$$E = \sum_{KL} C_K^* C_L \frac{D_{KL}}{\sqrt{D_{KK} D_{LL}}} \left[ H_0 + \int \left\{ H_1 + \int \frac{d\tau_{1'}}{r_{1'1}} \varrho^i(1'' | 1'') - \right. \right. \\ \left. \left. - \int \frac{d\tau_{1'}}{r_{1'1}} \varrho^i(1 | 1') \right\} \varrho_{KL}^v(1' | 1) d\tau_1 + \frac{1}{2} \int \frac{1}{r_{12}} \begin{vmatrix} \varrho_{KL}^v(1 | 1) & \varrho_{KL}^v(1 | 2) \\ \varrho_{KL}^v(2 | 1) & \varrho_{KL}^v(2 | 2) \end{vmatrix} d\tau_1 d\tau_2 \right] + \\ + \int V_p(1) \varrho^i(1 | 1) d\tau_1 + E^i. \quad (23)$$

(In the second term of the bracketed expression first the integrations contained in the operator have to be carried out, then the external integration after having equated the primed indices with the unprimed ones.)

$E^i$  is the energy of the core which can be taken as the zero point of the energy scale. In this case the energy of the valence shells is given by the other terms relative to that of the core as zero point. The second term of the bracketed operator of (23) (Coulomb interaction of the inner shells and valence shells) is a simple spherically symmetric potential, whereas the third term (the exchange interaction of the inner shells and valence shells) depends also after carrying out the inner integration on the angles.

### 9. Neglect of inner shells. Repulsive potential

In the preceding paragraph we saw that the following should be kept in mind if the inner closed shells are to be neglected.

a) The Coulomb interaction of the inner shells and the valence shells should be taken into consideration. The exact calculation of it is not too cumbersome. With a rough approximation it may be taken into account, so that the atomic number of the central nucleus is decreased by the number of electrons of the inner shell.

b) The exchange interaction of the inner shells and valence shells has to be taken into account. If there are many inner electrons, then its exact calculation encounters difficulties. Approximately it can be calculated with the following simple potential [27]:

$$-\frac{4}{3}\kappa_a(\varrho^i(1|1))^{\frac{1}{3}}, \quad \kappa_a = \frac{3}{4} \left( \frac{3}{\pi} \right)^{\frac{1}{3}}.$$

This should be added to  $H_1$ .

c) The interaction of electrons of the inner shell and the four protons has to be taken into consideration. Also this may be easily computed exactly, but fusing the inner electrons into the central nucleus this term does not even occur.

d) Orbitals of valence shells have to be orthogonalized to every inner orbital.

If the valence orbitals are not orthogonalized to the inner orbitals, then the variational method cannot be used, namely a function  $\Phi$  on which a special condition is not imposed, approximates the lowest eigenstate of the operator  $H$ . For instance in case of atoms, each function  $\Phi$  the angular part of which belongs to a given azimuthal quantum number  $l$  approaches the lowest state of that  $l$  (in case of  $l = 0$  the state  $1s$ , in case of  $l = 1$  the state  $2p$  etc.) if it is not required to be orthogonal to orbitals belonging to the same  $l$  below it.

This requirement gives connections between the variational parameters, hence these cannot be varied independently from each other. In order to avoid this a repulsive potential has been derived statistically by GOMBÁS [30, 31] adding it to the operator  $H$  and thus calculating the energy, the orthogonality has become unnecessary. Later the method was further improved by him with the grouping of the core electrons according to the azimuthal quantum number. This method can be more comfortably applied to real calculations than the preceding one.

Let  $D_l$  be the radial density of the inner electrons of azimuthal quantum number  $l$ . According to GOMBÁS if a valence electron of azimuthal quantum number is to be placed at a distance  $r$  from the nucleus of the core then an energy  $G_l(r)$  has to be expended, independently from the electrostatical interactions, which is obtained as

$$G_l(r) = \frac{\pi^2}{8(2l+1)} D_l^2(r) + \frac{1}{4r^2}. \quad (24)$$

Since in case of molecules  $l$  is not a "good quantum number", the orbitals  $\psi$  for the valence electrons have to be expanded in the eigenfunctions  $\varphi_l$  of the operator  $l$ :

$$\psi = \sum_l a_l \varphi_l,$$

and to the individual terms the corresponding operator  $G_l$  has to be applied (see also [33]). The method can be formally simplified so that  $G_l$  is at the same time considered as a projection operator by which  $\psi$  is transformed into  $a_l G_l \varphi_l$ . Then  $\psi$  is transformed by  $\sum_l G_l$  into  $\sum_l a_l G_l \varphi_l$  which, multiplying by  $\psi^*$  from left and integrating over the coordinates of the corresponding electron, furnishes the correct expression  $\int \sum_l |a_l|^2 \varphi^* G_l \varphi_l d\tau$ .

Hence the total repulsive potential to be added to the operator  $H$  is

$$\sum_i \sum_l G_l(r_i). \quad (25)$$

The summation has to be extended over the valence electrons (over  $i$ ) and the azimuthal quantum numbers of the inner shells (over  $l$ ).

#### REFERENCES

1. J. H. VAN VLECK, J. Chem. Phys., **1**, 177, 219, 1933; **2**, 20, 1934.
2. H. J. WOODS, Trans. Far. Soc., **28**, 877, 1932.
3. H. EYRING, A. FROST, J. TURKEVICH, J. Chem. Phys., **1**, 777, 1933.
4. F. SEITZ, A. SHERMANN, J. Chem. Phys., **2**, 11, 1934.
5. H. H. VOGEL, J. Chem. Phys., **4**, 581, 1936.

6. R. S. MULLIKEN, J. Chem. Phys., **3**, 375, 1935.
7. R. S. MULLIKEN, J. Chem. Phys., **3**, 573, 586, 1935.
8. C. A. COULSON, Trans. Far. Soc., **33**, 388, 1937.
9. R. S. MULLIKEN, J. Chem. Phys., **1**, 492, 1933.
10. R. A. BUCKINGHAM, H. S. W. MASSEY, E. R. TIBBS, Proc. Roy. Soc. A, **178**, 119, 1941.
11. H. Z. HARTMANN, Zs. f. Naturforschung, **2a**, 489, 1947.
12. M. J. M. BERNAL, Proc. Phys. Soc. A, **66**, 514, 1953.
13. C. CARTER, Proc. Roy. Soc. A, **235**, 321, 1956.
14. M. BORN, K. HUANG, Dynamical Theory of Crystal Lattices, University Press, Oxford, 1954.
15. H. EYRING, J. WALTER, G. E. KIMBALL, Quantum Chemistry, Wiley, New York, 1944.
16. P. GOMBÁS, Theorie und Lösungsmethoden des Mehrteilchenproblems der Wellenmechanik, Birkhäuser, Basel, 1950.
17. P. A. M. DIRAC, The Principles of Quantum Mechanics, University Press, Oxford, 1947.
18. G. RUMER, E. TELLER, A. WEYL, Gött. Nachr., 499, 1932.
19. E. WIGNER, Gruppentheorie und ihre Anwendungen auf die Atomspektren, Vieweg, Braunschweig, 1931.
20. R. S. MULLIKEN, J. Chem. Phys., **23**, 1997, 1955.
21. B. HIGMAN, Applied Group Theoretic and Matrix Methods, University Press, Oxford, 1955.
22. M. A. MELVIN, Rev. Mod. Phys., **28**, 16, 1956.
23. C. C. J. ROOTHAAN, Rev. Mod. Phys., **23**, 69, 1951.
24. J. C. SLATER, Phys. Rev., **37**, 481, 1931; **38**, 1109, 1931.
25. L. PAULING, J. Am. Chem. Soc., **53**, 1367, 1931.
26. G. E. KIMBALL, J. Chem. Phys., **8**, 188, 1940.
27. P. A. M. DIRAC, Proc. Camb. Phil. Soc., **26**, 376, 1930.
28. P. O. LÖWDIN, Phys. Rev., **97**, 1474, 1490, 1509, 1955.
29. P. A. M. DIRAC, Proc Camb. Phil. Soc., **27**, 240, 1931.
30. P. GOMBÁS, Zs. f. Phys., **118**, 164, 1941.
31. P. GOMBÁS, Die statistische Theorie des Atoms und ihre Anwendungen, Springer, Wien, 1949.
32. P. GOMBÁS, Acta Phys. Hung., **1**, 285, 1952.
33. R. GÁSPÁR, Acta Phys. Hung., **2**, 31, 1952.

## ПРИМЕНЕНИЕ ОДНОЦЕНТРОВОЙ ВОЛНОВОЙ ФУНКЦИИ К МОЛЕКУЛАМ ГИДРИДОВ С ТЕТРАЭДРИЧЕСКОЙ СИММЕТРИЕЙ

### I. Теоретические основы метода

Э. КАПУИ

### Резюме

Количественное толкование многоатомных молекул встречается с большими трудностями метематического характера. Значительная часть этих трудностей при применении одноцентровых волновых функций отпадает. В случае молекул с симметрией высшей степени этот метод может применяться с успехом. Настоящая работа рассматривает применение этого метода к молекулам гибридов с тетраэдрической симметрией; даются способы для построения волновой функции и упрощения вычислений.





# ON THE STATISTICAL TREATMENT OF THE FERMION GAS II

By  
P. SZÉPFALUSY

PHYSICAL INSTITUTE OF THE UNIVERSITY FOR TECHNICAL SCIENCES, BUDAPEST

(Presented by A. Kónya. — Received: 1. VIII. 1958)

In a previous paper we derived a new statistical model in the one-dimensional case. In the present paper the method is described in the three-dimensional case.

## I. Introduction

In a previous paper [1] (hereafter referred to as I) we derived a new statistical model in the one-dimensional case. The present paper treats the same method in the three-dimensional case. As was shown in I the method is essentially independent of the interaction of the particles, thus the system to be considered is again one consisting of particles with spin  $1/2$  without interaction. Assuming the outer potential to be spherically symmetrical and grouping the particles according to their orbital angular momentum quantum numbers we obtain a problem which is essentially one-dimensional, thus the procedure discussed in I can be directly applied to this case. Therefore we may omit most of the details of the calculation and restrict ourselves to giving the results.

## II. Wave functions of the one-particle states

The Schrödinger equation of  $n$  particles in the potential field  $V(r)$  is

$$\sum_{i=1}^n H(r) \Phi = \mathcal{E} \Phi, \quad (1)$$

where

$$H(r) = -\frac{\hbar^2}{2m} \Delta + V(r),$$

$\Delta$  is the Laplace operator.

By introducing spherical polar coordinates  $(r, \vartheta, \varphi)$  and disregarding

the normalization constant the antisymmetrical solution of this equation can be written in the form

$$\Phi = \text{Det} \left[ \frac{R_l(r_j)}{r_j} Y_{l_l}^{m_l}(\vartheta_j, \varphi_j) \chi_{m_s l}(\sigma_j) \right]. \quad (2)$$

Here  $Y_l^m$  is the spherical harmonics relating to the orbital angular momentum quantum number  $l$  and the magnetic quantum number  $m$ .  $\chi_{m_s}$  is the spin function,  $\sigma$  is the spin variable. In the bound state the functions  $R_l$  are real, thus the wave function of the one-particle states will be normalized, if

$$\int (Y_{l_l}^{m_l})^* Y_{l_k}^{m_k} d\omega = 4\pi \delta_{l_l l_k} \delta_{m_l m_k} \\ (d\omega = \sin \vartheta d\vartheta d\varphi)$$

and

$$\int R_l^2 dr = 1.$$

Define  $G_l$  in the following manner

$$G_l = \frac{n_l + q_l}{2(2l + 1)}, \quad (3)$$

where  $n_l$  is the number of particles with the orbital angular momentum quantum number  $l$ ;  $q_l = 0$  if all  $l$  groups are closed and in general  $q_l$  gives the number of particles wanted for the  $l$  group of highest energy to be closed.

If the system involves incompletely filled  $l$  groups, the general solution is obtained from a linear combination of determinants of type (2). However, as the interaction of the particles has not been taken into account, wave function (2) also gives the correct energy eigenvalue. In addition as our purpose is to determine the spherically symmetrized radial density only, expression (2) of the wave function will be satisfactory.

By substituting wave function (2) into equation (1) the following system of equations is obtained for the radial parts of the one-particle wave functions with the same orbital angular momentum quantum number :

$$\left[ -\frac{\hbar}{2m} \frac{d^2}{dr^2} + V_r \right] R_l = \sum_{k=1}^{G_l} R_k \epsilon_{kl} \quad (4) \\ (i = 1, 2, \dots, G_l).$$

where

$$V_r = V(r) + \frac{\hbar^2}{2m} \frac{l(l+1)}{r^2}.$$

The energy eigenvalue is

$$\mathcal{E} = \sum_l \mathcal{E}_l,$$

where

$$\mathcal{E}_l = 2(2l+1) \sum_{k=1}^{G_l} \epsilon_{kk} - q_l \in_{G_l G_l}. \quad (5)$$

The wave functions  $R_i$  are not uniquely determined; from any of the solutions of the system of equations (4) we may form, by linear transformation, further radial wave functions with which wave function (2) is a solution for equation (1). Thus, it can readily be seen that the radial wave functions can be chosen to be orthogonal to each other

$$\int R_i^0 R_k^0 dr = \delta_{ik}$$

and

$$R_l = \sum_{k=1}^{G_l} R_k^0 C_{kl}^0. \quad (6)$$

Then equations (4) and (5) are modified in the following way:

$$\left[ -\frac{\hbar^2}{2m} \frac{d^2}{dr^2} + V_r \right] R_i^0 = R_i^0 E_i, \quad (4')$$

$$\mathcal{E}_l = 2(2l+1) \sum_{i=1}^{G_l} E_i - q_l E_{G_l G_l}. \quad (5')$$

In perfect analogy to I we may write

$$\left[ -\frac{\hbar^2}{2m} \frac{d^2}{dr^2} + O_i V_r \right] R_i = R_i E_i, \quad (7)$$

where  $O_i$  may be the integral operator

$$O_i R_i = \int \sum_{k=1}^{G_l} (E_i - E_k) R_k^0(r') R_k^0(r) R_i(r') dr'.$$

In the case if

$$O_i = \frac{1}{2m} (p_{ri}^2 - \pi_{ri}^2), \quad (8)$$

where

$$\begin{aligned} -\hbar^2 \frac{d^2 R_i^0}{dr^2} &= p_{ri}^2 R_i^0, \\ -\hbar^2 \frac{d^2 R_i}{dr^2} &= \pi_{ri}^2 R_i, \end{aligned}$$

equation (7) is a trivial transformation of (4).

The coefficients  $C_{kl}^0$  in equation (6) must be chosen so that  
a) the wave functions  $R_i$  are nodeless,

b) the one-particle densities  $R_l^2$  average the one-particle densities  $R_l^{02}$  as well as possible (thus  $R_l^2 \equiv R_l^{02}$ ).<sup>1</sup>

Then the form of  $O_i$  in (8), as will be seen, can be expressed in the semi-classical approximation by the wave functions  $R_k$  and equation (7) can be used for the determination of the wave functions  $R_l$  and the eigenvalues  $E_l$ .

■

Denote by  $\varrho_l(r)$  the density of the particles with the orbital angular momentum quantum number  $l$ , which is generally not spherically symmetrical. Define the radial density  $\varrho_r(r)$  in the following manner

$$\varrho_r(r) = 4\pi r^2 \int \varrho_l(r) d\omega,$$

which can be expressed by the wave functions  $R_l^0$  in a simple way

$$\varrho_r = 2(2l+1) \sum_{i=1}^{G_l} R_l^{02} - q_l R_{G_l}^2.$$

However, according to the condition b) imposed on the wave functions  $R_l$

$$D_l(r) = 2(2l+1) \sum_{i=1}^{G_l} R_l^2 - q_l R_{G_l}^2 \quad (9)$$

and  $\varrho_r$  can be taken approximately as equal. Thus in the following  $D_l$  will be regarded as the radial density and the statistical model derived will be suitable for the determination of this spherically symmetrized density.

### III. Semi-classical approximation

In the way described in I, by using the WKB method we obtain

$$\begin{aligned} O_i &= \frac{1}{2m} P_{ri}^2 = \frac{\hbar^2}{32m(2l+1)} D_{li}^2, \quad V_r < E_i, \\ O_i &= 0, \quad V_r > E_i, \\ (i &\geq 2). \end{aligned} \quad (8')$$

Here  $P_{ri} = (p_{ri} + p_{r,i+1})/2$  can be regarded as the maximum radial momentum of the particles which fill the  $l$  groups of an energy lower than that of the  $(i+1)$ -th  $l$  group.  $D_{li}$  denotes the density of these particles

$$D_{li} = 2(2l+1) \sum_{k=1}^i R_k^2$$

<sup>1</sup> See I, chapter 2, the conditions a) and b).

and

$$P_{rl} = \frac{\hbar}{4(2l+1)} D_{ll}. \quad (10)$$

The case  $i = G_l$  must be considered separately. If this  $l$  group of maximum energy is incompletely filled ( $q_l \neq 0$ )  $D_{lG_l} \neq D_l$  and if  $q_l > 1$  one or more phase cells in this group are empty. To obtain a correct scheme for the distribution of the phase cells in the momentum space the fact must be kept in mind that the radial kinetic energies of the particles in the same  $l$  group agree and are independent of the fact whether this group is closed or not. Thus in the  $G_l$ -th group the maximum radial momentum at the filled phase cells in the momentum space will be  $P_{rG_l}$ , while at the empty phase cells it will be  $P_{r, G_l-1}$ . We have therefore modified the relation between the momentum  $P_{rG_l} = P_r$  and the density  $D_l$  in a former paper [2] in the following manner

$$P_r = \frac{\hbar}{2} \frac{G_l}{n_l} D_l. \quad (10')$$

If  $q_l = 0$  (10) goes over into the relation (10) set up for the  $i = G_l$ -th state.

By substituting the form of  $O_i$  in (8') into equation (7) we obtain a system of equations from which the wave functions  $R_i$  and the eigenvalues  $E_i$  can already be determined:

$$-\frac{\hbar^2}{2m} \frac{1}{R_i} \frac{d^2 R_i}{dr^2} + \frac{1}{2m} P_{ri}^2 + V_r = E_i, \quad V_r < E_i, \quad (7')$$

$$-\frac{\hbar^2}{2m} \frac{1}{R_i} \frac{d^2 R_i}{dr^2} + V_r = E_i, \quad V_r > E_i, \quad (7'')$$

$$(i \geq 2)$$

$$-\frac{\hbar^2}{2m} \frac{1}{R_1} \frac{d^2 R_1}{dr^2} + V_r = E_1.$$

On the basis of equations (7') and (7'') and the approximations

$$R_i = \text{const.}/D_{li}, \quad V_r < E_i,$$

$$R_i = \text{const. } D_{li}, \quad V_r > E_i,$$

which can be accounted for in a manner completely analogous to I, we obtain for the density  $D_{li}$  the following equations

$$-\frac{\hbar^2}{2m} D_{li}^{1/3} \frac{d^2 D_{li}^{-1/2}}{dr^2} + \frac{1}{2m} P_{ri}^2 + V_r = E_i, \quad V_r < E_i, \quad (11)$$

$$-\frac{\hbar^2}{2m} D_{li}^{1/2} \frac{d^2 D_{li}^{1/2}}{dr^2} + V_r = E_i, \quad V_r > E_i. \quad (11')$$

Equation (11') agrees with PLASKETT's equation [3]; the restriction of the validity of the equation to the region  $V_r < E_i$  and equation (11'') mean an improvement upon PLASKETT's method.

By introducing further approximations in a manner completely analogous to I we obtain the following equation, valid for the whole space

$$-\frac{\hbar^2}{2m} D_{li}^{-1/2} \frac{d^2 D_{li}^{1/2}}{dr^2} + \frac{1}{2m} P_{r, i-1}^2 + V_r = E_i.$$

In the case  $i = 1$  this equation goes over into the exact wave mechanical equation.

#### IV. The statistical energy expression

Calculate  $E_i$  from equation (12) by multiplying both sides of the equation by  $D_{li}/2 (2l+1) i$  and integrating over  $r$ . Introduce the approximation

$$D_{li} = \frac{2(l+1)i}{n_l} D_l$$

and form the energy of the particles with the orbital angular momentum quantum number  $l$  according to relation (5'):

$$\mathcal{E}_l = \mathcal{E}_{lw} + \mathcal{E}_{lkr} + \mathcal{E}_{lka} + \mathcal{E}_{lP}, \quad (13)$$

where

$$\mathcal{E}_{lw} = -\frac{\hbar^2}{2m} \int D_l^{1/2} \frac{d^2 D_l^{1/2}}{dr^2} dr - \frac{\hbar^2}{8m} \int \frac{1}{D_l} \left( \frac{dD_l}{dr} \right)^2 dr,$$

$$\mathcal{E}_{lkr} = \frac{\hbar^2}{8m} \frac{1}{n_l^3} \left[ \frac{(2l+1)(G_l-1)G_l(2G_l-1)}{2} - q_l(G_l-1)^2 \right] \int D_l^3 dr,$$

$$\mathcal{E}_{lka} = \frac{\hbar^2}{2m} l(l+1) \int \frac{1}{r^2} dr,$$

$$\mathcal{E}_{lP} = \int V D_l dr.$$

$\mathcal{E}_{lw}$  is the Weizsäcker inhomogeneity correction of the radial part of the zero point kinetic energy. It is practicable to compare the radial kinetic energy with the radial part of the Fermi zero point kinetic energy. In a former paper [2] the latter was modified in such a way that we replaced the integration over the momentum space by summing exactly over the states, under the same conditions as here

$$\mathcal{E}_{lkr}^0 = \frac{\hbar^2}{8m} \frac{1}{n_l^3} \left[ \frac{(2l+1)G_l(4G_l^2-1)}{6} - q_l(G_l-1/2)^2 \right] \int D_l^3 dr.$$



The comparison of the expressions of  $\mathcal{E}_{lkr}$  and  $\mathcal{E}_{lkr}^0$  yields

$$\mathcal{E}_{lkr} = i\mathcal{E}_{lkr}^0,$$

where

$$i = \frac{2(2l+1)(G_l-1)G_l(2G_l-1) - 6q_l(G_l-1)^2}{(2l+1)G_l(4G_l^2-1) - 6q_l(G_l-1/2)^2}.$$

If  $G_l = 1$ , i. e. particles can be found in the  $l$  group of lowest energy only,  $\mathcal{E}_{lkr} = 0$ . In the latter case the total radial kinetic energy is represented by the Weizsäcker correction term only and the relations go over into the exact wave mechanical expressions.

### V. Determination of the radial density

The statistical equation determining the radial density  $D_l$  is obtained by searching for the density for which  $\mathcal{E}_l$  is a minimum, taking the restriction  $\int D_l dr = n_l$  into account. Elementary calculation yields

$$-\frac{\hbar^2}{2m} D_l^{1/2} \frac{d^2 D_l^{1/2}}{dr^2} + \frac{1}{2m} \frac{1}{G_l^2 n_l} [(2l+1)(G_l-1)G_l(2G_l-1) - 3q_l(G_l-1)^2] P_r^2 + V_r = V_{0l}, \quad (13)$$

where  $V_{0l}$  is the Lagrange multiplier.

The determination of the radial density will be more accurate if the following procedure is applied. Writing equations (11) and (11') for the  $G_l$ -th state and using the approximation  $D_{lG_l} = \frac{n_l + q_l}{n_l} D_l$

$$-\frac{\hbar^2}{2m} D_l^{1/2} \frac{d^2 D_l^{-1/2}}{dr^2} + \frac{1}{2m} P_r^2 + V_r = E_{G_l}, \quad V_r < E_{G_l} \quad (14)$$

$$-\frac{\hbar^2}{2m} D_l^{-1/2} \frac{d^2 D_l^{1/2}}{dr^2} + V_r = E_{G_l}, \quad V_r > E_{G_l}. \quad (14')$$

Instead of solving PLASKETT's equation (14) we may proceed in the following manner. Equation (7') for the  $G_l$ -th state is

$$-\frac{\hbar^2}{2m} \frac{1}{R_{G_l}} \frac{d^2 R_{G_l}}{dr^2} + \frac{1}{2m} P_r^2 + V_r = E_{G_l}. \quad (15)$$

Calculate the radial density from equation (13) for the case when the number of particles with the orbital angular momentum quantum number  $l$  is  $n_l$  and  $n_l - 1$ , respectively. The difference between these two will yield approximately  $R_{G_l}^2$ . Knowing  $R_{G_l}$  and using (10') from equation (15) we may express  $D_l$ .

$$D_l = \frac{2}{h} \frac{n_l}{G_l} \left\{ 2m \left[ E_{G_l} - V_r + \frac{\hbar^2}{2m} \frac{1}{R_{G_l}} \frac{d^2 R_{G_l}}{dr^2} \right] \right\}^{1/2}. \quad (15')$$

Equations (14) and (15') are both approximations of equation (15).

Finally, if  $n_l$  is large, we may obtain a partial differential equation for  $D_l$  as the continuous function of  $n_l$ . Regarding  $D_l$  as the derivable function of  $n_l$   $R_{G_l}^2 = \int_{n_l-1}^{n_l} \frac{\partial D_l}{\partial k_l} dk_l$  and if  $n_l$  is large  $R_{G_l}^2 = \frac{\partial D_l}{\partial n_l}$ , which, substituted into equation (15) yields

$$\begin{aligned} -\frac{\hbar^2}{4m} \frac{\partial D_l}{\partial n_l} - \frac{\partial^3 D_l}{\partial r^2 \partial n_l} + \frac{\hbar^2}{8m} \left( \frac{\partial^2 D_l}{\partial r \partial n_l} \right)^2 + \frac{\hbar^2}{8m} \frac{G_l^2}{n_l^2} D_l^2 \left( \frac{\partial D_l}{\partial n_l} \right)^2 + \\ + V_r \left( \frac{\partial D_l}{\partial n_l} \right)^2 = E_{G_l} \left( \frac{\partial D_l}{\partial n_l} \right)^2, \\ (V < E_{G_l}) \end{aligned}$$

Similarly, starting from equation (7'') assumed for the  $G_l$ -th state

$$\begin{aligned} -\frac{\hbar^2}{4m} \frac{\partial D_l}{\partial n_l} - \frac{\partial^3 D_l}{\partial r^2 \partial n_l} + \frac{\hbar^2}{8m} \left( \frac{\partial^2 D_l}{\partial r \partial n_l} \right)^2 + V_r \left( \frac{\partial D_l}{\partial n_l} \right)^2 = E_{G_l} \left( \frac{\partial D_l}{\partial n_l} \right)^2 \\ (V > E_{G_l}). \end{aligned}$$

### Acknowledgement

Thanks are due to Professor P. GOMBÁS for his continuous interest in this work.

### REFERENCES

1. P. SZÉPFALUSY, Acta Phys. Hung., **9**, 203, 1958.
2. P. SZÉPFALUSY, Acta Phys. Hung., **7**, 433, 1957.
3. J. S. PLASKETT, Proc. Phys. Soc. A, **66**, 178, 1953.

### О СТАТИСТИЧЕСКОЙ ТРАКТОВКЕ ФЕРМИОН-ГАЗА II.

П. СЕПФАЛУШИ

### Резюме

В первой части работы выведена новая статистическая модель и одномерном случае. В настоящей работе рассматривается полученный метод, в трехмерном случае.

FATIGUE EFFECTS ON THE CATHODE  
OF SELF-QUENCHING GM COUNTERS

By

O. ORIENT

CENTRAL RESEARCH INSTITUTE OF PHYSICS, DEPT. FOR RADIOLOGY, BUDAPEST

(Received : 4. XI. 1957)

Fatigue effects occur on the photo-cathodes of vacuum and gas-filled phototubes upon prolonged operation [1]. According to observations the sensitivity range of the photo-cathode will shift gradually towards shorter wavelengths in the course of a steady high-intensity illumination. Likewise, the cathode of self-quenching counters is also exposed to strong effects due to  $10^9$  "organic ions" impinging on the cathode after each pulse. These ions extract electrons from the cathode surface, remain in an excited state for a very short period ( $10^{-13}$  sec) and then dissociate and radiate. In addition, photons of other origin also reach the cathode. We may, therefore assume fatigue effects to occur not only in the gas mixture but on the cathode of self-quenching counters in the case of prolonged operation.

Work functions of Cu and Ni cathode tubes and the behaviour of the characteristics (plateau length, plateau slope) of counters after prolonged operation (fatigue) were studied by the author. The tubes were of identical geometry with a cathode diameter of 20 mms, a sensitive anode length of 80 mms and gas volume of about 25 cc. The measurements were carried out on two pairs of counters of the Ni cathode and the Cu cathode type, respectively. The GM tubes, made of C9 hard glass were sealed onto a manifold connected to a glass recipient of 1.5 litres volume. The tubes, the manifold and the glass form a single system which could be detached from the pump after evacuating and filling. In this way all tubes contained a gas mixture of the same composition and pressure throughout the measurements. This mixture did not change essentially in the course of the fatigue process, the volume of the whole system being sixty times that of a tube.

The evacuating and filling of the system was performed as follows : the adsorbed gases were removed by degassing, which took 6 hours at a temperature of  $400^\circ$  C and a pressure of  $10^{-5}$  mm Hg. After cooling down the system was filled up with A to 150 mm Hg and with ethyl bromide to 10 mm Hg. The plateau length and slope of these tubes were measured with a scale-of-1000 having a dead time of less than 5  $\mu$ secs. The work functions

of the cathodes were measured by means of the monochromator of a Beckmann spectrometer, applying the method described by the author in a previous paper [2].

One specimen each of the Ni and Cu cathode tubes was operated continuously using a Co-60 sample. During the fatigue process these tubes counted  $6.10^4$  pulses per minute and a current of  $5\mu\text{A}$  flowed through them. Another pair of Ni and Cu tubes was not subjected to the fatigue process for control purposes. As the object of this study was the tube characteristics, the plateau lengths, the plateau slopes and work functions correspondig to the consecutive fatigue phases were not registered until 24 hours following the fatigue irradiation.

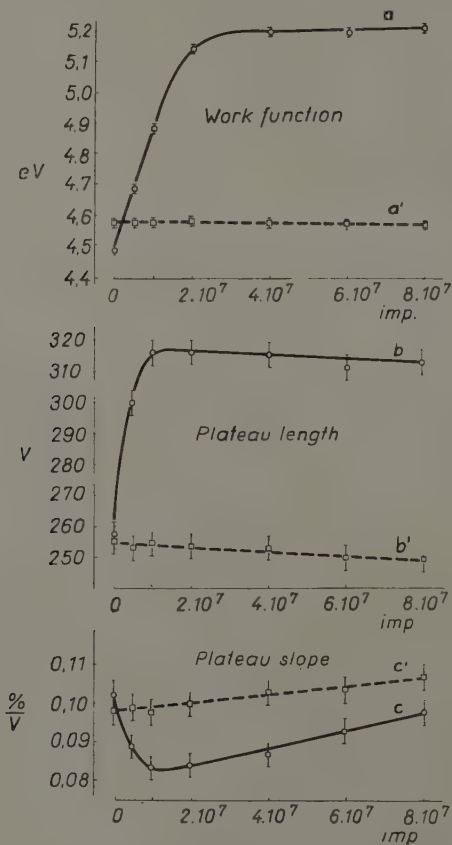


Fig. 1

The results obtained for the Ni cathode tube are shown in Fig. 1. The changes in the cathode work function are shown by curve *a*. In the course of

fatigue operation the work function increases rather quickly at first, while later on the rate of increase becomes gradually slower. Curve *b* gives the variation of the plateau length during the fatigue process, curve *c* indicates that of the plateau slope. Like the work function, the plateau length increases rapidly at the beginning of the fatigue process and the slope of the plateau shows a strong decrease. After  $2.10^7$  pulses the plateau becomes slightly shorter and steeper again on continuing the fatigue.

The work function of the Ni cathode control tube did not change during the fatigue of the operated Ni cathode tube (curve *a'* is a straight line). The change in the plateau length of the control tube during the fatigue of the first tube is given by curve *b'*, that in the plateau slope is given by curve *c'* (The Ni cathode control tube has not been fatigued.). The data of this control tube as measured after each pass of the fatigue process are shown below above the corresponding values of the fatigued tube. Curves *b'* and *c'* indicate a slight decrease in the plateau length and some increase in the plateau slope of the control tube as the fatigue of the first tube progressed.

Analogous measurements were carried out in the two Cu cathode tubes, the results being similar to those of the Ni tube measurements.

The fatigue of phototubes is caused by the change in the crystal structure of the photo-cathode according to the explanation given in the literature [1]. The gradual increase in the work function of the counter is presumably due to cathode surface structure changes brought about by ion and photon bombardment.

According to former measurements of the author [2] higher work functions of a particular cathode in tubes of given pressure and geometry always correspond to longer plateaus. Accordingly, the improvement of tube characteristics (plateau length and slope) in the first period of the fatigue process is caused by the increase in the work function value.

We did not succeed in eliminating the deterioration of the gas filling in the course of our fatigue investigations. It was this circumstance which caused the slight decrease in the plateau length of the control tubes as well as the increase of the starting voltage from 1020 V to 1040 V and the slight deterioration of the operational data of the fatigued Ni tube after  $2.10^7$  pulses — despite the further small increase in the work function.

The improvement of the operational properties at the beginning of the fatigue process could not be observed in counters without spare gas container, supposedly because the deterioration of the quenching properties of the gas mixture compensated the improvement due to the increase in the work function value.

#### REFERENCES

1. J. H. DE BOER and M. C. TEVES, *Zs. f. Phys.*, **74**, 604, 1932. W. KLUGE and S. WEBER, *Zs. f. angew. Phys.*, **7**, 123, 1955.
2. O. ORIENT, *Acta Phys. Hung.*, **7**, 199, 1957.





# FURTHER INVESTIGATION OF EXTENSIVE AIR SHOWERS CONTAINING NUCLEAR ACTIVE PARTICLES

By

G. BOZÓKI, E. FENYVES, T. SÁNDOR and A. SOMOGYI

CENTRAL RESEARCH INSTITUTE OF PHYSICS, DEPARTMENT FOR COSMIC RAYS, BUDAPEST

(Received : 17. XI. 1958)

We have published recently [1] the results of our measurements concerning the density spectrum of extensive air showers containing nuclear active particles. We have found that the exponent of the density spectrum of the electronic component was  $\gamma = 1,34 \pm 0,08$  and that the density spectrum

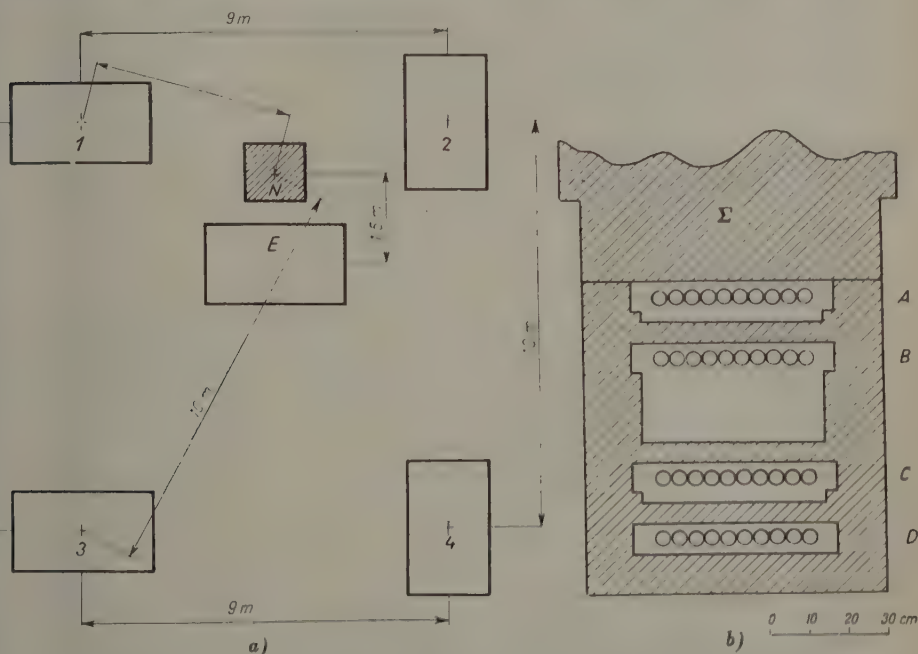


Fig. 1. a) The extensive air shower arrangement with the nuclear active particle detector N.  
b) The nuclear active particle detector N.

of the nuclear active component has the form of a power law approximately with the same exponent.

The measurements were carried out with an extensive penetrating shower arrangement (Fig. 1a) and  $\gamma$  was determined by measuring the rate of extensive penetrating showers ( $c/h$ ) as a function of the size of the surface ( $S$ ) of the electron detector counter set. As it was shown in [1] the exponent of the  $c/h$  vs.  $S$  curve gives the value of  $(\gamma - 1)$  and thus the exponent of the density spectrum of the electronic component can be determined. The

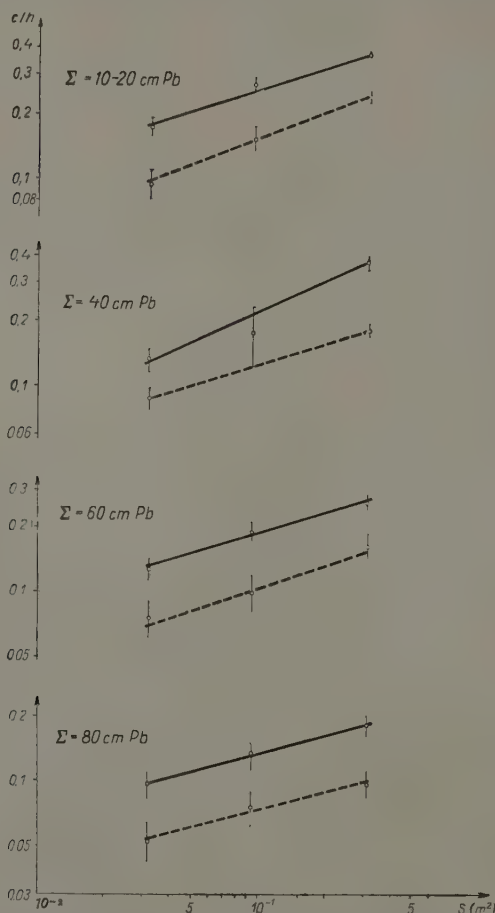


Fig. 2. The rate in  $c/h$  of coincidences vs. the surface of the unshielded counter trays for different absorber thicknesses above the nuclear active particle detector N. The solid lines correspond to coincidences of the  $(N_2, 1)$  type, while the dotted lines correspond to coincidences of the  $(N_3, 1)$  type.

nuclear active component was detected with a penetrating shower arrangement such as is commonly used (Fig. 1b) which was covered with lead absorbers

of thicknesses ( $\Sigma$ ) varying from 10 to 20 cm<sup>1</sup>. Lately further measurements were carried out with the same apparatus the thickness of the lead absorber above the penetrating shower detector being, however, increased to  $\Sigma = 40, 60$  and 80 cm. The same coincidence combinations were measured as earlier and in Fig. 2 the rate of coincidences ( $N_1, 1$ ) and ( $N_3, 1$ )<sup>2</sup> are plotted against the size of the surface of the electron detector 1 for 40, 60 and 80 cm lead absorber and for comparison the data obtained earlier for 10–20 cm are also plotted. The  $(\gamma - 1)$  exponents corresponding to these curves were calculated by the method of least squares; the values obtained are given in Table 1.

Table I

Thickness of the lead absorber (cm)	Type of coincidences	Exponent corresponding to the $c/h$ vs. $S$ curve
10–20 (ref. [1])	( $N_2, 1$ )	$0,32 \pm 0,09$
	( $N_3, 1$ )	$0,39 \pm 0,16$
40	( $N_2, 1$ )	$0,45 \pm 0,15$
	( $N_3, 1$ )	$0,32 \pm 0,14$
60	( $N_2, 1$ )	$0,29 \pm 0,16$
	( $N_3, 1$ )	$0,33 \pm 0,24$
80	( $N_2, 1$ )	$0,27 \pm 0,20$
	( $N_3, 1$ )	$0,26 \pm 0,25$

It can be seen from the Table that the values of the exponents obtained with different absorber thicknesses and different types of coincidences ( $N_2$  and  $N_3$ ) recorded by the penetrating shower detector are the same inside the limits of statistical error. Thus the best value of  $\gamma$  may be evaluated by calculating the weighted mean value of the exponents for the different absorber thicknesses resulting in

$$\gamma - 1 = 0,33 \pm 0,05,$$

i. e.

$$\gamma = 1,33 \pm 0,05.$$

This value is -- inside the limits of statistical error -- equal to the value of  $\gamma$  obtained earlier [2, 3] with the same apparatus using only the

<sup>1</sup> For a detailed description of the method used and the experiments carried out see [1].

<sup>2</sup>  $N_2$  and  $N_3$  refer to the recorded rates of penetrating showers discharging two or more resp. three or more counters in each of the four counter trays (A, B, C and D) of the penetrating shower arrangement; ( $N_2, 1$ ) and ( $N_3, 1$ ) refer correspondingly to coincidences between the penetrating shower detector and the electron detector 1.

electron detectors ( $\gamma = 1,43 \pm 0,02$ ).<sup>1</sup> The equality of the two exponents leads to the conclusion as discussed in [1] that for distances from the shower core and shower energies as selected with our apparatus the spectrum of the nuclear active particles has also the form of a power law with approximately the same exponent as that obtained for the electronic component.

We have also measured the change of the rate of coincidences with the distances between electron detector and penetrating shower detector (Fig. 3). The decoherence curve can be roughly approximated in the usual way by a

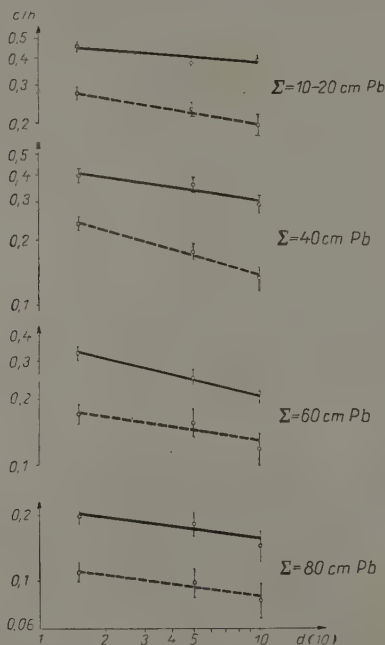


Fig. 3. The rate in  $c/h$  of coincidences vs. the distance  $d$  between the electron and nuclear active particle detectors for different absorber thicknesses above the nuclear active particle detector N. The solid lines correspond to coincidences  $N_2$  and the dotted lines to coincidences  $N_3$  recorded by the nuclear active particle detector.

power-law expression (see eq. (3) of [1]) the exponent  $\beta$  of which can be determined from the experimental data. The experimental curves of Fig. 3 do not deviate significantly from each other and the weighted mean value of  $\beta$  can be estimated as

$$\beta = 0,15 \pm 0,01,$$

<sup>1</sup> The  $\gamma$  value found in the present experiment is also in good agreement with the best  $\gamma$  values given in the literature for extensive air showers at low densities [3, 4, 5].

in good agreement with the exponent of the decoherence curve measured earlier by two of the authors [6, 7] with the electron detectors only ( $\beta = 0,20 \pm 0,01$ ).

Summarizing our results we have confirmed our earlier results published in [1] and furthermore we have shown that the density spectrum of the electronic component and the decoherence curve of extensive air showers containing nuclear active particles does not depend on the thickness of the absorber, under which the nuclear active particles are detected.

#### REFERENCES

1. G. BOZÓKI, E. FENYVES, T. SÁNDOR and A. SOMOGYI, Nucl. Phys., **7**, 677, 1958.
2. J. KOCH, T. SÁNDOR, A. SOMOGYI and J. SZIVEK, Reports of the Central Research Institute of Physics, **1**, 61, 1953.
3. K. GREISEN, Progress in Cosmic Ray Physics, **3**, 3, 1956.
4. A. ZAWADZKI, Bull. Acad. Polon. Sci. Cl. 3, **5**, 147, 1956.
5. H. S. MURDOCH, Nucl. Phys., **8**, 157, 1958.
6. L. JÁNOSSY, Nuovo Cim. Suppl., **1**, 247, 1955.
7. T. SÁNDOR and A. SOMOGYI, Reports of the Central Research Institute of Physics, **2**, 466, 1954.

A kiadásért felel az Akadémiai Kiadó igazgatója

Műszaki felelős: Farkas Sándor

A kézirat nyomdába érkezett: 1958. XII. 29. — Terjedelem: 9,25 (A/5) ív, 11 ábra

---

Akadémiai Nyomda, Budapest, V., Gerlőczy utca 2. — 47715/59 — Felelős vezető: Bernát György



# FURTHER STUDIES OF COSMIC RAY BURSTS WITH SOLAR ACTIVITY

By

S. L. MALURKAR

COLABA OBSERVATORY, BOMBAY 5, INDIA

(Presented by L. Jánosy. — Received: 14. III. 1958)

Among the upper air observations of cosmic ray intensity, POMERANTZ after a preliminary choice selected nine instances to relate them to solar flares, giving corresponding radio data and reproducing the cosmic ray records. As these were events described in some detail, it was considered desirable to examine them with reference to the evolution of corresponding solar active regions. As evolution of the region was considered, the use of available solar magnetic data previous and subsequent to the actual flares would be unobjectionable. Solar magnetic data were also available for one of the five very large solar flares connected with cosmic ray bursts and allowed good comparison. The examination has not indicated any modification of the conclusions drawn earlier.

The five recorded very big cosmic ray bursts at the time of solar flares were shown to have occurred when a particularly long-lived and continuously active solar region showed intense eruptions either at the time of its central meridian passage or at the time of its disappearance at the western limb of the sun [1]. The high-energy particles from these active solar regions would belong to a much heavier element than normally and be positively charged.

POMERANTZ in 1956 [2] examined from among the high altitude observations from balloons of cosmic ray increases and solar disturbances nine instances and concluded that on four occasions cosmic rays increased at high altitudes and that it was normal on five occasions when "r/f radio disturbances and/or visually observed solar flares occurred". While in the very big five events, the high-energy particles had definite sectors of emission, it cannot be excluded a priori that smaller events cannot occur under different conditions. Particles of lighter elements may be emitted with less over-all energy which might affect the cosmic ray reception at the surface of the earth or change the geomagnetic field. It appeared desirable to re-examine POMERANTZ's instances by the method used earlier.

The big cosmic ray bursts depend on the evolution and nature of the associated solar active regions. On many occasions it has not been possible to obtain these data for epochs of cosmic ray bursts. Since evolution of the active region was considered apart from the instantaneous situation, cognate data for days just preceding and days just following the events could also be utilized for confirmatory evidence. The data on the nature of the active region and the distribution of the magnetic field and the photographs in it are from

8

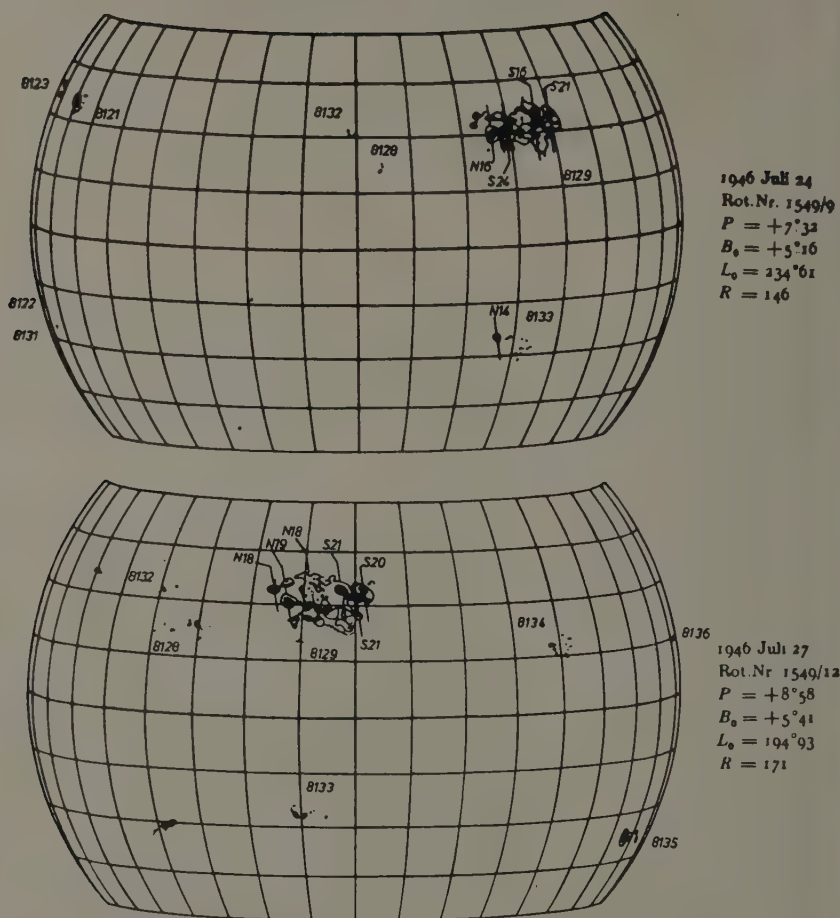


Fig. 1. Magnetic field strengths in solar active regions (from Potsdam Obsy. Publ.).

Potsdam [3]\*. The classification of sun-spot groups after Quart. Bull. Solar Activity [4] saves detailed description. As a sort of comparison the events of July 25, 1946 — one of the historically recorded major events — has also been considered here.

\* The diagrams have been reproduced with the permission of the Director, Astrophysical Obsy, Potsdam, whom I thank.

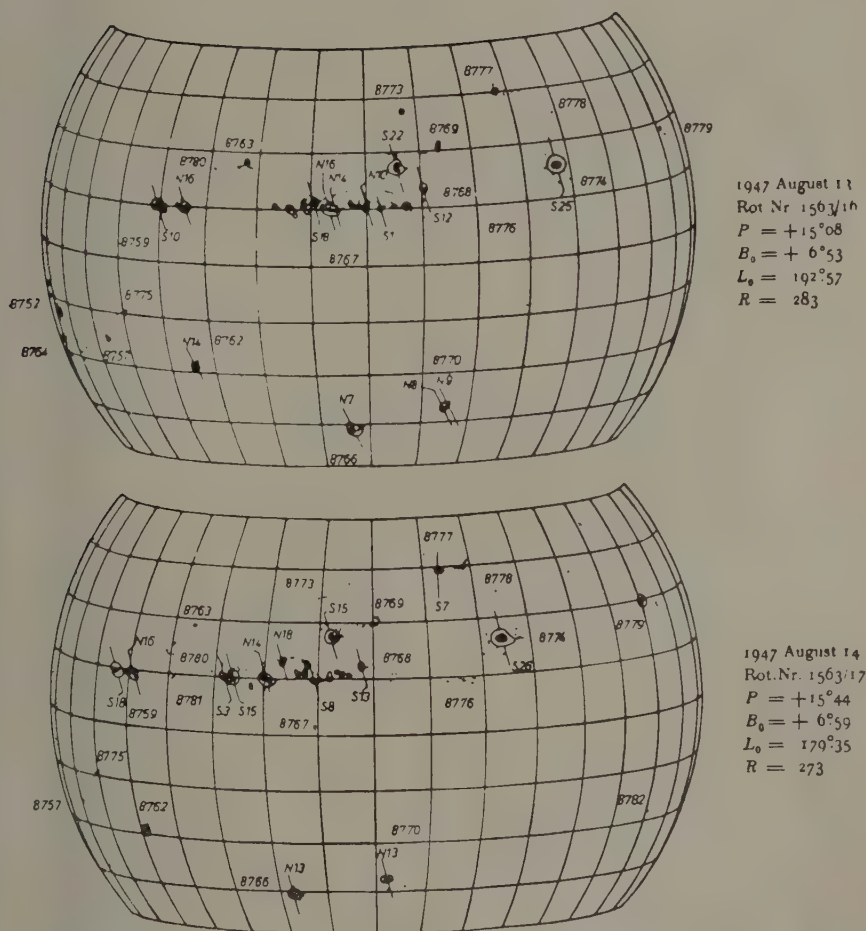


Fig. 2. Magnetic field strengths in solar active regions (from Potsdam Obsy. Publ.)

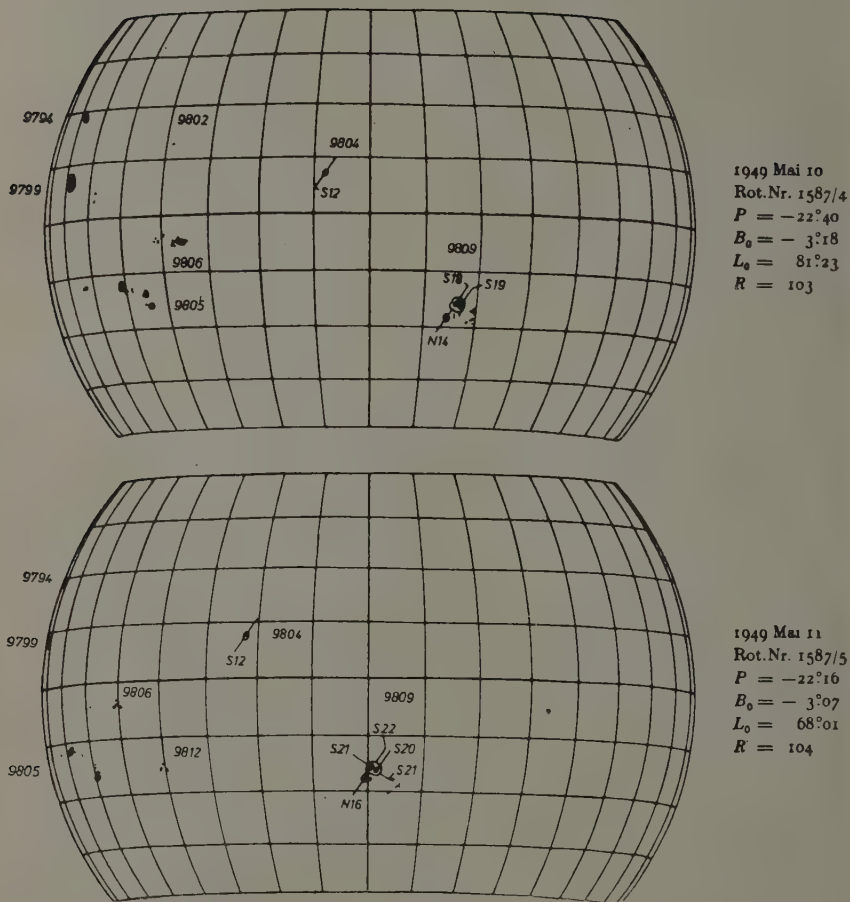


Fig. 3. Magnetic field strengths in solar active regions (from Potsdam Obsy. Publ.)

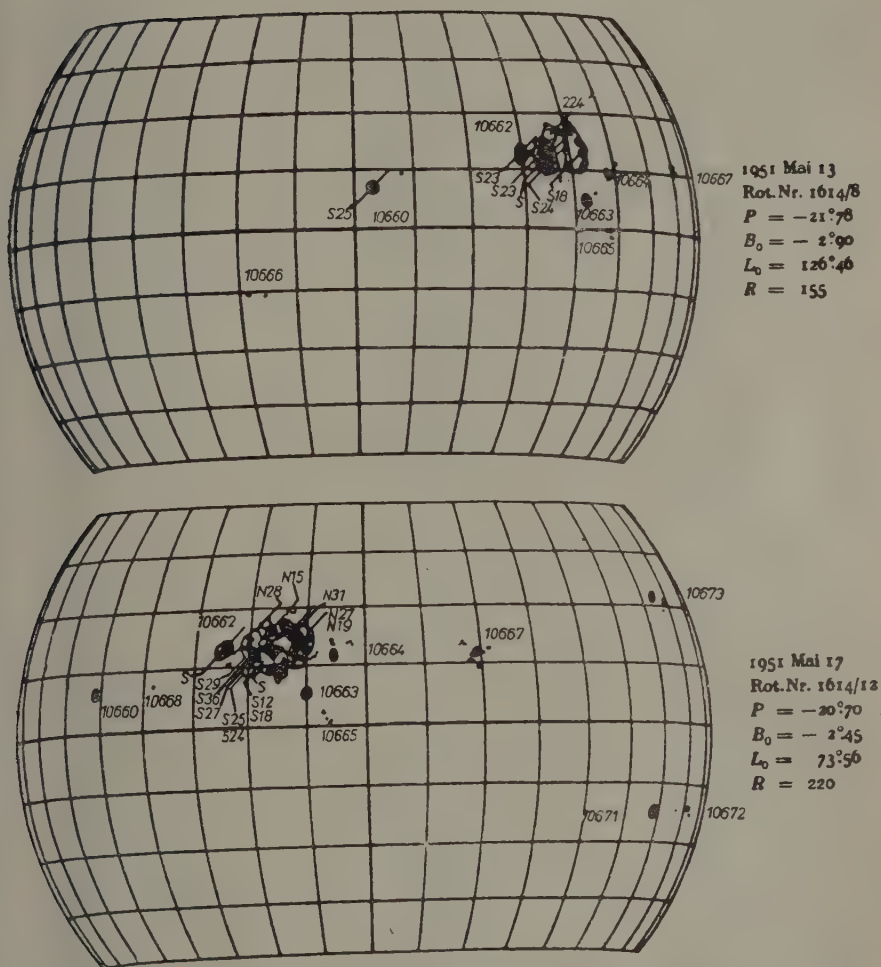


Fig. 4. Magnetic field strengths in solar active regions (from Potsdam Obsy. Publ.)

Date	Station	Time (U. T.)	Co-ordinates		Imp.
			$\varnothing$	C. M. Dist.	
1947					
Aug. 8.	Canberra	0607—0625	12 N	71 E	1
	Zürich	1547—1555	10 N	70 E	2
	McMath	1610—1625	10 N	70 E	1
	"	1705	5 N	55 E	1
9.	Wendelstein	0540—0550	8 N	63 E?	1
	"	0605—0800	15 N	61 E	1—2
	Schauinsland	0735—0750	18 N	58 E	1
	Wendelstein	1055—1115	8 N	63 E	1—2
	"	1237—1310	8 N	48 E	1
	"	1425—1640	15 N	61 E	1—2
	"	1620—1635	8 N	48 E	1
10.	Wendelstein	0630—0750	11 N	46 E	1
	"	0630—0730	20 N	50 E	2
	"	0810—0830	12 N	51 E	2
	"	0926—0944	11 N	46 E	1
	"	0959—1010	12 N	51 E	1
	"	1213—1315	10 N	37 E	2
	"	1515—1630	11 N	46 E	1
	"	1604—1630	12 N	51 E	1—2
	McMath	1635—1715	15 N	50 E	2
11.	Sherborne	0954—1010	13 N	40 E	1
	Schauinsland	1215—1222	8 N	12 E	1
	McMath	1705	10 N	10 E	1
	"	2018	10 N	30 E	1
12.	Zürich	0700—0740	11 N	11 E	1
	Schauinsland	0710—0836	10 N	4 E	2
	Wendelstein	0710—0836	10 N	4 E	2
	Zürich	0834—0839	13 N	2 W	1
	Sherborne	1154—1213	9 N	0	1
		(Max. 1157)			
	Zürich	1204—1215	9 N	4 E	1
	Greenwich	1400—1501	13 N	24 E	3
		(Max. 1409)			
	McMath	1403	10 N	15 E	2
	Schauinsland	1437—1530	11 N	21 E	2
	McMath	1605	10 N	15 E	1
	Sherborne	1730—1740	13 N	10 E	1
	McMath	1830	10 N	5 E	1
	"	2000	10 N	15 E	1
13.	Canberra	0100—0110	9 N	5 W	1
	Schauinsland	0602—0645	13 N	16 E	2
	Wendelstein	0602—0645	13 N	16 E	2
	Zürich	0623—0635	11 N	12 E	2
	Muswell Hill	0640—0700	3 N	15 E	1
		(Max. 0645)			
	"	0700	10 N	0	2
	Greenwich	1034—1100	9 N	7 W	2
	Muswell Hill	1045—1100	10 N	7 W	2
	Meudon	1048—1055	10 N	10 W	1
	Arcetri	1053—1058	10 N	6 W	2
	Schauinsland	1155—1200	9 N	2 W	1
14.	Schauinsland	1233—1240	9 N	19 W	2
	Wendelstein	1440—1450	11 N	35 W	1
	McMath	1443	13 N	30 W	1
	McMath	1640	15 N	30 W	1



Date	Station	Time (U. T.)	Co-ordinates		Imp.
			$\alpha$	C. M. Dist.	
Aug. 14.	Wendelstein	1740—1815	11 N	34 W	1—2
	Mt. Wilson	1740—1745	10 N	34 W	1
	McMath	1745	15 N	30 W	2
	Meudon	1750—1756	11 N	30 W	2
15.	Schauinsland	0540—0553	14 N	31 W	1
	"	0545—0620	9 N	40 W	2
	Wendelstein	0545—0620	9 N	40 W	2
	Muswell Hill	1100—1200 (Max. 1145)	10 N	50 W	1
16.	Wendelstein	0705—0738	11 N	56 W	1
	"	0807—0815	10 N	49 W	1
	Schauinsland	0852	7 N	45 W	1
	Greenwich	1005—1015	9 N	57 W	1
17.	Wendelstein	1008—1016	10 N	50 W	2
	"	1342—1350	9 N	43 W	1
	"	1705—1725	9 N	38 W	1—2
	"	1630—1642	10 N	70 W	1
18.	Mt. Wilson	1650	15 N	60 W	1
	McMath	1740—1755	12 N	62 W	1
	Wendelstein	1747—1800	11 N	64 W	3
	Zürich	0618—0705	10 N	61 W	2
19.	Schauinsland	0627—0740	9 N	63 W	1
	Arcetri	0943—0948	13 N	90 W	1
	"	0943—0948	10 N	60 W	1
	Arcetri	1338—1543	10 N	90 W	1
1949					
May 5.	Ondrejov	1300	17 S	75 E	1+
	"	0725—0748	18 S	62 E	1
	"	0833—0910	15 S	71 E	1
	"	(Max. 0838)			
6.	Edinburgh	0855—0920	15 S	75 E	1
	Kodaikanal	0900	17 S	70 E	1
	Mt. Wilson	1735—1750	17 S	70 E	1
	"	(Max. 1745)			
7.	McMath	2045	23 S	55 E	2
	Mitaka	2219—2300	18 S	45 E	1
8.	Mt. Wilson	1524—1716	16 S	40 E	2+
	"	(Max. 1556)			
	McMath	1528—1720	24 S	37 E	3—
	Schauinsland	1529—1645	13 S	46 E	2
9.	"	(Max. 1531)			
	Huancayo	1545—1648	18 S	31 E	1
	Kanzelhöhe	1646—1735	18 S	37 E	1
	Meudon	1715—1804	17 S	40 E	2
10.	Mt. Wilson	1951—2006	17 S	39 E	2
	"	(Max. 1953)			
	McMath	1958—	24 S	37 E	2
	Mitaka	0000—0015	20 S	27 E	1
9.	"	0353—0428	18 S	28 E	1
	Kanzelhöhe	0635—0647	17 S	27 E	1
	Mt. Wilson	1508—1518	17 S	25 E	1
	"	(Max. 1514)			
10.	Kodaikanal	0330—0430	17 S	20 E	2
	"	(Max. 0345)			
	Canberra	0330—0350	18 S	18 E	2

Date	Station	Time (U. T.)	Co-ordinates		Imp.
			$\varnothing$	C. M. Dist.	
May 10.	McMath	2002—2220 (Max. 2011)	20 S	12 E	3+
	Mitaka	2108—2217	18 S	5 E	1—2
16.	Ondrejov	0921—0935	21 S	64 W	1
Aug. 12.	Cambridge	0944—1004	12 N	90 E	1
15.	Mitaka	0450—0610	14 N	60 E	1
16.	Wendelstein	1657—1741 (Max. 1712)	16 N	29 E	1—2
	McMath	1700—1830 (Max. 1748)	13 N	22 E	2?
	Mt. Wilson	1709—1900 (Max. 1759)	11 N	30 E	2
18.	McMath	1953—2020	14 N	10 E	1
	Mt. Wilson	2151—2204 (Max. 2153)	14 N	7 E	1
19.	Kodaikanal	0250—0315	12 N	5 W	1
	Meudon	0722	14 N	2 E	1
	Mt. Wilson	2105—2150 (Max. 2111)	16 N	9 W	2
	McMath	2105—2206 (Max. 2110)	13 N	10 W	3
	Mt. Wilson	2337—2341	15 N	7 W	1
20.	McMath	1550—	12 N	10 W	1
	Mitaka	2350—2355	12 N	28 W	1
21.	Mitaka	0050—0102	12 N	28 W	1
	Mitaka	0350—0415	14 N	26 W	1
	Zürich	1110—1118	15 N	25 W	1
23.	Ondrejov	1235—1250	12 N	55 W	1
24.	Mitaka	0324—0334	9 N	68 W	1
25.	Kanzelhöhe	1430—1434	10 N	90 W	1
Oct. 1.	Kodaikanal	0418—0423	10 N	80 E	1
	Greenwich	1018—1026	9 N	85 E	?
	McMath	1415—	5 N	85 E	1+
	Mt. Wilson	1705—1723 (Max. 1710)	8 N	76 E	1
	Mitaka	2154—2202	9 N	69 E	1
2.	Mitaka	0035—0119	5 N	70 E	1
	"	0246—0309	7 N	69 E	1
	"	0410—0437	9 N	69 E	1
	Schauinsland	1345—1437 (Max. 1405)	9 N	68 E	2
	Mt. Wilson	1822—1836 (Max. 1827)	7 N	64 E	1
	"	2339—2357 (Max. 2349)	8 N	62 E	1
	Mitaka	2341—2349	8 N	60 E	1
3.	Kodaikanal	0314—0530 (Max. 0318)	8 N	50 E	3
	Mitaka	0317—0336	7 N	50 E	2
	Carter, N. Z.	0339—0424	9 N	52 E	2
	Wendelstein	1053—1104	6 N	49 E	1—2
	Edinburgh	1114—1226 (Max. 1156)	8 N	50 E	2
	Wendelstein	1144—1219 (Max. 1158)	5 N	50 E	2
	Kanzelhöhe	1609—1614	8 N	47 E	1

Date	Station	Time (U. T.)	Co-ordinates		Imp.
			$\varnothing$	C. M. Dist.	
Oct. 3.	Mt. Wilson	1736—1842 (Max. 1756)	8 N	48 E	1
	Mt. Wilson	2302—2352 (Max. 2333)	8 N	44 E	1
4.	Kanzelhöhe	0555—0635	7 N	43 E	1
	"	0741—0755 (Max. 0747)	6 N	38 E	1+
	"	0755—0810	11 N	39 E	1
	Arcetri	0800	8 N	47 E	1
	Wendelstein	1309—1346 (Max. 1317)	11 N	35 E	2
	Zürich	1310—1337 (Max. 1317)	10 N	37 E	1
	Kanzelhöhe	1320—1338 (Max. 1324)	10 N	35 E	1+
	Greenwich	1323—1342 (Max. 1324)	13 N	36 E	2-1
	Mt. Wilson	1610—1637 (Max. 1623)	14 N	30 E	2
	Kanzelhöhe	1618—1628	13 N	33 E	1
	Mt. Wilson	1900—1917 (Max. 1908)	6 N	32 E	1
	Muswell Hill	1105—1130	5 N	30 E	1
		1111—1134 (Max. 1120)	5 N	31 E	1—2
	Greenwich	1114—1126 (Max. 1119)	9 N	25 E	2
	Edinburgh	1114—1135 (Max. 1120)	11 N	32 E	1
6.	Kanzelhöhe	1120—1135	8 N	31 E	1+
	Kodaikanal	0452	8 N	17 E	1
	Canberra	0455—0505	8 N	25 E	1
	Kanzelhöhe	0920—0952 (Max. 0923)	10 N	11 E	1
	Ondrejov	0920—0934 (Max. 0925)	13 N	10 E	1
	Wendelstein	1121—1200 (Max. 1138)	11 N	10 E	1—2
	Kanzelhöhe	1130—1210 (Max. 1142)	11 N	11 E	1
	Ondrejov	1134—1201 (Max. 1135)	15 N	8 E	1
	Greenwich	1136—1203 (Max. 1142)	11 N	11 E	2
	Kanzelhöhe	1230—1234	9 N	8 E	1
	Wendelstein	1316—1336 (Max. 1324)	7 N	10 E	1
	Kanzelhöhe	1326—1403	6 N	10 E	1+
	Greenwich	1338—1348	6 N	9 E	2?
	Mitaka	0232—0238	11 N	4 E	1
	Ondrejov	0950—1010 (Max. 0953)	17 N	58 W	1+
11.	"	0750—0805 (Max. 0753)	14 N	55 W	2
	Wendelstein	0757—0811	11 N	52 W	1
	Ondrejov	1422—1430	8 N	61 W	1

Date	Station	Time (U. T.)	Co-ordinates		Imp.
			$\varnothing$	C. M. Dist.	
Oct. 11.	Mt. Wilson	2116—2437? (Max. 2120)	8 N	60 W	1
8.	Kodaikanal	0452	18 N	71 E	2
	Ondrejov	1017—1028 (Max. 1021)	16 N	65 E	1
	Schauinsland	1310—1331	21 N	62 E	2
	Ondrejov	1312—1335 (Max. 1316)	22 N	78 E	2
9.	Kanzelhöhe	0829—0843	19 N	47 E	1
	"	0937—0950	18 N	54 E	1
10.	Mitaka	0427—0437	17 N	45 E	1
	"	0628—0638	17 N	45 E	1
11.	"	0124—0135	16 N	32 E	1
	Carter, N. Z.	0207—0228	18 N	27 E	2
	Canberra	—0235	22 N	53 E	1
	Kodaikanal	0235—0240	14 N	31 E	1
	Wendelstein	1139—1323 (Max. 1150)	20 N	25 E	2
	Ondrejov	1514—1540 (Max. 1523)	19 N	22 E	2
	Wendelstein	1516—1527	21 N	23 E	2
	Mt. Wilson	1539—1654 (Max. 1551)	19 N	22 E	2
12.	Ondrejov	0722—0729	22 N	12 E	1
	Kanzelhöhe	1131—1250	19 N	12 E	1
	Greenwich	1140—1220	19 N	9 E	1+
13.	Ondrejov	1118—1251 (Max. 1147)	21 N	4 W	2
	Kanzelhöhe	1130—1246 (Max. 1150)	19 N	1 E	2+
	Zürich	1225—1252	18 N	2 E	2
15.	Arcetri	0846	20 N	27 W	2
	Edinburgh	1048—1151 (Max. 1058)	19 N	28 W	1
	Greenwich	1055—1125 (Max. 1101)	19 N	27 W	2—
	Wendelstein	1058—1120 (Max. 1104)	21 N	25 W	1
	Ondrejov	1242—1248 (Max. 1246)	21 N	35 W	1
	Kanzelhöhe	1456—1542	20 N	30 W	1
	Mt. Wilson	1536—2000 (Max. 1640)	20 N	31 W	1+
	Huancayo	1630—1700 (Max. 1640)	25 N	38 W	2+
	Mt. Wilson	1630—1640 (Max. 1635)	21 N	42 W	1
16.	Mitaka	0127—0135	18 N	33 W	1
	Kodaikanal	0225	18 N	40 W	1
	Schauinsland	0736—0805	20 N	40 W	1
	Ondrejov	0746—0807	22 N	39 W	1
	Arcetri	0821	20 N	39 W	2
	Edinburgh	1456—1516 (Max. 1500)	20 N	44 W	1
	Kanzelhöhe	1500—1512	21 N	44 W	1+
	Ondrejov	1502—1515	19 N	37 W	1+

Date	Station	Time (U. T.)	Co-ordinates		Imp.
			$\varnothing$	C. M. Dist.	
Oct. 16.	Mt. Wilson	1716—1840	20 N	48 W	1
17.	Mt. Wilson	1724—1734	20 N	58 W	1+
18.	Zürich	0940—0955	19 N	65 W	1
1951		(Max. 0945)			
Nr. (5)					
Jan. 27.	Edinburgh	1204—1245	8 N	8 E	1
	"	1530—1600	8 N	6 E	1
		(Max. 1534)			
28.	Mitaka	2343—2354	11 N	11 W	1
Feb. 2.	Mitaka	0121—0124	10 N	60 W	1
Nr. (6)					
Jan. 22.	Huancayo	1630—1700	10 S	90 E	1
27.	Edinburgh	1515—1535	12 S	17 E	1
		(Max. 1517)			
	Mt. Wilson	1956—2438	10 S	9 E	2
Nr. (7)					
Jan. 24.	Mitaka	0524—0544	8 N	76 E	1
25.	"	0158—0203	10 N	60 E	1
	"	0302—0308	8 N	62 E	1
	"	1028	7 N	58 E	1+
	Meudon	1043—1118	8 N	62 E	1
	Schauinsland	2330—2350	8 N	49 E	1
	Mitaka	0512—0527	7 N	40 E	1
26.	Mitaka	0250—0255	9 N	25 E	1
27.	Mitaka	0418—0435	8 N	23 E	1
	"	1048—1120	9 N	28 E	1
28.	Edinburgh	2338—2343	14 N	0	1
29.	Mitaka	0953—1005	18 N	10 W	1
		(Max. 0956)			
	Herstmonceux	0149—0201	8 N	29 W	1
Feb. 1.	Herstmonceux	0040—0052	4 N	40 W	1
	Mitaka	0149—0201	8 N	29 W	1
	"				
Nr. (13)					
May 8.	McMath	1505	10 N	90 E	2
	Mt. Wilson	1506—1514	12 N	90 E	1
		(1508)			
10.	Herstmonceux	1012—1024	12 N	73 E	2—
11.	Canberra	0120—0131	10 N	65 E	1
	"	0153—0215	0	70 E	1
	"	0610—0615	10 N	70 E	1
	"	1015—1026	17 N	59 E	1
	Herstmonceux	(Max. 1018)			
12.	Kodaikanal	0215—0240	15 N	55 E	1
	Arcetri	0933	15 N	45 E	1
	McMath	1255	12 N	50 E	1
	"	1920	12 N	50 E	1
13.	Meudon	0705	10 N	40 E	1+
	Zürich	0943—1005	15 N	37 E	2
	Ondrejov	1254—1316	14 N	36 E	1
	McMath	1314	10 N	35 E	1+
14.	Kodaikanal	0240	12 N	35 E	1
	Kanzelhöhe	1146—1204	16 N	26 E	1
	Mt. Wilson	2245—2322	14 N	19 E	2
		(Max. 2253)			
15.	McMath	1315—1415	16 N	10 E	1+
		(Max. 1330)			

Date	Station	Time (U. T.)	Co-ordinates		Imp.
			$\varnothing$	C. M. Dist.	
May 15.	Canberra	2332—2415	5 N	0	1
	Arcetri	0938	12 N	15 W	1
16.	Edinburgh	1016—1031	15 N	2 W	1
		(Max. 1023)			
	Herstmonceux	1025—1032	15 N	3 W	1
	McMath	1659—1810	15 N	5 W	2
17.	Canberra	0108—0125	15 N	10 W	1
	Meudon	1442—1455	12 N	20 W	1
	Herstmonceux	1447—1525	15 N	16 W	1
		(Max. 1451)			
	Edinburgh	1504—1524	21 N	15 W	1
		1527—1601	13 N	17 W	1
	Herstmonceux	1533—1548	15 N	16 W	1
		(Max. 1535)			
	Huancayo	1637—1643	15 N	21 W	1
	Canberra	2333—2358	10 N	20 W	1
18.	Canberra	0145—0153	12 N	25 W	1
		0201—0227	20 N	20 W	2
	Kodaikanal	0215—0315	16 N	22 W	1
	Canberra	0314—0325	16 N	30 W	1
	Kanzelhöhe	0725—0949	15 N	28 W	1
	Ondrejov	0739—0758	15 N?	28 W?	1+
		(Max. 0743)			
	Cambridge	1020—1225	12 N	35 W	?
		(Max. 1050)			
	Edinburgh	1021—1337	16 N	30 W	3
		(Max. 1028)			
	Kanzelhöhe	1022—1258	15 N	29 W	2
		(Max. 1050)			
	Ondrejov	1025—1154	12 N	26 W	2
	Zürich	1028—1320	15 N	29 W	3
	Herstmonceux	1043—1316	13 N	29 W	3
		(Max. 1112)			
	Saltsjobaden	1045	15 N	30 W	3
	McMath	1155—1415	11 N	30 W	2+
	Creteil	1300	18 N	35 E	3
	Meudon	1303—1330	15 N	33 W	2
	Kanzelhöhe	1621—1623	19 N	28 W	1
	McMath	1956—2100	17 N	35 W	2+
		(Max. 2000)			
	Mt. Wilson	1959—2050	17 N	43 W	1
		(Max. 2010)			
19.	Kanzelhöhe	0445—0452	14 N	46 W	1+
	Zürich	0734—0745	7 N	39 W	1
		0832—0845	16 N	37 W	1
		0858—0937	13 N	39 W	1
	Kanzelhöhe	0901—0930	16 N	41 W	1
	Ondrejov	1345—1421	18 N	45 W	1
		(Max. 1351)			
	Schauinsland	1350—1430	18 N	38 W	2
	Edinburgh	1415—1425	20 N	45 W	1
	McMath	1949—2040	12 N	43 W	3—
		(Max. 1957)			
	Ondrejov	0431—0509	6 N	69 W	1
20.		(Max. 0447)			
		0657—0718	13 N	55 W	1
		(Max. 0703)			



Date	Station	Time (U. T.)	Co-ordinates		Imp.
			$\lambda$	C. M. Dist.	
May 20.	Kanzelhöhe	0817—0845	16 N	58 W	2
	Ondrejov	0819—0850	12 N	65 W	1
		(Max. 0832)			
	Meudon	0843	17 N	60 W	1+
	Mt. Wilson	1956—2014	13 N	68 W	1
		(Max. 2000)			
	McMath	1957	12 N	60 W	2—
	Kodaikanal	0218—0310	8 N	67 W	1
	Zürich	1255—1303	8 N	75 W	1
	Herstmonceux	1308—1337	11 N	75 W	1+
21.		(Max. 1313)			
	Kanzelhöhe	1320—1323	4 N	68 W	1
	Arcetri	1336	6 N	72 W	2
	Herstmonceux	1612—1623	11 N	76 W	1
		(Max. 1615)			
	Kanzelhöhe	0439—0442	11 N	85 W	1
	Ondrejov	0918	6 N	84 W	1
	Zürich	1540—1545	14 N	80 W	1
	McMath	1310	13 N	90 W	1
Nr. (16) May 15.	Ondrejov	1127—1145	13 N	18 E	2+
	McMath	1150	12 N	17 E	2
	Mt. Wilson	2307—2330	10 N	18 E	1
		(Max. 2315)			
	McMath	1409—1529	10 N	5 E	1
		(Max. 1418)			
	"	1558—1647	10 N	5 E	1
	"	2047	10 N	5 E	1
	Herstmonceux	1754—1815	11 N	10 W	2
		(Max. 1758)			
17.	Edinburgh	1759—1845	12 N	9 W	2

Summary Table

Year	No.	Co-ordinates			C. M. Passage	No. of Distinct Obsd. Places	Type of Active Region	Field in 100 Overeds	Date Balloon Ascent	C. M. Dist.	Cosmic Ray Change	Geomagnetic Change Later	Dates of Solar Field
		$\phi$	L	Date at	Age at								
1946	7	21 N	198	Jul. 26. 8	> 6	37	F. - A large classification	24	—	—	Flare enhanced even <i>ground</i>	a storm	July 24, 27
1947	32	10 N	190	Aug. 13. 2	> 6	53	E. - Nowhere of much area line of spots	18	Aug. 12	—	normal	s. c. 12. 3	Aug. 13, 14
1949/2	30	17 S	60	May 11. 6	+7?	15	D or C, prob. fading after May 10th	22	May 11	—	enhanced	s. c. 11. 2 plus storm	May 10, 11
1949/3 1949	26	15 N	178	Aug. 19. 5	> 6	17	D type following B type one. Not very active	—	Aug. 19	—	normal	nil	—
1949/4	7	9 N	254	Oct. 7. 3	> 6	35	D type. Not very active	25	Oct. 4 (nearly three days before C. M. passage)	—	normal	s. c. 4. 2	—
1949/4	8	20 N	172	Oct. 13. 5	5	27	C type becoming D and later degrading to B	—	Oct. 11 (two days before CM passage)	—	normal	s. c. 11. 4	—
1951/1	5	9 N	68	Jan. 28. 2	+5?	4)	No data	—	Jan. 27	—	enhanced	nil	—
	6	10 S	66	Jan. 28. 4	> 6	3)							
	7	8 N	52	Jan. 29. 5	> 6	14)							
1951/2	13	14 N	85	May 16. 1	> 6	49	E type. No > 2	36	May 17	—	enhanced	nil	May 13, 17
1951/2	16	12 N	72	May 17. 1	> 6	6	Flare till 18th						
1952				No Data Reported					Jan. 17 1952	—	enhanced		

*July 26, 1946.*

This has been described earlier [1] as one of the five very large recorded solar flare periods when a cosmic ray burst occurred. The solar active region had a long history of great activity and the large flare near the C. M. passage of the sun gave rise to a cosmic ray burst followed by a cosmic ray related geomagnetic storm. From the photographs from Potsdam, the region was of very large type with a marked magnetic field.

*Aug. 12, 1947.*

The activity and the largest magnetic field of the related region was less than the previous one. The active region is a linear one with a relatively small breadth. The balloon ascent took place near about the time of the C. M. passage of the centre of the group of linear smaller regions. The geomagnetic storm occurred about the same time.

*May 11, 1949.*

The solar active region is a small one, though the largest magnetic field as measured on the sun is relatively large. After the big flares on 10th May, nearly a day before the C. M. passage, there has been only one recorded flare on the 16th. The region was apparently dissolving itself. Has a resemblance to those regions [1] when only geomagnetic storms were reported on the ground, without a cosmic ray burst at the time of a flare.

*Aug. 19, 1949.*

Though the active region was observed from limb to limb of the sun, the eruptions are not very marked and the region was of small type. It produced no ground effects and no upper air cosmic ray changes.

*Oct. 4, 1949.*

The solar active region observed from 80 E to 60 W. Though the highest observed magnetic field was quite marked the extent of the region is a small one. Balloon ascent nearly three days before the C. M. passage of the region which was decreasing in importance from 4th. After the C. M. passage flares observed towards end of its life.

*Oct. 11, 1949.*

Solar active region observed from 71 E to 65 W. C type region becoming D, degrading later to one of B. Balloon ascent two days before the C. M. passage. The activity of the region not marked.

*Jan. 27, 1951.*

Three minor solar active regions were approaching the C. M. of the sun. There are no solar magnetic data. Upper air cosmic ray *enhancement*.

*May 17, 1951.*

A large E type spot with a very marked magnetic field. Up to the day of balloon ascent the eruptions not very marked. Next day when the region had passed nearly 30° away from the C. M. the flares of importance 3 were observed twice *independently*. No geomagnetic storm followed. Upper air cosmic ray *enhanced*.

*Jan. 17, 1952.*

No solar active region reported and there was no geomagnetic disturbance. Radio disturbance has been quoted by POMERANTZ at the time of upper air cosmic ray *enhancement*.

In the instances given by POMERANTZ, none of the related solar active regions were markedly active over an extended period, compared with the five very big regions quoted earlier: except in the case of May, 1949; among the four occasions when cosmic ray increases were recorded no geomagnetic storm has been recorded at about the epoch. Whether *M* regions of Bartels are responsible for events of Jan. 17, 1952 would be a difficult question to decide. The study of emission of particles which might have given rise to

enhancement of upper air cosmic rays would be possible if more data than at present available could be collated. The facts presented here do not contradict or come in the way of the arguments used about the very large solar flares when cosmic bursts also occurred simultaneously. It would be necessary to examine all relevant data so as to obtain a picture of the geophysical and extra-terrestrial control of emission from the sun.

The cosmic ray enhancements have belonged to compact large area active regions in the sun with strong magnetic fields. A loosely distributed area of active region has produced little effect. This in an additional criterion to those already given [1]: of long life and of exceptional activity on the sun at the stage of C.M. passage or near the western limb.

#### REFERENCES

1. S. L. MALURKAR, *Acta Phys. Hung.*, **3**, 285, 1958.
2. M. A. POMERANTZ, *Phys. Rev.*, **102**, 870, 1956.
3. Publikation des Astrophys. Obs. Potsdam, **29**, Nr. 97, Heft 4. — (W. GROTRIAN, Polaritäten und Maximalwerte. Magnetische Feldstärken von Sonnenflecken in den Jahren 1946—1951. Akademie-Verlag, Berlin. — Sec. 5. Graphische Darstellung der Beobachtungsergebnisse and subsequent numbers by H. KUNZEL.)
4. Qr. Bull. Solar Activity. Int. Astro. U. Zürich.

#### ДАЛЬНЕЙШИЕ ИССЛЕДОВАНИЯ ЛИВНЕЙ КОСМИЧЕСКОГО ИЗЛУЧЕНИЯ, СВЯЗАННЫХ С СОЛНЕЧНОЙ АКТИВНОСТЬЮ

Ш. Л. МАЛУРКАР

#### Резюме

Из наблюдений интенсивности космического излучения в стратосфере Померанц выбрал после предварительной селекции девять случаев, связанных с солнечными вспышками, приводя соответствующие радио-данные и воспроизводя записи космического излучения. Так как они являются случаями, описанными детально, мы сочли желательным их исследование с учетом эволюции соответствующей активной солнечной области.

Так как была исследована эволюция области, солнечные магнитные данные до и после самой вспышки считались безупречными. Солнечные магнитные данные были доступны также в случае одной из пяти самых больших вспышек, связанных с ливнями космического излучения, и этот факт дал хорошую возможность для сравнения. Результаты исследования не потребовали внести изменение в наши предыдущие выводы.

# DETERMINATION OF ELECTROSTATIC POTENTIALS BY SERIES

By

R. GÁSPÁR, B. KOLTAY-GYARMATI and I. TAMÁSSY-LENTEI

INSTITUTE OF THEORETICAL PHYSICS, KOSSUTH LAJOS UNIVERSITY, DEBRECEN

(Presented by A. Kónya. — Received 20. III. 1958)

By using the solutions of eigenvalue problems often occurring in the various fields of theoretical physics the method of series, already used in certain cases for solving the Poisson equation, has been reformulated. In case the charge distribution can be expressed by the Dirac  $\delta$ -function, the potential distribution can be given in the form of a series, the convergence of which is sufficiently rapid. For simple cases the formulae can be analytically reduced to the known solutions of corresponding problems (e. g. in the case III/1). In other cases (III/2) the calculated potential distribution coincides with the potential distribution obtained by electrolytic tank measurements. In the case of the cylinder lens of electron optics (III/3) the method yields the potential distribution and the corresponding electrode shape for arbitrary slit width.

## I. Introduction

The well-known task of electrostatics is the determination of the electric field of charge distributions, when the electrode arrangements are given in advance. For the solution of the problem several methods have been worked out [1]. A common feature of most of these methods is that an electrode arrangement of particular symmetry is assumed and that for the individual arrangements the solutions are given separately in an explicit form. Thus these methods are in general too specialized for application to the actual electrode arrangement (required by some practical problems). The last possibility remaining in such cases is the experimental determination by electrolytic tanks which, however, may in cases not having symmetry properties prove to be a very complicated undertaking.

The solution of the fundamental problem of electrostatics in explicit form could be immediately given (although the possibility of its practical evaluation in slightly more complicated cases seems somewhat doubtful), if the distribution of the surface charge density on the metal electrodes were known. For a quite general electrode arrangement such an assumption would be indeed very audacious. In several cases of practical importance, however, the distribution of the surface charge density is exactly or at least approximately known. In the latter case when the distribution is approximately known one can proceed also in such a manner as to base the final execution of the shape of the electrode system on the equipotential surfaces of the field determined previously.

The basic idea of the method is the following. Let us consider an electrode system of which the distribution of the surface charge density is given and a closed surface on which the values of the electrostatic potential is prescribed. Knowing the latter the Green function of the fundamental equation of electrostatics can be determined and hereby the solution produced in the form of a series. In many instances a considerable reduction of analytical formulae can be achieved by producing the series in finite form.

The method developed is specialized first for the case of axially symmetric fields, then we show on a very simple example, the case of a cylinder capacitor, how the method may be applied. Afterwards the fields of three-electrode arrangements are determined which are used in the Penning's vacuum gauge, resp. which are differing from it in the placing of the anode and the cathode. These results are compared with the distributions measured by an electrolytic tank. Finally the potential field of an electrode arrangement important in electron optics (the two-cylinder lens of finite slit width) is determined in the form of a series.

It may be finally mentioned that the mathematical method applied here has recently been widely used for numerous problems [2]. Thus for instance also for the solution of the fundamental electrostatic problem in the case of simpler electrode arrangement [3].

## II. General part. Survey of the method.

The fundamental problem of electrostatics is the determination of the solution of the Poisson equation,

$$\Delta\Phi = -4\pi\rho, \quad (1)$$

i. e. determination of the potential distribution  $\Phi$  for given boundary conditions, if the space charge density  $\rho$ , respectively in other cases the surface charge density  $\sigma$ , the line densities  $\gamma$  or the dipole momenta of the surface double layers are known. In principle  $\Phi$  can be determined from equation (1) when the above quantities are known, practically, however, it depends on the charge distribution and the boundary conditions whether the solution can be given. In the present paper the method is described for the case of all those potential distributions for which the charge distribution can be written down by the Dirac  $\delta$ -function. (Hence for instance for any point charge distribution, for a surface and line charge distribution, provided they have suitable symmetry, etc.) In the following after the description of the general method we shall apply it to some actual instances.

The charge density of a single point charge occurring in the Poisson equation can be taken in the following form

$$\rho = e_0 \delta(\mathbf{r} - \mathbf{r}_0), \quad (2)$$



where  $q_0$  is the charge at the point  $r_0$ . Hence equation (1) takes the following form

$$\Delta\Phi = -4\pi q_0 \delta(r - r_0), \quad (1a)$$

The boundary conditions are that the potential shall on a closed or open surface take up a value determined in advance.

The solutions  $\Phi_i$  of the eigenvalue equation

$$\Delta\Phi = E\Phi \quad (2)$$

by which the above boundary conditions are satisfied, belong to the eigenvalues  $E_i$ . The Laplace operator is hermitian, and its eigenfunctions  $\Phi_i$  form an orthonormal complete set of functions. As is well known the Dirac  $\delta$ -function can be expanded in a complete set of orthonormalized functions, hence

$$\delta(r - r_0) = \sum_i \Phi_i^*(r_0) \Phi_i(r). \quad (4)$$

The functions  $\Phi_i$  satisfy the same boundary conditions as the potential  $\Phi$  which is to be determined, the latter can be expanded in the  $\Phi_i$ -s

$$\Phi(r) = \sum_i c_i \Phi_i(r). \quad (5)$$

Substituting (5) and (4) into (1a) owing to the linearity of the Laplace operator

$$\sum_i c_i \Delta\Phi_i = -4\pi q_0 \sum_i \Phi_i^*(r_0) \Phi_i(r). \quad (1b)$$

Using equation (3) from the comparison of the coefficients

$$c_i = -4\pi q_0 \frac{\Phi_i^*(r_0)}{E_i} \quad (6)$$

is obtained. Thus the potential is

$$\Phi(r) = -4\pi q_0 \sum_i \frac{\Phi_i^*(r_0) \Phi_i(r)}{E_i}.$$

(More generally see for instance [2].)

The method can be generalized without difficulties for the case of many point charges. Similarly all problems can be dealt with for which the charge

density can be written as the superposition of terms of the form (2). In this case the determination of the potential can be reduced to the search of solutions of (3) satisfying suitable boundary conditions.

### III. Special problems

In the following some axial symmetrical problems will be dealt with, on the one hand because of their physical importance (calculation of electron-optical cylinder lenses etc.) on the other because also from other sides the necessity of the solution of similar problems emerged. As a matter of course the method is also suitable for electrode arrangements having other adequate symmetries.

For axially symmetrical arrangements equation (3) can be written in the following form

$$\frac{\partial^2 \Phi}{\partial r^2} + \frac{1}{r} \frac{\partial \Phi}{\partial r} + \frac{\partial^2 \Phi}{\partial z^2} = E\Phi, \quad (3a)$$

$r$  and  $z$  are the well-known cylinder coordinates. In the following the solution of some special problem is searched.

1. As a first application such an electrode arrangement is dealt with for which calculations can easily be carried out also otherwise. An infinitely long metal cylinder of radius  $R_1$  the axis of which coincides with the  $z$  axis of the system of coordinates is first considered. The surface charge density on the cylinder be  $\sigma_0$ . It is surrounded by an earthed metal cylinder of radius  $R$  (cylinder capacitor). In the case of this arrangement the charge density is

$$\sigma = \sigma_0 \delta(r - R_1).$$

The potential depends owing to the symmetry properties only on  $r$ , and as is known

$$\left. \begin{aligned} \Phi &= 4\pi\sigma_0 \log \frac{R}{r}, & \text{if } R_1 \leq r \leq R, \\ \Phi &= 4\pi\sigma_0 \log \frac{R}{R_1}, & \text{if } 0 \leq r \leq R_1. \end{aligned} \right\} \quad (7)$$

Considering that the potential does not depend on  $z$ , the normalized solution of equation (3a) which vanishes at  $r = R$  is

$$\Phi_i(r) = \frac{\sqrt{2}}{R J'_0(k_i)} J_0\left(\frac{k_i}{R} r\right)$$

for the eigenvalues

$$E_i = -\frac{k_i^2}{R^2},$$

where  $J_0$  is the Bessel function of first kind of order zero and the  $k_i$ -s are the roots of this Bessel function. The dash means derivation into the argument. The potential can be produced according to the method given in the general part in the form

$$\Phi = 8\pi\sigma_0 \sum_i \frac{J_0\left(\frac{k_i}{R}R_1\right)J_0\left(\frac{k_i}{R}r\right)}{k_i^2 J_0'^2(k_i)}. \quad (8)$$

As can be easily seen by integration (8) is the expansion of (7) in a series of Bessel functions of different argument and order zero.

The fact that the series is convergent can be easily rendered plausible. According to the well-known asymptotical formula [4] referring to the Bessel functions of  $p$ th order

$$J_p(x) \approx \frac{\cos \varphi}{\sqrt{1/2 \pi x}} \quad \text{and} \quad \varphi = x - (p - 0.5) \frac{\pi}{2}, \quad (x)$$

if  $x \rightarrow \infty$ . Thus

$$J_0\left(\frac{k_i}{R}R_1\right)J_0\left(\frac{k_i}{R}r\right) \approx \frac{R}{\pi\sqrt{R_1 r k_i}} \left\{ \cos\left[\frac{k_i}{R}(R_1 - r)\right] + \sin\left[\frac{k_i}{R}(R_1 + r)\right] \right\}.$$

On the other hand it can be demonstrated also by (x) that for sufficiently great  $i$

$$J_1^2(k_i)k_i \approx \frac{2}{\pi}.$$

Thus the series is

$$\Phi(r) \approx \frac{4R\sigma_0\pi}{\sqrt{R_1}r} \sum_i \frac{\cos\left[\frac{k_i}{R}(R_1 - r)\right] + \sin\left[\frac{k_i}{R}(R_1 + r)\right]}{k_i^2}.$$

Substituting the highest possible value of cos resp. sin, i. e. 1, and considering the asymptotical behaviour of the roots of the Bessel functions

$$k_i \approx \left(i - \frac{1}{4}\right)\pi, \quad \text{if } i \rightarrow \infty,$$

it can be seen that the series can be majorized by the absolutely convergent series  $\sum_i \frac{1}{i^\alpha}$  ( $\alpha > 1$ ), which is a sufficient condition for convergence [5].

2. Let us calculate as another special problem the potential field of the following electrode arrangement: In a closed earthed cylinder of radius  $R$  and height  $l$  are placed in planes parallel with the base circle-shaped electrodes of radius  $R_1$  provided with a charge density  $\gamma$  as illustrated in Figure 1 [electrode arrangement of the Penning's vacuum gauge]. Rotating the Figure around the  $z$  axis the electrode arrangement above described is obtained. In the case *a*) two rings of radius  $R_1$  placed in heights  $z_1$  and  $l-z_1$  have been applied with the charge density  $\gamma_A = \gamma_B$ . Case *b*) — where in the middle plane of the cylinder one ring is present with a charge density  $\gamma_A$  — is, as can be seen, a special case of *a*). Case *c*) is a combination of cases *a*) and *b*) where a ring having a charge density  $\gamma_C$  is placed in the middle plane while in the planes in heights  $z_1$  and  $l-z_1$  there are rings bearing charge densities  $\gamma_A = \gamma_B$ .

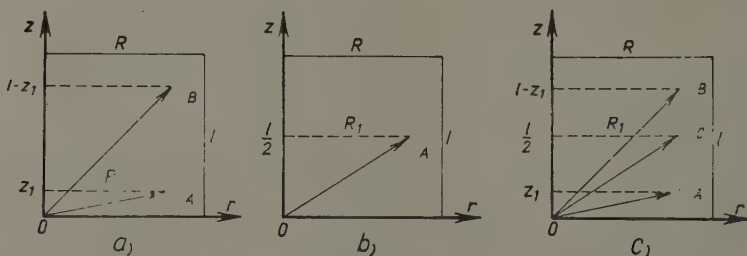


Fig. 1. Scheme of the electrode arrangement of the Penning type vacuum gauge

It can be immediately seen that in all the three cases the charge densities occurring in the Poisson equation can be expressed by one, two resp. three  $\delta$ -functions and the charge density  $\gamma$ . The part depending on  $r$  of the solution of equation (3a) satisfying the boundary conditions will be also now the system of Bessel functions of order zero,  $J_0\left(\frac{k_i}{R}r\right)$ , whereas the part depending on  $z$  is produced by the set of function  $\sin\left(n\frac{\pi}{l}z\right)$ .

Taking into consideration the symmetry of the arrangement the following expressions are obtained for the potential distribution:

$$\left. \begin{aligned}
 a) \quad \Phi &= \sum_{i,n} \frac{32 \pi \gamma_A}{l R^2 J_0'^2(k_i)} \frac{\sin\left(n \frac{\pi}{l} z_1\right) \sin\left(n \frac{\pi}{l} z\right) J_0\left(\frac{k_i}{R} R_1\right) J_0\left(\frac{k_i}{R} r\right)}{\frac{k_i^2}{R^2} + n^2 \frac{\pi^2}{l^2}}, \\
 b) \quad \Phi &= \sum_{i,n} \frac{16 \pi \gamma_A}{l R^2 J_0'^2(k_i)} \frac{\sin\left(n \frac{\pi}{2}\right) \sin\left(n \frac{\pi}{l} z\right) J_0\left(\frac{k_i}{R} R_1\right) J_0\left(\frac{k_i}{R} r\right)}{\frac{k_i^2}{R} + n^2 \frac{\pi^2}{l^2}}, \\
 c) \quad \Phi &= \sum_{i,n} \frac{16 \pi \gamma_A}{l R^2 J_0'^2(k_i)} \frac{\sin\left(n \frac{\pi}{l} z\right) J_0\left(\frac{k_i}{R} R_1\right) J_0\left(\frac{k_i}{R} r\right)}{\frac{k_i}{R^2} + n^2 \frac{\pi^2}{l^2}} \left[ \frac{\gamma_c}{\gamma_A} \sin\left(n \frac{\pi}{2}\right) + \right. \\
 &\quad \left. + 2 \sin\left(n \frac{\pi}{l} z_1\right) \right].
 \end{aligned} \right\} (9)$$

( $n$  is odd in all three cases).

It should be mentioned, although this is not essential for the method, but is of considerable importance from the point of view of the numerical calculations, that in the double sum the summation over  $n$  can be easily carried out. The formulae (9) can be thus brought to the following form:

$$\left. \begin{aligned}
 a) \quad \Phi &= \frac{8 \pi \gamma_A}{R} \sum_i \frac{J_0\left(\frac{k_i}{R} R_1\right) J_0\left(\frac{k_i}{R} r\right)}{k_i J_0'^2(k_i) \operatorname{ch}\left(\frac{k_i l}{2 R}\right)} \left[ \operatorname{sh}\left(\frac{k_i}{R} z\right) \operatorname{ch}\left[\frac{k_i}{R}\left(z_1 - \frac{l}{2}\right)\right], \text{ if } z_1 > z > 0, \right. \\
 &\quad \left. \operatorname{sh}\left(\frac{k_i}{R} z_1\right) \operatorname{ch}\left[\frac{k_i}{R}\left(z - \frac{l}{2}\right)\right], \text{ if } l - z_1 \geq z \geq z_1, \right. \\
 b) \quad \Phi &= \frac{4 \pi \gamma_A}{R} \sum_i \frac{J_0\left(\frac{k_i}{R} R_1\right) J_0\left(\frac{k_i}{R} r\right)}{k_i J_0'^2(k_i) \operatorname{ch}\left(\frac{k_i l}{2 R}\right)} \left[ \operatorname{sh}\left(\frac{k_i}{R} z\right), \text{ if } \frac{l}{2} > z, \right. \\
 &\quad \left. \operatorname{sh}\left[\frac{k_i}{R}(l - z)\right], \text{ if } \frac{l}{2} < z, \right. \\
 c) \quad \Phi &= \frac{4 \pi \gamma_A}{R} \sum_i \frac{J_0\left(\frac{k_i}{R} R_1\right) J_0\left(\frac{k_i}{R} r\right)}{k_i J_0'^2(k_i) \operatorname{ch}\left(\frac{k_i l}{2 R}\right)} \times \\
 &\quad \left\{ \frac{\gamma_c}{\gamma_A} \operatorname{sh}\left(\frac{k_i}{R} z\right) + 2 \operatorname{sh}\left(\frac{k_i}{R} z\right) \operatorname{ch}\left[\frac{k_i}{R}\left(z_1 - \frac{l}{2}\right)\right], \text{ if } z_1 > z > 0, \right. \\
 &\quad \left. \frac{\gamma_c}{\gamma_A} \operatorname{sh}\left[\frac{k_i}{R}(l - z)\right] + 2 \operatorname{sh}\left(\frac{k_i}{R} z_1\right) \operatorname{ch}\left[\frac{k_i}{R}\left(z - \frac{l}{2}\right)\right], \text{ if } l - z_1 \geq z \geq \frac{l}{2} \right\}.
 \end{aligned} \right\} (9a)$$

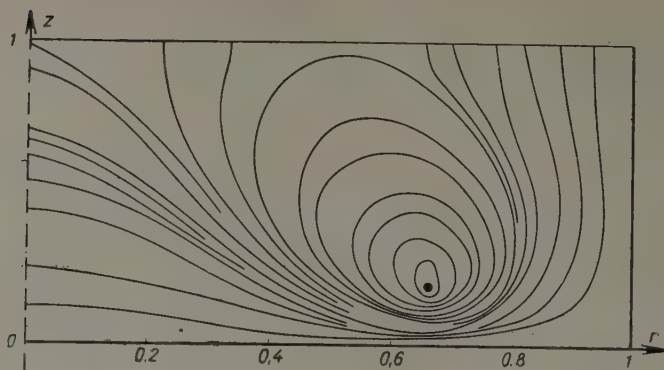


Fig. 2. Relative potential distribution obtained with the method in case of the electrode arrangement of Figure 1a. Along the  $r$  axis measurements are given in  $R$  units, whereas along the  $z$  axis in  $l_2$  units. The equipotential lines correspond (starting from the cylinder with the value 0% towards the thread corresponding to 100%) to the following relative potential values: 2.5%; 5%; 7.5%; 8.75%; 9.37%; 9.66%; 10%; 11.25%; 11.40%; 12.5%; 13.75%; 15%; 17.5%; 20%; 25%; 30%; 40%; 60%

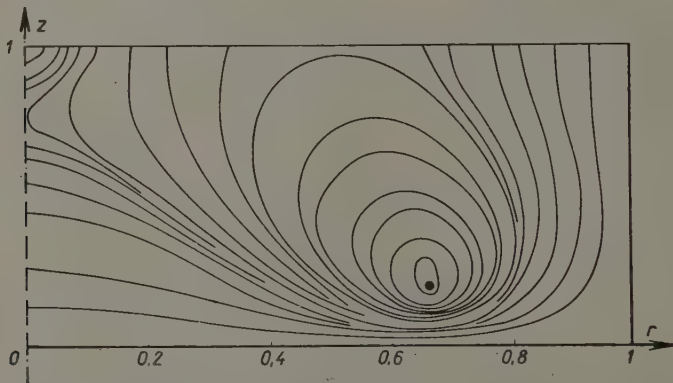


Fig. 3. The relative potential distribution measured in the electrolytic tank in the case of the electrode arrangement of Figure 1a. Denotations as in Figure 2. The relative potential values are: 2.5%; 5%; 7.5%; 8.75%; 9.37%; 9.68%; 9.84%; 10%; 11.25%; 12.05%; 13.75%; 15%; 17.50%; 20%; 25%; 30%; 40%; 60%

The problem of the convergence of the series can be dealt with also here in a way analogous to the case 1 by taking into account the asymptotical expressions for the functions  $shx$  and  $chx$ .

The potential distributions obtained for the case of electrode arrangements dealt with here were compared with the corresponding potential distributions measured in an electrolytic tank.\* Measurements were carried

\* We are indebted to Mr. E. KOLTAY pre "candidate" fellow for carrying out the measurements.



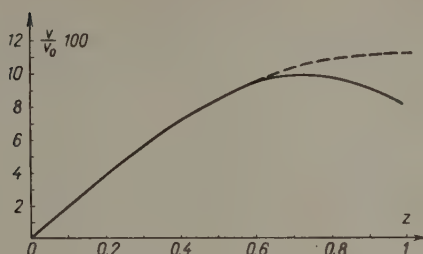


Fig. 4. The dependence of the relative value of the potential on  $z$  in case of  $r = 0$ . The full drawn line corresponds to the potential values obtained experimentally and the dotted to that obtained by the method

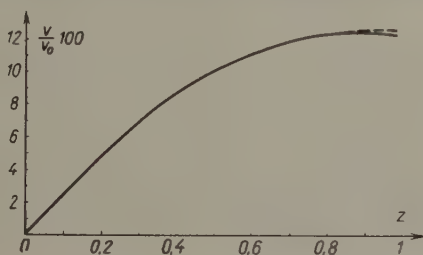


Fig. 5. The dependence of the relative value of the potential on  $z$ , in case of  $r = 0.22$ . Denotations as in Figure 4

out in the so-called tank with tilted bottom. By this modelling procedure the rotational symmetry of the electrode system is used for a simpler realization of the problem. Its drawback is, however, that due to the capillar phenomena appearing in the tank the accuracy of the method strongly decreases near the symmetry axis [6]. The potential distributions obtained by calculation and measurement are presented for case *a*) in Figures 2 and 3. Disregarding the surroundings of the  $z$  axis, agreement of the calculated and measured potential distributions within the limit of errors is found. The explanation of the differences observable near the axis may be found in what has been said above about the measuring accuracy. In Figures 4 resp. 5 so as to illustrate the agreement found the dependence of the relative potential value  $\frac{V}{V_0} \cdot 100$

on the  $z$  coordinate has been plotted for the values  $r = 0$  resp.  $r = 0.22$  ( $V_0$  is the potential of the circle). Along the  $r$  axis of the Figures values are given in units  $R$  along the  $z$  axis in units  $l/2$ , corresponding to the denotations of Figure 1. The experimental curve shown by the full line tends when further away from the axis towards the theoretical curve shown by the dotted line. For small values of  $z$  the agreement is good also for small values of  $r$ .

3. Now we determine the potential field of the electrooptical two-cylinder lens so important in practical physics. The electrode arrangement

is the following: Two cylindrical electrodes of radius  $R_1$  and length  $z_0 - \frac{d}{2}$  are placed along the  $z$  axis at a distance  $d$  from each other as illustrated in Figure 6. They are surrounded by an earthed metal cylinder of radius  $R$ . The cylinders are charged so that their surface charge densities are  $\sigma_1$  resp.

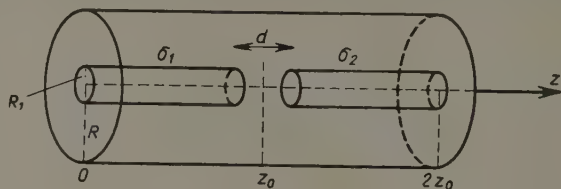


Fig. 6. The scheme of an electrode arrangement of the type of an electrooptical two-cylinder lens

$\sigma_2$ . The solution of equation (3a) satisfying the boundary conditions is now the complete set of functions

$$\left. \begin{aligned} \Phi_{i0} &= \frac{1}{R J_0'(k_i) \sqrt{z_0}} J_0 \left( \frac{k_i}{R} r \right) \\ \Phi_{in}^s &= \sqrt{2} \Phi_{i0}(r) \sin \left( n \frac{\pi}{2 z_0} z \right) \\ \Phi_{in}^c &= \sqrt{2} \Phi_{i0}(r) \cos \left( n \frac{\pi}{2 z_0} z \right) \end{aligned} \right\} . \quad (10)$$

Hereby the sum of the potentials of rings of surface charge densities  $\sigma_1$  and  $\sigma_2$  becomes

$$\begin{aligned} \varphi = & \sum_i \left\{ \frac{4\pi}{z_0 k_i^2 J_0'^2(k_i)} (\sigma_1 + \sigma_2) \left( z_0 - \frac{d}{2} \right) J_0 \left( \frac{k_i}{R} R_1 \right) J_0 \left( \frac{k_i}{R} r \right) + \right. \\ & + \sum_{n=1}^{\infty} \frac{16}{R^2 J_0'^2(k_i) n} \frac{J_0 \left( \frac{k_i}{R} R_1 \right) J_0 \left( \frac{k_i}{R} r \right)}{\frac{k_i^2}{R^2} + \left( n \frac{\pi}{2 z_0} \right)^2} \left[ \cos \left( n \frac{\pi}{2 z_0} z \right) \left[ \sigma_1 \sin n \frac{\pi}{2 z_0} \left( z_0 - \frac{d}{2} \right) - \right. \right. \\ & - \sigma_2 \sin n \frac{\pi}{2 z_0} \left( z_0 + \frac{d}{2} \right) \right] - \sin \left( n \frac{\pi}{2 z_0} z \right) \left[ \sigma_1 \left( \cos n \frac{\pi}{2 z_0} \left( z_0 - \frac{d}{2} \right) - 1 \right) + \right. \\ & \left. \left. + \sigma_2 \left( (-1)^n - \cos n \frac{\pi}{2 z_0} \left( z_0 + \frac{d}{2} \right) \right) \right] \right] \right\} . \quad (11) \end{aligned}$$

The summation over  $n$  can be carried out. We consider the effect of the whole cylinder surface by integrating over the correspondig values of the  $z$  coordinate and we obtain the formula

$$\Phi = \sum_i \frac{8\pi R z_0}{k_i} \frac{\Phi_{i0}(r) \Phi_{i0}(R_1)}{\frac{2 k_i z_0}{\text{sh} \frac{2 k_i z_0}{R}}} \left\{ \sigma_1 \int_0^{z_0 - \frac{d}{2}} \text{ch} \frac{k_i}{R} (2z_0 - |z - z_1|) dz_1 + \right. \\ \left. + \sigma_2 \int_{z_0 + \frac{d}{2}}^{2z_0} \text{ch} \frac{k_i}{R} (2z_0 - |z - z'_1|) dz'_1 \right\}, \quad \text{if } 0 < |z \pm z_1| < 4z_0 \quad (11a)$$

or in integrated form

$$\Phi = 8\pi R^2 z_0 \sum_i \frac{\Phi_{i0}(r) \Phi_{i0}(R_1)}{k_i^2 \text{sh} \frac{2 k_i z_0}{R}} \left\{ \sigma_1 \left[ 2 \text{sh} \left( \frac{k_i}{R} 2z_0 \right) - \text{sh} \frac{k_i}{R} (2z_0 - z) - \text{sh} \frac{k_i}{R} \left( z + z_0 + \frac{d}{2} \right) \right] + \sigma_2 \left[ \text{sh} \frac{k_i}{R} \left( z + z_0 - \frac{d}{2} \right) - \right. \right. \\ \left. \left. - \text{sh} \left( \frac{k_i}{R} z \right) \right], \quad \text{if } 0 < z < z_0 - \frac{d}{2}, \right. \\ \sigma_1 \left[ \text{sh} \frac{k_i}{R} \left( 3z_0 - z - \frac{d}{2} \right) - \text{sh} \frac{k_i}{R} (2z_0 - z) \right] + \\ \left. + \sigma_2 \left[ \text{sh} \frac{k_i}{R} \left( z + z_0 - \frac{d}{2} \right) - \text{sh} \left( \frac{k_i}{R} z \right) \right], \right. \\ \left. \text{if } z_0 - \frac{d}{2} < z < z_0 + \frac{d}{2}, \right. \quad (11b) \\ \sigma_1 \left[ \text{sh} \frac{k_i}{R} \left( 3z_0 - z - \frac{d}{2} \right) - \text{sh} \frac{k_i}{R} (2z_0 - z) \right] + \\ \left. + \sigma_2 \left[ 2 \text{sh} \left( \frac{k_i}{R} 2z_0 \right) - \text{sh} \frac{k_i}{R} \left( 3z_0 - z + \frac{d}{2} \right) - \right. \right. \\ \left. \left. - \text{sh} \left( \frac{k_i}{R} z \right) \right], \quad \text{if } z_0 + \frac{d}{2} < z < 2z_0. \right\}$$

The potential of an infinitely long cylinder capacitor dealt with in 1. is evidently contained in (11b) when  $z_0 \rightarrow \infty$ . As can easily be seen

$$\lim_{z_0 \rightarrow \infty} \Phi(r, z)_{z=0} = 8\pi k^2 z_0 \sum_i \frac{\Phi_{i0}(r) \Phi_{i0}(R_1)}{k_i^2} \sigma_1, \quad \text{if } \frac{\sigma_1}{\sigma_2} \neq 0,$$

resp.

$$\lim_{z_0 \rightarrow -\infty} \Phi(r, z)_{z=2z_0} = 8\pi R^2 z_0 \sum_i \frac{\Phi_{i0}(r) \Phi_{i0}(R_1)}{k_i^2} \sigma_{2i} \quad \text{if} \quad \frac{\sigma_2}{\sigma_1} \neq 0.$$

From the formula (11b) the potential distribution of the two-cylinder lens used in electron optics is obtained for the case  $R \gg R_1$ .

The result thus obtained is of interest as — in contrast to any other method applied to the calculation of the field of the electrooptical two-cylinder lens — no stipulation was made during the calculation concerning the width  $d$  of the slit. Other methods used for the solution of the problem fail if the width of the slit is of the order of magnitude of the tube diameter.

For the first two cases mentioned as examples in III the formula is exact, whereas in the case of the electrooptical two-cylinder lens it has to be considered as approximative, since for the calculation we started from the assumption that the charge distribution is uniform on the cylinder surfaces. The accuracy of the approximation can be estimated from the equipotential surface running near the cylinder surface.

#### REFERENCES

1. W. R. SMYTHE, Static and Dynamic Electricity, McGraw Hill Book Company, Inc. New York, 1939.
2. Д. Иваненко и А. Соколов, Классическая Теория Поля; Государственное издательство технико-теоретической литературы, Москва, 1951.
3. P. H. M. MORSE and H. FESHBACH, Methods of Theoretical Physics, McGraw Hill Book Company, Inc. London, 1953.
4. See for instance E. JAHNKE-F. EMDE, Tables of Functions, page 203, Teubner Vlg. Leipzig, 1933.
5. See for instance E. MADELUNG, Die mathematischen Hilfsmittel des Physikers, page 56, Springer, Berlin, 1950.
6. V. E. COSSLETT, Introduction to Electron Optics, Section II. § 4; Clarendon Press, Oxford, 1946.

#### ОПРЕДЕЛЕНИЕ ЭЛЕКТРОСТАТИЧЕСКИХ ПОТЕНЦИАЛОВ С ПОМОЩЬЮ РЯДОВ

Р. ГАШПАР, В. КОЛТАЙ-ДЯРМАТИ и И. ТАМАШИ-ЛЕНТЕИ

#### Резюме

Мы реформулировали метод рядов для решения уравнения Пуассона, пользуясь решениями задач по собственным значениям, часто встречающихся в разных областях теоретической физики. Если распределение заряда соответствует  $\delta$ -функции Дирака, то решение получается в форме одного, довольно хорошо сходящегося ряда. В простых случаях наши решения аналитически трансформируемы в хорошо известные решения (напр. в случае III/1). В других случаях (III/2) вычисленное распределение потенциала совпадает с полученным из измерений в электролитическом ванне. В случае электрооптической цилиндрической линзы, (III/3) наш метод дает распределение потенциала для какой-либо ширины щели и соответствующую форму электродов.

# EINIGE ZWEIZENTRENINTEGRALE ZU RECHNUNGEN AUF GRUND DER METHODE DER KORRELATIONSMÄSSIGEN MOLEKÜLBAHN

Von

F. BERENCZ

INSTITUT FÜR THEORETISCHE PHYSIK DER UNIVERSITÄT, SZEGED

(Vorgelegt von A. Kónya. — Eingegangen 8. IV. 1958)

Die numerischen Werte der Integrale

$$I_{iklm}^n = \int \psi_1^2 (\psi_2 + \psi_3 + \psi_4 + \psi_5)^2 \mu_1^i \mu_2^k \nu_1^l \nu_2^m r_{12}^n d\tau,$$

$$J_{iklm}^n = \int \psi_1^2 (\psi_2 + \psi_3 + \psi_4 + \psi_5) (\psi_2 \pm \psi_3 - \psi_4 \mp \psi_5) \mu_1^i \mu_2^k \nu_1^l \nu_2^m r_{12}^n d\tau,$$

wo

$$\psi_1 = \exp[-\alpha(\mu_1 + \mu_2)], \quad \psi_2 = \exp[\beta(\nu_1 + \nu_2)], \quad \psi_3 = \exp[\beta(\nu_1 - \nu_2)],$$

$$\psi_4 = \exp[-\beta(\nu_1 + \nu_2)], \quad \psi_5 = \exp[-\beta(\nu_1 - \nu_2)]$$

und wo  $i, k, l, m, n = 0, 1, 2$  sein kann, wurden in Tafeln zusammengestellt.

In einer früheren Arbeit [1] wurde die Dissoziationsenergie des  $H_2$ -Moleküls mit einer solchen Näherungsfunktion berechnet, welche den folgenden Korrelationsfaktor enthält:

$$\Psi = N\psi_1(\psi_2 + \psi_3 + \psi_4 + \psi_5)(1 + p r_{12}),$$

wo

$$\psi_1 = \exp[-\alpha(\mu_1 + \mu_2)],$$

$$\psi_2 = \exp[\beta(\nu_1 + \nu_2)],$$

$$\psi_3 = \exp[\beta(\nu_1 - \nu_2)],$$

$$\psi_4 = \exp[-\beta(\nu_1 + \nu_2)],$$

$$\psi_5 = \exp[-\beta(\nu_1 - \nu_2)].$$

Unter den Integralen in dem Energieausdruck, der zum Minimum gemacht werden soll, sind diejenigen in der Literatur noch nicht vorgekommen, in welchen der Integrand die gegenseitige Entfernung  $r_{12}$  der beiden Elektronen in einer gewissen Potenz enthält. Diese Zweizentrenintegrale können in die folgenden zwei Gruppen eingeteilt werden:

$$I_{iklm}^n = \int \psi_1^2 (\psi_2 + \psi_3 + \psi_4 + \psi_5)^2 \mu_1^i \mu_2^k \nu_1^l \nu_2^m r_{12}^n d\tau,$$

$$J_{iklm}^n = \int \psi_1^2 (\psi_2 + \psi_3 + \psi_4 + \psi_5) (\psi_2 \pm \psi_3 - \psi_4 \mp \psi_5) \mu_1^i \mu_2^k \nu_1^l \nu_2^m r_{12}^n d\tau,$$

wo  $i, k, l, m, n = 0, 1, 2$  sein kann.

Bei der Berechnung der Integrale wird die Methode von KOTANI und seinen Mitarbeitern [2] benutzt, die schon bei SUGIURA [3] zu finden ist. Der Integrand wird in elliptischen Koordinaten hergeleitet und die gegenseitige Entfernung der beiden Elektronen durch den Kosinussatz

$$r_{12}^2 = \frac{R^2}{4} [\mu_1^2 + \mu_2^2 + \nu_1^2 + \nu_2^2 - 2\mu_1\mu_2\nu_1\nu_2 - 2 - 2\sqrt{(\mu_1^2 - 1)(\mu_2^2 - 1)(1 - \nu_1^2)(1 - \nu_2^2)} \cos(\varphi_1 - \varphi_2)],$$

sowie durch die Neumannsche Reihenentwicklung [4]

$$\frac{1}{r_{12}} = \frac{2}{R} \sum_{\tau=0}^{\infty} \sum_{\nu=0}^{\tau} D_{\tau\nu} Q_{\tau}^{\nu}(\mu_1) P_{\tau}^{\nu}(\mu_2) P_{\tau}^{\nu}(\nu_1) P_{\tau}^{\nu}(\nu_2) \cos(\varphi_1 - \varphi_2)$$

berücksichtigt, wo

$$D_{\tau 0} = 2\tau + 1 \quad \text{und} \quad D_{\tau\nu} = (-1)^{\nu} 2(2\tau + 1) \left[ \frac{(\tau - \nu)!}{(\tau + \nu)!} \right]^2, \nu = 1.$$

$\mu_+$  und  $\mu_-$  bezeichnen den grösseren, bzw. den kleineren Wert von  $\mu_1$  und  $\mu_2$ .  $P_{\tau}^{\nu}$  und  $Q_{\tau}^{\nu}$  bedeuten Legendresche Polynome erster und zweiter Art. Die unendliche Neumannsche Reihenentwicklung macht bei der Berechnung der Integrale keine besondere Schwierigkeit, weil die Integranden die  $\varphi_i$  entweder nicht enthalten oder nur im Ausdruck  $\sin \varphi_i$  und  $\cos \varphi_i$ . In diesem Falle kann in der zweiten Summe nur  $\nu = 0$  oder  $\nu = 1$  sein. Mit dem oben angegebenen Ausdruck für  $r_{12}^2$  bekommt man ein Polynom von sechs Integrationsvariablen ( $\mu_1, \nu_1, \varphi_1; \mu_2, \nu_2, \varphi_2$ ), und die Integration wird in gewöhnlicher Weise sukzessive durchführbar.

Bei der Durchführung der Integrationen werden die folgenden grundlegenden Integrale verwendet:

$$A_n(\alpha) = \int_1^{\infty} e^{-\alpha\mu} \mu^n d\mu,$$

$$B_n(\beta) = \int_{-1}^1 e^{-\beta\nu} \nu^n d\nu,$$

$$G_{\tau}^{\nu}(l, \beta) = \int_1^1 P_{\tau}^{\nu}(\nu_l) e^{-\beta\nu_l} \nu_l^l (1 - \nu_l^2)^{\frac{\tau}{2}} d\nu_l$$

$$W_{\tau}^{\nu}(i, k, \alpha) = \int_1^{\infty} \int_1^{\infty} Q_{\tau}^{\nu}(\mu_1) P_{\tau}^{\nu}(\mu_2) e^{-\alpha(\mu_1 + \mu_2)} \mu_1^i \mu_2^k (\mu_1^2 - 1)^{\frac{\tau}{2}} (\mu_2^2 - 1)^{\frac{\tau}{2}} d\mu_1 d\mu_2.$$

Die numerischen Werte der obigen Grundintegrale wurden von KOTANI, AMEMIYA und SIMOSE in Tafeln zusammengestellt.

Die analytischen Ausdrücke der Integrale sind in der Arbeit [1] zu finden; hier folgen die numerischen Werte in Tafeln zusammengestellt.



$\beta$	$\alpha$	0,5	0,75	1,00	1,25	1,5	1,75	2,00	2,25	2,5
0,5		2,39304057	0,30823904	0,05511129	0,01168467	0,00276572	0,00070447	0,00019303	0,00005288	0,00001959
0,75		3,18422573	0,41059112	0,07333562	0,01559278	0,00369351	0,00094141	0,00025848	0,00007074	0,00002680
1,00		4,70366564	0,60730466	0,10859710	0,02311376	0,00547995	0,00139786	0,00038483	0,00010518	0,00004100
1,25		7,63934825	0,98771031	0,17684263	0,03768065	0,00894225	0,00228300	0,00063013	0,00017203	0,00006931
1,5		13,4842656	1,74581554	0,31297209	0,06676078	0,01585908	0,00405245	0,00112229	0,00030500	0,00012758
1,75		25,5446579	3,31159367	0,59439882	0,12693079	0,03018177	0,00771899	0,00214249	0,00058338	0,00025182
2,00		51,2943948	6,65778013	1,19640815	0,25575495	0,05775968	0,01558099	0,00433588	0,00117930	0,00052543
2,25		108,307647	14,0248981	2,52309262	0,53990286	0,16038371	0,03294927	0,00919078	0,00249754	0,00114458
2,5		235,656654	30,6518001	5,52014883	1,18237508	0,28192066	0,07228192	0,02020503	0,00548699	0,00332177

$\beta$	$\alpha$	0,5	0,75	1,00	1,25	1,5	1,75	2,00	2,25	2,5
0,5	0,84999163	0,11684993	0,01972636	0,00420741	0,00099934	0,00009934	0,00025532	0,00007074	0,00001926	0,00000811
0,75	1,21434464	0,15733844	0,02822344	0,00602348	0,00143148	0,00036591	0,00010154	0,00002763	0,00001204	0,00000511
1,00	1,95682990	0,25376982	0,04556054	0,00973103	0,00231417	0,00059190	0,00016455	0,00004474	0,00001991	0,00000862
1,25	3,48982078	0,45301130	0,08140844	0,01740239	0,00414169	0,00106007	0,00029529	0,00008022	0,00003652	0,00001623
1,5	6,75295881	0,87744174	0,15783592	0,03377018	0,00804370	0,00206032	0,00057504	0,00015612	0,00007263	0,00003362
1,75	13,9207990	1,81047475	0,32599373	0,06981220	0,01664243	0,00426610	0,00119289	0,00032371	0,00015362	0,00007562
2,00	30,10118303	3,91829523	0,70621735	0,15137521	0,03611661	0,00926537	0,00259527	0,00070406	0,00034004	0,00018303
2,25	67,4431405	9,84509920	1,58517176	0,34008226	0,08120880	0,02084988	0,00584943	0,00158665	0,00077809	0,00040004
2,5	155,141590	20,2282808	3,65280583	0,78437090	0,18745900	0,04816732	0,01353309	0,00367087	0,00182396	0,00092396

$$\frac{8}{R^2} I_{0200}^1$$

$\beta$	$\alpha$	0,5	0,75	1,00	1,25	1,5	1,75	2,00	2,25	2,5
0,5	46,3971917	3,49460895	0,45311156	0,07792728	0,01588165	0,00287850	0,00087247	0,00023287	0,00006351	
0,75	57,4845804	4,33577386	0,56299858	0,09696264	0,01978716	0,00352997	0,00109078	0,00029111	0,00007943	
1,00	77,8402041	5,88136001	0,76508501	0,13199876	0,02698115	0,00471192	0,00149377	0,00039859	0,00010875	
1,25	115,168853	8,71838445	1,13640573	0,19643866	0,04022465	0,00684659	0,00223754	0,00059690	0,00016269	
1,5	185,529168	14,0712982	1,83887986	0,31828398	0,06739077	0,01137915	0,00364913	0,00097314	0,00026468	
1,75	323,154226	24,5521015	3,21252855	0,55736545	0,11452205	0,01840628	0,00642940	0,00171394	0,00046471	
2,00	602,798336	45,8688091	6,01155719	1,04464341	0,23290881	0,03015848	0,01211691	0,00322895	0,00087209	
2,25	1191,31790	90,7709848	11,9134115	1,64738847	0,42714239	0,06498749	0,02416362	0,00643721	0,00173127	
2,5	2468,20384	188,275531	24,7413056	4,31059637	0,88917770	0,13212065	0,05046056	0,01343970	0,00359934	

$$\frac{8}{R^2} I_{0220}^1$$

$\beta$	$\alpha$	0,5	0,75	1,00	1,25	1,5	1,75	2,00	2,25	2,5
0,5	16,6051699	1,31835643	0,16449170	0,02848658	0,00584342	0,00097977	0,00031976	0,00008651	0,00002382	0,000003179
0,75	22,0763646	1,76243736	0,21907374	0,03797187	0,00779536	0,00128817	0,00043441	0,00011555	0,00004711	0,000007670
1,00	32,5777190	2,61975010	0,32396581	0,05621136	0,01155097	0,00187308	0,00064527	0,00017148	0,000027986	0,000013565
1,25	52,8536673	4,28658296	0,52678120	0,09150449	0,01882302	0,00298641	0,00105482	0,00049635	0,00025726	0,00013565
1,5	93,1929382	7,62793604	0,93091108	0,16188615	0,03333596	0,00516760	0,00187228	0,00094463	0,00051730	0,00025726
1,75	176,362883	12,8819380	1,76546040	0,30734977	0,06335498	0,00959654	0,00356767	0,00190520	0,00108967	0,00051730
2,00	353,788949	25,7490399	3,54864085	0,61842551	0,12760334	0,01891124	0,00720381	0,00402594	0,00238202	0,00108967
2,25	743,730933	53,9475430	7,48865156	1,30375259	0,26926422	0,03912646	0,01523766	0,00882618	0,00238202	0,00108967
2,5	1622,26155	123,996957	16,3307705	2,85145101	0,58944434	0,08418563	0,03343257	0,00882618	0,00238202	0,00108967

$\frac{\alpha}{\beta}$		$\frac{8}{R\pi^2} I_{1002}^1$								
		0,5	0,75	1,00	1,25	1,5	1,75	2,00	2,25	2,5
0,5		2,81994848	0,56978466	0,08916347	0,01738075	0,00387206	0,00094294	0,00024601	0,00006644	0,00001876
0,75		3,75189134	0,75856401	0,11881875	0,02318164	0,00516839	0,00125950	0,00032871	0,00008884	0,00002510
1,00		5,54004034	1,12123889	0,17581126	0,03434087	0,00766357	0,00186913	0,00048801	0,00013201	0,00003732
1,25		8,99095269	1,82224724	0,28611934	0,05594439	0,01249734	0,00305084	0,00079690	0,00021576	0,00006105
1,5		15,8528582	3,21854843	0,50599481	0,09904964	0,02214934	0,00541205	0,00141429	0,00038327	0,00010854
1,75		29,9930545	6,10089195	0,96029939	0,18819048	0,04212528	0,01030239	0,00269347	0,00073058	0,00020708
2,00		60,1456543	12,2573157	1,93156479	0,37893398	0,08490457	0,02078308	0,00543609	0,00147577	0,00041868
2,25		126,397557	25,8042430	4,07077757	0,79941757	0,17928680	0,04392393	0,01149453	0,00312315	0,00088681
2,5		275,653715	56,3620842	8,90062272	1,74960531	0,39271348	0,09630035	0,02521410	0,00685654	0,00194856

$\frac{\alpha}{\beta}$		$\frac{8}{R\pi^2} I_{1200}$									
		0,5	0,75	1,00	1,25	1,5	1,75	2,00	2,25	2,5	
0,5		101,159628	6,25288542	0,72103494	0,11466593	0,02209370	0,00482678	0,00115111	0,00029270	0,00007814	
0,75		125,294232	7,75462839	0,89543705	0,14259598	0,02751094	0,00601761	0,00144092	0,00036570	0,00009772	
1,00		169,585835	10,5128334	1,21603882	0,19398297	0,03610437	0,00821188	0,00196334	0,00050039	0,00013387	
1,25		250,767453	15,5791854	1,80483429	0,28845074	0,05584031	0,01225290	0,00293392	0,00074880	0,00020058	
1,5		403,698960	25,1158083	2,91638230	0,47065631	0,09056208	0,01990441	0,00477321	0,00121989	0,00032718	
1,75		702,652139	43,7892468	5,09391904	0,81710065	0,15872471	0,03493909	0,00839034	0,00214705	0,00057651	
2,00		1309,74868	81,7477628	9,52506354	1,53032034	0,29771407	0,06562406	0,01470598	0,00404237	0,00108656	
2,25		2586,68587	161,663758	18,8636386	3,03492502	0,59120335	0,13047546	0,03140696	0,00805434	0,00216697	
2,5		5355,86898	335,120878	39,1521976	6,30685187	1,23000528	0,27174950	0,06547861	0,01680749	0,00452579	

$\frac{\alpha}{\beta}$		0,5	0,75	1,00	1,25	1,5	1,75	2,00	2,25	2,5
		$\frac{8}{R^{12}} I_{2200}^1$								
0,5		284,669273	13,3237669	1,30177440	0,18554631	0,03309095	0,00682751	0,00155842	0,00038281	0,00009939
0,75		352,471729	16,5156220	1,61568147	0,23059010	0,04117684	0,00850617	0,00194380	0,00047799	0,00012422
1,00		476,860332	22,3757511	2,19248420	0,31342693	0,05605883	0,01159801	0,00265408	0,00065350	0,00017004
1,25		704,755740	33,1218859	3,25125190	0,46563030	0,08342844	0,01728918	0,00396256	0,00097707	0,00025457
1,5		1133,86801	53,3758035	5,24889973	0,75310695	0,13517533	0,02805937	0,00644088	0,00159041	0,00041490
1,75		1972,52280	92,9894971	9,16006336	1,31655664	0,23670198	0,04921039	0,01131219	0,00279693	0,00073653
2,00		3674,09546	173,467543	17,1145784	2,46369328	0,44360767	0,09235510	0,02125742	0,00526211	0,00137590
2,25		7252,04052	342,821939	33,8698273	4,88238957	0,88027591	0,18349223	0,04228283	0,01047781	0,00274232
2,5		15008,1282	710,241182	70,2540011	10,1394825	1,83024005	0,38192926	0,08809926	0,02185189	0,00572421

$\frac{\alpha}{\beta}$		0,5	0,75	1,00	1,25	1,5	1,75	2,00	2,25	2,5
		$\frac{1}{4R^{12}} I_{0002}^2$								
0,5		8,16370764	0,80578392	0,12227174	0,02327899	0,00509117	0,00122168	0,00031317	0,00008433	0,00002358
0,75		10,9067899	1,08001059	0,16436762	0,03137528	0,00687755	0,00165365	0,00042465	0,00011452	0,00003207
1,00		16,1988451	1,61052161	0,24600625	0,04711040	0,01035578	0,00249607	0,00064235	0,00017356	0,00004869
1,25		26,4789037	2,64437801	0,40555747	0,07793819	0,01718459	0,00415298	0,00107121	0,00029002	0,00008150
1,5		47,0644795	4,72165647	0,72709363	0,14022303	0,03101171	0,00751419	0,00194259	0,00052698	0,00014835
1,75		89,7813942	9,04649396	1,39847081	0,27059821	0,06001568	0,01457735	0,00377649	0,00102634	0,00028940
2,00		181,461280	18,3572549	2,84774811	0,55267793	0,12288990	0,02991383	0,00776411	0,00211346	0,00059677
2,25		384,050393	38,9890417	6,06697957	1,18053131	0,26307581	0,06415813	0,01667894	0,00454645	0,00128532
2,5		842,652719	85,8085038	13,3878832	2,61089557	0,59292375	0,14238866	0,03706664	0,01011570	0,00286269

$$\frac{1}{4R^{2\pi^2}} I_{0022}^2$$

$\beta$	$\alpha$	0,5	0,75	1,00	1,25	1,5	1,75	2,00	2,25	2,5
0,5		2,98464540	0,3006012	0,04629309	0,00894221	0,00198039	0,00048042	0,00012433	0,00003376	0,00000951
0,75		4,28004215	0,43133153	0,06668765	0,01290533	0,00286255	0,00069535	0,00018016	0,00004896	0,00001381
1,00		6,92779931	0,70015630	0,10852182	0,02104606	0,00467677	0,00113782	0,00029519	0,00008032	0,00002267
1,25		12,4124938	1,25878656	0,19552066	0,03800178	0,00846039	0,00206162	0,00053558	0,00014590	0,00004123
1,5		24,1246602	2,45235501	0,38203814	0,07440961	0,01659526	0,00404998	0,00105347	0,00028731	0,00008126
1,75		49,9265470	5,08843868	0,79448757	0,15503685	0,03463252	0,00846330	0,00220399	0,00060168	0,00017032
2,00		108,316842	11,0650908	1,73110969	0,33837678	0,07569372	0,01851951	0,00482767	0,00131906	0,00037367
2,25		243,354329	24,9104333	3,90399313	0,76422200	0,17116264	0,04192027	0,01093731	0,00299063	0,00084775
2,5		561,027366	57,5306485	9,03001051	1,76990714	0,39682565	0,09727493	0,02539883	0,00694936	0,00197101

$$\frac{1}{4R^{2\pi^2}} I_{0200}^2$$

$\beta$	$\alpha$	0,5	0,75	1,00	1,25	1,5	1,75	2,00	2,25	2,5
0,5		214,008089	11,3405838	1,17219796	0,17202524	0,03119233	0,00650106	0,00149359	0,00036851	0,00009597
0,75		265,621547	14,1195875	1,46449902	0,21567240	0,03923778	0,00820355	0,00189019	0,00046760	0,00012207
1,00		360,649733	19,2492219	2,00552371	0,29667560	0,05420613	0,01137812	0,00263121	0,00065308	0,00017101
1,25		535,547935	28,7192792	3,00761312	0,44718741	0,08210052	0,01730981	0,00401908	0,00100119	0,00026303
1,5		866,601223	46,7046815	4,91754049	0,73503724	0,13561553	0,02872178	0,00669590	0,00167411	0,00044126
1,75		1517,04578	82,1622128	8,69638860	1,30650816	0,24219142	0,05151225	0,01205487	0,00302420	0,00079951
2,00		2844,60952	154,767653	16,4606586	2,48449602	0,46252444	0,09875160	0,02318820	0,00583467	0,00154663
2,25		5650,28649	308,673036	32,9703405	4,99670400	0,93365882	0,19999913	0,04709902	0,01188147	0,00315657
2,5		11760,8376	644,767242	69,1237382	10,5123263	1,97045957	0,42326559	0,09992020	0,02526016	0,00672346



$$\frac{1}{4R^{2\alpha,2}} I^{220}$$

$\beta$	$\alpha$	0,5	0,75	1,00	1,25	1,5	1,75	2,00	2,25	2,5
0,5		77,2170710	4,15402123	0,43652638	0,06512464	0,01199432	0,00253616	0,00059040	0,00014742	0,00003881
0,75		102,923579	5,55077679	0,58487220	0,08748508	0,01615190	0,00342285	0,00079840	0,00019971	0,00005266
1,00		152,416859	8,24585528	0,87176881	0,13082481	0,02422648	0,00514802	0,00120374	0,00030176	0,00007973
1,25		248,331767	13,4820889	1,43066995	0,21546998	0,04003318	0,00853214	0,00200031	0,00050262	0,00013307
1,5		439,917095	23,9694696	2,55321998	0,38593325	0,07194247	0,01537833	0,00361481	0,00091041	0,00024152
1,75		836,489990	45,7356963	4,88947730	0,74162601	0,13868112	0,02972677	0,00700465	0,00176794	0,00046991
2,00		1685,64719	92,4587768	9,91738358	1,50896860	0,28296911	0,06080679	0,01435948	0,00363119	0,00096676
2,25		3558,11905	195,720782	21,0553246	3,21249060	0,60391178	0,13005555	0,03077067	0,00779405	0,00207805
2,5		7788,92311	429,507656	46,3236442	7,08459870	1,33465189	0,28795789	0,06823964	0,01730893	0,00462054

$$\frac{1}{4P^{2,2}} I^{1002}$$

$\alpha$	0,5	0,75	1,00	1,25	1,5	1,75	2,00	2,25	2,5
0,5	21,7871952	1,65155559	0,21419515	0,03676584	0,00747409	0,00169914	0,00041789	0,00010891	0,00002967
0,75	29,2672633	2,21025912	0,28748158	0,04947614	0,01008189	0,00229684	0,00056795	0,00014774	0,00004031
1,00	43,1110952	3,28971532	0,42942189	0,07414741	0,01515354	0,00346121	0,00085480	0,00022360	0,00006111
1,25	70,3483947	5,39019878	0,70640121	0,12241256	0,02509742	0,00574857	0,00142320	0,00037309	0,00010216
1,5	124,818164	9,60395676	1,26369594	0,21978118	0,04520418	0,01038290	0,00257681	0,00067694	0,00018571
1,75	237,700241	18,3633723	2,42554156	0,42329691	0,08732422	0,02010969	0,00500209	0,00131666	0,00036183
2,00	479,673679	37,1941047	4,92997823	0,86303212	0,17851966	0,04120662	0,01027038	0,00270812	0,00074536
2,25	1013,78085	78,8673770	10,4858518	1,84062260	0,38163048	0,08826741	0,02203812	0,00581981	0,00160390
2,5	2221,65437	173,328186	23,1062803	4,06541559	0,84460868	0,19568605	0,04893000	0,01293788	0,00356952



		$\frac{1}{4R^{2\alpha-2}} I_{1200}^2$									
$\beta$	$\alpha$	0,5	0,75	1,00	1,25	1,5	1,75	2,00	2,25	2,5	
0,5		504,856849	21,6997782	1,97494807	0,26575056	0,04523640	0,00898551	0,00198789	0,00047579	0,00012087	
0,75		625,314645	26,9954831	2,46480135	0,33276787	0,05682886	0,01132319	0,00251232	0,00060293	0,00015354	
1,00		849,847243	36,7641945	3,37072411	0,45702685	0,07837534	0,01567794	0,00349127	0,00084068	0,00021475	
1,25		1261,05723	54,7845201	5,04701289	0,68765645	0,11848236	0,02380551	0,00532274	0,00128646	0,00032972	
1,5		2038,99715	88,9792447	8,23849434	1,12820463	0,19533283	0,03942323	0,00885102	0,00214718	0,00055218	
1,75		3566,64782	156,334576	14,5461173	2,00179027	0,34819544	0,07057559	0,01590651	0,00387222	0,00099892	
2,00		6682,97815	294,142259	27,4928769	3,80051612	0,66386013	0,13507523	0,03054884	0,00745965	0,00192965	
2,25		13658,8037	586,038404	54,9966656	7,63262721	1,33814612	0,27317827	0,06196601	0,01517123	0,00393364	
2,5		27596,7712	1223,04127	115,175279	16,0385874	2,82067147	0,57745062	0,13131206	0,03222016	0,00837038	

		$\frac{1}{4R^{2\alpha-2}} I_{2200}^2$									
$\beta$	$\alpha$	0,5	0,75	1,00	1,25	1,5	1,75	2,00	2,25	2,5	
0,5		1582,31158	50,6691830	3,85126219	0,45881768	0,07156050	0,01331309	0,00279987	0,00064378	0,00015832	
0,75		1961,91808	62,9755319	4,80047264	0,57368116	0,08975677	0,01674937	0,00353278	0,00081451	0,00020081	
1,00		2660,23385	89,6590207	6,55417307	0,78641385	0,12353777	0,02314317	0,00489934	0,00113346	0,00028033	
1,25		3944,14873	127,464652	9,79530395	1,18072602	0,18633079	0,03505985	0,00745258	0,00173069	0,00042953	
1,5		6371,63749	206,713793	15,9581316	1,93285499	0,30647136	0,05792490	0,01236436	0,00288234	0,00071784	
1,75		11135,6040	362,656376	28,1223876	3,42213957	0,54508769	0,10346696	0,02217278	0,00518741	0,00129611	
2,00		20848,1084	681,400251	53,0596749	6,48414344	1,03714838	0,19763141	0,04250191	0,00997527	0,00249955	
2,25		41353,4818	1355,93857	105,975759	13,0003696	2,08690591	0,39900407	0,08607034	0,02025618	0,00508810	
2,5		85971,4948	2826,79739	221,640453	27,2778249	4,39240520	0,84219757	0,18214014	0,04296410	0,01081407	

$$\frac{8}{R\pi^2} J_{0012}^1$$

$\alpha$	0,5	0,75	1,00	1,25	1,5	1,75	2,00	2,25	2,5
0,5	0,38503109	0,04839070	0,00843595	0,00175346	0,00040664	0,00010161	0,00002748	0,00000736	0,00000335
0,75	0,78452996	0,09917238	0,01738518	0,00363264	0,00084662	0,00021254	0,00005783	0,00001554	0,00000711
1,00	1,62704244	0,21082702	0,03783802	0,00807918	0,00192082	0,00049117	0,00013645	0,00003711	0,00001638
1,25	3,30978980	0,42944084	0,07713668	0,01648229	0,00392122	0,00100329	0,00027920	0,00007588	0,00003417
1,5	6,95451070	0,90311737	0,16236640	0,03471920	0,00826568	0,00211622	0,00058995	0,00016023	0,00007359
1,75	15,0696245	1,95861113	0,35783052	0,07542283	0,01796924	0,00460368	0,00128561	0,00034898	0,00016332
2,00	33,2389713	4,30190763	0,77120942	0,16450745	0,03907820	0,00998529	0,00278371	0,00075348	0,00036327
2,25	76,2741115	9,92950711	1,78981394	0,35367224	0,09154742	0,02348731	0,00657986	0,00178499	0,00086322
2,5	176,654794	23,0227889	4,15502655	0,89174113	0,21301590	0,05470944	0,01335244	0,00416605	0,00204076

$$\frac{8}{R\pi^2} J_{0210}^1$$

$\alpha$	0,5	0,75	1,00	1,25	1,5	1,75	2,00	2,25	2,5
0,5	7,90370966	0,59940130	0,07827233	0,01355330	0,00271129	0,00046683	0,00015455	0,00004114	0,00001133
0,75	14,8615085	1,12787969	0,14739567	0,02554111	0,00524211	0,00086907	0,00029195	0,00007767	0,00002137
1,00	27,0673952	2,05605587	0,26894918	0,04664691	0,00958203	0,00156182	0,00053481	0,00014215	0,00003904
1,25	50,1173515	3,81070946	0,49899993	0,08663556	0,01781321	0,00284589	0,00099664	0,00026461	0,00007253
1,5	95,9717528	7,30466722	0,95756704	0,16642711	0,03419661	0,00535465	0,00192131	0,00050951	0,00013929
1,75	190,958648	14,5486835	1,90071538	0,33217552	0,06843313	0,01046397	0,00384824	0,00101929	0,00027784
2,00	394,327092	30,0709680	3,95029052	0,68798154	0,14186943	0,02123607	0,00799737	0,00211587	0,00057501
2,25	841,696191	64,2429735	8,44907052	1,47263480	0,30395176	0,04461207	0,01717421	0,00453926	0,00122992
2,5	1848,06873	141,170344	18,5799912	3,24197942	0,66973468	0,09658750	0,03792632	0,00109836	0,00270628

$\beta$	$\alpha$	0,5	0,75	1,00	1,25	1,5	1,75	2,00	2,25	2,5
$\frac{1}{4R^{2\pi\alpha}}J_{0012}^1$										
0,5		1,45254171	0,14802694	0,02311043	0,00450948	0,00100728	0,00024614	0,00006410	0,00001750	0,00000495
0,75		2,87868675	0,28989829	0,04479241	0,00866348	0,00192077	0,00046640	0,00012080	0,00003282	0,00000925
1,00		5,74758792	0,58024124	0,08984873	0,01741038	0,00386616	0,00094004	0,00024375	0,00006630	0,00001871
1,25		11,7459295	1,18892296	0,18452698	0,03582706	0,00796908	0,00194041	0,00050376	0,00013716	0,00003874
1,5		24,7809987	2,51488100	0,39121174	0,07610305	0,01695542	0,00413426	0,00107459	0,00029288	0,00008279
1,75		53,9021960	5,48371921	0,85486831	0,16660012	0,03717441	0,00907598	0,00236167	0,00064428	0,00018227
2,00		120,352085	12,2717338	1,91681656	0,37417356	0,08360720	0,02043626	0,00532304	0,00145341	0,00041148
2,25		274,534970	28,0504855	4,38916568	0,85806123	0,19196765	0,04697210	0,01224571	0,00334613	0,00094797
2,5		637,130233	65,2186101	10,2211618	2,00083628	0,44812756	0,10975326	0,02863546	0,00782990	0,00221953

$\beta$	$\alpha$	0,5	0,75	1,00	1,25	1,5	1,75	2,00	2,25	2,5
$\frac{1}{4R^{2\pi\alpha}}J_{0210}^2$										
0,5		36,7477561	1,97631948	0,20761547	0,03096408	0,00570113	0,00120517	0,00028049	0,00007002	0,00001843
0,75		69,2610842	3,73308388	0,39309352	0,05876201	0,01084260	0,00229651	0,00053542	0,00013387	0,00003529
1,00		126,553399	6,84034586	0,72246792	0,10831675	0,02004082	0,00425522	0,00099428	0,00024910	0,00006577
1,25		235,24398	12,7563036	1,35194076	0,20336516	0,03774201	0,00803578	0,00188227	0,00047259	0,00012503
1,5		452,446267	24,617766	2,61843038	0,39523591	0,07358256	0,01571102	0,00368930	0,00092834	0,00024609
1,75		904,321903	49,3697188	5,26964732	0,79809282	0,14903790	0,03190840	0,00751078	0,00189393	0,00050298
2,00		1875,56403	102,715914	10,9998181	1,67112142	0,31294808	0,06716782	0,01584490	0,00400313	0,00106492
2,25		4019,61358	220,765553	23,7118545	3,61242118	0,67818893	0,14588068	0,03447967	0,00872577	0,00232467
2,5		8857,44692	487,703382	52,5199239	8,02080997	1,50910635	0,32523644	0,07699968	0,01951460	0,00520555

Der Verfasser dankt auch an dieser Stelle Fräulein M. BLAZSÓ für ihre Hilfe bei den numerischen Rechnungen.

# LITERATUR

1. F. BERENCZ, Acta Phys. Hung., **6**, 243, 1957.
2. M. KOTANI, A. AMEMIYA und T. SIMOSE, Proc. Phys. Math. Soc., Japan, **20**, extra No 1 (1938). 22. extra No. (1940).
3. Y. SUGIURA, Z. Physik, **45**, 484, 1927.
4. F. NEUMANN, Vorlesungen über die Theorie des Potentials und der Kugelfunktionen, Teubner, Leipzig, 1887.

## НЕКОТОРЫЕ БИПОЛЯРНЫЕ ИНТЕГРАЛЫ ДЛЯ ИСЧИСЛЕНИЙ НА ОСНОВЕ МЕТОДА КОРРЕЛИРОВАННЫХ МОЛЕКУЛЯРНЫХ ОРБИТ

Ф. БЕРЕНЦ

### Резюме

Табулированы нумерические значения интегралов

$$I_{iklm}^n = \int \psi_1^2 (\psi_2 + \psi_3 + \psi_4 + \psi_5)^2 \mu_1^i \mu_2^k v_1^l v_2^m r_{12}^n d\tau,$$

$$J_{iklm}^n = \int \psi_1^2 (\psi_2 + \psi_3 + \psi_4 + \psi_5) (\psi_2 \pm \psi_3 - \psi_4 \mp \psi_5) \mu_1^i \mu_2^k v_1^l v_2^m r_{12}^n d\tau,$$

$$\psi_1 = \exp[-\alpha(\mu_1 + \mu_3)], \quad \psi_2 = \exp[\beta(v_1 - v_2)], \quad \psi_3 = \exp[\beta(v_1 - v_3)],$$

$$\psi_4 = \exp[-\beta(v_1 - v_2)], \quad \psi_5 = \exp[-\beta(v_1 - v_2)]$$

и  $i, k, l, m, n = 0, 1, 2$ .

# THE FUNDAMENTAL THEOREM OF CONTINUOUS TRANSFORMATIONS IN THE QUANTUM THEORY

By

G. MARX

INSTITUTE FOR THEORETICAL PHYSICS OF THE ROLAND EÖTVÖS UNIVERSITY,  
CENTRAL RESEARCH INSTITUTE OF PHYSICS, BUDAPEST

(Presented by K. F. Novobátzky. — Received 18. VII. 1958)

The unitary operator, the generator of symmetry transformations in the Hilbert-space, will be formed on the basis of the field equations together with the commutation law. Our method is the reversal of SCHWINGER's method used in the covariant formulation of the quantum theory and eliminates some insufficiencies of the previous treatments.

§ 1. The present paper deals with a problem of methodological interest, across which the author came in the course of his university lectures.

The transformations leaving the field equations (Lagrangian) as well as the commutation laws invariant play a significant role in the quantum theory. Such transformations of the coordinates  $x_i$  and of the field quantities  $\psi_\mu$

$$x_i \rightarrow x'_i, \quad \psi_\mu(x) \rightarrow \psi'_\mu(x') \quad (1)$$

are the so-called symmetry transformations. In the Hilbert-space the generator of a transformation which does not affect the commutation rules is a unitary operator:

$$\psi'(x) = U \psi(x) U^{-1}, \quad (2)$$

In the course of quantum theoretical applications the explicit form of the generator  $U$  becomes important. As is well known [1] in the classical theory always a conservation law corresponds to every symmetry transformation. There exists a close relation between this conservation law and the form of the unitary generator  $U$ . This operator gives the transition between the two state vectors with which observers in different "systems of reference" describe the same physical state:

$$|>' = U |>. \quad (3)$$

It is very remarkable that *in case the Lagrangian is known a method can be given for the unambiguous formation of the generator of a continuous symmetry transformation.* This method can be obtained by the aid of the *fundamental theorem of continuous transformations.*

In the SCHWINGER's covariant formulation of the quantum theory this fundamental theorem is regarded as an axiom of the theory and the form

of the commutation rule was deduced from it [2]; in addition it is possible to deduce also the field equations. However, the reversed process can also be considered: the fundamental theorem can be deduced from the field equations and the commutation law. These latter can be introduced more easily in a correspondence-like way, therefore this kind of treatment seems to be methodically more advantageous (although SCHWINGER's method is mathematically more elegant). The deduction of the fundamental theorem from the commutation law has already been treated in the special case when the symmetry transformation does not affect the space coordinates (e.g. gauge transformation, the transformations of the isotopic space) and formerly the general case was handled, too, but in a rather indirect and cumbersome way [3]. The author, however, has not read any plain direct deduction of the fundamental theorem in a covariant manner which would be valid for all kinds of continuous symmetry transformations. This paper aims at presenting such a deduction which is of general validity. Only then will the equivalence (resp. the extent of the equivalence) of the Hamilton principle and the commutation law with the fundamental theorem become quite clear.

§ 2. As starting point for the covariant formulation of the theory serves the Lagrangian  $L$ . For the sake of simplicity let us assume that  $L$  is built up from the field quantities and their first derivatives. The physical field is described (in the classical theory as well as in the Heisenberg picture of the quantum theory) by such field quantities for which the integral

$$\int_W L(\psi(y), \partial \psi(y)) dy \quad (3)$$

is stationary (i.e. its first variation is zero) for values  $\psi_\mu(x)$  fixed on the boundary of the four-dimensional domain  $W$ . This Hamilton principle will be regarded as the first axiom of the theory; from this the Lagrangian form of the field equation can be obtained:

$$\frac{\partial L}{\partial \psi_\mu} - \partial_i \frac{\partial L}{\partial \partial_i \psi_\mu} = 0. \quad (4)$$

When substituting the expression for  $\psi_\mu(y)$  determined from (4) for the inner region of  $W$  into (3), we get the action integral

$$S = \frac{1}{ic} \int_W L(\psi(y), \partial \psi(y)) dy, \quad (5)$$

which depends only on the extent of  $W$  and on the specific value of  $\psi_\mu$  prescribed on the boundary of  $W$ .



Varying the four-dimensional domain  $W$  a surface point with coordinate  $x_i$  becomes a surface point with coordinate  $\bar{x}_i = x_i + \delta x_i$ . The value of the field quantity in this boundary surface point be also changed from  $\psi_\mu(x)$  to  $\bar{\psi}_\mu(\bar{x}) = \psi_\mu(x) + \delta\psi_\mu(x)$ . (By using the changed functions  $\bar{\psi}(\bar{y})$  corresponding to the modified boundary conditions the action integral  $S$  becomes of course stationary in the interior of the domain.) The variation of the boundary conditions modifies also the value of the action integral. The variation of  $S$  (according to the boundary formula of the variation calculus) can be transformed into a surface integral:

$$\delta S = \frac{1}{ic} \oint_H \left\{ \frac{\partial L}{\partial \partial_k \psi_\mu} \delta \psi_\mu + \Theta_{ik} \delta x_i \right\} dF_k = \oint_H (\pi_\mu \delta \psi_\mu + p_i \delta x_i) dF, \quad (6)$$

(where the domain of integration  $H$  is the boundary surface of  $W$ ). Let us use the following notations:

$$\Theta_{ik}(x) = L \delta_{ik} - \partial_i \psi_\mu \frac{\partial L}{\partial \partial_k \psi_\mu} \quad (7)$$

is the canonical energy momentum tensor,  $N_k$  is the normal unit vector of the surface element  $dF_k$  (i.e.  $dF_k = N_k dF$ ,  $N_k N_k = +1$ ). According to PIERRE WEISS the quantity

$$\pi_\mu(x) = \frac{1}{ic} \frac{\partial L}{\partial \partial_k \psi_\mu} N_k \quad (8)$$

will be regarded as the canonical conjugate of the field quantity  $\psi_\mu(x)$  and the function

$$p_i(x) = \frac{1}{ic} \Theta_{ik} N_k \quad (9)$$

as the canonical conjugate of the independent variable  $x_i$  [4]. (It should be noted that  $\pi_\mu(x)$  and  $p_i(x)$  are not pure local functions but they depend on the direction of the surface element at the point  $x$ .) They can be designated canonical conjugates as (in the classical theory as well as in the quantum theory) canonical equations can be deduced for them.

Let  $f_i(x)$  be four arbitrarily given coordinate functions and let us form the integral

$$B = \int_F p_i(y) f_i(y) dF = \frac{1}{ic} \int_F \Theta_{ik}(y) f_i(y) dF_k = \int_F \left( \frac{1}{ic} L N_i - \partial_i \psi_\mu \cdot \pi_\mu \right) f_i dF \quad (10)$$

for an arbitrary three-dimensional not-bounded space-like hyperplane  $F$ . The integrand is a given expression of  $\psi_\mu(y)$ ,  $\partial_i \psi_\mu(y)$  and  $\pi_\mu(y)$ . Using (8) the normal derivate of  $\psi_\mu$  can be expressed by  $\psi_\mu$  and  $\pi_\mu$  and thus  $B$  can be regarded as a functional of the values of  $\psi_\mu$  and  $\pi_\mu$  taken on the plane  $F$ .

By varying the values of  $\psi_\mu(y)$  and  $\pi_\mu(y)$  prescribed on the hyperplane we get for the variation of  $B$  (after identical transformations) :

$$\begin{aligned} \delta B[\psi, \pi] = & \frac{1}{ic} \int \left( \frac{\partial L}{\partial \psi_\mu} - \partial_i \frac{\partial L}{\partial \partial_i \psi_\mu} \right) \delta \psi_\mu dF + \\ & + \int_F \left( \frac{1}{ic} \frac{\partial L}{\partial \partial_r \psi_\mu} N_i f_i \delta \psi_\mu - \pi_\mu \delta \psi_\mu f_r \right) dF + \\ & + \int_F \left\{ \left[ \partial_i (f_i \pi_\mu) - \frac{1}{ic} \frac{\partial L}{\partial \partial_r \psi_\mu} N_i \partial_r f_i \right] \delta \psi_\mu - [\partial_i \psi_\mu f_i] \delta \pi_\mu \right\} dF. \end{aligned} \quad (11)$$

The first integral becomes zero due to (4), the second one is also zero (in spite of the fact that it is a four-sum) due to the vanishing of  $\psi_\mu$  in the space-like infinity. From the remaining expression we can see that the functional derivatives are the following :

$$\frac{\delta B}{\delta \psi_\mu(x)} = \partial_i (f_i \pi_\mu) - \frac{1}{ic} \frac{\partial L}{\partial \partial_r \psi_\mu} N_i \partial_r f_i, \quad (12)$$

$$\frac{\delta B}{\delta \pi_\mu(x)} = -f_i \partial_i \psi_\mu. \quad (13)$$

In the special case when  $f_i = \delta_{ik}$  (12) and (13) lead to the following canonical equation

$$\frac{\delta P_k}{\delta \psi_\mu(x)} = \partial_k \pi_\mu(x), \quad \frac{\delta P_k}{\delta \pi_\mu(x)} = -\partial_k \psi_\mu(x), \quad (14)$$

where

$$P_k = \frac{1}{ic} \int_F \Theta_{ik} dF_k = \int_F p_i dF \quad (15)$$

is the four-momentum of the system.

§ 3. A symmetry transformation has to be regarded as continuous if 1) it is a differentiable function of the parameter  $a$ , 2) it turns into identical transformation when  $a = 0$  and 3) the parameter can be chosen so that the successive transformations with parameter  $a_1$  and  $a_2$  correspond to a transformation with parameter  $a_1 + a_2$ .

The transformation changes the field quantity components  $\psi_\mu$  in the given geometrical point  $P$ : they combine with each other

$$\psi'_\mu(P) = \sigma_{\mu\nu} \psi_\nu(P). \quad (16)$$

$\sigma_{\mu\nu}$  and thus also  $\psi'_\mu$  are functions of the parameter  $a$ .

$$\sigma_{\mu\nu}(0) = \delta_{\mu\nu}, \quad \sigma_{\mu'_2}(a_2) \sigma_{\nu'_1}(a_1) = \sigma_{\mu\nu}(a_2 + a_1). \quad (17)$$

Let us form the following expressions:

$$\Delta\sigma_{\mu\nu} = \left[ \frac{d\sigma_{\mu\nu}}{da} \right]_{a=0} = I_{\mu\nu}, \quad (18)$$

$$\Delta\psi_\mu(x) = \left[ \frac{d\psi'_\mu(x')}{da} \right]_{a=0} = I_{\mu\nu} \psi_\nu(x). \quad (19)$$

$I_{\mu\nu}$  is the matrix of the infinitesimal transformation.

The symmetry transformation can change the coordinates of the point  $P$  too:  $x \rightarrow x'(a) = sx$ . Let us deal now with the following expression:

$$\Delta x_i = \left[ \frac{dx'_i}{da} \right]_{a=0}. \quad (20)$$

If we regard the arguments of the field quantities in (16).

$$\psi'_\mu(x') = \sigma_{\mu\nu} \psi_\nu(x), \quad (21)$$

i.e.

$$\psi'_\mu(x') = \sigma_{\mu\nu} \psi_\nu(s^{-1}x')$$

and change the notation of the independent variable  $x'_i \rightarrow x_i$ , we get:

$$\psi'_\mu(x) = \sigma_{\mu\nu} \psi_\nu(s^{-1}x). \quad (22)$$

Thus, comparing the *functional forms* of the field quantities (i.e. their dependence on the coordinates as independent variables) instead of comparing their values taken at a given geometrical point according to (16) we can see that the expression  $\psi_\mu(x)$  will be altered by the transformation due to two reasons: the components of the field quantities combine in a given point ( $\sigma$ ) and the coordinates of this point will be changed in the argument ( $s$ ). Thus the derivative of  $\psi_\mu(x)$  with respect to the transformation parameter consists of two parts:

$$\begin{aligned} \Delta^* \psi_\mu(x) &= \left[ \frac{d\psi'_\mu(x)}{da} \right]_{a=0} = \left[ \frac{d\sigma_{\mu\nu}}{da} \right]_{a=0} \psi_\nu(x) + \partial_i \psi_\nu(x) \left[ \frac{d(s^{-1}x)_i}{da} \right]_{a=0} = \\ &= \Delta \psi_\mu(x) - \partial_i \psi_\mu(x) \cdot \Delta x_i. \end{aligned} \quad (23)$$

Let us consider now, following E. NOETHER [1], the action integral after the transformation as a function of the transformation parameter  $a$  :

$$S(a) = \frac{1}{ic} \int_W L(\psi'(y'), \partial' \psi'(y')) dy'.$$

As the transformation is a symmetry transformation the action integral has to be equal to the non-transformed expression  $S(0)$ , i.e.

$$\Delta S = \left[ \frac{dS(a)}{da} \right]_{a=0} = \int_W \partial_k \left[ \frac{1}{ic} \left( \frac{\partial L}{\partial \partial_k \psi_\mu} \Delta \psi_\mu + \Theta_{ik} \Delta x_i \right) \right] dx = 0. \quad (24)$$

This relation, however, is valid for an arbitrary domain  $W$  only when

$$\partial_k j_k = 0,$$

where

$$j_k(x) = \frac{i}{c} \left( \frac{\partial L}{\partial \partial_k \psi_\mu} \Delta \psi_\mu + \Theta_{ik} \Delta x_i \right). \quad (25)$$

To every symmetry transformation corresponds a conservation law. The differential form of a conservation law is given in (25). This is *Noether's theorem*. The current density  $j_k(x)$  is a pure local function independent of the transformation parameter and the surface direction.

Let us choose the four-dimensional domain  $W$  in (28) as the four-volume between the two hyperplanes  $F_0$  and  $F$  and assume the normals of the hyperplanes as directed into the "future". Then using the Gauss theorem and the fact that the field quantities vanish in the space-like infinity, we get for (24)

$$\Delta S = Q(F_0) - Q(F) = 0,$$

i. e.

$$Q = \int_F j_k dF_k = - \int_F (\pi_\mu \Delta \psi_\mu + p_i \Delta x_i) dF \quad (26)$$

is independent of the hyperplane, i. e. it is a constant of motion and it can be transformed like a contravariant quantity with respect to the transformation parameter  $a$ . The form of  $Q$  can be written down directly when  $L$  is known. This is the integral form of NOETHER's theorem.

§ 4. In quantum theory besides the field equations the commutation laws must also be known. Let us consider a hyperplane  $F$ . The following commutation laws are valid for the field quantities taken at two points  $x, y$  of the hyperplane :

$$\{\psi_\mu(x), \pi_\nu(y)\} = i\hbar \delta_{\mu\nu} \delta(x - y), \quad \{\pi_\mu(x), \pi_\nu(y)\} = 0, \quad \{\psi_\mu(x), \psi_\nu(y)\} = 0. \quad (27)$$

Here

$$\{A, B\} = AB \pm BA,$$

where the sign depends on the statistics of the field investigated. The definition of the surface function  $\delta(x)$  is the relation

$$\int_F f(y) \delta(y - x) dF(y) = f(x).$$

The "simultaneous" commutation rule (27) refers to the hyperplane  $F$  (due to the quantities  $\pi_\mu, \delta(x)$  and to the assumption  $x, y \in F$ ). Comparing (27) and the field equations (4) the commutator  $\{\psi_\mu(x), \psi_\nu(z)\}$  at two points of arbitrary location can be obtained and its value is already independent of  $F$ .

The results of the classical theory obtained in the above two paragraphs are valid also in the quantum theory as operator relations if we take care of the sequence of operators in the course of differentiations. The most obvious way is to regard all the products as ordered products.

§ 5. As the transformations dealt with are symmetry transformations the operators  $\psi'_\mu(x)$  satisfy the same commutation rules as the operators  $\psi_\mu(x)$  (the transformation is canonical). Thus the two operators can be related to each other by a unitary perator  $U$ , namely :

$$\psi'_\mu(x) = U \psi_\mu(x) U^{-1}. \quad (28)$$

Our main task is to determine the explicit form of the generator  $U$ . For the transformations dealt with here we can write

$$U(a_2)U(a_1) = U(a_2 + a_1), \quad U(0) = 1.$$

Be

$$\Delta U = \left[ \frac{dU}{da} \right]_{a=0}. \quad (29)$$

Differentiating (28) with respect to  $a$  and taking the derivative for  $a = 0$  we get by taking into account (23) and (29)

$$\Delta^* \psi_\mu(x) = [\Delta U, \psi_\mu(x)]. \quad (30)$$

([...] means a minus commutator.) Evidently, if the operator  $\Delta U$  satisfying (30), is determined, the operator  $U$  can easily be obtained. In the case of a very small transformation parameter one can write :

$$U(a) \approx U(0) + a \left( \frac{dU}{da} \right)_{a=0} = 1 + a \Delta U.$$

The relation becomes exact if  $a \rightarrow 0$ . The generator of a transformation with a finite parameter  $a$  can be obtained from the generator of a transformation having as parameter  $a/n$  in the following way:

$$U(a) = U\left(\frac{a}{n}\right)^n,$$

and if  $n$  is large enough

$$U\left(\frac{a}{n}\right) \approx 1 + \frac{a}{n} \Delta U, \quad \text{thus} \quad U(a) \approx \left(1 + \frac{a}{n} \Delta U\right)^n.$$

The equality sign applies if  $\frac{a}{n} \rightarrow 0$ , i.e. if  $n \rightarrow \infty$ . Thus we can write symbolically

$$U(a) = \lim_{n \rightarrow \infty} \left(1 + \frac{a}{n} \Delta U\right)^n = e^{a \Delta U}. \quad (31)$$

As a preparation for the determination of  $\Delta U$  the commutators of  $Q$  and  $\psi_\mu(x)$  have to be formed:

$$[Q, \psi_\mu(x)] = - \int [\pi_\nu(y) \Delta \psi_\nu(y), \psi_\mu(x)] dF(y) - [B, \psi_\mu(x)]. \quad (32)$$

Here

$$B = \int_F p_i(y) \Delta y_i dF. \quad (33)$$

As  $Q$  is independent of the position of  $F$  we have chosen a hyperplane laid through the fixed point  $x$ . For the evaluation of the first term on the right hand side of (32) the algebraic identity

$$[AB, C] = A\{B, C\} - \{C, A\}B \quad (34)$$

can be used and for the second term the general mathematical relation

$$[B, \psi_\mu(x)] = \frac{\hbar}{i} \frac{\delta B}{\delta \pi_\mu(x)} \quad (35)$$

which is valid as a result of (27) for all expressions  $B$  of interest. (It must be taken into account that only even number fermion operators can occur in  $B$ .) Thus we get

$$[Q, \psi_\mu(x)] = \int \left\{ \psi_\mu(x), \pi_\nu(y) \right\} \Delta \psi_\nu(y) - \pi_\nu(y) I_{\nu\mu} \left\{ \psi_\nu(y), \psi_\mu(x) \right\} dF(y) + i \hbar \frac{\delta B}{\delta \pi_\mu(x)}.$$



From the commutation laws (27) and from the general canonical equations (13) (by choosing  $f_i(y) = \Delta y_i$ ) we get

$$[Q, \psi_\mu(x)] = i\hbar (\Delta \psi_\mu(x) - \partial_i \psi_\mu(x) \Delta x_i) = i\hbar \Delta^* \psi_\mu(x). \quad (36)$$

Comparing (30) and (36) we get for the operator  $\Delta U$ :

$$\Delta U = -\frac{i}{\hbar} Q = \frac{i}{\hbar} \int (\pi_\mu \Delta \psi_\mu + p_i \Delta x_i) dF \quad (37)$$

and the generator of the finite symmetry transformation becomes

$$U(a) = e^{-a \frac{i}{\hbar} Q} = \exp \frac{ia}{\hbar} \int_F (\pi_\mu \Delta \psi_\mu + p_i \Delta x_i) dF = \exp \frac{a}{\hbar c} \int_F \left( \frac{\partial L}{\partial \partial_k \psi_\mu} \Delta \psi_\mu + \right. \\ \left. + L \Delta x_k - \frac{\partial L}{\partial \partial_k \psi_\mu} \partial_i \psi_\mu \Delta x_i \right) dF_k. \quad (38)$$

Thus we have succeeded in obtaining the generator of an arbitrary continuous symmetry transformation by the aid of the field equations and the commutation law. The generator is, according to § 3, a Lorentz invariant constant of motion, which is independent of  $F$ .

§ 6. As we mentioned already in the introduction, the fundamental theorem expressed by (28) and (38) was regarded by J. SCHWINGER as an axiom of the quantum theory from which the commutation law can be deduced.

Indeed: Let us consider such a symmetry transformation, for which  $\Delta x_i = 0$ . In this case it follows from the expression (37) (which is accepted as an axiom) that

$$\Delta \psi_\mu = \Delta^* \psi_\mu = [\Delta U, \psi_\mu(x)] = \frac{i}{\hbar} \int_F [\pi_\nu(y) \psi_\nu(y), \psi_\mu(x)] I_{\nu 0} dF(y) = \\ = \frac{i}{\hbar} \int (\pi_\nu(y) \{\psi_\nu(y), \psi_\mu(x)\} - \{\psi_\mu(x), \pi_\nu(y)\} \psi_\nu(y)) I_{\nu 0} dF(y).$$

This requirement can be fulfilled for many possible expressions  $I_{\nu 0}$  and point  $x$  and hyperplane  $F$  by choosing

$$\{\psi_\nu(y), \psi_\mu(x)\} = 0, \quad \{\psi_\mu(x), \pi_\nu(y)\} = i\hbar \delta_{\mu\nu} \delta(x - y).$$

Of course the fundamental theorem does not affect the type of the statistics. Conclusions can be drawn from the fundamental theorem also regarding

the field equation. The theory is invariant against the displacement of the origo of the coordinate system, i.e.

$$x'_i = x_i - a_i, \quad \psi'_\mu(x') = \psi_\mu(x) \quad (39)$$

are symmetry transformations. From this follows according to (26) the conservation of the field momentum  $P_i$ , the form of which can be obtained directly from (15) if the Lagrangian is known.

Applying (30) to the transformation (39) we get

$$i\hbar [P_i, \psi_\mu(x)] = \partial_i \psi_\mu(x). \quad (40)$$

(40) determines the space and time variations of the field quantities and thus leads to the field equations.

#### REFERENCES

1. E. NOETHER, Gött. Nachr., 235, 1918.
2. J. SCHWINGER, Phys. Rev., **82**, 914, 1951.
3. See e.g. L. ROSENFELD, Ann. Phys., **5**, 113, 1930.  
R. UTIYAMA, Progr. Theor. Phys., **5**, 437, 1950.  
M. JAUCH-R. ROHRLICH, Quantum Theory of Photons and Electrons, Addison-Wesley Publ. Co. Cambridge, Mass. 1955.  
P. T. MATTHEWS, The Relativistic Quantum Theory of Elementary Particles, Rochester Lectures, 1957. Preprint.  
J. SCHWINGER, Annals of Physics, **2**, 407, 1957.
4. P. WEISS, Proc. Roy. Soc. A, **169**, 102, 1938.

#### О ФУНДАМЕНТАЛЬНОЙ ТЕОРЕМЕ НЕПРЕРЫВНЫХ ПРЕОБРАЗОВАНИЙ В КВАНТОВОЙ ТЕОРИИ

Г. МАРКС

#### Резюме

Унитарный оператор, производящий преобразования симметрии в гильбертовом пространстве, строится на базе уравнений поля и перестановочных соотношений. Наш метод является обращением метода Швингера и он устраняет некоторые недостатки предыдущих трактовок.

# ZUSAMMENHANG ZWISCHEN DER STRUKTUR UND DEN PHYSIKALISCHEN EIGENSCHAFTEN DES GLASES.

## III. DIE WÄRMEAUSDEHNUNG DES GLASES

Von

I. NÁRAY-SZABÓ

CHEMISCHES ZENTRALFORSCHUNGSINSTITUT DER UNGARISCHEN AKADEMIE DER WISSENSCHAFTEN,  
BUDAPEST

(Vorgelegt von Z. Gyulai. — Eingegangen: 23. VII. 1958)

1. Die vorhandenen Messungen von Wärmeausdehnungskoeffizienten von Gläsern bekannter Zusammensetzung werden durch lineare Gleichungen berechnet, die von den bisher benutzten sich hauptsächlich darin unterscheiden, dass die netzbildenden Oxyde  $\text{SiO}_2$ ,  $\text{Al}_2\text{O}_3$  und  $\text{B}_2\text{O}_3$  keinen Anteil an der Ausdehnung haben, dass ihnen also ein Faktor Null zukommt. Die Wärmeausdehnung wird nach dieser Auffassung praktisch nur durch gerüstmodifizierende Ionen hervorgerufen, in erster Linie durch die Alkalien.

2. Die Gleichungen enthalten eine additive Konstante, die durch den Typ des Glases bestimmt ist.

3. Die Abweichungen zwischen den mit diesen Gleichungen berechneten und den gemessenen Ausdehnungskoeffizienten betragen im Mittel etwa 1—3 Prozent, also bedeutend weniger als die früheren, die übrigens nur auf gewisse Glassorten anwendbar sind.

4. Eine kurze Diskussion über den Zusammenhang zwischen der Wärmeausdehnung und den Eigenschaften des Glasgerüsts wird hier gegeben.

Wegen der praktischen Wichtigkeit der Wärmeausdehnung des Glases wurden viele Messungen auf diesem Gebiet durchgeführt und unter ihnen befindet sich eine ziemliche Anzahl solcher, die an zwei- und dreikomponentigen Gläsern mit systematisch variiertem Zusammensetzung vorgenommen wurden. Schon die frühen Arbeiten von WINKELMANN und SCHOTT [1] geben eine additive Gleichung an, die zur Berechnung der Wärmeausdehnung aus der chemischen Zusammensetzung dient; ihre Ergebnisse weichen von den gemessenen Werten im Mittel um etwa 5%, maximal um 11% ab. ENGLISH und TURNER [2] haben genaue Messungen an mehreren Serien ausgeführt und dabei die von WINKELMANN und SCHOTT angegebenen Faktoren sehr stark abgeändert. Wieder andere Rechnungsverfahren wurden von GILARD und DUBRUL [3] und von BLAU [4] angegeben, die eine quadratische bzw. eine mit vielen Faktoren operierende Gleichung empfehlen. Schon HALL [5] hat den Anteil des Siliciumdioxids an der Wärmeausdehnung für vernachlässigbar gehalten und entsprechende Faktoren angegeben. R. SCHMIDT [6] rechnet in fast gleicher Weise. Doch gab es bisher keine solchen Faktoren, die allgemein anwendbar gewesen wären, ohne von den experimentellen Werten allzu grosse Abweichungen zu ergeben.

Da die Möglichkeit einer genaueren und allgemein verwendbaren Gleichung von grossem praktischen und auch theoretischem Wert ist, habe ich das vorhandene publizierte Material samt einer Anzahl unpublizierter Mes-

sungen aus der Industrie durchgearbeitet und daraus eine allgemeine Gleichung aufgestellt, die für den Ausdehnungskoeffizienten ( $10^8 \alpha = 10^8 \cdot \Delta l / l \cdot \Delta t$ ) von gewöhnlicher Temperatur bis 90 oder 100° C gültig ist. Dabei bin ich von den einfachsten Systemen ausgehend auf solche mit mehreren Komponenten vorgedrungen.

Quarzglas hat eine sehr kleine Wärmeausdehnung, zwischen 0—100°  $10^{-8} \cdot 48,7$  pro C°. Glasiges Bortrioxyd hat dagegen einen ausgesprochen grossen  $\alpha$ -Wert von  $1510 \cdot 10^{-8}$  pro C° (zwischen 0—100°). Die aus diesen Oxyden hergestellten gemischten Gläser weisen eine desto höhere Ausdehnung auf je mehr Bortrioxyd in ihnen enthalten ist, der Zusammenhang ist aber keineswegs linear.

Tabelle I

Wärmeausdehnung von  $\text{SiO}_2$ — $\text{B}_2\text{O}_3$ -Gläsern [7]

$\text{SiO}_2\%$	$\text{B}_2\text{O}_3\%$	$10^8 \alpha$ gem.
0	100	1510
6,46	93,54	1317
9,99	90,01	1181
14,81	85,19	1114
24,45	75,55	870
38,03	61,97	719
45,51	54,49	576
52,17	47,83	498
57,24	42,76	475
100	0	48,7

Tabelle 2

Wärmeausdehnung von  $\text{Na}_2\text{O}$ — $\text{SiO}_2$ -Gläsern (25—90°) [8]

$\text{SiO}_2\%$	$\text{Na}_2\text{O}\%$	$10^8 \alpha$ gem.	$10^8 \alpha$ ber.	Diff. %
66,91	33,09	1346	1351	+0,4
70,38	29,62	1240	1231	—0,7
74,05	25,95	1138	1103	—3,1
76,27	23,73	1035	1025	—1,0
79,13	20,87	917	925	+0,9
81,34	18,66	849	848	—0,1
82,83	17,17	755	785	+4,0

Die Wärmeausdehnung von anderen, aus mehreren gerüstbildenden Oxyden hergestellten Gläsern wurde nicht gemessen.

Bei der Betrachtung der Wärmeausdehnung von einfachen Natron-silikatgläsern fällt es auf, dass diese eine enge Parallelität mit dem Natrongehalt zeigt.

(Die geringen Verunreinigungen — einige Zehntelprozent — wurden zum  $\text{Na}_2\text{O}$  gerechnet.)

Bezeichnet man die Prozentzahlen eines Oxyds mit der in runden Klammern gesetzten Formel — wie es im folgenden stets gemacht wird — so finden wir, dass auf Grund der Gleichung

$$10^8 \alpha = 35 (\text{Na}_2\text{O}) + 185$$

die gemessenen Werte mit einer maximalen Abweichung von 4,0% berechnet werden können. Die durchschnittliche Abweichung ist weniger als 1,5%.

Leider haben wir keine Daten für  $\text{K}_2\text{O}-\text{SiO}_2$  und andere binäre Gläser. Dagegen stehen uns eine Anzahl von Messreihen von dreikomponentigen Natrongläsern zur Verfügung. — Betrachten wir zunächst jene, die neben  $\text{SiO}_2$  noch ein anderes gerüstbildendes Oxyd enthalten, so sehen wir, dass  $\text{BeO}$  nur die additive Konstante der Gleichung verändert, der Faktor von  $\text{Na}_2\text{O}$  aber bleibt erhalten.

Tabelle 3

Wärmeausdehnung von  $\text{Na}_2\text{O}-\text{BeO}-\text{SiO}_2$ -Gläsern (20—400°) [9]

$\text{SiO}_2\%$	$\text{BeO}\%$	$\text{Na}_2\text{O}\%$	$10^8\alpha$		Diff. %
			gem.	ber.	
80,0	7,5	12,5	740	758	+2,4
75,0	12,5	12,5	780	758	-2,8
74,0	11,0	15,0	840	845	+0,6
72,0	12,0	16,0	880	880	$\pm 0$
72,0	10,0	18,0	960	950	-1,0
76,0	5,0	19,0	1000	985	-1,5
66,0	14,0	20,0	1000	1020	+2,0
74,0	3,5	22,5	1090	1107	+1,6
69,0	7,5	23,5	1120	1123	+0,3
71,0	3,0	26,0	1180	1210	+2,5
62,5	11,0	26,5	1220	1228	+0,7
64,5	7,0	28,6	1280	1298	+1,4

Obzwar hier die Temperaturgrenzen sehr verschieden sind, bleibt der Koeffizient des  $\text{Na}_2\text{O}$  derselbe, und wir erhalten die Gleichung

$$10^8 \alpha = 35 (\text{Na}_2\text{O}) + 320.$$

Die maximale Abweichung beträgt 2,8% und die durchschnittliche 1,4%.

Es ist sehr interessant, dass auch die Wärmeausdehnung von Borosilikatgläsern analog berechnen kann, dass also  $\text{B}_2\text{O}_3$  keinen starken Einfluss darauf ausübt.

Tabelle 4

Wärmeausdehnung von  $\text{Na}_2\text{O}-\text{B}_2\text{O}_3-\text{SiO}_2$ -Gläsern (25—90°) [10]

$\text{SiO}_2\%$	$\text{B}_2\text{O}_3\%$	$\text{Na}_2\text{O}\%$	$10^8 \alpha$		Diff. %
			gem.	ber.	
70,75	18,71	9,89	498	496	—0,4
67,18	21,81	10,26	497	504	+1,4
61,94	25,82	11,33	521	547	+5,0
74,91	12,45	11,36	578	548	—5,2
71,51	8,28	18,86	817	810	—0,9
61,28	18,84	19,04	805	816	—1,3
68,39	11,29	19,04	813	816	—0,4
74,22	4,46	19,92	840	847	+0,8
64,72	14,45	20,09	837	953	+1,9
50,04	28,83	20,44	814	866	+5,0

(Der geringe  $\text{CaO}$ -Gehalt wurde zum  $\text{Na}_2\text{O}$  gerechnet)

So lassen sich bis 30%  $\text{B}_2\text{O}_3$  enthaltende Gläser bei maximalem Fehler von 5,2% berechnen, wobei der durchschnittliche Fehler 1,93% beträgt.

Eine andere Messreihe gibt die Wärmeausdehnung von Natronborosilikatgläsern zwischen anderen Temperaturgrenzen, daher muss die additive Konstante der Gleichung etwas modifiziert werden. Wir erhalten mit der Gleichung

$$10^8 \alpha = 35(\text{Na}_2\text{O}) + 200$$

eine maximale Abweichung von 5,3% (durchschnittlich 2,5%). Man muss beachten, dass der  $\text{Na}_2\text{O}$ -Gehalt hier bis zu 32% reicht.



Tabelle 5

Wärmeausdehnung von  $\text{Na}_2\text{O}-\text{B}_2\text{O}_3-\text{SiO}_2$ -Gläsern (25–150°) [11]

$\text{SiO}_2\%$	$\text{B}_2\text{O}_3\%$	$\text{Na}_2\text{O}\%$	$10^\circ\alpha$		Diff. %
			gem.	ber.	
63,81	4,33	31,86	1333	1314	—1,4
61,57	8,28	30,15	1247	1254	+0,2
59,53	11,33	29,14	1181	1219	+3,2
53,66	18,05	28,29	1151	1189	+3,3
55,15	17,60	27,25	1108	1153	+4,0
55,74	18,29	25,97	1052	1108	+5,3
65,49	10,12	24,39	1054	1052	—0,2
61,27	14,57	24,16	1009	1041	+3,5
55,72	30,17	24,11	1007	1043	+3,6
51,00	24,86	24,14	1004	1044	+4,0
76,99	4,68	18,33	882	841	—4,7
73,38	8,71	17,91	833	826	—0,8
70,05	12,79	17,16	788	800	+1,5
67,55	16,29	16,16	740	765	+3,4
65,65	19,33	15,02	721	726	+0,7
62,04	22,80	15,16	723	730	+1,0

Im Falle von Aluminiumoxyd kann man ebenso verfahren :

Tabelle 6

Wärmeausdehnung von  $\text{Na}_2\text{O}-\text{Al}_2\text{O}_3-\text{SiO}_2$ -Gläsern [12]

$\text{SiO}_2\%$	$\text{Al}_2\text{O}_3\%$	$\text{Na}_2\text{O}\%$	$10^\circ\alpha$		Diff. %
			gem.	ber.	
75,12	6,54	18,38	853	862	+1,1
70,76	10,58	18,56	870	877	+0,8
66,17	15,62	18,20	860	856	—0,5
62,25	19,79	18,01	863	850	—1,5
79,21	6,62	14,36	730	722	—1,1
74,72	10,69	14,81	723	738	+2,1
69,99	15,57	14,52	727	729	+0,3

(Der geringe  $\text{CaO}$ -Gehalt wurde zu  $\text{Na}_2\text{O}$ ,  $\text{Fe}_2\text{O}_3$  zu  $\text{Al}_2\text{O}_3$  gerechnet.)

Mit der Gleichung

$$10^8\alpha = 35(\text{Na}_2\text{O}) + 220$$

erhalten wir eine vorzügliche Übereinstimmung; der maximale Fehler beträgt 2,1% und der durchschnittliche 1,0%. Bei einer anderen Messreihe (13) erhält man ebenfalls ziemlich gute Übereinstimmung — allerdings mit einer etwas modifizierten additiven Konstante — bis zu einem  $\text{Na}_2\text{O}$ -Gehalt von 21%, darüber hinaus werden die Abweichungen grösser.

### Gläser mit zwei gerüstmodifizierenden Oxyden

Wir haben einige wenige Daten für die Wärmeausdehnung von Lithium-aluminumsilikatgläsern.

Tabelle 7

Wärmeausdehnung von  $\text{Li}_2\text{O}-\text{Al}_2\text{O}_3-\text{SiO}_2$ -Gläsern (30—500°) [14]

$\text{SiO}_2\%$	$\text{Al}_2\text{O}_3\%$	$\text{Li}_2\text{O}\%$	$10^8\alpha$		Diff. %
			ber.	gem.	
49,6	42,14	8,26	760	—	—
66,3	28,1	5,52	666	662	—0,6
74,9	21,0	4,15	525	525	$\pm 0$
79,8	16,9	3,32	436	442	+1,4
83,1	14,1	2,77	393	387	—1,5

Bis zu einem  $\text{Li}_2\text{O}$ -Gehalt von 6% kann man diese mit der Gleichung

$$10^8\alpha = 100(\text{Li}_2\text{O}) + 110$$

berechnen, wobei sich eine maximale Differenz von 1,5% und eine durchschnittliche von 0,9% ergibt. — Aus diesen Daten sieht man aber auch, dass sich  $\text{Li}_2\text{O}$  den Alkalien ähnlich verhält, d. h. eine grosse Wärmeausdehnung verursacht, es gehört also keineswegs zu den gerüstbildenden Oxyden, obzwar  $\text{Li}^+$  in Viererkoordination im  $\text{Li}_2\text{SiO}_3$  auftritt [15].

Betrachten wir die Ausdehnung von  $\text{MgO}$  enthaltenden Gläsern, so sehen wir, dass  $\text{MgO}$  die Ausdehnung verringert.

Tabelle 8

Wärmeausdehnung von  $\text{Na}_2\text{O}$ — $\text{MgO}$ — $\text{SiO}_2$ -Gläsern (25—90°) [16]

$\text{SiO}_2\%$	$\text{MgO}\%$	$\text{Na}_2\text{O}\%$	$10^8\alpha$		Diff. %
			ber.	gem.	
74,07	1,10	24,23	1104	1099	—0,5
75,00	2,49	22,12	1005	1013	+0,8
75,19	4,20	19,83	895	920	+2,8
77,09	6,10	16,05	784	773	—1,4
76,86	7,46	14,55	710	708	—0,3
78,28	9,30	11,76	594	598	+0,7

Wir benützen für  $\alpha$  eine Gleichung

$$10^8\alpha = 35(\text{Na}_2\text{O}) - 8(\text{MgO}) + 260$$

und erhalten damit eine maximale Abweichung von 2,8% und eine durchschnittliche von 1,3%.

Die wichtigen Natronkalksilikatgläser zeigen, dass  $\text{CaO}$  einen positiven Beitrag zur Wärmeausdehnung liefert.

Tabelle 9

Wärmeausdehnung von  $\text{Na}_2\text{O}$ — $\text{CaO}$ — $\text{SiO}_2$ -Gläsern (0—75°) [17]

$\text{SiO}_2\%$	$\text{CaO}\%$	$\text{Na}_2\text{O}\%$	$10^8\alpha$		Diff. %
			gem.	ber.	
75,94	12,04	12,00	744	755	+1,5
75,25	9,37	15,38	844	850	+0,7
74,70	6,91	18,39	916	927	+1,2
74,75	4,80	19,91	998	960	—3,8
74,65	2,69	22,66	1054	1034	—1,9
76,00	12,26	11,74	723	749	+3,6
75,80	10,21	13,99	796	807	+1,3
81,19	8,07	10,52	658	664	+0,9
74,07	10,01	15,45	858	855	—0,3
70,27	14,08	15,49	898	897	—0,1
72,87	10,06	16,96	895	910	+1,7
70,64	14,41	15,00	874	884	+1,1

Die Gleichung

$$10^8\alpha = 35(\text{Na}_2\text{O}_3 + 10(\text{CaO}) + 215$$

gestattet eine Berechnung der Werte von  $\alpha$  mit einer maximalen Abweichung von 3,8%, wobei die durchschnittliche Abweichung 1,5% beträgt.

Die Ergebnisse einer anderen Messreihe finden sich in der folgenden Tabelle.

Tabelle 9/a

Wärmeausdehnung von  $\text{Na}_2\text{O}-\text{CaO}-\text{SiO}_2$ -Gläsern (25–90°) [18]

$\text{SiO}_2\%$	$\text{Na}_2\text{O}\%$	$\text{CaO}\%$	$10^3\alpha$		Diff. %
			gem.	ber.	
73,92	23,80	1,50	1106	1073	—3,0
74,08	23,00	2,61	1065	1056	—0,8
74,07	21,50	3,81	1021	1015	—0,6
73,78	20,87	4,50	988	997	+0,9
74,41	17,20	7,45	911	902	—1,0
74,99	16,00	8,16	870	867	—0,3
74,94	14,88	9,36	844	840	—0,5
74,59	14,22	10,38	810	826	+2,0
74,93	13,02	11,68	769	798	+3,8
66,71	12,72	18,17	882	853	—3,3
69,73	11,22	17,38	801	792	—1,1

Hier wurde die additive Konstante zu 225 angenommen; die berechneten Werte zeigen eine maximale Abweichung von 3,8% und eine mittlere von 1,6%.

Barium hat eine mit dem Kalzium vergleichbare positive Wirkung.

Tabelle 10

Wärmeausdehnung von  $\text{Na}_2\text{O}-\text{BaO}-\text{SiO}_2$ -Gläsern (25–90°) [19]

$\text{SiO}_2\%$	$\text{BaO}\%$	$\text{Na}_2\text{O}\%$	$10^3\alpha$		Diff. %
			gem.	ber.	
72,86	3,03	23,30	1102	1099	—0,3
71,46	5,98	20,95	1068	1077	+0,8
70,83	8,59	21,11	1048	1033	—1,4
68,72	11,07	19,49	1034	1053	+1,8
68,33	14,16	17,39	1001	988	—1,3
66,33	17,28	15,89	950	961	+1,1
64,94	19,38	14,98	956	938	—1,9
63,18	22,37	12,52	888	877	—1,2
62,67	24,25	11,72	884	864	—2,2

Die Rechnung wurde mit der Gleichung

$$10^8\alpha = 35(\text{Na}_2\text{O}) + 8(\text{BaO}) + 260$$

durchgeführt; der maximale Fehler ist 2,2% und der durchschnittliche 1,3%. Bleioxyd wirkt noch weniger als Bariumoxyd.

Tabelle 11

Wärmeausdehnung von  $\text{Na}_2\text{O}$ — $\text{PbO}$ — $\text{SiO}_2$ -Gläsern [20]

$\text{SiO}_2\%$	$\text{PbO}\%$	$\text{Na}_2\text{O}\%$	$10^8\alpha$		Diff. %
			gem.	ber.	
51,21	41,83	5,61	705	715	+1,4
52,61	39,24	6,90	729	748	+2,6
53,58	37,45	7,88	761	773	+1,6
54,10	36,60	8,27	781	783	+0,3
54,84	33,96	10,02	844	831	—1,5
55,87	31,57	11,35	880	864	—1,8
58,52	28,01	12,40	903	884	—2,2
60,30	24,33	13,83	934	915	—2,1
61,67	22,94	14,06	929	916	—1,4
65,95	16,35	16,34	966	964	—0,2

Hier wurde mit der Gleichung

$$10^8\alpha = 35(\text{Na}_2\text{O}) + 6(\text{PbO}) + 280$$

gerechnet, die maximale Abweichung beträgt 2,6%, die durchschnittliche 1,5%.

Untersuchen wir zinkoxydhaltige Natrongläser, so ergibt sich, das  $\text{ZnO}$  keine Wirkung auf die Wärmeausdehnung ausübt.

Tabelle 12

Wärmeausdehnung von  $\text{Na}_2\text{O}$ — $\text{ZnO}$ — $\text{SiO}_2$ -Gläsern (25—90°) [21]

$\text{SiO}_2\%$	$\text{Na}_2\text{O}\%$	$\text{ZnO}\%$	$10^8\alpha$		Diff. %
			gem.	ber.	
74,09	24,12	1,29	1081	1090	+0,8
73,48	21,95	3,51	1016	1018	+0,2
73,52	20,69	4,55	959	974	+1,6
73,36	19,52	6,12	917	932	+1,6
75,06	17,12	6,70	842	848	+0,7
72,11	17,28	9,24	875	854	—2,4
72,46	15,46	11,13	779	790	+1,4

Die Gleichung ist

$$10^8\alpha = 35(\text{Na}_2\text{O}) + 250,$$

und die Rechnung zeigt eine maximale Abweichung von 2,4%, während die durchschnittliche Differenz 1,2% beträgt.

Eine andere Serie solcher Gläser wurde zwischen 20—100° gemessen; hier muss die additive Konstante etwas modifiziert werden.

Tabelle 13

Wärmeausdehnung von  $\text{Na}_2\text{O}$ — $\text{ZnO}$ — $\text{SiO}_2$ -Gläsern (20—100°) [22]

$\text{SiO}_2\%$	$\text{Na}_2\text{O}\%$	$\text{ZnO}\%$	$10^8\alpha$		Diff. %
			gem.	ber.	
59,7	32,9	5,8	1451	1440	—0,8
59,9	27,6	11,9	1257	1255	—0,2
59,1	21,6	17,4	1085	1046	—3,6
59,1	16,5	23,8	873	867	—0,7
58,8	10,9	29,7	632	672	+3,2

Hier haben wir die Gleichung

$$10^8\alpha = 35(\text{Na}_2\text{O}) + 290,$$

welche eine maximale Abweichung von 3,6% und eine durchschnittliche von 1,7% ergibt.

Das vierwertige Titan hat keinen Einfluss auf die Wärmeausdehnung, wie dies aus Tabelle 14 ersichtlich ist.

Tabelle 14

Wärmeausdehnung von  $\text{Na}_2\text{O}$ — $\text{TiO}_2$ — $\text{SiO}_2$ -Gläsern (25—90°) [23]

$\text{SiO}_2\%$	$\text{Na}_2\text{O}\%$	$\text{TiO}_2\%$	$10^8\alpha$		Diff. %
			gem.	ber.	
73,42	23,68	1,94	1035	1019	—1,5
72,88	23,16	3,01	990	1000	+1,0
72,82	21,82	4,95	903	954	+5,6
73,30	18,78	6,88	874	846	—3,2
72,61	16,31	10,03	807	761	—5,6
72,41	11,90	14,91	619	606	—2,1



In diesem Fall kann dieselbe Gleichung benützt werden, die für einfache Natronsilikatgläser gilt; die maximale Abweichung beträgt 5,6% und die durchschnittliche 3,3%.

Bei zirkoniumdioxydhaltigen Gläsern muss man eine geringe negative Korrektur in der Gleichung anwenden:

$$10^3\alpha = 35(\text{Na}_2\text{O}) - 6(\text{ZrO}_2) + 255;$$

man erhält auf diese Weise eine maximale Differenz von 2,8% und eine durchschnittliche von 1,2%.

Tabelle 15

Wärmeausdehnung von  $\text{Na}_2\text{O}-\text{ZrO}_2-\text{SiO}_2$ -Gläsern (25—90°) [24]

SiO <sub>2</sub> %	Na <sub>2</sub> O%	ZrO <sub>2</sub> %	10 <sup>3</sup> α		Diff.%
			gem.	ber.	
73,77	24,70	0,95	1106	1114	+0,7
74,14	22,60	2,67	1028	1030	+0,2
72,80	22,15	3,54	1006	1009	+0,3
72,88	20,69	4,67	961	952	+0,9
72,96	20,19	5,39	935	928	—0,8
71,89	19,32	6,97	885	889	+0,4
71,97	18,90	8,25	844	867	+2,7
72,10	16,89	10,33	808	785	—2,8
71,01	22,45	5,35	1015	1010	—0,5
65,59	21,40	11,13	935	936	+0,1
61,10	21,75	15,15	910	925	+1,6
56,38	21,09	20,59	859	870	+1,1
75,00	18,74	5,80	871	875	+0,5
69,32	18,42	11,73	801	810	+1,1
65,08	18,78	14,80	845	822	—2,7

Leider haben wir keine Daten für Kaligläser, die eine dritte Komponente enthalten. Dagegen gibt es Daten für vier- und fünfkomponentige Gläser. Diese zeigen, dass die Faktoren, die oben für die dreikomponentigen Gläser angegeben wurden, ohne weiteres für mehrkomponentige Gläser gültig bleiben. Natürlich gelten sie nur bis zu gewissen Grenzen; sie können z. B. auf ein 80% PbO enthaltendes, natronfreies Glas nicht mehr angewandt werden. Im folgenden führen wir die zur Verfügung stehenden Daten von vier- und fünfkomponentigen Gläsern an. Die Ausdehnung eines MgO- und CaO-haltigen Natronglases kann durch die Gleichung

$$10^3\alpha = 35(\text{Na}_2\text{O}) - 8(\text{MgO}) + 10(\text{CaO}) + 220$$

ausgedrückt werden, die eine maximale Differenz von 3,1% und eine durchschnittliche von 1,8% liefert.

Tabelle 16

Wärmeausdehnung von  $\text{Na}_2\text{O}$ — $\text{MgO}$ — $\text{CaO}$ — $\text{SiO}_2$ -Gläsern (25—90°) [25]

$\text{SiO}_2\%$	$\text{Na}_2\text{O}\%$	$\text{MgO}\%$	$\text{CaO}\%$	$10^3\alpha$		Diff. %
				gem.	ber.	
74,76	14,84	1,64	7,52	781	802	+2,6
74,74	14,98	2,58	6,43	779	789	+1,3
75,58	14,48	3,66	5,48	775	751	—3,1
76,32	14,58	4,10	3,82	746	735	—1,5
76,00	14,98	4,85	3,14	739	737	—0,3

In eisenhaltigen Gläsern kommen immer  $\text{FeO}$  und  $\text{Fe}_2\text{O}_3$  nebeneinander vor; solche Natrongläser sehen wir in der folgenden Tabelle.

Tabelle 17

Wärmeausdehnung von  $\text{Na}_2\text{O}$ — $\text{FeO}$ — $\text{Fe}_2\text{O}_3$ — $\text{SiO}_2$ -Gläsern [26]

$\text{SiO}_2\%$	$\text{Na}_2\text{O}\%$	$\text{FeO}\%$	$\text{Fe}_2\text{O}_3\%$	$10^3\alpha$		Diff. %
				gem.	ber.	
72,18	23,80	0,63	2,21	1050	1071	+2,6
71,33	21,36	0,84	4,84	990	996	+0,2
69,02	22,36	1,05	6,52	999	1038	+3,9
70,00	17,38	1,05	9,95	862	878	+2,2
69,25	17,20	1,89	10,16	833	872	+3,9
66,63	15,34	1,78	15,42	839	828	—1,3
65,64	14,46	4,20	15,03	769	796	+3,5
63,72	13,66	3,88	17,19	799	777	—2,8
63,69	11,54	3,36	20,50	739	718	—2,8
62,97	10,64	3,99	21,90	673	691	+2,6

Man kann die gefundenen Ausdehnungskoeffizienten durch die Gleichung

$$10^3\alpha = 35(\text{Na}_2\text{O}) + 4(\text{Fe}_2\text{O}_3) + 230$$

ausdrücken, wobei der maximale Fehler 3,9% und der durchschnittliche 2,6% beträgt. Ferrooxyd übt also praktisch keinen Einfluss auf die Wärmeausdehnung aus.

Magnesiumoxyd und Zirkoniumdioxid enthaltende Gläser können auch mit den oben gefundenen Faktoren berechnet werden.

Tabelle 18

Wärmeausdehnung von  $\text{Na}_2\text{O}$ — $\text{MgO}$ — $\text{ZrO}_2$ — $\text{SiO}_2$ —Gläsern (25—90°) [24]

$\text{SiO}_2\%$	$\text{Na}_2\text{O}\%$	$\text{MgO}\%$	$\text{ZrO}_2\%$	$10^8\alpha$		Diff. %
				gem.	ber.	
72,77	20,42	3,24	—	939	943	+0,4
72,42	18,50	4,96	1,83	871	850	—2,4
73,15	18,40	3,46	3,74	863	856	—0,8
72,36	19,11	1,83	5,95	849	871	+2,6
71,34	18,82	0,23	8,01	848	863	+1,8
74,58	20,00	2,56	2,24	910	922	+1,3

Die Gleichung ist

$$10^8\alpha = 35(\text{Na}_2\text{O}) - 8(\text{MgO}) - 6(\text{ZrO}_2) + 255,$$

die maximale Abweichung beträgt 2,6% und die durchschnittliche 1,6%.  
Fünfkomponentige Gläser finden sich in Tabelle 19.

Tabelle 19

Wärmeausdehnung von  $\text{Na}_2\text{O}$ — $\text{K}_2\text{O}$ — $\text{CaO}$ — $\text{B}_2\text{O}_3$ — $\text{SiO}_2$ —Gläsern (25—90°) [27]

$\text{SiO}_2\%$	$\text{B}_2\text{O}_3\%$	$\text{Na}_2\text{O}\%$	$\text{K}_2\text{O}\%$	$\text{CaO}\%$	$10^8\alpha$		Diff. %
					gem.	ber.	
75,82	—	6,86	7,90	8,56	802	778	—3,0
75,38	0,66	6,84	8,02	8,52	795	780	—1,9
73,38	2,05	6,14	9,38	8,40	785	795	+1,2
69,06	5,44	7,54	8,22	8,64	746	751	+0,8
68,20	7,90	7,00	7,56	8,40	734	709	—3,4
66,50	9,58	7,04	7,40	8,72	714	710	—0,5
64,58	10,78	7,50	7,42	8,60	701	725	+3,4
62,42	13,65	6,26	8,06	8,90	693	705	+1,7
56,76	19,43	7,38	7,14	8,54	695	713	+2,6
53,26	22,54	6,74	6,98	9,10	694	692	—0,3
49,50	25,70	7,00	7,50	9,08	700	716	+2,3
41,98	33,79	6,52	7,38	8,56	739	691	—6,5

Die Rechnung kann mit Hilfe der Gleichung

$$10^8\alpha = 35(\text{Na}_2\text{O}) + 10(\text{K}_2\text{O}) + 10(\text{CaO}) + 215$$

erfolgen, solange der Anteil des Bortrioxys nicht über 2,5% liegt; ist er grösser, so wird die additive Konstante 190. Man erhält eine durchschnittliche Abweichung von 1,9% und eine maximale von 3,4%, bis zu etwa 30%  $\text{B}_2\text{O}_3$ ; darüber hinaus werden die Abweichungen grösser.

Es stehen auch Messungen der Ausdehnungskoeffizienten von industriellen Gläsern zur Verfügung. Man muss zu diesen bemerken, dass die Temperaturgrenzen oft nicht genügend sicher bekannt sind, und daher nehmen wir im allgemeinen die Grenzen 20—100° an. Zwischen anderen Grenzen wird man naturgemäss andere additiven Konstanten benützen.

Von WINKELMANN und SCHOTT [1] wurden bereits zahlreiche industrielle Gläser untersucht, deren Zusammensetzungen sie auch bestimmten. Aus ihren Messungen haben sie Faktoren zur Berechnung von  $\alpha$  abgeleitet, die aber keine sehr gute Annäherung erlauben; von späteren Autoren wurden diese vielfach modifiziert.

Wir benützen die verallgemeinerte Gleichung

$$10^8\alpha = 35(\text{Na}_2\text{O}) + 30(\text{K}_2\text{O}) - 8(\text{MgO}) + 10(\text{BaO}) + 6(\text{PbO}) + 10(\text{Fe}_2\text{O}_3) - 6(\text{ZrO}_2) + A,$$

wo für die additive Konstante  $A$  folgende Werte gelten:

bei Bleigläsern	(>5% PbO)	280,
bei Ba-Gläsern	(>50 BaO)	220,
bei Zn-Gläsern	(>5% ZnO)	250 und
bei weniger als 5% obiger Oxyde enthaltenden Gläsern		200.

Zuerst ziehen wir  $\text{PbO}$ , dann  $\text{BaO}$  und zuletzt  $\text{ZnO}$  in Betracht; wenn also ein Glas z. B. 8%  $\text{PbO}$  und 6%  $\text{BaO}$  enthält, so wird die Konstante 280; bei 4%  $\text{PbO}$  und 7%  $\text{ZnO}$  250 usw.

Wir sehen, dass man mit den für drei- und vierkomponentigen Gläsern gefundenen Faktoren eine bessere Übereinstimmung als mit den alten Faktoren von WINKELMANN und SCHOTT erhält; mit den neuen Faktoren ergibt sich eine maximale Differenz von 4,8% und im Mittel 2,4%. Nur bei einem Glas, das mehr als 30%  $\text{B}_2\text{O}_3$  enthält, ergibt sich eine Differenz von 6,1%.

Eine andere Serie wurde von PETERS und CRAGOE gemessen, hier sind aber die Temperaturgrenzen sehr verschieden, nämlich von etwa 20° bis 402—513°. Wir benützen hier grössere additive Konstanten und zwar für gewöhnliche Gläser 400, für Blei- und Borosilikatgläser (mit weniger als 6%  $\text{B}_2\text{O}_3$ ) 380 und für mehr als 6%  $\text{B}_2\text{O}_3$  enthaltende Gläser 300. Die Faktoren der Oxyde bleiben dieselben.

Tabelle 20

Wärmeausdehnung der Gläser von WINKELMANN und SCHOTT [1]

SiO <sub>2</sub> %	B <sub>2</sub> O <sub>3</sub> %	Al <sub>2</sub> O <sub>3</sub> %	Na <sub>2</sub> O%	K <sub>2</sub> O%	CaO%	BaO%	ZnO%	PbO%	10 <sup>6</sup> α		Diff%
									gem.	ber.	
51,3	14	4,5	—	—	—	25	5	—	457	470	+2,8
32,8	31	7	1	3	—	—	—	25	523	555	+6,1
72	12	5	11	—	—	—	—	—	590	585	—0,8
45,2	—	0,5	0,2	7,5	—	—	—	46,4	787	790	+0,4
54,3	1,5	—	3	8	—	—	—	33	793	823	+3,8
48,8	3	—	1,0	7,5	—	29	10,3	—	793	770	—2,9
68,3	10	—	10	9,5	—	—	2	—	797	835	+4,8
28,4	—	—	—	2,5	—	—	—	69	803	769	—4,2
67,5	2	2,5	14	—	7	—	7	—	803	810	+0,9
69,1	2,5	—	4	16	8	—	—	—	883	900	+1,9
51,7	—	—	1,5	9,5	—	20	7	10	900	878	—2,4
68,2	—	—	16,5	—	—	—	2	13,1	903	935	+3,5
68,1	3,5	—	5	16	—	—	7	—	917	905	—1,3
73,2	—	—	18,5	—	8	—	—	—	967	928	—4,2
65,5	2,5	—	5	15	—	9,6	2	—	963	941	—1,9
64,3	1,5	—	3	20	11	—	—	—	973	1015	+4,3
71,7	—	2	10	13	3	—	—	—	1000	970	—3,0
54,8	—	2,5	6	11,5	—	—	—	25	1017	985	—3,0
69,7	—	—	—	25	5	—	—	—	1017	1000	—1,7
64,3	—	2,5	9	15	9	—	—	—	1047	1055	+0,8
58,8	—	4	10	14	—	—	8	6	1080	1086	+0,6
43,0	—	4	8	11	—	—	—	34	1093	1094	+0,1
57	—	12	13	13	—	—	5	—	1123	1095	—2,7

(Der geringe Arsengehalt einiger Gläser wurde nicht beachtet.)

Bei dem zehnten Glas der Tabelle (mit 54,0% SiO<sub>2</sub>) ist der gemessene Wert offenbar falsch, da das vorangehende Glas, dessen Zusammensetzung kaum davon abweicht, eine um mehr als 20% grössere Ausdehnung (gemessen) hat, welche gut mit dem berechneten Wert übereinstimmt. Von diesem Glas abgesehen erhalten wir eine maximale Abweichung von 3,5% und eine durchschnittliche von 1,4%. Der geringe As<sub>2</sub>O<sub>3</sub>- und Fe<sub>2</sub>O<sub>3</sub>-Gehalt einiger Gläser wurde ausser acht gelassen.

Zuletzt teile ich die Ausdehnungskoeffizienten einiger Gläser aus der Industrie mit, die zwischen 20—300° gemessen wurden; die additive Konstante beträgt bei gewöhnlichen Gläsern 300, bei hochtonerdehaltigen Gläsern 280, bei PbO-Gläsern (über 5% PbO) 360 und bei mehr als 10% B<sub>2</sub>O<sub>3</sub> enthaltenden Gläsern 180.

Tabelle 21

Wärmeausdehnung der Gläser von PETERS und CRAGOE (20—402 bis 513°) [28]

SiO <sub>2</sub> %	B <sub>2</sub> O <sub>3</sub> %	Na <sub>2</sub> O%	K <sub>2</sub> O%	MgO%	CaO%	BaO%	ZnO%	PbO%	10 <sup>a</sup> α		Diff. %
									gem.	ber.	
71,7	—	13,4	0,1	0,3	12,5	—	—	—	990	995	+0,7
72,0	—	16,2	0,3	—	10,2	—	—	—	1080	1074	—0,6
72,0	—	13,7	—	—	12,4	—	—	—	1010	1004	—0,6
72,5	—	13,8	0,2	—	11,5	—	—	—	990	1004	+1,4
71,3	—	10,4	0,4	—	14,7	—	—	—	940	923	—1,8
44,3	—	3,5	5,0	—	3,0	—	—	44,0	970	946	—2,5
58,8	1,7	1,7	8,3	—	—	14,3	2,5	12,7	880	908	+3,5
47,6	4,0	2,0	6,0	—	—	29,2	9,9	—	900	922	+2,4
53,9	—	1,0	7,6	—	2,0	—	—	35,2	880	874	—0,7
54,0	—	1,0	6,0	—	2,0	—	—	36,7	700	837	+19,6
68,5	3,5	12,0	5,0	—	—	9,7	1,0	—	1020	1028	+0,8
67,0	3,5	12,0	5,0	—	—	10,6	1,5	—	1040	1035	—0,5
66,5	7,8	9,8	5,9	—	—	7,8	2,0	—	900	898	—0,2
74,0	—	17,1	—	3,1	5,8	—	—	—	1070	1055	—1,4
74,3	—	17,2	—	3,0	5,5	—	—	—	1030	1055	+2,4
74,0	—	16,1	—	2,7	7,2	—	—	—	1020	1034	+1,4

Tabelle 22

Die Wärmeausdehnung einiger industrieller Gläser (20—300°)

SiO <sub>2</sub> %	B <sub>2</sub> O <sub>3</sub> %	Al <sub>2</sub> O <sub>3</sub> %	Na <sub>2</sub> O%	K <sub>2</sub> O%	MgO%	CaO%	BaO%	PbO%	10 <sup>a</sup> α		Diff. %
									gem.	ber.	
73,0	14,0	1,7	4,4	—	—	—	—	5,7	360	368	+2,2
80,0	13	2	4	—	—	—	—	—	330	320	—3,0
74,6	18	1,0	4,2	1,7	—	0,3	—	—	370	381	+3,0
77,3	12,8	1,7	1,4	6,6	—	—	—	—	413	427	+3,4
58,5	3	22,4	—	0,8	8,9	6,3	—	—	370	367	—0,8
51,3*	1,0	25,3	—	—	4,2	8,3	5,3	—	415	416	+0,2
67,5	22	2	6,5	2	—	—	—	—	460	467	+1,8
70,5	—	1,0	16,0	1,0	3,9	5,4	2,0	—	890	934	+4,9
55,6	—	—	4,0	8,0	—	—	—	32,4	920	934	+1,5
62,09	—	0,60	6,7	8,26	—	—	—	21,75	960	973	+1,4
57,4	—	1,3	3,9	7,6	—	—	—	29,3	900	900	±0
53,9	—	1,2	5,3	7,5	—	—	3,6	28,5	990	978	—1,2
70,7	—	1,9	15,7	—	3,9	7,6	—	—	950	896	—5,7

\* Dieses Glas enthält 4,6% P<sub>2</sub>O<sub>5</sub>, das auf die Wärmeausdehnung keinen Einfluss ausübt.  
(Der geringe As<sub>2</sub>O<sub>5</sub>- bzw. Sb<sub>2</sub>O<sub>5</sub>-Gehalt wurde ausser acht gelassen.)



Auch bei diesen Gläsern beträgt die maximale Abweichung nicht mehr als 5,7% und die durchschnittliche Abweichung ist 2,2%.

### Die Deutung der Wärmeausdehnung

Aus den mitgeteilten Berechnungen, die etwa 230 verschiedene Gläser erfassen, lassen sich folgende Schlüsse ziehen :

1. Man kann die Wärmeausdehnung verschiedenster Gläser durch Gleichungen vom Typ

$$10^8\alpha = a(\text{Na}_2\text{O}) + b(\text{K}_2\text{O}) + c(\text{MgO}) + \dots + A$$

mit guter Annäherung berechnen, wo die in Klammer gesetzten Formeln die Prozentzahlen der betreffenden Oxyde,  $a$ ,  $b$ ,  $c$  usw. konstante Faktoren und  $A$  eine additive Konstante bedeuten, die vom chemischen Typ des Glases und von den Temperaturgrenzen der Messung abhängt.

2. Die Einwirkung der gerüstbildenden Oxyde ( $\text{SiO}_2$ ,  $\text{B}_2\text{O}_3$ ,  $\text{BeO}$ ,  $\text{Al}_2\text{O}_3$ ,  $\text{P}_2\text{O}_5$ ) äussert sich nur in der additiven Konstante  $A$  der Gleichungen.

3. Von den gerüstmodifizierenden Oxyden übt  $\text{Li}_2\text{O}$  die grösste Wirkung aus, dann folgen  $\text{Na}_2\text{O}$  und  $\text{K}_2\text{O}$ . Die zweiwertigen Ionen sind von geringerer Wirkung. Drei- und vierwertige Ionen üben nur ausnahmsweise eine Wirkung aus, die positiv oder negativ sein kann, aber in beiden Fällen gering bleibt.

Bekanntlich ist die Bindung zwischen dem Zentralion der glasbildenden Oxyde und dem Sauerstoffion sehr stark\*. Die Abstände Si-O etc. werden auch bei erhöhter Temperatur kaum vergrössert und wegen der unregelmässigen Zusammenknüpfung der  $\text{SiO}_4$ -etc.- Tetraeder können keine »kooperativen« Drehungen vorkommen, die eine bedeutende Wärmeausdehnung hervorrufen würden. Daher wäre die Wärmeausdehnung des Glasgerüstes an sich (ohne die gerüstmodifizierenden Kationen) sehr gering und für unsere Zwecke vernachlässigbar.

Dagegen werden die gerüstmodifizierenden Kationen (Alkalien, Erdalkalien usw.) eine Wärmebewegung ausführen, die wegen ihrer schwachen Bindung sehr intensiv ist ; je leichter das Ion und je schwächer seine Bindung ist, desto intensivere Schwingungen wird es ausführen. Es ist zu erwarten, dass die intensivere Wärmebewegung eine Verlängerung des Abstandes M-O (die die Schwächung der Bindung bedeutet) hervorrufen wird. Man findet im allgemeinen, dass die Zusammenwirkung von Ionengewicht und Ionenradius die Einwirkung eines Ions auf die Wärmeausdehnung bestimmt. Die mehr-

\* Die Bindungsstärke allein liefert aber keine Erklärung für die Glasbindung ; auch die Bindungen S—O und Cl—O sind sehr stark, es gibt aber keine Sulfat- oder Perchloratgläser.

wertigen Kationen üben wegen der stärkeren Anziehung zwischen dem Kation und dem  $O^{2-}$ -Ion eine weit geringere Wirkung aus, so ist z. B. die von Titan zu vernachlässigen, die von Zirkonium sogar negativ.

Nach der Theorie von DEBYE wird die Wärmeausdehnung durch die Anharmonizität der Schwingungen verursacht.

Zusammenfassend kann man sagen, dass die neuen Gleichungen es gestatten, die Berechnung der Wärmeausdehnung mit einer die bisherige übertreffenden Genauigkeit für Gläser im Zusammenhang mit ihrer chemischen Zusammensetzung auszuführen. Darüber hinaus wird die verschiedenartige Rolle der gerüstbildenden und gerüstmodifizierenden Ionen bzw. Oxyde im Glas durch diese Gleichungen geklärt.

### LITERATUR

1. A. WINKELMANN und O. SCHOTT, *Ann. Phys.*, **51**, 735, 1894.
2. S. ENGLISH, W. E. S. TURNER, *J. Am. Ceram. Soc.*, **10**, 551, 1927; **12**, 760, 1929.
3. P. GILARD und L. DUBRUL, *Verr. silicat. ind.*, **5**, 122, 1934.
4. H. H. BLAU, *J. Soc. Glass Techn.*, **35**, 304, 1951.
5. F. P. HALL, *J. Am. Ceram. Soc.*, **13**, 182, 1930.
6. R. SCHMIDT, *Der praktische Glasschmelzer*, 5. Aufl. Fachbuchverlag, Leipzig, 1953; S. 133.
7. A. COUSEN und W. E. S. TURNER, *J. Soc. Glass Techn.*, **12**, 169, 1928.
8. S. ENGLISH und W. E. S. TURNER, *J. Soc. Glass Techn.*, **5**, 121, 1921.
9. E. RENCKER, *C. r.* **197**, 840, 1933.
10. S. ENGLISH und W. E. S. TURNER, *J. Soc. Glass Techn.*, **7**, 155, 1923.
11. R. WENIG und E. ZSCHIMMER, *Sprechsaal*, **62**, 855; 874; 889; 1929.
12. V. DIMBLEBY, S. ENGLISH, F. W. HODKIN und W. E. S. TURNER, *J. Soc. Glass Techn.*, **8**, 173, 1924.
13. S. ENGLISH und W. E. S. TURNER, *J. Soc. Glass Techn.*, **5**, 183, 1921.
14. C. E. BRACKBILL, H. A. MCKINSTRY und F. A. HUMMEL, *J. Am. Ceram. Soc.*, **34**, 107, 1951.
15. H. SEEMANN, *Acta Cryst.*, **9**, 251, 1956.
16. S. ENGLISH und W. E. S. TURNER, *J. Soc. Glass Techn.*, **4**, 115, 1920.
17. E. SEDDON, W. E. S. TURNER und F. WINKS, *J. Soc. Glass Techn.*, **13**, 5, 1934.
18. S. ENGLISH und W. E. S. TURNER, *J. Soc. Glass Techn.*, **4**, 126, 1920.
19. S. ENGLISH und W. E. S. TURNER, *J. Soc. Glass Techn.*, **11**, 425, 1927.
20. J. MORI, *J. Japan. Cer. Ass.*, **368**, 176, 1923.
21. S. ENGLISH, W. E. S. TURNER und F. WINKS, *J. Soc. Glass Techn.*, **12**, 287, 1928.
22. L. D. FETTEROLF und C. W. PARMELEE, *J. Am. Ceram. Soc.*, **12**, 193, 1929.
23. A. R. SHEEN und W. E. S. TURNER, *J. Soc. Glass Techn.*, **8**, 187, 1924.
24. V. DIMBLEBY, S. ENGLISH, E. M. FIRTH, F. W. HODKIN und W. E. S. TURNER, *J. Soc. Glass Techn.*, **11**, 52, 1927.
25. S. ENGLISH und W. E. S. TURNER, *J. Soc. Glass Techn.*, **6**, 228, 1922.
26. S. ENGLISH, H. W. HOWES, W. E. S. TURNER und F. WINKS, *J. Soc. Glass Techn.*, **12**, 31, 1928.
27. W. E. S. TURNER und F. WINKS, *J. Soc. Glass Techn.*, **9**, 389, 1925.
28. C. G. PETERS und C. H. CRAGOE, *J. Optic. Soc. Am.*, **4**, 105, 1920.

# СВЯЗЬ МЕЖДУ СТРУКТУРОЙ И ФИЗИЧЕСКИМИ СВОЙСТВАМИ СТЕКЛА

## III. Термическое расширение стекла

И. НАРАИ—САБО

### Резюме

1. Результаты существующих измерений коэффициента термического расширения стекол с известным составом обрабатываются с помощью линейных уравнений; эти уравнения отличаются от других известных уравнений существенно тем, что образующие решетку оксиды  $\text{SiO}_2$  и  $\text{B}_2\text{O}_3$  не принимают участие в расширении, т. е. им соответствует фактор, равный нулю. Термическое расширение в таком понятии происходит практически только из-за наличия скелетомодифицирующих ионов, главным образом щелочных.
2. В уравнениях имеется аддитивная постоянная, определенная типом стекла.
3. Различия между измеренными и вычисленными на основании этих уравнений коэффициентами расширения составляют в среднем около 1—3 процента, т. е. значительно меньше чем между вычисленными с помощью других известных уравнений, которые впрочем были применимы только к определенным сортам стекол.
4. Кратко дискутируется связь между термическим расширением и свойствами скелета стекла.



# INTENSITY FORMULAE FOR ${}^7\Pi \leftrightarrow {}^7\Sigma$ BAND

By

I. KOVÁCS and O. SCARI

DEPARTMENT OF ATOMIC PHYSICS, TECHNICAL UNIVERSITY, BUDAPEST

(Received: 1. VIII. 1958)

Explicit expressions are given concerning the intensity distribution occurring in the branches of bands  ${}^7\Pi(a) \leftrightarrow {}^7\Sigma$ ,  ${}^7\Pi(b) \leftrightarrow {}^7\Sigma$ . The intensity distribution calculated on the basis of the established formulae is compared with measurements carried out on the  ${}^7\Pi \rightarrow {}^7\Sigma$  bands of MnH and relatively good agreement is found.

## 1. §.

The problem of intensity distribution occurring in the rotational spectra of multiplet bands has already been dealt with by many researchers, from the theoretical [1] as well as from the experimental point of view [2]. In general the theoretical investigations relate to a wider field than the experimental data, providing hereby the experimental researcher with some guidance in case of an analysis of a new kind [3]. The reverse rarely occurs, when namely the analysis of the band and the intensity distribution are known from the experimental side, but the appropriate theoretical formulae are missing. An example for such a case is NEVIN's work [4], which contains the analysis of a  ${}^7\Pi \rightarrow {}^7\Sigma$  band in the spectrum of MnH as well as the estimation of the intensity of the observed spectrum lines. The purpose of the present paper is to give the lacking theoretical intensity formulae and to compare these with the experiment.

## 2. §.

As is known, in case of the thermal equilibrium the intensity of the lines of emission bands can be given by the following expression:

$$I = g' \nu^4 i e^{-\frac{E_i}{kT}}, \quad (1)$$

where  $g'$  is constant inside each band, whereas the other symbols have the usual meaning. The task of the theory is the calculation of the  $i$  factors for all branches occurring in the rotational transitions. For this the corresponding expressions for the amplitudes

$$z_a({}^7\Pi_\Omega {}^7\Sigma_\Omega') = \int \Psi_a^*({}^7\Pi_\Omega) z \Psi_a({}^7\Sigma_\Omega') d\tau \quad (2)$$

are used, the absolute values of which may be found in a paper by KRONIG [5]. It is, however, known, that the  $\Sigma$  terms exist only in HUND's case  $b$ ), therefore

concerning the  ${}^7\Sigma$  term the eigenfunctions of case  $b)$  of the following form are introduced:

$$\Psi_b({}^7\Sigma_{K'}) = \sum_{\Omega=-3}^{-3} S_{\Omega, K'}(\Sigma) \Psi_a({}^7\Sigma_{\Omega}); \quad (3)$$

hereby the amplitudes become

$$z({}^7\Pi_{\Omega} {}^7\Sigma_{K'}) = \int \Psi_a^*({}^7\Pi_{\Omega}) z \Psi_b({}^7\Sigma_{K'}) d\tau; \quad (4)$$

the threefold square of which summed over the magnetic quantum numbers give the  $i$  factors referring to the transitions  ${}^7\Pi(a) \leftrightarrow {}^7\Sigma(b)$ . The transformation matrix elements  $S_{\Omega, K}(\Sigma)$  occurring in (3) for the  ${}^7\Sigma$  terms were already earlier published by us [6]. Part of the  $i$  factors which can be obtained on the basis of (4) occur in the third column of Table I. According to detailed calculations in the above case 147 branches can exist, from among which the  $i$  factors of the branches  ${}^R P_{64}, {}^N P_{24}, {}^S Q_{64}, {}^O Q_{24}, {}^T R_{64}, {}^P R_{24}$  are proportional to  $\frac{1}{J}$ , the intensity of the branches  ${}^N P_{46}, P_4, {}^R P_{42}, {}^O Q_{46}, Q_4, {}^S Q_{42}, {}^P R_{46}, R_4, {}^T R_{42}$  is zero, whereas the  $i$  factors of the other not enumerated branches are directly proportional to  $J$ . As regards branches with an intensity differing from zero, the rule holds that the intensity of the  $Q$  branches to good approximation is twice the intensity of the corresponding  $P$  resp.  $R$  branches. So as to save space, however, from among the 147 branches the  $i$  factors of those 55 branches only are given the intensity of which in case of a transition  ${}^7\Pi(b) \leftrightarrow {}^7\Sigma(b)$  does not differ from zero.

The  ${}^7\Pi$  terms can in general be rendered well by the formulae of HUND's case  $a)$  only in the range of the lower rotational quantum numbers. With increasing rotational quantum numbers namely starts the transition towards the case  $b)$  and the difficulty in describing the conditions consists in that no expression is known concerning the  ${}^7\Pi$  energies valid with a satisfactory accuracy for any value of the binding constant  $Y = A/B$ . Thus we have to content ourselves with the knowledge of the energies of the relatively simple case  $b)$ , respectively with the amplitudes produced by the use of the transformation matrix elements calculated with their aid

$$z({}^7\Pi_K {}^7\Sigma_{K'}) = \int \Psi_b^*({}^7\Pi_K) z \Psi_b({}^7\Sigma_{K'}) d\tau, \quad (5)$$

where

$$\Psi_b({}^7\Pi_K) = \sum_{\Omega=-3}^{-3} S_{\Omega, K}(\Pi) \Psi_a({}^7\Pi_{\Omega}), \quad (6)$$

and the elements of the transformation of  ${}^7\Pi$  state are the following



$$S_{4,J+3} = + \sqrt{\frac{(J-3)(J-2)(J-1)J}{8(J+3)(2J+1)(2J+3)(2J+5)}};$$

$$S_{3,J+3} = + \sqrt{\frac{3(J-2)(J-1)(J+4)}{4(J+3)(2J+1)(2J+3)(2J+5)}};$$

$$S_{2,J+3} = + \sqrt{\frac{15(J-1)J(J+4)}{8(2J+1)(2J+3)(2J+5)}};$$

$$S_{1,J+3} = + \sqrt{\frac{5J(J+2)(J+4)}{2(2J+1)(2J+3)(2J+5)}};$$

$$S_{0,J+3} = + \sqrt{\frac{15(J+1)(J+2)(J+4)}{8(2J+1)(2J+3)(2J+5)}};$$

$$S_{-1,J+3} = + \sqrt{\frac{3J(J+2)(J+4)}{4(2J+1)(2J+3)(2J+5)}};$$

$$S_{-2,J+3} = + \sqrt{\frac{(J-1)J(J+4)}{8(2J+1)(2J+3)(2J+5)}};$$

$$S_{4,J+2} = - \sqrt{\frac{3(J-3)(J-2)(J-1)(J+4)}{8(J+2)(J+3)(2J+1)(2J+3)}};$$

$$S_{3,J+2} = - \sqrt{\frac{(J-2)(J-1)(2J+9)^2}{4(J+2)(J+3)(2J+1)(2J+3)}};$$

$$S_{2,J+2} = - \sqrt{\frac{5(J-1)(J+6)^2}{8(J+2)(2J+1)(2J+3)}};$$

$$S_{1,J+2} = - \sqrt{\frac{15}{2(2J+1)(2J+3)}};$$

$$S_{0,J+2} = + \sqrt{\frac{5J(J+1)}{8(2J+1)(2J+3)}};$$

$$S_{-1,J+2} = + \sqrt{\frac{2J+3}{4(2J+1)}};$$

$$S_{-2,J+2} = + \sqrt{\frac{3(J-1)(J+2)}{8(2J+1)(2J+3)}};$$

$$S_{4,J+1} = + \sqrt{\frac{15(J-3)(J-2)(J-1)(J+3)(J+4)}{8(J+1)(J+2)(2J-1)(2J+1)(2J+5)}};$$

$$S_{3,J+1} = + \sqrt{\frac{5(J-2)(J-1)(J+3)(J+7)^2}{4(J+1)(J+2)(2J-1)(2J+1)(2J+5)}};$$

$$S_{2,J+1} = - \sqrt{\frac{(J-1)(J^2-13J-50)^2}{8(J+1)(J+2)(2J-1)(2J+1)(2J+5)}};$$

$$S_{1,J+1} = - \sqrt{\frac{3(J^2+2J-5)^2}{2(J+1)(2J-1)(2J+1)(2J+5)}};$$

$$S_{0,J+1} = - \sqrt{\frac{J(J+7)^2}{8(2J-1)(2J+1)(2J+5)}};$$

$$S_{-1,J+1} = + \sqrt{\frac{5(J+1)^3}{4(2J-1)(2J+1)(2J+5)}};$$

$$S_{-2,J+1} = + \sqrt{\frac{15(J-1)(J+1)(J+2)}{8(2J-1)(2J+1)(2J+5)}};$$

$$S_{4,J} = - \sqrt{\frac{5(J-3)(J-2)(J+3)(J+4)}{4J(J+1)(2J-1)(2J+3)}};$$

$$S_{3,J} = - \sqrt{\frac{30(J-2)(J+3)}{J(J+1)(2J-1)(2J+3)}};$$

$$S_{2,J} = + \sqrt{\frac{3(J-3)^2(J+4)^2}{4J(J+1)(2J-1)(2J+3)}};$$

$$S_{1,J} = + \sqrt{\frac{9(J-1)(J+2)}{J(J+1)(2J-1)(2J+3)}};$$

$$S_{0,J} = - \sqrt{\frac{3(J-1)(J+2)}{4(2J-1)(2J+3)}};$$

$$S_{-1,J} = 0$$

$$S_{-2,J} = + \sqrt{\frac{5J(J+1)}{4(2J-1)(2J+3)}};$$

$$S_{4,J-1} = + \sqrt{\frac{15(J-3)(J-2)(J+2)(J+3)(J+4)}{8(J-1)J(2J-3)(2J+1)(2J+3)}};$$

$$S_{3,J-1} = - \sqrt{\frac{5(J-6)^2(J-2)(J+2)(J+3)}{4(J-1)J(2J-3)(2J+1)(2J+3)}};$$

$$S_{2,J-1} = - \sqrt{\frac{(J+2)(J^2+15J-36)^2}{8(J-1)J(2J-3)(2J+1)(2J+3)}};$$

$$S_{1,J-1} = + \sqrt{\frac{3(J^2-6)^2}{2J(2J-3)(2J+1)(2J+3)}};$$

$$S_{0,J-1} = - \sqrt{\frac{(J-6)^2(J+1)}{8(2J-3)(2J+1)(2J+3)}};$$

$$S_{-1,J-1} = - \sqrt{\frac{5J^3}{4(2J-3)(2J+1)(2J+3)}};$$

$$S_{-2,J-1} = + \sqrt{\frac{15(J-1)J(J+2)}{8(2J-3)(2J+1)(2J+3)}};$$

$$S_{4,J-2} = - \sqrt{\frac{3(J-3)(J+2)(J+3)(J+4)}{8(J-2)(J-1)(2J-1)(2J+1)}};$$

$$S_{3,J-2} = + \sqrt{\frac{(J+2)(J+3)(2J-7)^2}{4(J-2)(J-1)(2J-1)(2J+1)}};$$

$$S_{2,J-2} = - \sqrt{\frac{5(J-5)^2(J+2)}{8(J-1)(2J-1)(2J+1)}};$$

$$S_{1,J-2} = - \sqrt{\frac{15}{2(2J-1)(2J+1)}};$$

$$S_{0,J-2} = + \sqrt{\frac{5J(J+1)}{8(2J-1)(2J+1)}};$$

$$S_{-1,J-2} = - \sqrt{\frac{2J-1}{4(2J+1)}};$$

$$S_{-2,J-2} = + \sqrt{\frac{3(J-1)(J+2)}{8(2J-1)(2J+1)}};$$

$$S_{4,J-3} = + \sqrt{\frac{(J+1)(J+2)(J+3)(J+4)}{8(J-2)(2J-3)(2J-1)(2J+1)}};$$

$$S_{3,J-3} = - \sqrt{\frac{3(J-3)(J+1)(J+2)(J+3)}{4(J-2)(2J-3)(2J-1)(2J+1)}};$$

$$S_{2,J-3} = + \sqrt{\frac{15(J-3)(J+1)(J+2)}{8(2J-3)(2J-1)(2J+1)}};$$

$$S_{1,J-3} = - \sqrt{\frac{5(J-3)(J-1)(J+1)}{2(2J-3)(2J-1)(2J+1)}};$$

$$S_{0,J-3} = + \sqrt{\frac{15(J-3)(J-1)J}{8(2J-3)(2J-1)(2J+1)}};$$

$$S_{-1,J-3} = - \sqrt{\frac{3(J-3)(J-1)(J+1)}{4(2J-3)(2J-1)(2J+1)}};$$

$$S_{-2,J-3} = + \sqrt{\frac{(J-3)(J+1)(J+2)}{8(2J-3)(2J-1)(2J+1)}}.$$

From (5) the  $i$  factors relative to the transitions  ${}^2\Pi(b) \leftrightarrow {}^2\Sigma(b)$  can be calculated. Those differing from zero are to be found in the fourth column of Table I. Apart from the selection rule  $\Delta J = 0, \pm 1$  valid for case  $a$ ) also the condition  $\Delta K = 0, \pm 1$  is characteristic for the latter. It can be stated in general that if the  ${}^2\Pi$  term is belonging to the case  $b$ ), then the  $i$  factors of the main branches ( $\Delta J - \Delta K = 0$ ) are proportional to  $J$ , among the satellite branches those, for which  $\Delta J - \Delta K = \pm 1$ , are proportional to  $1/J$ , whereas those, for which  $\Delta J - \Delta K = \pm 2$ , are proportional to  $1/J^3$ . In the main branches the intensity of the  $Q$  branches is here also approximately twice that of the corresponding  $P$  respectively  $R$  branches, but in the satellite branches, if there exist corresponding branches, the situation is just the opposite.

Table I  
Intensity factors for  ${}^7\Pi \leftrightarrow {}^7\Sigma$  bands

Branches		i-factors	
${}^7\Pi \rightarrow {}^7\Sigma$	${}^7\Sigma \rightarrow {}^7\Pi$	${}^7\Pi(a)$	${}^7\Pi(b)$
$P_1(J)$	$R_1(J-1)$	$\frac{(J+1)(J+2)^2(J+3)^2}{8J(2J-3)(2J-1)(2J+1)}$	$\frac{(J-4)(2J+1)}{2J-5}$
$Q_1(J)$	$Q_1(J)$	$\frac{(J-2)(J+2)(J+3)^2}{8J(2J-3)(2J-1)}$	$\frac{(J-3)(J+1)(2J+1)}{(J-2)J}$
$R_1(J)$	$P_1(J+1)$	$\frac{(J-2)(J-1)(J+2)(J+3)}{8(2J-3)(2J-1)(2J+1)}$	$\frac{(J-1)(2J+3)}{2J-3}$
${}^qP_{21}(J)$	${}^qR_{12}(J-1)$	$\frac{3(J-2)(J+1)^2(J+2)^2}{4J(2J-3)(2J-1)(2J+1)}$	$\frac{3(2J+1)}{(J-2)J}$
${}^RP_{21}(J)$	${}^PQ_{12}(J)$	$\frac{3(J-2)(J-1)(J+2)^2}{4J(2J-3)(2J-1)}$	$\frac{3(J-1)(2J+1)}{(J-2)J(2J-3)}$
${}^RP_{31}(J)$	${}^PR_{13}(J-1)$	$\frac{15(J-2)(J-1)J(J+1)^2}{8J(2J-3)(2J-1)(2J+1)}$	$\frac{15(J-1)}{(J-2)J(2J-5)(2J-3)}$
${}^PQ_{12}(J)$	${}^RQ_{21}(J)$	$\frac{3(J-2)(J+2)(J+3)^2}{8J(J+1)(2J-1)}$	$\frac{3(J-3)(2J+1)}{(J-2)J(2J-3)}$
${}^qR_{12}(J)$	${}^qP_{21}(J+1)$	$\frac{3(J-2)(J-1)(J+2)(J+3)}{8(J+1)(2J-1)(2J+1)}$	$\frac{3(2J+3)}{(J-1)(J+2)}$
$P_2(J)$	$R_2(J-1)$	$\frac{(J-2)(J+1)(J+2)^2}{J(2J-1)(2J+1)}$	$\frac{(J-3)^2(J+1)(2J+1)}{(J-2)J(2J-3)}$
$Q_2(J)$	$Q_2(J)$	$\frac{(J-2)(J-1)(J+2)^2}{J(J+1)(2J-1)}$	$\frac{(J^2-J-5)^2(2J+1)}{(J-2)(J-1)J(J+1)}$
$R_2(J)$	$P_2(J+1)$	$\frac{(J-2)(J-1)J(J+2)}{(J+1)(2J-1)(2J+1)}$	$\frac{(J-2)J(J+2)(2J+3)}{(J-1)(J+1)(2J-1)}$
$P_{32}(J)$	${}^qR_{23}(J-1)$	$\frac{5(J-2)(J-1)(J+1)}{8(2J-1)(2J+1)}$	$\frac{5(J+1)(2J-5)}{(J-2)(J-1)J}$
${}^RQ_{32}(J)$	${}^PQ_{23}(J)$	$\frac{5(J-2)(J-1)}{8(2J-1)}$	$\frac{5(J-2)(2J+1)(2J+3)}{(J-1)(J+1)(2J-3)(2J-1)}$
${}^RP_{42}(J)$	${}^PR_{24}(J-1)$	0	$\frac{30}{(J-1)(2J-3)(2J-1)}$

Branches		i-factors	
${}^7\Pi \rightarrow {}^7\Sigma$	${}^7\Sigma \rightarrow {}^7\Pi$	${}^7\Pi(a)$	${}^7\Pi(b)$
${}^PR_{13}(J)$	${}^RP_{31}(J+1)$	$\frac{15(J-2)^2(J-1)(J+2)(J+3)}{8(J+1)(2J-3)(2J+1)(2J+3)}$	$\frac{15(J-2)}{(J-1)(J+1)(2J-3)(2J-1)}$
${}^PQ_{23}(J)$	${}^RQ_{32}(J)$	$\frac{5(J-3)^2(J-1)(J+2)^2}{4J(J+1)(2J-3)(2J+3)}$	$\frac{5(J-2)^2(2J+1)(2J+3)}{(J-1)J(J+1)(2J-3)(2J-1)}$
${}^eR_{23}(J)$	${}^eP_{32}(J+1)$	$\frac{5(J-3)^2(J-1)J(J+2)}{4(J+1)(2J-3)(2J+1)(2J+3)}$	$\frac{5(J+2)(2J-3)}{(J-1)J(J+1)}$
$P_3(J)$	$R_3(J-1)$	$\frac{(J-1)(J+1)(J+6)^2}{8(2J-3)(2J+1)(2J+3)}$	$\frac{(J-2)^2(J+1)(2J-5)(2J+3)}{(J-1)J(2J-3)(2J-1)}$
$Q_3(J)$	$Q_3(J)$	$\frac{(J-1)(J+6)^2}{8(2J-3)(2J+3)}$	$\frac{(J^2-6)^2(2J+1)}{(J-1)J^2(J+1)}$
$R_3(J)$	$P_3(J+1)$	$\frac{(J-1)J(J+6)^2}{8(2J-3)(2J+1)(2J+3)}$	$\frac{(J-1)(J+2)(2J-3)(2J+5)}{J(2J-1)(2J+1)}$
${}^eP_{43}(J)$	${}^eR_{34}(J-1)$	$\frac{3(J-1)^2J(J+1)}{2(2J-3)(2J+1)(2J+3)}$	$\frac{6(J-2)(2J+3)}{(J-1)J^2}$
${}^RQ_{43}(J)$	${}^PQ_{34}(J)$	$\frac{3(J-1)J(J+1)}{2(2J-3)(2J+3)}$	$\frac{6(J+2)(2J-3)}{J^2(2J-1)}$
${}^RP_{53}(J)$	${}^PR_{35}(J-1)$	$\frac{(J-2)(J-1)^2(J+6)^2}{8J(2J-3)(2J+1)(2J+3)}$	$\frac{36(J+1)}{J^2(2J-1)(2J+1)}$
${}^PR_{24}(J)$	${}^RP_{42}(J+1)$	$\frac{15(J-1)J}{2(J+1)(2J-1)(2J+3)}$	$\frac{30(J-1)}{J(J+1)(2J-1)(2J+1)}$
${}^PQ_{34}(J)$	${}^RQ_{43}(J)$	$\frac{3(J-1)(J+2)(2J+1)}{4(2J-1)(2J+3)}$	$\frac{6(J-1)(J+2)(2J-3)}{J^2(J+1)(2J-1)}$
${}^eR_{34}(J)$	${}^eP_{43}(J+1)$	$\frac{3(J-1)J(J+2)}{4(2J-1)(2J+3)}$	$\frac{6(J-1)(2J+5)}{J(J+1)^2}$
$P_4(J)$	$R_4(J-1)$	0	$\frac{(J-2)(J-1)(J+2)(2J-3)(2J+3)}{J^2(2J-1)(2J+1)}$
$Q_4(J)$	$Q_4(J)$	0	$\frac{(J-2)^2(J+3)^2(2J+1)}{J^2(J+1)^2}$
$R_4(J)$	$P_4(J+1)$	0	$\frac{(J-1)(J+2)(J+3)(2J-1)(2J+5)}{(J+1)^2(2J+1)(2J+3)}$
${}^eP_{54}(J)$	${}^eR_{45}(J-1)$	$\frac{3(J-2)(J-1)^2(J+2)}{4J(2J-1)(2J+3)}$	$\frac{6(J+2)(2J-3)}{J^2(J+1)}$



Branches		i-factors	
${}^3\Pi \rightarrow {}^3\Sigma$	${}^3\Sigma \rightarrow {}^3\Pi$	${}^3\Pi(a)$	${}^3\Pi(b)$
${}^RQ_{54}(J)$	${}^PQ_{45}(J)$	$\frac{3(J-1)^2(J+2)(2J+1)}{4J(J+1)(2J-1)(2J+3)}$	$\frac{6(J-1)(J+2)(2J+5)}{J(J+1)^2(2J+3)}$
${}^RP_{64}(J)$	${}^PR_{46}(J-1)$	$\frac{15(J-3)(J-2)}{2J(2J-1)(2J+3)}$	$\frac{30(J+2)}{J(J+1)(2J+1)(2J+3)}$
${}^PR_{35}(J)$	${}^RP_{53}(J+1)$	$\frac{(J-5)^2J(J+2)}{8(2J-1)(2J+1)(2J+5)}$	$\frac{36J}{(J+1)^2(2J+1)(2J+3)}$
${}^PQ_{45}(J)$	${}^RQ_{54}(J)$	$\frac{3J(J+1)(J+2)}{2(2J-1)(2J+5)}$	$\frac{6(J-1)(2J+5)}{(J+1)^2(2J+3)}$
${}^Q R_{45}(J)$	${}^Q P_{64}(J+1)$	$\frac{3J(J+1)(J+2)^2}{2(2J-1)(2J+1)(2J+5)}$	$\frac{6(J+3)(2J+1)}{(J+1)^2(J+2)}$
$P_5(J)$	$R_5(J-1)$	$\frac{(J-5)^2(J-2)(J-1)(J+2)}{8J(2J-1)(2J+1)(2J+5)}$	$\frac{(J-1)(J+2)(2J-3)(2J+5)}{(J+1)(2J+1)(2J+3)}$
$Q_5(J)$	$Q_5(J)$	$\frac{(J-5)^2(J-1)(J+2)^2}{8J(J+1)(2J-1)(2J+5)}$	$\frac{(J^2+2J-5)^2(2J+1)}{J(J+1)^2(J+2)}$
$R_5(J)$	$P_6(J+1)$	$\frac{(J-5)^2(J+2)^2(J+3)}{8(J+1)(2J-1)(2J+1)(2J+5)}$	$\frac{J(J+3)^2(2J-1)(2J+7)}{(J+1)(J+2)(2J+3)(2J+5)}$
${}^Q P_{65}(J)$	${}^Q R_{56}(J-1)$	$\frac{5(J-3)(J-2)(J-1)(J+4)^2}{4J(2J-1)(2J+1)(2J+5)}$	$\frac{5(J-1)(2J+5)}{J(J+1)(J+2)}$
${}^Q Q_{65}(J)$	${}^P Q_{56}(J)$	$\frac{5(J-2)(J-1)(J+3)(J+4)^2}{4J(J+1)(2J-1)(2J+5)}$	$\frac{5(J+3)^2(2J-1)(2J+1)}{J(J+1)(J+2)(2J+3)(2J+5)}$
${}^RP_{75}(J)$	${}^PR_{57}(J-1)$	$\frac{15(J-4)(J-3)(J-2)(J-1)(J-3)}{8J(2J-1)(2J+1)(2J+5)}$	$\frac{15(J+3)}{J(J+2)(2J+3)(2J+5)}$
${}^PR_{46}(J)$	${}^RP_{64}(J+1)$	0	$\frac{30}{(J+2)(2J+3)(2J+5)}$
${}^PQ_{56}(J)$	${}^RQ_{65}(J)$	$\frac{5(J-1)(J+2)^2(J+3)}{8J(J+1)(2J+3)}$	$\frac{5(J+3)(2J-1)(2J+1)}{J(J+2)(2J+3)(2J+5)}$
${}^Q R_{56}(J)$	${}^Q P_{65}(J+1)$	$\frac{5(J+2)^2(J+3)^2}{8(J+1)(2J+1)(2J+3)}$	$\frac{5J(2J+7)}{(J+1)(J+2)(J+3)}$
$P_6(J)$	$R_6(J-1)$	$\frac{(J-3)(J-2)(J-1)(J+3)}{J(2J+1)(2J+3)}$	$\frac{(J-1)(J+1)(J+3)(2J-1)}{J(J+2)(2J+3)}$

Branches		i-factors	
${}^7\Pi \rightarrow {}^7\Sigma$	${}^7\Sigma \rightarrow {}^7\Pi$	${}^7\Pi(a)$	${}^7\Pi(b)$
$Q_6(J)$	$Q_6(J)$	$\frac{(J-2)(J-1)(J+3)^2}{J(J+1)(2J+3)}$	$\frac{(J^2+3J-3)^2(2J+1)}{J(J+1)(J+2)(J+3)}$
$R_6(J)$	$P_6(J+1)$	$\frac{(J-1)(J+3)^2(J+4)}{(J+1)(2J+1)(2J+3)}$	$\frac{J(J+4)^2(2J+1)}{(J+1)(J+3)(2J+5)}$
${}^oP_{76}(J)$	${}^oR_{67}(J-1)$	$\frac{3(J-4)(J-3)(J-2)(J-1)}{8J(2J+1)(2J+3)}$	$\frac{3(2J-1)}{J(J+1)}$
${}^pQ_{76}(J)$	${}^pQ_{67}(J)$	$\frac{3(J-3)(J-2)(J-1)(J+4)}{8J(J+1)(2J+3)}$	$\frac{3(J+4)(2J+1)}{(J+1)(J+3)(2J+5)}$
${}^pR_{57}(J)$	${}^pP_{75}(J+1)$	$\frac{15J(J+2)^2(J+3)^2}{8(J+1)(2J+1)(2J+3)(2J+5)}$	$\frac{15(J+2)}{(J+1)(J+3)(2J+5)(2J+7)}$
${}^pQ_{67}(J)$	${}^pQ_{76}(J)$	$\frac{3(J-3)(J-2)(J-1)(J+4)}{4(J+1)(2J+3)(2J+5)}$	$\frac{3(J+2)(2J+1)}{(J+1)(J+3)(2J+5)}$
${}^oR_{67}(J)$	${}^oP_{76}(J+1)$	$\frac{3(J-2)(J-1)J(J+4)(J+5)}{4(J+1)(2J+1)(2J+3)(2J+5)}$	$\frac{3(2J+1)}{(J+1)(2J+3)}$
$P_7(J)$	$R_7(J-1)$	$\frac{(J-4)(J-3)(J-2)(J-1)}{8(2J+1)(2J+3)(2J+5)}$	$\frac{(J+2)(2J-1)}{2J+5}$
$Q_7(J)$	$Q_7(J)$	$\frac{(J-3)(J-2)(J-1)(J+4)}{8(J+1)(2J+3)(2J+5)}$	$\frac{J(J+4)(2J+1)}{(J+1)(J+3)}$
$R_7(J)$	$P_7(J+1)$	$\frac{(J-2)(J-1)J(J+4)(J+5)}{8(J+1)(2J+1)(2J+3)(2J+5)}$	$\frac{(J+5)(2J+1)}{2J+7}$

In Table I the  ${}^7\Pi$  term was assumed to be normal. In case of inverted terms  $\Omega = 4$  corresponds not to the state  $K = J + 3$ , but to  $K = J - 3$  and for the transition  ${}^7\Pi(a) \rightarrow {}^7\Sigma(b)$  the first indices 1, 2, ... 7 in the denotation of the branches should be replaced by the denotation 7, 6, ... 1. (For  ${}^7\Sigma(b) \rightarrow {}^7\Pi(a)$  the second.)

### 3. §. Comparison with the experiment

Two  ${}^7\Pi \rightarrow {}^7\Sigma$  bands were analysed by NEVIN in the spectrum of MnH for wave lengths  $\lambda = 5677 \text{ \AA}$  and  $\lambda = 6237 \text{ \AA}$ , which arise from the transitions (0,0) and (0,1) [4]. For the comparison of the theoretical values with the ex-

periment the intensity values which were estimated with the eye and which are written up beside the spectrum lines of the (0,0) band were used. The total intensity distribution of the rotational spectrum lines is given by formula (1), the exponent of which contains the effective arc temperature. This has been determined from experimental data by means of the method published by NOLAN and JENKINS [2]. Computing the arc temperature from the branches belonging to the individual term components owing to the dispersion of the measuring data the following values are obtained:

$${}^7\Pi_4: 3706 \text{ K}^\circ; {}^7\Pi_3: 3812 \text{ K}^\circ; {}^7\Pi_2: 3733 \text{ K}^\circ; {}^7\Pi_1: 3869 \text{ K}^\circ; \\ {}^7\Pi_0: 3863 \text{ K}^\circ; {}^7\Pi_{-1}: 3863 \text{ K}^\circ; {}^7\Pi_{-2}: 3781 \text{ K}^\circ.$$

The exponential factor was computed with their arithmetic mean i. e. 3803 K $^\circ$ , and the intensity values belonging to the individual lines divided by it. The circles in the Figure give separately for every branch observed by NEVIN [4] the dependence of the experimental  $i$  factors on  $K$ . By the continuous line the values of the theoretical  $i$  factors computed from Table I are given in case  ${}^7\Pi(b) \leftrightarrow {}^7\Sigma$  against the rotational quantum numbers. The proportionality factor given here has been chosen so that the observed and the computed intensity values of the  $Q_2$  branch overlap as well as possible.

The dispersion of the experimental values is rather considerable which can be attributed to the fact that the employed experimental data do not arise from quantitative intensity measurements, but were estimated by NEVIN during the analysis with the naked eye only and characterized by whole numbers from 0—50.

It should be noted that there exist also rotational lines the wave length of which coincides with the wave length of the line of some other branch, moreover even three and fourfold coincidences might occur. The intensities of these of course add up and in the experimental data for each term of such coinciding line pair or group always the joint intensity occurs. If these lines had always been taken into account with the given intensity values, then in our Figures numerous line intensities protruding to a high extent would have appeared and finally would have led to the falsification of the real situation. In order to avoid this the experimental intensity values for such line ensembles were divided up between the terms of the group in the proportion of the intensities expected from the theoretical calculations. Hereby several projecting points could be eliminated (101 double, 13 triple, 2 quadruple groups).

Detailed investigation of the course of terms shows that the term  ${}^7\Pi$  can be considered from about  $K = 15$ —20 to a good approximation as case  $b$ ), that means that in case of  $K > 20$  the conditions are correctly described by the  $i$  factors of case  $b$ ). In case of  $K > 20$  the theoretical and experimental  $i$  factors of the main branches are in good agreement and here — under the

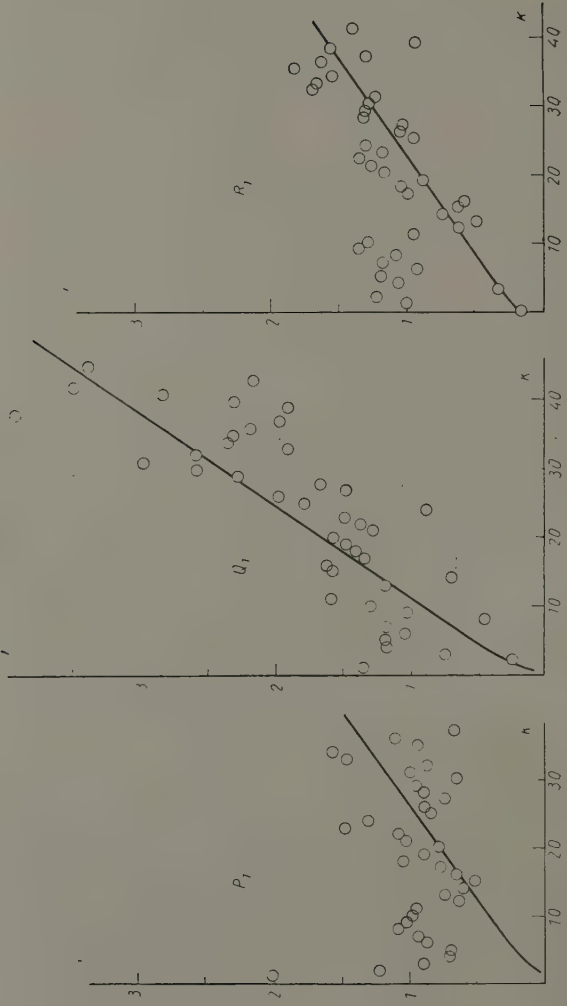


Fig. I

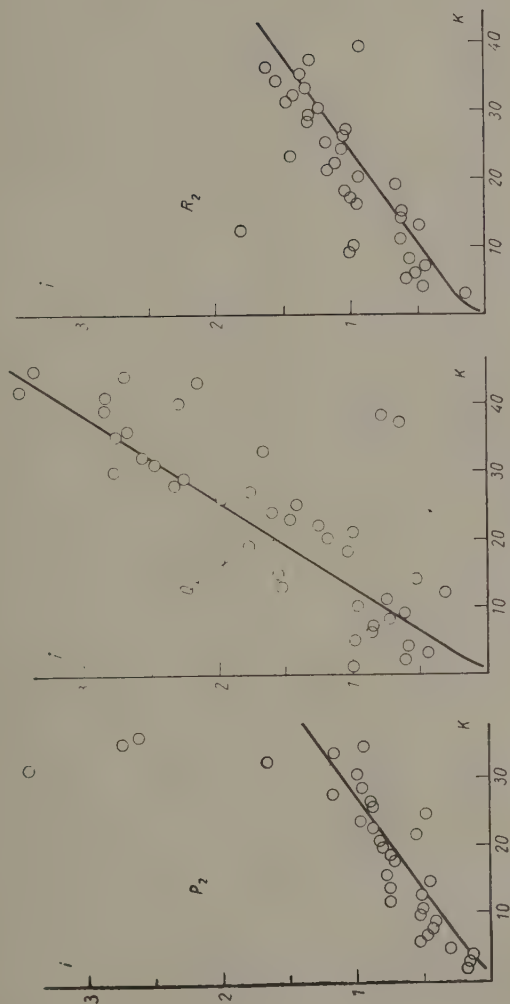


Fig. 2

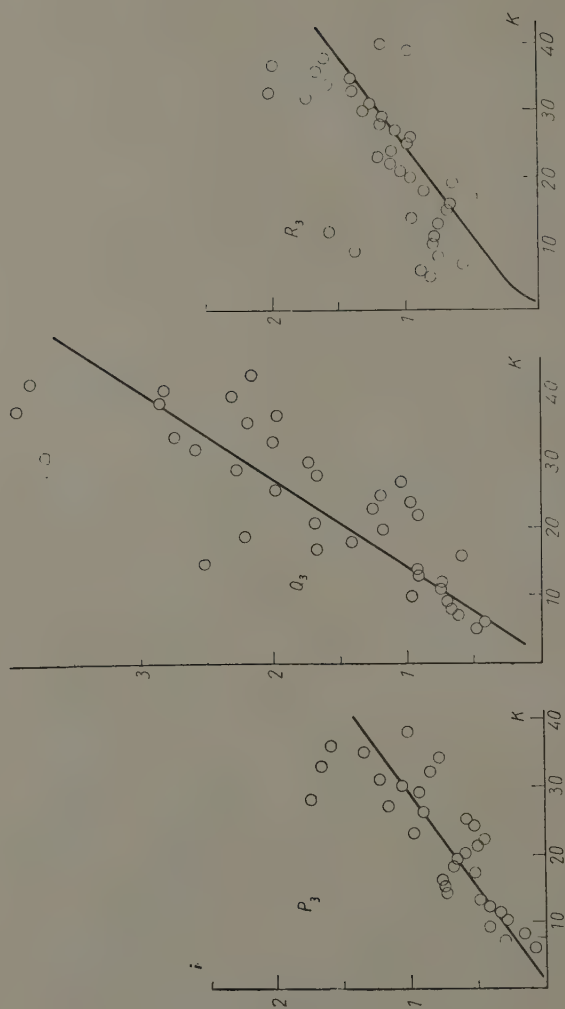


Fig. 3



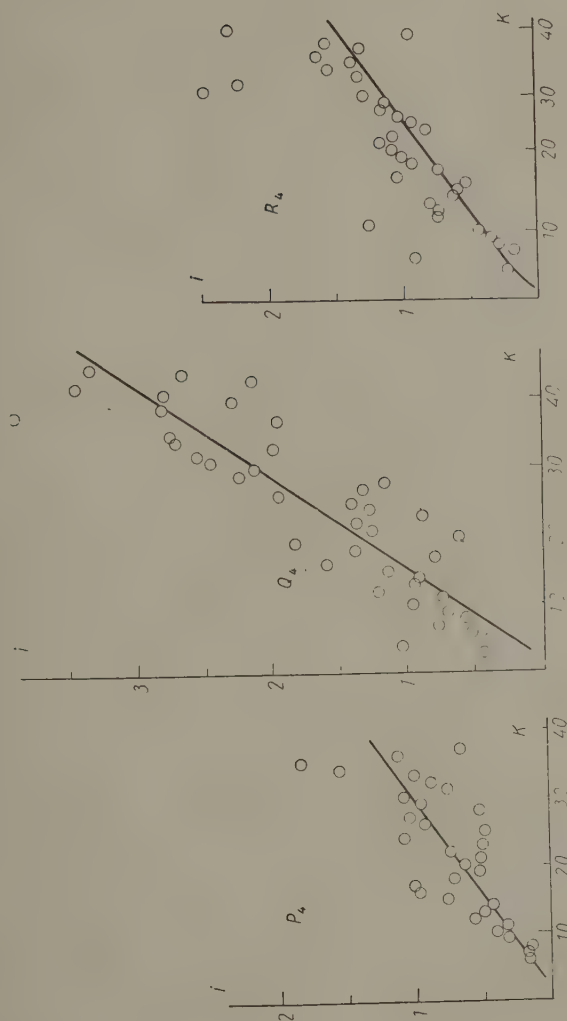


Fig. 4

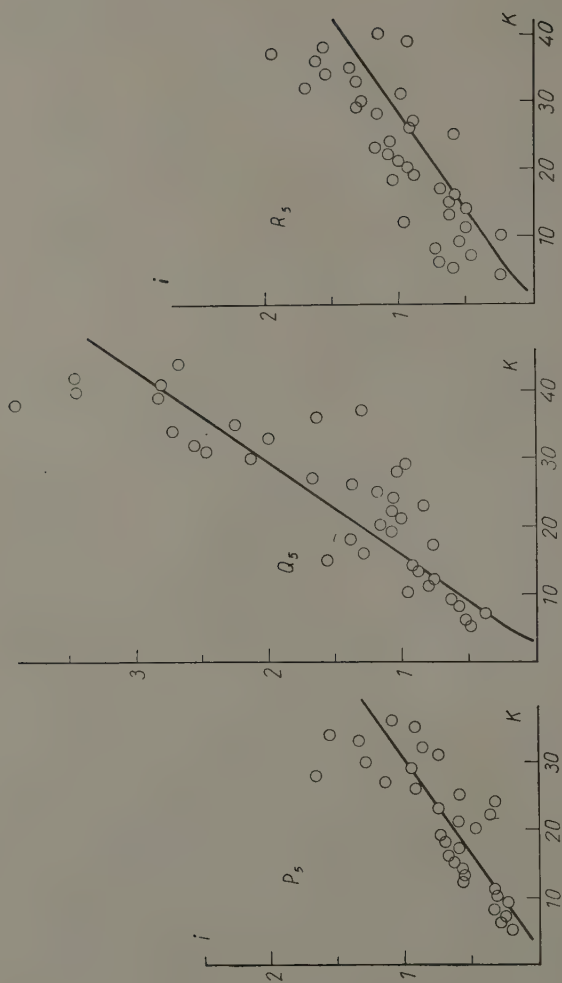


Fig. 5

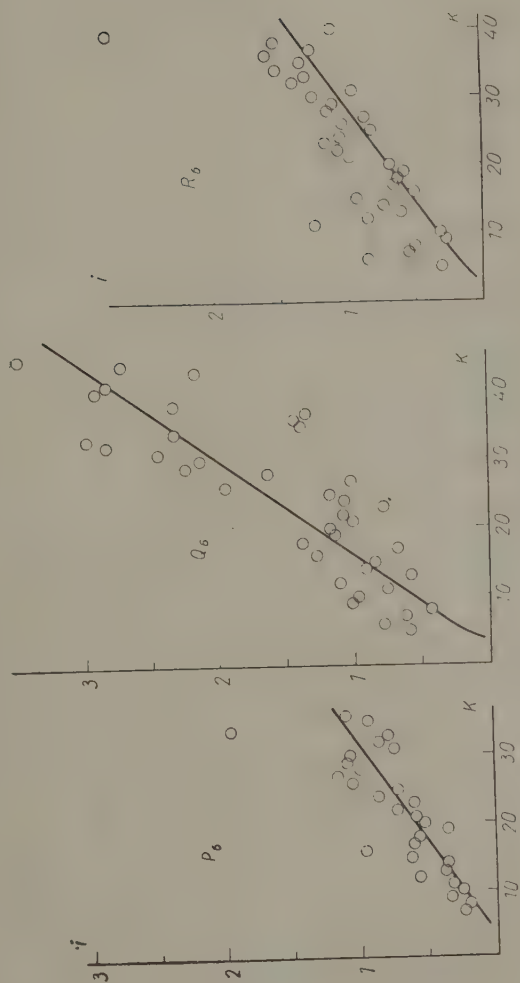


Fig. 6

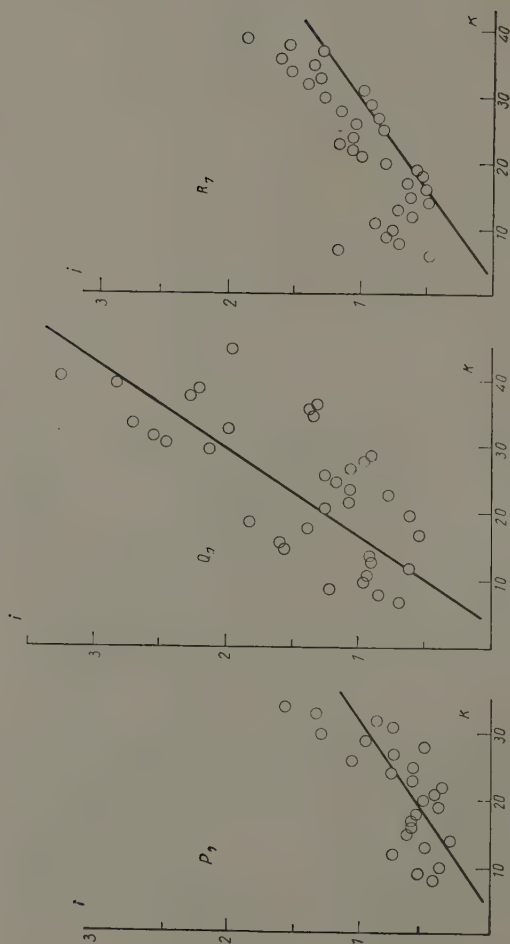


Fig. 7

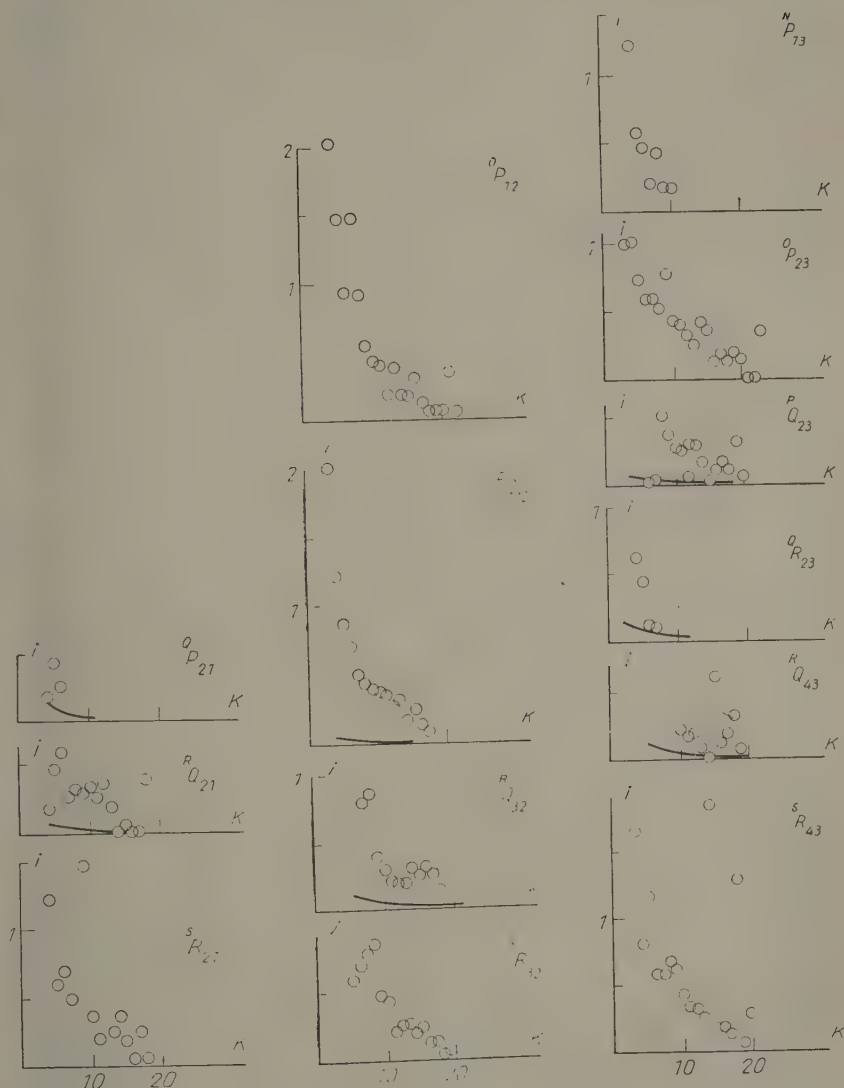


Fig. 8

usually occurring conditions — the intensity of the satellite branches is according to the theory already below the limit of measurability and indeed in this region observations do not exist. In case of  $K < 20$  two effects mix: the first is the transition towards case *a*), the consequence of which is the breaking

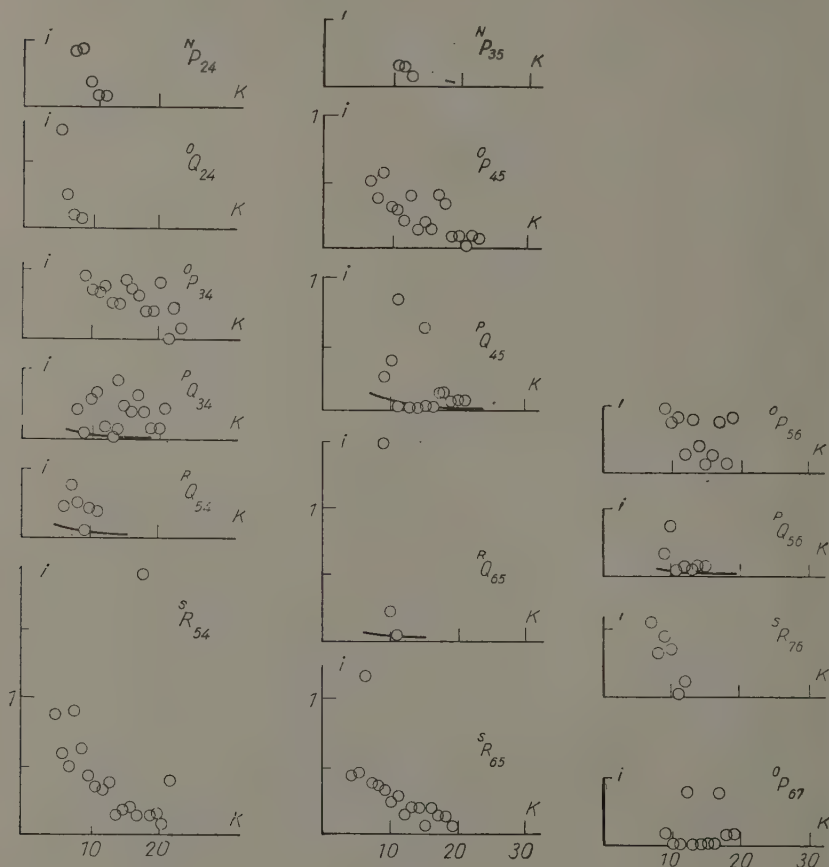


Fig. 9

down of the selection rule  $\Delta K = 0, \pm 1$  and hereby the appearance of further satellite branches differing from those permitted in case *b*), whereas the other effect is the strong perturbation appearing in the  $\Pi$  term for low quantum numbers. The latter results in deviations from the theoretical intensity values of case *a*), which can be particularly well observed on the main branches  $P_1, R_1$  as well as on some satellite branches. The exact interpretation of these



deviations is possible only after detailed investigation of the occurring perturbations, if at the same time quantitative measurement of the intensity values are available. Considering what has been said above the agreement of the theoretical and experimental results can be considered as fairly good.

## REFERENCES

1. E. L. HILL and J. H. VAN VLECK, *Phys. Rev.*, **32**, 250, 1928; A. BUDÓ, *Zs. f. Phys.*, **105**, 73, 579, 1937; D. PREMASWARUP, *Ind. Journ. of Phys.*, **27**, 415, 578, 1953.
2. R. SCHMID, T. NEUGEBAUER, D. FARKAS and CH. BARABÁS, *Zs. f. Phys.*, **65**, 541, 1930; W. KAPUSCINKI and J. G. EYMERS, *Zs. f. Phys.*, **54**, 246, 1929; J. G. EYMERS, *Zs. f. Phys.*, **63**, 396, 1930; LESTER T. EARLS, *Phys. Rev.*, **48**, 423, 1935; W. R. VAN WIJK, *Zs. f. Phys.*, **59**, 313, 1930; PH. NOLAN and F. A. JENKINS, *Phys. Rev.*, **50**, 943, 1936.
3. I. KOVÁCS and A. BUDÓ, *Zs. f. Phys.*, **116**, 693, 1940; **117**, 612, 1941; B. KLEMAN and E. WERHAGEN, *Ark. f. Phys.*, **6**, 399, 1953; I. KOVÁCS and O. SCARI, *Acta Phys. Hung.*, **8**, 425, 1958.
4. T. E. NEVIN, *Proc. Roy. Ir. Acad.*, **48A**, 1, 1942; **50A**, 123, 1945.
5. R. L. KRONIG, *Zs. f. Phys.*, **45**, 458, 1927.
6. I. KOVÁCS, *Proc. Roy. Ir. Acad.*, in press, 1959.

## ФОРМУЛЫ ИНТЕНСИВНОСТЕЙ СЕПТЕТНЫХ ПОЛОС

И. КОВАЧ и О. СҚАРИ

## Резюме

Даны явные выражения для распределения интенсивностей в ветвях полос  ${}^7\Pi(a) \leftrightarrow {}^7\Sigma$ ,  ${}^7\Pi(b) \leftrightarrow {}^7\Sigma$ . Распределения вычислены по формулам, сравнены с результатами измерений на полосах  ${}^7\Pi \rightarrow {}^7\Sigma$  в спектре MnH, и найдено удовлетворительное согласие.



# APPLICATION OF ONE-CENTER WAVE FUNCTIONS TO TETRAHEDRAL SYMMETRIC HYDRID MOLECULES II. NUMERICAL COMPUTATIONS FOR METHANE

By

E. KAPUY

RESEARCH GROUP FOR THEORETICAL PHYSICS OF THE HUNGARIAN ACADEMY OF SCIENCES, BUDAPEST

(Presented by A. Kónya. — Received 1. IX. 1958)

Two different types of one-center wave functions are used to calculate several physical constants of the  $\text{CH}_4$  molecule. In spite of the great simplifications fairly good results are obtained for energy, bond length and vibrational frequency etc. The method, however, cannot predict a correct binding energy.

The sources of the inadequacies and the possibilities of improvement are investigated.

## 1. One-center MO method with single Slater orbitals

According to the MO method the electronic ground term  $^1A_1$  of  $\text{CH}_4$  can be represented by a simple electron configuration :  $(1a_1)^2(2a_1)^2(1f_2)^6$ . To a first approximation, single Slater orbitals  $1s$ ,  $2s$ ,  $2p$  are used for the molecular orbits  $1a_1$ ,  $2a_1$ ,  $1f_2$  resp. (see [1] 6.) :

$$\begin{aligned} \sqrt{\frac{\gamma^3}{\pi}} e^{-\gamma r} &= 1a_1, & \sqrt{\frac{\delta^5}{\pi}} r e^{-\delta r} &\begin{cases} \sin \vartheta \cos \varphi = 1f_{21}, \\ \sin \vartheta \sin \varphi = 1f_{22}, \\ \cos \vartheta = 1f_{23}. \end{cases} \\ \sqrt{\frac{\delta^5}{3\pi}} r e^{-\delta r} &= 2a_1, \end{aligned} \quad (1)$$

The  $\gamma$  and the  $\delta$ -s in the exponent are considered as variational parameters. The orbital exponents of  $2a_1$  and  $1f_2$  might be varied also separately. Computations carried out, however, for atoms of similar atomic number have shown that from the point of view of energy only an irrelevant improvement is obtained (some thousandth a. u.), whereas the work is considerably increased. It is proved also by calculations carried out for atoms that on the one hand the energy obtained with Slater orbitals is to a slight extent closer to the empirical value than that obtained with hydrogen-like orbitals, on the other hand the use of Morse-Young-Haurwitz orbitals yield some thousandth a. u. improvement whereas the application of the Hartree-Fock SCF method makes the result better by maximally some tenth a. u., with considerably more work.

From the five orbitals which are provided by the  $\alpha$  and  $\beta$  spin functions respectively, the following wave function is built up :

$${}^1\Psi^{A_1} = \frac{1}{\sqrt{D}\sqrt{10!}} \det \left[ \begin{array}{ccccc} 1s\alpha, 2s\alpha, 2p_x\alpha, 2p_y\alpha, 2p_z\alpha & 1s\beta, 2s\beta, 2p_x\beta, 2p_y\beta, 2p_z\beta \end{array} \right]. \quad (2)$$

Since  $2s$  and  $1s$  are not orthogonal, the first order density matrix consists of 14 terms. It means a great simplification that its diagonal part (i. e.  $\varrho(1|1) \equiv \varrho(1)$ ) is spherically symmetric, namely in (2) all the three  $2p$  functions occur twice. By the formation of  $\varrho(1|1)$  the angular parts drop out because

$$\sin^2 \vartheta \cos \varphi + \sin^2 \vartheta \sin^2 \varphi + \cos^2 \vartheta = 1.$$

The Hamiltonian of  $\text{CH}_4$  is the following

$$H = -\frac{1}{2} \sum_{i=1}^{10} \Delta_i - \sum_{i=1}^{10} \frac{6}{r_i} - \sum_{i=1}^{10} \sum_{p=1}^4 \frac{1}{r_{ip}} + \sum_{1=i < j}^{10} \frac{1}{r_{ij}} + \frac{1}{R} \left( 24 + \frac{3\sqrt{6}}{2} \right). \quad (3)$$

The calculation can be easily carried out according to what has been said in [1]8. No particular difficulties are met with in the integration,  $\frac{1}{r_{12}}$  occurring in the integrand is expanded in the spherical harmonics [2] :

$$\begin{aligned} \frac{1}{r_{12}} = & \begin{cases} \frac{1}{r_1} \sum_{l=0}^{\infty} \left( \frac{r_2}{r_1} \right)^l P_l(\cos \vartheta), & r_1 > r_2; \\ \frac{1}{r_2} \sum_{l=0}^{\infty} \left( \frac{r_1}{r_2} \right)^l P_l(\cos \vartheta), & r_2 > r_1; \end{cases} \\ & P_l(\cos \vartheta) = P_l(\cos \vartheta_1) P_l(\cos \vartheta_2) + \\ & + 2 \sum_{m=1}^l \frac{(l-m)!}{(l+m)!} P_l^m(\cos \vartheta_1) P_l^m(\cos \vartheta_2) \cos m(\varphi_1 - \varphi_2). \end{aligned} \quad (4)$$

Finally, the analytical energy expression obtained is a function of three parameters :

$$E = E(\gamma, \delta, R).$$

The numerical calculation has been carried out so that the values of  $\gamma$  and  $\delta$  minimizing the energy were determined for  $R = 2,00$  a. u. Afterwards by fixing the  $\gamma$ , the energy minimum was determined by variation of  $\delta$  for different values of  $R$ . Since in the proximity of the equilibrium nuclear distance ( $R_0 \sim 2$  a. u.) the density of  $1s$  electrons may be practically considered as zero, for a slight variation of  $R$  the value of  $\gamma$  at the energy minimum already does not alter considerably. The results are given in the following Table toge-

ther with calculation to be found in the literature as well as with the empirical values :

	$E$	$R_0$	$\chi_{\text{mol}}$
BUCKINGHAM, MASSEY, TIBBS [3]	-40,37 a. u.	2,16 a. u.	-33,2 · 10 <sup>-6</sup>
BERNAL [4]	-39,33 a. u.	1,975 a. u.	—
Present work	-39,39 <sub>5</sub> a. u.	1,993 a. u.	-26,7 · 10 <sup>-6</sup>
Empirical	-40,54 a. u. *	2,067 a. u. [6]	-12,2 · 10 <sup>-6</sup> [6]

\* See Appendix

Knowing the values  $\gamma = 5,69$  and  $\delta = 1,34$  corresponding to the energy minimum, the diamagnetic susceptibility [5] of the molecule ( $\chi_{\text{mol}}$ ) can be computed, and this can be compared with the empirical value. (See the above Table.)

The computed value, however, has to be corrected by the so called high-frequency paramagnetism. This is the consequence of the deviation from spherical symmetry and its value is always positive. Since the wave function of our model is at the same time also an eigenfunction of the total angular momentum operator of the electrons (and belongs to the 0 eigenvalue of it) it cannot account for the high-frequency paramagnetism. Its value is for the  $\text{CH}_4 + 9,3 \cdot 10^{-6}$  [7], which has to be subtracted from the computed value.

Also the so-called "vertical ionization energy" can be easily computed. It means the energy which has to be expended in order to remove an electron from a given orbital leaving the positions of the nuclei and the other orbitals unchanged.

	$I_{2a_1}$	$I_{1f_2}$
computed	23,1 eV	11,2 eV
empirical [8]	20~ eV	13,0 eV

Finally knowing the function  $E(R)$ , the totally symmetrical normal frequency of  $\text{CH}_4$  can be computed :

$$\nu^* = \frac{1}{2\pi c} \sqrt{\frac{d^2 E}{dR^2}} \cdot \frac{1}{4M}$$

( $c$  is the velocity of light, whereas  $M$  is the mass of the proton.)

The result is the following :

$$\nu^{\square} \left\{ \begin{array}{ll} \text{computed} & : \quad 3400 \text{ cm}^{-1}, \\ \text{empirical [9]} & : \quad 2914 \text{ cm}^{-1}. \end{array} \right.$$

From the comparison of the computed and empirical data the following may be concluded :

a) The deviation of the computed energy value from the empirical value is in absolute value not high (2,8%), but no account is given by the method for the stability of the molecule. In a similar approximation we obtain for the  $^3P$  state of the C atom about  $-37,6$  a. u. (for instance TUBIS [10] obtained  $-37,629$  a.u. with Morse-Young-Haurwitz orbitals), hence  $+0,2$  a.u. is obtained for the binding energy, whereas the empirical value is :  $-0,670$  a.u.\* Neither variation of the radial parts nor application of the Hartree-Fock method would help, namely according to calculations carried out for atoms of similar atomic numbers, in the best case an improvement of 1—2 tenth a. u. could be attained. Hence the calculations of BUCKINGHAM, MASSEY and TIBBS have to contain an error somewhere, as is confirmed also by [11]. The apparently satisfactory result of HARTMANN [12] may be ascribed to the fact that the hydrogen-like  $2s$  orbitals were not orthogonalized to the  $1s$  orbitals which were neglected by him. Considering only the valence electrons an energy  $E^v = 7,05$  a. u. is obtained by our method. Hence HARTMANN's result of  $E^v = -7,70$  a. u. is due to the lack of the orthogonality. (See [1] 9.)

b) The computed value of the equilibrium nuclear distance can be considered as satisfactory considering the simplicity of calculation.

c) The computed value of the diamagnetic susceptibility is large even after considering the high-frequency paramagnetism. Hereby it is proved that the calculated electron density is too diffuse, i. e. in regions farther from the center it exceeds the real electron density.

d) The agreement of the "vertical ionization energies" with experience can be considered also fairly satisfactory. It should be, however, noted that their values are very sensitive to slight variations of the parameter  $\delta$ . If, for instance,  $\delta$  is increased from 1,30 to 1,35, then  $I_{2a_1}$  decreases by 5 percent and  $I_{1f_2}$  by 13 percent.

e) The wave number of the totally symmetrical vibration is about 17 percent higher than the empirical value. By the one-center wave function namely the real situation is well approximated only if  $R \rightarrow 0$ . (In this case our model turns into the corresponding united atom : Ne.) Increasing  $R$  the approximation becomes ever worse since the wave function of  $\text{CH}_4$  goes over into that one of  $\text{C}^{4-} + 4\text{H}^+$  and not into that of  $\text{C} + 4\text{H}$ .

\* See Appendix.

Summarizing the conclusions drawn above: the method in this approximation gives relatively good results for some properties of the  $\text{CH}_4$  molecule but it has to be sufficiently modified to give better values for the binding energy.

## 2. Possible improvements

As it was seen in [1] there are two different ways for improving the approximation.

a) If we intend to keep to the MO method, then on the one hand the used orbitals have to be modified, namely so that beside of  $s$  and  $p$  we use also the functions  $d$  and  $f$ , on the other hand the configurational interaction has to be taken into account as well. According to CARTER [11] the energy of  $\text{CH}_4$  improves by about 0,2 a. u. when taking the  $d$  orbitals into account.

The drawback of this method is that considerably more calculation is required because the diagonal part of the first order density matrix is no longer spherically symmetric and also the number of the variational parameters increases.

b) The other possibility is given by the VB method. The orbitals of the four hydrogens are for instance expanded in the Slater orbitals. In general this calculation would be a lengthy one. If, however, in the expansion only terms of character  $s$  and  $p$  are kept, and the four hydrogen orbitals thus obtained are orthogonalized to one another, the diagonal part of the first order density matrix remains also further spherically symmetric which means a considerable simplification. This method will be followed.

## 3. One-center VB method in "spherically symmetric density" approximation

Again Slater orbitals are used, the center of which is the nucleus of the C atom. The two 1s electrons of C are placed on orbital:  $\sqrt{\frac{\gamma^3}{\pi}} e^{-\gamma r}$ . The four protons are situated, according to Figure 1 at the four corners of the tetrahedron at a distance  $R$  from the nucleus of the atom C. The  $(x, y, z)$  coordinates of the proton are in turn:

$$\begin{aligned} 1: & \left( +\frac{R}{\sqrt{3}}, +\frac{R}{\sqrt{3}}, +\frac{R}{\sqrt{3}} \right); \quad 2: \left( -\frac{R}{\sqrt{3}}, +\frac{R}{\sqrt{3}}, -\frac{R}{\sqrt{3}} \right); \\ 3: & \left( -\frac{R}{\sqrt{3}}, -\frac{R}{\sqrt{3}}, +\frac{R}{\sqrt{3}} \right); \quad 4: \left( +\frac{R}{\sqrt{3}}, -\frac{R}{\sqrt{3}}, -\frac{R}{\sqrt{3}} \right). \end{aligned}$$

The four valence electrons of the C atom are situated on four hybrid orbitals:  $\varphi_i$  ( $i = 1, 2, 3, 4$ ), the radial part of which is common, whereas the



angular parts are such combinations of those of the orbitals  $p_x, p_y, p_z$  which are equivalent and are directed towards the corners of the tetrahedron [13]:

$$\begin{aligned}
 1: & \quad 1 + \sqrt{3} (+ \sin \vartheta \cos \varphi + \sin \vartheta \sin \varphi + \cos \vartheta), \\
 2: & \quad 1 + \sqrt{3} (- \sin \vartheta \cos \varphi + \sin \vartheta \sin \varphi - \cos \vartheta), \\
 3: & \quad 1 + \sqrt{3} (- \sin \vartheta \cos \varphi - \sin \vartheta \sin \varphi + \cos \vartheta), \\
 4: & \quad 1 + \sqrt{3} (+ \sin \vartheta \cos \varphi - \sin \vartheta \sin \varphi - \cos \vartheta).
 \end{aligned} \tag{5}$$

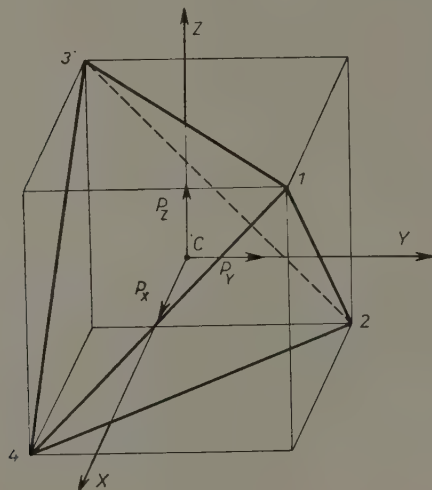


Fig. 1

If the orbitals  $\varphi'_i$  ( $i = 1, 2, 3, 4$ ) of the four hydrogen atoms are chosen so that the corresponding angular parts are identical with those of (5), then the four orbitals are orthogonal to one another, whereas the diagonal part of the first order density matrix is spherically symmetric. The common radial part of the hydrogen orbitals is taken in the form:  $\frac{1}{2} \sqrt{\frac{\delta'^5}{3\pi}} r e^{-\delta' r}$ .

Since the radial parts can be factored out, the eight orbitals are orthogonal to one another with the exception of those pointing into the same corner of the tetrahedron:

$$\begin{aligned}
 \int \varphi_i \varphi_k dv &= \delta_{ik}, \\
 \int \varphi'_i \varphi'_k dv &= \delta_{ik}, \quad (i, k = 1, 2, 3, 4) \\
 \int \varphi'_i \varphi_k dv &= A \delta_{ik},
 \end{aligned}$$

where

$$A = \frac{\sqrt{\delta^5 \delta'^5}}{\left(\frac{\delta + \delta'}{2}\right)^5}.$$

Afterwards from the two 1s orbitals and the eight free valence orbitals such determinants are formed which belong to the 0 eigenvalue of  $S_z$ . From these, according to [1] 4., such combination is formed in which orbitals directed towards the same corner of the tetrahedron are forming singlet pairs.

This belongs as we have seen in [1] 7. at the same time to the irreducible representation  $A_1$  of the point group  $T_d$ . This combination consisting of 16 determinants which correspond essentially to the so-called "Perfect Pairing" approximation is the following:

$$\begin{aligned} 1\Psi^{A_1} = & (\varphi_1 \varphi_2 \varphi_3 \varphi_4 | \varphi'_1 \varphi'_2 \varphi'_3 \varphi'_4) + (\varphi'_1 \varphi_2 \varphi_3 \varphi_4 | \varphi_1 \varphi'_2 \varphi'_3 \varphi'_4) + \\ & + (\varphi_1 \varphi'_2 \varphi_3 \varphi_4 | \varphi'_1 \varphi_2 \varphi'_3 \varphi'_4) + (\varphi_1 \varphi_2 \varphi'_3 \varphi_4 | \varphi'_1 \varphi'_2 \varphi_3 \varphi'_4) + \\ & + (\varphi_1 \varphi_2 \varphi_3 \varphi'_4 | \varphi'_1 \varphi'_2 \varphi'_3 \varphi_4) + (\varphi'_1 \varphi'_2 \varphi_3 \varphi_4 | \varphi_1 \varphi_2 \varphi'_3 \varphi'_4) + \\ & + (\varphi'_1 \varphi_2 \varphi'_3 \varphi_4 | \varphi_3 \varphi'_2 \varphi_3 \varphi'_4) + (\varphi'_2 \varphi_2 \varphi_3 \varphi'_4 | \varphi_1 \varphi'_2 \varphi'_3 \varphi_4) + \\ & + (\varphi_1 \varphi'_2 \varphi'_3 \varphi_4 | \varphi'_1 \varphi_2 \varphi_3 \varphi'_4) + (\varphi_1 \varphi'_2 \varphi_3 \varphi'_4 | \varphi'_1 \varphi'_2 \varphi_3 \varphi'_4) + \\ & + (\varphi_1 \varphi_2 \varphi'_3 \varphi'_4 | \varphi'_1 \varphi'_2 \varphi_3 \varphi_4) + (\varphi'_1 \varphi'_2 \varphi'_3 \varphi_4 | \varphi_1 \varphi_2 \varphi_3 \varphi'_4) + \\ & + (\varphi'_1 \varphi'_2 \varphi_3 \varphi'_4 | \varphi_1 \varphi_2 \varphi'_3 \varphi_4) + (\varphi'_1 \varphi_2 \varphi'_3 \varphi'_4 | \varphi_1 \varphi'_2 \varphi_3 \varphi_4) + \\ & + (\varphi_1 \varphi'_3 \varphi'_2 \varphi'_4 | \varphi'_1 \varphi_2 \varphi_3 \varphi_4) + (\varphi'_1 \varphi'_2 \varphi'_3 \varphi'_4 | \varphi_1 \varphi_2 \varphi_3 \varphi_4). \end{aligned} \quad (6)$$

The two 1s orbitals are not indicated, whereas the first four orbitals are always provided with  $\alpha$  and the second four always with  $\beta$  spin functions.

The energy expression is computed according to [1] 6. Since the orbital  $\varphi_{1s}$  is not orthogonal to the orbitals  $\varphi_i$  and  $\varphi'_i$  (more exactly to the  $s$  components of these) therefore the determinants  $D_{KL}$  will have 26 elements differing from zero, this means that the  $\varrho_{KL}$ -s consist also of 26 terms. If orthogonality would exist then the  $\varrho_{KL}$ -s would have 10 terms only by which the calculation would be simplified to a considerable extent. This may be attained by assuming the  $\varphi_i$ -s as well as the  $\varphi'_i$ -s orthogonal to  $\varphi_{1s}$  (though in reality they are not), i. e. for the calculation of the determinants  $D_{KL}$  the elements  $\int \varphi_i \varphi_{1s} dv$  and  $\int \varphi'_i \varphi_{1s} dv$  ( $i = 1, 2, 3, 4$ ) are taken for zero, and the repulsive potential derived by GOMBÁS is added to the operator (3) and the energy is computed by this so-called "modified Hamilton operator". In our case the potential:

$$G(r_i) = \sum_{i=1}^{10} \left\{ 8\pi^2 \gamma^6 r_i^4 e^{-2\gamma r_i} + \frac{1}{4r_i^2} \right\}$$

should be added to the H operator, but care should be taken that this acts only upon the valence orbitals and also only on the 2s components of them, hence it behaves like a projection operator ([1] 9.).

Applying the repulsive potential, on the one hand, the theorem is no longer valid according to which the energy value obtained by the variational method is always above the empirical value, on the other hand, the wave function changes also. This can be studied on the most simple model, i. e. on the Li atom. Taking the Slater orbital  $\sqrt{\frac{\gamma^3}{\pi}} e^{-\gamma r}$  as the 1s orbital, and the Slater orbital  $\sqrt{\frac{\delta^5}{3\pi}} r e^{-\delta r}$  as 2s orbital:

a) Taking into account that 2s is not orthogonal to 1s we obtain [15] :

$E$	$\gamma$	$\delta$
-7,4179 a. u.	2,688	0,630

b) Assuming that 2s is orthogonal to 1s and applying the potential  $G$  we obtain :

$E$	$\gamma$	$\delta$
-7,4360 a. u.	2,690	0,745

We see that the calculation carried out with the potential  $G$  produces a slightly lower value but which in this approximation does not decrease below the experimental value :  $E_{Li} = -7,4837$  a. u. [6].

The increase of the parameter  $\delta$  indicates that the maximum of the radial density of the electrons has got nearer to the nucleus. In the proximity of the nucleus the electron densities obtained by the two methods differ from each other to a greater extent, but since we are interested in the region far from the nucleus only (in the valence shell) this does not cause any difficulties.

If  $\text{CH}_4$  is dealt with exactly in the way as described in 1.) but assuming the orthogonality of 2s to 1s and using the potential  $G$  the following results are obtained :

$E$	$R_0$	$Z_{\text{mol}}$	$\nu^*$	$\gamma$	$\delta$
-39,46 a. u.	1,930 a. u.	$-25,0 \cdot 10^{-8}$	3750 $\text{cm}^{-1}$	5,696	1,38

For the calculation of the energy expression corresponding to the trial functions (6) the terms in which the diagonal part of the first order density matrix occur can be easily computed due to the spherical symmetry. The Coulomb and exchange interaction of the electrons of the valence orbitals consists of integrals of the form :

$$\int \frac{\varphi_i(1) \varphi_k(1) \varphi_i(2) \varphi_k(2)}{r_{12}} d\tau_1 d\tau_2.$$

These contain each  $4^4 = 256$  terms, because the number of the angular terms of the orbitals  $\varphi_i$  is 4. In order to simplify these integrals by decreasing the number of the terms the coordinate system is changed. First the  $x$  and  $y$  axes are turned round the  $z$  axis counter-clockwise by  $135^\circ$ , then round the new  $x'$  axis the  $z$  axis (as a matter of course together with the  $y$  axis) is turned by  $54^\circ 44'$  so as to point towards the hydrogen atom 1 (see Figure 2).

The matrix of the coordinate transformation corresponding to this rotation is the following :

$$\begin{pmatrix} -\frac{\sqrt{2}}{2} & -\frac{1}{2} \frac{\sqrt{2}}{\sqrt{3}} & +\frac{1}{\sqrt{3}} \\ +\frac{\sqrt{2}}{2} & -\frac{1}{2} \frac{\sqrt{2}}{\sqrt{3}} & +\frac{1}{\sqrt{3}} \\ 0 & +\frac{\sqrt{2}}{\sqrt{3}} & +\frac{1}{\sqrt{3}} \end{pmatrix} :$$

The  $s$  orbitals are invariant against rotations, whereas the orbitals  $p_x$ ,  $p_y$ ,  $p_z$  are transformed in the same way as the coordinates  $x$ ,  $y$ ,  $z$ . The angular parts in (5) can be expressed by the orbitals  $p'_x$ ,  $p'_y$ ,  $p'_z$  of the new system of coordinates as follows :

$$\begin{aligned} 1: & \{1 + 3 \cos \vartheta\}, \\ 2: & \{1 + \sqrt{6} \sin \vartheta \cos \varphi - \sqrt{2} \sin \vartheta \sin \varphi - \cos \vartheta\}, \\ 3: & \{1 + 2\sqrt{2} \sin \vartheta \sin \varphi - \cos \vartheta\}, \\ 4: & \{1 - \sqrt{6} \sin \vartheta \cos \varphi - \sqrt{2} \sin \vartheta \sin \varphi - \cos \vartheta\}. \end{aligned} \quad (8)$$

Owing to the symmetry of  $\text{CH}_4$  all the four angular parts are equivalent. Hence for the calculation of the integrals of form

$$\int \frac{\varphi_i(1) \varphi_k(1) \varphi_i(2) \varphi_k(2)}{r_{12}} d\tau_1 d\tau_2,$$

it is best to use the first and third term of (8). Thus the integral consists altogether of 36 terms instead of 256, as it was the case in the former system of coordinates. Among the 136 different  $\varrho_{KL}$  there are also equivalent ones, which give after integration identical results. All the Coulomb and exchange integrals containing  $\frac{1}{r_{12}}$  can be reduced to 28 types of basic integrals.

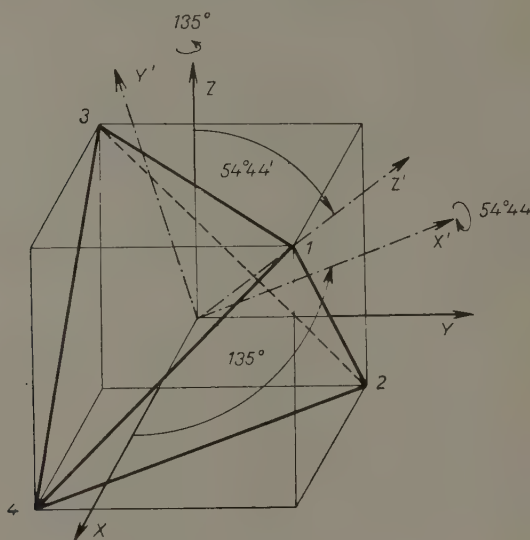


Fig. 2

The four-parameter function of the energy expression is :

$$E = E(\gamma, \delta, \delta', R).$$

$\gamma$  and  $R$  are not varied but fixed at a probable value :  $\gamma = 5,70$  and  $R = 2,00$ .

a) Equating in the energy expression  $\delta'$  with  $\delta$  we get back to the preceding calculation with the difference that now  $\gamma$  and  $R$  are not varied. Varying  $\delta$  we obtain :

$E$	$\chi_{\text{mol}}$	$\delta$
-39,459 a. u.	$-25,8 \cdot 10^{-6}$	1,36

The radial density  $D(r) = \int \varrho r^2 \sin \vartheta d\vartheta d\varphi$  is illustrated in Figure 3 by curve "a".

b) Varying  $\delta$  and  $\delta'$  separately the following result is obtained :

$E$	$\chi_{\text{mol}}$	$\delta'$	$\delta$
-39,527 a. u.	$-28,6 \cdot 10^{-6}$	1,02	1,72

The energy has become lower by 0,068 a. u. relative to the preceding value, whereas the diamagnetic susceptibility has increased, which is due to the flattening of the radial density. (See curve "b" of Figure 3.)

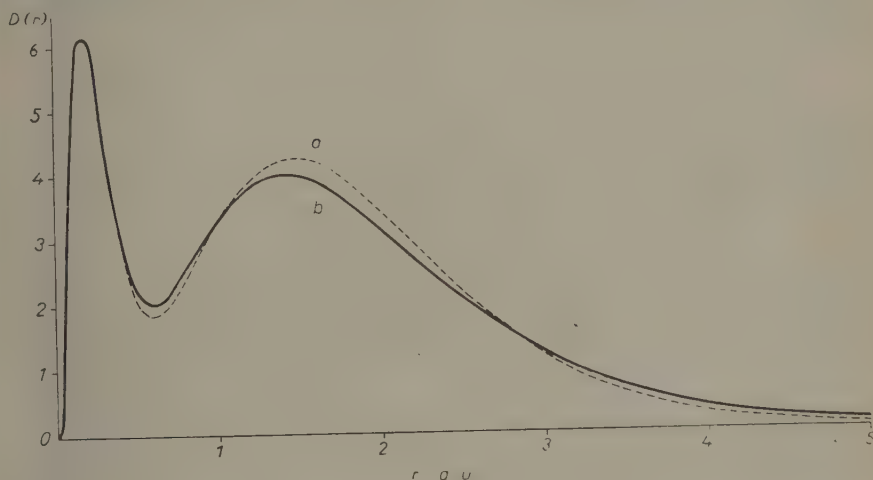


Fig. 3

Probably for the same reason also the equilibrium nuclear distance has increased to a slight extent and got nearer to the empirical value.

c) Calculating the energy alone with the aid of the first term of (6) no improvement can be obtained varying  $\delta$  and  $\delta'$  separately, which proves that the lowering of the energy is mainly caused by terms of the form

$$\int \varphi'_i(1) \varphi_i(1) H \varphi'_i(2) \varphi_i(2) d\tau_1 d\tau_2.$$

### Conclusions

The difference between the calculated and the empirical values of the energy, considering even the result of (3) is more than 2,5 percent. The contribution of the inner shell to this deviation is about 7 percent only, the valence

shell has to account for the remaining 93 percent. Further improvement might be attained by not confining ourselves to the combination (6), but taking into account also the two combinations which can be constructed from the further 13 singlets of the given 8 free orbitals. Hereby, however, our work would be increased to a great extent and at best would yield an energy improvement of about 0,1—0,15 a. u. only. No greater improvement may be expected from the altering of the radial part. The main source of the deviation as it can be easily shown, is that bad approximation is obtained by the given combination of the orbitals of types *s* and *p* for the 1*s* orbitals of the H atoms. Let an atom H be at a distance  $R = 2,00$  a. u. from the center on the *z* axis. To approximate this orbital we have in 3. used the function

$$\frac{1}{2} \sqrt{\frac{\delta'^5}{3\pi}} r e^{-\delta' r} (1 + 3 \cos \vartheta).$$

The Hamilton operator of the atom H is

$$-\frac{1}{2} \Delta - \frac{1}{\sqrt{R^2 + r^2 - 2Rr \cos \vartheta}}.$$

Calculating the energy expression and minimizing the energy we obtain

$$E_H = -0,26603 \text{ a. u.}; \quad \delta' = 0,72. \quad (10)$$

The deviation from the empirical value ( $-0,50000$  a. u.) is 47 percent.

We have seen that neither the method described in 1. nor that in 3. gives negative binding energy for  $\text{CH}_4$ . The situation, however, will be different if consistently energy values calculated with the same method are used in the calculation of the binding energy ( $E_B = E_{\text{CH}_4} - E_C - 4E_H$ ).

The ground state  $^3P$  of the atom C can be described by a single determinant

$$^3\Psi^P = \frac{1}{\sqrt{6!}} \det \left[ 1s\alpha, 1s\beta, 2s\alpha, 2s\beta, 2p_0\alpha, 2p_+\alpha \right].$$

Let us use similarly to  $\text{CH}_4$  the following orbitals:

$$\begin{aligned} \sqrt{\frac{\gamma^3}{\pi}} e^{-\gamma r} &= 1s, \\ \sqrt{\frac{\delta^5}{3\pi}} r e^{-\delta r} &= 2s, \\ \begin{cases} \cos \vartheta &= 2p_0, \\ \frac{1}{\sqrt{2}} \sin \vartheta e^{+i\varphi} &= 2p_+. \end{cases} \end{aligned}$$



$3\psi^P$  is at the same time eigenfunction of the operators  $L^2$ ,  $L_z$ ,  $S^2$ ,  $S_z$ .

The calculation is carried out as in 3., namely assuming the orbital  $2s$  orthogonal to  $1s$  and using the potential  $G$ . With the variation of  $\gamma$  and  $\delta$  we obtain :

	$E_c$	$\gamma$	$\delta$
Calculated	-37,811 a. u.	5,738	1,676
Empirical	-37,87 a. u.*	—	—

\* See Appendix

Using the energy value of (9), (10) and (11) we obtain for the binding energy  $-0,612$  a. u., whereas the empirical value is  $-0,670$  a. u. Hence a relatively better value is obtained by this method for the binding energy than for the energy of the H atoms.

If our aim is to decrease the deviation of the calculated energy of  $\text{CH}_4$  from the measured value, there remains nothing else but to give up the "spherically symmetric density" approximation and to consider possibly also functions  $d$  and  $f$ . Thus the convergence will be probably more rapid than if only the radial parts were enlarged. It is advisable to examine the suitability of the function in question separately for the H atoms before the calculations are carried out for the  $\text{CH}_4$ .

The calculation carried out in 3. can be applied apart from  $\text{CH}_4$  also to  $\text{SiH}_4$  and  $\text{GeH}_4$ .

Then, however, it is advisable to omit the electrons of the inner shells from the trial function; the interaction of the inner shells and the valence shell should be taken into account by some approximative method. Here the difference between the empirical and the computed values will be even higher than for the  $\text{CH}_4$  because, on the one hand, the Slater orbitals are already less good, for higher atomic numbers, on the other hand, because of the interaction of the valence electrons with the many inner electrons no such big separation of  $\delta$  and  $\delta'$  is allowed as for the  $\text{CH}_4$ .

Instead of the simple Slater orbitals the linear combination of several such orbitals should be used and it is also advisable to vary the power exponents of  $r$  as well.

I should like to express my grateful thanks to Prof. P. GOMBÁS for his help and his valuable advice.

## Appendix

The calculation of the energy of  $\text{CH}_4$  and C as well as of the binding energy of  $\text{CH}_4$  from empirical data.

The binding energy of  $\text{CH}_4$  at  $0^\circ$  Kelvin:  $\text{C}(^3\text{P}) + 4\text{H}(^2\text{S}) \rightarrow \text{CH}_4(^1\text{A}_1)$

The sublimation energy of graphite:  $-170,0$  Kcal/mol

The dissociation energy of two  $\text{H}_2$  [6]:  $-206,4$  Kcal/mol

The heat of formation of  $\text{CH}_4$  [16]:  $-16,0$  Kcal/mol

$$\underline{-392,4 \text{ Kcal/mol} = -17,02 \text{ eV}}$$

$$\underline{-17,02 \text{ eV}}$$

The zero point vibration energy of  $\text{CH}_4$  [9]:  $-1,18 \text{ eV}$

The binding energy of  $\text{CH}_4$ : .....  $\underline{-18,20 \text{ eV} = -0,670 \text{ a. u.}}$

The sublimation energy of C is uncertain. In the literature from 125 Kcal up to 180 Kcal numerous values occur. By recent measurements a value about 170 Kcal is rendered probable.

The energy of the valence electrons of  $\text{CH}_4$ :  $4\text{H}^+ + \text{C}^{4+}(^1\text{S}) + 8e^- \rightarrow \text{CH}_4(^1\text{A}_1)$

The ionisation energies of the C atom [6]:

$$\begin{cases} -11,27 \text{ eV} \\ -24,80 \text{ ,,} \\ -47,90 \text{ ,,} \\ -64,50 \text{ ,,} \end{cases}$$

$$\underline{-148,47 \text{ eV}}$$

The binding energy of  $\text{CH}_4$ : .....  $\underline{-18,20 \text{ ,,}}$

$$\underline{-166,67 \text{ eV} = -6,128 \text{ a. u.}}$$

The ionisation energy of the four H atoms: .....  $\underline{-2,000 \text{ ,, ,}}$

The energy of the valence electrons of  $\text{CH}_4$ : .....  $\underline{-8,128 \text{ a. u.}}$

The energy of the valence electrons of the C atom:  $\text{C}^{4+}(^1\text{S}) + 4e^- \rightarrow \text{C}(^3\text{P})$

$$\underline{-148,5 \text{ eV} = -5,459 \text{ a. u.}}$$

The total energy of  $\text{CH}_4$  and C is obtained by adding to the energy of the valence electrons the ionisation energy (with opposite sign) of the two electrons of the  $\text{C}^{4+}$  ion:

$$\underline{-392,0 \text{ eV} \quad [6]}$$

$$\underline{-489,6 \text{ ,,} \quad [\text{from the Schrödinger equation of } \text{C}^{5+}]}$$

$$\underline{-881,6 \text{ eV} = -32,41 \text{ a. u.}}$$

Hence the total energy of  $\text{CH}_4$ :  $\underline{-40,54 \text{ a. u.}}$

whereas that of the C atom:  $\underline{-37,87 \text{ a. u.}}$

## REFERENCES

1. E. KAPUY, *Acta Phys. Hung.*, **9**, 317, 1959. Part I of this work.
2. P. GOMBÁS, *Theorie und Lösungsmethoden des Mehrteilchenproblems der Wellenmechanik*, Birkhäuser, Basel, 1950.
3. R. A. BUCKINGHAM, H. S. W. MASSEY, E. R. TIBBS, *Proc. Roy. Soc. A*, **178**, 119, 1941.
4. M. J. M. BERNAL, *Proc. Phys. Soc. A*, **66**, 514, 1953.
5. J. H. VAN VLECK, *The Theory of Electric and Magnetic Susceptibilities*, Oxford, University Press, 1932.
6. LANDOLT and BÖRNSTEIN, *Zahlenwerte und Funktionen. Atom- und Molekularphysik. Part 1, 2, 3*, Springer, Berlin 1950.
7. W. WELTNER, *J. Chem. Phys.*, **24**, 518, 1956.
8. R. E. HONIG, *J. Chem. Phys.*, **16**, 105, 1948.
9. G. HERZBERG, *Infra-red and Raman Spectra*, Van Nostrand, Toronto, New York, London, 1945.
10. A. TUBIS, *Phys. Rev.*, **102**, 1049, 1956.
11. C. CARTER, *Proc. Roy. Soc. A*, **235**, 321, 1956.
12. H. Z. HARTMANN, *Zs. f. Naturforschung*, **2a**, 489, 1947.
13. G. E. KIMBALL, *J. Chem. Phys.*, **8**, 188, 1940.
14. P. GOMBÁS, *Acta Phys. Hung.*, **1**, 285, 1952.
15. E. B. WILSON, *J. Chem. Phys.*, **1**, 210, 1933.
16. H. H. VOGEL, *J. Chem. Phys.*, **16**, 984, 1948.

## ПРИМЕНЕНИЕ ОДНОЦЕНТРОВОЙ ВОЛНОВОЙ ФУНКЦИИ К МОЛЕКУЛАМ ГИДРИДОВ С ТЕТРАЭДРИЧЕСКОЙ СИММЕТРИЕЙ

### II. Нумерические вычисления для метана

Э. КАПУИ

#### Резюме

Для вычисления нескольких физических постоянных молекулы  $\text{CH}_4$  применяется одноцентровая волновая функция двух типов. Несмотря на большие упрощения, для энергии, длины связи, колебательной частоты и т. д. получаются довольно хорошие результаты. Но устойчивость молекулы нельзя объяснить данным методом.

Рассматриваются причины расхождения и возможность дальнейшего развития метода.



# STATISTISCHE BEHANDLUNGSWEISE DES N<sub>2</sub>-MOLEKÜLS

Von

P. GOMBÁS

PHYSIKALISCHES INSTITUT DER UNIVERSITÄT FÜR TECHNISCHE WISSENSCHAFTEN, BUDAPEST

(Eingegangen: 18. I. 1959)

Im Anschluss an eine vorangehende Arbeit<sup>1</sup> wird gezeigt, dass man im Rahmen des statistischen Atommodells bei Berücksichtigung des Weizsäckerschen kinetischen Energieanteils in der Wechselwirkungsenergie der beiden N-Atome die Bindung des N<sub>2</sub>-Moleküls erklären kann. Bei Voraussetzung einer einfachen Superposition der Elektronenwolken der Atome ergibt sich für den Kernabstand  $\delta_0 = 1,39 \text{ \AA}$  und für die Bindungsenergie  $D = 10,9 \text{ eV}$ . Während die Bindungsenergie mit der empirischen sehr gut übereinstimmt, ist der Kernabstand im Verhältnis zum empirischen um ca 30% zu gross. Diese Diskrepanz dürfte sich jedoch in den höheren Näherungen verringern.

## 1. Einleitung und Zusammenfassung

In einer vorangehenden kurzen Mitteilung<sup>1</sup> wurde gezeigt, dass man im Rahmen der statistischen Theorie der Atome für homöopolare Moleküle, so insbesondere für das N<sub>2</sub>-Molekül, eine Bindung erhält, sofern man in der Wechselwirkungsenergie die Weizsäckersche Inhomogenitätskorrektur der kinetischen Energie berücksichtigt. Die dort erhaltenen Resultate können nur als vorläufig betrachtet werden, denn es wurde erstens für die Elektronendichte der freien N-Atome — aus der wir durch einfache Superposition die Elektronendichte des Moleküls aufgebaut haben — nur eine grobe Näherung angesetzt und zweitens wurde zur Berechnung der Wechselwirkungsenergie der beiden N-Atome ein Näherungsausdruck herangezogen. Es ergab sich so für die Bindungsenergie des N<sub>2</sub>-Moleküls rund 20 eV, die rund um das Doppelte grösser ist als die experimentelle [man vgl. (21)]. Uns kam es dort nicht so sehr auf den genauen Wert der Bindungsenergie, sondern hauptsächlich darauf an zu zeigen, dass man bei Berücksichtigung der Weizsäckerschen Energie für das N<sub>2</sub>-Molekül eine Bindung erhält, die voraussichtlich auch von den genaueren Berechnungen bestätigt wird. Dass dies tatsächlich zutrifft, soll hier gezeigt werden.

Die Elektronendichte des N<sub>2</sub>-Moleküls wird auch hier als einfache Superposition der Elektronendichten der beiden freien N-Atome angesetzt; für die Elektronenverteilung der freien N-Atome wird jedoch nicht mehr eine Nähe-

<sup>1</sup> P. GOMBÁS, ZS. f. Phys. 152, 397, 1958.

ungsverteilung sondern die exakte Verteilung zugrunde gelegt. Weiterhin wird die Wechselwirkungsenergie der beiden N-Atome nicht mit dem in der vorangehenden Arbeit gebrauchten Näherungsausdruck sondern auf numerischem Wege exakt berechnet.

Die Berechnung der Wechselwirkungsenergie wird für mehrere Kernabstände durchgeführt; das Minimum der Wechselwirkungsenergie entspricht der stabilen Gleichgewichtslage. Demnach lässt sich aus der Wechselwirkungsenergie als Funktion des Kernabstandes der Kernabstand in der Gleichgewichtslage, sowie die Bindungsenergie, d. h. der Betrag der Wechselwirkungsenergie in der Gleichgewichtslage sofort feststellen. Die so erhaltene Bindungsenergie stimmt mit der experimentellen sehr gut überein, der Kernabstand ergibt sich jedoch um cca 30% als zu gross. Diese Abweichung dürfte hauptsächlich darauf zurückzuführen sein, dass wir die Elektronendichte des Moleküls hier grob als einfache Superposition der Elektronendichten der freien Atome ansetzten. Ein besserer Ansatz für die Elektronendichte wird den Kernabstand aller Wahrscheinlichkeit nach verkleinern, während sich im Wert der Bindungsenergie nicht viel ändern dürfte, da die Energie in bezug auf die zugrunde gelegte Dichteverteilung der Elektronen nicht sehr empfindlich ist.

## 2. Die Elektronendichte im freien N-Atom

Da wir die Elektronendichte im  $N_2$ -Molekül als einfache Superposition der Elektronendichten in den beiden freien N-Atomen ansetzen, müssen wir in erster Linie die Elektronendichte  $\varrho$  des freien N-Atoms festlegen. Diese bestimmen wir aus der mit der vollen Weizsäckerschen Korrektur erweiterten Grundgleichung des statistischen Atoms, die folgendermassen lautet

$$4\kappa_i \Delta\psi - \frac{5}{3}\kappa_k \psi^{7/3} + \frac{4}{3}\kappa_a \psi^{5/3} + (V - V_0) e\psi = 0 \quad (1)$$

und die man, da die Elektronendichte und das Potential nur von der Entfernung  $r$  vom Kern abhängen, in folgender Form

$$4\kappa_i \left( \psi'' + \frac{2}{r} \psi' \right) - \frac{5}{3}\kappa_k \psi^{7/3} + \frac{4}{3}\kappa_a \psi^{5/3} + (V - V_0) e\psi = 0 \quad (2)$$

schreiben kann. Hier ist

$$\psi = \varrho^{1/2}, \quad (3)$$

$\psi'$ ,  $\psi''$  die erste, bzw. zweite Ableitung von  $\psi$  nach  $r$  und  $V$  das Gesamtpotential des Atoms

$$V = \frac{Ze}{r} - e \int \frac{\psi^2(r')}{|r' - r|} dv' = Zeg(r), \quad (4)$$

wo  $Z$  die Ordnungszahl,  $Z_{\text{eff}}(r)$  die effektive Kernladung am Ort  $r$ ,  $r$  bzw.  $r'$  Ortsvektoren,  $e$  die positive Elementarladung und  $dv'$  das Volumenelement bezeichnet;  $V_0$  bedeutet eine Konstante, die aus der Normierungsbedingung

$$\int \psi^2 dv = N \quad (5)$$

festgelegt ist, in der  $N$  die Bedeutung der Elektronenzahl hat;  $\kappa_i$ ,  $\kappa_k$  und  $\kappa_a$  sind die folgenden Konstanten

$$\kappa_i = \frac{1}{8} e^2 a_0, \quad \kappa_k = \frac{3}{10} (3\pi^2)^{2/3} e^2 a_0, \quad \kappa_a = \frac{3}{4} \left( \frac{3}{\pi} \right)^{1/3} e^2, \quad (6)$$

wo  $a_0$  den ersten Bohrschen Wasserstoffradius bezeichnet.

Die Lösung der Gleichung (1), bzw. (2) hat mit den für das freie Atom geltenden Randbedingungen

$$\psi(0) = \text{const.}, \quad (7)$$

$$\psi(\infty) = 0, \quad (8)$$

$$\psi'(\infty) = 0 \quad (9)$$

zu erfolgen.

Die Lösung für das freie N-Atom wurde auf numerischem Wege mit demselben Verfahren festgestellt, das wir in einer früheren Arbeit<sup>2</sup> für andere Atome schon benutzten. Die Lösung, genauer die Funktion  $y(r) = r\psi(r)$ , sowie die radiale Elektronendichte  $D = 4\pi y^2$  ist tabellarisch im Anhang dargestellt.

### 3. Berechnung der Wechselwirkungsenergie

Wie schon gesagt, setzen wir die Elektronendichte  $\nu$  des N<sub>2</sub>-Moleküls als einfache Superposition der Elektronendichte  $\varrho_1$ , bzw.  $\varrho_2$  der beiden freien N-Atome an. Wir setzen also

$$\nu = \varrho_1 + \varrho_2. \quad (10)$$

Für diesen Fall kann man die Wechselwirkungsenergie der beiden N-Atome, d. h. die Energieänderung, die bei der Annäherung der beiden neutralen N-Atome zufolge der Überdeckung der Elektronenwolken entsteht, einfach berechnen<sup>3</sup>. Diese besteht aus mehreren Anteilen, die wir einzeln in Betracht ziehen wollen. Die Indices 1 und 2 weisen durchweg auf die beiden Atome hin.

<sup>2</sup> P. GOMBÁS, Acta Phys. Hung. 5, 483, 1956.

<sup>3</sup> H. JENSEN, ZS. f. Phys. 77, 722, 1932; P. GOMBÁS, ZS. f. Phys. 152, 397, 1958. Man vgl. auch P. GOMBÁS, Die statistische Theorie des Atoms und ihre Anwendungen, S. 143 ff., Springer, Wien, 1949.



Wir beginnen mit der elektrostatischen Wechselwirkungsenergie. Diese besteht aus zwei Teilen. Der eine Teil entsteht daraus, dass jeder der beiden Kerne in die Elektronenwolke des anderen Atoms eindringt und dort unter die Wirkung eines nicht-Coulombschen Potentials  $V$  von der effektiven Kernladung  $Zeg$  kommt. Hieraus resultiert die Energie

$$u_n = 2ZeV(\delta). \quad (11)$$

Der andere Teil der potentiellen Energie resultiert daraus, dass bei der Überdeckung der Elektronenwolken die Abstossungsenergie der Elektronenwolken nicht mehr  $Z^2e^2/\delta$  ist, sondern vermindert wird, denn die überlagerten Teile der Elektronenwolken tragen zur Abstossung nicht bei. Daraus ergibt sich die Energie

$$u_e = -ZeV(\delta) - \frac{1}{2}e \int V_1 \varrho_2 dv - \frac{1}{2}e \int V_2 \varrho_1 dv, \quad (12)$$

die man aus Symmetriegründen auch in der einfacheren Form

$$u_e = -ZeV(\delta) - e \int V_1 \varrho_2 dv \quad (13)$$

schreiben kann.

Der kinetische Anteil der Wechselwirkungsenergie besteht ebenfalls aus zwei Teilen, aus dem Fermischen und aus dem Weizsäckerschen Anteil. Der Fermische Anteil gestaltet sich folgendermassen

$$u_k = \kappa_k \int [(\varrho_1 + \varrho_2)^{5/3} - \varrho_1^{5/3} - \varrho_2^{5/3}] dv. \quad (14)$$

Für den Weizsäckerschen Anteil ergibt sich

$$\begin{aligned} u_i = & \kappa_i \int \frac{(\text{grad } \varrho_1)^2}{\varrho_1 + \varrho_2} dv - \kappa_i \int \frac{(\text{grad } \varrho_1)^2}{\varrho_1} dv + \\ & + \kappa_i \int \frac{(\text{grad } \varrho_2)^2}{\varrho_1 + \varrho_2} dv - \kappa_i \int \frac{(\text{grad } \varrho_2)^2}{\varrho_2} dv + \\ & + 2\kappa_i \int \frac{(\text{grad } \varrho_1, \text{grad } \varrho_2)}{\varrho_1 + \varrho_2} dv. \end{aligned} \quad (15)$$

Da  $\varrho_1$  und  $\varrho_2$  kugelsymmetrisch sind, ist  $\text{grad } \varrho_i = \partial \varrho_i / \partial r_i$  ( $i = 1, 2$ ), wo  $r$  die Entfernung vom Kern  $i$  bezeichnet.

Zu diesen Energieanteilen hat man noch die aus dem Elektronenaustausch resultierende Wechselwirkungsenergie zu addieren, für die man

$$u_a = -\kappa_a \int [(\varrho_1 + \varrho_2)^{4/3} - \varrho_1^{4/3} - \varrho_2^{4/3}] dv \quad (16)$$

erhält.

Für die gesamte Wechselwirkungsenergie der beiden N-Atome ergibt sich also in dieser Näherung

$$u = u_p + u_k + u_i + u_a. \quad (17)$$

Zu dieser käme noch die Korrelationsenergie hinzu; diese ist jedoch klein und kann in dieser Näherung vernachlässigt werden.

#### 4. Resultate.

##### Kernabstand und Bindungsenergie des N<sub>2</sub>-Moleküls

Zur Bestimmung des Kernabstandes und der Bindungsenergie in der stabilen Gleichgewichtslage hat man die Wechselwirkungsenergie  $u$  als Funktion des Kernabstandes  $\delta$  zu berechnen und das Minimum dieser Funktion festzustellen. Wenn man von der Nullpunktschwingung der Kerne absieht, so ist der Kernabstand beim Minimum dieser Funktion der Kernabstand des Moleküls in der stabilen Gleichgewichtslage und der Betrag des Minimums von  $u$  die Bindungsenergie des Moleküls in der stabilen Gleichgewichtslage. Die Berechnungen wurden für die in der Tabelle 1 angegebenen Kernabstände durchgeführt, die Resultate sind in derselben Tabelle angegeben.

Tabelle 1

Die Wechselwirkungsenergie zweier N-Atome, sowie ihre Anteile für verschiedene Werte des Kernabstandes. Der Kernabstand in  $a_0$ - und die Energien in  $e^2/a_0$ -Einheiten

$\delta$	2,25	2,43	2,55	2,67	2,70	2,85	3,09
$u_n$	1,52	1,09	0,878	0,705	0,669	0,506	0,319
$u_e$	-1,82	-1,38 <sub>5</sub>	-1,14	-0,936	-0,894	-0,702	-0,474
$u_k$	1,10 <sub>5</sub>	0,874	0,752	0,658	0,632	0,530	0,398
$u_i$	-0,872	-0,736	-0,682	-0,638	-0,622	-0,556	-0,470
$u_a$	-0,286	-0,230	-0,205	-0,188	-0,181	-0,159	-0,130
$u$	-0,35 <sub>3</sub>	-0,38 <sub>7</sub>	-0,39 <sub>7</sub>	-0,399	-0,396	-0,381	-0,357

Mit den in der Tabelle angegebenen Werten von  $u$  ergibt sich durch eine graphische Interpolation, dass das Minimum von  $u$  bei

$$\delta_0 = 2,62a_0 = 1,39 \text{ \AA} \quad (18)$$

liegt und den Wert  $u_0 = -0,400e^2/a_0$  hat. Der Betrag dieses Wertes

$$D = |u_0| = 0,400 \frac{e^2}{a_0} = 10,9 \text{ eV} \quad (19)$$

ist die Bindungsenergie des Moleküls.

Die entsprechenden empirischen Werte<sup>4</sup> sind

$$\delta_0 = 1,094 \text{ \AA} \quad (20)$$

und

$$D = 9,762 \text{ eV}, \quad (21)$$

mit denen wir unsere Resultate (18) und (19) vergleichen können.

## 5. Diskussion der Resultate

Die von uns eingeschlagene Näherung beruht auf einer einfachen Superposition der Elektronenwolken der beiden N-Atome. Dies kann man nur als eine grobe erste Näherung betrachten. Wesentlich ist, dass man schon in dieser Näherung eine Bindung erhält. Dies ist auf die Berücksichtigung der Weizsäckerschen Energie  $u_i$  im Ausdruck der Bindungsenergie zurückzuführen; ohne dieser wäre die Wechselwirkungsenergie der beiden N-Atome durchweg positiv, d. h. es käme keine Bindung zustande, die beiden N-Atome würden sich abstoßen.

Die von uns berechnete Bindungsenergie (19) stimmt mit dem experimentellen Wert sehr gut überein. In Anbetracht der zugrunde liegenden groben Näherung dürfte diese auffallend gute Übereinstimmung zum Teil auf Zufall beruhen. Weniger gut ist die Übereinstimmung beim Kernabstand und zwar erweist sich der theoretische Wert um cca 30% als zu gross. Bei einer genaueren Approximation der Elektronendichte des Moleküls wird sich der theoretische Kernabstand aller Wahrscheinlichkeit nach verkleinern, d. h. die Übereinstimmung mit dem empirischen Wert verbessern. Für die Bindungsenergie ist in den höheren Näherungen keine grössere Änderung zu erwarten, da die Energie in bezug auf die zugrunde gelegte Dichteverteilung der Elektronen ziemlich unempfindlich ist; die gute Übereinstimmung der hier berechneten Bindungsenergie mit der empirischen dürfte demnach erhalten bleiben.

Zusammenfassend lässt sich also feststellen, dass die auf den Resultaten der vorangehenden kurzen Mitteilung beruhende Erwartung, dass man bei Berücksichtigung der Weizsäckerschen Energiekorrektion für das  $\text{N}_2$ -Molekül eine Bindung erhält, durch die genaueren Berechnungen der vorliegenden Arbeit bestätigt wird. Unser weiteres Ziel ist nun die höheren Näherungen herzuleiten, denn die erzielten Resultate berechtigen zur Hoffnung, dass sich auf diesen Grundlagen eine brauchbare erste Näherung für die Bindung von Molekülen entwickeln lässt.

<sup>4</sup> Bezüglich des Kernabstandes vgl. man. LANDOLT-BÖRNSTEIN, Zahlenwerte u. Funktionen, 6. Aufl., Atom- u. Molekular-Physik, 3. Teil, Molekeln II, S. 10 u. 11, Springer, Berlin-Göttingen-Heidelberg, 1951; bezüglich der Dissoziationsenergie vgl. man A. G. GAYDON, Dissociation Energies, 2. Aufl., S. 152 f. u. 228, Chapman u. Hall, London, 1953. Die von verschiedenen Autoren auf empirischem Wege festgestellten Werte der Dissoziationsenergie weisen von einander grössere Abweichungen auf. Der im Text angegebene Wert scheint der zur Zeit genaueste empirische Wert zu sein.

## Anhang

Lösung der Grundgleichung (1) für  $N(Z=7)$ 

Die Funktion  $y = r\psi$  und die radiale Dichteverteilung der Elektronen  $D = 4\pi y^2$ . Die Funktion  $y$  in  $1/a_0^{1/2}$ - und  $D$  in  $1/a_0$ -Einheiten. (Der Parameter  $V_0$  beträgt  $V_0 = 0,16907 e/a_0$  und die in der in Fussnote 2 angeführten Arbeit definierten Parameter  $\alpha$  und  $\gamma$  haben die Werte:  $\alpha = 1,5163/a_0^{1/2}$  und  $\gamma = 0,5815/a_0$ .)

$r$	$y$	$D$
0	0	0
0,002	0,01151	0,001665
0,004	0,02554	0,008197
0,006	0,03924	0,01935
0,008	0,05258	0,03475
0,010	0,06557	0,05402
0,012	0,07823	0,07691
0,016	0,10260	0,13229
0,020	0,12574	0,19869
0,028	0,16863	0,35734
0,036	0,20743	0,54069
0,044	0,24259	0,73953
0,052	0,27453	0,94709
0,060	0,30360	1,1583
0,076	0,35430	1,5775
0,092	0,39668	1,9774
0,108	0,43228	2,3483
0,124	0,46228	2,6854
0,140	0,48764	2,9882
0,156	0,51009	3,2697
0,172	0,52826	3,5068
0,188	0,54365	3,7141
0,204	0,55665	3,8938
0,220	0,56760	4,0485
0,252	0,58446	4,2926
0,284	0,59596	4,4632
0,316	0,60335	4,5745
0,348	0,60757	4,6388
0,380	0,60930	4,6653
0,412	0,60908	4,6619
0,444	0,60731	4,6349
0,476	0,60431	4,5891
0,508	0,60034	4,5291
0,540	0,59559	4,4577
0,572	0,59021	4,3775
0,636	0,57810	4,1997
0,700	0,56477	4,0083
0,764	0,55074	3,8115
0,828	0,53635	3,6150
0,892	0,52184	3,4221
0,956	0,50738	3,2350
1,020	0,49308	3,0553
1,084	0,47902	2,8835

r	y	D
1,212	0,45182	2,5653
1,340	0,42598	2,2803
1,468	0,40155	2,0262
1,596	0,37851	1,8004
1,724	0,35681	1,5998
1,852	0,33637	1,4218
1,980	0,31711	1,2637
2,108	0,29895	1,1276
2,236	0,28181	0,99799
2,364	0,26562	0,88661
2,492	0,25032	0,78741
2,620	0,23585	0,69901
2,876	0,20920	0,54997
3,132	0,18532	0,43158
3,388	0,16391	0,33761
3,644	0,14474	0,26327
3,900	0,12759	0,20457
4,156	0,11228	0,15842
4,412	0,098648	0,12229
4,668	0,086526	0,094081
4,924	0,075775	0,072155
5,180	0,066262	0,055175
5,436	0,057864	0,042075
5,692	0,050466	0,032004
5,948	0,043961	0,024286
6,204	0,038253	0,018388
6,460	0,033253	0,013896
6,716	0,028881	0,010482
6,972	0,025064	0,0078942
7,228	0,021735	0,0059365
7,484	0,018836	0,0044584
7,740	0,016313	0,0033440
7,996	0,014121	0,0025057
8,252	0,012217	0,0018757
8,508	0,010566	0,0014029
8,764	0,0091341	0,0010484
9,020	0,0078934	0,00078296
9,276	0,0068190	0,00058433
9,532	0,0058890	0,00043580
9,788	0,0050844	0,00032485
10,044	0,0043886	0,00024203
10,300	0,0037870	0,00018021
10,556	0,0032671	0,00013413
10,812	0,0028178	0,000099777
11,068	0,0024296	0,000074179
11,324	0,0020942	0,000055112
11,580	0,0018044	0,000040915
11,836	0,0015549	0,000030382
12,092	0,0013399	0,000022560
12,348	0,0011545	0,000016750

СТАТИСТИЧЕСКАЯ ТРАКТОВКА МОЛЕКУЛЫ  $N_2$ 

П. ГОМБАШ

## Резюме

В связи с одной из предыдущих работ доказывается, что статистической теорией атома можно истолковать связь молекулы  $N_2$ , если в энергии взаимодействия обоих атомов  $N$  принимается во внимание и поправка Вейцеккера. При простой суперпозиции электронного облака обоих атомов  $N$  для расстояния между ядрами получается  $\delta_0 = 1,39 \text{ \AA}$ , а для энергии связи  $D = 10,9 \text{ eV}$ . Энергия связи очень хорошо согласуется с экспериментальным значением энергии, но расстояние между ядрами примерно на 30% больше. В высшего порядка приближениях для расстояния между ядрами можно ожидать значения, гораздо лучше согласующиеся с экспериментальными данными.





## ÜBER DAS SICHTBARMACHEN DER VERSETZUNGEN AN DEN GRENZEN DER SUBKÖRNER DER Fe—Cr- LEGIERUNGEN MITTELS BOMBARDIERUNG DURCH IONEN

Von

ALOIS MAŠÍN,

FORSCHUNGSINSTITUT FÜR VERKEHRSWESEN, PRAG, TSCHECHOSLOWAKEI

VLADIMÍR HAVEL,

FORSCHUNGSINSTITUT FÜR EISENMETALLURGIE, PRAG, TSCHECHOSLOWAKEI

(Eingegangen: 14. II. 1958)

In der letzten Zeit wurde bewiesen, dass zwischen der Verteilung der Ätzfiguren auf der Oberfläche der Metall- oder Ionen-Kristalle, die noch deformiert sind, und den Punkten, in denen die Versetzungen an die Oberfläche treten, ein enger Zusammenhang besteht. Ein Beispiel dafür sind die Ergebnisse der Arbeiten [1—8], in denen sowohl Versetzungen an den Grenzen der Körner, Subkörner und den Gleitlinien, als auch die Art der Versetzungen festgestellt wurde.

Gegenwärtig ist einstweilen noch nicht ganz klar, unter welchen Bedingungen diese Versetzungen geätzt werden. Wie FORTY und FRANK [9] und WYON und MARCHIN [6] bei reinem Aluminium gefunden haben, treten hier Versetzungen nur in dem Fall auf, wenn an ihm Verunreinigungen heften bleiben. DASH [10] gelang es, durch Anwendung von infrarotem Licht auf Kristallen von Silizium mit Kupferbeimischung zu beweisen, dass die Ätzgrüblein an den Stellen erscheinen, wo die Versetzungen an die Kristalloberfläche hervortreten und bei denen fadenähnliche Präzipitate von Kupfer ausgeschieden wurden. Ähnlich kann man bei Legierungen von Al-Mg (3% Mg), Al-Zn (6—12% Zn) und Al-Mn (0,56% Mn) [6] Reihen von Ätzfiguren, welche den Versetzungen in den Gleitlinien entsprechen, erst nach Ätern durch Verformung feststellen. Bei reinem Kupfer und bei hochreinem Aluminium gelang es dagegen nicht, die Versetzungen anzuätzen [11,6]. Es scheint also, das Anätzen der Versetzungen durch die Anwesenheit der Verunreinigungen bei diesen Versetzungen bedingt wird.

In der vorliegenden Arbeit möchten wir das Sichtbarmachen der Versetzungen an den Grenzen der Subkörner einer gehärteten Fe-Cr Legierung mittels Bombardierung durch Ionen beschreiben. Die experimentellen Arbeiten wurden auf einer Eisenlegierung mit 24% Cr, 0,14% C, 0,65% Si, 0,04% Mn durchgeführt. Die Proben hatten die Form von Walzen mit einem Durch-

messer von 8 mm und einer Höhe von 6 mm und wurden bei einer Temperatur von  $1100^{\circ}\text{C}$  in Wasser gehärtet. Die Oberfläche der Stirnseite der Probe wurde vor dem Bombardieren durch Ionen metallographisch geschliffen und mechanisch poliert.

Das Bombardieren durch Ionen wurde in einer Vakuum-Vorrichtung durchgeführt, die aus einer Glasröhre, welche an beiden Enden eingeschliffen wurde, bestand. In den Einschliff an dem einen Ende wurde ein Messinghalter mit der Probe gelegt und in den entgegengesetzten Einschliff die Anode, welche durch eine Aluminiumfolie gebildet wurde. Der Halter, welcher die Form des Kernes des Einschliffes hatte, wurde durch zirkulierendes Wasser gekühlt, sodass die Probe während des Bombardierens ununterbrochen ge-

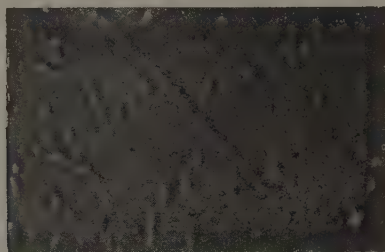


Abb. 1. Detail der angeätzten Spuren, entstanden durch Bombardierung durch Ionen (Ursprüngliche Vergrößerung  $1320\times$ )

kühlt wurde. Die Probe wurde in ihm derart befestigt, dass sie die Stirn des Halters um 0,15 mm überhöhte und, um das Bombardieren durch Ionen nur auf ihre Oberfläche zu konzentrieren, wurde die Stirn des Halters mit einer dünnen elektrischen Isolationsmasse bedeckt. Das Bombardieren durch Ionen wurde bei einer Spannung von 1700—1900 V Gleichstrom und einer Stromintensität von 3 mA durchgeführt. Die Ätzzeit bewegte sich zwischen 80—130 Minuten.

Nach einem zweistündigen Bombardieren der Oberfläche durch Ionen erschienen innerhalb der einzelnen Körner Ketten von Spuren, die an die Spuren der Versetzungen z. B. an den Grenzen der Subkörner oder an den Gleitlinien am Germanium, Siliziumeisen, Aluminium u. a. erinnern [1—8]. Ihre Ausbildungsform ist aus den Abbildungen 1 und 2 ersichtlich.

Die Ketten der Spuren umgrenzen meistens kleine Gebiete — die Subkörner innerhalb der Körner.

Da die Grenzen der Subkörner, wie bekannt [5], durch Versetzungen gebildet werden und da die durch Bombardierung der Ionen entstandenen Spuren mit den Spuren der Versetzungen an anderen Metallen identisch sind,

können sie auch hier den Versetzungen zusprechen, die an der Oberfläche zum Vorschein kommen.

Aus den Abbildungen 2 und 3 wird ersichtlich, dass die Versetzungen nur in den Gebieten sichtbar gemacht werden, wo keine grossen Karbidbestand-

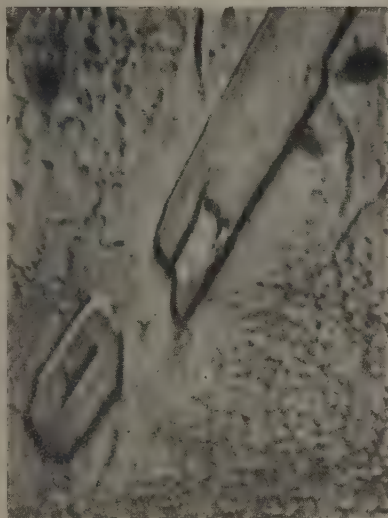


Abb. 2. Umgebung von karbidischen Bestandteilen ohne sichtbargemachte Versetzungen  
(Urspr. Vergrösserung 550  $\times$ )

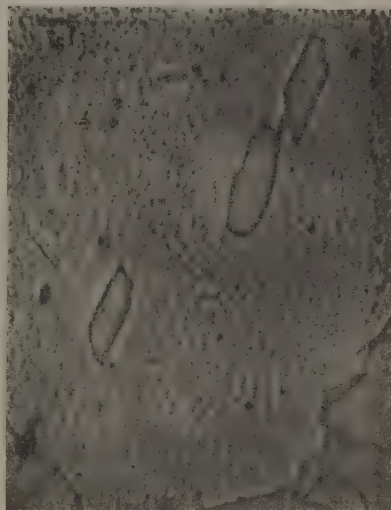


Abb. 3. Umgebung von karbidischen Bestandteilen ohne sichtbargemachte Versetzungen  
(Urspr. Vergrösserung 250  $\times$ )

teile ausgeschieden werden, trotzdem in der Umgebung dieser Bestandteile auch Versetzungen existieren müssen.

Dieses Ergebnis folgt als selbstverständlich aus der Annahme, dass das Sichtbarmachen der Versetzungen von der Anwesenheit von Verunreinigungsatomen — in unserem Fall des Kohlenstoffes — an diesen Versetzungen abhängig ist, wie aus [6, 9, 10, 11] folgt. Wie aus dem Gleichgewichtsdiagramm der angewandten Legierung folgt, ist bei der Temperatur von 1100° C, bei der das Härten der Proben durchgeführt wurde, die Lösbarkeit des Kohlenstoffes grösser, als bei normaler Temperatur. Beim Härten wird deswegen also ein Teil des Kohlenstoffes wegen der sich verringernden Lösbarkeit in Form von Karbiden ausscheiden und der übrige Teil des Kohlenstoffes in der festen Lösung festgehalten. Das während des Härten entstehende Karbid verbraucht dabei zu seiner Bildung den Kohlenstoff der ihm umgebenden, angrenzenden Gebiete und, da die grosse Geschwindigkeit des Temperatur-

sinkens beim Härten nicht mehr erlaubt, den entstandenen Konzentrationsunterschied durch Diffusionsvorgang auszugleichen, werden diese Stellen fast ohne Kohlenstoff sein. Wenn also die Bedingung für das Sichtbarmachen der Versetzungen die Anwesenheit der Kohlenstoffatome an ihnen ist, ob im freien Zustand oder am Anfang des Ausscheidungsstadiums feiner Präzipitate, dann müssen die Versetzungen in den Kornflächen ohne grosse karbidische Teilchen, wo der Kohlenstoff — eventuell schon in der Form von submikroskopischen Karbiden — bei den Versetzungen anwesend ist, angeätzt werden, dagegen in den Gebieten um die karbidischen Teilchen herum, wo der Kohlenstoff verbraucht wurde, werden sie nicht sichtbar gemacht. Das ist in völligem Einklang mit den Abbildungen 2, 3.

Aus der Lage und dem Aussehen der Schatten einzelner Versetzungsspuren, die den Schatten grosser karbidischer Teilchen gleichen, (siehe Abbildung 2) ist ersichtlich, dass einzelne Versetzungen an die Oberfläche hervortreten — Hügelchen bilden — im Gegensatz zum Germanium, Aluminium [1, 4—6] u. a., wo durch das Ätzen Grüblein entstanden sind. Dies bezeugt, dass entweder die Anwesenheit der Kohlenstoffatome um diese Versetzungen herum die Vergrösserung des Widerstandes dieser Stellen gegen die Zerstörung bei der Bombardierung durch Ionen zur Folge hat, oder dass es sich um sehr feine Präzipitate, welche bei diesen Versetzungen ausgeschieden wurden, handelt.

Der Möglichkeit, dass Versetzungen beim Ätzen nicht Grüblein sondern Hügelchen bilden müssen, begegnen wir auch in der Arbeit von COILEY und SMITH [12], welche die Struktur der Grenzen des Stahls mit niedrigem Kohlenstoffgehalt mittels eines Elektromikroskops studierten. Sie haben dabei festgestellt, dass die Grenze durch einen ganzen Kamm gebildet wird, der aus kleinen Hügelchen besteht. Diese Hügelchen erklären sie dann als Versetzungskanten, die die Grenze bilden, zu der die Kohlenstoffatome diffundieren.

#### LITERATURVERZEICHNIS

1. F. L. VOGEL, W. G. PFANN, H. E. COREY und E. E. THOMAS, *Phys. Rev.*, **90**, 489, 1953.
2. S. AMELICKX, *Acta Met.*, **2**, 848, 1954.
3. S. AMELICKX, *Phil. Mag.*, **1**, 269, 1956.
4. G. WYON und P. LACOMBE, *Rep. Bristol. Conf. Phys. Soc.*, 187, 1955.
5. P. HIRSCH, R. HORNE und M. WHELAN, *Phil. Mag.*, **1**, 677, 1956.
6. G. WYON und J. MARCHIN, *Phil. Mag.*, **46**, 1119, 1955.
7. J. GILMAN und W. JOHNSTON, *J. of Appl. Phys.*, **27**, 1018, 1956.
8. C. G. DUNN und F. W. DANIELS, *Trans. AIME*, **191**, 147, 1951.
9. A. J. FORTY und F. C. FRANK, *J. Phys. Soc. Japan*, **10**, 656, 1955.
10. W. C. DASH, *J. of Appl. Phys.*, **27**, 1193, 1956.
11. P. A. JACQUET, *Acta Met.*, **2**, 752, 1954.
12. J. NUTTING, *Rev. Universelle des Mines*, 9. serie, **12**, 512, 1956.



# DIAMAGNETIC SUSCEPTIBILITY OF PERTURBED SYSTEMS

By

E. KAPUY

RESEARCH GROUP FOR THEORETICAL PHYSICS OF THE HUNGARIAN ACADEMY OF SCIENCES, BUDAPEST

(Received 27. X. 1958)

It is known that the computed value of the diamagnetic susceptibility is very sensitive to the wave function chosen for the calculation. Recently the exact eigenfunction of some states of the  $\text{HeH}^{2+}$  ion was determined for many different nuclear distances by BATES and CARSON [1]. The  $1s\sigma$  ground state of  $\text{HeH}^{2+}$  can be considered as the simplest model of a perturbed system.

If the high-frequency paramagnetism [2] is to be calculated with the aid of perturbation calculations, then the eigenfunctions of all the excited states of  $\text{HeH}^{2+}$  are needed. These, however, are not at our disposal. Therefore it is advisable to apply the variation method, which has been derived by TILLIEU [3] for the calculation of the magnetic susceptibility of systems having zero resultant electronic angular and spin momentum. (In our case the spin momentum is equal to  $\frac{\hbar}{2}$ , however, this is disregarded, because we are interested only in the diamagnetic susceptibility.)

According to TILLIEU the  $\chi_{ij}$  component of the susceptibility tensor is:

$$\chi_{ij} = -\frac{e^2}{4mc^2} \int \psi_0 [r^2 \delta_{ij} - x_i x_j] \psi_0 d\tau - \frac{e}{mc} \int \psi_0 [g_i L_j + g_j L_i] \psi_0 d\tau + \frac{\hbar}{m} \int \psi_0 [(\nabla g_i)(\nabla g_j)] \psi_0 d\tau. \quad (1)$$

Here by indices  $i, j=1, 2, 3$  the coordinates  $x, y, z$  are denoted (for instance  $\chi_{11} = \chi_{xx}$ ,  $L_1 = L_x = \frac{\hbar}{i} \left( y \frac{\partial}{\partial z} - z \frac{\partial}{\partial y} \right)$ ,  $x_1 = x$ ,  $x_2 = y$ ,  $x_3 = z$ ), whereas  $\psi_0$  is the wave function of the ground state of the system. The pure imaginary functions  $g_i (i = x, y, z)$  are the solutions of the following differential equations:

$$\frac{\hbar^2}{2m} \psi_0 \Delta g_i + \frac{\hbar^2}{m} (\nabla \psi_0)(\nabla g_i) = -\frac{e}{2mc} L_i \psi_0, \quad (i = x, y, z). \quad (2)$$

Instead of the solution of the differential equation (1) such functions  $g'_i = iG_i$  are chosen, which contain the variational parameters  $C_1, C_2, \dots, C_k$

and which conform to the symmetry required by equation (2). After that the components  $\chi_{ij}$  are calculated with the functions  $G_i$  ( $i = x, y, z$ ) and the  $C_k$ -s are determined so that the  $\chi_{ij}$ -s be maxima. (The susceptibility can namely be expressed with the aid of the energy:  $\sum_{i=1}^3 \sum_{j=1}^3 \chi_{ij} \mathfrak{H}_i \mathfrak{H}_j = 2E(0) - 2E(\mathfrak{H})$ , here  $\mathfrak{H}$  is the magnetic field strength.  $E(\mathfrak{H})$  and  $E(0)$  the energy of the system in a magnetic field of field strength  $\mathfrak{H}$  and without field, resp.).

He  $\text{H}^{2+}$  has  $C_{\infty v}$  symmetry. The center of the coordinate system be in the nucleus  $\text{He}^{2+}$ , and the  $z$  axis be directed towards the nucleus  $\text{H}^+$ . From  $L_z \psi_0 = 0$  follow  $G_z = 0$  and

$$\chi_{zz} = -\frac{e^2}{4mc^2} \int \psi_0 [x^2 + y^2] \psi_0 d\tau.$$

Since the problem is cylindrically symmetric :

$$\begin{aligned} \chi_{xx} = \chi_{yy} = & -\frac{e^2}{4mc^2} \int \psi_0 [y^2 + z^2] \psi_0 d\tau - \frac{2ie}{mc} \int \psi_0 G_x L_x \psi_0 d\tau - \\ & - \frac{\hbar^2}{m} \int \psi_0 |\nabla G_x|^2 \psi_0 d\tau, \end{aligned}$$

and the off-diagonal elements are equal to zero.

For the  $G_x$ -s the following expressions were chosen :

a) one-parameter expression :  $G_x^{(a)} = C_y$ ,

b) two-parameter expression :  $G_x^{(b)} = C_1 y + C_2 yz$ .

In both cases the calculation of the integrals is equivalent to the determination of the mean values  $\bar{z}$ ,  $\bar{z}^2$ ,  $\bar{x}^2$ ,  $\bar{y}^2$ . These, however, can be readily found in the literature for the ground state of  $\text{HeH}^{2+}$  [4].

In the following Table the average molar susceptibilities

$$\chi_{\text{mol}} = \frac{\chi_{xx} + \chi_{yy} + \chi_{zz}}{3} N$$

are to be found ( $N$  is Avogadro's number), namely separately the so-called Langevin term  $\chi_{\text{mol}}^L$  :

$$\chi_{\text{mol}}^L = -\frac{Ne^2}{6mc^2} \int \psi_0 r^2 \psi_0 d\tau,$$

the high-frequency term  $\chi_{\text{mol}}^{HF}$

$$\chi_{\text{mol}}^{HF} = -\frac{4ieN}{3mc} \int \psi_0 G_x L_x \psi_0 d\tau - \frac{2}{3} \frac{N\hbar^2}{m} \int \psi_0 |\nabla G_x|^2 \psi_0 d\tau$$

and the sum of both :

$$\chi_{\text{mol}} = \chi_{\text{mol}}^L + \chi_{\text{mol}}^{HF}$$

in electromagnetic units. (The quantities calculated with the one-parameter function  $G_x^{(a)}$ , and the two-parameter function  $G_x^{(b)}$  are denoted by  $\chi_{mol}^{HF(a)}$ ,  $\chi_{mol}^{(a)}$  and  $\chi_{mol}^{HF(b)}$ ,  $\chi_{mol}^{(b)}$  resp.)

Table

$R$ in a. u.	$\chi_{mol}^L \cdot 10^6$ in e. m. u.	$\chi_{mol}^{HF(a)} \cdot 10^6$ in e. m. u.	$\chi_{mol}^{(a)} \cdot 10^6$ in e. m. u.	$\chi_{mol}^{HF(b)} \cdot 10^6$ in e. m. u.	$\chi_{mol}^{(b)} \cdot 10^6$ in e. m. u.
0,0	-0,263	+0,000	-0,263	+0,000	-0,263
0,5	-0,399	+0,015	-0,384	+0,016	-0,383
1,0	-0,551	+0,025	-0,526	+0,031	-0,520
2,0	-0,620	+0,006	-0,614	+0,009	-0,611
3,0	-0,600	+0,001	-0,599	+0,002	-0,598
4,0	-0,595	+0,000	-0,595	+0,000	-0,595
5,0	-0,593	+0,000	-0,593	+0,000	-0,593
$\infty$	-0,593	+0,000	-0,593	+0,000	-0,593

If therefore the nucleus  $H^+$  approaches  $He^+$  from the infinite, then first of all the term  $\chi_{mol}^L$  begins to increase (from  $R = 4$ ), later also  $\chi_{mol}^{HF}$  increases (from  $R = 2$ ) and from  $R = 1,5$  (about the threefold Bohr radius of  $He^+$ )  $\chi_{mol}$  is already smaller than the susceptibility of  $He^+$ . For  $R = 0$ , of course,  $\chi_{mol}$  agrees with the susceptibility of  $Li^{2+}$ .

It is well known that the susceptibility of some diamagnetic substances (for instance water) increases suddenly at the melting point and then increases slowly with increasing temperature (in absolute value). This can be interpreted according to what has been said before in the following way:

Owing to the increasing disorder and the thermal expansion the distance between the groups perturbing each other increases,  $\chi_{mol}^{HF}$  decreases and thus  $\chi_{mol}$  increases.

## REFERENCES

1. D. R. BATES and T. R. CARSON, Proc. Roy. Soc. A, **234**, 207, 1956.
2. J. H. VAN VLECK, The Theory of Electric and Magnetic Susceptibilities, Oxford, University Press 1932.
3. J. TILLIEU, Ann. de Phys., 13. série **2**, 471, 631, 1957.
4. B. L. MOISEWITSCH and A. L. STEWART, Proc. Phys. Soc. **69**, 480, 1956.



A kiadásért felel az Akadémiai Kiadó igazgatója

Műszaki felelős: Farkas Sándor

A kézirat nyomdába érkezett: 1959. II. 5. — Terjedelem: 11 (A/5) ív, 33 ábra

---

Akadémiai Nyomda Budapest, V. Gerlőczy u. — 48111/58 — Felelős vezető: Bernát György